Copyright is owned by the Author of the thesis. Permission is given for a copy to be downloaded by an individual for the purpose of research and private study only. The thesis may not be reproduced elsewhere without the permission of the Author.

The Tale of the Shear-Thickening Mamaku Polysaccharide, from Forest to Gut

Akshay Bisht

Supervisor

A/Prof. Dr. Lara Matia-Merino
Associate Professor in Food Rheology & Colloid Science
Massey University

Co-supervisors

A/Prof. Dr. Kelvin K. T. Goh
Associate Professor in Food Technology
Academic Director, Singapore Institute of Technology-Massey Food Technology
Massey University

Dr. John A. Monro
Principal Scientist, Food Nutrition & Health
New Zealand Institute for Plant & Food Research Ltd.

Copyright © 2023 Akshay Bisht

Copyright is owned by the Author of the thesis. Permission is given for a copy to be downloaded by an individual for the purpose of research and private study only. The thesis may not be reproduced elsewhere without the prior permission of the Author.

The Tale of the Shear-Thickening Mamaku Polysaccharide from Forest to Gut

A thesis presented in partial fulfilment of the

requirements for the degree of

Doctor of Philosophy

(Food Technology)

Massey University

Palmerston North, New Zealand

Akshay Bisht

2023

Abstract

The New Zealand black tree fern (*Cyathea medullaris*, 'mamaku' in the Māori language) is grown across the Pacific Islands and has a long history of use for therapeutic benefits or as food by Māori people. The water-soluble gum extract from mamaku fern contains a novel glucuronomannan biomacromolecule, called mamaku polysaccharide (MP), which has been shown to exhibit a unique shear-thickening (*i.e.,* increase in viscosity on shearing) behaviour at a similar shear rate as that found in the human stomach. Herein, the objective was to gain a better technical and physiological understanding of MP for designing a novel shear-thickening ingredient for the industry with proven effects in humans.

The shear-thickening behaviour of MP was sensitive to the harvesting age of mamaku fronds and industrial operations such as high temperature and shear. With the increase in harvesting age, the molecular weight of MP reduced, which consequently reduced the shear viscosity. The shear-thickening behaviour was lost in MP from old fronds. Furthermore, the temperature treatment disintegrated the backbone of MP into smaller fragments which caused a reduction in viscosity and extent of shear-thickening. Similar rheological trends were observed post-shear treatment, however, there was no evidence of depolymerisation.

A combination of *in vitro* models revealed that mamaku gum extract could improve host gut functioning by reducing the activity of digestive enzymes (α-amylase, pepsin and lipase) and binding bile acids. Mamaku gum can act as a substrate for colonic fermentation, promote the production of short-chain fatty acids and alter the colonic microbial composition.

Upon ingesting mamaku gum, the shear-thickening behaviour may develop in the oesophagus causing a possible choking hazard. Therefore, the potential of using the whole pith—natural entrapment of MP in the tissue of pith—as an alternative to gum extract was studied. Freeze-dried pith was ground to powder. The powder particles swelled upon rehydration with water and released the water-soluble MP into the continuous phase in a time-dependent manner. The presence of enough MP in the continuous phase to form polymer-polymer interactions resulted in a shear-thickening behaviour of the pith powder suspension similar to the MP extract solution. Moreover, the co-consumption of 1 h pre-hydrated mamaku pith powder with a carbohydrate-rich meal significantly reduced the postprandial glycaemic response (blood glucose peak height) in human participants.

Additionally, the consumption of mamaku pith powder in rats could alter colonic microbiota. Interestingly, more than half of the MP (uronic acid) consumed by rats survived the gut transition and was obtained in faeces, suggesting that MP could potentially be used as a laxative.

Thus, mamaku pith could be used as an alternative to gum extract to develop a natural shear-thickening ingredient which may potentially help to manage diabetes and improve colon health.

Keywords**:** Mamaku polysaccharide, shear and extensional rheology, *in vitro* gastrointestinal digestion and fermentation, drying and powder processing, glycaemic response

Acknowledgements

I first dreamed of pursuing a doctoral degree in 2014 while helping with a project during my graduation days. I knew the journey I dreamt to embark upon would be challenging and was preparing for it since then. As I arrived in New Zealand on the 16th of March 2020 for PhD, a nationwide lockdown was announced. COVID came as a surprise (as to others) and most of the preparations I did were of no use. Because of these unprecedented times, the gratitude I feel is even stronger and deeper. For a long time, I have been looking forward to this moment when I could write these words of appreciation and now that the time has come, here it goes…

I am indebted to my supervisor, A/Prof. Dr. Lara Matia-Merino for giving me this opportunity to live my dream. I am grateful for your mentorship, guidance, encouragement, and feedback throughout my doctoral study. You gave me the freedom to explore the project in my way and supported my ideas. You were easily accessible and your doors were always open for me. I only had to knock on your door, cry out my questions and you would help. You not only helped me to be a better researcher but inspires me to be a good human being. Thank you for all the food you feed me, for pushing me to join BodyStep classes and for motivating me to have a life outside work. You have gone as far as doing groceries for me. Thank you for always being there and standing by me no matter what came our way.

I am grateful to A/Prof. Dr. Kelvin K. T. Goh, my co-supervisor, whom I never meet in person (as he is based in Singapore). But thanks to technology, you never let the distance be a problem. You were always an email away, willing to discuss things over a video call at any hour of the day. I am thankful for your bits of advice, motivation and valuable comments. Thank you for always checking on my health and well-being. On a lighter note, I thank you for your patience, especially when I speak fast. You would patiently listen to me, wait for me to stop and then ask me to repeat.

I would like to express my earnest gratitude towards Dr. John A. Monro, my other co-supervisor, for always inspiring me with his enthusiasm and passion for science. Thank you for always helping me with my queries, sharing your years of experience and knowledge and pushing me in the right direction to achieve a good thesis. Thank you for involving me

in human and rat studies. I always enjoyed your humour, especially at difficult times which we all want to forget.

I am thankful to the High-Value Nutrition (HVN) programme of The New Zealand National Science Challenges (Ministry of Business, Innovation and Employment) for funding the research project *Mamaku whakaoraora* (Contract no. AUAX1902). This doctoral thesis is a deliverable from the *Mamaku whakaoraora* project involving an industrial partner (Nga Uri o te Ngahere Trust), The New Zealand Institute for Plant and Food Research Ltd. and Massey University. The New Zealand Institute for Plant and Food Research Ltd. is acknowledged for financially supporting my doctoral studies (PFR Contract no. 38041). I am grateful to Massey University for providing Doctoral Conference Grant to attend an overseas conference.

To Prof. Dr. Nicholas (Nick) Rahiri Roskruge (Tahuri Whenua, National Māori Vegetable Growers Collective; School of Agriculture and Environment, Massey University) and Mr. Garry M. Watson (Nga Uri o te Ngahere Trust) for the cultural review of the project.

To Prof. Dr. Richard Archer for providing the mamaku fronds for this thesis. Thank you for helping with harvesting and for your hospitality. I always enjoyed our philosophical-*ish* conversations after the NZIFST events.

To people from the Food Innovation team (Ms. Janiene Gilliland, Mr. Chris Hall and Ms. Chanapha (Nok) Sawatdeenaruenat), technicians (Ms. Michelle Tamehana, Mr. Steve Glasgow and Mr. Warwick Johnson) and students (Ms. Phan Le Bao Ngoc, Mr. Jacob Jibi Peter, Ms. Sini Yi Quek, Mr. Edwin Susanto, Dr. Maryam Abshirini, Dr. Emmanual Kyere, Dr. Marzieh (Marzi) Eblaghi, Dr. Jolin Morel and Dr. Jiuk Kim) for their assistance during the harvesting and processing of mamaku fronds.

To Mr. Allan Hardacre for all the discussions we had. Thank you for teaching me mamaku gum extraction and for guidance on extrusion technology.

To Dr. Jason Hindmarsh for allowing me to use the in-house built extensional rheometer and helping with setting it up. Chapter 4 would have been incomplete without your support.

To Dr. Ian M. Sims for accommodating me at The Ferrier Research Institute, Victoria University of Wellington, teaching constituent sugar analysis and helping with interpreting NMR results.

To Dr. Patrick J. B. Edwards for assistance with NMR analysis and data interpretation.

To Dr. Janet Weber for discussions and suggestions while filling out the human ethics application for collecting faecal samples.

To Dr. Carlos Montoya from AgResearch Ltd. for proofreading Chapter 5. Your valuable comments helped me significantly improve the chapter.

To Prof. Dr. Anthony (Tony) Paterson and Dr. Qun (Jim) Chen for valuable discussions and insides on drying and powder technology. Thank you for proofreading Chapter 7.

To Prof. Dr. Matt Golding for comments on sections of the thesis.

To New Zealand eScience Infrastructure (NeSI; funded jointly by NeSI's collaborator institutions and through the Ministry of Business, Innovation and Employment's Research Infrastructure programme) for high-performance computing facility and training services specifically in genomics and bioinformatics. Special mention to Mr. Dinindu (Dini) Senanayake for always being there for troubleshooting. I am grateful to Dr. Valter Almeidax for guiding me at the beginning of bioinformatics analysis.

To Dr. Suman Mishra from The New Zealand Institute for Plant and Food Research Ltd. for managing the human trial and for all the laughter and food we shared.

To Dr. Andrew Carroll, Ms. Nayer Ngamatea, Ms. Sheridan Martell, Ms. Hannah Dinnan, Mr. Duncan Hedderley, Ms. Halina Stoklosinski and Ms. Sue Middlemiss-Kraak from The New Zealand Institute for Plant and Food Research Ltd. for their assistance with human and rat trails. I am also grateful to Dr. Caroline Kim for aiding me to set up *in vitro* colonic fermentation model.

To all the lab managers and technicians: Ms. Michelle Tamehana (Food Characterisation lab), Mr. Steve Glasgow (Food Chemistry lab), Ms. Ann-Marie Jackson, Dr. Baizura Md Zain and Ms. Kylie Evans (Microbiology lab), Ms. Rana Naser, Mr. Garry Radford, Mr. Warwick Johnson and Mr. Rob Gaw (FoodPilot), Ms. Inge Merts and Mr. John Edwards, (Bioprocess Engineering lab) and Ms. Anja Moebis (Soil and Earth Sciences). Thank you for providing me with training and advice, helping with procurement and facilitating my lab work. Thank you for being friendly and helpful.

To Dr. Matthew Savoian and Mr. Raoul Solomon (Manawatu Microscopy and Imaging Centre) for training and helping with confocal and scanning electron microscopy analysis.

To Ms. Maggie Zou, Dr. Zhigao Niu, Dr. Peter Zhu and Dr. Siqi Li from Riddet Institute for providing laboratory-related training.

To Pūhoro visiting intern (Ms. Shahanna Tahere) and graduate students (Ms. Megan Palmer and Ms. Teresa Sumich) for their assistance in new product development work.

To Massey Genome Service for performing amplicon sequencing.

To Massey Nutrition Laboratory for timely completion of chemical analysis.

To Dr. Russell Wilson for insights into commercialisation and intellectual property (IP) aspects of the project and to Mr. Carl Massarotto for handling the contractual side of the project.

To Mr. Tim O'Dea, Mr. Peter Jeffery, Mr. Nicholas Look and Mr. Mark Adams for resolving information technology (IT) related issues.

I am deeply thankful to my mentors in India, late A/Prof. Dr. Vijendra Mishra, A/Prof. Dr. Neetu K. Taneja and Dr. Divya Sachdev for always guiding me and inspiring me to dream big. You guys early on saw my passion for research and helped me to inculcate the required skills. I am grateful to Dr. Harinderjeet Bhullar (Harry Di) for allowing me to help her with her project which implanted the dream for a PhD and for motivating me to achieve it.

Thank you to my friends in New Zealand, Cai Ling, Haz, Feng Ming, Matthew, Anubhavi, Linda, Maru, John, Ngoc, Solita, Arthur, Emmanuel, Marzi, Jolin and Jiuk, for all the memories, laughter, and little social life I had. I am grateful to Cai Ling, Haz and Feng Ming for finding time to listen to me and help me resolve my curiosities. You three, thank you for feeding me, keeping an eye on my well-being and making me part of your journeys.

Friends from back home in India, Saummya and Sanju for always being a phone call away and helping me to cope with difficult times. Thank you for being my cheerleaders. Heartfelt thanks to Akansha, Ankit and Manasvi for their support and for checking on me.

Lastly, a big thank you to my parents and my sister in India, for putting up with my occasional tantrums and still loving and supporting me. Thank you for letting me pursue my dreams.

And, if I missed mentioning anyone who supported me or contributed directly or indirectly to this thesis, thank you.

My strengths are not from me alone but from the people around me!

To all those who loved me, motivated me, supported me, stood by me, taught me, cried with me, cried for me, fought with me, fought for me. People I call friends and family, some of whom may be lost in the process.

Table of contents

Abstract *i*
Acknowledgements *iii*
Table of contents *ix*
List of figures *xv*
List of tables *xxiii*
List of publications and conference proceedings *xxv*

Chapter 1: Introduction **1**
1.1 Background 1

Chapter 2: Literature review **7**
2.1 Introduction 8
2.2 Mamaku polysaccharide 10
2.2.1 Characterisation 10
2.2.2 Rheological behaviour 13
2.2.3 Shear-thickening behaviour 17
2.2.3.1 What is the reason for shear-thickening in mamaku polysaccharide? 20
2.2.4 Mamaku gum in the stomach 23
2.3 Powder production 25
2.3.1 Drying 25
2.3.1.1 Oven drying 31
2.3.1.2 Freeze drying 35
2.3.2 Powder properties 38
2.3.2.1 Particle size and distribution 39
2.3.2.2 Particle shape 40
2.3.2.3 Density 40
2.3.2.4 Microstructure and surface properties of powder 42
2.3.2.5 Powder rehydration 43
2.4 Possible physiological effects and health benefits of mamaku 48
2.4.1 Possible physiological effects 49

2.4.1.1 Physical structure of digesta 49
2.4.1.2 Binding ability of dietary fibres 50
2.4.1.3 Gut microbiota fermentation 51
2.4.2 Possible health benefits 53
2.5 Gaps in the literature 55

Chapter 3: Experimental techniques 57
3.1 Processing of mamaku fronds 58
3.1.1 Extraction of mamaku gum 59
3.1.2 Production of mamaku pith powder 60
3.2 Polysaccharide characterisation 62
3.2.1 Constituent sugar composition 62
3.2.2 Colorimetric quantification of uronic acid 64
3.2.3 Nuclear magnetic resonance spectroscopy 64
3.2.4 Size-exclusion chromatography coupled with multi-angle laser light scattering 66
3.2.5 Dynamic light scattering (Zetasizer) 68
3.3 Powder particle characterisation 69
3.3.1 Powder particle size 70
3.3.2 Scanning electron microscopy 71
3.4 Rheological characterisation 71
3.4.1 Shear rheology 71
3.4.1.1 Rotational shear rheology 71
3.4.1.2 Oscillatory shear rheology 75
3.4.2 Extensional rheology 77
3.5 *In vitro* studies 80
3.5.1 *In vitro* enzyme activity inhibition 80
3.5.2 *In vitro* static digestion 81
3.5.3 *In vitro* static colonic fermentation 83
3.6 Metagenomic analysis 85
3.7 Human trial 90

Chapter 4: Does harvesting age matter? Changes in structure and rheology of a shear-thickening polysaccharide from *Cyathea medullaris* as a function of age 93
4.1 Introduction 94
4.2 Materials and methods 95
4.2.1 Extraction and purification of mamaku gum 95
4.2.2 Chemical analysis 97
4.2.3 Constituent sugar analysis 97
4.2.4 Nuclear magnetic resonance spectroscopy 98

4.2.5 Size-exclusion chromatography coupled with multi-angle laser light scattering 98
4.2.6 Shear rheology 99
4.2.7 Extensional rheology 99
4.2.8 Statistical analysis 101
4.3 Results and discussion 101
4.3.1 Yield 101
4.3.2 Chemical composition 102
4.3.3 Nuclear magnetic resonance 104
4.3.4 Size-exclusion chromatography coupled with multi-angle laser light scattering 106
4.3.5 Shear rheology 108
4.3.6 Extensional rheology 112
4.4 General discussion 117

Chapter 5: The fate of mamaku gum in the gut: Effect on *in vitro* gastrointestinal function and colon fermentation by human faecal microbiota 123
5.1 Introduction 124
5.2 Materials and methods 126
5.2.1 Extraction of mamaku gum 126
5.2.2 Molecular weight analysis during *in vitro* simulated gastric and intestinal digestion 126
5.2.3 Effect on enzyme activity and bile acids binding ability 127
5.2.4 *In vitro* static colonic fermentation 129
5.2.4.1 Determination of pH and short-chain fatty acids 130
5.2.4.2 DNA extraction, amplification and 16S rRNA gene sequencing 131
5.2.4.3 Bioinformatic analysis 131
5.2.5 Rotational shear rheology 132
5.2.6 Statistical analysis 132
5.3 Results and discussion 133
5.3.1 Gastric and intestinal digestion of mamaku gum 133
5.3.2 Enzyme activity and bile acids binding ability 136
5.3.3 *In vitro* colonic fermentation 138
5.3.3.1 Short-chain fatty acids production and pH change 138
5.3.3.2 Effect on colonic microbiota 142
5.4 General discussion 146

Chapter 6: Shear and temperature sensitivity of a shear-thickening biopolymer from the New Zealand black tree fern 151
6.1 Introduction 152

6.2 Materials and methods 154
6.2.1 Extraction of mamaku gum 154
6.2.2 Shear and temperature treatments 155
6.2.3 Shear rheology 156
6.2.4 Size-exclusion chromatography coupled with multi-angle laser light scattering 156
6.2.5 Dynamic light scattering 157
6.2.6 Constituent sugar analysis and nuclear magnetic resonance spectroscopy 157
6.2.7 Urea treatment 157
6.2.8 Statistical analysis 157
6.3 Results and discussion 158
6.3.1 Rheological analysis 158
6.3.2 Molecular weight and size of mamaku polysaccharide 165
6.3.3 Constituent sugar composition and nuclear magnetic resonance 168
6.4 General discussion 170

Chapter 7: Process-structure-function relationship for mamaku suspension: Effect of drying methods on powder functionality 177
7.1 Introduction 178
7.2 Materials and methods 180
7.2.1 Mamaku pith powder 180
7.2.2 Powder characterisation 180
7.2.2.1 Chemical composition 180
7.2.2.2 Colour 181
7.2.2.3 Density of powder 181
7.2.2.4 Powder flow behaviour 182
7.2.2.5 Scanning electron microscopy 182
7.2.3 Powder rehydration 183
7.2.3.1 Wetting: Contact angle 183
7.2.3.2 Sinking time 183
7.2.3.3 Dispersion: Particle size measurements 183
7.2.3.4 Solubilisation 184
7.2.4 Shear rotational rheology 184
7.2.5 Release behaviour of mamaku polysaccharide 184
7.2.6 *In vitro* digestion of starch 184
7.2.7 Statistical analysis 185
7.3 Results and discussion 185
7.3.1 Chemical composition 185
7.3.2 Powder characterisation 186
7.3.2.1 Colour 186

7.3.2.2 Density and flow behaviour 186
7.3.2.3 Powder microstructure 187
7.3.3 Rehydration behaviour of powders 189
7.3.3.1 Wetting 189
7.3.3.2 Sinking 189
7.3.3.3 Dispersion and solubilisation 191
7.3.4 Rheological characterisation 192
7.3.5 Release of mamaku polysaccharide from powder particles 195
7.3.6 Effect of hydrated powders on *in vitro* starch digestion 198
7.4 General discussion 199

Chapter: 8 *In vivo* effects of mamaku pith powder on glycaemic, insulin and appetite responses and colonic fermentation 203
8.1 Introduction 204
8.2 Materials and methods 206
8.2.1 Human trial: Effect of mamaku pith powder on glycaemic, insulin and appetite responses 206
8.2.1.1 Participants 207
8.2.1.2 Study design 208
8.2.1.3 Data collection 208
8.2.2 Rat trial: Effect of mamaku pith powder on colon fermentation 209
8.2.2.1 Colonic microbiota analysis 210
8.2.2.2 Quantification of caecal short-chain fatty acids 211
8.2.2.3 Faecal uronic acid determination 212
8.2.3 Rotational rheology 212
8.2.4 Data processing and statistical analysis 213
8.3 Results 213
8.3.1 Human trial: Effect of mamaku pith powder on glycaemic, insulin and appetite responses 213
8.3.1.1 Postprandial blood glucose response 214
8.3.1.2 Postprandial insulin response 216
8.3.1.3 Subjective rating of appetite sensation 218
8.3.2: Rat trial: Effect of mamaku pith powder on colon fermentation 219
8.3.2.1 Colonic microbiota 219
8.3.2.2 Short-chain fatty acids production 220
8.3.2.3 Mamaku polysaccharide in faeces 222
8.4 Discussion 222

Chapter 9: Overall conclusions and recommendations for future work 227
9.1 Conclusions 228
9.1.1 Does the harvesting age of mamaku frond matter? 228

9.1.1.1 How does the structure and rheology of mamaku gum change with age? (Chapter 4) 228
9.1.1.2 How does mamaku gum affect the *in vitro* gastrointestinal function and colonic fermentation as a function of age? (Chapter 5) 230
9.1.2 Can mamaku gum/pith withstand industrial operations without compromising the shear-thickening behaviour? 231
9.1.2.1 Is mamaku gum sensitive to high shear and temperature treatments? (Chapter 6) 232
9.1.2.2 How does the drying method affect the functionality of the pith powder? (Chapter 7) 234
9.1.3 Will mamaku pith have an impact *in vivo*? 236
9.1.3.1 Can the consumption of pith powder have an impact on glycaemic response and colonic fermentation? (Chapter 8) 236
9.2 Recommendations 238

References *243*
Appendices *281*

List of figures

Figure 1.1: Overview of thesis structure. 5

Figure 2.1: (A) Picture of mamaku plant (*Cyathea medullaris*, New Zealand black tree fern), (B) young fronds: koru and (C) trunk with hexagonal patterns. 8

Figure 2.2: Possible structure of glucuronomannan polysaccharides extracted from (A) mamaku fern (Wee et al., 2014), (B) sesame leaves (Nep et al., 2016), (C) *Drosera* species (Erni et al., 2011) and (D) *Dicerocaryum zanguebaricum* (Barone et al., 1996). 12

Figure 2.3: Typical flow curve exhibited by mamaku gum. 14

Figure 2.4: Possible microstructural rearrangements in (A) particle suspensions, (B) micelle systems and (C) associative polymers, which leads to shear-thickening behaviour. (*): Beginning of shear-thickening behaviour. 18

Figure 2.5: Schematic illustration showing possible 'sticky' groups responsible for hydrogen bonding during shear-thickening in mamaku polysaccharide. GlcA, glucuronic acid. 22

Figure 2.6: Schematic diagram of an oven-dryer. 31

Figure 2.7: Micrographs of quince fruit during freeze and oven-drying. 34

Figure 2.8: (A) Schematic diagram of a freeze-dryer (A') showing dry layer formation during drying. (B) A typical product temperature, shelf temperature and pressure profiles during drying. 36

Figure 2.9: (A) Illustration of a particle with intraparticle pores. Consideration of different volumes (shown in dash lines) to calculate (B) particle and (C) bulk densities. 41

Figure 2.10: Schematic representation of rehydration of powder and hydration of released polysaccharide, showing (A) wetting, (B) sinking, (C) dispersion, (D) solubilising, (A') contact angle and (D') the interaction of water molecules with polysaccharide. 47

Figure 2.11: Overview of possible physiological effects and health benefits of mamaku. 53

Figure 3.1: Pictures from the field during the harvesting of mamaku fronds. 58

Figure 3.2: Processing of mamaku fern to obtain crude gum extract. 59

Figure 3.3: Processing of mamaku fern to obtain pith powder. 61

Figure 3.4: Particle size distribution of (A, A') freeze-dried and (B, B') oven-dried mamaku pith powder (dry powder) ground using a hammer mill (HM), pin mill (PM) and coffee grinder (CG). Values are plotted as means ± standard deviation (n=3). Values with the different superscripts are significantly different ($p \leq 0.05$) for a given parameter. 62

Figure 3.5: Schematic illustration of constituent sugar composition analysis with elution time for different sugars at different concentrations. Fuc, Fucose; Rha, Rhamnose; Ara, Arabinose; Gal, Galactose; Glc, Glucose; Man, Mannose; Xyl, Xylose; GalA, Galacturonic acid; GlcA, Glucuronic acid. 63

Figure 3.6: (A) Nuclear spins are oriented randomly in the absence of an external magnetic field but (B) on applying an external field the nuclei orient their own magnetic field to low and high energy states. The energy difference between the two states increases with increasing the strength of the applied magnetic field. (C) Irradiating the oriented nuclei with radio frequency cause the low-energy state 'spin-flip' to the higher-energy state. 65

Figure 3.7: Schematic illustration of (A) size-exclusion chromatography (SEC) of polymers of different molecular sizes and (B) multi-angle laser light scattering (MALLS) detector. 66

Figure 3.8: Movement of particles and intensity fluctuation over time for small and large particles. 69

Figure 3.9: Influence of particle size on the angle and the intensity of scattered light. 70

Figure 3.10: Flow of fluid between two parallel plates on applying force. 72

Figure 3.11: Sample expulsion observed for freeze-dried mamaku pith powder hydrated (2% w/w) overnight during viscosity measurement using plate-and-plate (A: smooth plate and B: serrated plate) at approximately 25 s^{-1}. 73

Figure 3.12: Sedimentation over 30 min at 25°C for (A) freeze-dried (0.75% w/w) and (B) oven-dried (1% w/w) mamaku pith powders hydrated overnight. Turbiscan Stability Index (TSI) at 0.5 is marked for both samples. 74

Figure 3.13: Rheological profile of overnight hydrated oven-dried mamaku pith powder (A: 0.5% w/w and B: 3% w/w) using cup-and-bod geometry and vane geometry. Measurements were taken at 20°C. 74

Figure 3.14: Response of elastic solids, viscous liquids and viscoelastic fluids to applied stress. The difference between the stress and strain waves is demoted by δ. 75

Figure 3.15: Linear and non-linear viscoelastic region (LVR and non-LVR). 77

Figure 3.16: Schematic illustration showing extensional deformation. 78

Figure 3.17: Schematic diagram of the capillary-breakup extensional rheometer. 79

Figure 3.18: Overview of Infogest 2.0 *in vitro* static digestion model showing oral, gastric and intestinal phases. SSF, simulated salivary fluid; SGF, simulated gastric fluid; SIF, simulated intestinal fluid. 83

Figure 3.19: Schematic illustration showing *in vitro* experimental sequence from digestion to fermentation. 84

Figure 3.20: Schematic illustration showing key steps during metagenomic analysis. 86

Figure 3.21: Pictorial representation showing the DNA sample used for amplicon and whole genome sequencing. 87

Figure 3.22: 16S rRNA gene of *E. coli* showing the hypervariable (V1-V9) and conserved regions. 88

Figure 3.23: A pictorial representation demonstrating species richness and evenness of a community. Each shape represents an organism. Different shapes represent different organisms. 89

Figure 4.1: Pictorial representation of mamaku frond with three stages of harvesting age (stage 1, stage 2 and stage 3). 96

Figure 4.2: (A) Selected region of ^{1}H spectra of purified mamaku gum. (B) Selected region of DEPT-edited HSQC spectrum of purified mamaku gum from stage 1. M, mannose; G, galactose; R, rhamnose; X, xylose; Ga, glucuronic acid; $COOCH_3$, methylesterification at C-6; $COCH_3$, O-methoxy group. 105

Figure 4.3: Light scattering (LS) signal and weighted-average molecular weight (M_w) analysis by size-exclusion chromatography coupled with multi-angle laser light scattering (SEC-MALLS) of purified mamaku gum. The two peaks for the stage 3 gum sample were deconvoluted using the Gaussian model (R^2 = 0.999) in Origin 2020 (Version 9.7.0.185 Academic). 107

Figure 4.4: Viscosity profiles of mamaku gum extracted from (A) stage 1, (B) stage 2 and (C) stage 3 as a function of shear rate. (D) Comparison of viscosity for mamaku gum extracted at 5% (w/w total solids), marked with η_{max}/η_{crit} ratios. Values are plotted as means ± standard deviation (n=3). Measurements were taken 109

using cup-and-bob geometry at 20°C. η_{max}, maximum viscosity (Pa.s); $\dot{\gamma}_{crit}$, critical shear rate (s^{-1}); η_{crit}, critical viscosity (Pa.s); η_{max}/η_{crit}, extent of shear-thickening.

Figure 4.5: Storage modulus (G', filled symbols) and loss modulus (G'', empty symbols) of mamaku gum extracted from (A) stage 1, (B) stage 2 and (C) stage 3 at 1%, 3%, 5% and 10% w/w total solids as a function of frequency. Oscillatory measurements (frequency sweep) were performed in the range of 0.01-20 Hz using a constant strain value of 5% (within the linear viscoelastic region) using the double gap geometry at 20°C. Values are plotted as means ± standard deviation (n=3) 111

Figure 4.6: Still images of the fluid filament during uniaxial extensional rheology experiment for mamaku gum from (A) stage 1, (B) stage 2 and (C) stage 3 as a function of time. The onset of the elastocapillary regime, characterised by a uniform fluid filament, is marked in-dash-boxes. The time is normalised by t_b, *i.e.*, $t^{'} = t/t_b$ (capillary breakup time, t_b, values are given in Table 4.7). The initial gap is $L_o = 1.5$ mm, the final gap $L_f = 4$ mm and the piston diameter $D_o = 4$ mm, giving initial and final aspect ratios of $\Lambda_o = 0.38$ and $\Lambda_f = 1$, respectively. 114

Figure 4.7: Dynamics of midfilament diameter as a function of time for mamaku gum extracted from (A) stage 1, (B) stage 2 and (C) stage 3. (D) Transient extensional viscosity of mamaku gum from stages 1 and 2 as a function of Hencky strain. λ_e, extensional relaxation time. 117

Figure 4.8: Viscosity profile of mamaku gum (5% w/w) from stage 1 after altering ionic strength by adding NaCl and $CaCl_2$. Native stage 1 and stage 2 mamaku gum (5% w/w) are shown for reference. 120

Figure 4.9: Schematic illustration showing the unfolding of mamaku polysaccharide chains from (A) stage 1, (B) stage 2 and (C) stage 3 on shearing or stretching and influence on intermolecular hydrogen bonds with neighbouring chains. 120

Figure 5.1: Light scattering (LS) signal and weighted-average molecular weight (M_w) analysis by size-exclusion chromatography coupled with multi-angle laser light scattering (SEC-MALLS) of purified mamaku gum (stage 1, 2 and 3) at 0, 1 and 2 h during (A) gastric and (B) intestinal digestion. 134

Figure 5.2: Effect of mamaku gum (from stage 1, 2 and 3 at initial concentrations of 1% and 4% w/w) on the activity of (A) α-amylase, (B) pepsin and (C) lipase and (D) relative bile acid binding ability. Water was used as a control for enzyme activity assays. Cholestyramine was used as a control for the bile acid binding assay. Values are plotted as means ± standard deviation (n=3). Bars with different letters are significantly different ($p \leq 0.05$). 137

Figure 5.3: Change in pH during *in vitro* fermentation (at 0 h, 6 h, 12 h and 24 h) in presence of water (blank), inulin, guar gum and mamaku gum (stage 1, 2 and 3). Values are expressed as means ± standard deviation (n=4). Different lowercase 141

letters indicate a significant difference ($p \leq 0.05$) between time points for the same group. Different capital letters indicate a significant difference ($p \leq 0.05$) between substrates at a specific time point.

Figure 5.4: Correlation between total short-chain fatty acid (SCFAs) and pH during *in vitro* colonic fermentation. 141

Figure 5.5: Alpha diversity of samples using (A) Faith's phylogenetic diversity (PD), (B) Observed features, (C) Pielou's evenness and (D) Shannon diversity metrics. Values are plotted as means ± standard deviation (n=3). Bars with different letters are significantly different ($p \leq 0.05$). (E) Beta diversity by principal coordinate analysis (PCoA) plot projecting Bray-Curtis distances ($p < 0.001$). 144

Figure 5.6: (A) Taxonomic composition of microbiota after 24 h *in vitro* fermentation at phylum level, (B) ratio of Firmicutes to Bacteroidetes and (C) heatmap of gut microbial composition at genus level in blank, inulin, guar gum and mamaku gum (stage 1, 2 and 3) groups. In (B) values are plotted as means ± standard deviation (n=3). Bars with different letters are significantly different ($p \leq 0.05$). 145

Figure 6.1: Viscosity profiles of crude mamaku gum (2% w/w total solids) after shear treatment at (A) 1k-8k rpm for 1 min and (B) 5k rpm for 30 sec-20 min. Dash lines (in A, B) represent the viscosity profile after 48 h storage at 4°C. Relative change (%) in viscosity at 1 s^{-1}, $\eta_{(1\,s^{-1})}$, and extent of shear-thickening, η_{max}/η_{crit}, after shear treatment at (C) 1k-8k rpm for 1 min and (D) 5k rpm for 30 sec-20 min. Values are plotted as means ± standard deviation (n=3). Measurements were taken using cup-and-bob geometry at 20°C. η_{max}, maximum viscosity (Pa.s); η_{crit}, critical viscosity (Pa.s). 159

Figure 6.2: (A) Viscosity profiles of crude mamaku gum (2% w/w total solids) after temperature treatment between 65-115°C for 30 min. (B) Relative change (%) in viscosity at 1 s^{-1}, $\eta_{(1\,s^{-1})}$, and extent of shear-thickening, η_{max}/η_{crit}, after temperature treatment. (*): Newtonian behaviour at 115°C treatment. Values are plotted as means ± standard deviation (n=3). Measurements were taken using cup-and-bob geometry at 20°C. η_{max}, maximum viscosity (Pa.s); η_{crit}, critical viscosity (Pa.s). 162

Figure 6.3: Storage modulus (G', filled symbols) and loss modulus (G'', empty symbols) of crude mamaku gum (2% w/w total solid) after shear and temperature treatment as a function of frequency. (*): G' was not detected. Values are plotted as means ± standard deviation (n=3). Measurements were taken using double gap geometry at 20°C. 164

Figure 6.4: Damping factor (ratio of G'' to G') of crude mamaku gum (2% w/w total solid) after shear and temperature treatment at 0.1 Hz frequency. (*): G' was not detected. Values are plotted as means ± standard deviation (n=3). Measurements were taken using double gap geometry at 20°C. Bars with different letters are significantly different ($p \leq 0.05$). 163

Figure 6.5: Light scattering (LS) signal and weighted-average molecular weight (M_w) analysis by size-exclusion chromatography coupled with multi-angle laser light scattering (SEC-MALLS) of purified mamaku gum after temperature treatment. 167

Figure 6.6: Effect of shear and temperature treatment on the z-average radius of purified mamaku gum. Values are plotted with mean ± standard deviation (n=5) obtained at 20°C. Bars with different letters are significantly different ($p \leq 0.05$). 168

Figure 6.7: Constituent sugar composition of purified mamaku gum after shear and temperature treatment. 169

Figure 6.8: Schematic illustration showing the effect of (A, B) shear treatment on the packing of mamaku polysaccharide molecules and (C) consequently limiting the unfolding during the rheological analysis. 172

Figure 6.9: Comparison between shear (5k- 20 min and 8k-1 min) and temperature (75°C- 30 min) treated mamaku gum samples (2% w/w total solids). η_{max}/η_{crit}, extent of shear-thickening; M_w, weighted-average molecular weight. 174

Figure 6.10: Effect of urea (5M) on the viscosity profile of shear-treated mamaku gum (2% w/w total solids). Measurements (n=3) were taken using cup-and-bob geometry at 20°C. 175

Figure 7.1: Micrographs of freeze-dried and oven-dried mamaku whole pith and their respective powder surfaces. 188

Figure 7.2: (A) Images showing the penetration of water droplet into freeze-dried (FDP) and oven-dried (ODP) mamaku pith powders at different time intervals. (B) Change in contact angle as a function of time at ~20°C. Values are plotted as means ± standard deviation (n=6). 190

Figure 7.3: Pictures of (A) oven-dried (ODP) and (B) freeze-dried (FDP) mamaku pith powders at the end of the sinking experiment. A gelatinous layer with aggregates was observed for FDP powder with no sinking for 60 min. 191

Figure 7.4: Change in (A) particle size (d 0.5) and (B) % solubilisation of freeze-dried (FDP) and oven-dried (ODP) mamaku pith powders in water at ~20°C as a function of time. Values are plotted as means ± standard deviation (n=6). 192

Figure 7.5: Viscosity profiles of (A) freeze-dried (FDP) and (B) oven-dried (ODP) mamaku pith powder suspensions (after 15 h hydration) as a function of shear rate. Values are plotted as means of triplicates (n=3). Measurements were taken using cup-and-bob geometry at 20°C. 8% (w/w) sample was measured using parallel plate geometry. 194

Figure 7.6: Amount of uronic acid in the continuous phase of freeze-dried (FDP) and oven-dried (ODP) mamaku pith powder suspension (1% w/w) as a function of 196

hydration time at ~20°C. Values are plotted as means ± standard deviation (n=3).

Figure 7.7: Time-dependent viscosity profiles of (A) freeze-dried (FDP) and (B) oven-dried (ODP) mamaku pith powder suspension (1% w/w) and their respective continuous phases (A': FDP; B': ODP). ODP continuous phase collected after 24 h of rehydration was concentrated using a vacuum evaporator: CF, concentrated fraction. Values are plotted as means ± standard deviation (n=3). Rheological measurements were taken using cup-and-bob (for suspension) or double gap geometry (for continuous phase) at 20°C. 197

Figure 7.8: *In vitro* digestion profiles for wheat biscuit alone (WB), and in the presence of 2.5% (w/v) freeze-dried (FDP) and oven-dried (ODP) mamaku pith powder. Values are plotted as means ± standard deviation (n=3). 198

Figure 7.9: (A) Rehydration of freeze-dried (FDP) and oven-dried (ODP) mamaku pith powder and release of mamaku polysaccharide (MP). (B) Interaction of MP with water in and outside the powder particle. 201

Figure 8.1: Trial design for mamaku pith powder testing in humans. 208

Figure 8.2: Trail design for mamaku pith powder colon fermentation in rats. 210

Figure 8.3: Consolidated Standards of Reporting Trials (CONSORT) diagram for the study trial. 214

Figure 8.4: Mean incremental change in blood glucose concentrations over baseline (T=0) after the consumption of wheat biscuit alone (WB), WB+ not-pre-hydrated mamaku pith powder (WB+MD), WB+ pre-hydrated mamaku pith powder (WB+MH) and WB+ guar gum (WB+GG). Values are reported as mean ± standard error mean (n=17). (*): Significant different observed ($p \leq 0.05$). 215

Figure 8.5: Mean incremental change in blood insulin concentrations over baseline (T=0) after the consumption of wheat biscuit alone (WB), WB+ not-pre-hydrated mamaku pith powder (WB+MD), WB+ pre-hydrated mamaku pith powder (WB+MH) and WB+ guar gum (WB+GG). Values are reported as mean ± standard error mean (n=17). (*): Significant different observed ($p \leq 0.05$). 217

Figure 8.6: Correlation between peak blood glucose and peak insulin responses for all four meals tested. WB, wheat biscuit alone; WB+MD, WB+ not-pre-hydrated mamaku pith powder; WB+MH, WB+ pre-hydrated mamaku pith powder; WB+GG, WB+ guar gum. 218

Figure 8.7: Changes in (A) hunger, (B) fullness, (C) satisfaction and (D) desire to eat after the consumption of wheat biscuit alone (WB), WB+ not-pre-hydrated mamaku pith powder (WB+MD), WB+ pre-hydrated mamaku pith powder (WB+MH) and WB+ guar gum (WB+GG). Values are reported as mean (n=17). 219

Figure 8.8: Alpha diversity analysis of colonic microbiota using (A) Faith's phylogenetic diversity (PD), (B) Observed features, (C) Pielou's evenness and (D) 221

Shannon diversity metrics in rats fed experimental diets. (E) Beta diversity by principal coordinate analysis (PCoA) plot projecting unweighted UniFrac distances ($p < 0.001$).

Figure 8.9: Viscosity profiles of guar gum (3 g in 250 ml water) and mamaku pith powder (5 g in 250 ml water, pre-hydrated at 20°C) at different time points (0, 1, 3, 6 and 24 h). Measurements were taken using cup-and-bob geometry at 37°C. 225

Figure 9.1: Schematic illustration showing the changes in size and rotational and extensional rheology of mamaku polysaccharide from different age fronds. Stage 1, young fronds; stage 2, fully grown fronds; stage 3, old fronds; M_w, weighted-average molecular weight; R_g, radius of gyration. 229

Figure 9.2: Schematic illustration showing the effects of mamaku gum in simulated gastric, small intestinal and colonic conditions. 231

Figure 9.3: Schematic illustration showing the effects of shear and temperature treatments on mamaku gum. 233

Figure 9.4: Schematic illustration showing the effects of freeze-drying and oven-drying methods on the functionality of mamaku pith powder. 235

Figure 9.5: Schematic illustration showing *in vivo* effects of consuming mamaku pith powder in humans and rats. 237

List of tables

Table 2.1: Proximate and mineral composition of freeze-dried mamaku gum. 11

Table 2.2: Molecular characterisation of the mamaku polysaccharide. 13

Table 2.3: Common drying methods used for food applications. 27

Table 2.4: Effect of oven-drying and freeze-drying on food commodities. 32

Table 2.5: Biological actions associated with the production of major short-chain fatty acids (SCFAs) in the colon. 52

Table 3.1: Composition of simulated fluids used during *in vitro* digestion. 83

Table 4.1: Yield of fresh mamaku extracts from fronds of different stages of harvesting age. 102

Table 4.2: Proximate, mineral and simple sugar composition of freeze-dried crude mamaku gum. 103

Table 4.3: Constituent sugar composition of purified mamaku gum. 104

Table 4.4: Molecular parameters of purified mamaku gum analysed by size-exclusion chromatography coupled with multi-angle laser light scattering (SEC-MALLS). 107

Table 4.5: Comparison of viscosities and critical shear rate for crude mamaku gum from stage 1 and stage 2 at 3%, 5% and 10% (w/w) total solids. 110

Table 4.6: Crossover frequency and relaxation time (λ_s) for crude mamaku gum from stage 1 and stage 2 at 5% and 10% (w/w) total solids. 112

Table 4.7: Capillary breakup time (t_b) and extensional relaxation time (λ_e) for crude mamaku gum samples from stage 1, stage 2 and stage 3 of harvesting age at 1, 3 and 5% (w/w) total solids concentration. 113

Table 5.1: Molecular parameters of purified mamaku gum (stage 1, 2 and 3) at 0, 1 and 2 h during gastric and intestinal digestion, analysed by size-exclusion 135

chromatography coupled with multi-angle laser light scattering (SEC-MALLS).

Table 5.2: Concentration of short-chain fatty acids (SCFAs) during *in vitro* fermentation in presence of water (blank), inulin, guar gum and mamaku gum (stage 1, 2 and 3). 139

Table 5.3: Relative abundances after 24 h *in vitro* fermentation of the top 21 genera in blank, inulin, guar gum and mamaku gum (stage 1, 2 and 3) groups. 146

Table 6.1: Comparison of viscosities and critical shear rate for crude mamaku gum (2% w/w total solids) after shear treatment for 1 min. 160

Table 6.2: Comparison of viscosities and critical shear rate for crude mamaku gum (2% w/w total solids) after shear treatment at 5k rpm for varying times. 160

Table 6.3: Comparison of viscosities and critical shear rate for crude mamaku gum (2% w/w total solids) after temperature treatment for 30 min. 162

Table 6.4: Molecular parameters of purified mamaku gum after shear treatment analysed by size-exclusion chromatography coupled with multi-angle laser light scattering (SEC-MALLS). 166

Table 6.5: Molecular parameters of purified mamaku gum after temperature treatment analysed by size-exclusion chromatography coupled with multi-angle laser light scattering (SEC-MALLS). 167

Table 7.1: Characterisation of freeze-dried (FDP) and oven-dried (ODP) mamaku pith powders. 187

Table 8.1: Composition of diets for rat trial. 211

Table 8.2: Peak height and mean incremental area under the blood glucose curve (iAUC) to 120 min and 180 min for meals. 215

Table 8.3: Peak height and mean incremental area under the insulin curve (iAUC) for meals. 217

Table 8.4: Short-chain fatty acids (SCFAs) in the caecum of rats fed the experimental diets. 220

Table 8.5: Survival of mamaku polysaccharide (MP) during gut transit estimated from dietary and faecal uronic acid. 222

List of publications and conference proceedings

- **Bisht, A.**, Goh, K. K. T., & Matia-Merino, L. (2023). The fate of mamaku gum in the gut: Effect on *in vitro* gastrointestinal function and colon fermentation by human faecal microbiota. *Food & Function*,14, 7024-7039.

- **Bisht, A.**, Goh, K. K. T., Sim, I. M., Edwards, P. J. B., & Matia-Merino, L. (2023). Shear and temperature sensitivity of a shear-thickening biopolymer from the New Zealand black tree fern. *Food Hydrocolloids*, 145, 109075.

- **Bisht, A.**, Goh, K. K. T., Sim, I. M., Edwards, P. J. B., & Matia-Merino, L. (2023). Does harvesting age matter? Changes in structure and rheology of a shear-thickening polysaccharide from *Cyathea medullaris* as a function of age. *Carbohydrate Polymers*. (*In submission*).

- **Bisht, A.**, Goh, K. K. T., Monro, J., Mishra, S., & Matia-Merino, L. (2023). Process-structure-function relationship for mamaku suspension: Effect of drying methods on powder functionality. *Food Hydrocolloids*. (*In submission*).

- Mishra, S., **Bisht, A.**, Matia-Merino, L., Ngamatea, N., Martell, S., Dinnan, H., … & Monro, J. (2023). Mamaku (*Cyathea medullaris*) pith effects on glycaemic, insulin and appetite responses to co-consumed wheat product. *British Journal of Nutrition*. (*In submission*).

- Monro, J., Paturi, G., Stoklosinski, H., Carroll, A., **Bisht, A.**, Mishra, S., … & Matia-Merino, L. (2023). *Cyathea medullaris* (mamaku) pith effects on faecal properties and hind-gut microbiota in the rat faecal bulking model. *Food & Function*. (*In submission*).

- Monro, J., **Bisht, A.**, Mishra, S., Goh, K. K. T., & Matia-Merino, L. (2023). *Cyathea medullaris* (mamaku) pith has functional attributes of potential importance to human health. *Plant Foods for Human Nutrition*. (*In submission*).

- **Bisht, A.**, Goh, K. K. T., Monro, J., & Matia-Merino, L. Shear-thickening behaviour for food and health: A case of mamaku polysaccharide. (*In preparation*).

- **Bisht, A.**, Goh, K. K. T., Sim, I. M., Edwards, P. J. B., & Matia-Merino, L. (2023). The tale of a shear-thickening biomacromolecule from the New Zealand black tree fern. [Oral presentation]. 21st Gums and Stabilisers for Food Industry Conference, The Food Hydrocolloids Trust, Thessaloniki, Greece.

- **Bisht, A.**, Goh K. K. T., & Matia-Merino, L. (2022). A shear-thickening biomacromolecule from the New Zealand black tree fern: A novel ingredient for managing diabetes? [Oral presentation]. International Conference on Key enabling technologies for sustainable agri-food chain, National Institute of Technology, Rourkela, India. (*Won Best Speaker Award*)

- **Bisht, A.**, Goh K. K. T., Monro, J., & Matia-Merino, L. (2022). Physical modification of a bio-polysaccharide from *Cyathea medullaris*. [Poster session]. New Zealand Institute of Food Science and Technology (NZIFST) Annual Conference, Rotorua, New Zealand.

- **Bisht, A.**, Goh K. K. T., Monro, J., Mishra S., & Matia-Merino, L. (2021). Mamaku polysaccharide functionality. [Poster session]. New Zealand Institute of Food Science and Technology (NZIFST) Annual Conference, Palmerston North, New Zealand.

Chapter 1

Introduction

1.1 Background

Over hundreds of years of practice, indigenous knowledge systems such as Ayurveda, traditional Chinese medicine, Siddha medicine, Jamu and Mātauranga Māori have successfully established the use of medicinal plants to manage a variety of diseases and promote human health. In Mātauranga Māori—the knowledge of indigenous Māori people of New Zealand—one such plant is the New Zealand black tree fern (*Cyathea medullaris*). The New Zealand black tree fern, commonly known as 'mamaku' in the Māori language is regarded as a Taonga (treasured) species by Māori people. Mamaku is a native fern to New Zealand and the Pacific Islands with a long history of use as a therapeutic remedy to treat skin conditions and gastrointestinal complaints and is traditionally consumed as a food. However, like many other traditional medicinal plants, the scientific understanding of mamaku is limited.

A water-soluble gum extract from mamaku fern was first reported by the Food Structure group at Massey University in 2007, and ever since then, it has been extensively characterised in terms of its physicochemical and rheological properties. Initial investigations have shown that mamaku gum exhibits unique and complex rheological properties such as Newtonian, shear-thickening, shear-thinning, thixotropic, and anti-thixotropic behaviour depending on the concentration and applied shear rate (Goh, Matia-Merino, Hall, Moughan, & Singh, 2007), indicating that the behaviour of mamaku gum is very diverse and may be manipulated as per requirement. This complex rheological behaviour is attributed to a one-of-a-kind biomacromolecule called *mamaku polysaccharide* (MP) present in the gum extract. The shear-thickening behaviour of mamaku gum, which is uncommon amongst natural polymers, develops at shear rates similar to those occurring in the human stomach and is responsible for altering the peristalsis contractions in an *ex vivo* rat stomach model (Lentle, Janssen, Goh, Chambers, & Hulls, 2010). This suggests that mamaku gum may significantly

delay the emptying of food from the stomach into the small intestine (*i.e.,* delaying gastric emptying), thus, suppressing appetite and delaying the digestion of food, which could help manage diseases such as obesity and type 2 diabetes. To date, no human trials have been carried out on mamaku. Furthermore, the search for natural polysaccharides with entirely novel functionalities (such as a shear-thickening behaviour as in the present thesis) is always a relevant topic within the food and nutraceutical industry.

Before using mamaku for commercial applications in the food industry, further scientific and technical understanding is necessary. For example, it is crucial to investigate the effect of the age of the fronds collected from mamaku fern on the functionality of the gum so that a consistent product can be supplied to industry (**Chapters 4** and **5**). During industrial processing of mamaku, the gum may be subjected to treatments such as high shear and temperature which could adversely affect the structural and rheological properties, thereby its physiological functionality (**Chapter 6**). In addition to delaying gastric emptying, polysaccharides can improve the host health by regulating enzyme activity, altering gut transit time, delaying the rate of absorption and acting as a substrate for colonic fermentation (Capuano, 2017). However, the possible effects of mamaku gum on gut function are unknown (**Chapter 5**).

The complex rheology that distinguishes mamaku gum from other polysaccharides poses a challenge in processing it into a safe deliverable form. The shear-thickening behaviour of mamaku gum may develop during oral processing and its transition through the oesophagus, causing a choking hazard. Therefore, taking inspiration from the way mamaku has been consumed by native Māori people for centuries—as raw or cooked pith (the white flesh from the fronds)—this thesis also explores the use of whole mamaku pith as an alternative to mamaku gum extract. Since MP is naturally present in the tissues of the pith, it was hypothesised that aqueous suspensions of pith tissue may also exhibit the complex rheological properties and therefore potential health benefits (**Chapters 7** and **8**). Using whole plant tissue is more sustainable and may represent a natural encapsulation of the gum, which could avoid many problems associated with working with the extracted gum, especially in concentrated form. Perhaps, doing *'less is more'*.

The overarching aim of this research was to provide an evidence-based foundation for using mamaku fern to make a natural and novel shear-thickening functional food ingredient with proven effects in humans. In order to do so, three major questions were investigated:

- **Does the harvesting age of mamaku frond matter?**
- **Can mamaku gum/pith withstand industrial operations without compromising the shear-thickening behaviour?**
- **Will mamaku pith have an impact *in vivo*?**

These research questions are addressed in **Chapters 4** to **8** using an interdisciplinary approach including fields such as rheology, molecular characterisation of polymer, *in vitro* digestion and fermentation, bioinformatics, powder technology, and *in vivo* human and rat trials. The fundamental background and relevant literature are presented in **Chapters 2** and **3**. The outline of the thesis is shown in **Figure 1.1**.

Answering these three questions covers the journey of the MP from its origin at the forest to its end effects on the human gut, and therefore the title of this thesis is '*The tale of the shear-thickening mamaku polysaccharide, from forest to gut*'.

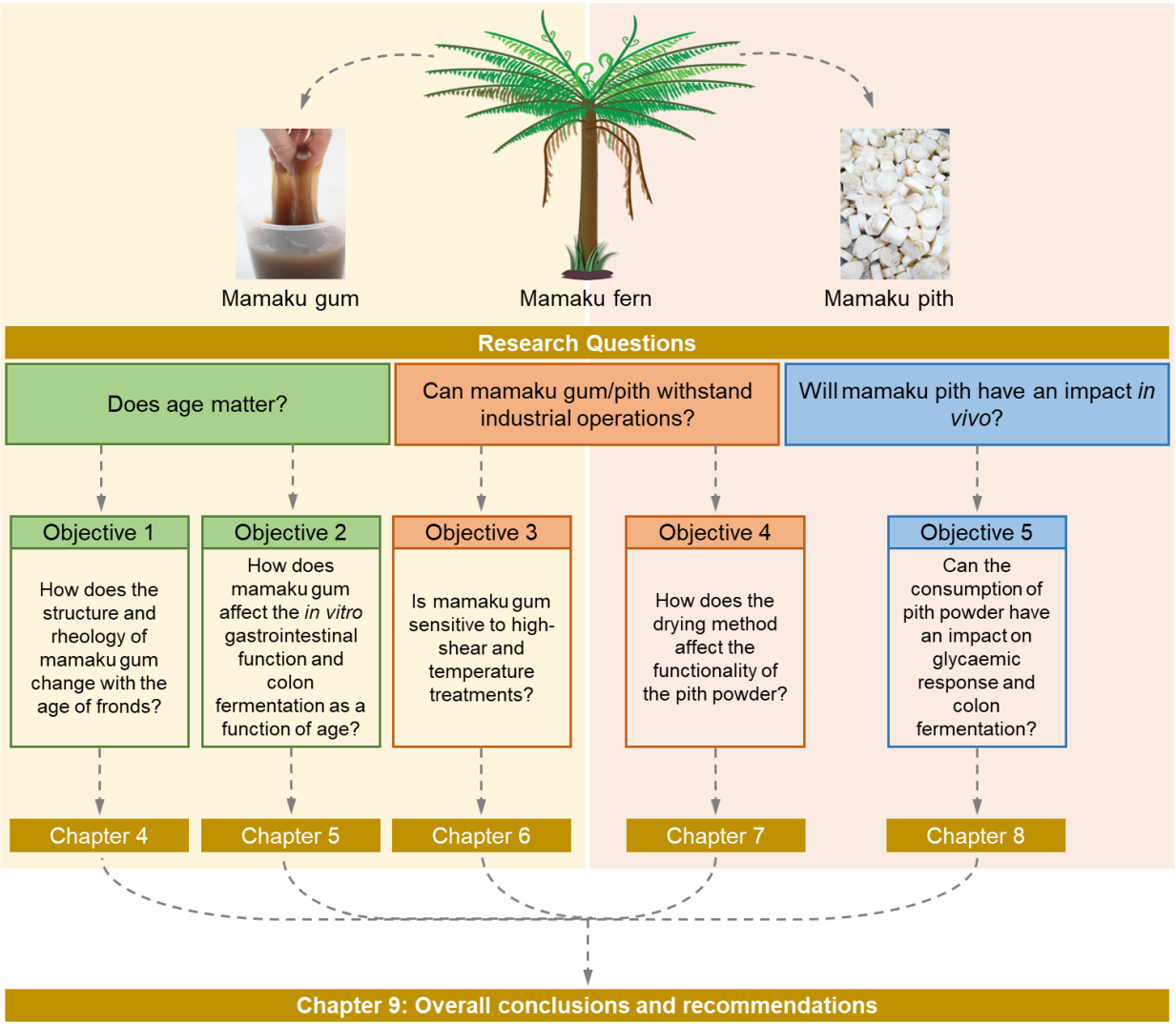


Figure 1.1: Overview of thesis structure.

Chapter 2

Literature review

2.1 Introduction

Cyathea medullaris (commonly known as 'mamaku' in Māori and locally also called körau, katätä and pïtau) is one of the world's tallest tree ferns indigenous to New Zealand and the Pacific Islands (**Figure 2.1**). The fern can grow to a height of up to 20 m in warm and humid conditions and often towers above the neighbouring flora (Crowe, 2004). It can easily be distinguished from other ferns of the same family such as silver fern (*Cyathea dealbata*) by the presence of distinctive hexagonal patterns left on the trunk by the old fronds as they fall apart (Esler, 1976). Mamaku can also be distinguished by its large, leafy and thick black fronds, which can grow up to 6 m long.

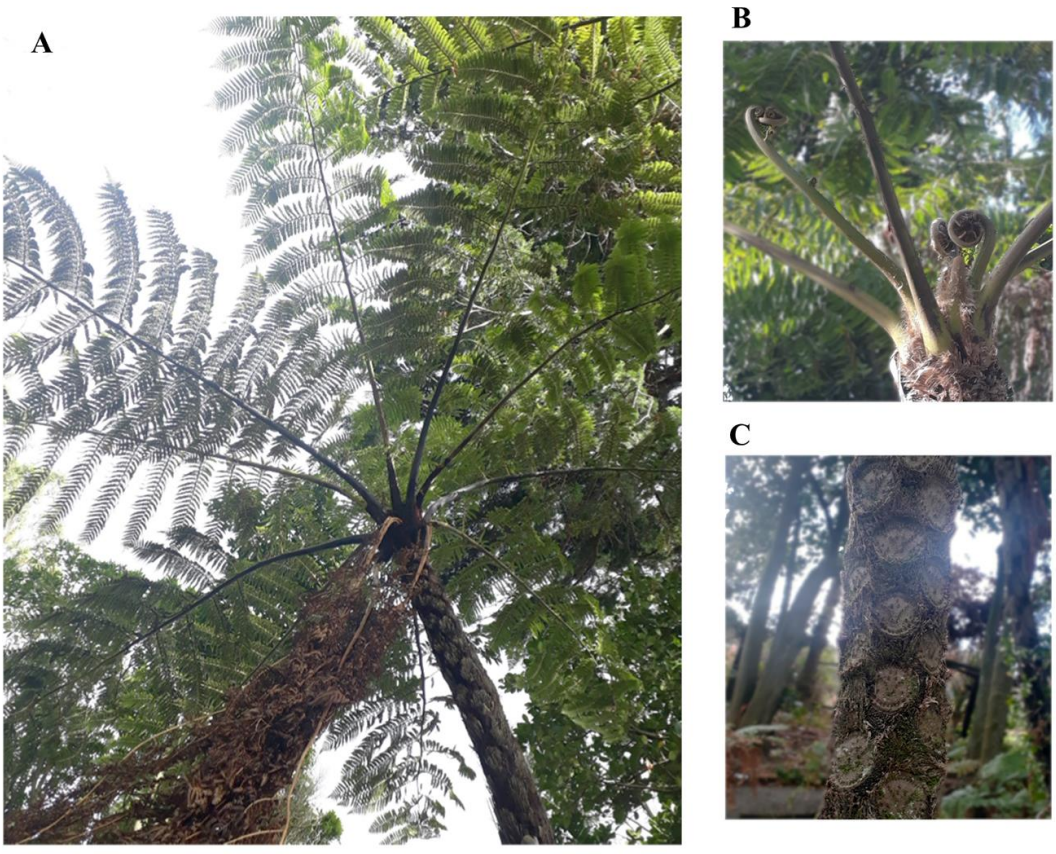


Figure 2.1: (**A**) Picture of mamaku plant (*Cyathea medullaris*, New Zealand black tree fern), (**B**) young fronds: koru and (**C**) trunk with hexagonal patterns.

Traditionally, the pith[1] (*medullaris* means "pithy") from the upper part of the trunk and stipes (mid-ribs) of young fronds was widely used for its therapeutic benefits, both for external and internal applications. Generally, the fresh slimy pith was directly rubbed, or maybe crushed and made into a poultice to apply as dressings for a variety of skin conditions such as wounds and bruises; swollen feet and eyes; inflamed breasts; to treat boils and facilitate pus eruptions. The pith was also boiled and administrated orally to treat gastric conditions such as sore stomach and as a remedy for diarrhoea (BPJ, 2008; Crowe, 2004; Foster, 2008; McGowan, 2014; Riley, 1994). It is commonly believed that the aforementioned health benefits of mamaku may be due to its immunological or anti-inflammatory potential although there is no scientific literature supporting this. Based on the long history of use by the Māori and the believed skin-related biomedical benefits, mamaku gum has been incorporated as a bioactive ingredient in several cosmetic products such as body cream by Ora skincare, mamaku magic face cream by Koko body, hydrating facial fluid and creams by Kanapa™, daily facial moisturiser for normal to dry skin by NZ native oils, repair balm by Real world® and face mask by Sothys Paris. Recently, as part of the marketing campaign, Ora Innovation New Zealand Ltd. asked 100 participants—with some underlying skin condition(s)—to apply a hydrogel containing mamaku gum twice daily for two weeks and reported that mamaku gum can potentially be used to treat skin conditions (Rademaker, Davis, & Harris, 2022). Though this study has many limitations, such as lack of a control group, analysis based on free-text commentary, photos provided by the participants, and no quantitative data was collected, it is still an important study in the direction of making claims on cosmetic products.

Other than for therapeutic use, mamaku pith has also been traditionally consumed fresh or boiled like vegetables (Best, 1977). However, the potential of mamaku pith as a functional food ingredient has not yet been explored and to the best of the author's knowledge, mamaku (pith or gum) is not being used as an ingredient in the food industry. Thus, this research plays a crucial role in comprehending mamaku, from its origin to end-use, and highlighting its potential as a food ingredient. Considering the broad spectrum of the thesis, the literature review is divided into three comprehensive sections, namely: (i) *Mamaku*

[1] Pith, or medulla is the soft and spongy central part in the stems of vascular plants, composed of parenchyma cells.

polysaccharide (MP)—structural and rheological properties of the polysaccharide; (ii) *Powder production*—drying techniques and powder properties; and (iii) *Possible physiological and health benefits of consuming mamaku*.

2.2 Mamaku Polysaccharide

2.2.1 Characterisation

Mamaku fern contains a slimy, reddish-brown, mucus-like mucilage, which can easily be extracted in water. The initial study which analysed the chemical composition of freeze-dried crude gum extracted from mamaku reported that it mainly consists of carbohydrates (~55% w/w) in the form of simple sugars and non-starch polysaccharide (~10% w/w) (Goh et al., 2007). The water-soluble non-starch polysaccharide present in mamaku gum, hereafter referred to as *mamaku polysaccharide* (MP), is the biomacromolecule of interest in this thesis. The crude gum is also rich in minerals (~16% w/w) with a major presence of potassium, sodium, calcium, magnesium and aluminium; while ~18% w/w gum extract remains unidentified (**Table 2.1**). Subsequently, it was reported that of the unknown fraction (~18% w/w), approximately 10.3% w/w is starch (Wee, Matia-Merino, Carnachan, Sims, & Goh, 2014).

The crude gum from mamaku was further purified and the chemical structure of MP was studied (Wee et al., 2014). MP comprises of ~90% carbohydrates, with *c.a.* 51-53% of uronic acid (mostly glucuronic acid) and the remaining fraction being neutral sugars (mostly galactose, mannose, glucose and xylose). A proportion of uronic acid was methylesterified. MP is a glucuronomannan polymer, possibly, consisting of a repeating backbone of β-1,4-linked methylesterified glucopyranosyl uronic acid and α-1,2-linked mannopyranosyl residues, branched at O-3 on 45% and at both O-3 and O-4 on 53% of the mannopyranosyl residues. The sidechain consists of galactose, arabinose, non-methylesterified glucuronic acid, xylose and other simple sugars. Polysaccharides with a similar repeating backbone structure, -4)-β-D-GlcpA-(1→2)-α-D-Manp-(1→, are reported in mucilages[2] and exudate[3] gums from different plant sources such as *Anogeissus latifolia* (gum ghatti; Aspinall, Hirst, & Wickstrøm, 1955), *Anogeissus leiocarpus* (Aspinall, Carlyle, McNab, & Rudowski, 1969),

[2] Water-soluble sticky material made of carbohydrates present in different parts of the plant.
[3] Substances/fluids that ooze out from the tissues of injured plant.

Actinidia deliciosa (kiwifruit; Redgwell, O'Neill, Selvendran, & Parsley, 1986; Ross, Redgwell, & MacRae, 1993), *Hakea* species (Eagles, Stephen, & Churms, 1993), *Dicerocaryum zanguebaricum* (Barone et al., 1996), *Drosera* species (sundew; Aspinall, Puvanesarajah, Reuter, & Schauer, 1984; Erni, Varagnat, Clasen, Crest, & McKinley, 2011; Rost & Schauer, 1977), *Vochysia tucanorum* (Wagner et al., 2007; Wagner et al., 2008), *Auricularia auricala* (Li et al., 2012), *Sesamum radiatum* (sesame leaves; Nep et al., 2016), *Sargassum fusiforme* (Jin et al., 2020). However, what differentiates MP from most of the glucuronomannans is the presence of branching (monosaccharide or short oligosaccharides) in all mannose residues and no sidechain is attached to methylesterified glucuronic acid residues (**Figure 2.2**). Also, in most of the glucuronomannans, glucuronic acid in the backbone is not methylesterified.

Table 2.1: Proximate and mineral composition of freeze-dried mamaku gum.

Composition	% (w/w)
Moisture	9.25
Ash	16.07
Crude protein	2.02
Fat	0.17
Crude fibre	0.24
Tannins	0.09
Sugars	44.3
Non-starch polysaccharides	9.80
Unknown	18.06
Minerals	**mg/kg**
Potassium	51800
Sodium	30400
Calcium	1200
Magnesium	1000
Aluminium	710
Zinc	54
Manganese	26
Iron	7.7
Copper	7.4
Selenium	0.28
Lead	0.072
Mercury	<0.01

Reprinted with permission from Goh et al. (2007). Copyright© 2007, American Chemical Society.

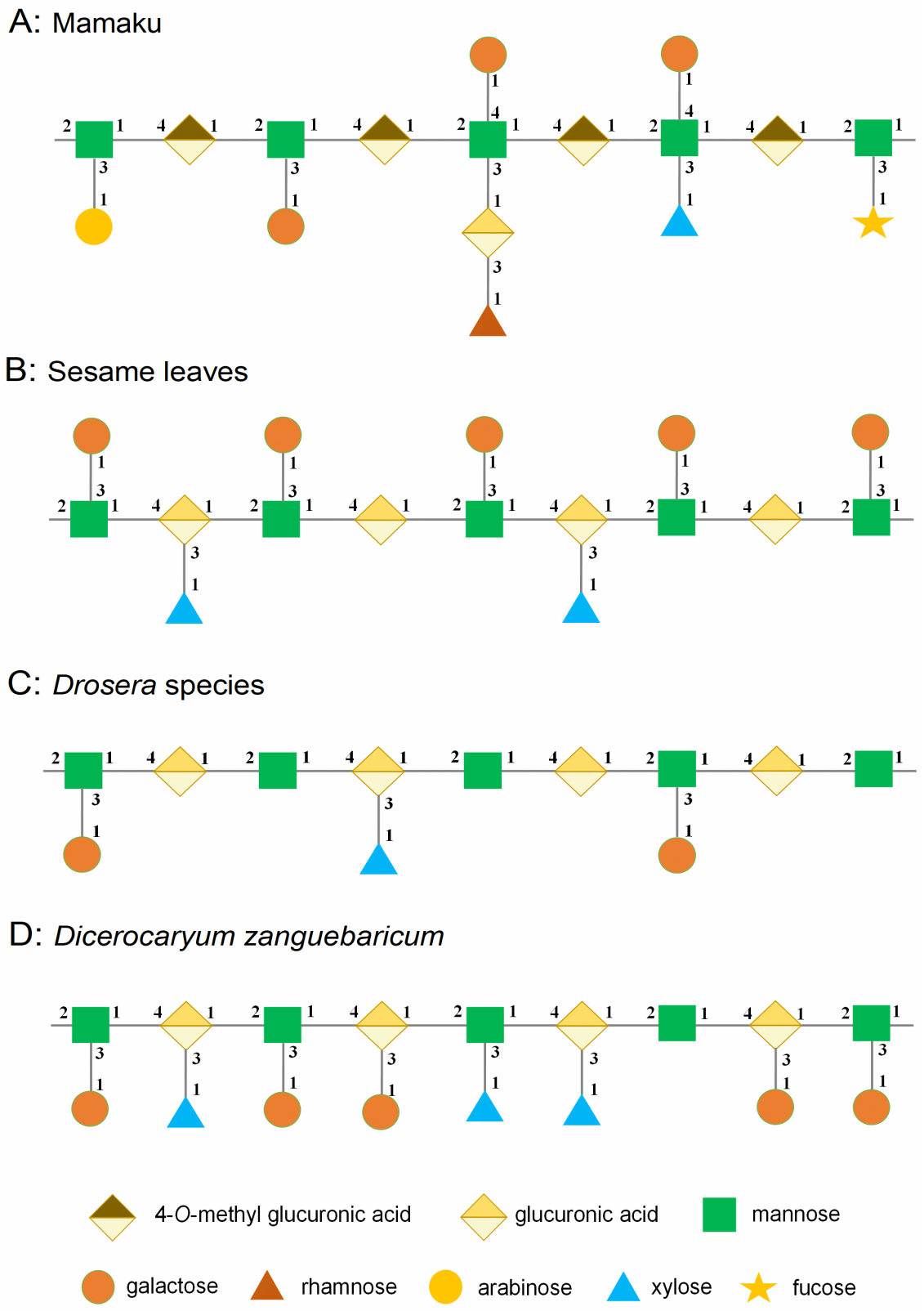


Figure 2.2: Possible structure of glucuronomannan polysaccharides extracted from (**A**) mamaku fern (Wee et al., 2014), (**B**) sesame leaves (Nep et al., 2016), (**C**) *Drosera* species (Erni et al., 2011) and (**D**) *Dicerocaryum zanguebaricum* (Barone et al., 1996).

At the molecular level, MP is a flexible random coil long-chain polymer of molecular weight (M_w) ~3x10^6 Da and radius of gyration (R_g) ~144 nm. Some of the molecule parameters of MP are summarised in **Table 2.2** (Goh, Matia-Merino, Pinder, Saavedra, & Singh, 2011). The high intrinsic viscosity ([η]) and the calculated value of Huggins constant (K': ~0.42) indicate that water is a good solvent for MP. Moreover, on introducing ions into the solvent (from various salts such as sodium chloride, NaCl), the [η] of the MP decreased in a concentration-dependent manner, indicating the anionic nature of the polymer. Na^+ acts as a counter ion, which reduces the negative charge on the polymer, thereby reducing intramolecular repulsive interactions and consequently, making the molecule more compact.

Table 2.2: Molecular characterisation of the mamaku polysaccharide.

Molecular parameter	Definition/ significance	Values for mamaku polysaccharide
Intrinsic viscosity, [η]	The hydrodynamic volume occupied by the individual polymer chain in the solvent.	2020±23 ml/g (in milli-Q water)
Weighted-average molecular weight, M_w	The molecular mass of the polymer chain averaged based on weight. It is more accurate for polymers with large polysaccharide chains.	3.20±0.11x10^6 Da (in 0.1M NaCl)
Radius of gyration, R_g	The distribution of components of an object around its axis.	144±1 nm (in 0.1 M NaCl)
Z-average radii	Hydrodynamic radii of polymer (calculated by equating to a sphere with similar Brownian motion).	~75 nm
Polydispersity index	It is the extent of molecular weight distribution.	1.08±0.05

Data sourced from Goh et al. (2011)

2.2.2 Rheological behaviour

Rheology is the science of deformation and flow of matter under applied stress or force and describes the interrelationship between force, deformation and time. Rheological analysis of a material can reveal many of its properties such as viscosity, flow behaviour, and viscoelasticity. These properties can help design equipment, predict performance during

processing, assess the quality and stability of food products or ingredients and predict the molecular structures of the macromolecules.

The unique rheological behaviour of mamaku gum (containing ~10% MP) was first described by Goh et al. (2007). These authors reported that mamaku gum demonstrates a region of Newtonian[4] behaviour at low shear, followed by a region of shear-thickening[5] at intermediate shear and then a region of shear-thinning[6] at higher shear. The typical flow curve of the mamaku gum is shown in **Figure 2.3**. Moreover, when an up-down viscosity sweep (*i.e.*, the sample is subjected to increasing shear rate—from low to high, and then immediately sheared back from high to low shear) was performed, mamaku gum showed its signature flow behaviour (Newtonian, shear-thickening and shear-thinning) with increasing shear rate; and on reducing the shear rate, thixotropic[7] and anti-thixotropic[8] behaviours were also observed. The change in its flow properties suggests that MP has undergone different conformations and intermolecular interactions at different shear conditions and its rheology is time-dependent.

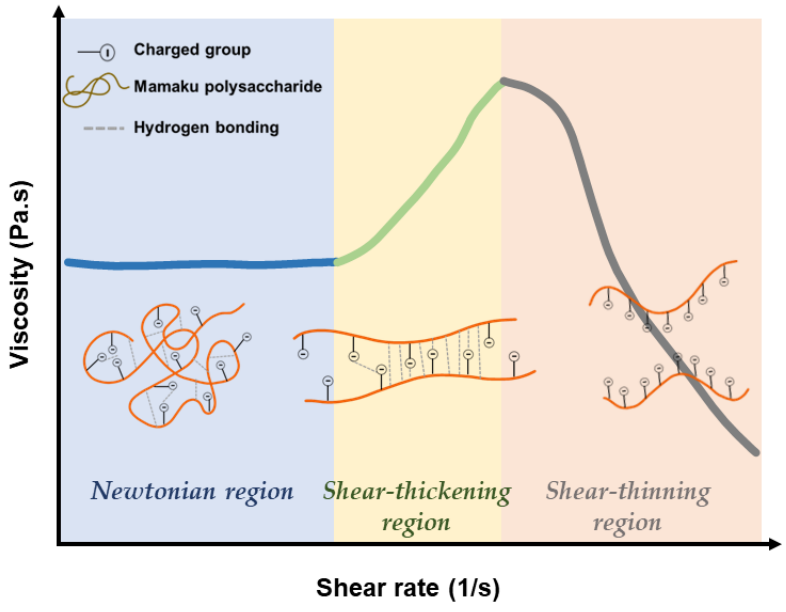


Figure 2.3: Typical flow curve exhibited by mamaku gum.

Adapted from Wee, Matia-Merino, and Goh (2015a)

[4] Fluid with constant viscosity over a range of shear rate and time.
[5] Increase in apparent viscosity with increase in shear rate.
[6] Decrease in apparent viscosity with increase in shear rate.
[7] Decrease in apparent viscosity with increase in time under constant shear rate.
[8] Increase in apparent viscosity with increase in time under constant shear rate.

Furthermore, Weissenberg (rod-climbing)[9] and self-siphoning[10] effects were also observed on shearing mamaku gum, suggesting that the shear can stretch and orient the MP chains creating normal forces[11]. The presence of normal forces indicates the elastic behaviour of mamaku solutions, suggesting that shear-thickening can also arise from the partial elastic property (extension) of the polysaccharide causing an increase in intermolecular linkages (Goh et al., 2007). The extensional rheology of mamaku gum was studied using a Capillary Breakup Extensional rheometer (CaBER™—the polymer is stretched between two parallel plates and change in filament diameter is studied) and two key observations were reported: (i) the intermolecular interactions in mamaku gum during extension are significantly strong and are evident in both dilute and semi-dilute concentration region; (ii) increasing the concentration of mamaku gum has a more pronounced effect on the shear response of the polymer than on the extensional response (Jaishankar, Wee, Matia-Merino, Goh, & McKinley, 2015). Thus, considering the extensional behaviour of mamaku gum may be useful while designing its applications.

The rheological behaviour of polymers is likely to be affected by their external environment. A small change in the pH and/or ionic strength and/or temperature and/or shear can induce significant changes in the physical properties of the polymers and thereby their functionality. The polymers with charged groups are specifically sensitive to pH and ionic strength. Thus, the rheological behaviour of mamaku gum (*i.e.*, Newtonian, shear-thickening and shear-thinning) was investigated under different conditions:

(i) Effect of pH: The native pH of mamaku gum extract is ~5.2, and any deviation from its native pH, in the range between pH 3 to 9 did not have any effect on the viscosity profiles. However, under highly acidic conditions (pH: 1-2) or highly alkaline conditions (pH: 10-12) significant decrease or increase in the viscosity, respectively, was observed (Matia-Merino, Goh, & Singh, 2012). The low viscosity under highly acidic conditions was attributed to the

[9] For elastic polymers, when a spinning rod is inserted into the solution, the polymer chains are pulled towards the rod and starts to rise around it instead of being pushed towards the walls of the container.
[10] For long polymers, when one end of the chain is pulled, the other part of the chain pulls the surrounding chains. For mamaku gum it was studied by pulling the gum using a syringe. Even after the syringe was lifted above the gum interface, the pulling continues (Goh et al., 2007).
[11] When elastic polymers are subjected to shear, they tend to store energy. At sufficiently high shear the energy is released, and the polymer returns to its entropically favourable conformation. The release of energy takes place in a direction perpendicular to the shear direction, which results in a force in the normal direction *i.e.*, normal force.

reduction in the charge on the polymer, reducing its effective volume, and leading to aggregation. The charge density on the MP (*c.a.* -30 mV) was significantly reduced on increasing the acidity of the solution. The increase in viscosity above pH 9 was thought to be related to chemical degradation as a weak gel was observed in excess of sodium hydroxide (NaOH). Overall, it has been shown that mamaku gum is stable over a wide pH range.

(ii) Effect of ions: On adding NaCl to mamaku gum, at concentrations above 0.5 M, the viscosity and shear-thickening effect were enhanced but remained unaffected at lower concentrations (Matia-Merino et al., 2012). The addition of salts reduced the charge density of the polymer, which shields the intramolecular repulsion and enhances intermolecular interactions. The increase in viscosity after adding NaCl indicated that the interaction between polymer chains may be due to hydrogen bonding or hydrophobic interactions and not electrostatic interactions. However, on increasing the concentration of mamaku gum towards the semi-diluted region, the viscosity was hardly affected by the presence of salts, suggesting the mamaku gum has high salt resistance.

(iii) Effect of temperature: The viscosity profiles of mamaku gum at different temperatures (from 5 to 80°C) were studied and significant changes in the viscosity were observed (Matia-Merino et al., 2012; Wee et al., 2015a). With the increase in temperature, a decrease in viscosity and a delay in the onset of shear-thickening behaviour (*i.e.*, at a higher shear rate) were observed; above 50°C shear-thickening phenomena disappeared. The increase in temperature increases the mobility of polymer chains, which in turn can hinder the intermolecular associations thereby reducing or preventing (above 50°C) the shear-thickening phenomenon. These studies highlighted the temperature dependency of the rheological behaviour of mamaku gum and the lack of contribution of hydrophobic interactions to the thickening effect, however, they were not very representative of real processing conditions during food manufacture. In these studies, mamaku gum was heated up to different temperatures and the rheological behaviour was studied at that specific temperature, whereas in reality during food processing, the product is first heated to a specific temperature (and maybe held at that temperature for some time) then cooled down (maybe at room temperature). The heating and holding of polymers at high temperatures may lead to irreversible thermal degradation (Liang, Han, Chen, Su, & Feng, 2019;

Nachtigall, Rohm, & Jaros, 2021). Therefore, the rheological behaviour of the polymers once back to the lower temperature may be very different to what it was before heating. Thus, the rheological behaviour of heat-treated mamaku gum, measured at temperature which is normally used (*i.e.*, 20°C) should also be considered.

(iv) Effect of shear: The use of high shear is another common practice during the processing of food. DNA was the first biomacromolecule reported to decrease in M_w after high shear treatment (Cavalieri & Rosenberg, 1959); and ever since shear treatment is used to modify the structure of polymers. However, the mechanical degradation of polymers on exposure to high shear is not always desired and may be an unwelcome consequence of processing conditions. Shear sensitivity of several polysaccharides such as tragacanth gum (Silvestri & Gabrielson, 1991), starch (Nilsson, Leeman, Wahlund, & Bergenståhl, 2006), β-glucan (Kivelä, Pitkänen, Laine, Aseyev, & Sontag-Strohm, 2010), pectin (Xie et al., 2018), xanthan (Laneuville, Turgeon, & Paquin, 2013), cashew tree gum (Porto, Augusto, Terekhov, Hamaker, & Cristianini, 2015) and puka gum (Riana, Sims, & Matia-Merino, 2022) has been reported in the literature. However, the effect of high shear treatment on the structure and rheology of mamaku gum has yet not been investigated.

2.2.3 Shear-thickening behaviour

Shear-thickening refers to an increase in the viscosity of fluid when a shear force is applied. The increase in viscosity, on shearing, does not necessarily happen throughout the whole shear rate range but may be observed only when a critical shear rate is achieved and may only occur within a specific shear rate range. Once the critical shear rate is achieved there may be some microstructural rearrangements in the fluid, leading to shear-thickening. Materials showing a shear-thickening effect can broadly be classified into three categories, namely: *particle suspensions, micelle systems* and *associative polymers* (**Figure 2.4**).

Particle suspensions: Concentrated suspensions of hard particles (such as silicon dioxide, SiO_2; calcium carbonate, $CaCO_3$; titanium oxide, TiO_2; and corn starch) dispersed in a liquid (such as water, ethylene glycol, polyethylene glycol and polypropylene glycol) usually exhibit shear-thickening behaviour (Ding et al., 2013; Gürgen, Li, & Kuşhan, 2016; Haleem & Nott, 2009; Jiang & Zukoski, 2012; Warren et al., 2015). It is widely accepted that once the critical

shear rate is achieved, the particle with repulsive interaction in the suspension can form temporary force-bearing aggregates, called hydroclusters, as a result of short-range hydrodynamic lubrication or frictional contact forces, which leads to shear-thickening. The chains of hydroclusters grow with the increase in shear rate, resulting in larger aggregates which can jam the flow (**Figure 2.4A**) (Ding et al., 2013; Egres, Nettesheim, & Wagner, 2006; Wei, Lin, & Sun, 2022). After the shear force is removed the particles can go back to their equilibrium state.

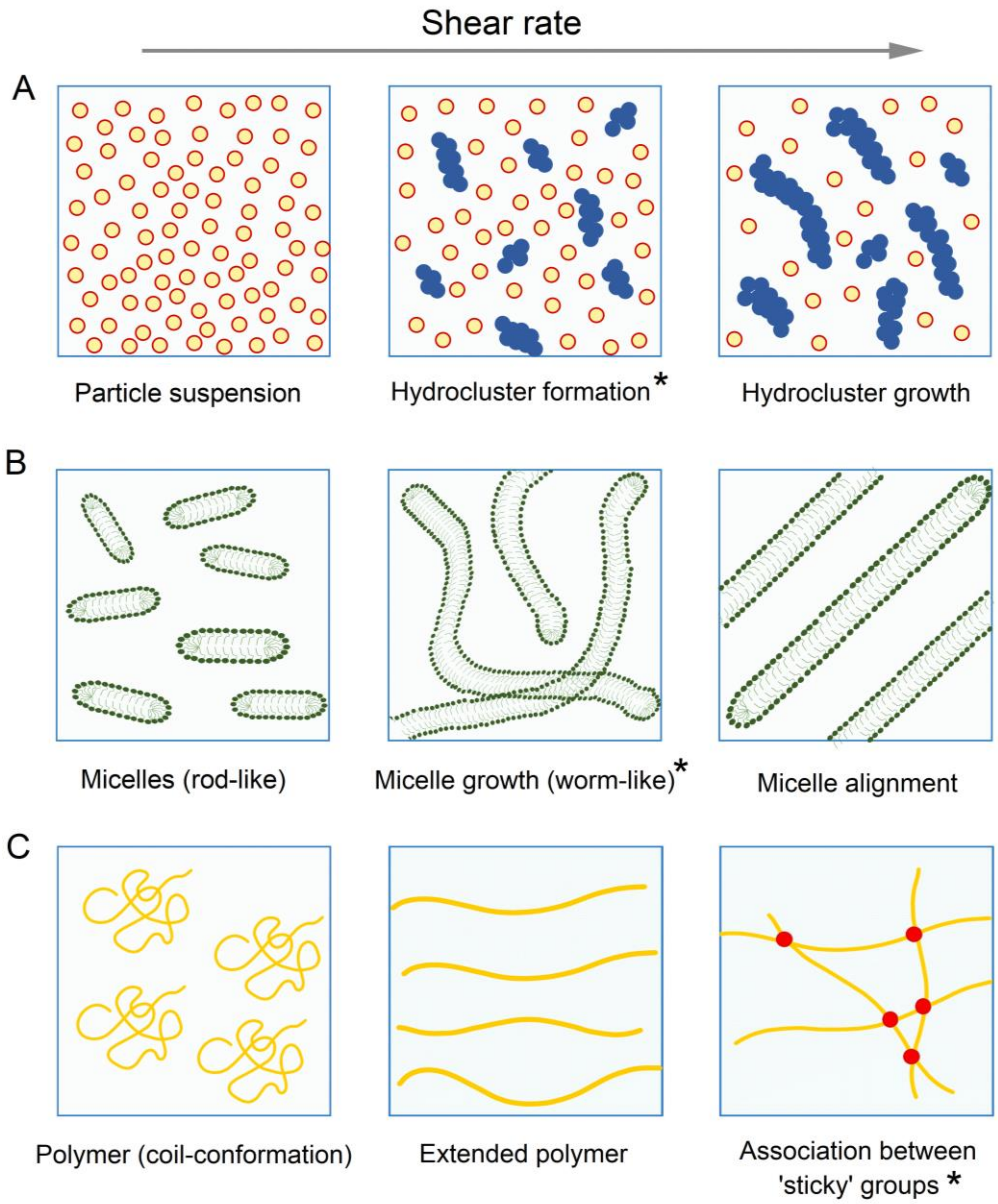


Figure 2.4: Possible microstructural rearrangements in (**A**) particle suspensions, (**B**) micelle systems and (**C**) associative polymers, which leads to shear-thickening behaviour. (*): beginning of shear-thickening behaviour.

Micelle systems: Micelles formed by self-organised aggregates of surfactant molecules in an aqueous solution can also exhibit shear-thickening behaviour. Shear-thicking behaviour is reported for several micelle systems such as cetylpyridiniumsalicylate (CPySal)/ sodium salicylate (NaSal) (Marín-Santibáñez, Pérez-González, & Rodríguez-González, 2014; Rehage & Hoffmann, 1982), cetyltrimethylammonium tosylate (CTAT) (Bautista et al., 2016; Berret, Gamez-Corrales, Lerouge, & Decruppe, 2000), cetyltrimethylammonium bromide (CTAB)/ NaSal (Dehmoune, Decruppe, Greffier, & Xu, 2007; Kim & Yang, 2000), 1-hexadecyl-3-methylimidazolium tetrafluoroborate ($C_{16}mimBF_4$)/ NaSal (Wang et al., 2021) and dimethyl amidopropyl hydroxyl sulfobetaine (AHSB)/ sodium dodecyl sulfate (SDS) (Lu et al., 2022). The origin of shear-thickening behaviour in micelles is not well understood but is commonly argued to be related to shear-induced structural growth at the critical shear rate and transition from rod-like micelles systems to longer worm-like morphologies (Berret, Gamez-Corrales, Séréro, Molino, & Lindner, 2001; Walker, 2001; Wei et al., 2022). During shear-thickening, the worm-like micelles formed align perfectly to the direction of flow (**Figure 2.4B**) (Dehmoune et al., 2007; Lu et al., 2022).

Associative polymers: Shear-thickening behaviour is generally reported for synthetic polymers such as hydrolyzed polyacrylamide (Hu, Wang, & Jamieson, 1995), hydrophobically modified urethane–ethoxylate (Tam, Jenkins, Winnik, & Bassett, 1998), hydrophobically modified alkali-soluble emulsion (Tan, Tam, & Jenkins, 2001), hydrophobically end-capped poly(ethylene oxide) (Ma & Cooper, 2001), cross-linked supramolecular polymer (Xu, Hawk, Loveless, Jeon, & Craig, 2010) and polyimide/cyclohexanone solutions (Chen et al., 2019) and for physically (starch; Ang, Goh, Lim, & Matia-Merino, 2021), or chemically (hydrophobically modified alginate/cyclodextrin; Burckbuchler et al., 2006), or enzymatically (dextran; Sabatie, Choplin, Paul, & Monsan, 1986) modified natural polymers. However, shear-thickening is a rarely encountered phenomenon in unmodified natural polymers. Other than MP, *Ulva fasciata* polysaccharide (Shao, Qin, Han, & Sun, 2014), *Rosa acicularis* polysaccharide (Wang, Guo, Zhang, & Zhao, 2021) and bacterial exopolysaccharides (Ayyash et al., 2020; Li, Hou, & Zhang, 2011; Sahana & Rekha, 2019) are reported to exhibit shear-thickening behaviour.

The shear-thickening behaviour of polymers can be attributed to the presence of 'sticky' groups on the polymer, which tend to associate together during shearing (**Figure 2.4C**). The 'sticky' groups are usually hydrophobic or ionic groups or groups capable of forming hydrogen bonding or dipolar bonds with other groups. The 'sticky' groups on the polymer may be present as a single block or two end blocks or many randomly distributed groups throughout the polymer (Chassenieux, Nicolai, & Benyahia, 2011). There are several theoretical models that predict the molecular origin of shear-thickening behaviour in polymers, but shear-induced cross-linking and transient network theory are the most widely accepted mechanisms. According to the shear-induced cross-linking model, the probability of intermolecular associations increases at the expense of intramolecular associations due to the elongation of chains upon shearing. When at rest, the polymer chains are in a coiled conformation with intramolecular interactions. These interactions are broken during shearing as polymer chains adopt an extended conformation, allowing the formation of intermolecular interactions and therefore increase in viscosity (**Figure 2.4C**) (Ballard, Buscall, & Waite, 1988; Witten Jr & Cohen, 1985). However, this model does not explain any shear-thinning behaviour that may follow the shear-thickening region. Transient network theory, on the other hand, argues that the 'sticky' groups present in the elastic strands (polymer chains) continuously join and destruct to form a temporary reversible junction, which leads to a transient network. The elastic strands can be effective (*i.e.*, both ends of the chain are attached to the network), dangling (*i.e.*, only one end of the stand is attached to the network), and free (*i.e.*, not attached to a junction). When sheared, the free stands attach to the network and the shear-thickening behaviour is observed. At the high shear rate, the rate of chains detaching from the network increases resulting in shear-thinning behaviour (Koga & Tanaka, 2005; Wang, 1992). This theory only accounts for associative polymers with 'sticky' groups present at the chain ends whereas polymers with 'sticky' groups randomly distributed throughout the chain may behave differently.

2.2.3.1 What is the reason for shear-thickening in mamaku polysaccharide?

The uncommon shear-thickening behaviour of mamaku gum was thought to be due to shear-induced microstructural changes. These structural changes can be explained using the energetically crosslinked transient network (ECTN) model. According to this model, the

association between polymer chains is due to thermodynamically driven energetic transient crosslinking (H-bonding). When shear is applied, the polymer chains mobilise, stretch and orient to build up intermolecular crosslinking. The zipping of elongated polymer chains *via* intermolecular crosslinking leads to the formation of a ladder-like structure, thus a rapid increase in viscosity (Lele & Mashelkar, 1998). In the case of mamaku gum, Newtonian behaviour was observed at a low shear rate, which could be due to a compact folded polymer structure with the dominance of intramolecular interactions over intermolecular interactions (**Figure 2.3**). The rate of formation of intermolecular linkages will be equal to the rate of bond disruption, thus, constant viscosity was observed at low shear. On increasing the shear to the intermediate range, the compact structure starts to unfold and stretch, exposing more 'sticky' groups. This promotes intermolecular interactions, leading to a zipped ladder-like structure, which results in a shear-thickening effect. Finally, at a higher shear rate, intermolecular interactions start to break much faster than they are reformed, so the rate of dissociation dominates the rate of association, unzipping the ladder-like structure, leading to shear-thinning behaviour (Goh et al., 2007; Matia-Merino et al., 2012; Wee, Matia-Merino, & Goh, 2015b).

The temporary crosslinking of functional groups leading to a shear-thickening effect can arise because of different types of interactions, namely: (i) electrostatic interactions; (ii) hydrophobic interaction; and (iii) hydrogen bonding. Usually, if hydrophobic interaction is the main reason for the development of temporary junctions the viscosity of the system becomes more pronounced with an increase in temperature (Burckbuchler et al., 2006). As stated previously, in the case of mamaku gum, with an increase in temperature the thickening phenomenon was reduced, thus, indicating that interaction between MP chains was not likely to be caused by hydrophobic interactions getting stronger. To elucidate these interactions, a pure fraction of polysaccharide was collected by enzymatically treating and further dialysing (to remove salts) the mamaku gum extract. After dialysing the gum, the purified fraction did not show any shear-thickening behaviour, highlighting the need for the ions to be present, in order to observe this effect. In the absence of ions, the repulsion occurring between strong negatively charged chains (*c.a.* -60 mV) prevents any interaction. On adding back salts (mono-, di- and trivalent) to the purified MP, the shear-thickening behaviour was recovered. It can be argued that the presence of cations (di- and trivalent)

may possibly cause an ion-bridging effect (electrostatic interactions) between MP chains leading to the shear-thickening, but this could not explain the recovery of thickening, in the presence of monovalent salts. Alternatively, cations can interact with the MP chains and reduce their electrostatic repulsion, allowing intermolecular interactions to take place which would lead to the shear-thickening behaviour (Wee et al., 2015a). Thus, it was thought that intermolecular interactions which could be involved were likely to be hydrogen bonds. To confirm the occurrence of hydrogen bonding in MP chains, MP was treated with urea (which disrupts hydrogen bonds) and a loss in the shear-thickening phenomenon was observed (Jaishankar et al., 2015). Thus, it was concluded that the shear-induced transition from intra- to intermolecular hydrogen bonding in presence of cations is the main cause of the shear-thickening effect observed in MP solutions. Moreover, based on the chemical structure of MP, it was suggested that carbonyl and carboxyl groups of glucuronic acid and the hydroxyl group of mannose and other sugars can act as 'sticky' groups which interact with each other *via* hydrogen bonding (**Figure 2.5**) (Wee et al., 2015a).

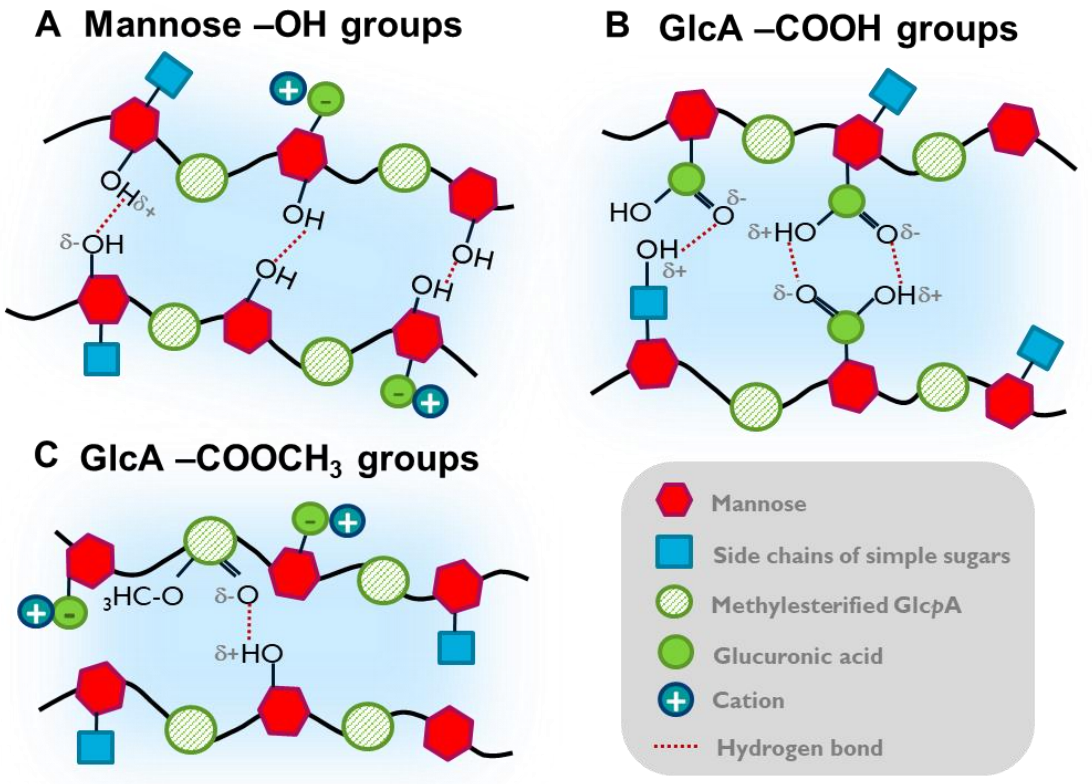


Figure 2.5: Schematic illustration showing possible 'sticky' groups responsible for hydrogen bonding during shear-thickening in mamaku polysaccharide. GlcA, glucuronic acid.

Reprinted from Wee et al. (2015a), with permission from Elsevier.

2.2.4 Mamaku gum in the stomach

The stomach is a muscular bag which primarily receives food from the oesophagus and passes it on to the small intestine. The gastric function is complicated by the occurrence of simultaneous events such as accommodation of the incoming food, digestion, size reduction of bigger particles and selective passage of finer particles (Lentle & Janssen, 2011; Schulze, 2006). In general, the incoming bolus is received and stored at the upper end of the stomach called the fundus by receptive relaxation, and subsequently, the fundus promotes the outflow of food by reducing its volume (*i.e.,* increase in fundus tone) (Hausken, Mundt, & Samsom, 2002; Pal et al., 2004). The outflow is mainly facilitated by the antral contraction waves which promote the flow towards the pylorus (end part of the stomach) and reduce the pressure gradient immediately distal to the fundus (Lentle & Janssen, 2011). The bolus from the fundus enters the body of the stomach where it is mixed with gastric juices and partially digested, forming the chyme. The digesta (chyme) is then pushed into the pylorus. As the contraction wave approaches towards the end of the pylorus, the digesta is pushed through the pyloric sphincter into the duodenum. The emptying of digesta from the stomach into the duodenum (*i.e.,* gastric emptying) can be affected by altering the rheological behaviour of digesta (normally shear thinning) (Lentle & Janssen, 2011; Marciani et al., 2001).

The effect of mamaku gum on gastric emptying was studied using an *ex vivo* rat stomach model and compared with guar gum at a similar viscosity (Lentle, Janssen, Goh, Chambers, & Hulls, 2010). When mamaku gum (~16.4% w/w) was perfused into the stomach, the wall activity response of the stomach was significantly different from its response to guar gum. In the presence of mamaku, the contraction waves were no longer consistently linear and the site of initiation and direction of propagation of the contraction was different. It was believed that the elastic nature of mamaku causes residual stress to persist within the solution after each contraction, which subsequently altered the antrocorporal contractions, thereby possibly delaying gastric emptying.

A subsequent *in vivo* rat trial was conducted by Wee, Lentle, Goh, and Matia-Merino (2017) to investigate the effect of mamaku gum on delaying gastric emptying. Briefly, mamaku gum (~15% w/w) or deionised water was gavaged to rats for five times each on alternative days over two weeks, and body weight and food intake were recorded daily. The rats were

euthanised 2 h after the final gavage and the stomach content was quantified. Authors reported that rats consumed less food on the days of gavage, and the food consumption was lower in rats gavaged with mamaku even after 24 h compared to rats gavaged with deionised water. Furthermore, after 24 h of gavage, the body weight gain in rats gavaged with mamaku was significantly lower than the rats gavaged with water. The weight of the content retrieved from the stomach of mamaku-gavaged rats was significantly higher than the weight of the content of those gavaged with water. Based on these observations, the authors suggested that mamaku gum engendered daylong gastric satiety by delaying gastric emptying.

In both of the above studies, the fresh mamaku gum was directly administrated into the stomach and then its effects were studied. However, in reality, mamaku gum needs to travel from the mouth *via* the oesophagus before it reaches the stomach. During oral processing of mamaku gum and its flow through the oesophagus, shear-thickening may develop which could pose an undesirable choking hazard. Efforts have been made to encapsulate mamaku gum for improving its delivery to the stomach, but due to its complex viscosity, the gum has still not been efficiently encapsulated (unpublished data). In addition, both studies mentioned were carried out at a high concentration of mamaku gum (more than ~15% w/w), which may not be a realistic concentration to deliver to humans if used in food systems.

Therefore, taking inspiration from the way mamaku is consumed by the native Māori people, this research explores the development of ingredients using the whole pith from mamaku fronds, as an alternative to gum extract. As MP is trapped in the tissue of the pith, it is hypothesised that the whole mamaku pith may still exhibit shear-thickening behaviour and have the desired effect in the stomach. Thus, whole pith will be processed into powders which could then be more easily incorporated into various food systems at various concentrations. However, in order to produce a stable powder for the food industry, which can maintain the desired functionality when consumed, the basis of powder technology need to be understood.

2.3 Powder Production

Processing food materials into powders is a common industrial operation. Food products are dehydrated to develop high-value products with low moisture and water activity (a_w) and an extended shelf-life. In some cases, the drying operation may be followed by a grinding operation to reduce particle size.

2.3.1 Drying

The first documented dried vegetable traces back to the 1700s, suggesting that drying is an age-old technique used for the preservation of food products. During the drying process, the moist food is heated to an appropriate temperature such that the moisture is reduced to the level where microbial growth and the rate of chemical reactions are inhibited or minimised (Barbosa-Canovas, Ortega-Rivas, Juliano, & Yan, 2005b). The moisture removal from the food involves two basic phenomena: (i) vaporisation of the surface moisture; and (ii) migration of moisture from the interior of the food to the surface, *via* diffusion, pressure gradient and cell contraction (Kaur, Sharanagat, & Nema, 2018). In addition to preservation, drying is also advantageous in reducing the bulk volume thus, reducing the cost of packaging, transportation, handling and distribution. It also helps in making seasonal products available throughout the year.

Traditionally, sun drying was used to remove moisture from foods, however, over time, new methods such as oven-drying, drum-drying, spray-drying, osmotic dehydration, pneumatic-drying, microwave-drying, freeze-drying and vacuum-drying have been developed. Drying methods commonly used for food applications are summarised in **Table 2.3**. The selection of an appropriate drying method depends on many factors such as cost, holding capacity, the efficiency of the process, ease of handling equipment, initial product quality and functionality of the final product. In this thesis, based on the initial solid-like state of the raw material and availability of equipment, hot air oven-drying and freeze-drying methods were selected. One may argue that the initial solid-like state of mamaku pith can be converted into a liquid or semi-liquid state by mincing with water and then, the paste could be used for methods such as drum drying and spray drying. Since the core purpose of drying is to remove moisture, adding extra water to change the state of mamaku pith to achieve

optimum pre-drying conditions, only to have to remove it by drying afterwards, will not be economical. Furthermore, operations like mincing, blending and cutting employed in reducing the solid-like pith will exert pressure on the MP which may affect the rheological profile in the final product (as reported in this thesis). Moreover, the presence of high fibre content in the pith can limit the application of a drying method, as fibres can block the nozzle of the spray dryer (Anthony Paterson, personal communication, 28th October 2020). Thus, oven-drying and freeze-drying methods were selected as potentially suitable drying methods.

Table 2.3: Common drying methods used for food applications.

Drying method	Mechanism of drying	Advantage	Disadvantages	Reference
Sun drying	Solid feed is spread in a thin layer and heated under the sun to evaporate moisture.	◦ Simple and inexpensive method ◦ Low initial and operational cost ◦ Can accommodate a large volume of product	◦ Nearly impossible to control the temperature and humidity ◦ Difficult to have a consistent product due to variations in weather ◦ Long drying time ◦ High risk of contamination from microorganisms, insects, pests and dust	-
Solar drying	Inlet air is heated by solar radiation and circulated over the moist food product in the drying chamber.	◦ Easy to use ◦ Low initial and operational cost ◦ More hygienic than sun drying	◦ Long drying time ◦ Dependent on day-to-day weather conditions ◦ Can only handle small quaintly of product	Tripathy (2018)
Hot air drying (Oven/tray/cabinet drying)	The product is held in the trays and exposed to hot air to remove moisture.	◦ Easy to operate ◦ Can be used for a vast type of products (as suitable for both solid and liquid products) ◦ Less capital cost	◦ Non-uniform drying of products at different locations ◦ Collapse and case hardening defects ◦ Loss of nutrition due to high temperature ◦ Time-consuming process	Karam, Petit, Zimmer, Djantou, and Scher (2016)
Spray drying	Liquid state feed is atomised into a hot drying medium, leading to moisture removal and formation of powder	◦ Relative short drying contact time, therefore, can be used for temperature-sensitive products ◦ Great control over the size and morphology of the product ◦ Suitable to produce high-quality fine powder	◦ Feed with high viscosity and stickiness may not be suitable ◦ Not an energy-efficient process ◦ Some products like high fat and sugar products may stick to the wall of dries ◦ Nozzle may block due to high fibres	Haque, Timilsena, and Adhikari (2018); Woo and Bhandari (2013)

		◦ Continuous operation	in the feed ◦ Requires a trained operator	
Drum drying	Viscous or sticky liquid is deposited on the surface of the drum and is heated from inside throughout the drum wall. Upon drying, the product is scraped off using a blade.	◦ High drying rate and thermal efficiency ◦ Can be used for small or medium production runs ◦ One of the inexpensive methods of drying	◦ The feed material that cannot adhere to the surface of the drum cannot be processed using drum drying ◦ Sugar-rich material can stick to the surface ◦ High temperature may lead to unwanted cooking ◦ Milk and milk products develop cooked flavour with some browning due to the Maillard reaction ◦ Denaturation of proteins at high temperature	Courtois (2013)
Fluidized bed drying	Small size solid particles are rested on a perforated plate and hot air (or gas) is passed through the particle bed, making particles move *i.e.,* fluidize. The hot air carries moisture with itself.	◦ High heat and mass transfer, so faster drying rate ◦ Uniform temperature leads to uniform drying	◦ Not suitable for liquid and sticky products ◦ Particle break down is common ◦ Continuous moment of the particles in hot air may lead to the generation of surface charges	Buck and Tsotsas (2018)
Osmotic drying	Moist food product is immersed in a hypertonic solution and because of the osmosis pressure gradient water is diffused from the tissues into the solution, resulting in a partially dehydrated product.	◦ Operates at moderate temperature, therefore heat damage to the product is minimised ◦ Energy-efficient process ◦ Improve the quality of the product	◦ Along with water, solutes (pigments, flavours, minerals, organic acid and sugars) may also leach into the solution, thereby affecting the nutritional and organoleptic properties of food ◦ Further drying step is needed after osmotic drying ◦ Mass transfer is slow ◦ Sugars/salts from hypertonic solution	Rastogi, Adsare, Karley, Raghavarao, and Niranjan (2018)

			may penetrate the product	
Freeze drying	The frozen material (containing moisture as ice) is directly converted to vapour, at low pressure, without entering the liquid phase (*i.e.*, sublimation).	◦ Yields a high-nutritional quality product because most of the deteriorative reactions are minimised/ stop in absence of free water and oxygen at low temperature ◦ Can be used for a vast type of products (as suitable for both solid and liquid products) ◦ Retain the original shape and size of the product ◦ Highly porous product is produced with good reconstitution properties	◦ High initial and operational cost ◦ Long process time due to freezing followed by slow drying ◦ Mostly the resultant products are hygroscopic, so need proper storage	Verma and Sharma (2018)
Vacuum drying	Product is kept at a pressure lower than the atmospheric pressure, causing the lowering of boiling point water.	◦ Fast drying rate ◦ High-quality product ◦ Low drying temperature ◦ Oxygen deficient processing environment ◦ Dried products have good rehydration property	◦ Expensive	Mohapatra (2018)
Microwave drying	Electromagnetic energy is converted to thermal energy by molecular agitation (dipole rotation and oscillatory migration of ions), causing an increase in product temperature. Whole mass of food is heated simultaneously.	◦ Microwaves penetrate deep inside the material and heat is generated uniformly through the substance ◦ Fast drying rate ◦ Precise control over process requirements ◦ High-quality product	◦ Hot and cold spots in food ◦ High initial investment ◦ Requires a trained operator ◦ Specific sample shape and size may be required for efficient drying	Changrue, Raghavan, Orsat, and Vijaya Raghavan (2006)

Infrared drying	Infrared radiations are absorbed by the molecules on the surface of food, causing molecules to vibrate. When molecules return to their ground state heat is generated. Heat is then transferred to the interior by conduction.	◦ Fast drying rate ◦ Uniform heating ◦ High degree of process control ◦ Increased energy efficiency ◦ Better retention of nutrients	◦ Surface hardening ◦ Low rehydration rates ◦ Fracture of material during long drying ◦ Difficult for thick products	Huang, Yang, Tang, Luo, and Sunden (2021)

2.3.1.1 Oven drying

Oven drying is a straightforward drying method that has been successfully applied to several food commodities such as mushrooms, pomegranates, oranges, chokeberries and bananas (**Table 2.4**). During oven drying, the product is held in trays and exposed to hot air in an enclosed space (**Figure 2.6**). The air entering the cabinet is heated to about 50-70°C (and at low relative humidity) and circulated around the product. The heated air comes in contact with the surface of the wet product, which transfers heat into the product matrix by conduction. The liquid migrates toward the surface by diffusion and/or hydrostatic pressure gradient and is transported away by air convection (Karam et al., 2016). The moist air is then again recirculated after heating or is removed from the system. Air is circulated at a relatively high speed (usually greater than 2 m/s) to ensure efficient heat and mass transfer occur (Singh & Heldman, 2001).

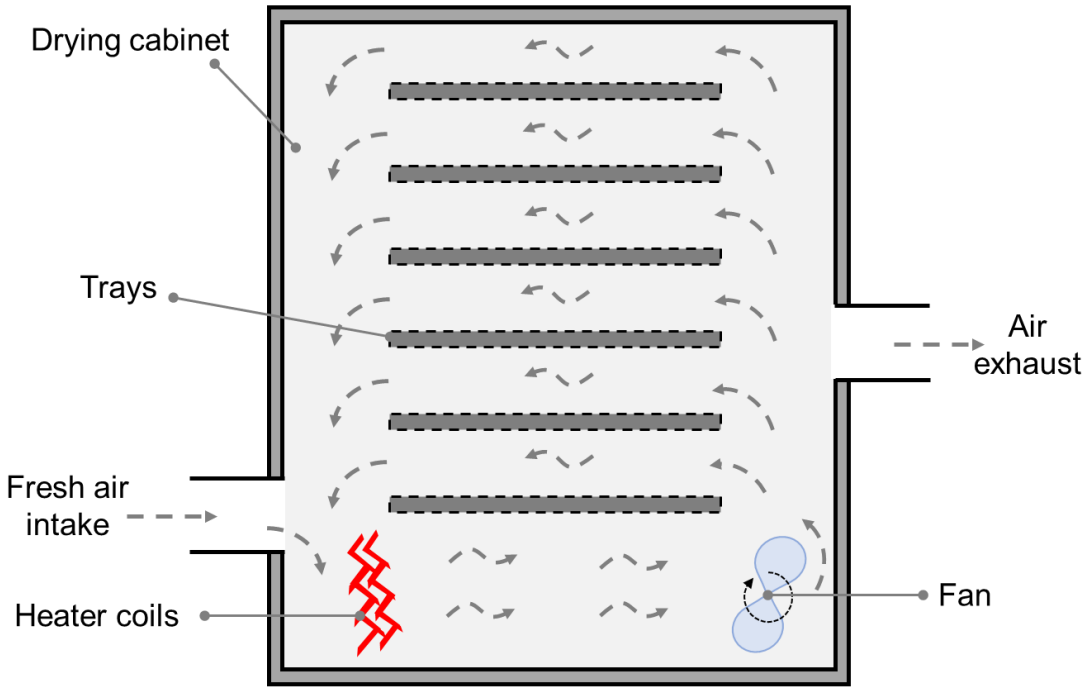


Figure 2.6: Schematic diagram of an oven-dryer.

Table 2.4: Effect of oven-drying and freeze-drying on food commodities.

Food commodity	Sample preparation	Drying conditions		Product quality	Reference
		Oven-drying*	Freeze-drying**		
Button mushrooms	Sliced to 5 mm thickness	60°C	50°C, 100 Pa	◦ Degradation of colour in OD sample ◦ OD sample has high density ◦ FD sample has high porosity ◦ FD sample has better rehydration in water ◦ OD sample has a dense microstructure	Argyropoulos, Heindl, and Müller (2011)
Pumpkin and green pepper	Sliced to 2x2 cm squares	30-70°C	T not reported, 0.666 Pa	◦ Degradation of colour in OD sample ◦ OD sample has high hardness	Guiné and Barroca (2012)
Pomegranate	Arils were separated Rind was cut into 1x1 cm squares	50-70°C	30°C, 65 Pa	◦ OD sample has high density ◦ FD sample has high phenolic compounds ◦ OD sample has a burnt odour	Calín-Sánchez et al. (2013)
Tomatoes and ginger	Sliced to 2x2 cm squares	60°C	T not reported, 13.3 Pa	◦ FD sample has high phenolic compounds, vitamin C and antioxidant activity	Gümüşay, Borazan, Ercal, and Demirkol (2015)
Chokeberries	-	60°C	30°C, 65 Pa	◦ FD sample has high porosity ◦ OD sample has high density ◦ OD sample has high hardness ◦ FD sample has better sensory attributes	Calín-Sánchez et al. (2015)
Jujube	Cut in pieces and pitted	50-70°C	26°C, 0.96 kPa	◦ FD sample has high phenolic compounds and antioxidant activity ◦ Degradation of colour in OD sample ◦ OD sample has high hardness	Wojdyło et al. (2016)
Blackcurrant	Fruits were grounded	50-90°C	T not reported,	◦ FD sample has high porosity	Michalska, Wojdyło,

pomace	and pressed		65 Pa	◦ FD sample has high phenolic compounds and antioxidant activity ◦ Degradation of colour in OD sample ◦ FD sample has high solubility	Lech, Łysiak, and Figiel (2017)
Green banana	Peeled and sliced to 7 mm thickness	55°C	T not reported, 0.7 Pa	◦ OD sample has high density ◦ OD sample was darker in colour ◦ No effect on crystallinity ◦ FD sample has a higher water-holding capacity	Ahmed, Thomas, and Khashawi (2020)
Orange	Peels were cut into small pieces	45-60°C	T not reported, 12.5 Pa	◦ OD sample has high density ◦ OD sample was darker in colour ◦ FD sample has a high yield of essential oils ◦ FD sample has high phenolic compounds and antioxidant activity	Farahmandfar, Tirgarian, Dehghan, and Nemati (2020)

* Air temperature in the oven; ** Shelf temperature, pressure in the chamber; OD, Oven-dried; FD, Freeze-dried

Shrinkage of the product (*i.e.*, collapse) and hardening of the outer surface (*i.e.*, case hardening) are common phenomena associated with oven drying. Many authors have reported shrinkage during oven-drying (Karam et al., 2016), which can be up to 80%, for instance in kiwifruit and berries (Jankovie, 1993; Maskan, 2001). Both of these phenomena are closely associated with the *glass transition temperature* (T_g). T_g can be defined as the temperature at which the amorphous material changes from a glassy state into a rubbery state (Rahman, 2009). As the temperature of the product increases above T_g, the hard and glassy state of the material changes to a soft and rubbery state leading to the loss of structure. **Figure 2.7** shows the loss of porous structure in quince fruit with increasing oven-drying temperature. However, as the moisture is continuously reduced during drying, the material properties significantly transform from soft, and rubbery to hard and glassy, leading to case hardening (Gulati & Datta, 2015). Case hardening is usually the result of faster drying at the outer surface of the product than at the core, thus, entering into a glassy state (Achanta, Okos, Cushman, & Kessler, 1997). As a result of the collapse and case hardening, the rehydration properties of oven-dried materials are often poor, therefore other drying methods like freeze-drying are commonly used for high-value products (**Table 2.4** and **Figure 2.7**).

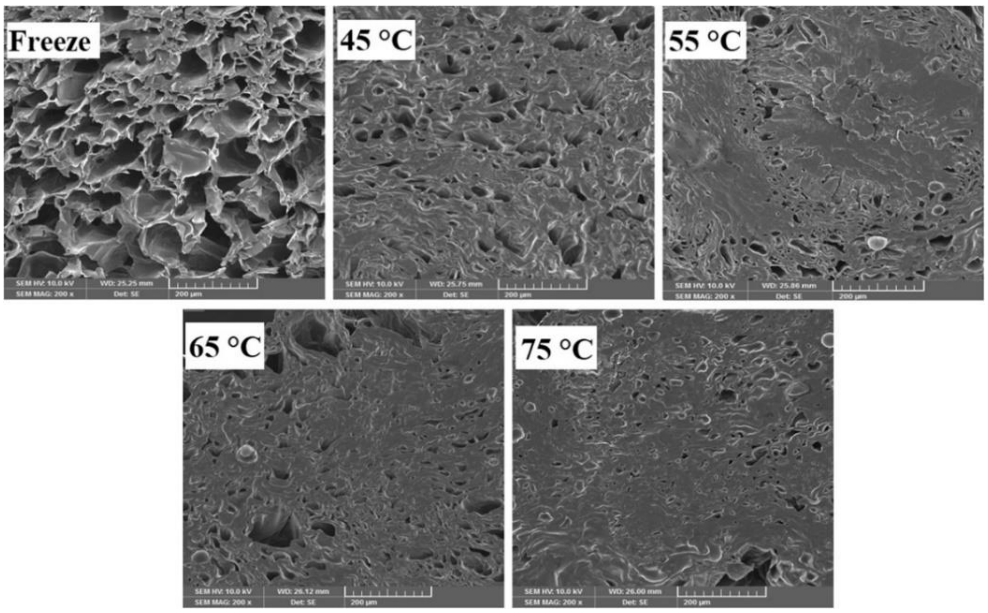


Figure 2.7: Micrographs of quince fruit during freeze and oven-drying.

Reprinted from Izli and Polat (2019), with permission from Springer Nature.

2.3.1.2 Freeze drying

Similar to oven-drying, freeze-drying is also applied for various plant-based food commodities such as blackcurrant, pumpkin, tomatoes, pomegranates, oranges, and jujube (**Table 2.4**). Freeze-drying is a low-temperature drying method in which the frozen product is dehydrated by sublimation[12]. During freeze-drying, the moisture, in the form of ice in a frozen material is directly converted to vapour, at low pressure, without entering the liquid phase. The freeze-drying process comprises three steps: (i) the product is frozen by reducing the temperature; (ii) then the pressure in the chamber is reduced below the triple point[13]; and (iii) finally, heat is supplied to convert the ice into vapour, leading to moisture removal (Verma & Sharma, 2018). A schematic diagram of the freeze-dryer and a typical product temperature profile during freeze-drying is shown in **Figure 2.8**.

(i) Freezing: Freezing is a crucial step in freeze-drying but is sometimes disregarded. During freezing, the initial temperature of the food product is reduced by decreasing the temperature (from point a to b in **Figure 2.8B**). Freezing can be performed outside the dryer (in a separate unit), but in most industrial applications it is done directly in the freeze-dryer chamber. The food undergoing freeze-drying constitutes water as a solvent with other materials suspended in it as solutes. The presence of solutes in the food system decreases the freezing point more than that of pure water *i.e.,* causing freezing point depression. Upon reducing the temperature, the water separates, and ice crystals are formed, creating a higher concentration of solutes in regions left unfrozen. Although at this point the product may appear frozen, the temperature is further reduced to freeze the unfrozen solute regions. The frozen product may also be maintained at the specific subfreezing temperature for some time (a process called annealing) to ensure proper freezing of the more concentrated regions (from point b to c in **Figure 2.8B**) (Ratti, 2013). Freezing rate is another important parameter as it may affect the cellular structure of the food and thereby the quality of the final product. If the freezing rate is slow, it causes the formation of large extracellular ice crystals leading to tissue damage. On the contrary, the rapid freezing rate will promote intensive nucleation and the formation of many small intra- and extracellular ice crystals (Fernández, Otero,

[12] The process of directly converting a solid into a vapour, without transforming it into a liquid.
[13] The point at which all the three phases *i.e.,* solid, liquid and gas coexist in thermodynamic equilibrium. It has a unique value to temperature and pressure, 0.01°C and 612 Pa, respectively.

Guignon, & Sanz, 2006). Though the small ice crystals help to preserve the structure of the product, they are difficult to dry; on the other hand, the larger crystals can easily sublimate during drying due to a lower presence of restrictive channels, improving the rate of primary drying (Verma & Sharma, 2018).

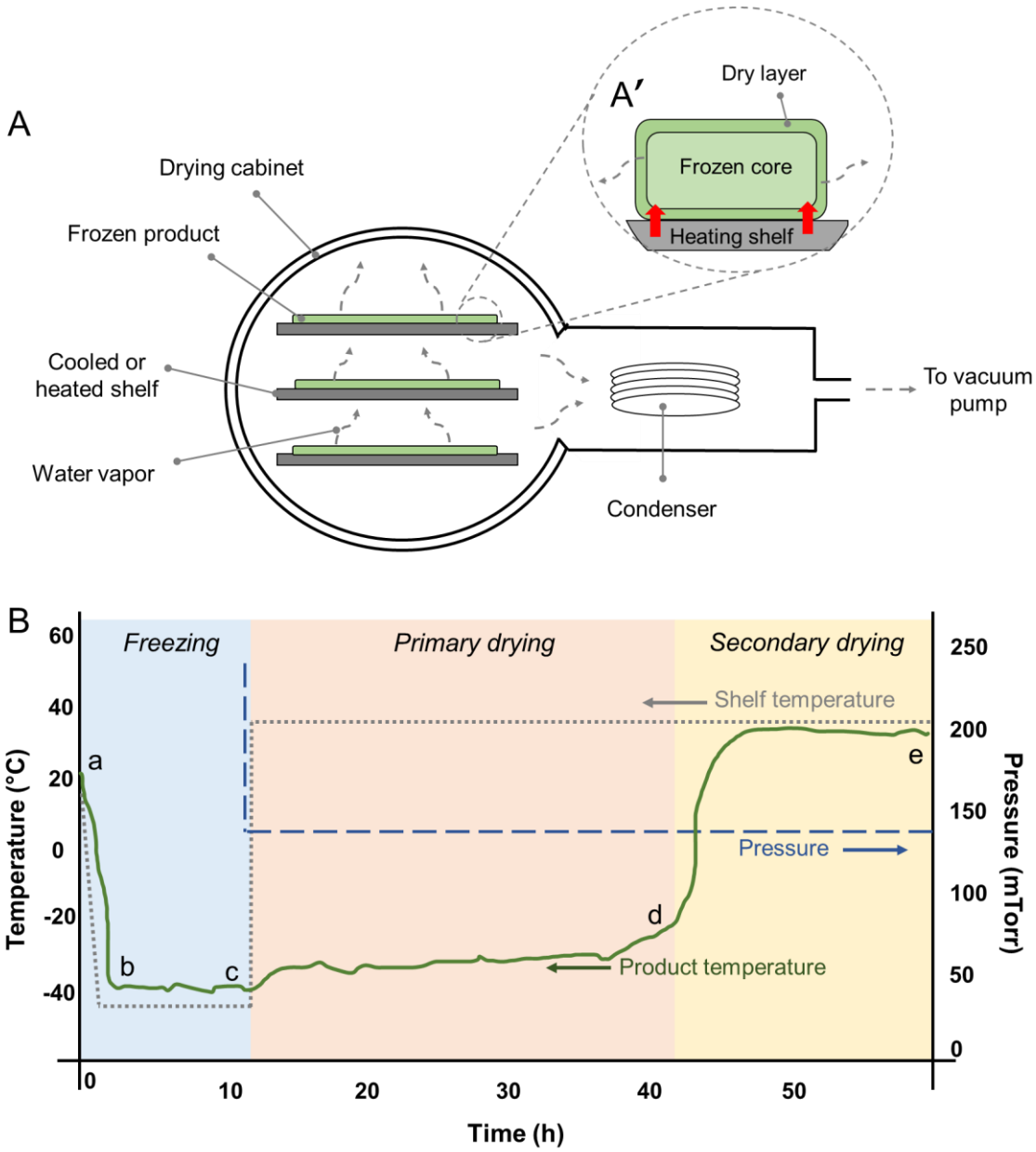


Figure 2.8: (**A**) Schematic diagram of a freeze-dryer (**A′**) showing dry layer formation during drying. (**B**) A typical product temperature, shelf temperature and pressure profiles during drying.

Adapted from Ratti (2013)

(ii) Primary drying: Once the product is frozen, the pressure in the drying chamber is reduced and the temperature of the shelf is increased to initiate sublimation. The driving force for

sublimation is the pressure difference between the water vapour pressure at the ice front (in/on food) and the vapour pressure in the drying chamber (Barbosa-Canovas et al., 2005b). As sublimation begins, the ice from the outer surface of the product in contact with heat will convert into vapour, leaving behind a porous dry layer; with the progression of sublimation, the thickness of the porous dry layer increases (moves from the surface to the inner core of the product) (**Figure 2.8A'**). The thick dry layer surrounding the frozen core of the product acts as an insulator and restricts the heat transfer to the ice and mass transfer from the ice, thereby reducing the drying rate. Although heat is supplied to the product, the temperature of the product is significantly lower than the temperature of the shelf due to the enormous latent heat of sublimation (from point c to d in **Figure 2.8B**) (Ratti, 2013). By the end of this drying step, a maximum fraction of the moisture has been removed from the product, and the temperature significantly starts to increase, marking the beginning of the secondary drying (from point d to e in **Figure 2.8B**).

(iii) Secondary drying: During the secondary drying, the bound water which could not freeze during the freezing step, leaves the product matrix by desorption. In order to break the bonds between the water and the food matrix, more energy is needed, so the temperature may be slightly increased keeping the same vacuum as during the primary drying (Verma & Sharma, 2018). A resultant food product with 2-10% moisture content is usually recommended (Barbosa-Canovas et al., 2005b).

The temperature of the product is critical during primary and secondary drying as it should be below the critical limit where the product quality may deteriorate. However, it should be high enough to lead to an efficient sublimation. Although critical, the product temperature cannot be manipulated directly but it can be adjusted by adjusting the temperature of the shelf and pressure in the cabinet; therefore, with an increase in pressure, the product temperature will increase (at constant shelf temperature) leading to an increased sublimation rate and *vice versa* (Ratti, 2013). If the product temperature is above the critical limit then it may result in collapse, causing sealing of the capillaries, reducing the pore size and leading to loss of structure (as in the case of oven-dried products); therefore, the product temperature should always be lower than the collapse temperature (Oyinloye & Yoon, 2020). The collapse temperature during drying can be analysed by trial and error or by using

methods like specific volume determination. Levi and Karel (1995) showed that the collapse in sucrose:raffinose mixtures, increased as the drying temperature increased above the T_g. Thus, T_g can be considered as the theoretical maximum temperature limit that should not be exceeded during drying (Oyinloye & Yoon, 2020). If the process parameters are correctly maintained during drying, the resultant product will retain its original shape and size with a highly porous structure (**Table 2.4**). High porosity increases the surface area of the product, enabling it to rehydrate easily and quickly when a solvent is reintroduced. However, high porosity also implies a shorter shelf-life due to more surface exposure to the external environment.

Mamaku pith after drying either by oven-drying or freeze-drying needs to be reduced in size to have a usable form, thus, grinding operation is essential. During grinding, the material is subjected to mechanical stress leading to an increase in energy thereby fragmentation (Karam et al., 2016). The stress applied to the dry solid surface will create a network of cracks that will determine the shape and size of the fragments after the breakdown (Oyinloye & Yoon, 2020). The creation of cracks and breakdown into fragments is strongly influenced by the properties of the food material. For instance, brittle materials like grains, coffee and sugar will absorb little energy and break into finer pieces that can be reassembled to form the original structure; while in semi-brittle materials, first, a cut will appear which will lead to breaking with an increase in stress. The extreme behaviour corresponds to that of plastic materials like dried leaves, fruits and herbs, which will deform before reaching the breaking point (Baudelaire, 2013). Thus, depending on the nature of the food material different types of grinding forces (such as shearing, impact and cutting) may be needed for size reduction. Different grinding forces may be achieved by using different types of equipment such as ball mill, hammer mill, knifes mill, roller mill and disc mill (Gao, Chen, Wang, & Meng, 2020). However, there is limited information in the literature on the effect of the grinding process on the overall quality of powders.

2.3.2 Powder properties

The resulting solid-state particles, after drying and grinding, with sizes ranging from nano to micrometres are commonly referred to as powder. The properties of powder can be classified into three categories, namely: (i) *Fundamental properties* such as particle size, distribution,

shape, moisture, density, surface characteristics, composition and T_g; (ii) *Functional properties* (depending on application) such as flowability, mixing, compressibility and rehydration properties; and (iii) *Defective properties* such as caking, stickiness and dusting (Bhandari, 2013). The functional and defective properties are directly influenced by the combination of different fundamental properties. Powder properties can also be classified as: (i) *Particle properties* such as particle size, particle density, and particle shape; and (ii) *Bulk properties* such as particle size distribution, bulk density, porosity, flow and rehydration (Shah, Karde, Ghoroi, & Heng, 2017). In general, the fundamental properties can be related to the properties of individual particles which together govern the bulk powder properties. It is vital to measure the particle and bulk properties as they are often used as quality parameters and are critical for designing a good process as well as helping in decoding the events during the powder formation process.

2.3.2.1 Particle size and distribution

Particle size is the most important particle property as it can influence many characteristics of bulk powder, such as flowability, compression and rehydration; primarily because particle size can influence the surface area of a particle which determines particle-particle interactions as well as particle-surrounding solvent interactions (Fitzpatrick, 2013). Although an important parameter, describing the size of particles by a single number is not simple, as particles rarely have a regular shape. Different approaches are used to describe the diameter of irregular particles leading to different sizes used to describe the same particle. The first approach (statistical diameter) is to measure one linear dimension of a particle in a fixed direction (usually by a microscope). The second approach (equivalent circle diameter) is to equate the diameter of a circle that would have the same properties to the projected area or perimeter of a particle on a surface. Both these approaches are slow and only a limited number of particles may be considered while measuring the size. Furthermore, the particles are three-dimensional objects and should be compared with another three-dimensional object. Thus, the third approach (equivalent sphere diameter) where the diameter of a particle is measured by equating it to a sphere of similar surface area, volume and surface-to-volume ratio, is a commonly used method (Allen, 1981; Barbosa-Canovas, Ortega-Rivas, Juliano, & Yan, 2005c; Fitzpatrick, 2013; Hawkins, 1990). The size of the particles in bulk

powder is not uniform so there is a need to describe the distribution of the particles. To quantitatively express the distribution, mean and median are often used, enabling one to express the size of the population using a single number (Fitzpatrick, 2013). However, this does not give any indication of the size variation in the population. The size and distribution of particles are commonly measured using the laser diffraction technique (discussed in **Chapter 3**).

2.3.2.2 Particle shape

Particle shape is another important property along with particle size, that can influence the packaging behaviour of the bulk powder and therefore, the bulk density. It can also affect the flowability and handling operation of the powders by influencing the surface contact between particles; irregular and uneven particles can interact by mechanical interlocking. The shape of particles can be described using words like irregular (lacking any symmetry), fibrous (thread-like), acicular (needle-shaped), dendritic (branched crystalline shape) and spherical (Allen, 1981). These can be useful in describing the particles with a more regular shape without much variation through the population. The shape of the particle is generally quantified by measuring the ratio of length to breadth or width. However, different shape particles can have the same length-to-breadth ratio, leading to ambiguity. Nevertheless, the knowledge of the shape and aggregation state of particles derived from purely observing them under the microscope, without any quantification, can be beneficial (Barbosa-Canovas et al., 2005c; Fitzpatrick, 2013; Hawkins, 1990).

2.3.2.3 Density

The density of a particle is defined as the ratio of mass to volume and it indicates how the matter is arranged in the particle. A high-density value means a compact molecular arrangement and *vice-versa* (Singh & Heldman, 2001). Depending on how the volume is measured, density can be defined differently for the same particle. Food particles are mostly porous *i.e.,* there are voids in the particle. These voids can be open (pores which are exposed to the exterior environment) or closed (pores buried inside the particle and not connected to the exterior of the particle) (**Figure 2.9A**). When calculating density, if the volume occupied by the open and closed pores is not considered, then the *true particle density* (ρ_s) is calculated.

Therefore, true density is the density of the solid material of which the particle is composed. *Apparent particle density* (or particle density, ρ_p) is defined as the ratio of the mass of the particle to the volume of the particle, excluding the open pores. Apparent density is commonly measured using a gas pycnometer, with helium or nitrogen gas. If there is a particle without any closed pores, then ρ_s and ρ_p will be equal. If all the voids in the particle are considered, then it is called *effective particle density* (ρ_e) (**Figure 2.9B**) (Barbosa-Canovas et al., 2005c; Kousaka & Endo, 2006).

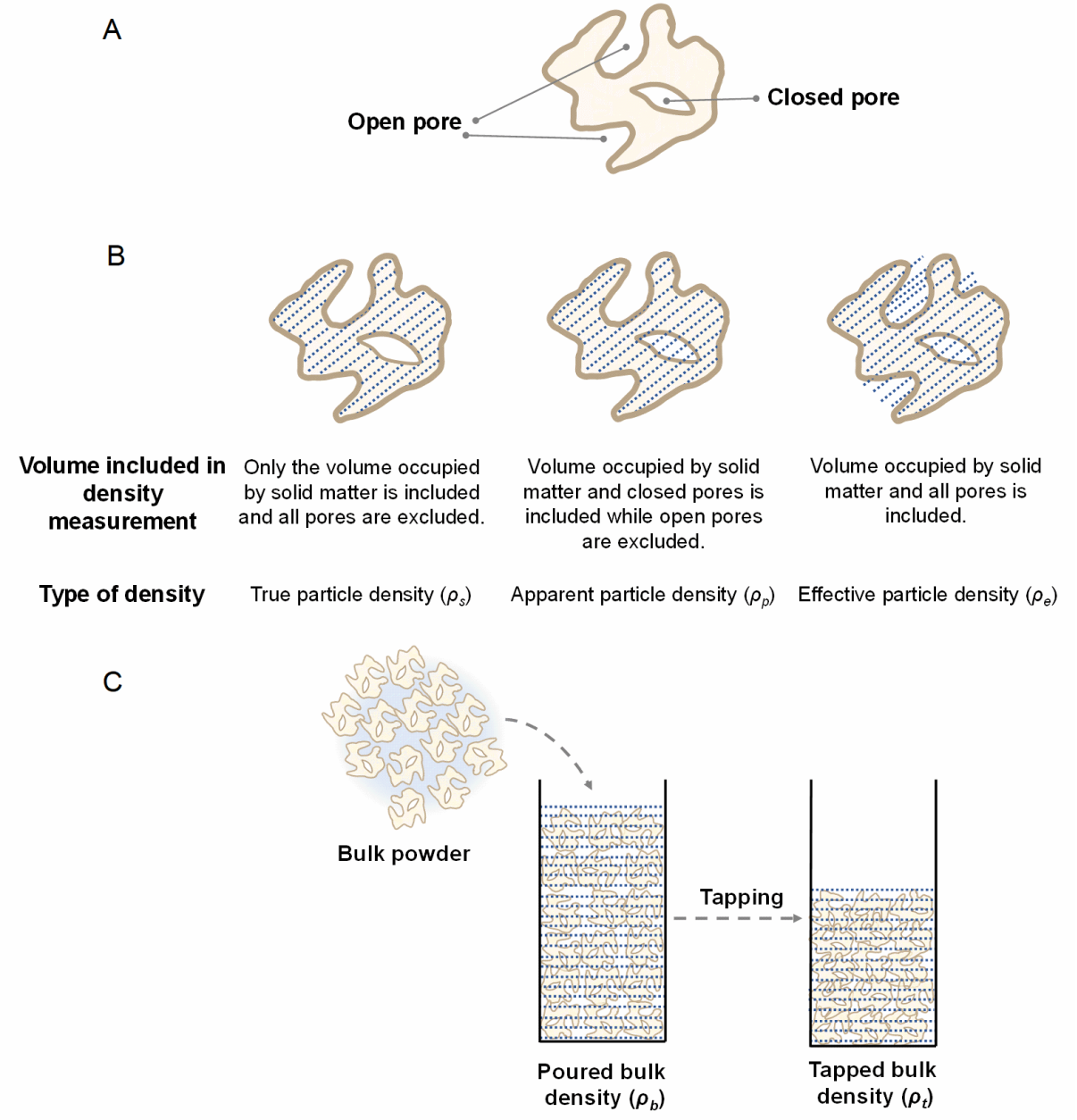


Figure 2.9: (**A**) Illustration of a particle with intraparticle pores. Consideration of different volumes (shown in dash lines) to calculate (**B**) particle and (**C**) bulk densities.

When considering the bulk powder, in addition to intraparticle spaces (voids), interparticle space will also exist. The bulk powder is a mixture of particles and gas, where gas occupies the space between the individual particles. If the density is calculated for the bulk powder bed by dividing the mass of powder by its bulk volume, including interparticle space, then it is called *poured bulk density* (ρ_b). However, if the powder is compressed by tapping *i.e.,* removing the interparticle space then the calculated density is called *tapped bulk density* (ρ_t) (**Figure 2.9C**) (Barbosa-Canovas, Ortega-Rivas, Juliano, & Yan, 2005a). The bulk density of the powder is influenced by the size distribution and shape of the particles. Powders with wider size distribution will have lower poured bulk density due to the fitting of smaller particles in the interparticle voids and *vice-versa*.

2.3.2.4 Microstructure and surface properties of powder

The microstructure of powder impacts its functional properties and stability. At the microstructural level, the powder can be crystalline or amorphous. The microstructure development of powders is strongly dependent on the rate of drying since slow drying results in a crystalline structure while rapid drying tends to result in an amorphous one. Crystalline structures (such as in sugars) have a well-defined tightly packed ordered molecular alignment, and as a result, the molecules only at the air-solid interface can interact with the environment, making the powder less susceptible to exposure to water and air (Bhandari, 2013). Consequently, crystalline powders need high energy and a longer time to dissolve in water *i.e.,* have poor rehydration properties. On the contrary, the amorphous structures (such as in fruit juice powders and protein powders) have a randomly disordered molecular structure with more open voids. Due to the presence of pores, there are more sites for interaction with the external environment, thus, the powders can absorb water rapidly. The amorphous structure may be suitable for food powders where easy rehydration of powder is needed but will hinder powder stability (Hedegaard & Skibsted, 2013). Thermodynamically, the immobilised glassy state of amorphous material has higher Gibbs free energy than the crystalline state, thus, there is always a driving force towards the crystalline form; however, the shift from an amorphous to a crystalline structure is a very slow process (Bhandari & Howes, 1999). The transition to the crystalline structure can be promoted by increasing the temperature or a_w, leading to the deterioration of the powder.

As the temperature of amorphous powder increases above the T_g, the glassy state converts to a more flowing rubbery state which promotes molecular diffusion and may initiate crystallisation (Bhandari, 2013; Hedegaard & Skibsted, 2013). Moreover, with the increase in the a_w of powder, the T_g will decrease, and the rate of crystallisation will increase. Thus, controlling temperature fluctuations and limiting the a_w are necessary for the optimal storage of powders.

Functional and defective properties such as caking, rehydration, sticking and flowability are also strongly influenced by the surface properties of particles (Gaiani, Burgain, & Scher, 2013). Based on the powder-making process and composition of the raw material, the surface of the particle can be smooth (rarely), wrinkled, dented, cracked or shrivelled. Despite variation in the surface morphology, all the particle surfaces are broken structures, leading the surface molecules to behave differently due to broken chemical bonds with other molecules (Bhandari, 2013). This confers the surface molecules with higher reactivity, resulting in more interactions with the environment (gas and water vapours). Increased moisture on the surface will increase the cohesion between the particles leading to caking and reducing the flowability. In addition to surface structure, the surface composition of the powder is also critical (Shah et al., 2017). The surface composition of the particle can be different when compared to the bulk composition. For instance, the surface of whole milk powder is reported to have higher fat content, due to fat migration during the drying process and storage (Kim, Chen, & Pearce, 2009). The high-fat content on the surface of the particles introduces more hydrophobic sites, leading to poor powder reconstitution in water (Gaiani et al., 2010). High surface fat also makes the powder more prone to deteriorate *via* lipid oxidation (Kim, Chen, & Pearce, 2002).

2.3.2.5 Powder rehydration

Food powders are consumed either as the main ingredient (such as milk powders, coffee powders and flour) or as a functional ingredient in products (such as hydrocolloids in ice cream and bread). In either case, rehydration of powders in water is the primary step for incorporating powder into the food system (Selomulya & Fang, 2013). Desirable rehydration properties can be described as the quick dissolution of powder upon introducing water, without forming lumps or sediments. A delay in the dissolution of powder may lead to

prolonged processing time, possibly poor quality and increased production cost (Saggin & Coupland, 2002). In general, rehydration of powders can be divided into four sequential steps: (i) *wetting*, (ii) *sinking*, (iii) *dispersion* and (iv) *particle solubilisation* into solutions (Crowley, Kelly, Schuck, Jeantet, & O'mahony, 2016; Fang, Selomulya, & Chen, 2007; Wangler & Kohlus, 2018); however, these steps tend to overlap with each other, making it nearly impossible to observe each phase independently (**Figure 2.10**) (Schubert, 1993).

Wettability is the tendency of the liquid phase to replace the gaseous phase on the surface of a solid substance and is generally considered the rate-limiting step of powder rehydration (**Figure 2.10A**) (Kirchberg, Abdin, & Ziegmann, 2011; Vega & Roos, 2006). During wetting, the liquid has to penetrate the porous arrangement of the bulk powder, thus, it is influenced by the interfacial tension between solid and liquid (**Figure 2.10A'**) (Wangler & Kohlus, 2017). Many efforts had been made to model the kinetics of wetting of powders (Asthana, 2000; Good & Lin, 1976; Lavi & Marmur, 2006), and most of these models have been developed based on the Washburn equation (**Equation 2.1**) to analyse the water uptake by the capillary rise (Washburn, 1921).

$$\frac{dl}{dt} = \frac{r\sigma}{\eta 4l} cos\theta \qquad \textbf{Equation 2.1}$$

where, $\frac{dl}{dt}$ is the velocity of the liquid penetrating the capillary of radius, r. η and σ are the viscosity and surface tension of the surrounding liquid. l is the penetrating distance of liquid and θ is the contact angle. From **Equation 2.1**, it can be inferred that large pores (due to large particle size) and small contact angle will favour wetting. Wetting of powders is a dynamic process, leading to continuous changes in η, σ, r and θ (Selomulya & Fang, 2013). For instance, upon wetting milk powders, the surface tension will continuously change due to dissolution of several components such as lactose, salts and whey proteins which also change the viscosity of the liquid. As lactose dissolves, the radius of the pores will also increase. With progression in wetting the interface of solid and liquid will change, thus, altering the contact angle (Fang et al., 2007; Wangler & Kohlus, 2017). Therefore, quantifying wettability is difficult and methods available are limited and dependent on powder type.

Once the gaseous phase around the powder particles is replaced by water, particles or part of the bulk powder starts to sink; this is termed sinkability (**Figure 2.10B**). Sinkability can be

defined as the falling of powder below the surface of the liquid (Crowley et al., 2016). For good sinkability, the weight force must be higher than the buoyancy force *i.e.*, the density of the particle (or bulk powder) must exceed the density of the liquid (Wangler & Kohlus, 2017). The high density of powder particles along with a low quantity of air enclosed in the particle will result in faster sinking. The density of the particle, in addition to its composition, is also influenced by the water uptake during wetting. As wetting progresses the density of particles increases, and sinking will start (Masters, 1985). During absorption of water, the particles may also swell, which results in delaying the sinking. At the bulk powder level, the presence of agglomerates will accelerate the sinking process due to a high aggregate density, thus, aggregation of powders is a common method used for making instantaneous powders (Forny, Marabi, & Palzer, 2011; Ji, Cronin, Fitzpatrick, Fenelon, & Miao, 2015). In general, a powder is considered wet from the point at which it starts to sink in the liquid; thus, wettability and sinkability are often used interchangeably (Fang et al., 2007).

After the aggregated particles have sunk, they will break up and start to disperse into individual particles (**Figure 2.10C**) (Fang, Selomulya, Ainsworth, Palmer, & Chen, 2011). The rate of particle dispersion is shown to increase with particle size and decrease with a high fraction of finer particles (≤90 μm) in milk powders (Vojdani, 1996). Poor dispersion can lead to the formation of large lumps and slurry settling at the bottom of the container (Selomulya & Fang, 2013). Finally, the components of the particle will diffuse and attain maximum solubility in the rehydrating liquid (**Figure 2.10D**) (Fang et al., 2007).

After the dissolution of powder particles in the solvent, the rehydration process is complete. However, the intended functionality of the polysaccharide may yet not be fully achieved. For instance, when polysaccharides are mixed in water, the solution usually takes time to attain its maximum viscosity. Wang, Ellis, and Ross-Murphy (2002) showed that on dispersing 1% (w/w) guar gum in water, the viscosity of the solution increased over 5 h of study. This enhancement in viscosity over time can be due to the interaction between the polysaccharide and water at the molecular level *i.e.*, hydration of the individual polysaccharide chains or aggregates. Here, the hydration of polysaccharides refers to the interfacial hydrogen bond network formed between water molecules and the actual macromolecules (Grossutti & Dutcher, 2020). These associations are due to polar groups present on the polymer, and take

place in two steps: (i) the water molecules bind to polymer-specific sites and then (ii) more water molecules attach to initially bound water resulting in the formation of a big water cluster, or hydration shell, often referred to as the swelling of a polysaccharide (Despond, Espuche, Cartier, & Domard, 2005; Fringant et al., 1996). Based on this interaction, the water around a polymer can be characterised as: (i) n*on-freezable bound water:* it forms a strong bond with the surface of the polymer and has very low mobility, with very weak water-water interactions; (ii) *intermediate bound water:* it presents moderate interaction with the surface of the polymer and other water molecules, and has slightly higher mobility being able to freeze below 0°C; and (iii) *free water:* has high mobility and similar freezing temperature as the bulk water, hardly interacts with the surface of the polymer (**Figure 2.10D'**) (Bag & Valenzuela, 2017). The degree of hydration and the extent of the different types of water molecules surrounding a polymer is strongly dependent on the structural parameters of the polymer (Bag & Valenzuela, 2017; Despond et al., 2005), however, the current understanding in this area is still limited. From the viscosity perspective, it may be interpreted that as the hydration proceeds the hydrodynamic volume around the polysaccharide will increase, leading to an increase in the intrinsic viscosity; thus, viscosity-enhancement is observed over time (Premathasan & Taylor, 2018; Wangler & Kohlus, 2018). During hydration, some conformational changes may also have occurred in the polymer which will further contribute to the viscosity enhancement. Thus, in addition to quick powder rehydration, the hydration of a polysaccharide must be considered, in order to achieve the intended functionality of the biopolymer under study. This is crucial when exploring possible applications of powders made from mamaku pith, as in the present thesis.

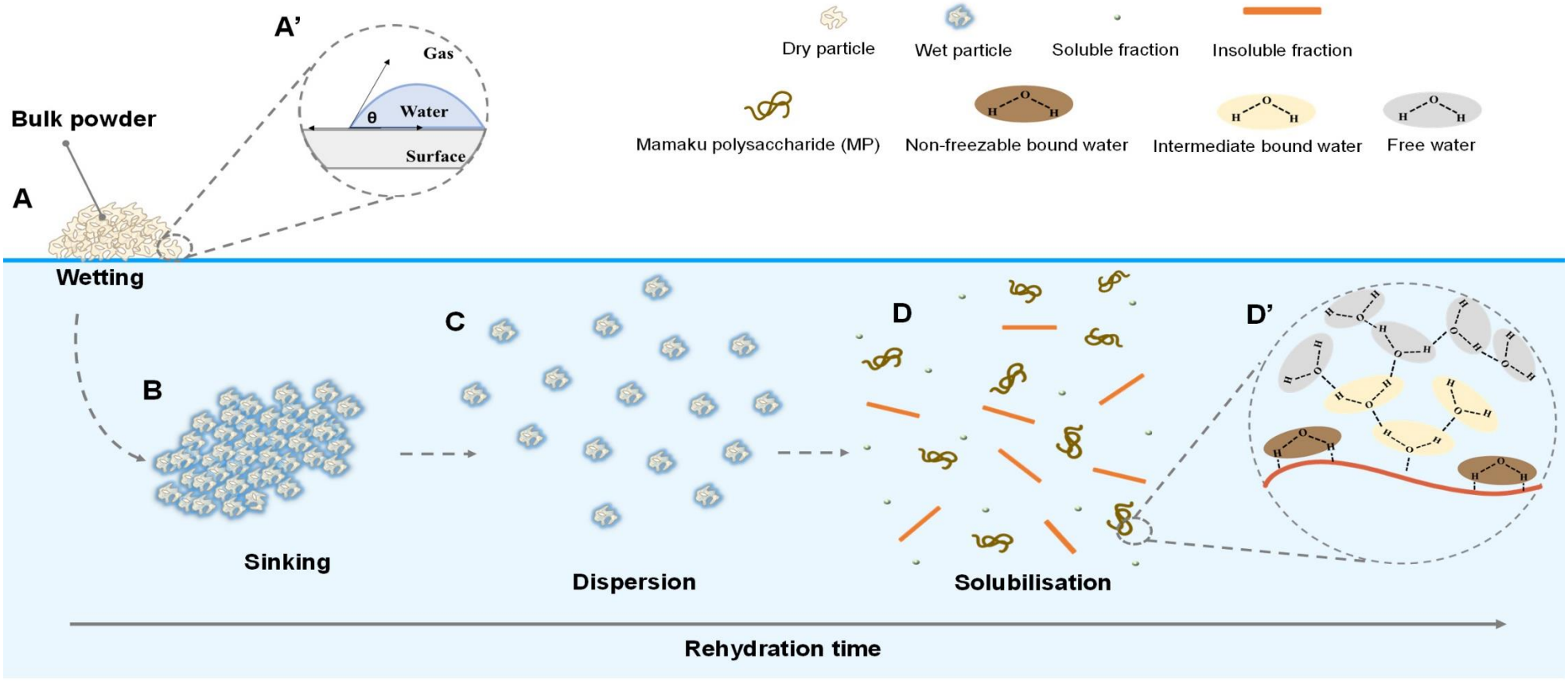


Figure 2.10: Schematic representation of rehydration of powder and hydration of released polysaccharide, showing (**A**) wetting, (**B**) sinking, (**C**) dispersion, (**D**) solubilising, (**A'**) contact angle and (**D'**) the interaction of water molecules with polysaccharide.

2.4 Possible Physiological Effects and Health Benefits of Mamaku

The therapeutic effects exhibited by a non-digestible, non-absorbable food product/ ingredient are primarily governed by its composition and behaviour in the human gastrointestinal tract (GIT). In general, under gastrointestinal conditions, the macronutrients (protein, fat and carbohydrates) in the product are broken into their simpler units, absorbed into the bloodstream, and transported to their respective destinations to perform specific functions; meanwhile, the remnant after digestion, which includes dietary fibre, passes through the colon where some may be fermented, and the remainder is excreted. The remnant fraction that escapes digestion and absorption in the foregut is normally referred to as dietary fibre and the vast majority of this is made of polysaccharides (Mishra & Monro, 2012). CODEX Alimentarius defines the dietary fibre as "…*carbohydrate polymers with 10 or more monomeric units, which are not hydrolysed by the endogenous enzymes in the small intestine of humans and belong to the following categories: (i) Edible carbohydrate polymers naturally occurring in the food as consumed, (ii) Carbohydrate polymers, which have been obtained from food raw material by physical, enzymatic or chemical means and which have been shown to have a physiological effect or benefit to health as demonstrated by generally accepted scientific evidence to competent authorities, (iii) Synthetic carbohydrate polymers, which have been shown to have a physiological effect of benefit to health as demonstrated by generally accepted scientific evidence to competent authorities*" (Codex Alimentarius, 2010).

Many epidemiological studies have shown the positive effects of consuming food rich in dietary fibre on the incidence of diseases such as obesity, type 2 diabetes, cardiovascular disease (CVD) and several forms of cancers (Astorg et al., 2002; Bazzano et al., 2002; Chajès & Romieu, 2014; Chuang et al., 2012; Feskens, Sluik, & Du, 2014; Franco et al., 2014; Hosseinpour-Niazi, Mirmiran, Mirzaei, & Azizi, 2015; Kochar, Gaziano, & Djoussé, 2011; Mao, Huang, Zhu, Wei, & Chen, 2021; Reynolds, Temple, Robertson, & Mann, 2001); and, thus, this has been the focus of research for decades. As mamaku powder will be prepared using whole pith, which includes entire cell walls as well as MP, it is expected to be a rich source of dietary fibre. Since there is no scientific literature on the therapeutic effects of mamaku, efforts are made in the following section to identify the possible benefits of

consuming mamaku by comparing it to other non-starch polysaccharide dietary fibres such as pectin, guar gum and cellulose, which are well-known for not being digested by humans.

2.4.1 Possible physiological effects

Dietary fibres can alter the physiology of GIT by: (i) changing the physical state of digesta leading to the alteration of the gastric transition time, and retarding physical processes governing digestion rate, such as mixing and diffusion; (ii) binding with enzymes and bile acids, thereby, hindering the digestion and absorption process; and (iii) acting as a substrate for fermentation in the colon (Brownlee, 2011; Capuano, 2017; Williams, Mikkelsen, Flanagan, & Gidley, 2019); (iv) contributing to hydrated faecal mass which is a stimulus for evacuation and distal transfer of fermentation. These physiological effects of dietary fibres are governed by their physicochemical properties such as hydration, solubility and viscosity (Edwards & Garcia, 2009; Guillon & Champ, 2000).

2.4.1.1 Physical structure of digesta

Dietary fibres can interact with digestive fluids and/or components of the food, thus contributing to the rheological properties of digesta. Viscosity development is the most investigated property. Dietary fibres can alter the viscosity either by solubilising in the liquid phase of the digesta or by affecting the physical properties of the digesta matter (Lentle & Janssen, 2008). Increased digesta viscosity in the stomach may change the flow behaviour and delay gastric emptying, hence, the rate of nutrients entering the small intestine may be delayed (Capuano, 2017). An increase in digesta viscosity is reported to reduce starch hydrolysis and glucose diffusion coefficient, which could lead to a decrease in postprandial blood glucose level (Dhital, Dolan, Stokes, & Gidley, 2014). Viscosity development will also influence the mixing process in the stomach, which may influence the particle size reduction rate, and therefore to some extent, may contribute to gastric emptying (Pera et al., 2002).

Chyme leaving the stomach is mixed with pancreatic juice and bile acids in the small intestine, and several enzymes are introduced to carry out digestion and facilitate absorption processes. As in the stomach, the mixing process in the small intestine may also be impeded, increasing the unstirred water layer, and leading to lowering enzymatic activity (Edwards & Garcia, 2009). The viscous chyme may delay the movement of enzymes to the substrate;

and/or may delay the diffusion of nutrients to the absorption site (Brownlee, 2011). However, the viscosity and absorption processes are not always interrelated. It was reported that during *in vitro* small intestine digestion of starch-guar gum mixtures, a decrease in the viscosity of digesta did not alter the rate of starch hydrolysis (Hardacre, Yap, Lentle, & Monro, 2015). Furthermore, the prolonged delay in the release and absorption of nutrients will trigger appetite-regulating hormonal feedback, which results in the inhibition of gastrointestinal mobility (ileal break), contributing to a delay in gastric emptying (Brownlee, 2011; Marciani et al., 2001).

2.4.1.2 Binding ability of dietary fibres

In addition to viscosity development in the small intestine, dietary fibres are reported to bind with bile acids and gastric enzymes which can also explain their physiological effects. Bile acids help in the emulsification of lipids and micelle formation essential for the absorption of lipids. Interaction of dietary fibres with bile acids can have significant consequences; primarily making the bile acids unavailable to act as surfactants, thus, hindering micelle formation and absorption of lipids into the body and consequently, lowering the level of blood lipids. More than 95% of the parental bile acids that do not participate in micelle formation are re-absorbed in the distal part of the small intestine. The bile acids bound to dietary fibres will escape re-absorption which facilitates elimination of bile acids in the faeces. This will reduce the bile acids pool in the body; thus, the liver will use endogenous cholesterol to replenish the pool, resulting in a reduction of the blood lipid levels (Brownlee, 2011; Capuano, 2017). For example, lignin has excellent bile acids absorption capacity due to the formation of hydrophobic interactions (Kosikova, Slamenova, Mikulasova, Horvathova, & Labaj, 2002). Chitosan can electrostatically interact with negatively charged bile acids at neutral pH (Thongngam & McClements, 2005). Other dietary fibres such as pectin, guar gum and β-glucan are reported to increase bile acids in faeces and lower cholesterol levels (Butt, Shahzadi, Sharif, & Nasir, 2007; Ellegard & Andersson, 2007; Theuwissen & Mensink, 2008), however, the actual mechanism is yet not fully understood, although effects of hydrocolloids on chyme viscosity may be accentuated in the terminal ileum as available food components are absorbed and soluble dietary fibres become concentrated.

Dietary fibres can directly interact with enzymes and inhibit their activity by: (i) altering the enzyme conformation due to bonding; or (ii) competing with the substrate for the active site of the enzyme (Capuano, 2017). Guar gum and pectin can form a complex with α-amylase and lipase, respectively, inhibiting their activity (Hardacre et al., 2015; Kumar & Chauhan, 2010). Alginate is reported to selectively inhibit pepsin but not trypsin, due to possible electrostatic interaction between positively charged pepsin and negatively charged alginate at acidic pH (Chater, Wilcox, Brownlee, & Pearson, 2015). Most of the studies advocating the binding effect of dietary fibres are conducted in a '*well-controlled clean environment*' using *in vitro* models where the purest form of the compounds of interest are set to interact with enzymes. However, the incorporation of dietary fibres in the food matrix may not result in a binding effect as the site for interaction may be occupied before the fibre reaches the GIT. Thus, on consuming a meal high in dietary fibre, reduction in bile acids and inhibition of enzyme activity is most likely to be due to the entrapment of molecules in the viscous matrix instead of interactions at the molecular level.

2.4.1.3 Gut microbiota fermentation

Food remnants that resist digestion in the small intestine reach the colon where some of them perform the very relevant role of being substrates for fermentation, leading to a shift in bacterial diversity and production of short-chain fatty acids (SCFAs). The unfermented material adds to faecal mass and hydration, which has its own influence on colonic processes (Monro, 2000, 2001; Monro et al., 2012). The human colon hosts a complex bacterial ecosystem with more than 1000 species of bacteria majorly belonging to phylum Firmicutes (58-88%), Bacteroidetes (8.5-28%), Proteobacteria (0.1-8%) and Actinobacteria (2.5-5%) (Williams, Grant, Gidley, & Mikkelsen, 2017). When dietary fibre enters the colon, different bacteria either from the same species or from different species use polysaccharide-digesting enzymes to hydrolyse it into simple sugars which will then be utilised for fermentation. Since a specific type of dietary fibre is normally fermented by a specific species of bacterium, it is expected that a high intake of one type of dietary fibre can improve the activity of specifically associated bacteria, thereby, changing the microbiota composition (Edwards & Garcia, 2009). In the absence of dietary fibres, the bacterial community will utilise large

intestinal mucus and then the underlying mucosa as a source of energy (Brownlee, 2011); hence, dietary fibres are necessary to maintain good colon health.

The fermentation of dietary fibres in the anaerobic environment of the colon produces several SCFAs, namely acetate, butyrate, propionate, valerate, isovalerate and isobutyrate, along with gases (carbon dioxide, hydrogen and methane) (Williams et al., 2017). The yield and proportion of the type of SCFAs produced during fermentation depend on the composition of the dietary fibre consumed. Pectin increases the production of acetate, and guar gum increases acetate and propionate while arabinoxylan yields more acetate and butyrate (Englyst & Hudson, 1987; Hughes et al., 2007; Hughes, Shewry, Gibson, McCleary, & Rastall, 2008). Acetate, butyrate and propionate are the principal SCFAs that are produced in large quantities and have significant effects on the host. The beneficial effects of SCFAs are summarised in **Table 2.5**. Butyrate is the primary energy source for the colon epithelial cells and is known for its anti-inflammatory and anti-carcinogenic effects (Canani et al., 2011; Hugenholtz, Mullaney, Kleerebezem, Smidt, & Rosendale, 2013). Associated with these effects, butyrate can increase the proliferation of intestine cells, promote colon healing post-injury and induce apoptosis in colon cancer cells (Fava, Lovegrove, Tuohy, & Gibson, 2009). Moreover, propionate is reported to improve glucose tolerance and satiety in the host (Arora, Sharma, & Frost, 2011; Williams et al., 2019). Some of these effects are also exhibited by other SCFAs, though less prominent, such as acetate and propionate which may also have some anti-inflammatory effects (Tedelind, Westberg, Kjerrulf, & Vidal, 2007).

Table 2.5: Biological actions associated with the production of major short-chain fatty acids (SCFAs) in the colon.

Biological action	Short-chain fatty acids (SCFAs)		
	Acetate	Butyrate	Propionate
Source of energy to brain, heart and muscles	+		+
Source of energy to colonocytes		+	
Decrease pH of the gut	+	+	+
Anti-carcinogenic effect		+	
Anti-inflammatory effect		+	
Lipid metabolism	+		+
Increased leptin production			+

Adapted from Hugenholtz et al. (2013) with data sourced from Fava et al. (2009) and Rosendale, Cookson, Roy, and Vetharaniam (2011)

2.4.2 Possible health benefits

Based on the above-discussed physiological effects of dietary fibres, the possible health benefits can be related to: (i) *body weight management*—implications for obesity; (ii) *regulating blood glucose*—implications for diabetes; (iii) *regulating blood lipid levels*—implications for CVD; and (iv) *colonic health* (**Figure 2.11**).

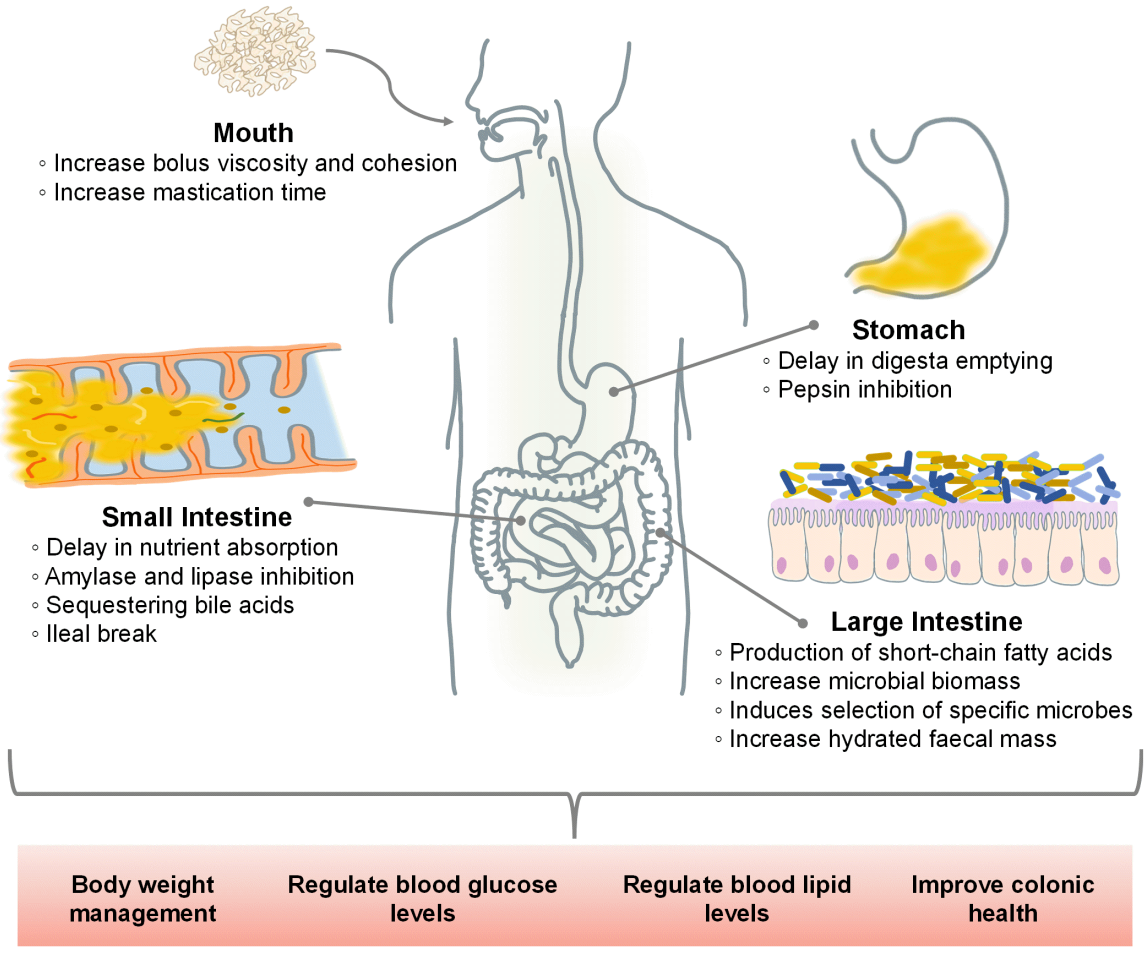


Figure 2.11: Overview of possible physiological effects and health benefits of mamaku.

A major cause of being overweight or obese is a poor energy balance, where energy intake exceeds energy expenditure by large. Energy intake can be limited by regulating the appetite in individuals. Several studies advocating the effectiveness of consuming dietary fibres for bodyweight management by controlling satiety are reported in the literature (Dreher, 2015;

Feskens et al., 2014; Kristensen & Jensen, 2011; Wang et al., 2007). Viscous dietary fibres can regulate satiety by: (i) increasing oral mastication time and inducing sensory-specific satiety; (ii) delaying gastric emptying; (iii) delaying the nutrient absorption in the small intestine (particularly postprandial glucose and insulin responses), which will signal the release of appetite-controlling hormones (such as CCK, cholecystokinin; GLP-1, glucagon-like peptide 1; and PYY, peptide YY); and (iv) producing SCFAs during fermentation in the colon, which can regulate the secretion of satiety hormones (such as GLP-1 and PYY) (Brownlee, 2011; Edwards & Garcia, 2009; Ho, Matia-Merino, & Huffman, 2015; Howarth, Saltzman, & Roberts, 2001). Prolonged consumption of dietary fibres may potentially be used to aid weight management however, their role in treating obesity is still controversial.

High glucose and insulin levels in the blood are the primary indicators of glucose intolerance, insulin resistance and type 2 diabetes (Edwards & Garcia, 2009). Dietary fibre consumption has been consistently shown to lower postprandial glucose levels. Consumption of pectin from soybean was reported to reduce the mean glucose incremental area under the curve (iAUC) by 13.2% in 15 healthy male subjects (Jones, 2015). Adding xanthan gum to cooked rice has been shown to suppress the glucose level in 11 healthy female subjects (Fuwa, Nakanishi, & Moritaka, 2016). Maki et al. (2008) reported that, in 50 healthy subjects, administration of hydroxypropylmethylcellulose (HPMC) and methylcellulose (MC) reduced iAUC ranging from 7-48% in a dose-dependent manner. A short delay in postprandial insulin has also been observed, which is consistent with a delay in glucose absorption. A similar glucose-lowering effect was observed in 30 participants with and without type 2 diabetes on consuming dietary fibre-fortified protein bars; however, no effect was observed on insulin levels (Bae, Kim, Min, Ahn, & Cho, 2018). The lowering of glucose and insulin level in blood after supplementation with dietary fibres is thought to be related to the following: (i) a delay in gastric emptying, as a result, the digesta is not quickly available for digestion and therefore absorption; (ii) binding/trapping of enzymes leading to inhibiting enzyme activity; (iii) a reduction in mixing or movement of nutrients in the small intestine; and (iv) the upregulation of GLP-1 hormone by SCFAs which suppresses glucagon secretion along with suppressing appetite (Capuano, 2017; Cassidy, McSorley, & Allsopp, 2018; Lovegrove et al., 2017).

The hypocholesterolaemia effect of soluble dietary fibre has also been well-reported and agreed upon for several years (Rideout, Harding, Jones, & Fan, 2008; Soliman, 2019; Surampudi, Enkhmaa, Anuurad, & Berglund, 2016). Consumption of oat β-glucan (6 g/day for 6 weeks) by hypercholesterolemic subjects has been shown to reduce the total and low-density lipoprotein (LDL) cholesterol by 0.3 mmol/l from baseline in comparison to control (Queenan et al., 2007). Supplementation with arabinoxylan (15 g/day for 6 weeks) in obese and impaired glucose tolerance subjects resulted in lowering postprandial responses in serum glucose, insulin and triglycerides when compared with control (Garcia et al., 2007). The main cause for the reduction in blood lipid levels on supplementation with dietary fibres, in addition to the viscosity and fermentation effect of digesta, is thought to be related to the hindrance in re-absorption of the parental bile acids in the small intestine, resulting in utilising the stored cholesterol for synthesising new bile acids (Brownlee, 2011; Madar & Stark, 1995).

Lastly, dietary fibres play a key role in improving colon health. As discussed earlier, the colon is the main site for the action of dietary fibres where they can ferment. Dietary fibres can function as prebiotics and promote the growth of specific beneficial bacteria. The production of SCFAs can have anti-inflammatory and anti-carcinogenic effects in the colon but also can stimulate the secretion of different hormones which affects the body as a whole. For instance, colon fermentation may indirectly regulate the secretion of hormones from the pancreas and adipose tissues which can regulate energy metabolism (Nilsson, Ostman, Holst, & Björck, 2008). Some dietary fibres may not be able to ferment in the colon but may still be beneficial in protection against disorders such as colorectal cancer by improving bowel movement and stool quality through their hydrating and lubricating effects.

2.5 Gaps in the Literature

Based on the literature review presented above, it is clear that there is limited information available on mamaku, when dealing with its preparation as a food ingredient—targeting the effects of processing—as well as its functionality regarding possible health benefits in human. To be specific, currently, there are only ten scientific publications, mostly revolving around the rheology and structure analysis of mamaku gum and no published information on the use of mamaku pith. In order to bridge the knowledge gap between the fundamental

understanding of mamaku and its industrial applications, the following research areas of interest—leading this thesis—have been identified:

- Environmental factors such as geographical location, soil conditions and harvesting season, and harvesting age of plants can affect the structure of the extracted biomacromolecule, however, they are mostly ignored. The effects of these factors on the structure and rheology of mamaku gum are currently unknown.
- During industrial processing, the polymers may be subjected to varying conditions such as changes in pH and salts, and high temperature and shear, which can adversely affect their functionality. In general, the effects of pH, salts and certain aspects of temperature sensitivity have been studied for mamaku, but the understanding of exposure to high shear is limited.
- Different drying methods can have a significant effect on the physicochemical properties and rehydration behaviour of the powders. Though the effects on the physicochemical properties of dried plant material are reported in the literature, the rehydration behaviour of whole plant powders is poorly understood. There is no available information on mamaku powder.
- Food matrixes are commonly used to deliver 'functional' powder ingredients to the gut, but the selection of an appropriate delivery medium is important to achieve the intended functionality in humans. Mamaku has not yet been incorporated into any food matrixes.
- There are two studies describing the physiological effect of fresh mamaku gum on delaying gastric emptying, one *ex vivo* rat, the other *in vivo* rat. However, a wider understanding of the effects of mamaku gum on gut health including the rate of digestion, enzyme activity, growth of colon bacteria and SCFAs production is required.
- Mamaku has been traditionally used for several therapeutic benefits, but there is no human intervention study to establish the health benefits of consuming mamaku, and its effectiveness *in vivo* compared with other well-characterised dietary fibres.

Chapter 3

Experimental techniques

3.1 Processing of Mamaku Fronds

Mamaku fronds (~1,000 kg) were harvested from a farm in Waverley, Taranaki region of New Zealand between the 10th and 30th of October 2020, following local traditional practices (**Appendix A**). During harvesting, the leaves on the fronds were removed and the fronds were chopped into manageable lengths (~50 cm). The surface of the chopped fronds was cleaned by submerging them in hydrogen peroxide (~2% w/w) for 1 min and then washed with fresh water. The chopped fronds were packed in plastic bags, transported to the Pilot Plant at Massey University, Palmerston North, stored at refrigerated conditions (4°C) and processed within three days from harvesting (**Figure 3.1**).



Figure 3.1: Pictures from the field during the harvesting of mamaku fronds.

3.1.1 Extraction of mamaku gum

The harvested fronds were mulched (Crushing shredder, Ryobi, Fuchu, Japan) and mixed with an equal amount of water (w/w) at 4°C for ~24 h. The soaked fronds (along with water) were blended in a wet disintegrator (for 5 min, Jeffco, Dry Creek, Kilburn, Australia), followed by heating the mixture in a steam-jacketed pan (~55°C for 5 min) with continuous stirring. The heated mixture was then transferred into mesh bags, sealed and pressed to recover the liquid portion using a wine press. The water-soluble crude gum extract was collected (**Figure 3.2**). The left-over pulp was reheated in water, and the extract was collected until no visual viscous consistency of the flowing liquid was observed. This was repeated an average of 3-5 cycles. The pooled extracts were left undisturbed overnight at 4°C for the remnants of pulp to sediment by gravity followed by separating the clearer top layer using a siphon. The collected *'crude gum extract'* was either freeze-died or concentrated using a vacuum evaporator (temperature between 50-57°C and pressure between 70-55 mbar, BÜCHI Labortechnik AG, Flawil, Switzerland) and stored at -18°C until use.

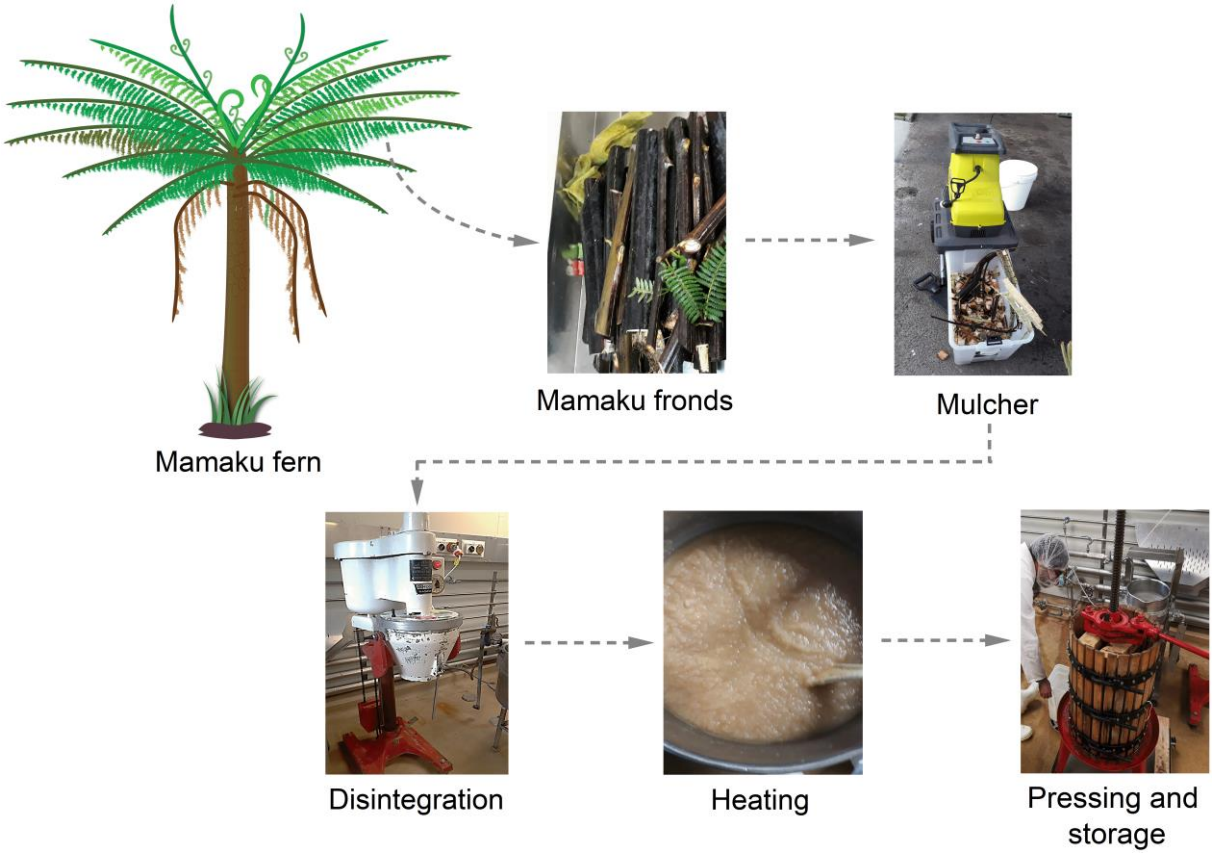


Figure 3.2: Processing of mamaku fern to obtain crude gum extract.

3.1.2 Production of mamaku pith powder

The harvested fronds were peeled with a sharp knife to remove the external rind. This yielded ~40% (w/w) of pith, which was cut into slices (~0.5-1 cm in thickness). The sliced pith was transferred on aluminium trays in a single layer and dried using either a freeze-dryer or an oven-dryer (**Figure 3.3**). For freeze-drying, the sample trays were stored at -15°C overnight and then loaded into a freeze-dryer (FD18ISLA, Cuddon Freeze Dry, Blenheim, New Zealand). The temperature of the freeze-dryer was reduced to -35°C and held for 2 h. The primary drying was initiated by reducing the pressure in the chamber to 1.8 mbar and gradually increasing the chamber temperature from -35°C to 20°C in 4 h. The temperature and pressure of the chamber were maintained at 20°C and 1.8 mbar until the secondary drying was completed (about 40 h). For oven-drying, the sample trays were exposed to continuous circulating air at ~50°C for about 30-35 h in an oven-drier (Inoxtrend, Treviso, Italy). Both freeze-drying and oven-drying were terminated once the final moisture content of the pith was reduced to ~5%. This yielded ~9.5% (w/w) dried pith from sliced fresh pith.

The dried pith was ground using a hammer mill (Siemens-Schuckert, Germany) or a pin mill (Grain Tech Engineering Ltd., Auckland, New Zealand) or a coffee grinder (Breville, Australia). Three different types of equipment were used to obtain powders of different size fractions [d(0.5) of 181.8±23.14 μm, 105.5±0.5 μm, and 48.45±0.35 μm for freeze-dried pith powders and 171±11 μm, 104.75±9.7 μm and 97±0.35 μm for oven-dried pith powders using a hammer mill, a pin mill and a coffee grinder respectively (**Figure 3.4**)]. Since the d(0.5) values were similar for freeze-dried (105.5±0.5 μm) and oven-dried (104.75±9.7 μm) pith powders produced using a pin mill, these powders were used in further studies comparing the two drying methods. The powder was stored in sealed aluminium bags until use.

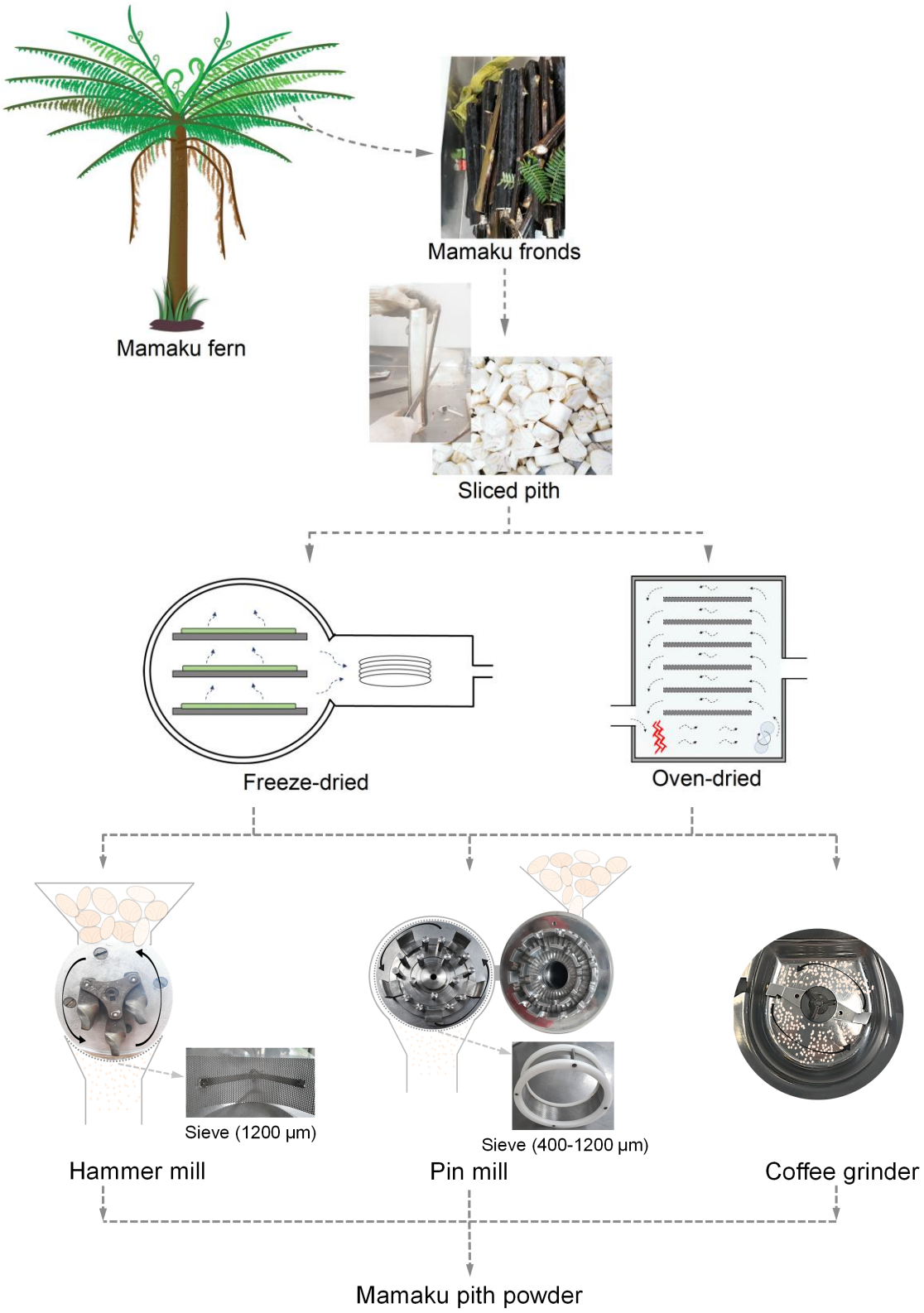


Figure 3.3: Processing of mamaku fern to obtain pith powder.

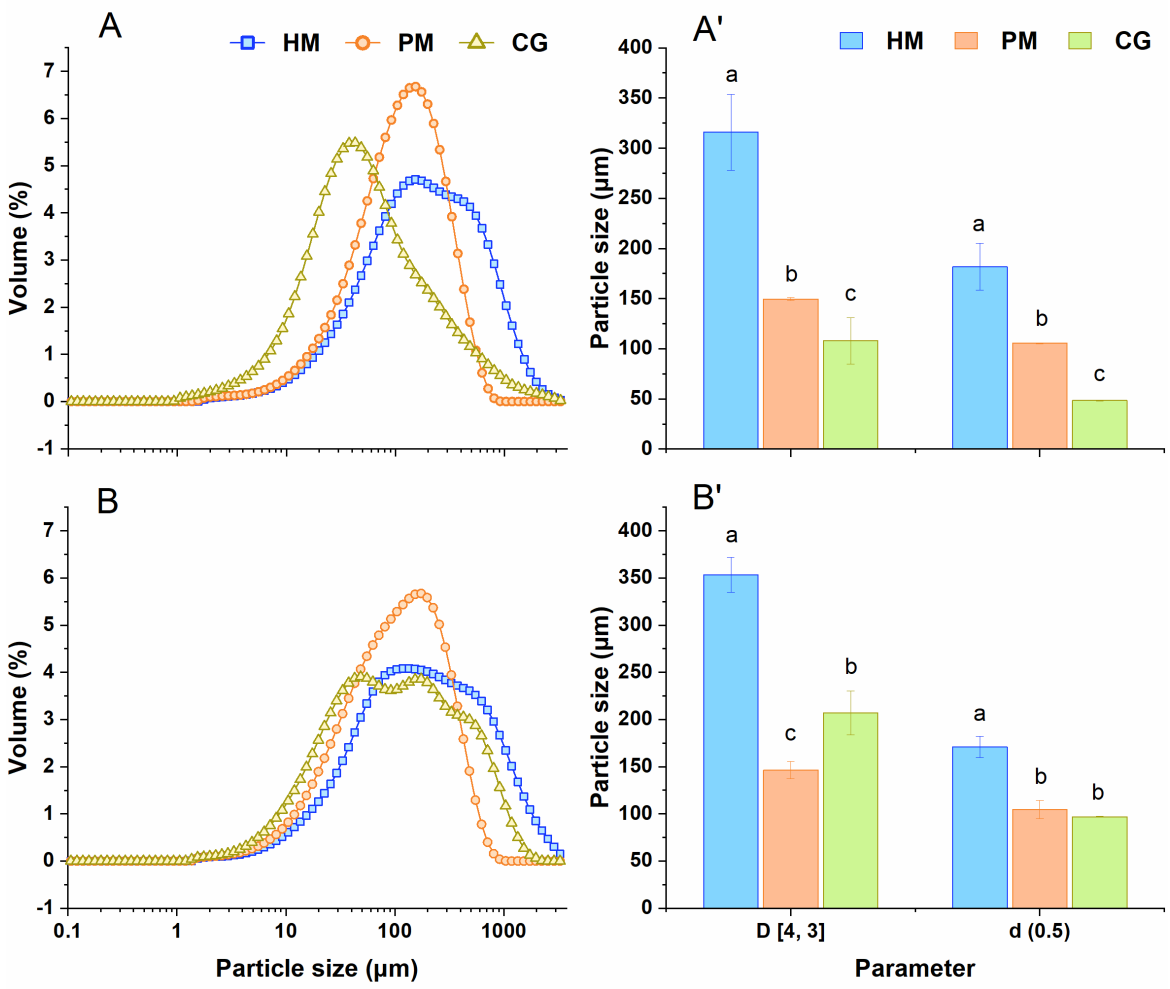


Figure 3.4: Particle size distribution of (**A**, **A'**) freeze-dried and (**B**, **B'**) oven-dried mamaku pith powder (dry powder) ground using a hammer mill (HM), pin mill (PM) and coffee grinder (CG). Values are plotted as means ± standard deviation (n=3). Values with the different superscripts are significantly different ($p \leq 0.05$) for a given parameter.

3.2 Polysaccharide Characterisation

The mamaku polysaccharide (MP) was characterised using a combination of techniques such as constituent sugar composition, nuclear magnetic resonance (NMR), size-exclusion chromatography coupled with multi-angle laser light scattering (SEC-MALLS), and Zetasizer, as described below.

3.2.1 Constituent sugar composition

A polysaccharide is an assembly of multiple sugar units linked together by various α or β glycosidic bonds. The analysis of constituent sugar units that make up the polysaccharide is generally initiated with hydrolysis (**Figure 3.5**). Hydrolysis can be performed using acids

such as sulfuric (H_2SO_4), hydrochloric (HCl) or trifluoroacetic (TFA) but the type of acid used can affect the yield of constituent sugar units (monosaccharides) (Panagiotopoulos & Sempéré, 2005). A two-step mild hydrolysis involving methanolic HCl hydrolysis preceding TFA hydrolysis was used for hydrolysing MP as it can result in complete hydrolysis with the minimum decomposition of liberated monosaccharides (De Ruiter, Schols, Voragen, & Rombouts, 1992). The hydrolysis step releases a pool of individual monosaccharides that were subsequently quantified using high-performance anion-exchange chromatography (HPAEC) as it enables direct chromatographic separation of sugars without derivatisation. For HPAEC, neutral sugars (uncharged) are partially ionised to weak acids (negative charge) at high pH (> 12) and thus can be separated as anions. The more acidic the sugars are more tightly bound to the column, therefore, delaying the elution (Corradini, Cavazza, & Bignardi, 2012; Rohrer, 2021). The difference in eluting time was used to identify different sugars which were then quantified using calibration curves.

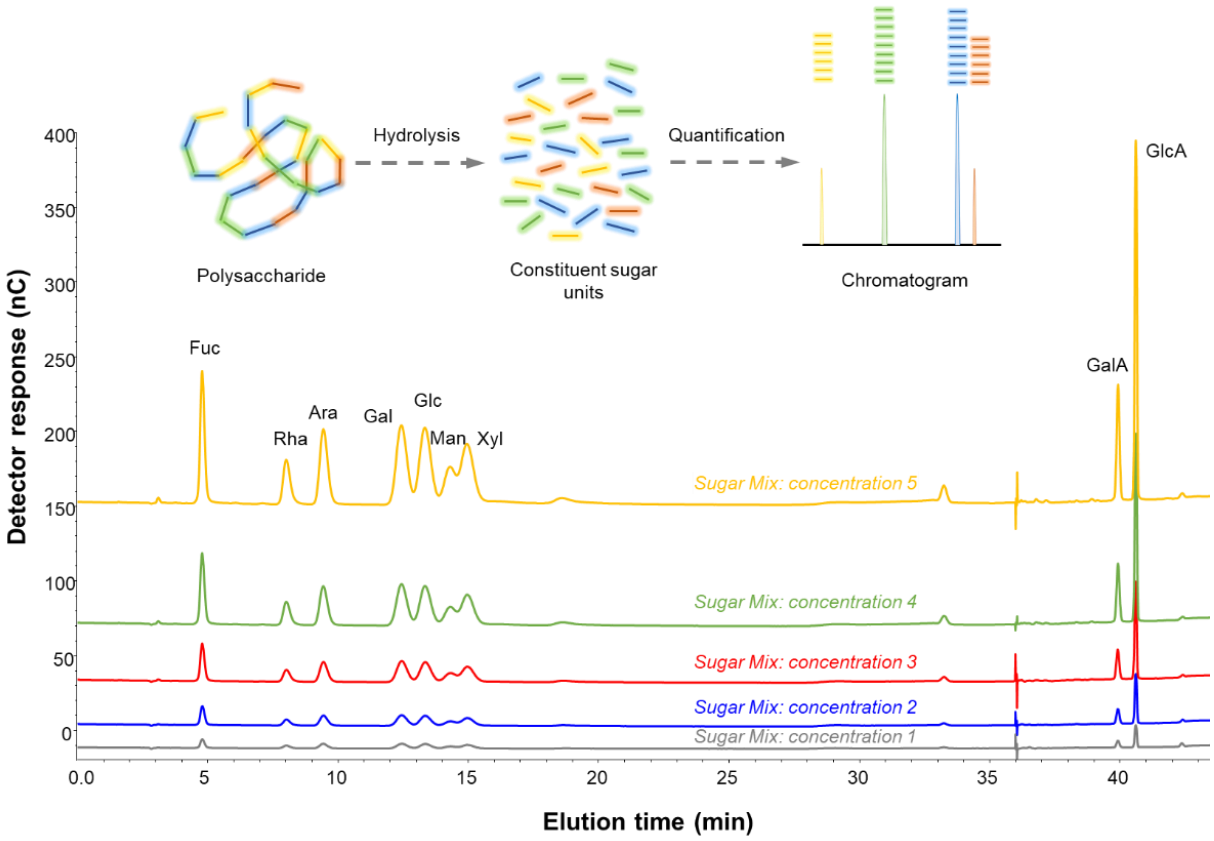


Figure 3.5: Schematic illustration of constituent sugar composition analysis with elution time for different sugars at different concentrations. Fuc, Fucose; Rha, Rhamnose; Ara, Arabinose; Gal, Galactose; Glc, Glucose; Man, Mannose; Xyl, Xylose; GalA, Galacturonic acid; GlcA, Glucuronic acid.

3.2.2 Colorimetric quantification of uronic acid

MP is considered to have a backbone composed of repeating units of glucuronic acid and mannose. Quantifying the amount of glucuronic acid in the solution can indicate the amount of MP in the solution. Glucuronic acid content was quantified spectrophotometrically as described by Blumenkrantz and Asboe-Hansen (1973). In this method, the MP was hydrolysed in concentrated H_2SO_4 and sodium tetraborate solution at high temperatures to obtain free glucuronic acid. Glucuronic acid reacts with H_2SO_4 to produce 5-formyl-2-furancarboxylic acid (5FF). Neutral hexoses and pentoses released at the same time as glucuronic acid produces 5-hydroxymethyl-2-furancarboxaldehyde and 2-furancarboxaldehyde, respectively, on reacting with H_2SO_4 (Scott, 1979). The addition of borate during hydrolysis increases the rate of 5FF formation. A colorimetric reagent *i.e.*, *m*-hydroxydiphenyl (3-phenylphenol) specific to 5FF was added and the developed pink coloured was measured using UV/Vs spectrophotometer at λ_{520} nm.

3.2.3 Nuclear magnetic resonance spectroscopy

Nuclear magnetic resonance (NMR) spectroscopy is used to determine the molecular structure at the atomic level. It helps to map the chemical environment of nuclei in the molecule. The fundamental concept of NMR is that the atomic nuclei are positively charged and any charged body in movement generates a magnetic field. Many kinds of nuclei can spin about an axis (*i.e.*, are spin-active nuclei[14]) and thus, generate their own magnetic field and behave like a tiny magnetic bar. When spin-active nuclei (oriented randomly) are placed in the strong external magnetic field the nuclei adopt a specific orientation, just as a compass needle to earth's magnetic field. The nuclei can orient so that their own magnetic field aligns to (parallel spin) or against (antiparallel spin) the external magnetic field. The former orientation has slightly lower energy, making it slightly more favoured than the latter. The oriented nuclei can now be exposed to radiation (radio frequency) providing energy equivalent to the energy difference (ΔE) between two orientation spins, energy absorption occurs, and nuclei are shifted from low-energy spin state to higher-energy spin state (*spin-flip*) (**Figure 3.6**). The exact frequency necessary for the resonance depends both on the strength of the external magnetic field and the identity of the nuclei. If a very strong

[14] Magnetic properties are common for all nuclei with an odd number of protons (*e.g.*, ^{1}H, ^{2}H, ^{14}N, ^{19}F and ^{31}P) or neutrons (*e.g.*, ^{13}C) but for nuclei with even number of both protons and neutrons (*e.g.*, ^{12}C and ^{16}O).

magnetic field is applied, the energy difference between the two spin states is large and higher-frequency (higher energy) radiation is required for a spin-flip. The frequency of radiation that is absorbed by the nuclei is expressed as a *chemical shift*[15] (δ, ppm) and appears as a peak in the NMR spectra (McMurry, 2008).

Polysaccharides have abundant hydrogen and carbon atoms, thus ^{1}H and ^{13}C NMR are commonly used for their structural analysis (Nep et al., 2016). Polysaccharides such as MP have a high molecular weight and consequently viscosity which leads to broad resonances in NMR spectra. Higher temperatures and higher magnetic fields help produce better-resolved spectra (Cheng & Neiss, 2012). ^{1}H and ^{13}C NMR spectra of MP were obtained on a Bruker Avance Neo 700 MHz NMR spectrometer (Bruker BioSpin, Rheinstetten, Germany) at 65°C and interpreted by comparing the chemical shift values with the literature.

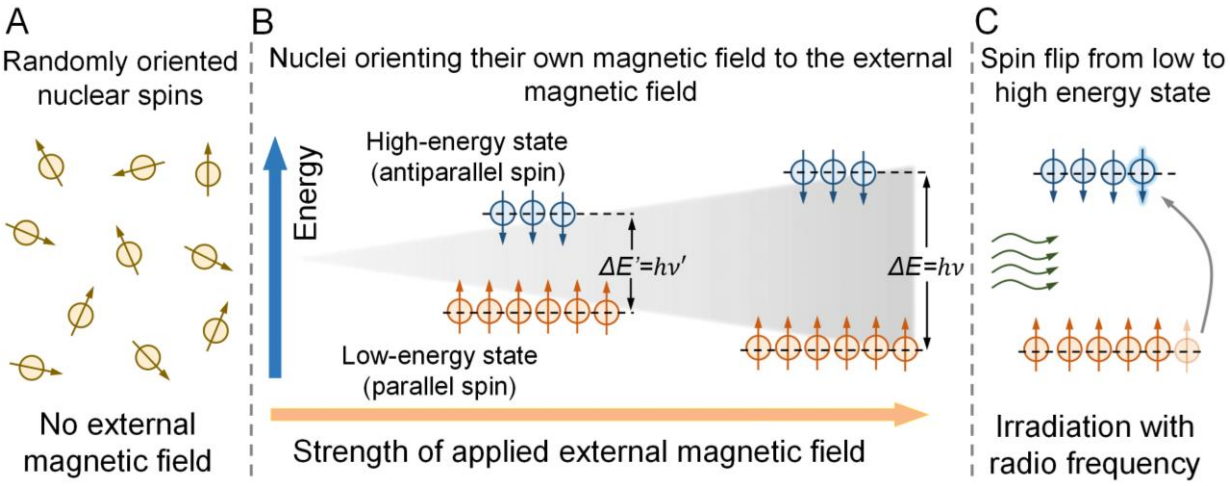


Figure 3.6: (**A**) Nuclear spins are oriented randomly in the absence of an external magnetic field but (**B**) on applying an external field the nuclei orient their own magnetic field to low and high energy states. The energy difference between the two states increases with increasing the strength of the applied magnetic field. (**C**) Irradiating the oriented nuclei with radio frequency cause the low-energy state 'spin-flip' to the higher-energy state.

[15] The resonant frequency of an atomic nucleus relative to a standard in a magnetic field.

3.2.4 Size-exclusion chromatography coupled with multi-angle laser light scattering

The molecular weight, size and conformation of MP were determined using size-exclusion chromatography coupled with multi-angle laser light scattering (SEC-MALLS). Size-exclusion chromatography (SEC) is a technique that separates the polysaccharide based on the size (hydrodynamic) when passed through the columns packed with porous particles (**Figure 3.7A**). The mobile phase carries polysaccharides of different sizes and the polysaccharides that are larger than the column pores will not have access to pores as a result will be eluted first. The smallest size polysaccharide will access all pores and will travel a longer distance, so eluted last. The polysaccharide of intermediate size will have partial access to pores and will be eluted in between. Columns of different sizes can be combined to get a better separation if needed.

The polysaccharide separated into different size fractions in SEC subsequently enters the multi-angle laser light scattering (MALLS) detector that employs the static light scattering technique for characterisation (**Figure 3.7B**). The advantage of MALLS is that it does not require calibration against standards of known size and no assumption is made about the molecular conformation (Philip, 2003).

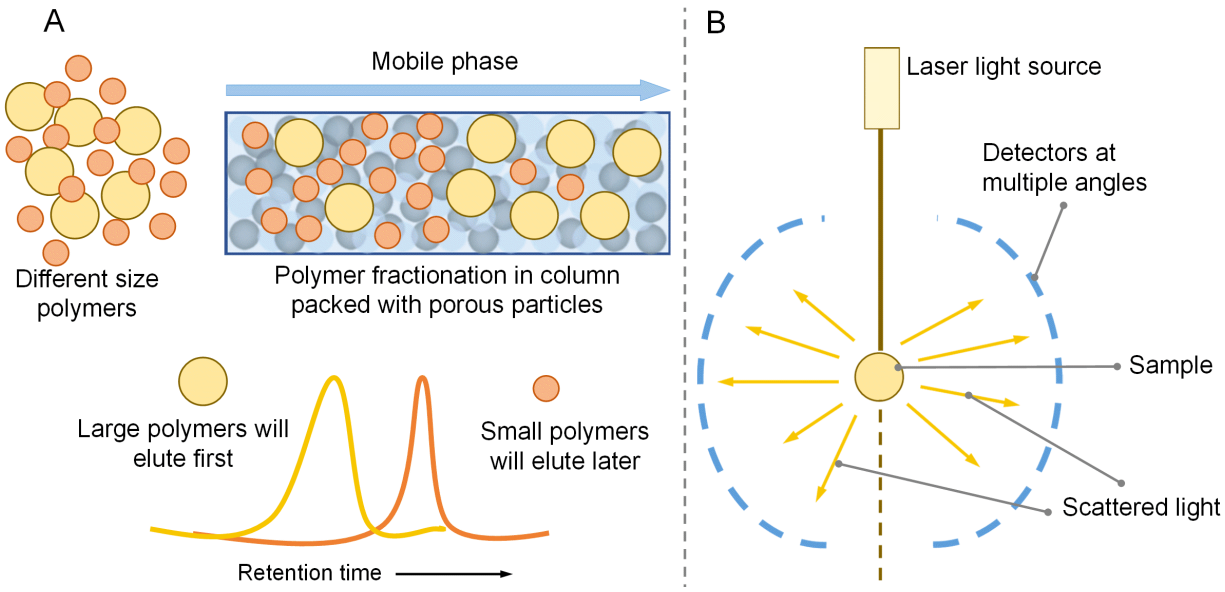


Figure 3.7: Schematic illustration of (**A**) size-exclusion chromatography (SEC) of polymers of different molecular sizes and (**B**) multi-angle laser light scattering (MALLS) detector.

Fundamentally, when monochromatic laser light is passed through the polysaccharide solution, some of the light is scattered from its original direction. The amount of light scattered is directly proportional to the molecular weight and solute concentration (assuming no absorption by the polysaccharide). Furthermore, the angular variation of scattered light is directly related to the size of the molecule. This can be embodied in the Rayleigh-Debye-Gans model as follows:

$$\left(\frac{Kc}{R_\theta}\right) = \frac{1}{M_i}\left(1 + \frac{16\pi^2}{3\lambda^2}\ \langle r_g^2\rangle_i\ sin^2\left(\frac{\theta}{2}\right) - \ 2A_2M_ic_i\ \right) \qquad \textbf{Equation 3.1}$$

where, K is the optical constant, R_θ is the Rayleigh excess scattering or excess intensity of scattered light at angle θ (*i.e.*, intensity due to solute), λ is the wavelength of the incident laser beam (632.8 nm), A_2 is the second viral coefficient (assumes to be 0 due to the low concentration), $\langle r_g^2\rangle_i$ is the mean square radius, M_i is molecular weight and c_i is the sample concentration of the i^{th} slice.

MALLS measure the intensity of scattered light at multiple angles (typically between 15-160°) while the concentration is measured using a separate differential reflective index (DRI) detector. Then using different fitting models namely Zimm, Debye and Berry, based on **Equation 3.1**, plots of $sin^2\left(\frac{\theta}{2}\right)$ against $\frac{Kc}{R_\theta}$ or $\frac{R_\theta}{Kc}$ or $\sqrt{\frac{Kc}{R_\theta}}$, respectively, can be generated. The intercept of the plot *via* extrapolation to zero degrees angle and zero concentration is used to determine the molecular weight (M_i). Polysaccharides commonly consist of a mixture of chains with different numbers of monomer units, so molecular weight is often expressed as an average value. In this thesis, molecular weight is expressed as a *weighted-average molecular weight* (M_w) as it is most commonly used for polysaccharides:

$$M_w = \frac{\sum(c_iM_i)}{\sum c_i} \qquad \textbf{Equation 3.2}$$

where, c_i is the sample concentration and M_i is the molecular weight of the i^{th} slice.

The spread of molecular weight distribution is given by the *polydispersity index*. It is calculated by the ratio of M_w/M_n where M_n is the number-average molecular weight ($M_n = \frac{\sum c_i}{\sum c_i/M_i}$). Generally, for polysaccharides polydispersity index is between 1.5 to 2 (Wang & Cui, 2005).

Furthermore, the slope of the fitted plot gives the mean square radius ($\langle r_g^2 \rangle_i$). The mean square radius is defined as "*the distance from the centre of mass of the body at which the whole mass could be concentrated without changing its moment of rotational inertia about an axis through the centre of mass*" (Rudin, 1998). It is given as the sum of all the intramolecular distances in the polymer from the centre of the mass. The mean square radius is presented as the root-mean-square (RMS, $\sqrt{\langle r_g^2 \rangle_i}$) radius and is called the *radius of gyration* (R_g).

The conformation of a polysaccharide can be deduced from the M_w dependency of R_g and can be described by the power-law behaviour:

$$R_g = KM_w^v \qquad \textbf{Equation 3.3}$$

where, K and v are the intercept and slope from the log-log plot of R_g as a function of M_w, respectively. The slope values of ~0.33, ~0.6 and ~1 correspond to the spherical, random coil and stiff rod-like molecular shapes, respectively (Morris, Adams, & Harding, 2014).

3.2.5 Dynamic light scattering (Zetasizer)

The size of MP can also be measured using a Zetasizer which is based on the principle of dynamic light scattering. Dynamic light scattering measures the speed at which the molecules/particles suspended in liquid are diffusing due to the Brownian motion[16] and relates it to the size of the particle. The instrument illuminates the particles with laser light and analyses the time-dependent fluctuation in the intensity of the scattered light at a fixed angle. The fluctuation in the intensity of the scattered light is dependent on the rate of diffusion of particles. The small particles can diffuse faster and cause rapid fluctuation in the intensity of scattered light, and *vice versa* (**Figure 3.8**) (Lim, Yeap, Che, & Low, 2013). The size of the particle is calculated from the diffusion coefficient by using the Stokes-Einstein equation:

$$d(H) = \frac{kT}{3\pi\eta D} \qquad \textbf{Equation 3.4}$$

where, $d(H)$ is hydrodynamic diameter, k is Boltzmann's constant ($1.38064852 \times 10^{-23}$ J/K), T is absolute temperature, η is the viscosity of suspending liquid and D is diffusion coefficient.

[16] The random movement of particles due to the bombardment by the solvent molecule that surrounds them.

The fluctuation in the light intensity over time is used by the instrument to determine the rate of fluctuation which is used to determine the weighted mean particle size, known as the *Z-average size*. The Z-average size of the particle is described as the size of a sphere that diffuses at the same rate as the particle being measured ('the equivalent sphere theory'). Currently, the dynamic light scattering technique can measure particles in the range of 0.3 nm to 5 µm (Malvern Panalytical Ltd., 2023).

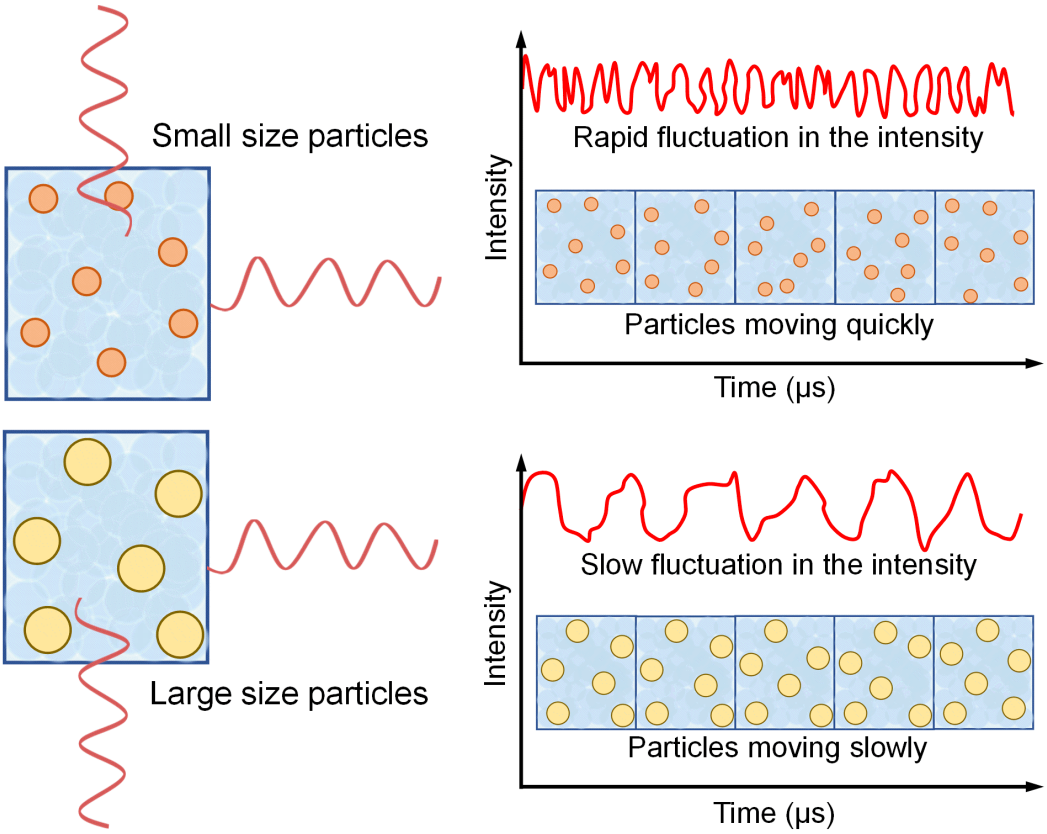


Figure 3.8: Movement of particles and intensity fluctuation over time for small and large particles.

3.3 Powder Particle Characterisation

The mamaku pith powders were prepared after drying the fresh mamaku pith using a freeze-dryer or oven-dried. The resulting powders were characterised for density, rehydration behaviour in water, particle size and surface morphology. The former two were explained in **Chapter 2**. The following section discusses the powder particle size measurements using laser diffraction and surface morphology using scanning electron microscopy (SEM).

3.3.1 Powder particle size

The size of powder particles was determined using low-angle laser light scattering (LALLS) known as laser diffraction. In principle, the angular variation of scattered light is related to the size of the particle. Large-size particles scatter the light more intensely mainly in the forward direction, *i.e.*, at a small angle. In contrast, the small-size particles scatter light at wider angles, but this scattered light has a much lower intensity that the forward scattered light (**Figure 3.9**) (Tekade, 2018). The difference in the angular scattering intensity is used to determine the particle size (the scattering angle is inversely proportional to the particle size).

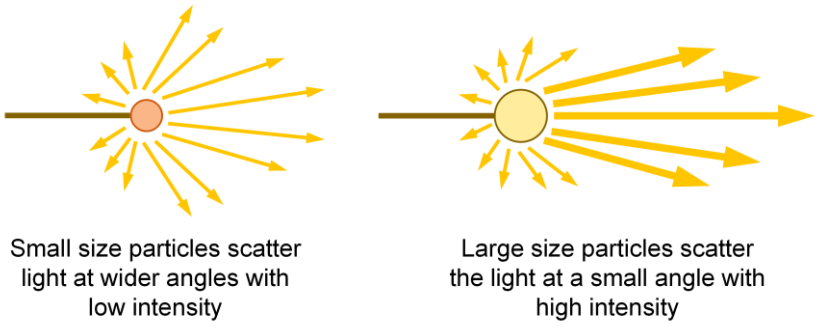


Figure 3.9: Influence of particle size on the angle and the intensity of scattered light.

Mie theory of light scattering is used to calculate the particle-size distribution. This theory assumes that (i) the particles being measured are spherical, (ii) the suspension is dilute so that the light is scattered by an individual particle, (iii) particles with varying optical properties will scatter light differently and (iv) the particles are homogeneous. The differences in refractive indices of particles and their dispersing medium are used to calculate the intensity of the scattered light. During measurement, red (λ = 633 nm) and blue leaser (λ = 466 nm) light sources are used. The latter helps to detect very small signals produced from sub-micron particles, improving the resolution. This allows the detection of particle size over a wide range from 0.1 to 3000 μm (Malvern Panalytical Ltd., 2020). This technique can be used for measuring the size of wet or dry systems *i.e.*, powder dispersed in water or not. Once the powder particles come in contact with water the powder starts to hydrate and the particle size changes. In this thesis, the size of mamaku pith powder was determined using the dry system and the changes during hydration were monitored using the wet system.

3.3.2 Scanning electron microscopy

Scanning electron microscopy (SEM) is a powerful technique to examine the surface of a sample. This technique uses a focused beam of high-energy electrons bombarded on the sample. The electron beam interacts with the sample and dissipates energy, generating secondary electrons[17], backscattered electrons[18], and heat. Secondary electrons (closer to the surface, ~5-50 nm) are most valuable for revealing the morphology and topography of samples. Backscattered electrons (from the deeper depth) help with the contrasts in samples. The obtained images can be magnified from 20X to approximately 30,000X which can show detail down to 25 Angstroms, or better.

3.4 Rheological Characterisation

In this thesis, the rheological behaviour of MP and hydrated mamaku pith powders was characterised using shear and/or extensional rheology methods. As names suggest, during shear rheology, the sample is subjected to shear deformation, causing it to rotate or oscillate, while during extensional rheology the sample is subjected to elongational deformation so molecules can stretch, possibly to full extension. The type of method used for characterisation can reveal different properties of the material, as discussed below.

3.4.1 Shear rheology

3.4.1.1 Rotational shear rheology

When the fluid flows, the molecules generate a frictional force that resists flow. This resistance to flow is called *viscosity*. Shear viscosity (η_s) is defined as the ratio of shear stress (τ) to shear rate ($\dot{\gamma}$):

$$\eta_s = \frac{\tau}{\dot{\gamma}} \qquad \textbf{Equation 3.5}$$

Shear stress and shear rate are commonly described using the two-parallel-plate model, where the fluid is placed between a moving top plate and stationary bottom plate separated by a distance, h (**Figure 3.10**). The fluid is sheared by applying a force, F, on the top plate of area A resulting in a velocity v. Shear stress (τ) is defined as the force over the area (**Equation**

[17] The energy from the electron beam is transferred to the specimen atom which leads to a potential expulsion of an electron from that same atom.

[18] The electron beam interacts with the electric field of the nucleus of a specimen atom, resulting in a change in direction of the electron beam without a significant change in the energy of the electron beam. If the scattered beam electron is deflected back out of the specimen, the electron is termed a backscattered electron.

3.6) while shear rate ($\dot{\gamma}$) is the resulting velocity over the distance between the plates (Equation 3.7).

$$\tau = \frac{F}{A} \qquad \text{Equation 3.6}$$

$$\dot{\gamma} = \frac{v}{h} \qquad \text{Equation 3.7}$$

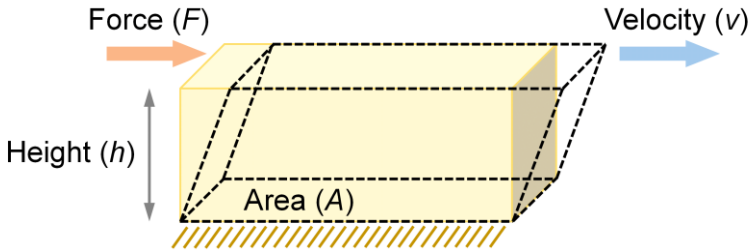


Figure 3.10: Flow of fluid between two parallel plates on applying force.

As evident from Equation 3.5, η_s of a fluid is dependent on the applied $\dot{\gamma}$, therefore it is apparent viscosity. If the η_s of the fluid is constant (independent of shear stress, shear rate and time) at a given temperature, then the fluid is called Newtonian. However, for most polysaccharide solutions the η_s is shear-dependent above certain concentrations, making them non-Newtonian fluids. The η_s of non-Newtonian fluids can decrease or increase with shear and the fluids are termed as shear-thinning or shear-thickening, respectively. The flow behaviour exhibited by a fluid is helpful to understand the molecular structure and the interactions between molecules. For example, shear-thinning behaviour is usually due to bond breakdown, while shear-thickening is attributed to associations upon shear.

Flow curve measurements were performed using a Paar Physica MCR 302 rheometer (Anton-Paar, Graz, Austria) in controlled shear rate (CSR) mode at 20°C. Measuring the unusual rheological properties of mamaku gum was challenging as sample expulsion was observed with cone-and-plate and plate-and-plate geometry even at low shear of 10 s^{-1}. Using the plate with a serrated texture did not appear to control expulsion (Figure 3.11). The contact between geometry and plate in both cases was rapidly changing, the results were considered invalid, as it was difficult to conclude whether the changes are because of the shear-induced transition or because of mechanical instabilities. The use of cup-and-bob geometry caused the rod climbing effect but was only significant at comparably high shear rates (above 50 s^{-1}). Furthermore, given the large contact area in the cup-and-bob geometry,

the small sample expulsion is less likely to affect the viscosity values in the range of the shear rate of interest (1-10 s^{-1}).

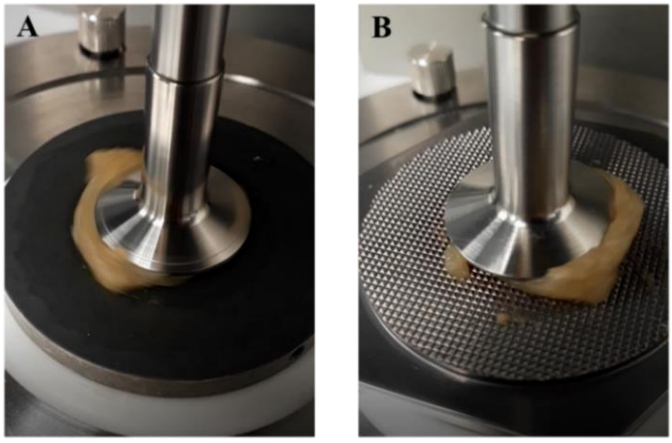


Figure 3.11: Sample expulsion observed for freeze-dried mamaku pith powder hydrated (2% w/w) overnight during viscosity measurement using plate-and-plate (**A**: smooth plate and **B**: serrated plate) at approximately 25 s^{-1}.

In addition to sample expulsion, sedimentation of the insoluble particles (from mamaku pith powder) during viscosity measurements at the low shear rates was another challenge—given the fact that high shears would keep any particle in suspension. The particle sedimentation was monitored for overnight hydrated powder samples by measuring transmittance and backscattering continuously after every 30 sec for 30 min using a Turbiscan (Formulaction Turbiscan LAB, Toulouse, France) at 25°C. Based on the collected data, the likeliness of sedimentation in hydrated mamaku pith powders dried using freeze-drier and oven-drier is shown in **Figure 3.12**. In order to quantify the time until no significant change in the system was observed, the Turbiscan Stability Index (TSI) scale was used and the time at which TSI equals 0.5 was calculated. For hydrated mamaku pith powder samples dried using freeze-drier and oven-drier, the time for TSI=0.5 was about 14 min and 9 min, respectively, indicating that viscosity measurements made before this time are likely to be free from any sedimentation effect. Furthermore, the rheological profiles generated using cup-and-bob geometry and vane geometry were comparable (**Figure 3.13**), eliminating the possibility of any sedimentation effects. In conclusion, due to: (i) more stable results at low shear, (ii) more

reproducible results and (iii) less sample volume required, cup-and-bob geometry was preferred over vane geometry.

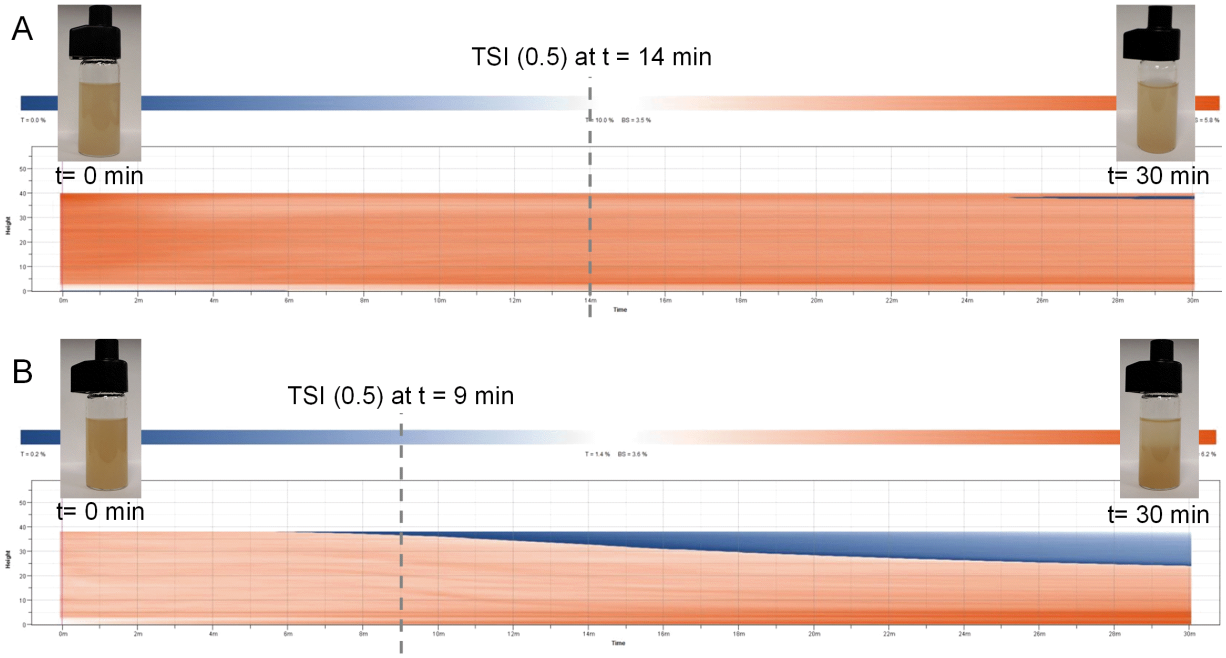


Figure 3.12: Sedimentation over 30 min at 25°C for (**A**) freeze-dried (0.75% w/w) and (**B**) oven-dried (1% w/w) mamaku pith powders hydrated overnight. Turbiscan Stability Index (TSI) at 0.5 is marked for both samples.

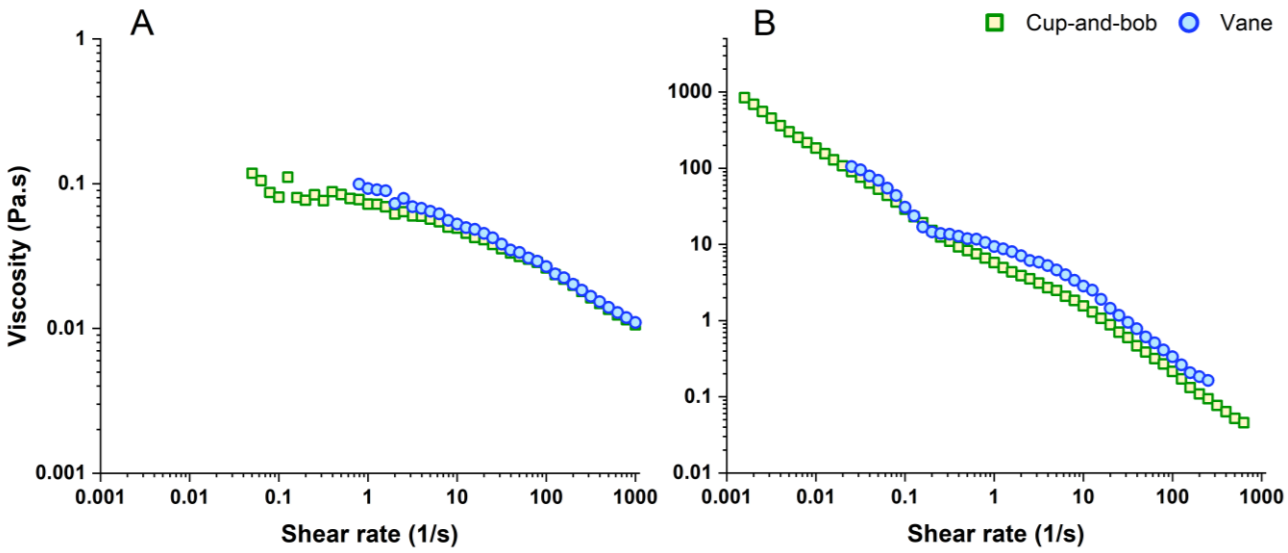


Figure 3.13: Rheological profile of overnight hydrated oven-dried mamaku pith powder (**A**: 0.5% w/w and **B**: 3% w/w) using cup-and-bod geometry and vane geometry. Measurements were taken at 20°C.

3.4.1.2 Oscillatory shear rheology

Typical viscosity measurements done using rotational shear rheology causes bonds to break at high shear. Studying the response of the material at low shear without breaking the bonds may provide further information on the material's properties. Contrary to rotational rheology, an oscillatory test is performed by applying small stress in a sinusoidal wave to incur a small deformation, and the resulting strain (γ) of the material is measured. The material deformed on applying stress can either recover to its original shape upon removal of the stress or may flow irreversibly (**Figure 3.14**). The former material is called an 'ideal solid' and the behaviour is called an *elastic* (solid-like) response, while the latter material is called an 'ideal liquid' and the behaviour is called a *viscous* (liquid-like) response. However, in reality, the ideal solid or ideal liquid materials do not exist. Most materials (and particularly food materials) exhibit a *viscoelastic* behaviour, where it behaves partially like a solid and partially like a liquid.

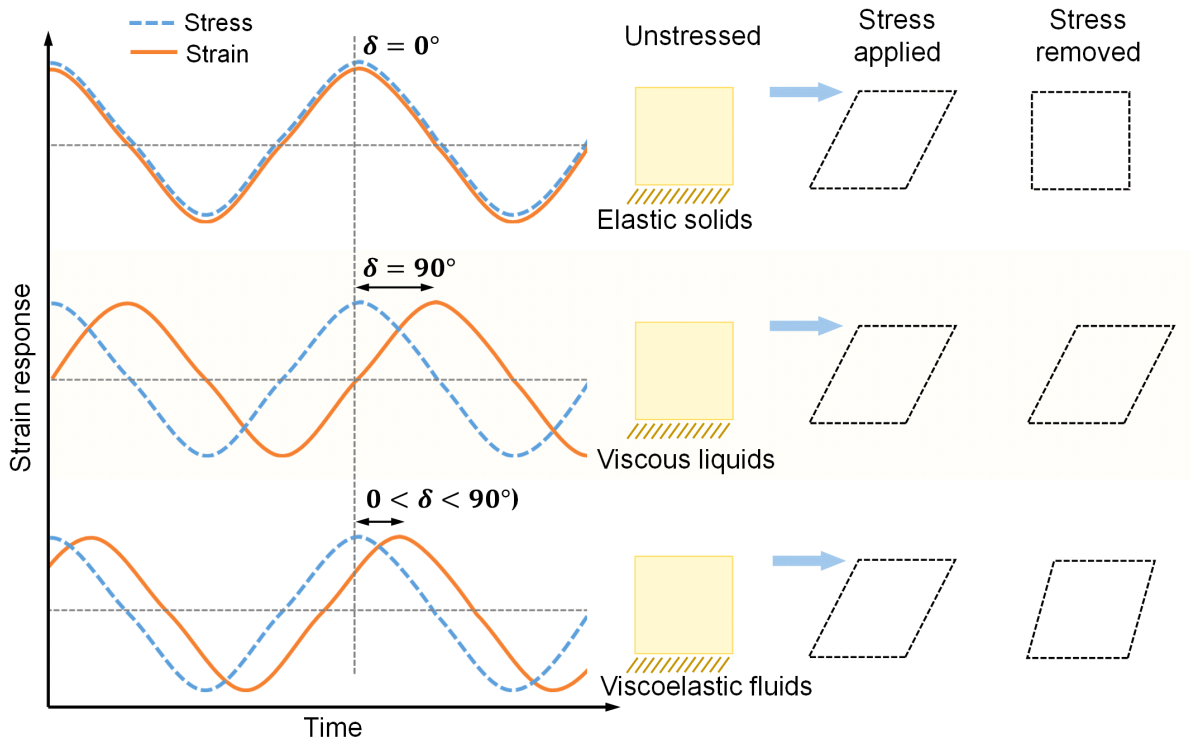


Figure 3.14: Response of elastic solids, viscous liquids and viscoelastic fluids to applied stress. The difference between the stress and strain waves is demoted by δ.

The perfectly elastic solids upon experiencing sinusoidal stress result in oscillating strain which is in phase with the stress wave. On the other hand, for perfectly viscous liquids the resultant strain is exactly 90° out-of-phase with the stress wave. For viscoelastic fluids, the difference between the input stress wave and resulting strain wave, demoted by the phase angle, δ, falls between the two extremes ($0 < \delta < 90°$) (**Figure 3.14**).

Using the two-parallel-plate model (**Figure 3.10**) for oscillatory measurements, sinusoidal stress is applied to the top plate at an angular frequency (ω), while the bottom plate remains stationary. The applied sinusoidal stress, $\tau(t)$, is given as:

$$\tau(t) = \tau_o \sin \omega t \qquad \textbf{Equation 3.8}$$

where, τ_o is maximum stress and t is the time. The resulting out-of-phase sinusoidal strain, $\gamma(t)$, is given as:

$$\gamma(t) = \gamma_o \sin(\omega t + \delta) \qquad \textbf{Equation 3.9}$$

where, γ_o is maximum strain and δ is the phase angle between the stress and strain waves. From here, *storage* (G') and *loss* (G'') moduli can be determined. The former represents the elastic component of the sample and indicates the energy stored during deformation, while the latter represents the viscous component of the sample and indicates the energy dissipated during deformation. Both the moduli can be calculated as:

$$G' = \frac{\tau_o \cos \delta}{\gamma_o} \qquad \textbf{Equation 3.10}$$

$$G'' = \frac{\tau_o \sin \delta}{\gamma_o} \qquad \textbf{Equation 3.11}$$

where, τ_o is maximum stress, γ_o is maximum strain and δ is the phase angle between the stress and strain waves. The ratio of two moduli (G''/G') is defined as a loss tangent or damping factor and is equal to $\tan \delta$. When viscous properties dominate over elastic ($G'' > G'$), $\tan \delta > 1$ and $\delta > 45°$. Conversely, when elastic properties dominate ($G' > G''$), $\tan \delta < 1$ and $\delta < 45°$. The point when $\tan \delta = 1$ or $G'' = G'$ is called the *crossover point* and the corresponding frequency is called the crossover frequency. The inverse of crossover frequency is the *shear relaxation time* (λ_s), which is generally defined as the time required for the applied stress to relax.

For G' and G'' to be measured correctly, the oscillatory rheology test must be conducted within a linear viscoelastic region (LVR). In LVR the strain response of the sample is

proportional to the applied stress and the sample properties are independent of the magnitude of the stress and deforming strain. Beyond this point, the moduli are no longer linear, and a decreasing trend indicates breakage in the structure. The LVR of mamaku gum was determined by subjecting the sample to an increasing deformation amplitude (amplitude sweep test) and the region with constant moduli values is regarded as LVR (**Figure 3.15**). Oscillatory measurements for mamaku gum were made at 5% strain.

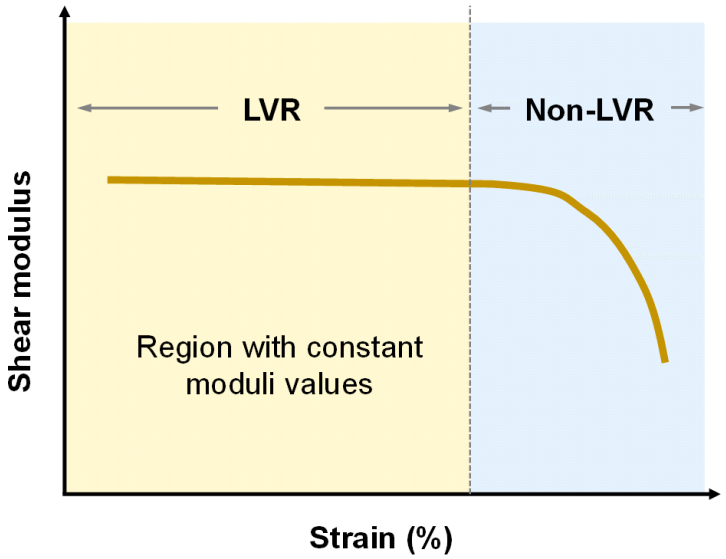


Figure 3.15: Linear and non-linear viscoelastic region (LVR and non-LVR).

3.4.2 Extensional rheology

Imagine holding a rubber band in your hand; you can either shear it between your palms or stretched it using your fingers, but the latter will provide more useful information. Likewise, physiological operations such as mixing of saliva during mastication (Haward, Odell, Berry, & Hall, 2011; Yuan, Ritzoulis, & Chen, 2018b), swallowing of food (Jimenez, Martínez Narváez, & Sharma, 2020; Marconati & Ramaioli, 2020; Tobin et al., 2020), peristaltic flow in stomach and intestine (Feigl & Tanner, 2022) and blood circulation (Lacombe & Essabbah, 1981), and industrial operations such as extrusion, coating, spraying and atomisation (Dinic, Zhang, Jimenez, & Sharma, 2015; Sharma et al., 2015) have a large extensional component that must be considered.

During steady-state uniaxial extensional deformation, the material is stretched in one direction, resulting in compression/shrinkage in the other two directions (**Figure 3.16**). The instantaneous length, $L(t)$, of the sample during extension is given as:

$$L(t) = L_O e^{\dot{\varepsilon} t} \qquad \textbf{Equation 3.12}$$

where, L_O is the initial length of the material being stretched, $\dot{\varepsilon}$ is instantaneous extension strain rate (*i.e.*, stretching rate) and t is time. Thus, the length of the material should increase exponentially with time to achieve a constant strain rate. The resistance offered by the material to stretching deformation is *extensional viscosity* (η_e), similar to η_s, and is given as:

$$\eta_e = \frac{\sigma_e}{\dot{\varepsilon}} \qquad \textbf{Equation 3.13}$$

where, σ_e is extensional stress and $\dot{\varepsilon}$ is instantaneous extension strain rate. However, during extensional behaviour steady-state deformation cannot be achieved in most cases, thus apparent transient extensional viscosity is used.

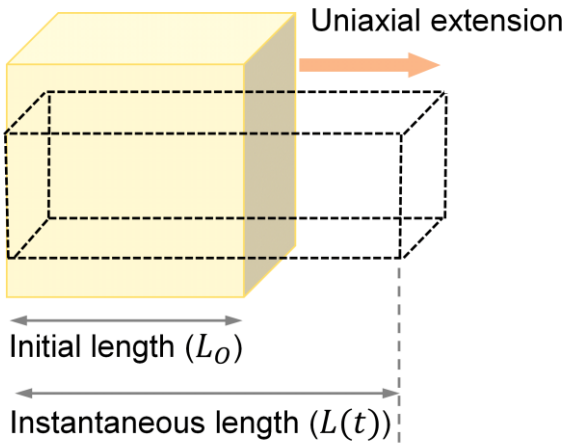


Figure 3.16: Schematic illustration showing extensional deformation.

Different techniques can be used to measure the extensional behaviour of a sample depending on its viscosity and elasticity. This thesis used the capillary-breakup extensional rheometer (CaBER™), first developed by McKinley and co-workers at MIT in conjunction with the Cambridge Polymer Group. The CaBER™ is suitable for low to moderate viscoelastic polysaccharides (Anna & McKinley, 2001; Rodd, Scott, Cooper-White, & McKinley, 2005; Vadillo, Mathues, & Clasen, 2012). For CaBER™, the mamaku gum was placed between two parallel plates, stretched rapidly, and then held at the fixed separation.

This forms an unstable fluid filament between two plates. The self-thinning dynamics of the stretched fluid filament as a function of time was monitored (**Figure 3.17**). The dynamics of stretched fluid with extensional properties pass through three stages: (i) the initial stretching phase characterised by a sharp decrease in diameter, (ii) the relaxation phase where diameter decreases exponentially, and (iii) lastly the breakup phase where the filament breaks. The longer the relaxation phase, the stronger the extensional behaviour.

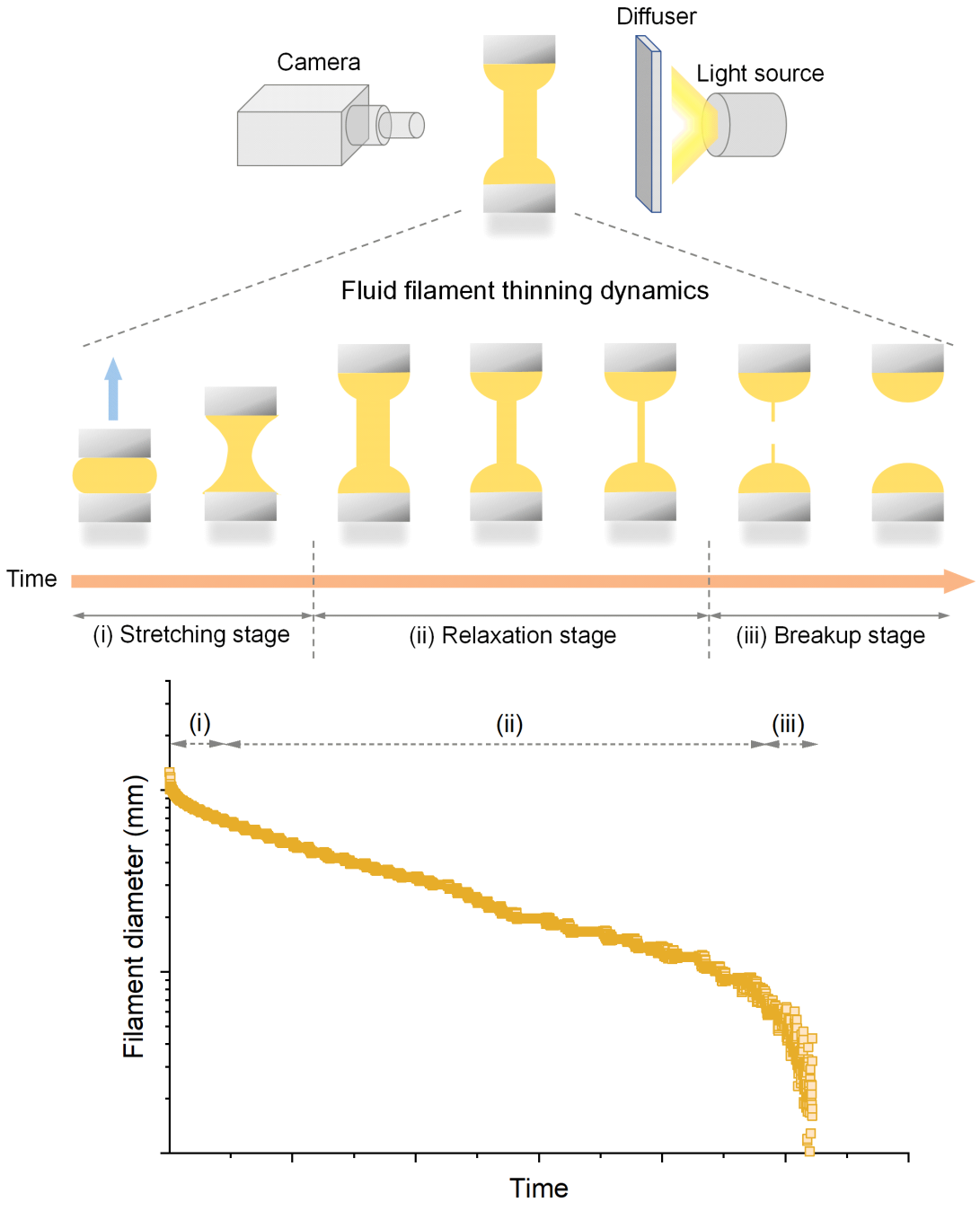


Figure 3.17: Schematic diagram of the capillary-breakup extensional rheometer.

The thinning of fluid filament is driven by capillary stresses and is restricted by the extensional stresses developed. The force balance between gravitational, inertial, viscous, elastic and capillary forces within the fluid filament is used to calculate η_e. The gravitational force is very small compared to others and thus neglected. The inertial and viscous forces are dominant at the beginning of the experiment. The elastic and capillary forces dominate thereafter as the filament thins and this region where elastic forces are balanced by the capillary forces is called the *elastocapillary* region (Anna & McKinley, 2001). The onset of this region is marked by the formation of uniform cylindrical filament (from image analysis). In the elastocapillary region, the filament diameter, $D(t)$, decreases exponentially following:

$$\frac{D(t)}{D_1} = \left(\frac{GD_1}{2\sigma}\right)^{1/3} \exp[-t/3\lambda_e] \qquad \textbf{Equation 3.14}$$

where, D_1 is the diameter of filament immediately after stretching; G is elastic modulus, σ is surface tension and λ_e is the longest *extensional relaxation time*. The relaxation time calculated from filament thinning measurement is usually greater than the relaxation time calculated from oscillatory rheology as the sample is largely deformed in the former.

3.5 *In Vitro* Studies

As discussed in **Chapter 2**, polysaccharides can have a range of physiological effects such as reduced enzyme activity, delayed digestion, and improved colonic fermentation in humans after consumption. However, testing all the physiological effects in human experimental trials is expensive, resource intensive and subjected to ethical considerations. Therefore, *in vitro* models—closely mimicking human physiological conditions—are used to test and compare the effect of polysaccharides. *In vitro* models have better reproducibility, require a small quantity of test material, are easier to collect the sample, quick and have better control of experimental conditions than in a human trial. The physiological effects of mamaku gum were studied using multiple *in vitro* models as discussed below.

3.5.1 *In vitro* enzyme activity inhibition

Enzymes such as α-amylase, pepsin and lipase play a key role in the digestion of food. Enzymes break down complex molecules to form simpler ones, which are then absorbed into the body. The *activity of enzymes*—generally relates to the units of product formed per ml from a substrate in a given time—can be inhibited by the addition of plant extracts during

digestion. The activity of α-amylase, pepsin and lipase in presence of mamaku gum was investigated (**Chapter 5**). Briefly, the enzymes were allowed to break down a specific substrate in presence of mamaku gum, and the amount of product formed was quantified. The principles involved in individual enzyme activity are as follows:

(i) α-amylase breaks down the starch molecule into maltose. The resulting maltose is a reducing sugar that can be determined colorimetrically. The maltose could be further broken down into glucose units using amyloglucosidase and then quantified colorimetrically.

(ii) Pepsin breaks down haemoglobin into peptides which are soluble in trichloroacetic acid (TCA) and can be quantified colorimetrically.

(iii) Lipase breaks down olive oil into oleic acid and glycerol. The free fatty acid is determined through titration.

The amount of digestion product from each enzyme hydrolysis was compared with the control (without mamaku gum).

3.5.2 *In vitro* static digestion

The digestion of food is a complex and dynamic process involving several events happening simultaneously at different rates such as the addition of enzymes and salts, gradual changes in pH, the transition of food, peristaltic movements and absorption of the products. It is broadly divided into three phases: oral, gastric and small intestine, representing different sites of the human gastrointestinal (GI) tract. The *in vitro* digestion models mimicking this complex process can be classified as dynamic, semi-dynamic and static, depending on the degree of simulation of physiological events. Amongst these, the dynamic model is closest to human physiology as the rate of enzyme addition, pH adjustment, gastric emptying, removal of the product and the peristaltic movements of the gut are often simulated (Dupont et al., 2019; Kong & Singh, 2010). However, the dynamic model is complex, expensive, time-consuming, and unavailable to many researchers. In a semi-dynamic model, the peristaltic movements are ignored and compromises may be made about gastric emptying; gradual pH adjustments and enzyme addition are typically maintained (Mulet-Cabero et al., 2020). This type of model is suitable for studying the possible changes in the food structure. The static models are designed to mimic only the biochemical environment of the compartments of the

GI tract. pH adjustments and enzyme addition occur at the beginning of the digestion phase (oral, gastric and small intestine) and gastric emptying and peristaltic movements are not considered (Mishra, Monro, & Hedderley, 2008). Static models are suitable to access the endpoint (digested products) resulting from the digestion of foods without considering the kinetics and possible structural changes.

The static *in vitro* models described in the literature are inconsistent. Apart from agreement on performing digestion at 37°C, there is great variation in pH, digestion time, enzyme source, concentration and activity, the inclusion of oral phase and sampling method used by different researchers (Hur, Lim, Decker, & McClements, 2011). This makes it difficult to compare and validate digestion results. Hence, a standardised digestion protocol for adults (Infogest model) was proposed by Minekus et al. (2014). This model was further refined and Infogest 2.0 was proposed (Brodkorb et al., 2019).

The Infogest 2.0 digestion process was used in this thesis (**Figure 3.18**). Infogest 2.0 model uses a constant ratio of food to enzymes and electrolytes, at constant pH of each digestive phase for a fixed time. Briefly, during the oral phase, the sample was mixed with simulated salivary fluid (1:1 w/w) with salivary amylase for 2 min at pH 7. The oral bolus was then diluted with simulated gastric fluid (1:1 v/v) with gastric enzymes and incubated with agitation for 2 h at pH 3 (gastric phase). The gastric chyme was then diluted with simulated intestinal fluid (1:1 v/v) containing pancreatic enzymes and bile salts and incubated with agitation for 2 h at pH 7 (small intestine phase). pH 3 during gastric phase is recommended taking into account the gradual secretion of hydrochloric acid, the buffering capacity of the food and the optimum activity of gastric pepsin (pH 2 to 4). The pH of chyme leaving the stomach is acidic as a result the pH in the duodenum is around 5, while in the jejunum and ileum, the pH is around pH 7. As the length of the duodenum is small compared to the latter parts, pH 7 is recommended for the intestinal phase. The composition of simulated fluids used in the Infogest 2.0 model is given in **Table 3.1**. The Infogest model does not account for the brush border enzymes such as amyloglucosidase which play a key role in starch digestion (Mishra et al., 2008; Warren, Zhang, Waltzer, Gidley, & Dhital, 2015). Thus, amyloglucosidase was introduced during intestinal digestion in this thesis.

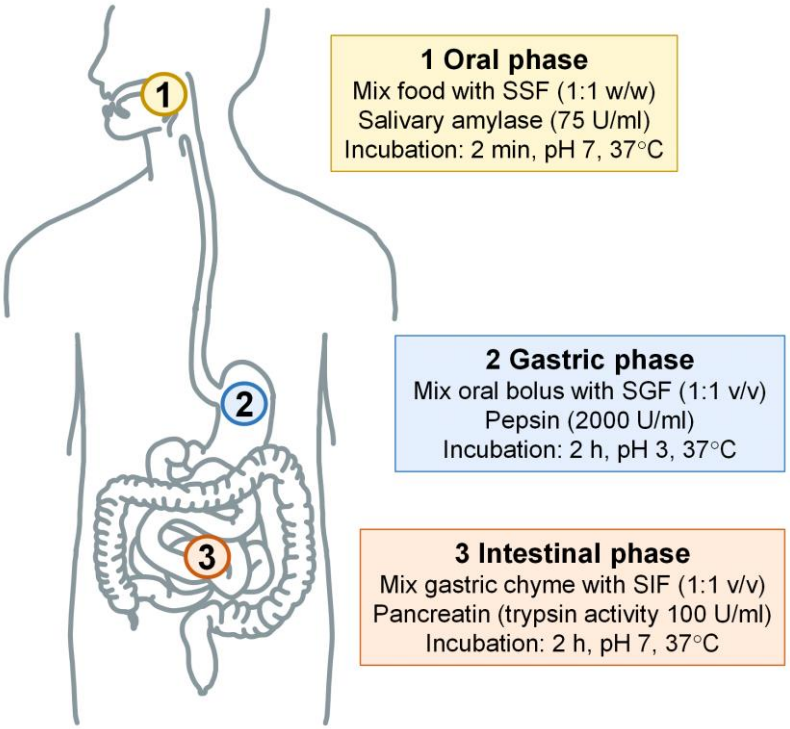


Figure 3.18: Overview of Infogest 2.0 *in vitro* static digestion model showing oral, gastric and intestinal phases. SSF, simulated salivary fluid; SGF, simulated gastric fluid; SIF, simulated intestinal fluid.

Table 3.1: Composition of simulated fluids used during *in vitro* digestion.

Salt	Concentration (mM)		
	SSF (pH 7)	SGF (pH 3)	SIF (pH 7)
KCl	15.1	6.9	6.8
KH_2PO_4	3.7	0.9	0.8
$NaHCO_3$	13.6	25	85
NaCl	-	47.2	38.4
$MgCl_2{\cdot}6H_2O$	0.15	0.12	0.33
$(NH_4)_2CO_3$	0.06	0.5	-
HCl	1.1	15.6	8.4
$CaCl_2{\cdot}2H_2O$	1.5	0.15	0.6

SSF, simulated salivary fluid; SGF, simulated gastric fluid; SIF, simulated intestinal fluid.

Data sourced from Brodkorb et al. (2019)

3.5.3 *In vitro* static colonic fermentation

In recent years, there has been a growing interest in understanding the effect of gut microbiota on human health. The gut microbiota is considered a 'forgotten organ' that is

reflective of our diet. The undigested food from the small intestine enters the colon, where colonic microbes can use it as a substrate for anaerobic fermentation. Different food types respond differently to colonic microbiota and thus cannot be generalised.

For performing *in vitro* colonic fermentation, the pre-digested sample collected after static digestion (using Infogest 2.0) was subjected to membrane dialysis to mimic the intestinal absorption process. After this, the microbial inoculum (human faeces) was added to the sample, mixed with carbohydrate-free basal nutrient growth media, and allowed to ferment under anaerobic conditions (**Figure 3.19**).

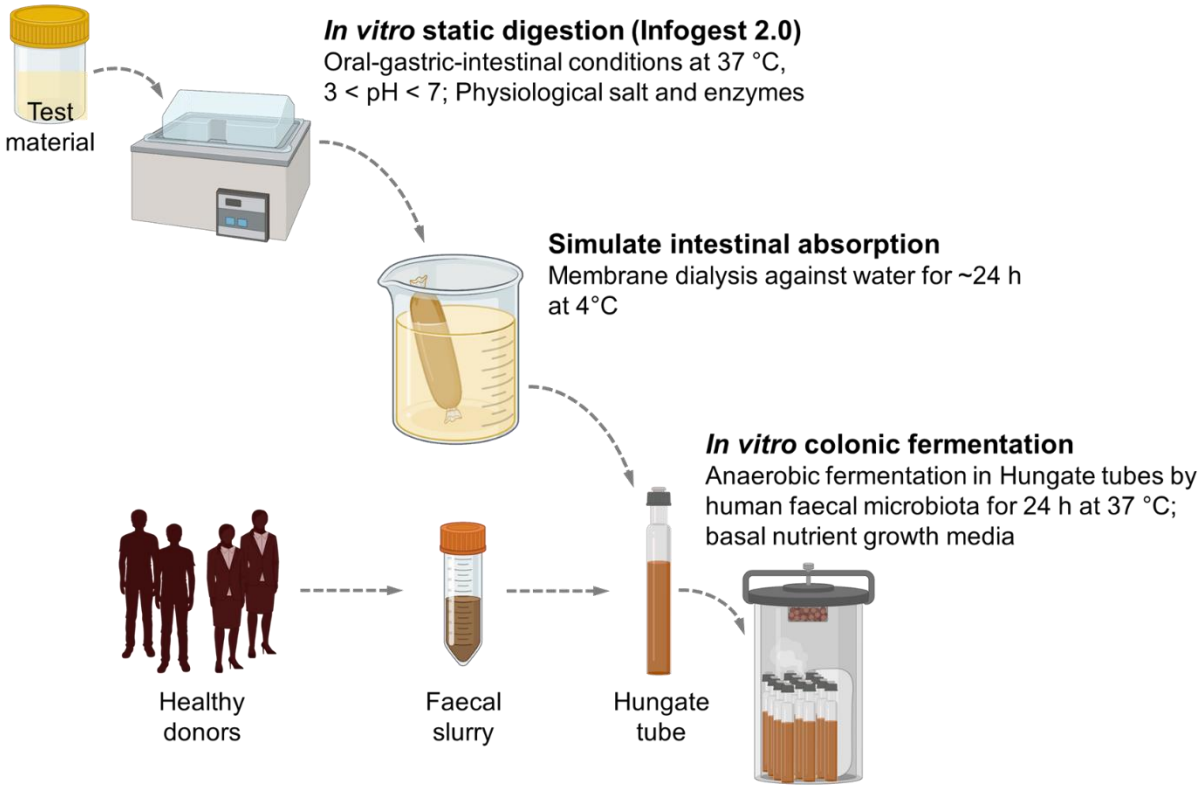


Figure 3.19: Schematic illustration showing *in vitro* experimental sequence from digestion to fermentation.

The batch fermentation method is commonly used to test the fermentability of foods despite its limitations. It is far less than ideal in mimicking the absorption of metabolite acids. The acids accumulate with fermentation, decreasing the pH. This affects the growth of acid-sensitive bacteria such as *Bacteroides*. The bicarbonate and phosphate added in basal nutrient growth media may however help with some pH control in short-term studies. Furthermore,

the polyphenols present in plant food can also modulate the colonic microbiota in addition to the dietary fibres. The dialysis step performed might potentially remove the polyphenols that might have reached the colon. When faecal samples from different individuals are used as microbial inoculum, the inter-individual heterogeneous composition of gut microbiota cannot be discounted (Parkar et al., 2018). To overcome this, the faecal sample from different individuals are pooled together to make an inoculum slurry. Also, using faecal samples is not representative of the entire colon as the microbial diversity varies throughout the colon.

During *in vitro* fermentation, the changes in short-chain fatty acids (SCFAs) production and microbial community were key parameters of interest. The former was analysed using a gas chromatogram, while the latter was more complicated and required metagenomic analysis.

3.6 Metagenomic Analysis

The traditional culture-based approaches utilising carefully formulated growth media are good to enumerate the known microorganism of interest. However, a large fraction of "viable but non-culturable" microbiota[19] (as in the case of human faeces) cannot be examined using traditional methods. Therefore, molecular based (such as genome sequencing) approaches are used. *Genome sequencing* is an umbrella term used to describe the initial purification of deoxyribonucleic acid (DNA) samples from microbiota at the site of interest, preparation of genomic DNA by fragmentation, followed by library preparation and amplification and then sequencing on a dedicated platform. DNA sequencing was initially performed manually using the pioneer Sanger sequencing method (first published in 1977). The development in technology, particularly polymerase chain reaction (PCR) led to the development of the first automated DNA sequencer in 1986 which was later used in the human genome sequencing project. This is considered the 'first-generation' technology. The need for new and improved techniques to sequence a large number of human genomes and simultaneous developments happening in the field of nanotechnology and computational biology to name some contributed to the development of 'second-generation' or High-throughput sequencing or *next-generation sequencing* (NGS) methods from Roche/454, Helicos BioSciences and Illumina/Solexa and Ion Torrent (Metzker, 2010; Pereira, Oliveira, & Sousa, 2020). The raw sequences collected from the sequencing platform are thereafter processed

[19] Total collection of microbial organisms within a community or sample.

and statistically analysed to interpret the biological data using high-performance computing, and this is known as *bioinformatics*. As a whole, this field of study of microbial communities sampled directly from the site of interest, typically relying on high-throughput sequencing and bioinformatics techniques is called *metagenomics* (**Figure 3.20**).

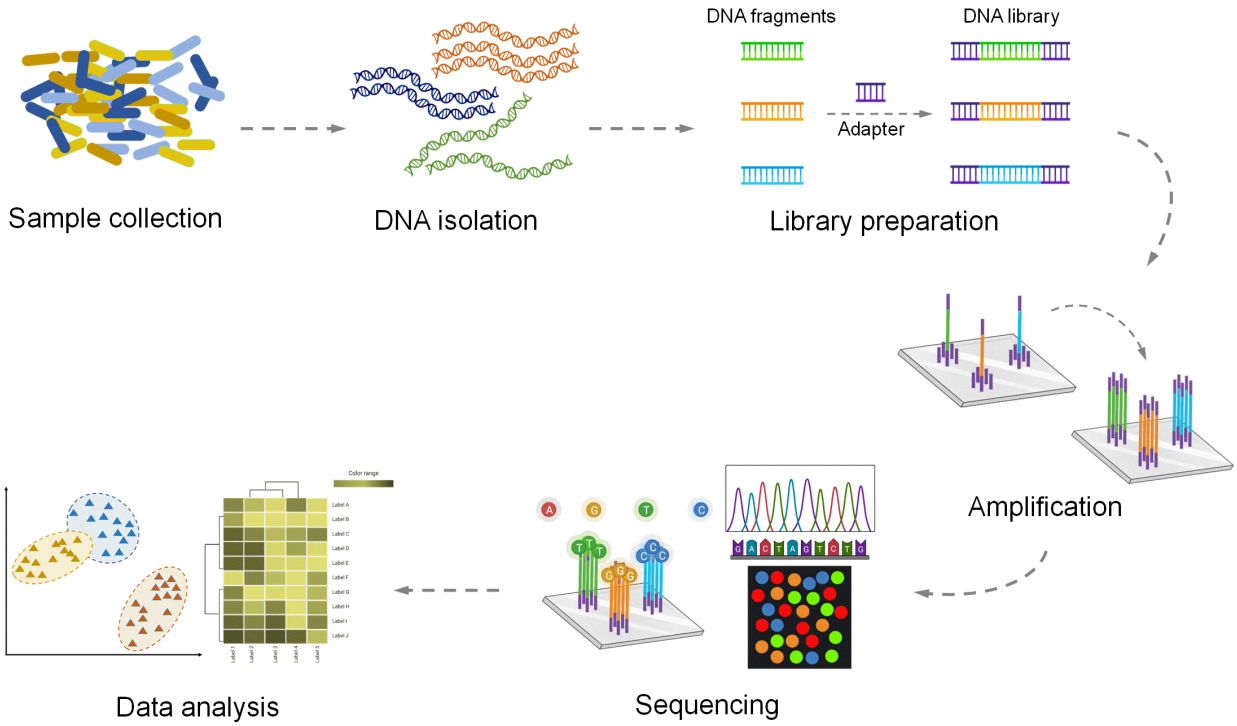


Figure 3.20: Schematic illustration showing key steps during metagenomic analysis.

The isolated DNA can be analysed using two different approaches (**Figure 3.21**): (i) The entire DNA content collected from a site, including extra-nuclear DNA from mitochondria and plasmids is used for sequencing, referred to as *whole genome sequencing* and (ii) Segment/region of DNA with a specific marker gene[20] that is commonly found in the broader community is sequenced, referred to as *amplicon sequencing* (Ranjan, Rani, Metwally, McGee, & Perkins, 2016). The former can provide more information and is less susceptible to bias but is slow and costly to sequence, computationally expensive, and require sequencing and bioinformatics expertise, thus the latter was used in this thesis.

[20] Specific gene or DNA sequence with a known location on the chromosome which can be used to identify individuals or species.

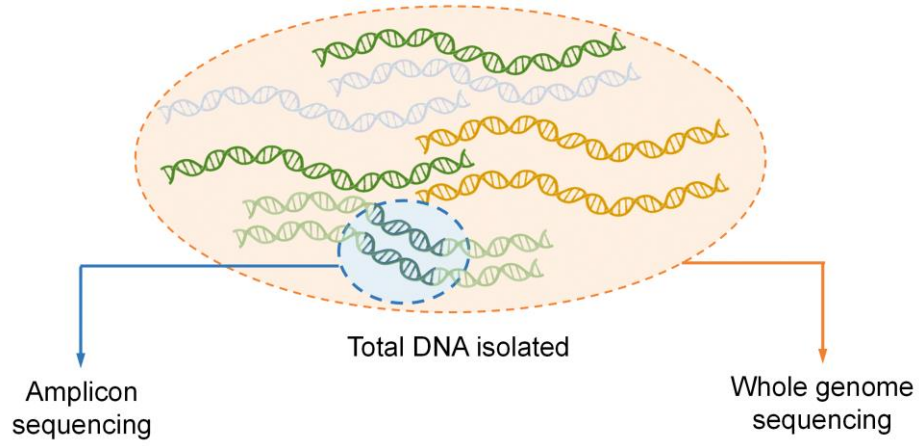


Figure 3.21: Pictorial representation showing the DNA sample used for amplicon and whole genome sequencing.

Amplicon sequencing is a fast and cost-effective way to gain insight into the taxonomic[21] composition of the community. It involves amplifying the marker gene *via* PCR which is subsequently sequenced and aligned to a reference database to gain information about the microbial community in the sample. Different marker genes can be used to study a microbial community in a sample, for example, the 16S small subunit ribosomal ribonucleic acid (rRNA) gene is used for bacteria and archaea, the 18S rRNA gene is used for eukaryotes and the Internal transcribed spacer (ITS) region for fungi. For colonic fermentation, *16S rRNA* is the most widely used marker gene, but it must be noted that it only provides information about the bacterial community and not about other significant partners fungi and viruses in the colon.

16S rRNA gene is a ~1,500 base pair long gene coding for an rRNA that is a part of the 30S ribosome (small) subunit which plays a role in protein synthesis. It is present in all prokaryotic cells and consists of both highly conserved regions (acting as a site for 'universal' primers to initiate targeted amplification) and nine hypervariable regions (allowing discrimination between different species) between species (Gao et al., 2021) (**Figure 3.22**). The second-generation sequencing platforms do not allow the sequencing of the entire 16S rRNA gene. As a result, one or more adjacent variable regions (~250-500 bp) are amplified and sequenced. Relying on some hypervariable regions limits the taxonomic resolution and different hypervariable regions within the sample 16S rRNA gene may result in some

[21] Classifying groups of biological organisms on basis of shared characteristics.

differences in taxonomic classification (Srinivasan et al., 2015). The selected region can then be amplified using universal primers and sequenced using a sequencing platform. Sequencing is mostly performed externally *via* a service provider, therefore not discussed here, interested readers are directed to other review articles (Metzker, 2010). In this thesis, the *V3-V4 region* was analysed using the Illumina MiSeq platform (Illumina Inc., San Diego, California, USA).

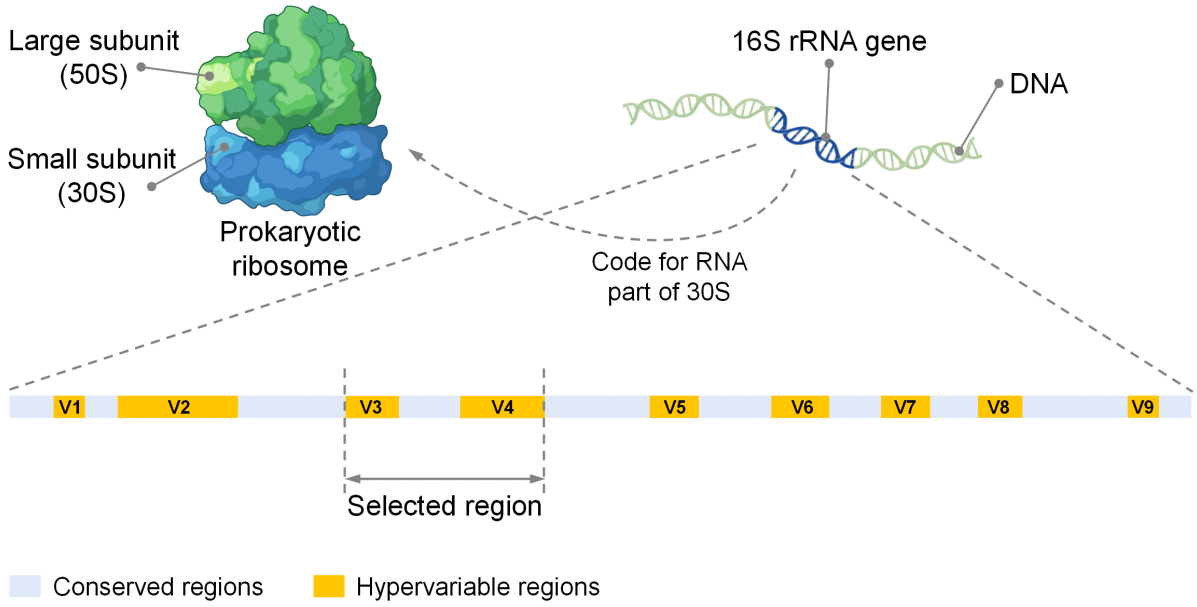


Figure 3.22: 16S rRNA gene of *E. coli* showing the hypervariable (V1-V9) and conserved regions.

The raw sequences are then processed using bioinformatic pipelines which bundle together different computational tools. Several pipelines such as QIIME, Mothur, DADA2, MG-rast and Keaken are available. For colonic bacteria analysis, *Quantitative Insights Into Microbial Ecology* (QIIME) is mostly used due to the availability of extensive documentation, the ease of use and the flexibility of processing and analysis methods; thus was used in here. Briefly, the raw reads[22] are sorted into separate files for each sample (demultiplexing), checked for quality and trimmed to remove low-quality base pairs (minimum quality score: 30), merged by aligning the forward and reverse reads, clustered based on similarity, annotated[23] against

[22] A sequence of nucleotides that is being sequenced after fragmentation.
[23] Assigning a taxonomic lineage or a function to a gene.

the reference database, filtered to remove low abundance reads, normalised and then analysed for statistical differences (Gao et al., 2021).

The data can be analysed for the *structural* (what bacteria are in a sample and their abundance) and *functional* (what is the bacterial community doing) potential of a bacterial community in the sample. The structural analysis involves taxonomic classification of the bacterial community and identifying the different bacteria. The 16S rRNA gene sequencing can identify and classify the community to the genus level. Structural characteristic is measured using diversity analysis. *Alpha-diversity* deals with how diverse a sample is *i.e.,* within sample diversity. It can be calculated either based on the *richness* of a sample, meaning how many different types of bacteria are present in one sample or based on the *evenness* of a sample, meaning how abundant are the community members in a sample (**Figure 3.23**). *Beta-diversity*, on the other hand, deals with how similar/different are two or more samples from each other *i.e.,* between sample diversity.

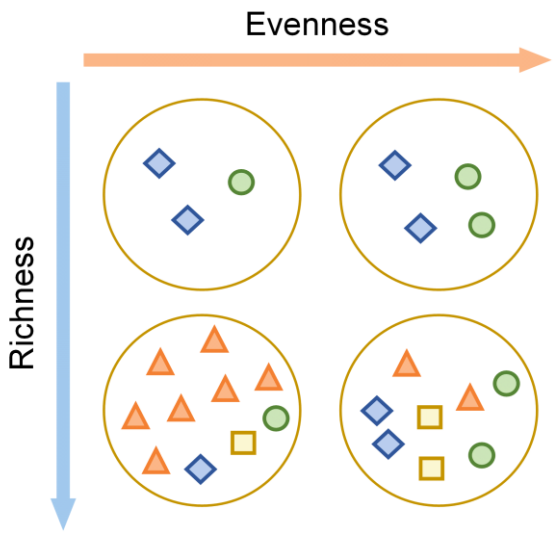


Figure 3.23: A pictorial representation demonstrating species richness and evenness of a community. Each shape represents an organism. Different shapes represent different organisms.

Functional analysis is used to predict the functional capacity of the community based on the genes identified *via* annotation. It must be noted that the presence of a gene does not mean that it is biologically active, other techniques such as metatranscriptomics and metaproteomics are used for that purpose, thus the functional analysis is predictive.

Functional analysis is mostly performed using whole genome sequencing, but bioinformatics tools like Phylogenetic Investigation of Communities by Reconstruction of Unobserved States (PICRUST) are developed to predict function using 16S rRNA gene data with a 75-85% accuracy for human microbiome (Langille et al., 2013).

3.7 Human Trial

The human body is more complex than what we can replicate in an *in vitro* model. Due to the lack of complexity of *in vitro* models, they cannot accurately demonstrate the full body's response to food. A very high correlation existed between *in vitro* glucose release from some starchy foods and glycaemic response[24] *in vivo* (Granfeldt, Wu, & Björck, 2006; Monro, Wallace, et al., 2010), but additional information about insulin response and appetite cannot be obtained from the former. Furthermore, human trials are a must for making health-related claims about food. A human trial should be conducted towards the later phase of the study based on the observations made using *in vitro* models. In this thesis, the effect of mamaku pith powder on glycaemic response was tested using human participants, whereby participants consumed a carbohydrate-rich meal with test material and changes in blood glucose were monitored.

International standard (ISO 26642:2010) developed in joint consultation with FAO/WHO is the most up-to-date document followed to determine the glycaemic response of a food. The key points to consider during the glycaemic response trial [summarised from Brouns et al. (2005) and Flavel, Jois, and Kitchen (2021)] are as follows:

- *Subject number and characteristics*: There should be a minimum of 10 subjects to get a reasonable degree of power and precision. The number can be increased if greater precision is required. Subject characteristics do not appear to significantly affect the mean values, but the variation of the value may differ in various groups. Healthy individuals are recommended for routine testing.
- *Reference food*: Glucose solution can be used to deliver a known amount of carbohydrates. However, sometimes subjects can get nauseous after drinking a concentrated glucose drink in the fasted state. Also, for practical reasons, white

[24] The effect of food or meal on blood glucose levels after consumption.

bread, wheat biscuits and rice or any other food which is more representative of a meal can be used as the reference food.

- *Available carbohydrates*: A dose of 50 g of available carbohydrates can be delivered to participants; above this, the glucose response curve tends to plateau. However, depending on the size of the meal, the amount of available carbohydrates can be adjusted between 25 to 50 g.
- *Ingestion time*: The fluid meal, 250 ml, should be ingested within 5-10 min, while solid and semi-solid meals should be ingested within 10-20 min. The first blood sample should be taken exactly 15 min after the first bite of the food.
- *Blood sampling*: The amount of glucose in the arterial blood is the principal measurement of interest as this is the concentration to which the tissues are exposed. However, collecting arterial blood is an invasive and painful procedure. Capillary blood (especially from the fingertip) is less painful and can be used when a low sample is required.
- *Data collection*: More than one baseline blood sample is recommended as it reduces variability. Post-prandial blood samples should be taken at 15, 30, 45, 60, 90 and 120 min.

This chapter has explained the basis of the techniques used in the subsequent chapters to answer all the stated research questions.

Chapter 4

Does harvesting age matter? Changes in structure and rheology of a shear-thickening polysaccharide from *Cyathea medullaris* as a function of age

4.1 Introduction

Consumer demand for minimally processed natural ingredients is recognised by the scientific community, and therefore attempts are constantly being made to seek novel ingredients, such as polysaccharides, to be used in the pharmaceutical, nutraceutical, cosmetic and food industries. Here, a novel water-soluble polysaccharide from the New Zealand black tree fern (*Cyathea medullaris*), commonly known as mamaku fern, is studied.

The reddish-brown mucilage extracted from mamaku fern has been reported to exhibit unique rheological properties such as Newtonian, shear-thickening, shear-thinning, thixotropic and anti-thixotropic behaviour (depending on concentration and shear rate) (Goh et al., 2007). Shear-thickening behaviour is generally reported for synthetic polymers (Chen et al., 2019; Hu et al., 1995; Ma & Cooper, 2001; Tam et al., 1998; Tan et al., 2001; Xu et al., 2010) and for physically/chemically modified natural polymers (Ang, Goh, Lim, & Matia-Merino, 2021; Burckbuchler et al., 2006; Kjøniksen, Hiorth, & Nyström, 2005); however, is not a common phenomenon in unmodified natural polymers. The complex rheological behaviour of mamaku mucilage has been attributed to the presence of a non-starch polysaccharide fraction referred to as mamaku polysaccharide (MP). MP is a long-chain glucuronomannan polymer comprising of a repeating backbone of β-1,4-linked methylesterified glucopyranosyl uronic acid and α-1,2-linked mannopyranosyl residues, branched at O-3 of 45% and at both O-3 and O-4 of 53% of the mannopyranosyl residues (Wee et al., 2014). The sidechain comprises galactose, arabinose, non-methylesterified glucuronic acid and other simple sugars. Furthermore, MP was reported to have strong extensional viscosity (η_e—of the order 10^3) (Jaishankar et al., 2015), indicating higher intermolecular interaction between MP chains during extension as compared to other polymers such as guar gum (Szopinski, Handge, Kulicke, Abetz, & Luinstra, 2016) or okra polysaccharide (Yuan, Ritzoulis, & Chen, 2018a).

Studies disclosing novel polysaccharides from natural sources are common in the literature, although, the relatively small amount of information available limits their use for commercial applications. It is vital to understand the properties of novel polysaccharides at all stages of their development, *i.e.*, from their origin to end-use. During biochemical and physiological developments in the plant, such as seed germination and fruit ripening, endogenous enzymes can cause structural changes in polysaccharides (Ward, Moo-Young, & Venkat, 1989), thereby affecting their functionality. During the ripening of fruits, the activity of several enzymes such as pectin esterases, responsible for the changes in pectin structure, increases significantly (Wang, Yeats, Uluisik, Rose, & Seymour, 2018). Changes in pectin during maturation may include shortening of the pectin chain, demethylation of carboxyl groups and deacetylation of hydroxyl groups (Ward et al., 1989). Therefore, it is important to understand the effect of mamaku frond age on the functionality of MP.

The working hypothesis was that the physicochemical properties of MP differ as a function of age, which affects its functionality (*e.g.*, shear and extensional rheology). This work not only provides useful knowledge on the appropriate and sustainable harvesting time but also on how to achieve product uniformity in large-scale production. To the best of the author's knowledge, there is no report characterising the changes in MP based on the age of fronds. This study presents a comprehensive analysis of the structural characterisation of MP extracted from three different age group fronds and its impact on shear and uniaxial extensional rheology.

4.2 Materials and Methods

4.2.1 Extraction and purification of mamaku gum

Mamaku fronds from three different age groups were harvested as described previously (**Section 3.1**). The harvesting stages were classified based on the significant visual changes in the growth of the fern. Stage 1 refers to young fronds (known as koru), stage 2 refers to fully grown fronds, and stage 3 refers to fronds starting to die, where brown sections were observed (**Figure 4.1**). Gum extraction was carried out as per **Section 3.1.1**. Briefly, after harvesting, the fronds were chopped, blended with water and heated to ~55°C for 5 min with continuous stirring. The exuded gum, separated from insoluble plant debris, was collected.

The left-over pulp was reheated in water and the extract was collected until no visual viscous consistency of the flowing liquid was observed. This was repeated an average of 3-5 cycles. The pooled extracts were left undisturbed overnight at 4°C for the remains of pulp to sediment by gravity. The clearer top layer was then separated using a siphon, and the 'crude gum extract' was freeze-dried.

The crude mamaku gum extract samples were hydrated overnight (5% w/w) and ultra-centrifuged (Sorvall WX Ultra 100, T-865 motor, Thermo-Fisher Scientific, Waltham, Massachusetts, USA) at 250,000 g for 1 h to remove large aggregates, dialysed (molecular weight cut-off: 12,000-14,000 Da) against reducing NaCl concentrations (0.01 M, 0.001 M and milli-Q water only) for ~42 h at 4°C, and the 'purified gum fraction' was freeze-dried.

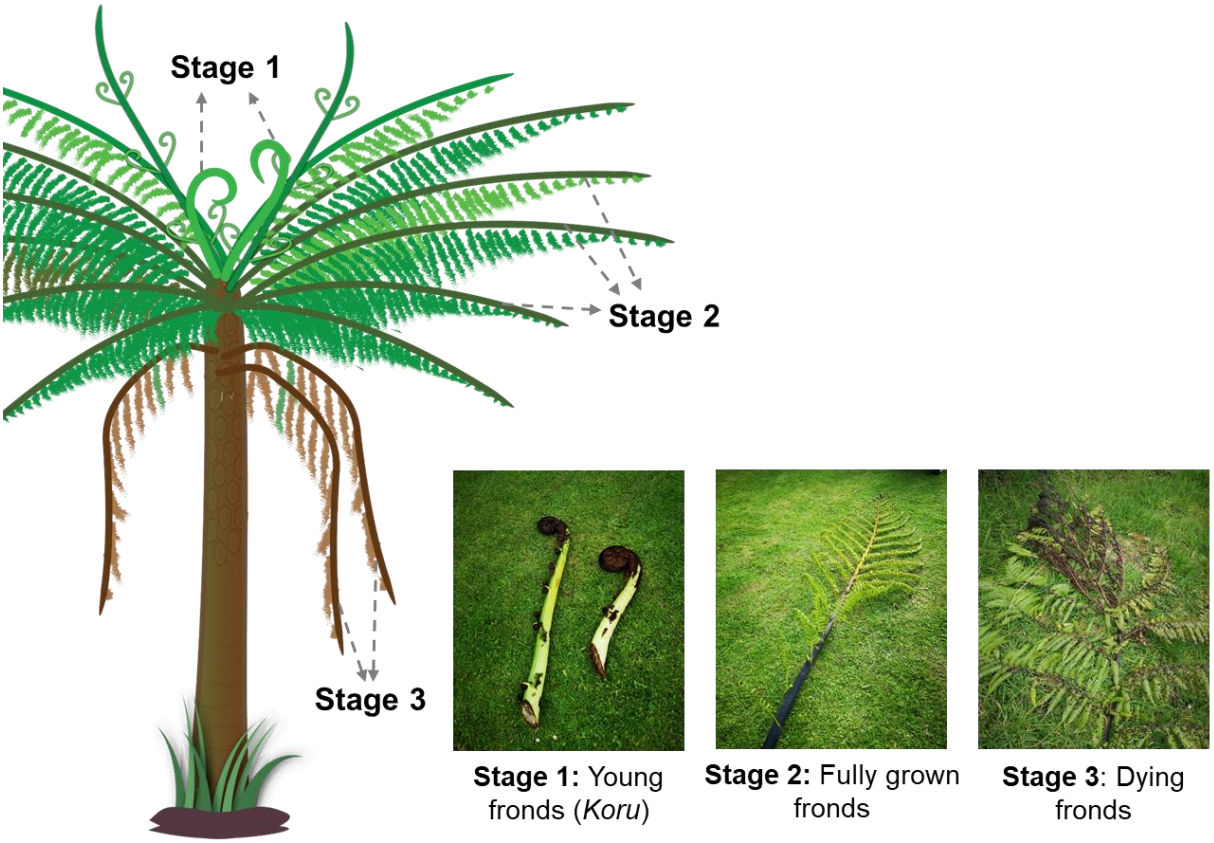


Figure 4.1: Pictorial representation of mamaku frond with three stages of harvesting age (stage 1, stage 2 and stage 3).

4.2.2 Chemical analysis

Quantification of total solids, ash, protein, fat, starch and dietary fibres (soluble and insoluble) was carried out on the crude gum extracts using AOAC 925.45A, AOAC 942.05, AOAC 968.06, AOAC 922.06, AOAC 996.11 (Megazyme kit) and AOAC 991.43 (Megazyme kit) methods, respectively. The mineral and sugar compositions were analysed using an inductively coupled plasma (ICP)-optical emission spectrometer and gas chromatography, respectively. The uronic acid content was quantified spectrophotometrically using the *m*-hydroxydiphenyl method with glucuronic acid as the standard (Blumenkrantz & Asboe-Hansen, 1973). The chemical analyses were conducted by an accredited Nutrition Laboratory, Massey University, Palmerston North, New Zealand.

4.2.3 Constituent sugar analysis

The constituent sugar composition of purified gum was determined using high-performance anion-exchange chromatography (HPAEC) after hydrolysis to its component monosaccharides, as described by De Ruiter et al. (1992) with modifications (Wee et al., 2014). Briefly, duplicate samples (400 μg) were hydrolysed with methanolic HCl (3 M, 500 μl, 80°C, 18 h), followed by aqueous trifluoroacetic acid (TFA, 2.5 M, 500 μl, 120°C, 1 h). The resulting hydrolysates were dried, diluted with Type 1 water (to 80 μg/ml) and analysed on a CarboPac PA-1 (4 × 250 mm) column equilibrated in 20 mM NaOH and eluted with a simultaneous gradient of NaOH (20 mM from 0-25 min, then 20→100 mM from 25-30 min and held to 50 min, then 100→200 mM from 50-52 min and held to 59 min, then 200→20 mM from 59-60 min and held to 75 min) and NaOAc (0 mM from 0-30 min, then 0→500 mM from 30-50 min, then 500→1000 mM from 50-52 min and held to 59 min, then 1000→0 mM from 59-60 min and held to 75 min) at 30°C and a flow rate of 1 ml/min. The sugars were identified from their elution times relative to a standard sugar mix (L-fucose, L-rhamnose, L-arabinose, D-galactose, D-glucose, D-mannose, D-xylose, D-galacturonic acid, and D-glucuronic acid), quantified from the response calibration curves of each sugar and converted wt% anhydrosugar.

4.2.4 Nuclear magnetic resonance spectroscopy

The purified mamaku gum samples were deuterium exchanged by freeze-drying twice with D_2O and dissolved in D_2O at 6.7 mg/ml, with the addition of acetone (0.4% v/v) as an internal standard, set at 31.45 ppm (^{13}C) and 2.225 ppm (^{1}H). NMR data were collected on a Bruker Avance Neo 700 MHz NMR spectrometer (Bruker BioSpin, Rheinstetten, Germany) equipped with a 5 mm TCI cryoprobe (fitted with a Z-gradient coil) at 65°C. 1D ^{1}H NMR spectra were recorded with a spectral width of 20 ppm, 65,536 complex data points, 30-degree excitation pulse, each with an acquisition time of 2.36 s and a 1 s recycle delay time. Phase-sensitive, sensitivity enhanced Heteronuclear single quantum coherence (HSQC) and double-quantum filtered correlation spectroscopy (DQF-COSY) experiments were carried out using standard Bruker pulse programs (*hsqcetgpsisp2.2* and *cosydfph*). The 2D spectra used spectral widths of 10.2 and 124.0 ppm for the ^{1}H and ^{13}C dimensions, respectively. The HSQC was digitized using 2048 x 320 points. The DQF-COSY was acquired using 50% non-uniform sampling in the indirect dimension, giving a final data matrix of 2048 x 400 points. Both 2D experiments used a recycle delay of 1.5 s. Spectra were analysed and processed in Mestranova (Version 14.1.2). Assignments were made by comparing the spectra with published data.

4.2.5 Size-exclusion chromatography coupled with multi-angle laser light scattering

The weighted-average molecular weight (M_w) and radius of gyration (R_g) for purified gum samples was determined using high-performance liquid chromatography (HPLC) system (Shimadzu, Kyoto, Japan) coupled with multi-angle laser light scattering (Dawn Heleos 8+, Wyatt Technology Corp., Goleta, California, USA), as described by Goh et al. (2011). Separation was achieved by connecting two size-exclusion columns in series with a guard column (OHpak SB-G, SB-804 HQ and SB-806M HQ columns, Shodex, Tokyo, Japan) at 25°C. The purified gum samples were centrifuged at 30,000 g for 1 h, followed by injection (20 µl) into the HPLC system at a flow rate of 0.5 ml/min and eluted with 0.1 M NaCl. The mobile phase was filtered through a 0.22 µm membrane filter followed by a 0.025 µm membrane filter (Millipore Corp., Burlington, Massachusetts, USA) and degassed under vacuum overnight at room temperature before use. The Astra software (Version 6.1.1.17, Wyatt

Technology) was used to analyse the light scattering peak using the Zimm plot at an incremental refractive index (dn/dc) of 0.178 ml/g.

4.2.6 Shear rheology

Freeze-dried crude gum extract was hydrated in milli-Q water at different total solid concentrations (w/w) for ~15 h at 20°C. Rheological measurements were performed using a Paar Physica MCR 302 rheometer (Anton-Paar, Graz, Austria) in controlled shear rate (CSR) mode using a log-ramp profile from 30 s to 2 s (initial to final) at 20.0±0.1°C. Viscosity profiles were measured using the cup-and-bob geometry (CC27 and C-PTD 200) and data were recorded using Rheoplus/32 software (Version 3.62).

Oscillatory measurements (frequency sweep) were performed in the range of 0.01-20 Hz using a constant strain value of 5% (within the linear viscoelastic region) using the double gap geometry (DG-26-7 and C-PTD 200). The samples after loading were allowed to rest for 5 min, before starting the experiment, to reduce any effect of shear-history and for temperature equilibration.

4.2.7 Extensional rheology

The extensional behaviour of crude gum extract was investigated using a portable capillary-breakup extensional rheometer, built in-house at Massey University based on the design described by Hallmark et al. (2016). The in-house built portable extensional rheometer was previously validated (Rozali, 2019). This instrument consists of two cylindrical pistons of diameter, D_o, 4 mm separated by an initial gap, L_o, 1.5 mm (giving initial aspect ratio, $\Lambda_o = L_o/D_o = 0.38$). The samples were loaded between the pistons (cylindrical volume of fluid ~0.02 ml) and the top piston was displaced instantaneously to the final separation, L_f, of 4 mm (giving final aspect ratio, $\Lambda_f = L_f/D_o = 1$) using a battery-powered solenoid to impose a predominantly uniaxial extensional deformation and, thus, create a liquid filament bridge between pistons. The subsequent evolution of the liquid filament diameter was monitored using a high-speed camera at 500 frames per second. MATLAB software was programmed to digitally analyse the measurements of the diameter in each frame. The experiment was repeated at least 10 times in a temperature-controlled room at 20°C.

The filament thinning experiment assumes axial symmetry about the midplane but is strongly influenced by gravitational force, causing filament sagging. In order to minimize gravitational sagging and obtain the initial filament configuration close to the cylinder, the experiment parameters were set such that $L_o \leq$ capillary length, $l_{cap} = \sqrt{\sigma}/\rho g \approx 2.5$ mm, or equivalently $2L_o/D_o \leq 1/\sqrt{B_o} \approx 0.75 \leq 1.3$; where σ is surface tension, ρ is density (assumed as 1000 kg/m^3), g is the acceleration due to gravity (9.18 m/s^2) and B_o is Bond number ($= \frac{\rho g {D_o}^2}{4\sigma} \approx 0.6$) (Rodd et al., 2005). The surface tension for all the samples was measured independently using a Tensiometer (Biolin Scientific Attention theta flex, ATA Scientific Instruments, Australia) (**Table B.1** in **Appendix B**).

The liquid filament thins under the action of viscous, elastic and capillary forces, and the midplane diameter, $D(t)$, of the filament varies as a function of time. Three characteristic diameters were recorded for analysis: D_o, the initial sample diameter (≈ piston diameter = 4 mm); D_1, the diameter of mid-filament immediately after stretching; and $D(t)$, is the change in filament diameter with time after stretching until breakup. For viscous Newtonian fluids of viscosity η_s and surface tension σ, the midplane diameter, $D(t)$, decays linearly with time until breakup according to:

$$D(t) = 0.0709 \frac{2\sigma}{\eta_s} (t_b - t) \qquad \textbf{Equation 4.1}$$

where, t_b is the capillary breakup time (McKinley & Tripathi, 2000). However, for viscoelastic fluids, the filament initially drains under capillary pressure which is restricted predominantly by viscosity stress. The extensional flow generated during thinning results in additional elastic stress, due to the deformation of microstructure, which grows with increasing strain and ultimately dominates the viscous stress. This point, when capillary pressure arising from surface tension is balanced purely by stress from elasticity, marks the onset of an elastocapillary regime (Anna & McKinley, 2001; Haward, Sharma, Butts, McKinley, & Rahatekar, 2012). For viscoelastic fluid in the elastocapillary region, the midplane diameter, $D(t)$, decays exponentially according to:

$$\frac{D(t)}{D_1} = \left(\frac{GD_1}{2\sigma}\right)^{1/3} \exp[-t/3\lambda_e] \qquad \textbf{Equation 4.2}$$

where, G is elastic modulus and λ_e is the longest extensional relaxation time. The instantaneous strain rate, $\dot{\varepsilon}$, of the thinning fluid filament is given by:

$$\dot{\varepsilon} = -\frac{2}{D(t)}\frac{dD(t)}{dt} \qquad \textbf{Equation 4.3}$$

Hencky strain, $\varepsilon_H(t)$, experienced by the thinning filament at the axial midplane at time t is then given by:

$$\varepsilon_H(\mathrm{t}) = \int_0^t \dot{\varepsilon}\,(t)d(t) = 2ln\left(\frac{D_1}{D(t)}\right) \qquad \textbf{Equation 4.4}$$

The apparent transient extensional viscosity, η_e, of the stretching fluid can be obtained using:

$$\eta_e = -\frac{\sigma}{dD(t)/dt} \qquad \textbf{Equation 4.5}$$

4.2.8 Statistical analysis

All the experiments were done in triplicate, otherwise specified. Statistical analysis was performed using a one-way analysis of variance (ANOVA) with Tukey HSD post-hoc test at a 95% confidence level using SPSS software (IBM SPSS Statistics, Version 28.0.1.1(15)).

4.3 Results and Discussion

4.3.1 Yield

The amount of total solids in fresh extracts decreased with the increase in fronds harvesting age. The yield of uronic acid obtained in fresh crude gum extracts reduced from ~0.17% (in stage 1 fronds) to ~0.1% (in stage 3 fronds) when compared to fresh whole fronds (**Table 4.1**). The decrease in the amount of uronic acid (and therefore the MP) can be related to the functionality of MP in plant. The young fronds may produce a high amount of MP as it may help keep the fronds hydrated or act as a lubricant to help transport water and minerals (Zimmermann et al., 1994). As the fronds mature, the plant cell structure becomes rigid (as in plants that bear flowers and fruits-angiosperms), which may trap the polysaccharide tighter in the matrix, thus hinder in extraction.

Table 4.1: Yield of fresh mamaku extracts from fronds of different stages of harvesting age.

	Stage 1	Stage 2	Stage 3
Yield (% Total solids)	2.85	1.82	1.32
Yield of uronic acid (%)	0.17	0.11	0.09

Yield is represented in terms of fresh whole fronds.

4.3.2 Chemical composition

The composition of freeze-dried crude mamaku gum from different stages is shown in **Table 4.2**. All the gum extracts had high proportion of free sugars (stage 1: ~35%; stage 2: ~40%; stage 3: ~48%) and ash (stage 1: ~14%; stage 2: ~24%; stage 3: ~25%). In all extracts, fructose and glucose were the prevalent sugars, while potassium, sodium, calcium, magnesium and aluminium were the predominant minerals. A similarly high ash and sugar content has been shown for extracts from sesame leaves (Nep et al., 2016) and durian seeds (Amid, Mirhosseini, & Kostadinović, 2012). The amount of ash and sugars remarkably increased with the increasing age of mamaku fronds, while the amount of protein was found to reduce. The extracts were low in fat (stage 1: ~0.5%; stage 2: ~1%; stage 3: ~2%) and starch (stage 1: ~2%; stage 2: ~2%; stage 3: ~1%). About 6-7% of uronic acid was present in all gum extracts. These results are comparable with the mamaku gum extract composition reported previously (Goh et al., 2007).

Constituent sugar analysis of purified mamaku gum showed that the total sugar content increased with the growth stage (from 57.4% in stage 1 to 68.5 % in stage 3), although the relative proportions of each of the sugars was similar at each stage (**Table 4.3**). The samples contained similar amounts of neutral sugars, mostly galactose, mannose and xylose, as reported previously, but the glucuronic acid content was considerably lower (Wee et al., 2014). However, a comparison of the normalised weight percentage of glucuronic acid (27.4–29.9 %, **Table 4.3**) with the relative amounts (mol%) of glucuronic acid linkages (36.1 %) shown by Wee et al. (2014), suggested that the uronic acid content was overestimated in this earlier work. In addition, the relative proportions of glucuronic acid and mannose observed in this current work (~1.2:1) were consistent with a repeating backbone of -4)-β-D-Gla*m*-(1→2)-α-D-Man*p*-(1→, as suggested previously for this and other glucuronomannans

(Aspinall et al., 1955; Barone et al., 1996; Erni et al., 2011; Lai & Liang, 2012; Nep et al., 2016; Wee et al., 2014).

Table 4.2: Proximate, mineral and simple sugar composition of freeze-dried crude mamaku gum.

	Stage 1	Stage 2	Stage 3
Composition (% w/w dry basis)			
Ash	14.2	23.9	25.0
Protein	5.2	2.2	1.6
Fat	0.5	1.2	2.1
Starch	2.4	1.9	1.3
Sugar	34.6	39.5	47.5
Total dietary fibres	15.5	15.4	18.3
Insoluble dietary fibres	1.6	1.4	1.5
Soluble dietary fibres	13.9	14.0	16.8
Uronic acid	5.8	5.7	6.8
Minerals (mg/kg)			
Potassium	62217.2	79382.6	45209.9
Sodium	4072.4	27563.4	44133.5
Calcium	904.9	3528	7642.6
Magnesium	2488.7	1212.8	1937.6
Aluminium	1934.4	2535.8	828.9
Zinc	40.7	71.7	28.0
Manganese	22.3	9.6	10.1
Iron	373.3	374.9	99.1
Copper	14.8	15.6	7.0
Selenium	<0.2	<0.2	<0.2
Lead	0.2	0.2	0.1
Mercury	<0.01	<0.01	<0.01
Free sugars (% w/w)			
Fructose	17.9	20.9	21.6
Glucose	16.1	17.9	25.4
Maltose	<0.1	<0.1	<0.1
Sucrose	<0.1	<0.1	<0.1
Galactose	0.68	0.69	0.43

Table 4.3: Constituent sugar composition of purified mamaku gum.

Monosaccharide	Amount (wt %)[a]			Normalised (wt %)		
	Stage 1	Stage 2	Stage 3	Stage 1	Stage 2	Stage 3
Fucose	0.8	0.6	0.7	1.5	1.0	1.0
Rhamnose	1.2	1.6	1.4	2.1	2.6	2.0
Arabinose	2.1	2.2	2.7	3.6	3.7	4.0
Xylose	5.7	5.9	6.6	9.9	9.7	9.6
Galactose	15.0	17.0	18.4	26.2	27.6	26.9
Glucose	2.6	0.6	1.8	4.6	1.0	2.7
Mannose	13.8	14.9	16.5	24.0	24.2	24.1
Galacturonic acid	0.5	0.2	0.4	0.8	0.3	0.5
Glucuronic acid	15.8	18.4	20.0	27.4	29.9	29.2
Total	57.4	61.4	68.5	100.0	100.0	100.0

[a] Values are the average of duplicate analyses (n=2).

4.3.3 Nuclear magnetic resonance

The ^{1}H and ^{13}C NMR spectra of purified mamaku gum from each of the three stages were almost indistinguishable from each other (**Figure 4.2A** shows ^{1}H spectra) and were very similar to those obtained previously (Wee et al., 2014). The HSQC spectrum of purified mamaku gum from stage 1 is shown in **Figure 4.2B**; the ^{1}H and ^{13}C chemical shifts were partially assigned on the basis of the HSQC and DFQ-COSY experiments and by comparison with published spectra of similar molecules (Barone et al., 1996; Nep et al., 2016; Wagner et al., 2007; Wagner et al., 2008; Wagner et al., 2004).

Signals at H-1/C-1 5.33–5.37/99.7 ppm, with H-3/C-3 3.74/84.4 ppm were assigned to α-D-Man*p* residues with O-3 substitution, as observed previously by glycosyl linkage analysis (Wee et al., 2014). Similarly, signals at H-1/C-1 4.58/102.9 ppm and 4.53/103.5 ppm were assigned to β-D-Glc*p*A residues, which was confirmed by the presence of a carbonyl signal in the ^{13}C NMR spectrum at 171.5 ppm, and by H-1/H-2 correlations in the DFQ-COSY spectrum with H-2 signals at 3.54 ppm (C-2 74.3 ppm) and 3.39 ppm (C-2 73.5 ppm), respectively. The upfield ^{13}C chemical shift of the GlcA carbonyl signal, together with an intense *O*-methyl signal (^{13}C 54.5 ppm, ^{1}H 3.87 ppm) was consistent with methylesterification of this residue. A signal at H-1/C-1 4.70/104.4 ppm was previously assigned as β-D-Gal*p* (Wee et al., 2014), but correlations in the DFQ-COSY spectrum enabled full assignment of the

chemical shifts, which were consistent with *β*-D-Xyl*p* residues (Sims & Newman, 2006). Signals at H-1/C-1 5.24/101.9 and 5.15/103.0 ppm were assigned to *α*-D-Gal*p* residues and a weak signal at H-1/C-1 4.90/99.2 ppm was assigned to *α*-L-Rha*p* residues (H-6/C-6 1.29/17.8 ppm). A signal at H/C 3.44/57.4 ppm suggested that some residues carry a methoxy substituent, such as 3-*O*-methyl rhamnose reported by Barone et al. (1994) for *Ceratozamia spinosa* mucilage.

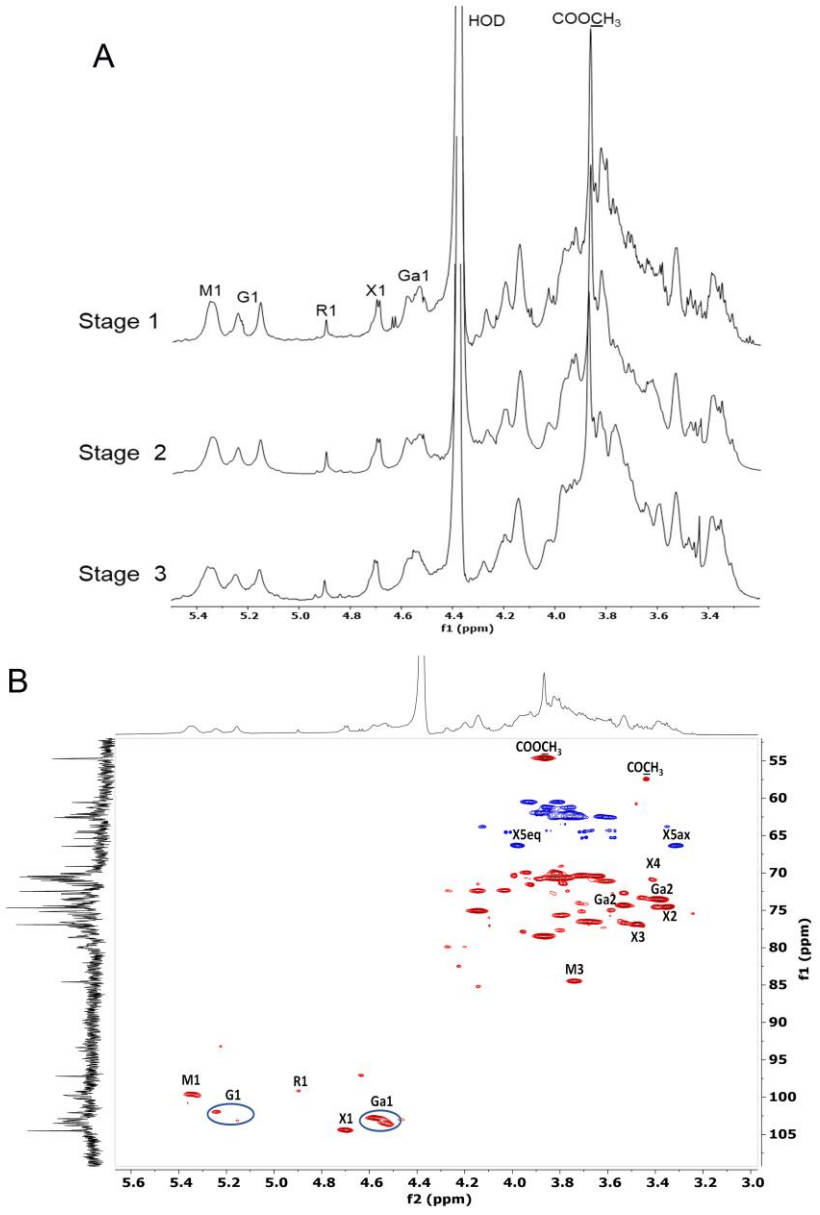


Figure 4.2: (**A**) Selected region of ^{1}H spectra of purified mamaku gum. (**B**) Selected region of DEPT-edited HSQC spectrum of purified mamaku gum from stage 1. M, mannose; G, galactose; R, rhamnose; X, xylose; Ga, glucuronic acid; COOCH$_3$, methylesterification at C-6; COCH$_3$, *O*-methoxy group.

4.3.4 Size-exclusion chromatography coupled with multi-angle laser light scattering

Figure 4.3 shows the chromatogram for purified mamaku gum from different stages at an elution time ranging between 20-30 min. A right-hand shift in eluting time can be observed with increasing age. M_w and R_g significantly decreased with an increase in age; M_w decreased from ~4.1x10^6 Da to ~2.1 x10^6 Da while R_g decreased from ~147 nm to ~108 nm from stage 1 to stage 3, respectively (**Table 4.4**). These results are consistent with Goh et al. (2011) who reported M_w = ~3.2x10^6 Da and R_g = ~144 nm for mamaku gum extracted from a mix of stage 1 and stage 2 fronds. On the other hand, Wee et al. (2014), reported M_w = ~2x10^6 Da and R_g = ~94 nm for mamaku gum extracted from a similar age mix fronds. The differences in these molecular parameters could be due to differences in frond maturity, harvesting season, sample preparation (heating at high temperature and ethanol precipitation) and/or differences in instrumental parameters (different analytical columns and mobile phase were used). Further, our results showed a shift from a monomodal peak to a bimodal peak (for the stage 3 gum) with increasing harvesting age (**Figure 4.3**). This shift in peaks profile was also accompanied by a significant increase in polydispersity index (M_w/M_n). These results suggest that MP undergoes (enzymatic) hydrolysis with the increase in frond maturity which may result in various molecular weight sizes of the polysaccharide. The hydrolysis of polysaccharides with plant ageing is a common phenomenon. There is a variety of enzymes such as β-glucosidase, α-glucosidase, β-mannanase, galacturonanase, β-1,3-glucanase, galactanase and β-xylosidase present in plants that are capable of hydrolysing most of the glycosidic bonds in the polysaccharides (Franková & Fry, 2013). In seeds like guar and locust, galactomannan is the main endosperm carbohydrate that is hydrolysed by enzymes such as 1,4-β-mannan hydrolase, β-mannosidase, and α-galactosidase during germination (McCleary & Matheson, 1974; Reid & Meier, 1973). However, further work is needed to identify enzymes specific to the hydrolysis of MP.

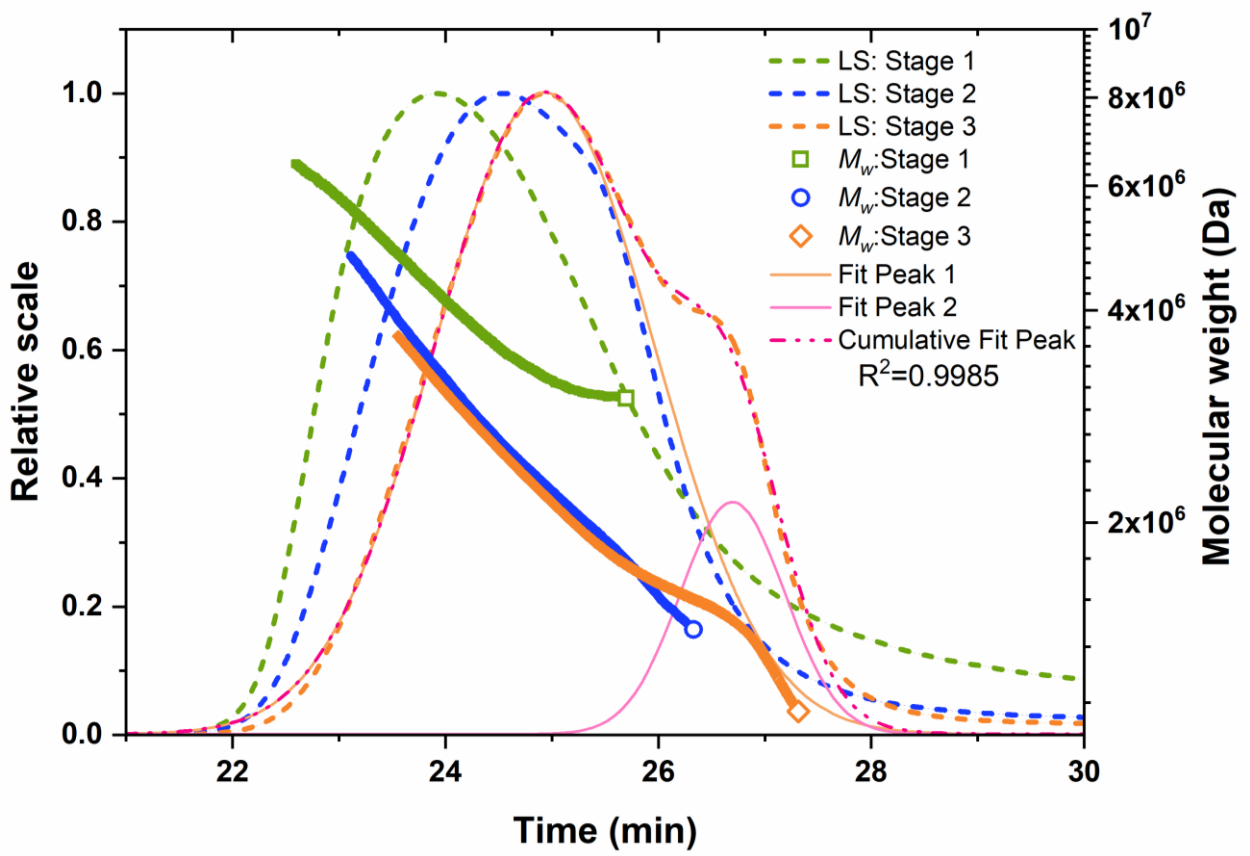


Figure 4.3: Light scattering (LS) signal and weighted-average molecular weight (M_w) analysis by size-exclusion chromatography coupled with multi-angle laser light scattering (SEC-MALLS) of purified mamaku gum. The two peaks for the stage 3 gum sample were deconvoluted using the Gaussian model ($R^2 = 0.999$) in Origin 2020 (Version 9.7.0.185 Academic).

Table 4.4: Molecular parameters of purified mamaku gum analysed by size-exclusion chromatography coupled with multi-angle laser light scattering (SEC-MALLS).

	Weighted-average molecular weight, M_w x 10^6 (Da)	Radius of gyration, R_g (nm)	Slope from the plot of M_w against R_g	Polydispersity, M_w/M_n
Stage 1	4.07±0.16^a	146.45±3.58^a	0.68±0.01^a	1.05±0.01^b
Stage 2	2.61±0.02^b	123.15±1.08^b	0.61±0.01^b	1.14±0.01^a
Stage 3	2.09±0.02^c	107.88±1.31^c	0.6±0.01^b	1.11±0.0^a

Values are expressed as means ± standard deviation (n=3). Values in the same column denoted with the different superscript letters are significantly different ($p \leq 0.05$).

4.3.5 Shear rheology

Shear rheology was performed to quantify the flow behaviour of the gums from the three different harvesting age stages. The viscosity profiles of crude mamaku gum (1%, 3%, 5% and 10% w/w total solids) extracted from the three stages are shown in **Figure 4.4**. Mamaku gum from stages 1 and 2 exhibited the unique rheological behaviour with three different regions—Newtonian region at the low shear rate, followed by a region of shear-thickening at intermediate shear rates, and shear-thinning at higher shear (**Figure 4.4A**, **B**). With the increase in gum concentration for both of these samples (stage 1 and 2), the viscosity increased across the whole shear rate range and the rate at the onset of shear-thickening (critical shear rate- $\dot{\gamma}_{crit}$) shifted to lower shear rates (stage 1: from 6.31 s^{-1} at 3% w/w to 2 s^{-1} at 5% w/w; stage 2: from 7.94 s^{-1} at 3% w/w to 2.51 s^{-1} at 5% w/w). The shear-thickening in MP has been proposed to be due to the unfolding of polymer chains and breaking of intramolecular bonds with increasing shear rate, leading to the formation of intermolecular hydrogen bonds with neighbouring polymer chains (Wee et al., 2015b). When the mamaku gum concentration is increased (*i.e.*, increased polymer concentration in solution), the free volume of the solution and the distance between polymer chains decreases, consequently leading to an increase in viscosity. The reduced distance between polymer chains in the solution facilitates hydrogen bonding between closely located (partially unfolded) polymer chains thereby decreasing the values of $\dot{\gamma}_{crit}$.

Despite similar viscosity profiles for stage 1 and stage 2 gum samples, two key differences were observed (**Table 4.5**); (i) The viscosity developed by the gum from stage 1 was higher than that from stage 2 at all ranges of applied shear. When comparing at 5% (w/w) total solids, the gums from stage 1 and stage 2 had similar uronic acid content (~0.3%) but the maximum viscosity (η_{max} -at the peak) for stage 1 gum was markedly higher, ~4.2 Pa.s (at 12 s^{-1}) compared to the η_{max} for stage 2 gum, ~1.4 Pa.s (at 13 s^{-1}) (**Figure 4.4D**). From this, it is obvious that the difference in viscosity between the two stages is not due to any changes in the uronic acid content (**Figure B.1** in **Appendix B**); (ii) The extent of shear-thickening, defined as the ratio between the peak viscosity during shear-thickening and the viscosity at the onset of shear-thickening (η_{max}/η_{crit}), was higher for stage 2 gum than for stage 1. For

instance, at 3% and 5% (w/w), the extent of shear-thickening for stage 2 gum was ~4.1 and ~3.9, respectively, while it was ~3.5 and ~3.3, respectively, for stage 1 gum.

Contrary to stages 1 and 2 gums, no shear-thickening was observed for the gum from stage 3, even at a high concentration of 10% (w/w) (corresponding to ~0.65% uronic acid) (**Figure 4.4C**). Furthermore, stage 3 gum had the lowest viscosity at all shear rates amongst all three gum samples (**Figure 4.4D**).

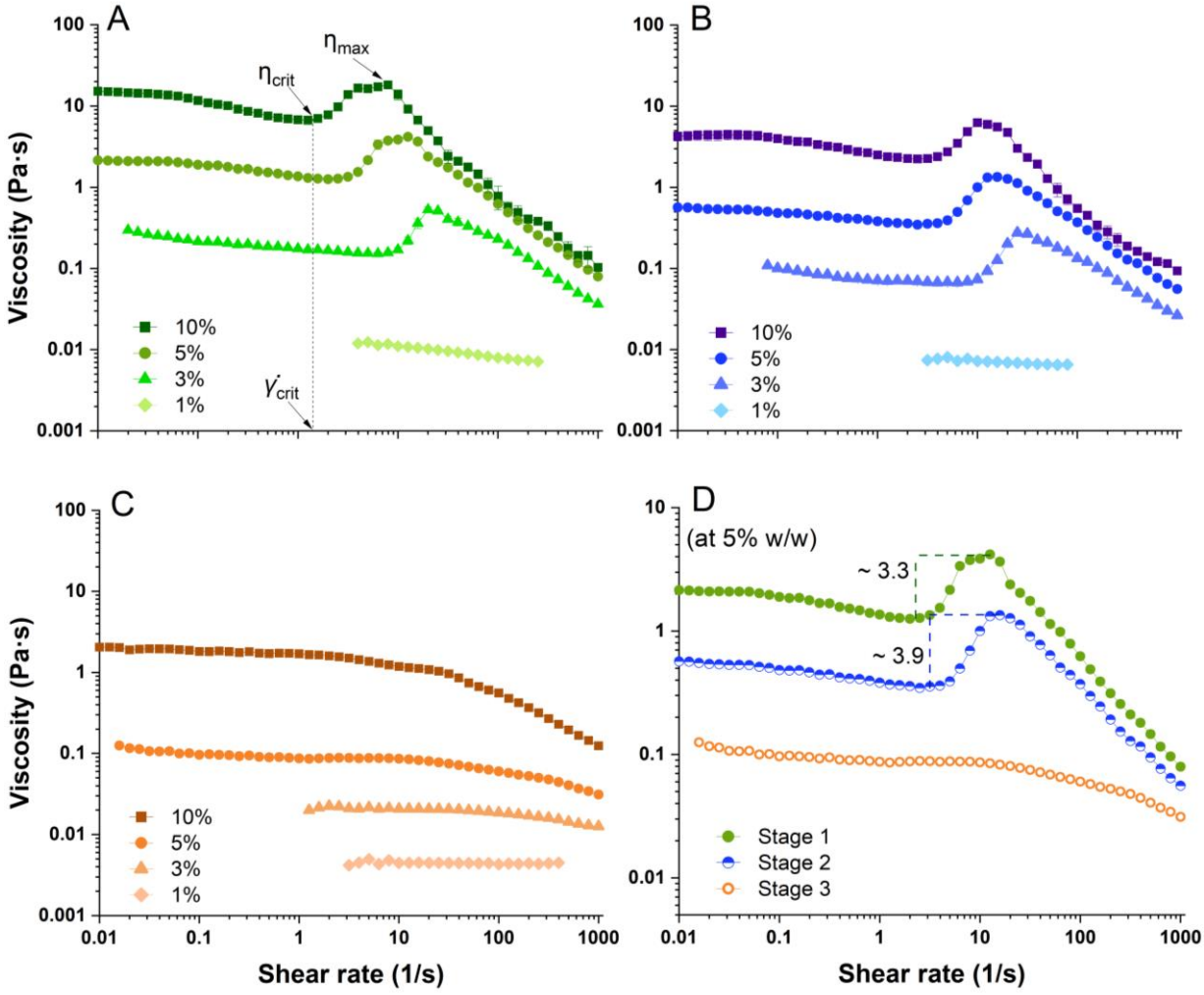


Figure 4.4: Viscosity profiles of mamaku gum extracted from (**A**) stage 1, (**B**) stage 2 and (**C**) stage 3 as a function of shear rate. (**D**) Comparison of viscosity for mamaku gum extracted at 5% (w/w total solids), marked with η_{max}/η_{crit} ratios. Values are plotted as means ± standard deviation (n=3). Measurements were taken using cup-and-bob geometry at 20°C. η_{max}, maximum viscosity (Pa.s); $\dot{\gamma}_{crit}$, critical shear rate (s^{-1}); η_{crit}, critical viscosity (Pa.s); η_{max}/η_{crit}, extent of shear-thickening.

Table 4.5. Comparison of viscosities and critical shear rate for crude mamaku gum from stage 1 and stage 2 at 3%, 5% and 10% (w/w) total solids.

	3%		5%		10%	
	Stage 1	**Stage 2**	**Stage 1**	**Stage 2**	**Stage 1**	**Stage 2**
$\eta_{(0.1\ s^{-1})}$	0.21	0.10	1.89	0.48	11.7	3.99
η_{max}	0.56	0.28	4.18	1.35	18.2	6.27
$\dot{\gamma}_{crit}$	6.31	7.94	2	2.51	1.26	2.51
η_{crit}	0.15	0.07	1.26	0.35	6.71	2.24
η_{max}/η_{crit}	3.47	4.11	3.33	3.89	2.71	2.80

$\eta_{(0.1\ s^{-1})}$, viscosity at 0.1 s^{-1} (Pa.s); η_{max}, maximum viscosity (Pa.s); $\dot{\gamma}_{crit}$, critical shear rate (s^{-1}); η_{crit}, critical viscosity (Pa.s); η_{max}/η_{crit}, extent of shear-thickening. Data extrapolated from graphs in **Figure 4.4**.

Crude mamaku gum from different stages of harvesting age was also subjected to frequency sweep at 5% strain- within the linear viscoelastic region (**Figure 4.5**). Storage (G') and loss moduli (G'') increased for all samples with increasing frequency and concentration. At low frequencies, G'' was above G' for all three samples, indicating a viscous flow behaviour, meaning that MP chains can relax to the original equilibrium configuration within the time scale. With an increase in frequency, for stage 1 and stage 2 gums at 5% and 10% (w/w), G' became dominant over G'' above the crossover frequency ($G' = G''$) (**Figure 4.5A**, **B**). G' greater than G'' indicates a change from viscous to 'gel-like' behaviour. The inverse of frequency at the crossover point is the shear relaxation time (λ_s). With the increase in concentration, the λ_s increased from 0.32 s at 5% to 20 s at 10% for stage 1 gum and from 0.12 s to 4 s for stage 2 (**Table 4.6**). The higher λ_s for stage 1 gum compared to stage 2, suggest that polymer chains in the stage 1 gum form a stronger network of inter- and intra-molecular interactions, thus, taking longer to relax. For stage 3 gum, G'' remained higher than G' for all the concentrations, indicating viscous fluid behaviour, due to limited polysaccharide linkages (**Figure 4.5C**). Similar to the viscosity trend observed above, G' and G'' decreased with an increase in the harvesting age, at a given frequency, as stage 1 > stage 2 > stage 3.

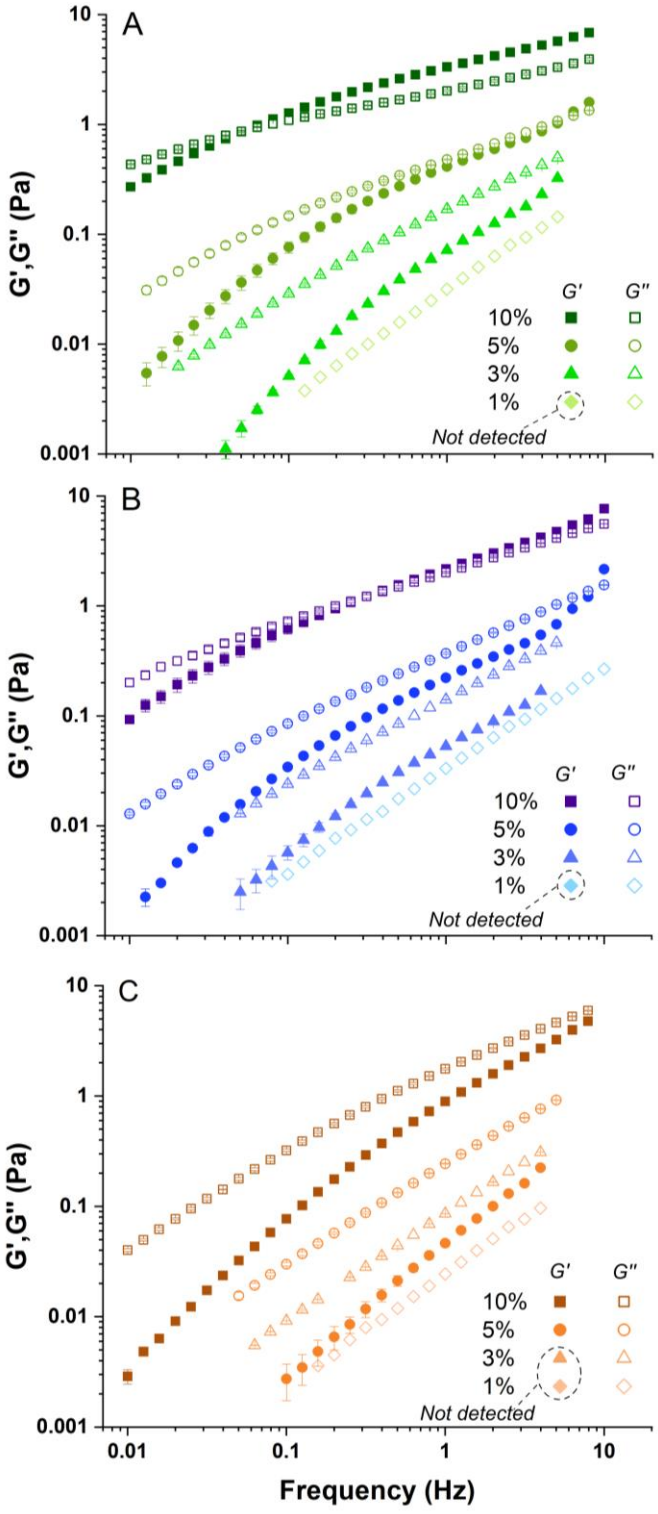


Figure 4.5: Storage modulus (G', filled symbols) and loss modulus (G'', empty symbols) of mamaku gum extracted from (**A**) stage 1, (**B**) stage 2 and (**C**) stage 3 at 1%, 3%, 5% and 10% w/w total solids as a function of frequency. Oscillatory measurements (frequency sweep) were performed in the range of 0.01-20 Hz using a constant strain value of 5% (within the linear viscoelastic region) using the double gap geometry at 20°C. Values are plotted as means ± standard deviation (n=3).

Table 4.6: Crossover frequency and relaxation time (λ_s) for crude mamaku gum from stage 1 and stage 2 at 5% and 10% (w/w) total solids.

Concentration	Stage 1		Stage 2	
	Crossover frequency (Hz)	Relaxation time, λ_s (s)	Crossover frequency (Hz)	Relaxation time, λ_s (s)
5%	3.16	0.317	7.94	0.123
10%	0.0501	20	0.251	3.984

No crossover was observed at 1% and 3% for stage 1 and stage 2 extracts. No crossover was observed at any concentration for stage 3 extract.

4.3.6 Extensional rheology

Figure 4.6 shows the sequence of images demonstrating the filament thinning dynamics as a function of time for crude gum samples from stage 1, stage 2 and stage 3 at 3% and 5% (w/w) total solids concentrations. The time in **Figure 4.6** is normalised by t_b, *i.e.*, $t^{'} = t/t_b$ (t_b values are given in **Table 4.7**). $t^{'} = 0$ is the instant when piston stretching ceases and corresponds to the starting time point of the experiment. Soon after the liquid bridge has been formed, the inertial stresses arising due to displacement of the piston are dominant (inertial regime). This is immediately followed by the viscocapillary regime, where capillary forces are balanced by the viscosity of the fluid. The filament diameter in the viscocapillary regime decreases linearly according to **Equation 4.1** (McKinley & Tripathi, 2000). Following the viscocapillary regime, is the exponential elastocapillary regime where filament diameter decays as $D(t) \sim \exp(-t/3\lambda_e)$ (from **Equation 4.2**) (Entov & Hinch, 1997). The onset of the elastocapillary regime can be viewed in images in **Figure 4.6** (marked in-dash-boxes), characterised by the presence of a stable axially uniform cylindrical fluid filament that thins with time. Mamaku gum from stage 1 and stage 2 enters into the elastocapillary regime faster than in stage 3. With the increase in concentration, the liquid bridge can sustain a thinner fluid filament without breaking; for example, for stage 2 gum, at $t^{'} = 0.65$, the filament diameter decreases with an increase in concentration—attributing to higher elastic stress at 5% (w/w) concentration that retards the breakup. Towards the breakup stage, the polymer chains become fully stretched and the elastic stress can no longer balance the increasing capillary stress, the filament behaves like a viscous Newtonian fluid and the diameter will decay linearly until breakup (Entov & Hinch, 1997). In order to predict the

evolution of diameter in both the elastocapillary and long-time viscous-like regimes, Anna and McKinley (2001) proposed a generalised form of **Equation 4.2** as:

$$D(t) = Ae^{-Bt} - Ct + D \qquad \textbf{Equation 4.6}$$

where A, B, C and D are fitting parameters. The value of B is related to the longest extensional relaxational time (λ_e) of the fluid ($B = 1/3\lambda_e$), and the value of C is related to the steady-state extensional viscosity plateau at larger Hencky strains ($C = \sigma/\eta_{e,\infty}$).

Table 4.7: Capillary breakup time (t_b) and extensional relaxation time (λ_e) for crude mamaku gum samples from stage 1, stage 2 and stage 3 of harvesting age at 1, 3 and 5% (w/w) total solids concentration.

Concentration	Capillary breakup time, t_b (s)			Extensional relaxation time, λ_e (s)		
	Stage 1	Stage 2	Stage 3	Stage 1	Stage 2	Stage 3
1%	0.05	0.08	0.02	0.01	0.01	0.01
3%	2.64	2.71	0.10	1.06	1.11	0.03
5%	10.44	18.15	0.50	3.23	6.8	0.21

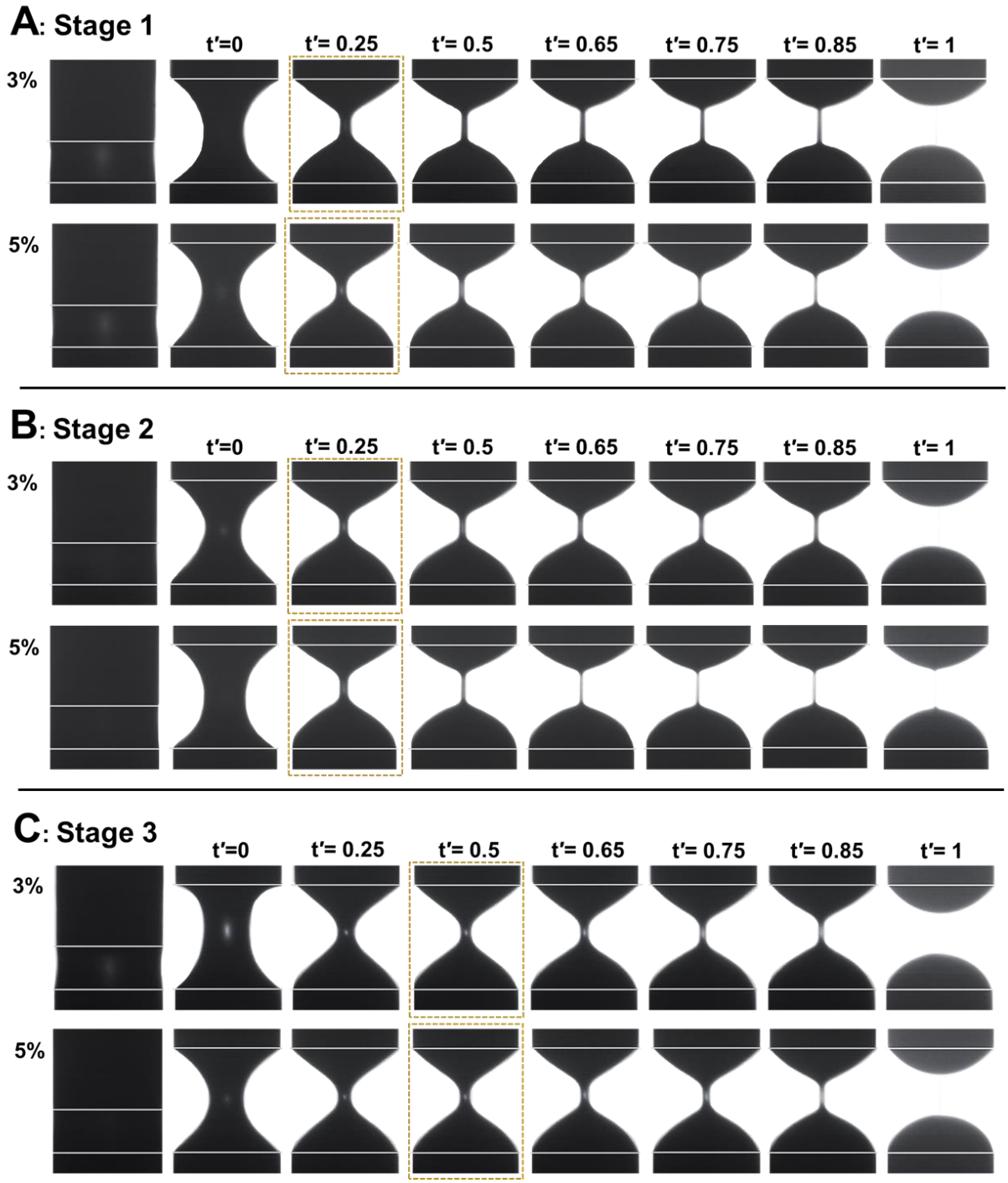


Figure 4.6: Still images of the fluid filament during uniaxial extensional rheology experiment for mamaku gum from (**A**) stage 1, (**B**) stage 2 and (**C**) stage 3 as a function of time. The onset of the elastocapillary regime, characterised by a uniform fluid filament, is marked in-dash-boxes. The time is normalised by t_b, *i.e.*, $t^{'} = t/t_b$ (capillary breakup time, t_b, values are given in **Table 4.7**). The initial gap is $L_o = 1.5$ mm, the final gap $L_f = 4$ mm and the piston diameter $D_o = 4$ mm, giving initial and final aspect ratios of $\Lambda_o = 0.38$ and $\Lambda_f = 1$, respectively.

The evolution of fluid filament diameter with time is shown in **Figure 4.7**. The decrease in filament diameter follows an exponential decay, characteristic of polymer fluids as reported previously for guar gum (Bourbon et al., 2010; Kongjaroen, Methacanon, & Gamonpilas, 2022; Piermaría, Bengoechea, Abraham, & Guerrero, 2016; Szopinski et al., 2016; Torres, Hallmark, & Wilson, 2014), xanthan (Choi, Mitchell, Gaddipati, Hill, & Wolf, 2014; Funami & Nakauma, 2021), mamaku (Jaishankar et al., 2015), locust bean gum (Bourbon et al., 2010; Funami & Nakauma, 2021; Piermaría et al., 2016), polystyrene (Clasen et al., 2006; Vadillo et al., 2012) and polyelectrolyte solutions (Jimenez, Dinic, Parsi, & Sharma, 2018). For mamaku gum extracted from different harvesting ages, t_b increased with an increase in concentration, indicating enhanced entanglement/interactions between stretched polymer chains in a concentration-dependent manner. At a given concentration, filament formed by stage 2 gum took the longest time to break (maximum t_b) while the breakup was fastest for stage 3 gum (minimum t_b). From the filament diameter *vs* time plot, using **Equation 4.2** in the elastocapillary regime, λ_e was calculated and values are given in **Figure 4.7** and **Table 4.7**. On comparing λ_e, stage 2 gum has higher λ_e followed by stage 1 and then stage 3 gum; at 5% (w/w) λ_e was 6.8 s, 3.2 s and 0.2 s respectively.

The relaxation time of a polysaccharide is related to the time taken by the polysaccharide chains to reach an equilibrium state after being disturbed. In this study, λ_s and λ_e were determined from oscillatory shear rheology and filament thinning diameter, respectively, and are given in **Tables 4.6** and **4.7**. At 5% (w/w) mamaku gum concentration for stage 1 and stage 2, λ_e was above λ_s. Similar observations, $\lambda_e > \lambda_s$, were made by Vadillo et al. (2012) and Clasen et al. (2006) for different molecular weight polystyrene solutions and by Szopinski et al. (2016) for carboxymethyl hydroxypropyl guar gum solution. On the contrary, Anna and McKinley (2001) demonstrated that $\lambda_e \approx \lambda_s$ for Boger fluids, while Yesilata, Clasen, and McKinley (2006) and Arnolds, Buggisch, Sachsenheimer, and Willenbacher (2010) showed $\lambda_e < \lambda_s$ for wormlike micelle solution based on erucyl bis(2-hydroxyethyl) methyl ammonium chloride (EHAC) and for poly(ethylene oxide) (PEO) solutions, respectively. The possible reason for the difference in λ_e and λ_s could be due to the difference in the mode of relaxation for shear and extensional flows. During extensional deformation, a single polysaccharide coil deforms and λ_e refers to the disentanglement of the entire polymer chain (Clasen et al., 2006; Szopinski et al., 2016). Whereas under shear

deformation, polysaccharide chain movements can be dominated by entanglements and λ_s refers to the time that a disentangled polymer requires to re-entangle with the neighbouring polymer molecules (Kongjaroen et al., 2022). In the case of mamaku, the possible reason for $\lambda_e > \lambda_s$ could be the more stretched MP under extensional flow—more sites for hydrogen bonding leading to greater intermolecular interactions—compared to partly stretched chains under oscillatory flow. During extensional behaviour, polymers are significantly stretched as they approach the elastocapillary regime, and they are further stretched as the filament evolves until a fully stretched polymer is achieved, thus, making intermolecular interactions significant, causing higher λ_e (Tirtaatmadja, McKinley, & Cooper-White, 2006). Interestingly, Bhardwaj, Miller, and Rothstein (2007), reported a concentration-dependent change in λ_e/λ_s for wormlike micelle solutions of cetylpyridinium chloride and sodium salicylate (NaSal) and cetyltrimethylammonium bromide and NaSal; at low concentration, λ_e was lower than λ_s, while at higher concentration λ_e was above λ_s. Mamaku concentration of 5% (w/w) is above the coil overlap concentration (c^*=2.2% (w/w) (Goh et al., 2007) so, $\lambda_e > \lambda_s$ for mamaku gum could also be a concentration effect, as λ_e is reported to be more sensitive to concentration than λ_s (Bhardwaj et al., 2007; Clasen et al., 2006; Tirtaatmadja et al., 2006). Since no crossover was observed at 1% and 3% concentrations from oscillatory data, λ_s was not determined and no comparison between λ_e and λ_s was made at lower concentrations.

The elastocapillary balance persists for sufficient time for stage 1 and stage 2 gum samples at 3% and 5% (w/w) concentrations, thus, 3% and 5% (w/w) concentrations were used to estimate apparent transient extensional viscosity, η_e, as a function of accumulated Hencky strain, $\varepsilon_H(t)$. A marked increase in η_e was observed for both sample types as $\varepsilon_H(t)$ increases in a concentration-dependent manner; ultimately reaching a plateau due to the molecules reaching their finite extensibility limit (**Figure 4.7D**). Similar to λ_e trend, η_e was higher for the gum from stage 2 than from stage 1, suggesting stronger extensional behaviour for the former. For both stage 1 and 2 gum, the η_e is considerably higher ($\eta_e > 200$ Pa.s) than other polymers such as guar gum ($\eta_e < 10$ Pa.s) (Torres et al., 2014), hydroxypropyl ether guar gum ($\eta_e < 10$ Pa.s) (Duxenneuner, Fischer, Windhab, & Cooper-White, 2008), and okra polysaccharide ($\eta_e < 100$ Pa.s) (Yuan et al., 2018a). Also, $\eta_e \gg \eta_s$ suggests that MP exhibits a more dramatic response to extensional deformation compared to shear deformation as the

association of MP chains is strengthened in extensional flow since the polymer is more stretched.

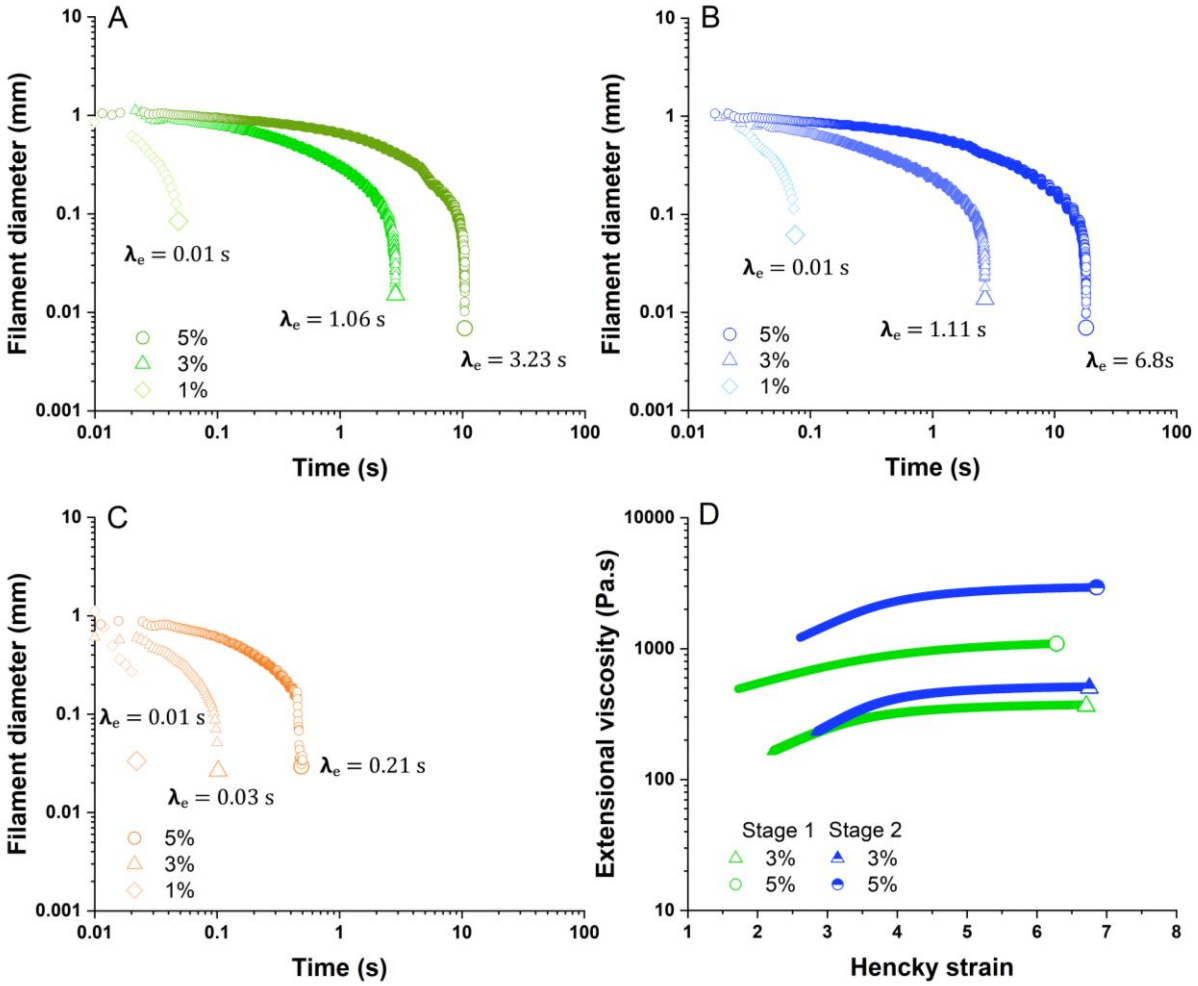


Figure 4.7: Dynamics of midfilament diameter as a function of time for mamaku gum extracted from (**A**) stage 1, (**B**) stage 2 and (**C**) stage 3. (**D**) Transient extensional viscosity of mamaku gum from stages 1 and 2 as a function of Hencky strain. λ_e, extensional relaxation time.

4.4 General Discussion

MP is a negatively charged biomacromolecule with unique rheological properties. Herein author showed that the rheological behaviour of MP is dependent on the harvesting age of the mamaku fronds. The molecular weight (chain length) of MP decreases (**Figure 4.3** and **Table 4.4**), with increasing harvest age without any apparent alteration in chemical structure (**Figure 4.2** and **Table 4.3**). The harvesting-age-dependent decrease in the chain length of MP

leads to a reduction in viscosity at all shear rates ($\eta_{s-Stage\,1} > \eta_{s-Stage\,2} > \eta_{s-Stage\,3}$, **Figure 4.4D**). A similar molecular weight-dependent decrease in viscosity was observed previously for xanthan gum (Holzwarth, 1978), guar gum (Beer, Wood, & Weisz, 1999) and starch (Iida, Tuziuti, Yasui, Towata, & Kozuka, 2008).

Despite MP from stage 1 having a higher molecular weight than that from stage 2, t_b, λ_e and η_e were greater for the latter (**Figure 4.7**). Furthermore, the trend for extensional behaviour is similar to the ratio η_{max}/η_{crit}, observed in shear rheology (stage 2 > stage 1) (**Figure 4.4D**). For extensional rheology, in general, t_b, λ_e and η_e increase with an increase in molecular weight (Anna & McKinley, 2001; Wunderlich et al., 2000). However, for polymers with complex architecture, the extensional behaviour can also be influenced by additional structural parameters like the rigidity of the backbone and the degree and length of branching, which can influence the interaction between the polymer chains. For example, in the case of polymer melts, the extensional behaviour was reported to be more pronounced for long-chain-branched polymer melts than linear polymer melts—explained by an increase in resistance to flow by the side branches after reaching a certain chain length sufficient for intermolecular entanglements (Vasilyev, Dreval, Malkin, & Kulichikhin, 2010; Wagner et al., 2000), and/or the ability of branches to distribute the stress into material leading to longer relaxation time (Kasehagen & Macosko, 1998). In this study, there was no difference in the chemical structure of the polysaccharide extracted from different harvesting ages, but only the size of the polysaccharide.

The observed behaviour suggests greater intermolecular interactions between polymer chains from stage 2 than in stage 1. The presence of high protein (~5.2% w/w dry bases, **Table 4.2**) in the stage 1 sample may interfere with the intermolecular interactions between MP chains, resulting in lower η_{max}/η_{crit}, t_b, λ_e and η_e, than stage 2 sample. Simultaneously, the difference in the ash content of stage 1 and stage 2 extracts (**Table 4.2**), resulting in different ionic strengths of ~14.8 mM and ~23 mM, respectively, might affect the screening of negative charges on MP. Wee et al. (2015a) reported that MP is very sensitive to the ionic strength of the system, especially at concentrations below 200 mM. With increasing ionic strength, intramolecular repulsion within the MP chains reduces, making them less extended, therefore decreasing viscosity. Thus, the effect of ionic strength on the viscosity of

the stage 1 sample was tested. The ionic strength of the stage 1 sample was increased to match the ionic strength of stage 2 sample by adding NaCl or $CaCl_2$. A decrease in the viscosity at low shear rates (0.01-1 s^{-1}) was observed (**Figure 4.8**); η_{crit} reduced on increasing ionic strength without affecting η_{max}, thereby increasing the η_{max}/η_{crit} (~3.9). The increased η_{max}/η_{crit} for stage 1 after adding salts was comparable to the native stage 2 sample. However, at similar ionic strength, one would expect higher η_{max}/η_{crit} for longer MP chains from the stage 1 sample, thus, the difference in ionic strength alone cannot explain the observed behaviour. Additionally, there may be a critical chain length of the polysaccharide where maximum intermolecular hydrogen bonding is achieved, resulting in stronger shear-thickening and extensional behaviours. The polysaccharide chains from stage 2 fronds, upon shearing/stretching, may unfold completely by disrupting intramolecular bonds. This will expose a greater number of associative groups, leading to the formation of intermolecular hydrogen bonding (**Figure 4.9B**). As the chain length increases above the critical length (in the case of stage 1), the intramolecular interactions per chain may also increase, which may limit the unfolding of the chains upon shearing/stretching. Thus, limiting the exposure of associative groups can result in reduced intermolecular interactions than for the shorter chain lengths of MP from stage 2 (**Figure 4.9A**). On the contrary, as the chain length decreases below the critical length, the polymer chains are likely to unfold completely upon shearing/stretching, however, the shear-thickening and extensional behaviours may reduce due to a decrease in the number of sites for intermolecular interaction. As the chain length decreases further, beyond a certain limit, there may be no intermolecular interaction between MP chains to cause shear-thickening behaviour as observed in the stage 3 MP (**Figure 4.9C**).

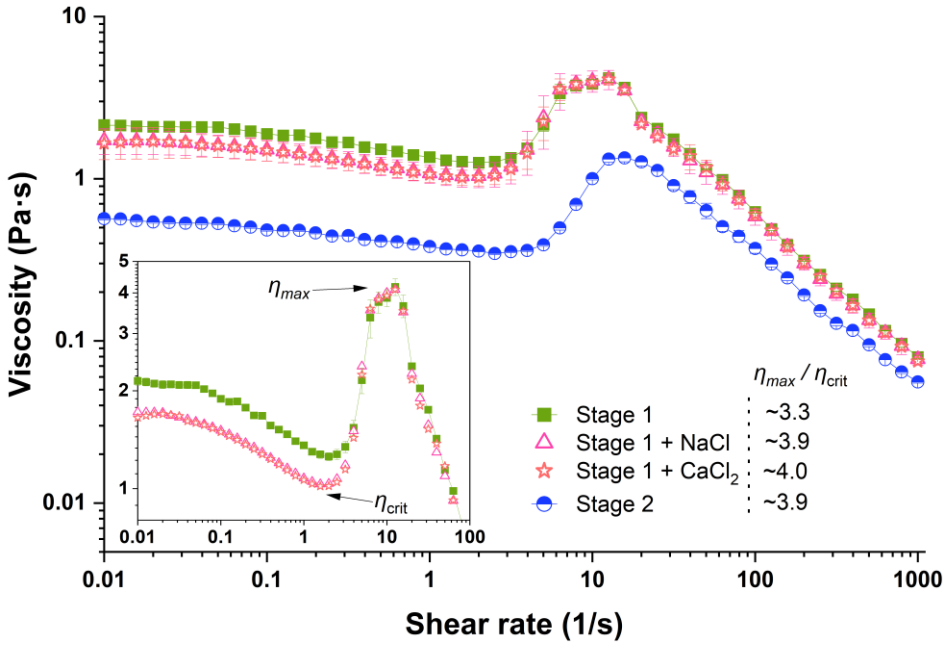


Figure 4.8: Viscosity profile of mamaku gum (5% w/w) from stage 1 after altering ionic strength by adding NaCl and $CaCl_2$. Native stage 1 and stage 2 mamaku gum (5% w/w) are shown for reference.

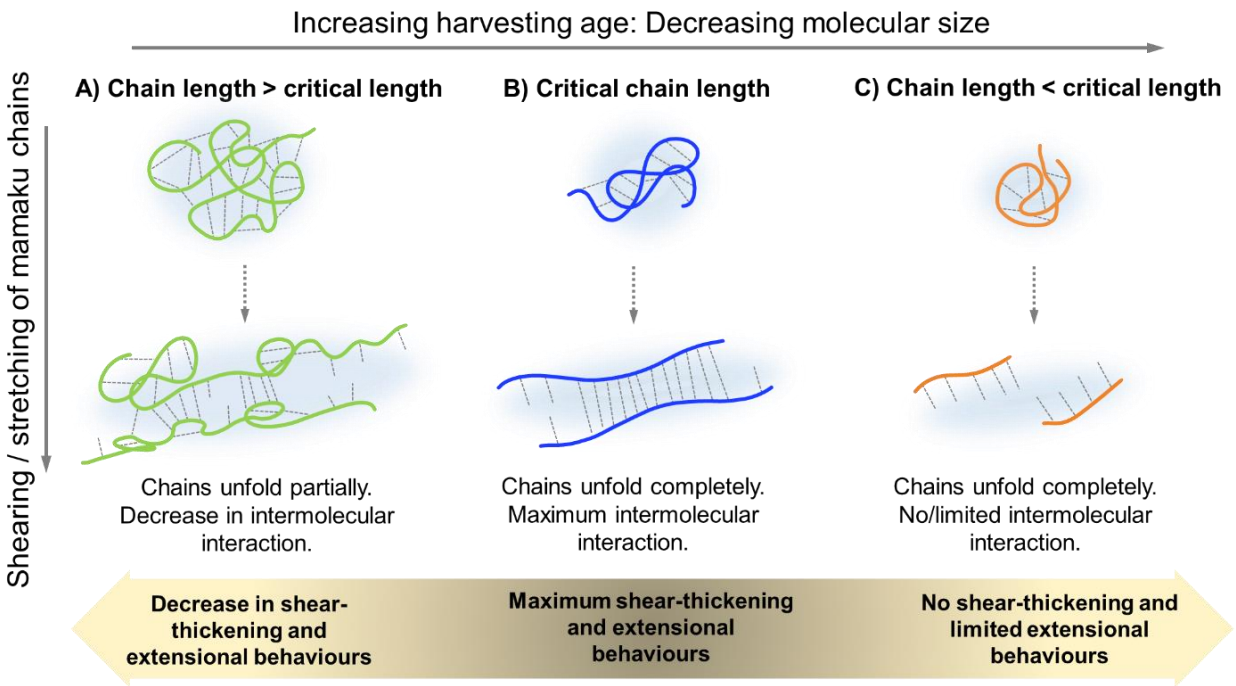


Figure 4.9: Schematic illustration showing the unfolding of mamaku polysaccharide chains from (**A**) stage 1, (**B**) stage 2 and (**C**) stage 3 on shearing or stretching and influence on intermolecular hydrogen bonds with neighbouring chains.

Interestingly, with the increase in the concentration of MP, the η_{max}/η_{crit} decreases and the difference between η_{max}/η_{crit} for the polymers from stage 1 and stage 2 reduces—at 10% (w/w) η_{max}/η_{crit} was ~2.7 for both gum samples (**Table 4.5**). The reduction in η_{max}/η_{crit} could be attributed to a decrease in free volume with an increase in concentration, which may limit the unfolding of MP chains and consequently, intermolecular interactions. On the other hand, the difference in extensional behaviour for stage 1 and stage 2 samples becomes more pronounced with an increase in concentration (**Figure 4.7** and **Table 4.7**). In addition to chain length, the extensional behaviour may also be affected by the number of polymer chains. At a given concentration of gum from stage 1 and stage 2, the gum from stage 2 will have a higher number of polymer chains—because of its smaller size—thus, have more load-bearing strands, which can result in stronger extensional behaviour when compared to stage 1 gum (Liu et al., 2013).

Overall, this study shows the age-dependent decrease in the molecular weight of the MP as the fronds mature, which impacted the shear and extensional behaviours, thus, confirming the original hypothesis. Based on these results, young and fully grown fronds may be harvested to extract MP with retained shear-thickening behaviour and longer capillary breaking time than MP from senescent (dying) frond. But will MP from different age fonds have any different impact on gut health is still unknown and is explored in the next chapter.

Chapter 5

The fate of mamaku gum in the gut: Effect on *in vitro* gastrointestinal function and colon fermentation by human faecal microbiota

5.1 Introduction

Mamaku gum has been traditionally used for treating wounds, bruises and boils and as a remedy for sore stomach and diarrhoea (Crowe, 2004; Foster, 2008; McGowan, 2014; Riley, 1994). Some of these physiological effects are commonly attributed to mamaku polysaccharide (MP), present in the gum. MP exhibits a unique rheological behaviour as shear-thickening develops at a shear rate similar to that occurring in the human gut (Goh et al., 2007; Matia-Merino et al., 2012). This shear-thickening behaviour altered the peristalsis contractions in an *ex vivo* rat stomach model when compared with guar gum at similar viscosity, suggesting a delay in the gastric emptying (Lentle et al., 2010). In a subsequent *in vivo* rat study, food consumption was reduced in rats gavaged with mamaku gum and the weight of the stomach content, retrieved 2 h after final gavage, was higher in the mamaku gum-treated group than in the control group (Wee et al., 2017).

In addition to delaying gastric emptying, non-starch polysaccharides are reported to enhance host health locally in various regions of the gastrointestinal tract (*e.g.*, enhancing the faecal excretion of bile acids, regulating the activity of digestive enzymes, influencing gut microbiota and microbial production of short-chain fatty acids), and systemically (*e.g.*, reducing blood cholesterol levels) (Brownlee, 2011; Capuano, 2017; Dikeman & Fahey Jr, 2006; Williams et al., 2019). For instance, in the upper gut, polysaccharides from *Dendrobium officinale* and *D. aphyllum* flowers and *β*-glucan from barley were shown to reduce the *in vitro* activity of *α*-amylase, pepsin and lipase enzymes (Wang, Liang, & Liu, 2019). The polysaccharide obtained from *Laminaria japonica* has also been shown to have bile acid-binding capacity (Gao, Lin, Sun, & Zhao, 2017).

In the lower gut, supplementation with konjac, guar gum or locust bean gum can differentially alter the gut microbiota composition and reduce the body weight gain in obese mice (Song et al., 2021). Likewise, supplementation with fructan has been reported to

increase the abundance of probiotic bacteria from *Bifidobacterium* and *Lactobacillus* genera and reduce body weight in obese-diabetic rats (Rendón-Huerta, Juárez-Flores, Pinos-Rodríguez, Aguirre-Rivera, & Delgado-Portales, 2012). The supply of non-digestible fermentable polysaccharides to the colon is an important factor that limits the growth and survival of gut microbiota. Microbes can enzymatically hydrolyse undigested polysaccharides or host mucin to extract energy and therefore, those bacteria that can consume available substrate most rapidly increase in abundance (Cummings & Macfarlane, 1991). During fermentation by gut microbiota, short-chain fatty acids (SCFAs) such as acetate, propionate and butyrate are major metabolites produced. SCFAs can benefit the host through anti-microbial, anti-carcinogenic and anti-inflammatory effects, lipid metabolism, improve immunity, maintain epithelial barrier function and act as a substrate for cross-feeding of colonic microbiota (Hugenholtz et al., 2013). SCFAs are also related to the expression of satiety hormones like glucagon-like peptide 1 (GLP-1) and peptide YY which may reduce the food intake in humans (Sánchez-Moya et al., 2017). However, the effects of MP on gut functioning are not known.

Furthermore, the conditions during gastric and intestinal digestion (pH, enzymes and bile acids) have been reported to alter the structure of the polysaccharides (Carnachan, Bootten, Mishra, Monro, & Sims, 2012; Tian et al., 2023). A study showed a decrease in molecular weight (M_w) of *Holothuria leucospilota* polysaccharide throughout gastrointestinal digestion (Yuan et al., 2019). Changes in the structural integrity, amongst other factors, can influence the biological functionality of polysaccharides through the gut, especially colonic fermentation. Thus, it is necessary to explore the effect of the gastrointestinal environment on the stability of polysaccharides.

Despite a few studies conducted with MP, it is unknown how MP can affect digestion in the upper gut and subsequent fermentation in the lower gut. As shown in **Chapter 4**, the rheological behaviour of MP changes with an increase in the harvesting age of fronds. The MP from old fronds loses the shear-thickening behaviour. Thus, this study aimed to explore the gastrointestinal and fermentation behaviours of MP extracted from three different age (stage 1, 2 and 3) fronds using *in vitro* models. It was hypothesised that MP is an indigestible

biomacromolecule that can reduce the activity of digestive enzymes (α-amylase, pepsin and lipase), bind to bile salts, and can be utilised by the colonic microbiota.

5.2 Materials and Methods

5.2.1 Extraction of mamaku gum

Mamaku fronds from three different age groups were harvested as described previously (**Section 3.1 and 4.2.1**). Stage 1 refers to young fronds, stage 2 refers to fully grown fronds, while stage 3 refers to fronds starting to die, where brown sections were observed (**Figure 4.1**). The fronds were chopped, blended with water, and heated to ~55°C for 5 min and the exuded gum was collected. The extracts were left undisturbed overnight at 4°C for the remains of pulp to sediment by gravity. The clearer top layer was then separated using a siphon, and the 'crude gum extract' was freeze-dried (**Section 3.1.1**).

5.2.2 Molecular weight analysis during *in vitro* simulated gastric and intestinal digestion

The crude gum samples from different age mamaku fronds were hydrated overnight (5% w/w) and ultra-centrifuged (250,000 *g*, 1 h, Sorvall WX Ultra 100, T-865 motor, Thermo-Fisher Scientific, Waltham, Massachusetts, USA), dialysed (molecular weight cut-off: 12,000-14,000 Da) against reducing NaCl concentrations (0.01 M, 0.001 M and milli-Q water only) for ~42 h at 4°C, and the 'purified gum fraction' was freeze-dried.

Overnight-hydrated purified gum (4% w/w) and freshly prepared simulated gastric fluid (SGF, **Table 3.1**) and simulated intestinal fluid (SIF, **Table 3.1**) were preheated to 37°C. Purified gum (10 ml) was mixed with SGF (10 ml) containing pepsin (porcine gastric mucosa pepsin, P7012, Sigma-Aldrich, Saint Louis, Missouri, USA, final concentration: 2,000 U/ml), and pH was adjusted to 3 using HCl (3 M). Gastric digestion was initiated by incubating the reaction tubes at 37°C in a shaking water bath for 2 h. For intestinal digestion, purified gum (10 ml) was mixed with SIF (10 ml) containing bile solution (porcine bile extract, B8631, Sigma-Aldrich, Saint Louis, Missouri, USA, final concentration: 10 mM) and pancreatin (porcine pancreas pancreatin, P7545, Sigma-Aldrich, Saint Louis, Missouri, USA, final concentration: 100 U/ml of trypsin). The pH was adjusted to 7 using NaOH (6 M) and reaction tubes were incubated at 37°C in a shaking water bath for 2 h (Brodkorb et al., 2019).

The mamaku gum samples were not digested sequentially from the gastric to intestinal phase to avoid the effect of dilution (dilution from one phase to another) and ionic strength (addition of more salts) on M_w determination. The activity of all enzymes was tested before use following Minekus et al. (2014).

After 0, 1 and 2 h of gastric and intestinal digestion, an aliquot (1 ml) was removed, centrifuged (10,000 *g*, 5 min at 4°C) and immediately analysed for M_w using high-performance liquid chromatography (HPLC) system (Shimadzu, Kyoto, Japan) coupled with multi-angle laser light scattering (Dawn Heleos 8+, Wyatt Technology Corp., California, USA), as described in **Section 4.2.5**.

5.2.3 Effect on enzyme activity and bile acids binding ability

The activity of α-amylase was assayed according to Deshpande, Sathe, Salunkhe, and Cornforth (1982) with modifications based on Infogest 2.0 (Brodkorb et al., 2019). Briefly, α-amylase solution (0.2 ml, porcine pancreatic α-amylase, E-PANAA, Megazyme, Bray, Ireland, final concentration: 200 U/ml) was mixed with potato starch slurry (4 ml, 1% w/v in SIF, Pre-gelatinised, P75, National Starch Food Innovation, Auckland, New Zealand) and overnight hydrated crude mamaku gum samples (0.8 ml, initial concentrations 1% or 4% w/w) at 37°C for 1 h in a shaking water bath. The reaction was stopped by mixing the sample (1 ml) with ethanol (4 ml). After centrifugation (5,000 *g*, 10 min at 4°C), a sub-sample (0.5 ml) was removed, and subsequent glucose content was determined using the 3,5-dinitrosalicylic acid (DNS) method (Mishra & Monro, 2012).

Pepsin activity was determined using a method described by Hu, Nie, Li, and Xie (2013) with modifications based on Infogest 2.0 (Brodkorb et al., 2019). Briefly, haemoglobin suspension (0.5 ml, 1% w/v in SGF, bovine blood haemoglobin, H2500, Sigma-Aldrich, Saint Louis, Missouri, USA) was mixed with pepsin (0.1 ml, final concentration: 2,000 U/ml) and overnight hydrated crude mamaku gum samples (0.5 ml, initial concentrations 1% or 4% w/w) at 37°C for 1 h in shaking water bath. The reaction was stopped by adding trichloroacetic acid (TCA, 0.9 ml, 5% w/v, T6399, Sigma-Aldrich, Saint Louis, Missouri, USA), followed by centrifugation (5,000 *g*, 10 min at 4°C). The protein content in the supernatant

was determined using a modified Lowry protein assay kit, as described by the manufacturer (Pierce™, 23240, Thermo-Fisher Scientific, Waltham, Massachusetts, USA).

Lipase activity was determined according to Shimura, Tsuzuki, Kobayashi, and Suzuki (1992) with modifications based on Infogest 2.0 (Brodkorb et al., 2019). Briefly, olive oil (1 ml, O1514, Sigma-Aldrich, Saint Louis, Missouri, USA) and overnight hydrated crude mamaku gum samples (1 ml, initial concentrations 1% or 4% w/w) were mixed with SIF (5 ml) at 37°C for 10 min, followed by addition of lipase solution (1 ml, Amano lipase A from *Aspergillus niger*, 534781, Sigma-Aldrich, Saint Louis, Missouri, USA, final concentration: 2,000 U/ml) at 37°C for 1 h in shaking water bath. The reaction was stopped by placing the tubes in a boiling water bath for 5 min and cooling them under running water. After centrifugation (5,000 *g*, 10 min at 4°C) the amount of free fatty acids (oleic acid) released in the reaction mixture was quantified by titration with NaOH (0.05 N) using phenolphthalein as an indicator.

Water (without mamaku gum) was used as a control for all enzyme activity assays. Samples without substrate were also tested and any contribution of mamaku gum to reaction products was subtracted. The residual enzyme activities were calculated using:

$$Residual\ enzyme\ activity = \frac{Amount\ of\ digestion\ product\ in\ sample}{Amount\ of\ digestion\ product\ in\ control} \times 100 \qquad \textbf{Equation 5.1}$$

The ability of mamaku gum to bind bile acids was determined using Huang, Chow, and Tsai (2012) with modifications based on Infogest 2.0 (Brodkorb et al., 2019). Briefly, bile solution (0.22 ml, prepared in SIF, final concentration: 10 mM), pancreatin (0.09 ml, prepared in SIF, final concentration: 100 U/ml of trypsin) and overnight hydrated crude mamaku gum samples (0.5 ml, initial concentrations 1% or 4% w/w) were mixed with SIF (2.7 ml) at 37°C for 1 h in shaking water bath. The reaction was stopped by adding ethanol (14 ml) to precipitate the mamaku gum, followed by centrifugation (5,000 *g*, 10 min at 4°C). The bile acids in the supernatant were measured using a total bile acids assay kit, as described by the manufacturer (DZ042A-KY1, Diazyme Laboratories, Poway, California, USA). The relative bile acids binding activity is expressed with reference to control (cholestyramine resin - bile acid sequestrant, 1% w/v, C4650, Sigma-Aldrich, Saint Louis, Missouri, USA; Cholestyramine

bile acids binding ability was defined as 100%). Water (without mamaku gum) was used as a reagent control.

5.2.4 *In vitro* static colonic fermentation

Crude mamaku gum (from stage 1, 2 and 3), inulin (I2255, Sigma-Aldrich, Saint Louis, Missouri, USA), guar gum (IngredietStop™, Hawkins Watts Ltd., Auckland, New Zealand) and water (blank- group without any carbon source) were subjected to *in vitro* static digestion following Infogest 2.0 (Brodkorb et al., 2019) and subsequent colonic fermentation as described previously (Liu et al., 2020; Parkar et al., 2012; Sánchez-Moya et al., 2017) with slight modifications (**Figure 3.19**). Briefly, the samples were digested for oral (using porcine pancreatic α-amylase, final concentration: 75 U/ml), gastric (**Section 5.2.2**) and intestinal (**Section 5.2.2**) phases. Amyloglucosidase (0.1 ml, from *Aspergillus niger*, E-AMGDF, Megazyme, Bray, Ireland) was also added during intestinal digestion to simulate secondary digestion. The digested samples were dialysed (molecular weight cut-off: 12,000-14,000 Da) for ~24 h at 4°C, with three changes of milli-Q water to stimulate intestinal absorption. An aliquot (1 ml) was collected after dialysis and the presence of simple sugars was tested using DNS assay; no simple sugar was detected in any sample. For the fermentation, sterile basal nutrient growth media (BNGM, pH 6.8, 5x concentrate) containing peptone (10 g), yeast extract (10 g), NaCl (0.5 g), KH_2PO_4 (0.2 g), K_2HPO_4 (0.2 g), $MgSO_4.7H_2O$ (0.05 g), $CaCl_2.6H_2O$ (0.05 g), $NaHCO_3$ (10 g), hemin (0.1 g), cysteine HCl (2.5 g), bile salts (2.5 g), Tween-80 (10 ml), vitamin K (50 µl) and resazurin dye (5 ml, 1% w/v solution) per litre was prepared.

Faecal samples were obtained from four healthy donors (two males and two females of Māori ethnicity, 18 to 40 years of age, non-smokers, not suffering from any colon disease) who were eating a regular diet with no history of antibiotic use for at least 3 months prior to the study. The volunteers gave informed written consent to the study protocol, as approved by Massey University Human Ethics Committee (SOA 20/51) (**Appendix C**). Fresh faecal samples were collected in a sterile container which was immediately transferred to an air-tight bag containing an anaerobic sachet (BD GasPak™ EZ Anaerobe Container System Sachets with Indicator, Franklin Lakes, New Jersey, USA). The faecal samples were stored at -80°C and used within three days. An equal amount of faeces from each volunteer were pooled and mixed in sterile phosphate buffer saline (PBS, 0.01 M, pH 7.4; faeces: PBS at 1:9

w/v) using a stomacher and centrifuged (350 *g*, 5 min) to separate the solid residues. The supernatant was immediately transferred to an anaerobic jar and used as a 'faecal slurry' for further experiments.

Fermentation was set up in sterile Hungate tubes (purged with CO_2) by mixing digested samples (5 ml, final concentration 1% w/w), with faecal slurry (1 ml, final concentration 1% w/v), sterile 5x BNGM (2 ml, final concentration 1x) and sterile distilled water (2 ml) and incubated in anaerobic jars at 37°C with shaking at 100 rpm for 24 h. Hungate tubes were withdrawn from anaerobic jars at 0, 6, 12 and 24 h and stored on ice for ~15 min before further analysis. Media (BNGM and PBS), substrate (digested samples) and distilled water used during fermentation were purged with CO_2 and pre-reduced in an anaerobic jar at room temperature for ~12 h and then at 37°C for ~1 h before initiating fermentation.

5.2.4.1 Determination of pH and short-chain fatty acids

The pH of fermented samples was measured using a pH meter (Mettler Toledo, Columbus, Ohio, USA). Fermented samples (1 ml) were centrifuged (15,000 *g*, 10 min at 4°C) and supernatants were collected for SCFAs quantification using a modified gas chromatography (GC) method (Richardson, Calder, Stewart, & Smith, 1989), while the precipitate was used for microbial analysis. The supernatant (100 µl) was mixed with 400 µl of 0.01 M PBS containing 2-ethylbutyric acid (6.25 mM, 109959, Sigma-Aldrich, Saint Louis, Missouri, USA) as an internal standard. This was acidified with 250 µl concentrated HCl followed by the addition of 1000 µl diethyl ether. The mix was vortexed (10 sec) and centrifuged (10,000 g, 5 min at 4°C). The diethyl ether phase was stored at -80°C until analysis on GC.

In a capped GC vial, 100 µl of the diethyl ether phase was derivatised with 20 µl N-tert-butyldimethylsilyl-N-methyltrifluoroacetamide with 1% tert-butyldimethylchlorosilane (MTBSTFA + TBDMSCI, 99:1; Sigma-Aldrich, Saint Louis, Missouri, USA) in a water bath at 80°C for 20 min. Once cooled the derivatised sample was transferred to a GC vial insert. To allow complete derivatisation the samples were left for 48 h at room temperature before analysis on GC. Standards containing 2-ethylbutyric acid (5 mM) as an internal standard were prepared for derivatisation alongside the samples.

GC analysis was performed using a Shimadzu capillary GC system (GC-2010 Plus, Tokyo, Japan) equipped with a flame ionization detector (FID) and Restek column (SH-Rtx-1, 30 m × 0.25 mm ID × 0.25 μm, Shimadzu, Kyoto, Japan). Helium was used as carrier gas with a flow rate of 21.2 ml/min and a pressure of 131.2 kPa. The temperature program began at 70°C, increased to 115°C at 6°C/min, with a final increase to 300°C at 60°C/min, and maintained for 3 min. Samples were injected (1 μl) with a split injection (split ratio 10:1). Injector temperature was 260°C and the detector temperature was 310°C. Data were processed using Shimadzu GC Work Station LabSolutions (Version 5.96). Acquired data were expressed as μmol acid/ml fermented sample.

5.2.4.2 DNA extraction, amplification and 16S rRNA gene sequencing

The precipitate collected in the SCFAs analysis was used to determine the relative bacterial abundance and diversity. The DNA was extracted using NucleoSpin® 96 Soil kit (Macherey-Nagel, Düren, Germany) according to the manufacturer's instructions. The DNA quantity and quality were determined using a Colibri spectrophotometer (Titertek Berthold, Pforzheim, Germany). V3-V4 hypervariable region of 16S rRNA gene was amplified using universal barcoded fusion primers:

16SF_V3 (5′-AATGATACGGCGACCACCGAGATCTACAC-barcode-TATGGTAATTGGCCTACGGGAGGCAGCAG-3′) and 16SR_V4 (5′-CAAGCAGAAGACGGCATACGAGAT-barcode-AGTCAGTCAGCCGGACTACHVGGGTWTCTAAT-3′)

and sequenced using 2x250 base paired-end read on Illumina MiSeq platform (Illumina Inc., San Diego, California, USA) at Massey Genome Service, Massey University, Palmerston North, New Zealand (Kozich, Westcott, Baxter, Highlander, & Schloss, 2013). An Illumina PhiX Control library was included as a sequencing control.

5.2.4.3 Bioinformatic analysis

Sequences were processed using Quantitative Insights Into Microbial Ecology 2 (QIIME2, Version 2021.11) (Bolyen et al., 2019). Demultiplexed sequences were denoised using the DADA2 pipeline (Callahan et al., 2016). Sequences were clustered into features and

annotated taxonomically using the embedded Naive Bayes fitted classifier trained on the SILVA (Version 138) database at 99% similarity (Bokulich et al., 2018; Pruesse et al., 2007; Quast et al., 2012). Data were filtered to remove features from mitochondria or chloroplast and low abundance (less than 4). Alpha rarefaction was performed at a sampling depth of 172,862 with 70.39% data coverage. Rarefaction curves reached a plateau, indicating that the data size was big enough to get the most biological information from each sample (**Figure D.1** in **Appendix D**). Alpha diversity (within a sample) was calculated using Faith's phylogenetic diversity (PD), Observed features, Pielou's evenness and Shannon diversity metrics. The beta diversity (between samples) was calculated using Bray-Curtis dissimilarity and plotted with principal coordinate analysis (PCoA). PCoA plot and Heatmap were created in R studio (Version 4.1.0) using pheatmap (Kolde, 2012), tidyverse (Wickham et al., 2019) and qiime2R (Bisanz, 2018) packages.

5.2.5 Rotational shear rheology

Viscosity measurements of crude mamaku gum samples were performed using a Paar Physica MCR 302 rheometer (Anton-Paar, Graz, Austria) in controlled shear rate (CSR) mode equipped with the double gap geometry (DG- 26-7 and C-PTD 200) at 20.0±0.1°C. Data was recorded using a log-ramp profile from 30 s to 2 s (initial to final).

5.2.6 Statistical analysis

All the experiments were done in triplicate unless otherwise specified. The results are expressed as mean ± standard deviation. The data were checked for normality using the Shapiro-Wilk test and for homoscedasticity using Levene's test. The difference amongst the treatments for M_w, relative enzyme activity and bile acid binding ability was analysed using a one-way analysis of variance (ANOVA) with Tukey HSD post-hoc test at a 95% confidence level using SPSS software (IBM SPSS Statistics, Version 28.0.1.1(15)). The difference amongst the treatments for pH and SCFAs were analysed using the two-way ANOVA with Tukey HSD post-hoc test at a 95% confidence level using Origin 2020 (OriginLab Corporation, Version 9.7.0.185). The significant differences in alpha and beta diversity metrics were calculated using the Kruskal-Wallis test and permutational multivariate analysis of variance (PERMANOVA), respectively.

5.3 Results and Discussion

5.3.1 Gastric and intestinal digestion of mamaku gum

The chromatogram of purified gum fractions during gastric and intestinal digestion is shown in **Figure 5.1**. A right-hand shift in eluting time from the size exclusion chromatogram was observed with increasing harvesting age, suggesting a decrease in M_w (from ~4.1x10^6 Da to ~2.1x10^6 Da from stage 1 to stage 3, respectively). However, no drastic changes in M_w were observed for any of the samples during gastric and intestinal digestion (**Table 5.1**). A similar resistance to gastrointestinal digestion was reported for polysaccharides extracted from *Lycium barbarum* (Ding et al., 2019) and *Camellia sinensis* (Chen et al., 2017a). On the contrary, a decrease in M_w during digestion was observed for polysaccharides extracted from *Craterellus cornucopioides* (Liu et al., 2020), *Oudemansiella radicata* (Liu et al., 2021) and *Dendrobium aphyllum* (Liu, Gong, Wei, & Wu, 2018). In these studies, it is unclear if the decrease in M_w was due to enzymatic degradation or conditions during digestion such as pH and presence of salts. In a study by Hu, Nie, Min, and Xie (2013) degradation of polysaccharide from *Plantago asiatica L.* seeds during gastrointestinal digestion (M_w reduced from 1,903 kDa to 39 kDa during gastric and to 7.2 kDa during intestinal digestion) was attributed to pH sensitivity of the polysaccharide and not to the enzymes. The viscosity profiles of mamaku gum were reported to be stable between pH 3 and pH 10 (Matia-Merino et al., 2012), implying possible retention of the molecular structure over the pH used here to simulate both gastric (pH 3) and small intestinal (pH 7) digestions, thus the stability of MP at pH during gastrointestinal digestion. For stage 2 and 3 samples, a slight increase in M_w was observed under intestinal conditions at all time points, even at the start of the intestinal digestion (0 h) (**Table 5.1**), suggesting some possible aggregation due to the presence of enzymes and bile salts.

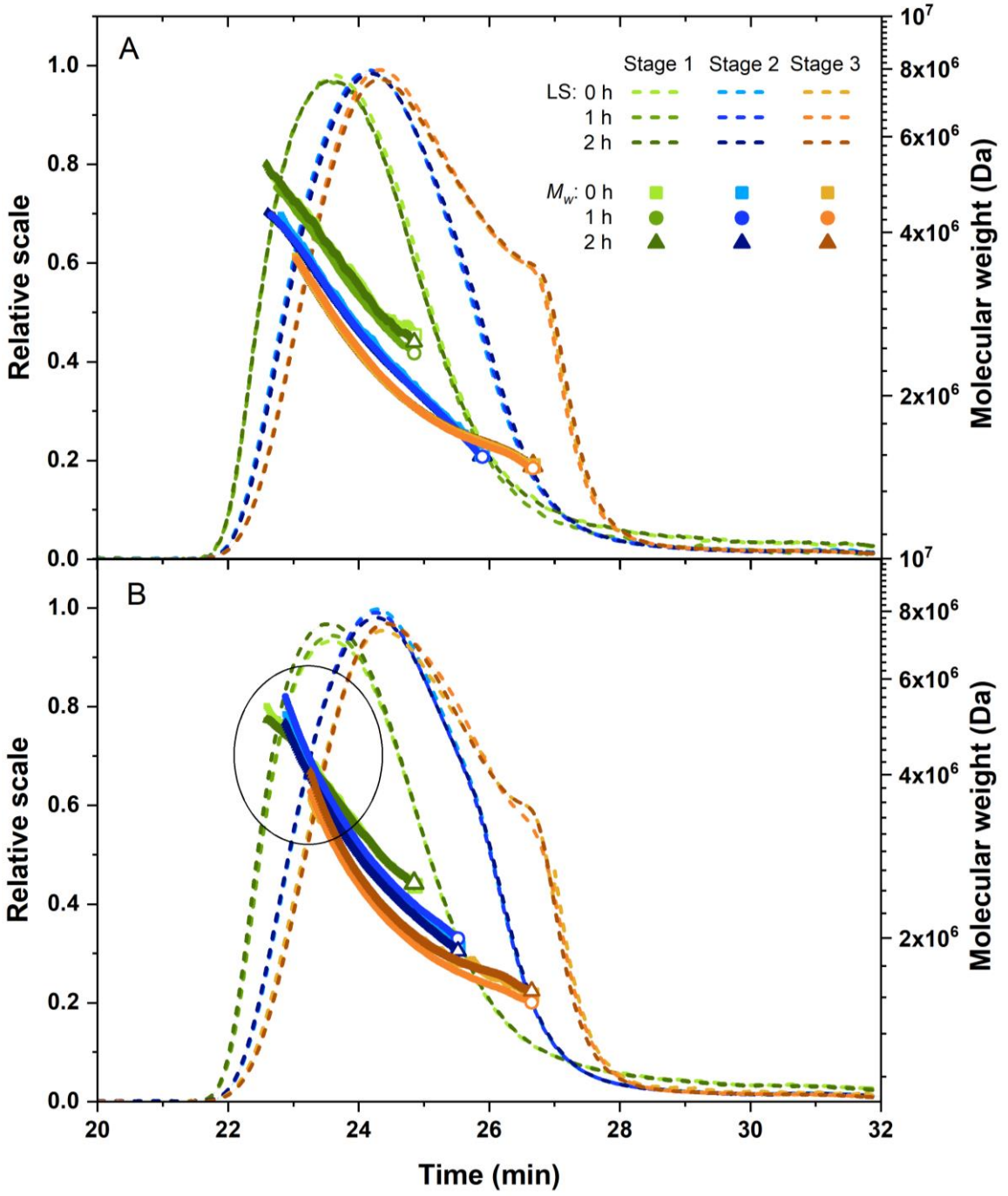


Figure 5.1: Light scattering (LS) signal and weighted-average molecular weight (M_w) analysis by size-exclusion chromatography coupled with multi-angle laser light scattering (SEC-MALLS) of purified mamaku gum (stage 1, 2 and 3) at 0, 1 and 2 h during (**A**) gastric and (**B**) intestinal digestion.

Table 5.1: Molecular parameters of purified mamaku gum (stage 1, 2 and 3) at 0, 1 and 2 h during gastric and intestinal digestion, analysed by size-exclusion chromatography coupled with multi-angle laser light scattering (SEC-MALLS).

	Weighted-average molecular weight, M_w x 10^6 (Da)	Radius of gyration, R_g (nm)	Polydispersity (M_w/M_n)
Gastric digestion			
Stage 1			
0 h	3.98±0.57^{a}	147.19±1.11^{a}	1.08±0.01^{a}
1 h	4.01±0.79^{a}	146.44±2.18^{a}	1.07±0.01^{a}
2 h	4.03±0.18^{a}	148.03±2.87^{a}	1.08±0.01^{a}
Stage 2			
0 h	2.51±0.04^{c}	124.05±3.35^{b}	1.11±0.01^{a}
1 h	2.45±0.14^{c}	122.27±1.01^{b}	1.12±0.01^{a}
2 h	2.44±0.06^{c}	122.57±1.27^{b}	1.12±0.01^{a}
Stage 3			
0 h	2.03±0.05^{e}	108.65±1.07^{c}	1.08±0.01^{a}
1 h	2.04±0.01^{e}	109.15±0.25^{c}	1.09±0.01^{a}
2 h	2.03±0.05^{e}	107.5±1.98^{c}	1.08±0.01^{a}
Intestinal digestion			
Stage 1			
0 h	4.06±0.17^{a}	148.17±4.11^{a}	1.09±0.01^{a}
1 h	4.12±0.06^{a}	147.04±1.18^{a}	1.08±0.01^{a}
2 h	4.11±0.1^{a}	147.64±2.87^{a}	1.08±0.01^{a}
Stage 2			
0 h	2.69±0.01^{b}	121.8±2.99^{b}	1.12±0.01^{a}
1 h	2.75±0.08^{b}	120.47±2.43^{b}	1.12±0.02^{a}
2 h	2.65±0.07^{b}	122.47±0.96^{b}	1.13±0.01^{a}
Stage 3			
0 h	2.20±0.08^{d}	107.7±1.27^{c}	1.1±0.01^{a}
1 h	2.15±0.07^{d}	106.75±1.91^{c}	1.1±0.02^{a}
2 h	2.23±0.95^{d}	106.2±2.65^{c}	1.1±0.01^{a}

Values are expressed as means ± standard deviation (n=3). Values in the same column denoted with different superscript letters are significantly different ($p \leq 0.05$).

5.3.2 Enzyme activity and bile acids binding ability

The effect of crude mamaku gum (stage 1, 2 and 3) on the activity of gastrointestinal enzymes (α-amylase, pepsin and lipase) is shown in **Figure 5.2**. When compared to the control, residual α-amylase and pepsin activities were reduced significantly in presence of mamaku gum (1% w/w) from stage 1 (by ~12 % and ~7%, respectively) and stage 2 (by ~10% and ~5%, respectively) but not for stage 3. The residual lipase activity was reduced significantly for all mamaku gum samples (1% w/w) in the order of stage 1 > stage 2 > stage 3. A similar reduction in *in vitro* α-amylase, pepsin and lipase activity was reported in presence of gum from *Cassia obtusifolia*, *C. tora* (Huang et al., 2012) and *P. asiatica L.* seeds (Hu, Nie, Li, et al., 2013). Enzyme activities were lower in the presence of mamaku gum from stage 1 (higher M_w) as compared to stage 3 (lower M_w). This is in contrast with Xu et al. (2018), who reported a higher α-amylase activity in presence of higher M_w polymer from blackcurrant than the degraded lower M_w polymer. Likewise, Xiao et al. (2020) showed higher α-amylase and lipase activity in presence of higher M_w β-glucan extracted from barley than the lower M_w β-glucan extracted post-fermentation of barley. In both of these studies, the difference in enzyme activity for high and low M_w polymers were attributed to the difference in chemical structure. However, the chemical structure is similar for mamaku gum from stage 1, 2 and 3 (**Chapter 4**).

The residual α-amylase and lipase activities were further reduced significantly by increasing the concentration of mamaku gum (4% w/w) for all sample types. For example, an increase in the concentration of mamaku gum from 1% to 4% (w/w) reduced the α-amylase and lipase activity by ~11% and ~7%, respectively, for the stage 1 sample. The dose-dependent reduction in pepsin activity was only significant for the stage 1 sample. This reduction in enzyme activity in the presence of mamaku gum could be due to interaction between polysaccharide-enzyme or polysaccharide-substrate, or the increase of viscosity of the reaction mixture (**Figure D.2** in **Appendix D**). With the increase in mamaku gum concentration, the number of sites for interaction between polysaccharide-enzyme or polysaccharide-substrate increases along with the viscosity, thus further lowering the enzyme activity. A similar dose-dependent decrease in enzyme activity was previously reported (Hu, Nie, Li, et al., 2013; Huang et al., 2012; Wang et al., 2019). Based on the results,

it is plausible that the stage 1 and 2 gum samples have a stronger influence on the activity of enzymes than the stage 3 sample. Here the focus was not enzyme kinetic so enzyme activity was analysed at a single substrate concentration, but further analysis using Michaelis–Menten kinetics would be useful.

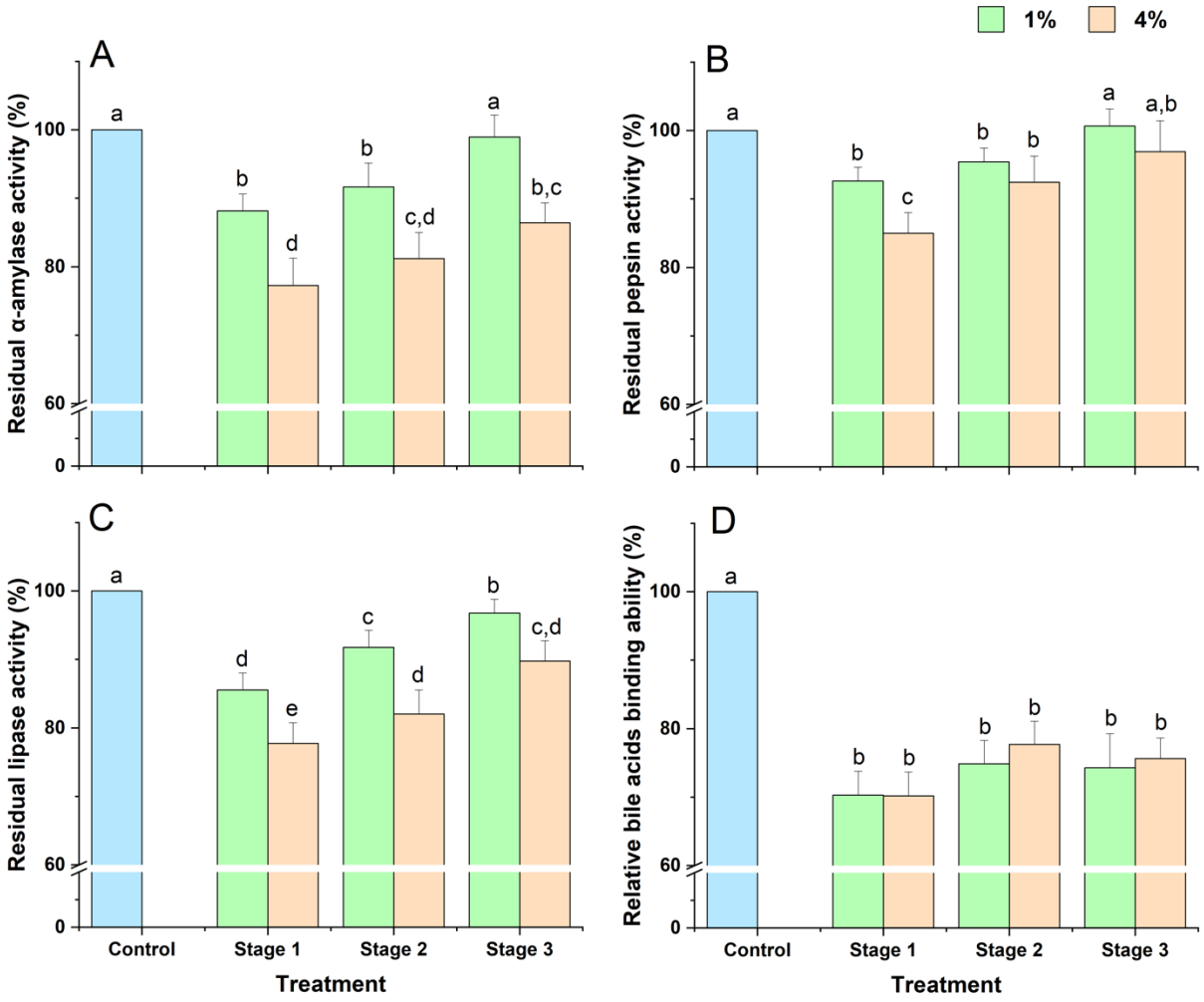


Figure 5.2: Effect of mamaku gum (from stage 1, 2 and 3 at initial concentrations of 1% and 4% w/w) on the activity of (**A**) *α*-amylase, (**B**) pepsin and (**C**) lipase and (**D**) relative bile acid binding ability. Water was used as a control for enzyme activity assays. Cholestyramine was used as a control for the bile acid binding assay. Values are plotted as means ± standard deviation (n=3). Bars with different letters are significantly different ($p \leq 0.05$).

Mamaku gum binds with bile acids (**Figure 5.2D**) and the binding ability was ~30% lower than the control (cholestyramine). The binding of bile acids could be a result of a direct interaction between segments of the polysaccharide and bile acids or it could be just the

entrapment of the bile acid in the viscous matrix (Gunness, Flanagan, & Gidley, 2010; Naumann, Haller, Eisner, & Schweiggert-Weisz, 2020). The concentration of mamaku gum did not affect the bile acid binding as reported elsewhere for polysaccharides from *C. obtusifolia* and *C. tora* seeds (Huang et al., 2012) and *P. asiatica L.* seeds (Hu, Nie, Li, et al., 2013). Kim and White (2010) reported a M_w dependent effect on the *in vitro* bile binding ability of β-glucan. Low and medium M_w β-glucan bound more bile acids than high M_w β-glucan, however, no such effect of M_w (stage 1, 2 and 3) was observed for mamaku gum.

5.3.3 *In vitro* colonic fermentation

5.3.3.1 Short-chain fatty acids production and pH change

The amount of SCFAs (acetic, n-butyric, propionic, succinic, formic and lactic acid) produced during the *in vitro* fermentation is shown in **Table 5.2**. At the end of 24 h fermentation, the production of total SCFAs was significantly higher in all treatment groups, compared with the blank group. For example, for mamaku gum, total SCFAs increased from 5.45±0.17 μg/ml (0 h) to 18.01±0.29 μg/ml (3.3-fold for stage 1), 14.97±0.58 μg/ml (2.8-fold for stage 2) and 14.85±0.88 μg/ml (2.7-fold for stage 3) at 24 h compared to the blank. The production of SCFAs was higher in stage 1 than in stage 2 and 3, and this is explained by a higher acetic and formic acid production. However, the increase in the total SCFAs was more pronounced for inulin (47.15±1.59 μg/ml, 8.7-fold) and guar gum (37.07±1.41 μg/ml, 6.8-fold) groups. In general, the production of formic and lactic acids increased during the first six hours of *in vitro* colonic fermentation, and then gradually decreased in most groups. A similar decline trend for formic and lactic acid has been reported previously (Zhu et al., 2013). Formic and lactic acids act as an intermediate product which could be used by colonic microbes (*e.g.*, acetogenic bacteria), as a precursor for the synthesis of other SCFAs such as acetate, propionate and butyrate (Louis, Hold, & Flint, 2014; Munoz-Tamayo et al., 2011). All three mamaku groups (stage 1, 2 and 3) had significantly higher levels of formic and acetic acid compared with the blank. For inulin and guar gum groups, in addition to formic and acetic acid, propionic, succinic, and lactic acid were also high after 24 h colonic *in vitro* fermentation compared to the blank. Meanwhile, with prolonged fermentation time, SCFAs levels also increased in the blank group which could be attributed to the degradation of the nutrients present in the anaerobic growth media and the faeces. In the growth media, it was expected

that protein and mannan (from yeast extract) are the main nutrients. There was no difference in the production of n-butyric acid between any treatment groups after 24 h of *in vitro* fermentation.

Table 5.2: Concentration of short-chain fatty acids (SCFAs) during *in vitro* fermentation in presence of water (blank), inulin, guar gum and mamaku gum (stage 1, 2 and 3).

SCFAs (µg/ml)	Treatment	Anaerobic fermentation time (h)			
		0	6	12	24
Acetic acid	Blank	2.62±0.21^{c}	3.99±0.15^{bB}	4.71±0.36^{abD}	5.65±0.37^{aE}
	Inulin	-	4.68±0.36^{cB}	11.42±1.10^{bA}	14.65±0.94^{aB}
	Guar gum	-	6.07±0.33^{cA}	9.81±1.88^{bB}	18.39±1.33^{aA}
	Stage 1	-	6.14±0.15^{bA}	7.96±0.59^{aC}	8.16±0.13^{aC}
	Stage 2	-	5.25±0.43^{bAB}	5.39±0.34^{bD}	6.99±0.12^{aD}
	Stage 3	-	4.89±0.63^{bAB}	5.02±1.01^{bD}	6.87±0.14^{aD}
***n*-Butyric acid**	Blank	ND	ND	ND	1.11±0.12^{aA}
	Inulin	-	ND	0.98±0.05^{aA}	1.11±0.21^{aA}
	Guar gum	-	ND	1.01±0.05^{aA}	1.21±0.01^{aA}
	Stage 1	-	ND	0.88±0.05^{aA}	1.22±0.05^{aA}
	Stage 2	-	ND	0.91±0.04^{aA}	1.11±0.15^{aA}
	Stage 3	-	ND	0.89±0.34^{aA}	1.21±0.32^{aA}
Propionic acid	Blank	0.42±0.01^{c}	0.42±0.01^{cA}	1.02±0.09^{bA}	2.80±0.25^{aBC}
	Inulin	-	0.41±0.01^{cA}	1.18±0.11^{bA}	3.44±1.13^{aB}
	Guar gum	-	0.43±0.02^{cA}	1.84±0.46^{bA}	7.95±1.75^{aA}
	Stage 1	-	0.45±0.06^{cA}	1.28±0.16^{bA}	2.41±0.23^{aC}
	Stage 2	-	0.45±0.04^{cA}	1.17±0.17^{bA}	2.51±0.24^{aC}
	Stage 3	-	0.42±0.03^{cA}	0.99±0.35^{bA}	2.51±0.27^{aC}
Succinic acid	Blank	0.30±0.01^{c}	1.01±0.11^{bB}	1.63±0.14^{aC}	1.84±0.11^{aC}
	Inulin	-	1.12±0.14^{cB}	4.95±0.46^{aA}	3.93±1.34^{bB}
	Guar gum	-	1.78±0.15^{bA}	5.24±1.58^{aA}	5.99±1.25^{aA}
	Stage 1	-	1.77±0.13^{bA}	2.68±0.23^{aB}	2.36±0.31^{aC}
	Stage 2	-	1.49±0.17^{aA}	2.01±0.31^{aBC}	1.92±0.31^{aC}
	Stage 3	-	1.38±0.26^{aAB}	1.72±0.61^{aBC}	1.65±0.42^{aC}
Formic acid	Blank	0.71±0.25^{b}	1.32±0.32^{aC}	0.89±0.11^{bD}	0.68±0.09^{bD}
	Inulin	-	2.09±0.12^{cB}	3.32±0.36^{aA}	2.55±0.19^{bA}
	Guar gum	-	2.17±0.24^{aB}	1.81±0.61^{aC}	1.69±0.31^{aB}
	Stage 1	-	3.65±0.07^{aA}	2.67±0.11^{bB}	2.26±0.17^{bA}
	Stage 2	-	2.27±0.24^{aB}	0.86±0.12^{bD}	1.08±0.11^{bC}
	Stage 3	-	2.22±0.27^{aB}	1.27±0.27^{cD}	1.73±0.10^{bB}
Lactic acid	Blank	0.73±0.35^{a}	0.79±0.22^{aB}	0.75±0.09^{aBC}	0.72±0.18^{aBC}
	Inulin	-	2.11±0.22^{cA}	9.21±1.31^{bA}	20.89±3.51^{aA}
	Guar gum	-	2.07±0.11^{aA}	1.78±0.46^{abB}	1.36±0.25^{bB}

	Stage 1	-	2.12±0.27^{aA}	1.11±0.15^{bB}	1.13±0.23^{bB}
	Stage 2	-	1.73±0.29^{aA}	1.06±0.46^{abBC}	0.78±0.21^{bBC}
	Stage 3	-	1.77±0.29^{aA}	0.64±0.28^{bC}	0.54±0.07^{bC}
Total	Blank	5.45±0.17^{c}	8.10±0.27^{bC}	9.39±0.27^{bE}	11.78±0.47^{aE}
	Inulin	-	11.06±0.17^{cB}	31.83±1.28^{bA}	47.15±1.59^{aA}
	Guar gum	-	15.18±0.57^{cA}	21.39±1.42^{bB}	37.07±1.41^{aB}
	Stage 1	-	14.85±0.16^{cA}	16.38±0.51^{bC}	18.01±0.29^{aC}
	Stage 2	-	11.88±0.71^{bB}	12.18±0.62^{bD}	14.97±0.58^{aD}
	Stage 3	-	10.35±0.31^{cB}	12.37±0.52^{bD}	14.85±0.88^{aD}

Values are expressed as means ± standard deviation (n=4). Different superscript lowercase letters within a row indicate a significant difference ($p \leq 0.05$) between time points for the same group. Different superscript capital letters within a column at a specific time point indicate a significant difference ($p \leq 0.05$) between substrates at the time point. ND = not detected. Valeric acid, isovaleric acid and isobutyric acid were not detected for any group and at any time point.

The production of SCFAs during *in vitro* fermentation reduces the pH of the medium. Changes in pH over 24 h of *in vitro* colonic fermentation are shown in **Figure 5.3**. The initial pH for each treatment group was ~6.8, which significantly reduced with increasing fermentation time for all groups. The pH of the blank (water) group was consistently higher than other treatment groups. After 24 h of fermentation, the pH of mamaku gum was reduced to ~6.1 with no difference between stages, while the pH for guar gum and inulin treatment groups was ~5.6 and ~5.3, respectively. Compared with 0 h, the change in pH (ΔpH) for blank, mamaku gum, inulin and guar gum groups were ~4%, ~10%, ~18% and ~22%, respectively. The significantly higher ΔpH for the mamaku gum treatment groups than the blank group, suggests that the former had an impact on the *in vitro* gut environment, although this impact was lower than the inulin and guar gum groups. The pH of the medium was significantly correlated (Pearson correlation of -0.90) to the amount of total SCFAs produced during *in vitro* fermentation (**Figure 5.4**). A similar high correlation between pH and SCFAs during fermentation was reported previously (Berggren, Björck, Nyman, & Eggum, 1993; Holmes et al., 2020; Salvador et al., 1993; Zhou, Cao, & Zhou, 2013).

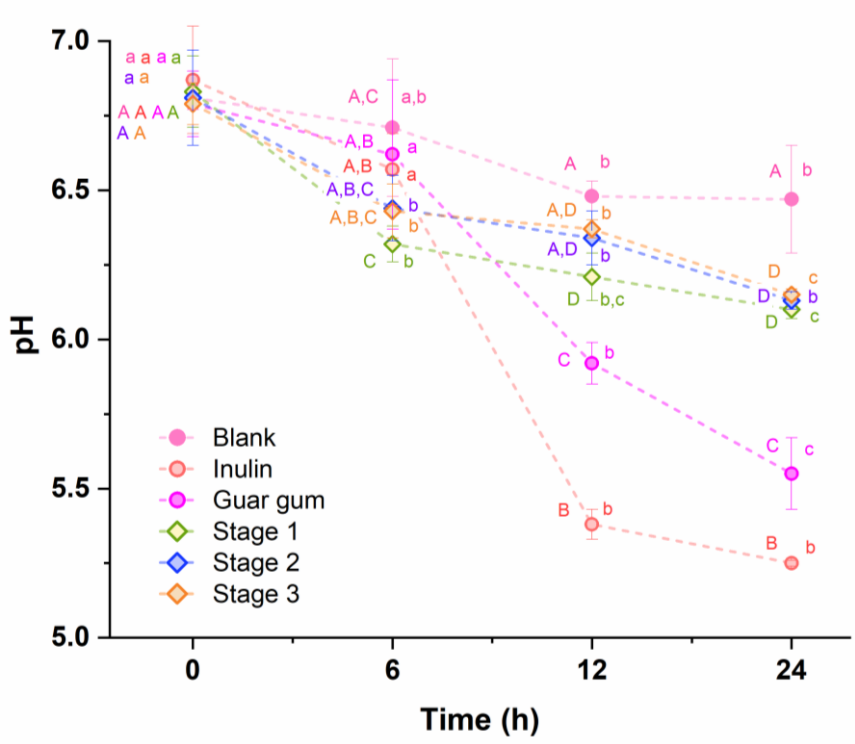


Figure 5.3: Change in pH during *in vitro* fermentation (at 0 h, 6 h, 12 h and 24 h) in presence of water (blank), inulin, guar gum and mamaku gum (stage 1, 2 and 3). Values are expressed as means ± standard deviation (n=4). Different lowercase letters indicate a significant difference ($p \leq 0.05$) between time points for the same group. Different capital letters indicate a significant difference ($p \leq 0.05$) between substrates at a specific time point.

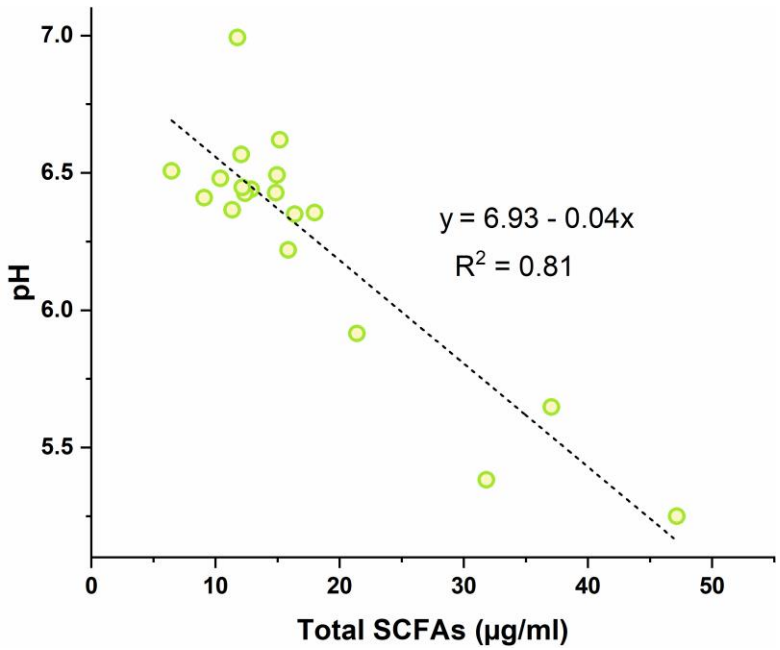


Figure 5.4: Correlation between total short-chain fatty acid (SCFAs) and pH during *in vitro* colonic fermentation.

5.3.3.2 Effect on colonic microbiota

The effect of mamaku gum on microbiota during *in vitro* colonic fermentation was investigated using high throughput amplicon sequencing analysis. The 16S rRNA gene analysis for 18 samples (6 groups, n=3) resulted in a total of 7,467,341 reads, with an average of 414,852 reads per sample. The reads after denoising and filtration were clustered, and 214 features were obtained. The alpha diversity of each group is shown in **Figure 5.5**. Faith's PD and Observed features indexes estimate the richness of the community, Pielou's evenness index estimates the evenness of the community, while Shannon diversity index accounts for both richness and evenness. After 24 h *in vitro* colonic fermentation, the community richness was in general maintained in mamaku gum (stage 1, 2 and 3) but reduced in inulin and guar gum groups (**Figure 5.5A**, **B**). Pielou's evenness index was significantly higher for the inulin group than the rest of the groups (**Figure 5.5C**). All mamaku gum-treated groups (stage 1, 2 and 3) had a Shannon index comparable to the inulin group and significantly higher than the guar gum group (**Figure 5.5D**). A high Shannon index indicates more diversity. High colonic microbial diversity has been considered a representation of health; for instance, slim individuals are reported to have higher gut diversity than obese individuals (Le Chatelier et al., 2013). Furthermore, the PCoA plot, with principal components covering ~88% total variation, showed treatment-induced separation in the composition of microbiota after the *in vitro* colonic fermentation (**Figure 5.5E**); the separation from the blank was more distinct for inulin and guar gum groups than for the mamaku gum (stage 1, 2 and 3).

Taxonomic profiling after 24 h *in vitro* colonic fermentation suggested that microbiota composition principally consisted of Proteobacteria, Firmicutes and Bacteroidetes phyla, accounting for more than 95% of the total phyla in all six groups (**Figure 5.6A**). Compared with the blank, a decline in the relative abundance of Firmicutes was observed in all groups, except inulin treated group, while Bacteroidetes increased in all treatment groups. This resulted in a significantly reduced Firmicutes/Bacteroidetes (F/B) ratio when guar gum and mamaku gum (stage 1, 2 and 3) were fermented (**Figure 5.6B**). A high F/B ratio has been related to health. For instance, a high F/B has been reported in obese individuals (Stojanov, Berlec, & Štrukelj, 2020). For inulin, the F/B ratio was not affected, which is in contrast with previous studies (Zhou et al., 2018), possibly due to the differences in the source and

structure of inulin used in this study. It was reported that mice fed with short-chain inulin had an increased F/B ratio while mice fed with long-chain inulin had a reduced F/B ratio (Li et al., 2020). Amongst all the treatment groups, inulin had higher Actinobacteria.

A closer look at the microbiota community revealed 45 main genera in the six groups (**Figure 5.6C**). Amongst these *Escherichia-Shigella*, *Bacteroides*, *Enterococcus*, *Streptococcus*, *Phascolarctobacterium*, *Dialister*, *Allisonella*, *Lactobacillus*, *Bifidobacterium* and *Eggerthella* were dominant genera. In order to uncover the differences in bacterial composition between groups, genera with relative abundance below 0.1% were excluded, resulting in 21 genera (**Table 5.3**). Compared with the blank, the relative abundance of four genera (*Bacteroides*, *Enterococcus*, *Paraprevotella* and *Parabacteroides*) significantly increased in at least two (of three) mamaku gum groups, while reduced for four genera (*Phascolarctobacterium*, *Eggerthella*, *Klebsiella* and *Bilophila*). The inulin group had a significantly higher relative abundance of six genera (*Bacteroides*, *Enterococcus*, *Streptococcus*, *Lactobacillus*, *Bifidobacterium* and *Collinsella*) and a lower relative abundance of eight genera (*Escherichia-Shigella*, *Phascolarctobacterium*, *Eggerthella*, *Allisonella*, *Alistipes*, *Burkholderia-Caballeronia-Paraburkholderia*, *Parabacteroides* and *Bilophila*) than the blank group. The guar gum group had a significantly higher relative abundance of two genera (*Bacteroides* and *Bifidobacterium*) and a lower relative abundance of five genera (*Phascolarctobacterium*, *Allisonella*, *Streptococcus*, *Parabacteroides* and *Bilophila*) than the blank group. The abundance of *Bacteroides* increased in all treatment groups, suggesting that the addition of fibres could largely promote the growth of *Bacteroides* during *in vitro* fermentation, as reported previously (Liu et al., 2020). On the contrary, the abundance of *Phascolarctobacterium* and *Bilophila* decreased in all treatment groups. The former is associated with better metabolic health and the production of SCFAs such as acetate and propionate (Wu et al., 2017), while the latter can cause inflammation and intestinal barrier dysfunction (Natividad et al., 2018). The growth of other intestinal pathogens such as *Escherichia-Shigella* and *Klebsiella* (both from Proteobacteria phylum) was also prevented in all treatment groups.

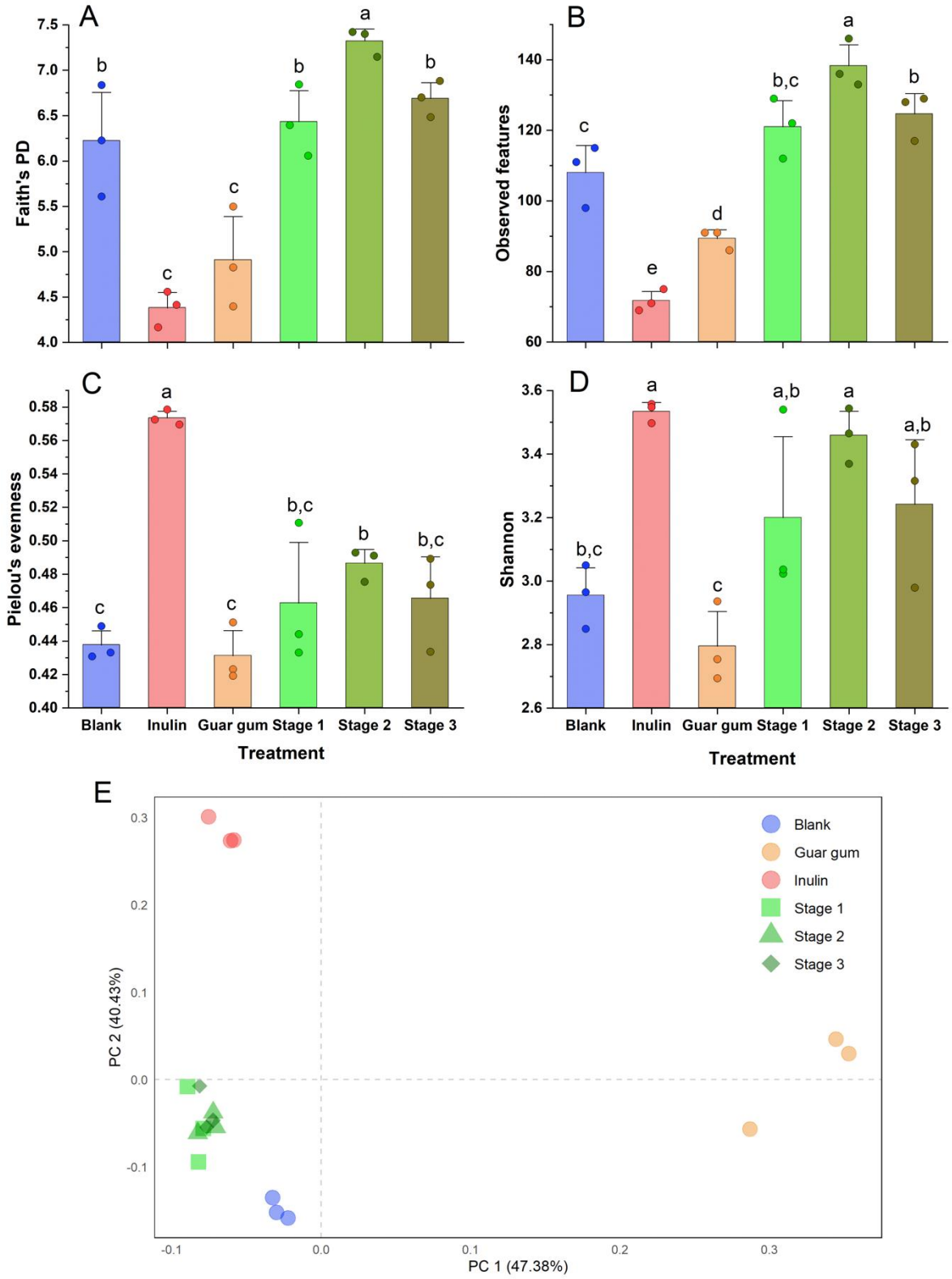


Figure 5.5: Alpha diversity of samples using (**A**) Faith's phylogenetic diversity (PD), (**B**) Observed features, (**C**) Pielou's evenness and (**D**) Shannon diversity metrics. Values are plotted as means ± standard deviation (n=3). Bars with different letters are significantly different ($p \leq 0.05$). (**E**) Beta diversity by principal coordinate analysis (PCoA) plot projecting Bray-Curtis distances ($p < 0.001$).

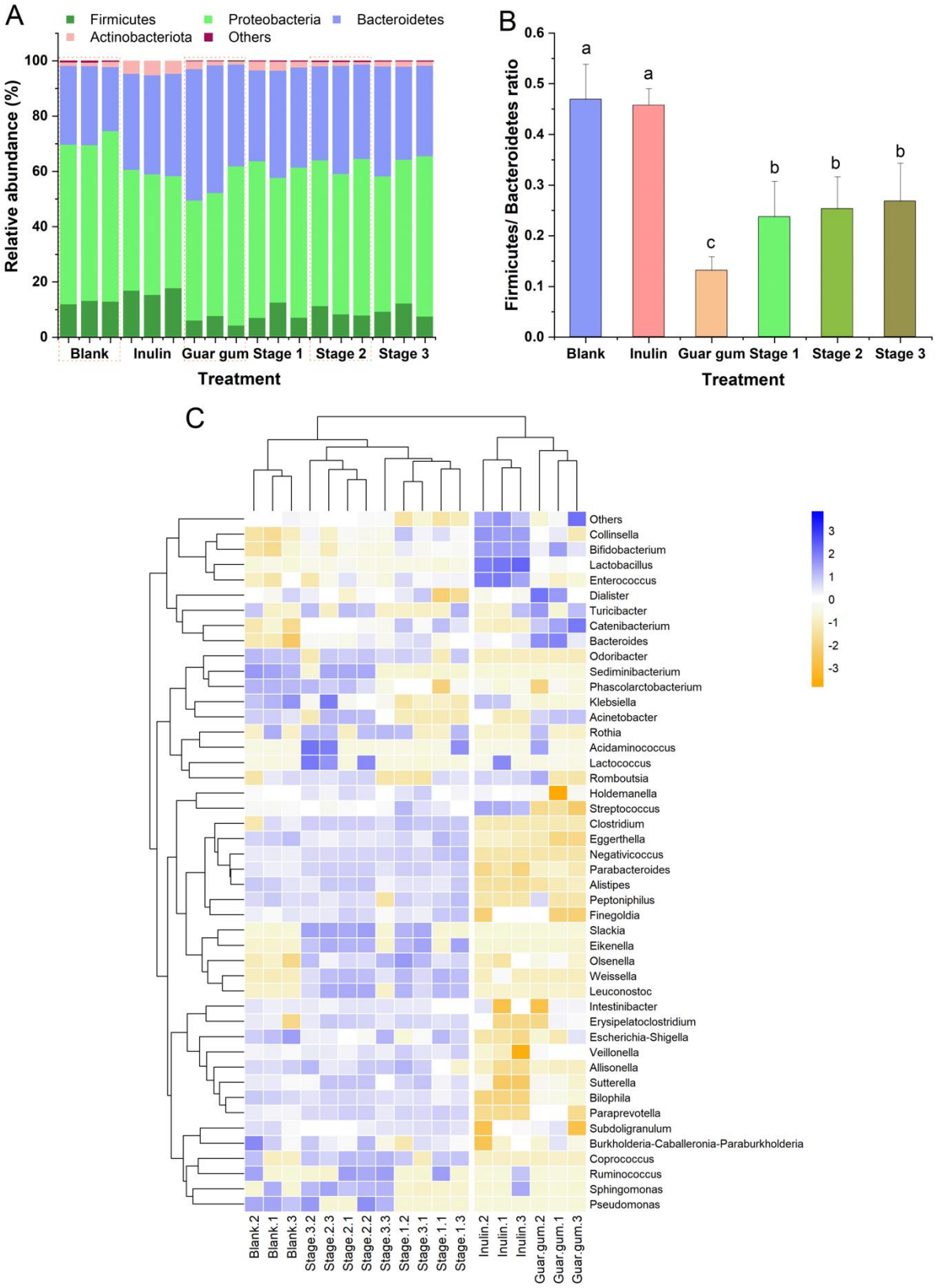


Figure 5.6: (**A**) Taxonomic composition of microbiota after 24 h *in vitro* fermentation at phylum level, (**B**) ratio of Firmicutes to Bacteroidetes and (**C**) heatmap of gut microbial composition at genus level in blank, inulin, guar gum and mamaku gum (stage 1, 2 and 3) groups. In (**B**) values are plotted as means ± standard deviation (n=3). Bars with different letters are significantly different ($p \leq 0.05$).

Table 5.3: Relative abundances after 24 h *in vitro* fermentation of the top 21 genera in blank, inulin, guar gum and mamaku gum (stage 1, 2 and 3) groups.

Genus	Treatment (Relative abundance %)					
	Blank	Inulin	Guar gum	Stage 1	Stage 2	Stage 3
Escherichia-Shigella	55.42±3.03^{a}	38.36±1.31^{b}	44.58±5.46^{ab}	50.55±6.2^{a}	47.77±2.19^{ab}	50.57±4.92^{a}
Bacteroides	26.11±2.87^{c}	35.97±1.15^{b}	43.54±5.84^{a}	34.48±3.02^{b}	33.88±2.74^{b}	34.52±3.47^{b}
Enterococcus	1.63±0.42^{c}	4.48±0.61^{a}	1.71±0.19^{c}	2.54±0.24^{b}	2.11±0.44^{b}	1.71±0.35^{c}
Streptococcus	1.65±0.28^{b}	3.99±0.45^{a}	0.55±0.14^{c}	2.61±1.03^{b}	1.73±0.28^{b}	2.12±0.38^{b}
Phascolarctobacterium	5.99±1.15^{a}	0.01±0.01^{b}	0.00±0.00^{b}	0.02±0.02^{b}	1.84±1.65^{b}	1.34±02.29^{b}
Dialister	1.29±0.45^{b}	0.98±0.12^{b}	2.81±1.55^{a}	0.75±0.66^{b}	0.96±0.22^{b}	1.41±0.45^{ab}
Allisonella	1.43±0.25^{a}	0.09±0.06^{b}	0.18±0.03^{b}	1.14±1.29^{ab}	1.33±0.48^{a}	1.98±0.41^{a}
Lactobacillus	0.11±0.01^{b}	6.86±2.19^{a}	0.25±0.07^{b}	0.13±0.02^{b}	0.14±0.02^{b}	0.13±0.01^{b}
Bifidobacterium	0.38±0.13^{d}	2.36±0.05^{a}	1.57±0.69^{b}	0.97±0.23^{c}	0.56±0.13^{cd}	0.67±0.06^{cd}
Eggerthella	1.20±0.19^{a}	0.14±0.02^{c}	0.07±0.03^{c}	1.28±0.36^{a}	0.7±0.11^{b}	0.72±0.09^{b}
Collinsella	0.09±0.03^{c}	2.39±0.27^{a}	0.39±0.27b^{c}	0.77±0.46^{b}	0.24±0.08^{c}	0.46±0.18^{bc}
Acinetobacter	0.31±0.21^{bc}	0.00±0.00^{c}	0.75±0.47^{b}	0.00±0.00^{c}	2.15±0.59^{a}	0.00±0.00^{c}
Paraprevotella	0.12±0.05^{c}	0.00±0.00^{c}	0.01±0.01^{c}	0.93±0.12^{a}	0.95±0.27^{a}	0.48±0.24^{b}
Sutterella	0.11±0.04^{b}	0.00±0.00^{b}	0.01±0.00^{b}	0.25±0.19^{b}	1.02±0.08^{a}	0.39±0.60^{b}
Veillonella	0.25±0.06^{bc}	0.01±0.01^{c}	0.10±0.03^{bc}	0.82±0.41^{a}	0.38±0.13^{b}	0.35±0.06^{b}
Alistipes	0.44±0.17^{ab}	0.00±0.00^{d}	0.01±0.00^{d}	0.35±0.22^{bc}	0.62±0.06^{a}	0.19±0.06^{cd}
Klebsiella	0.40±0.05^{a}	0.31±0.07^{abc}	0.21±0.01b^{c}	0.18±0.01^{c}	0.33±0.15^{ab}	0.22±0.02^{bc}
Burkholderia-Caballeronia-Paraburkholderia	0.37±0.26^{a}	0.11±0.08^{b}	0.16±0.09^{ab}	0.15±0.09^{ab}	0.28±0.11^{ab}	0.24±0.11^{ab}
Parabacteroides	0.16±0.03^{b}	0.00±0.00^{c}	0.01±0.00^{c}	0.31±0.09^{a}	0.33±0.01^{a}	0.29±0.09^{a}
Bilophila	0.38±0.14^{a}	0.00±0.00^{d}	0.00±0.00^{d}	0.09±0.03^{cd}	0.26±0.01^{b}	0.13±0.02^{c}
Negativicoccus	0.02±0.00^{b}	0.00±0.00^{b}	0.00±0.00^{b}	0.35±0.15^{a}	0.11±0.03^{b}	0.09±0.02^{b}

Genus with a relative abundance of 0.1% and above are presented. Values are expressed as means ± standard deviation (n=3). Values in the same row with the different superscript letters are significantly different ($p \leq 0.05$).

5.4 General Discussion

In this study, a combination of several *in vitro* models was used to unravel the fate of mamaku gum during its transition throughout the gut. Results showed that MP is a non-digestible polymer that can withstand conditions during *in vitro* gastrointestinal digestion and retain its molecular structure (**Figure 5.1** and **Table 5.1**). In the upper gut, mamaku gum can significantly reduce the *in vitro* activity of digestive enzymes such as α-amylase, pepsin and lipase (**Figure 5.2A**, **B**, **C**). The extent of reduction in enzyme activity was higher in mamaku gum from stage 1 and 2 than from stage 3.

Polysaccharides in general can potentially reduce enzyme activity through multiple mechanisms acting simultaneously. Polysaccharides may directly interact with enzymes (form enzyme-polysaccharide complex) or with the substrate (form substrate-polysaccharide complex), and as a result, hinder enzyme-substrate interactions and lower the rate of hydrolysis. For example, guar gum and cellulose are reported to bind with α-amylase and lower the rate of starch digestion (Dhital, Gidley, & Warren, 2015; Slaughter, Ellis, & Butterworth, 2001; Slaughter, Ellis, Jackson, & Butterworth, 2002). Pectin can interact with the protein, therefore making it less accessible to the enzyme (Girard, Turgeon, & Gauthier, 2002; Mouécoucou, Villaume, Sanchez, & Méjean, 2004). Naturally occurring metal ions (such as Ca^{2+}) and phenolic compounds (such as tannins) in gum extracts, may also indirectly affect enzyme activity. Ca^{2+} ions can form a complex with the free fatty acid produced during lipolysis and consequently, remove the fatty acid from the interface of the emulsion. This prevents the accumulation of the free fatty acid (product) at the interface, therefore, making the substrate accessible to the enzyme, and thus, promoting lipolysis to continue (Zangenberg, Müllertz, Kristensen, & Hovgaard, 2001). Additionally, Ca^{2+} ions provide structural integrity for the enzyme (Buisson, Duee, Haser, & Payan, 1987). Studies have shown that the removal of Ca^{2+} ions decreases the activity of α-amylase, which can partly be restored upon reintroducing Ca^{2+} ions (Buonocore, Poerio, Silano, & Tomasi, 1976; Nazmi, Reinisch, & Hinz, 2008). The fraction of Ca^{2+} ions present in the mamaku gum can possibly attached to anionic MP, which results in electrostatic interactions (bridge) between MP and enzymes. Thus, the difference in the concentration of Ca^{2+} ions (and metal ions in general), higher in stage 3 gum than in stage 1, may also influence the activity of enzymes (**Table 4.2**). Lastly, tannins can form complexes with proteins, making them inaccessible for enzymes and thus reducing the rate of proteolysis (Silanikove, Perevolotsky, & Provenza, 2001). Polysaccharides can also increase the viscosity of the system and consequently, lower the diffusion of enzyme, substrate and product; thus, indirectly reducing enzyme activity. The viscosity of the digestion mixtures containing mamaku gum samples from different stages at a given concentration was comparable, indicating that viscosity may not be the primary reason for the difference in reduced enzyme activity amongst sample types (**Figure D.2** in **Appendix D**). Further investigation on whether the effect of mamaku gum on enzyme activity is because of interactions or a mere physical hindrance between enzyme and

substrate is needed. Reduction in enzyme activity leads to delaying the digestion of food and consequently, its absorption, which may be beneficial in managing conditions such as type 2 diabetes by lowering postprandial glucose levels.

In addition to enzyme activity, mamaku gum can bind the bile acids *in vitro* (**Figure 5.2D**), possibly making them unavailable for fat micelle formation and hindering lipid absorption. The binding of bile acids to polymers is also reported to facilitate the removal of the former in faeces, as a result of which the endogenous cholesterol will be used by the liver to replenish bile acids, consequently reducing the blood lipid level (Capuano, 2017).

In the lower gut, undigested mamaku gum was found to alter the composition of colonic microbiota (**Figures 5.5** and **5.6**) and significantly increase the relative abundance of *Bacteroides*, *Enterococcus*, *Paraprevotella* and *Parabacteroides* genera (**Table 5.3**). *Bacteroides* spp. can rapidly utilise a range of simple and complex carbohydrates and promote substrate cross-feeding between different species, improve immune function, control competing pathogens in the gut and possibly play a key role in preventing obesity (Wexler, 2007). *Enterococcus* spp. limit gastrointestinal infections, improve the immune system and are used as a probiotic strain, but the benefits of a probiotic strain have been controversial (Krawczyk, Wityk, Gałęcka, & Michalik, 2021). *Paraprevotella* genus produces succinic and acetic acid as major fermentation products, however, the potential effects *Paraprevotella* spp. on human health are unknown (Bressa et al., 2017). *Parabacteroides* spp. can improve immunity, have anti-inflammatory effects, produce metabolic benefits such as anti-obesity and a decrease in hyperglycaemia in the host, and has application as a probiotic strain (Cui et al., 2022).

Mamaku gum fermentation also increased the production of total SCFAs compared to the blank group, resulting in reduced pH (**Table 5.2, Figures 5.3** and **5.4**). The changes in SCFAs and pH in the presence of mamaku gum were less prominent than in the presence of inulin and guar gum, suggesting lower fermentability of the former compared to the latter two. This difference in fermentability could be a result of differences in the chemical composition and structural features of treatment fibres, affecting their interaction with the gut microbiome (Jonathan et al., 2012; Payling et al., 2020). The monosaccharide composition of MP (mainly methylesterified glucuronic acid and mannose, and a small fraction of galactose, xylose, arabinose, glucose, non-methylesterified glucuronic acid, rhamnose and fucose) is far

more complex than inulin (fructose) and guar gum (mannose and galactose). Microbes can preferentially consume sugars differently when provided with more than one option. For instance, *E. coli* utilises glucose over lactose (Beisel & Afroz, 2016). Furthermore, the presence of methylesterified sugars is reported to delay the fermentation of high methylesterified pectin than low methylesterified pectin (Dongowski & Lorenz, 1998). Structural features such as M_w and developed viscosity have also been shown to impact fermentability. Reduced fermentation with an increase in M_w has been observed for Blackberry polysaccharide (Li et al., 2022) and guar gum (Stewart & Slavin, 2006), though no difference between the fermentability of different-size MP samples was observed. The viscosity of the medium during fermentation (differently influenced by fibres) can affect the availability of nutrients and water which can bring changes in the microbial composition. An increase in the viscosity of the fermentation media was shown to upregulate the growth of total anaerobes and *Clostridium* spp. and downregulate the growth of aerobes and *Enterococcus* (Tamargo et al., 2018). The exact consequences of polysaccharide sugar composition and structural features on fermentation are unknown and warrant further investigation.

In conclusion, MP was not degraded during gastric and intestinal digestion and can significantly reduce the activity of digestive enzymes and bind bile salts. Through colonic fermentation, mamaku gum significantly promoted the production of SCFAs, especially formic and acetic acids. Furthermore, mamaku gum could shape the colonic microbiota, primarily increasing *Bacteroides*, *Enterococcus*, *Paraprevotella* and *Parabacteroides* genera and decreasing *Phascolarctobacterium* and *Eggerthella*, *Klebsiella* and *Bilophila* genera. Thus, the results have provided scientific evidence for the potential application of mamaku gum as an alternative functional ingredient to improve gut health. Mamaku gum can be used to design functional food products, therefore, the sensitivity of MP to industrial operations such as high temperature and high shear, which are critical during the processing of MP for commercial applications, is explored in next chapter. Further preclinical and clinical studies are warranted to test the potential health benefits that may be achieved through dietary interventions using mamaku gum.

Chapter 6

Shear and temperature sensitivity of a shear-thickening biopolymer from the New Zealand black tree fern

6.1 Introduction

The novel shear-thickening behaviour of mamaku polysaccharides (MP) can potentially be used to develop food products that possess functionality suitable for satiety management to curb obesity epidemic (Wee et al., 2017); possibly reduce the glycaemic response for individuals suffering from diabetes or as a fibre to improve colon health. However, during manufacturing, MP may be subjected to treatments such as high shear and temperature which could adversely affect its structural and rheological properties, thereby limiting the use of MP as a potential natural active ingredient in food products. Thus, from both technological and physiological perspectives, understanding the effects of processing on MP is essential.

High shear equipment such as high-speed mixers, colloid mills, high-pressure homogenisers and microfluidizers are commonly used in the food industry for emulsification, particle size reduction and to modify textural properties of food products. Kivelä et al. (2010) investigated the effect of the use of a colloid mill, a homogeniser and a microfluidizer on the structure and rheology of oat β-glucan and reported a permanent decrease in viscosity with a simultaneous reduction in molecular weight (M_w), depending on the energy input. Several authors have reported shear- (from mechanical action) induced degradation of various polysaccharides, including flaxseed gum (Wang, Li, Wang, & Xue, 2011), cashew tree gum (Porto et al., 2015), acacia gum (Al-Assaf, Sakata, McKenna, Aoki, & Phillips, 2009), pectin (Corredig & Wicker, 2001; Shpigelman, Kyomugasho, Christiaens, Van Loey, & Hendrickx, 2015; Xie et al., 2018), xanthan (Eren, Santos, & Campanella, 2015; Harte & Venegas, 2010; Laneuville et al., 2013), tragacanth gum (Farzi, Yarmand, Safari, Emam-Djomeh, & Mohammadifar, 2015; Keivanfard, Nasirpour, Barekat, & Keramat, 2022), methylcellulose (Floury, Desrumaux, Axelos, & Legrand, 2002), k-carrageenan (Harte & Venegas, 2010), tamarind seed

polysaccharide (Xie et al., 2021), scleroglucan (Zeng, Wang, Shan, Yu, & Zhou, 2021) and exopolysaccharide from lactic acid bacteria (Nachtigall et al., 2019).

The shear sensitivity of a polysaccharide is not solely dependent on the imposed shear but is simultaneously governed by the structural features of the polymer. According to Pohl's equation, a polymer is affected by shear treatment if the threshold ($\eta \times \dot{\gamma} \times M_w^2$; where, η is viscosity, $\dot{\gamma}$ is shear rate and M_w is weighted-average molecular weight) is ≥ $1x10^{14}$, highlighting the strong dependence of shear susceptibility on the molecular weight of the polysaccharide (Mackenzie & Jemmett, 1971). This equation was first reported in 1943 for polymer blend oils, however the threshold value needs to be further examined and validated for a variety of polymers. Nevertheless, the molecular weight dependence of shear susceptibility is confirmed by many other authors (Kasaai, Charlet, Paquin, & Arul, 2003; Nilsson et al., 2006; Villay et al., 2012; Zaitoun et al., 2012), suggesting the frictional force experienced by the polymer is proportional to the macromolecule length. Furthermore, globular branched structures, such as that of gum arabic, were reported to be largely unaffected by shear treatment, while linear flexible polymers, such as guar gum, underwent depolymerisation (Villay et al., 2012). Likewise, apple pectin with a greater proportion of neutral sugars in the side chains—giving it a more compact structure than citrus pectin—was reported to resist depolymerisation on shearing (Shpigelman et al., 2015). The presence of large monomer units, the use of poor solvents and the specific pH of the system, all affect the flexibility of the polymer which can make it less sensitive to shear (Shpigelman et al., 2015; Zaitoun et al., 2012). Shear sensitivity is also affected by the inherent strength of the backbone molecules, for example, Si-O bonds (bond energy = 89.3 kcal/mol) are more resistant to shear than C-C bonds (58.6 kcal/mol) (Mackenzie & Jemmett, 1971).

High temperature treatments, such as those used during pasteurisation, sterilisation, blanching and drying for making food products microbiologically safe, inactivating enzymes, and cooking the product, may alter the structure and functionality of polysaccharides and, as a result, impact their functionality when used in food products (Keivanfard et al., 2022; Owen, Tung, & Paulson, 1992). Temperature-induced depolymerisation is commonly reported in literature *e.g.*, for β-glucan, detarium gum and dextran (Wang, Wood, Cui, & Ross-Murphy, 2001), diutan gum, xanthan, scleroglucan

(Liang et al., 2019) and exopolysaccharides from lactic acid bacteria (Nachtigall et al., 2021). However, the extent of thermal degradation of the polymer chain varies between different polymers. Robal, Truus, Volobujeva, Mellikov, and Tuvikene (2017) studied six different polysaccharides and observed that degradation at high-temperature decreased in the order of agaro > funoran > furcellaran > *k*-carrageenan > *λ*-carrageenan > *L*-carrageenan and attributed the greater stability to the presence of methoxy groups which stabilise the polymer chains.

Shear and temperature sensitivity for some macromolecules has been reported but cannot be generalised because of differences in the polymer structure. To the best of author's knowledge, there is no literature systematically describing the shear and temperature sensitivity of MP. It was hypothesised that shear and temperature treatment might degrade MP molecules causing fragmentation of the polymer chain and affecting rheological functionality. Therefore, the present work aimed to investigate the sensitivity of MP towards high shear and temperature, by characterizing the rheological properties, M_w, size and structural changes at the molecular level after various treatments.

6.2 Materials and Methods

6.2.1 Extraction of mamaku gum

Mamaku gum from young fronds (stage 1) was extracted as described in **Section 3.1.1**. Briefly, after harvesting, the fronds were chopped, blended with water and heated to ~55°C for 5 min with continuous stirring. The exuded gum, separated from insoluble plant debris, was collected. The left-over pulp was reheated in water and the extract was collected until no visual viscous consistency of the flowing liquid was observed. This was repeated an average of 3-5 cycles. The pooled extracts were left undisturbed overnight at 4°C for the remains of pulp to sediment by gravity. The clearer top layer was then separated using a siphon. The collected 'crude gum extract' was concentrated using a vacuum evaporator (BÜCHI Labortechnik AG, Flawil, Switzerland) and stored at -18°C until use.

6.2.2 Shear and temperature treatments

For the shear treatment, 300 ml of crude mamaku gum (2% w/w, total solids) was transferred into a beaker (17.5x8.7 cm) and subjected to different rotational speeds (1,000-8,000 rpm) for 1 min or at 5,000 rpm from 30 sec to 20 min using a bench-top high-shear mixer (Silverson, L4RT, Chesham, England—attached with emulsor screen of perforation ~1 mm and internal diameter ~3 cm). The temperature did not exceed 50°C during the shear treatment. The shear rate ($\dot{\gamma}$) developed between the high-shear mixer shaft and the beaker was calculated to be about 240-2,000 s^{-1} using the Magules equation:

$$\dot{\gamma} = \frac{2\omega}{1-\frac{r_1^2}{r_2^2}} \qquad \textbf{Equation 6.1}$$

where, ω is the angular velocity and r_1 and r_2 are the radius of the shaft and beaker respectively. However, the calculated value may not be a true representation of the shear experienced by the polysaccharides, as the flow of the fluid is non-uniformly distributed and there is additional shear developed within the hollow emulsor screen attached (Sisodia, Rajak, Pathak, & Guria, 2015). Additionally, to shear, centrifugal forces, suction, turbulence, and cavitation may also affect the polysaccharide—using one value of shear will not reflect all the events. Thus, in this chapter, shear treatment is represented in terms of the rotational speed of the instrument (*i.e.*, 1k-8k rpm) and not the true shear experienced by the polysaccharide. Shear-treated samples are labelled as rotational speed-treatment time, for example, 2k-1 min and 5k-20 min. Though efforts were made to study the effect of 'shear only' on the crude mamaku gum using a rheometer, the rod-climbing effect made it difficult as prolonged shearing caused the expulsion of the gum from the gap between the geometries. An in-house built capillary viscometer was also used to apply high shear, but the limited duration of the applied shear (fractions of a second) and the incorporation of air bubbles into the gum after shearing, hindered an accurate sample analysis.

For the temperature treatment, crude mamaku gum (100 ml, 2% w/w, total solids) was heated in a water bath at different temperatures (65-95°C) for a period of 30 mins each, and in the retort at 115°C for 30 min, followed by cooling to room temperature using an ice bath. This range of temperatures is commonly used in the food industry for food safety reasons. The untreated crude mamaku gum was used as a control.

The samples post shear or temperature treatment were immediately characterized in terms of their rheological properties and were further purified ('purified gum fraction') for molecular and structural analysis. The purification process involved ultra-centrifugation (Sorvall WX Ultra 100, T-865 motor, Thermo-Fisher Scientific Inc., Waltham, Massachusetts, USA) at 250,000 g for 1 h, followed by dialysis (molecular weight cut-off: 12,000-14,000 Da) in reducing NaCl concentrations (0.01 M, 0.001 M and milli-Q water only) for ~42 h at 4°C, then freeze-dried.

6.2.3 Shear rheology

Rheological measurements were performed using a Paar Physica MCR 302 rheometer (Anton-Paar, Graz, Austria) in controlled shear rate (CSR) mode at 20.0±0.1°C. Viscosity profiles were measured using a cup-and-bob geometry (CC27 and C-PTD 200) and data was recorded using Rheoplus/32 software (Version 3.62) using a log-ramp profile from 30 s to 2 s (initial to final). The relative change (%) in viscosity at a specific shear rate, with respect to the control, was calculated using:

$$Relative\ change = \frac{\eta_{control} - \eta_{treated}}{\eta_{control}} \times 100 \qquad \textbf{Equation 6.2}$$

where, $\eta_{control}$ is the viscosity of the control sample and $\eta_{treated}$ is the viscosity of each sample after the shear or temperature treatment.

Oscillatory measurements (frequency sweep) were performed in the range of 0.01-20 Hz at constant 5% strain (within the linear viscoelastic region) using the double gap geometry (DG-26-7 and C-PTD 200). Samples were allowed to rest for 5 min after being loaded, before the start of the experiment, reducing any shear history effect and allowing for temperature equilibration.

6.2.4 Size-exclusion chromatography coupled with multi-angle laser light scattering

Molecular weight analysis of temperature and shear-treated gum samples was performed using a high-performance liquid chromatography (HPLC) system (Shimadzu, Kyoto, Japan) coupled with multi-angle laser light scattering (Dawn Heleos 8+, Wyatt Technology Corp., Goleta, California, USA), as described in **Section 4.2.5**. Briefly, the purified gum samples

were centrifuged (30,000 *g*, 1 h), and injected (20 µl) into the HPLC system for separation using size-exclusion columns (OHpak SB-G, SB-804 HQ and SB-806M HQ) at 25°C with 0.1 M NaCl mobile phase at a flow rate of 0.5 ml/min. The Astra software (Version 6.1.1.17, Wyatt Technology) was used to analyse the light scattering peak.

6.2.5 Dynamic light scattering

The z-average radius of purified mamaku gum (0.5% w/w re-dispersed in 0.1 M NaCl overnight) was determined *via* dynamic light scattering using a Zetasizer Pro (Malvern Instruments Ltd., Malvern, England). Each sample was filled in low-volume polystyrene disposable cuvettes (ZEN0040) and the z-average readings were taken at 90° scattering light using a refractive index of 1.55 for MP. The reflective index of the dispersant (water) used was 1.33. The temperature of the samples was controlled at 20±0.1°C during the measurement. The zeta potential of MP was unaltered after a change in M_w (unpublished).

6.2.6 Constituent sugar analysis and nuclear magnetic resonance spectroscopy

The composition and structure of the purified mamaku gum after temperature and shear treatments were analysed as described previously. Constituent sugar compositions were determined using high-performance anion exchange chromatography (HPAEC) after hydrolysis of purified mamaku gums to their component monosaccharides (**Section 4.2.3**). Proton and carbon NMR data were collected on a Bruker Avance Neo 700 MHz NMR spectrometer (Bruker BioSpin, Rheinstetten, Germany) and assignments were made by comparing the spectra with published data (**Section 4.2.4**).

6.2.7 Urea treatment

The crude mamaku gum sample (4% w/w) was shear-treated and mixed with an equal volume of 10 M urea (to give a final concentration of 2% gum and 5 M urea) for 15 min at 200 rpm at 20°C, followed by rheological analysis.

6.2.8 Statistical analysis

All the experiments were done in triplicate with at least two measurements. The data are reported as mean ± standard deviation. Statistical analysis was performed using a one-way

analysis of variance (ANOVA) with Tukey HSD post-hoc test at 95% confidence level using SPSS software (IBM SPSS Statistics, Version 28.0.1.1(15)).

6.3 Results and Discussion

6.3.1 Rheological analysis

The effects of shear and temperature treatments on the rheological profile of crude mamaku gum (2% w/w, total solids) are shown in **Figures 6.1** and **6.2**. The control sample (no treatment) displayed the typical three-phase rheological behaviour of mamaku gum, namely Newtonian at a low shear rate (< 2 s^{-1}), shear-thickening at an intermediate shear rate (2-5 s^{-1}) and shear-thinning at higher shear rate (> 5 s^{-1}). This distinctive behaviour of MP has been attributed to transient molecular bonds being formed at specific shear rates. At low shear, the rate of formation of intermolecular linkages will be equal to the rate of bond disruption, thus, a constant viscosity is observed. As the shear rate increases, MP chains start to unfold and stretch, exposing sites for intermolecular interactions, and promoting the shear-thickening effect. Finally, at a higher shear rate, intermolecular interactions start to break much faster than they are formed again, leading to shear-thinning behaviour (Goh et al., 2007; Matia-Merino et al., 2012; Wee et al., 2015b).

Upon shear treatment, the rheological profile—including shear-thickening behaviour—of mamaku gum was retained but the following general trends (relative to the control) were observed with an increasing intensity of the shear (**Figure 6.1**, **Tables 6.1** and **6.2**): (i) viscosity decreased after MP was subjected to shear—the higher the intensity or time of shear, the lower is the viscosity of the MP. For example, at 1 s^{-1}, viscosity was reduced by ~56% and ~60% after treatment at 6k-1 min and 5k-5 min, respectively; (ii) the extent of shear-thickening, η_{max}/η_{crit} (defined as the ratio of maximum viscosity, η_{max}, to viscosity at the onset of shear-thickening, η_{crit}) was reduced by ~50% and ~52% after 8k-1 min and 5k-20 min treatment, respectively; (iii) an increase in the critical shear rate, $\dot{\gamma}_{crit}$, (defined as the shear rate at the onset of shear-thickening) from ~2.51 s^{-1} for control to ~12.6 s^{-1} after 8k-1 min and ~15.8 s^{-1} after 5k-20 min treatments, was observed.

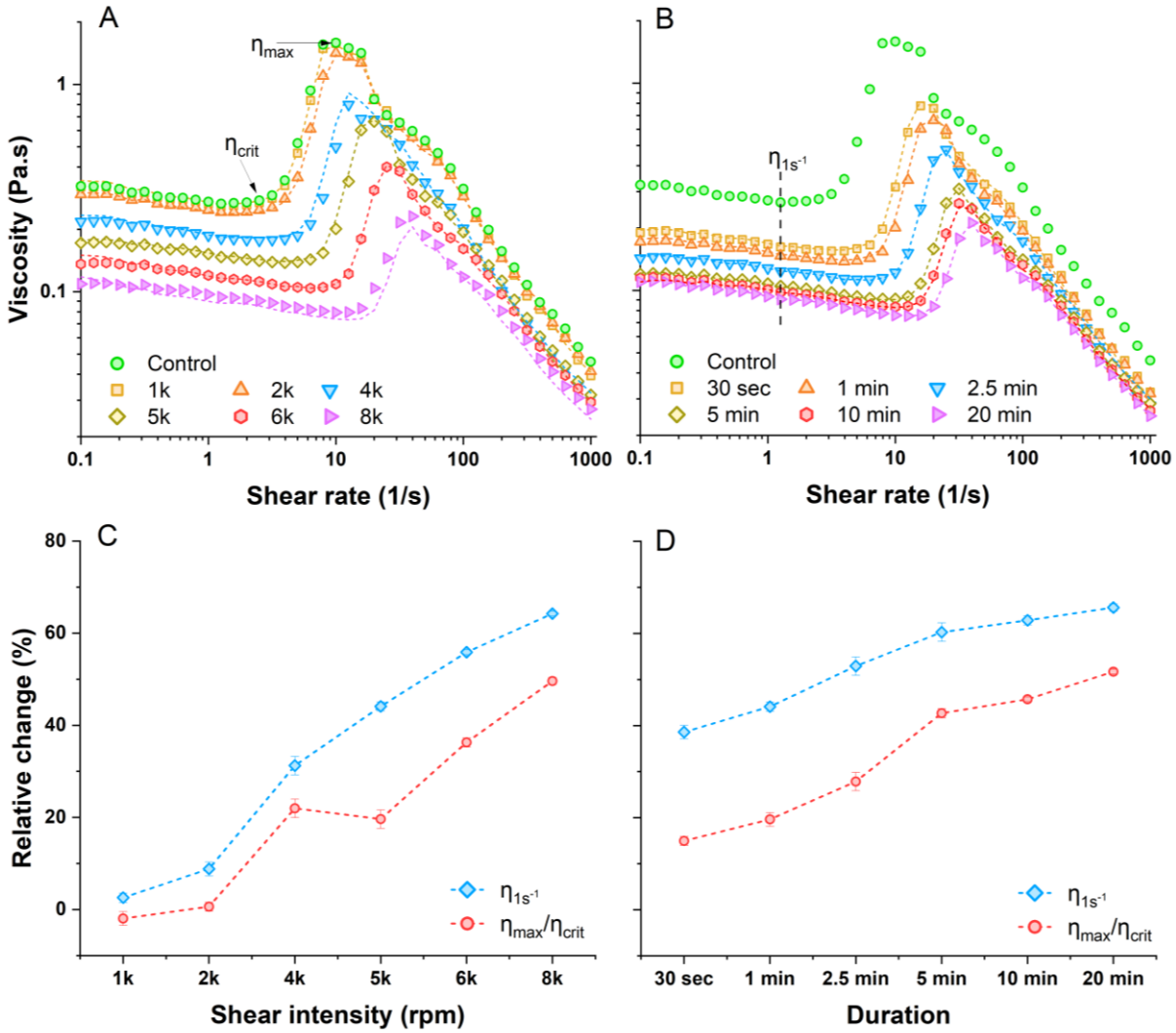


Figure 6.1: Viscosity profiles of crude mamaku gum (2% w/w total solids) after shear treatment at (**A**) 1k-8k rpm for 1 min and (**B**) 5k rpm for 30 sec-20 min. Dash lines (in **A**, **B**) represent the viscosity profile after 48 h storage at 4°C. Relative change (%) in viscosity at 1 s^{-1}, $\eta_{(1\,s^{-1})}$, and extent of shear-thickening, η_{max}/η_{crit}, after shear treatment at (**C**) 1k-8k rpm for 1 min and (**D**) 5k rpm for 30 sec-20 min. Values are plotted as means ± standard deviation (n=3). Measurements were taken using cup-and-bob geometry at 20°C. η_{max}, maximum viscosity (Pa.s); η_{crit}, critical viscosity (Pa.s).

The shear sensitivity of a biopolymer is affected by both the intensity of the applied shear and the duration of exposure. Interestingly, 5k treatment for 30 sec caused ~39% reduction in viscosity (measured at 1 s^{-1}) which was only further reduced an additional ~26% after 19 min, whereas 8k treatment, had ~65% reduction after 1 min indicating that the shear sensitivity of MP is influenced by both the applied shear and duration of the shear treatment, with the former having a stronger impact on the viscosity than the latter. These results are in

alignment with previous observations by Villay et al. (2012), who reported that for guar gum, sodium alginate, and gum arabica, the first cycle during high-pressure homogenization had a stronger impact on viscosity reduction than the subsequent cycles and the reduction increased with increasing pressure.

Table 6.1: Comparison of viscosities and critical shear rate for crude mamaku gum (2% w/w total solids) after shear treatment for 1 min.

	Control	1k	2k	4k	5k	6k	8k
$\eta_{(1\,s^{-1})}$	0.27	0.27	0.25	0.19	0.15	0.12	0.09
η_{max}	1.59	1.58	1.42	0.80	0.66	0.40	0.23
$\dot{\gamma}_{crit}$	2.51	2.51	2.51	3.16	6.31	10.00	12.60
η_{crit}	0.28	0.27	0.25	0.18	0.14	0.11	0.08
η_{max}/η_{crit}	5.76	5.87	5.73	4.49	4.63	3.67	2.90

$\eta_{(1\,s^{-1})}$, viscosity at 1 s^{-1} (Pa.s); η_{max}, maximum viscosity (Pa.s); $\dot{\gamma}_{crit}$, critical shear rate (s^{-1}); η_{crit}, critical viscosity (Pa.s); η_{max}/η_{crit}, extent of shear-thickening. Data extrapolated from graph in **Figure 6.1A**.

Table 6.2: Comparison of viscosities and critical shear rate for crude mamaku gum (2% w/w total solids) after shear treatment at 5k rpm for varying times.

	Control	30 sec	1 min	2.5 min	5 min	10 min	20 min
$\eta_{(1\,s^{-1})}$	0.272	0.167	0.152	0.128	0.108	0.101	0.094
η_{max}	1.59	0.779	0.662	0.478	0.309	0.263	0.212
$\dot{\gamma}_{crit}$	2.51	5.01	6.31	7.94	12.6	12.6	15.8
η_{crit}	0.276	0.159	0.143	0.115	0.094	0.084	0.076
η_{max}/η_{crit}	5.76	4.90	4.63	4.16	3.30	3.13	2.78

$\eta_{(1\,s^{-1})}$, viscosity at 1 s^{-1} (Pa.s); η_{max}, maximum viscosity (Pa.s); $\dot{\gamma}_{crit}$, critical shear rate (s^{-1}); η_{crit}, critical viscosity (Pa.s); η_{max}/η_{crit}, extent of shear-thickening. Data extrapolated from graph in **Figure 6.1B**.

In general, large and flexible macromolecules, such as MP, favour random coil conformations and have high entanglement density (Rudin & Schreiber, 1983). On subjecting them to high shear, the polysaccharide chain stretches, and the entanglement density reduces (*i.e.*, breakage of intermolecular interactions) causing a decrease in viscosity (**Figure 6.1**). However, this decrease in viscosity is typically temporary and will revert as the polymer returns to the original equilibrium state once the shear forces are removed. The rate of re-

entanglement is generally slower, as it depends on diffusion alone, compared to the rate of disentanglement which is favoured by applied shear (Rudin & Schreiber, 1983). Thus, the time-dependent recovery of mamaku gum after shear was tested. Samples were allowed to rest for 48 h at 4°C, after exposure to shear, and then again examined for rheological behaviour (shown as dash lines in **Figure 6.1A**, **B**). It is clear that there was no significant recovery in the viscosity for any of the samples after storage. This indicates that the loss of viscosity in mamaku gum was irreversible and remained somewhat permanent within the duration of our observation (48 h). Depending on the severity of shear treatment, the reduction in viscosity of a polysaccharide solution in general could be the result of one or more factor(s), such as disruption of aggregates or microgels, breakdown of double-strand structures (*e.g.*, for DNA and xanthan gum), reduction in M_w, changes in polydispersity and alteration in secondary structures (Eren et al., 2015; Harrington & Zimm, 1965; Laneuville et al., 2013). A similar reduction in viscosity has been reported for cashew tree gum (Porto et al., 2015), puka gum (Riana et al., 2022), pectin (Shpigelman et al., 2015; Xie et al., 2018) and tamarind seed polysaccharide (Xie et al., 2021) when subjected to shear (from mechanical action). These authors collectively suggested shear-led depolymerisation as the primary cause of viscosity reduction. On the contrary, an increase in viscosity for tragacanth gum due to the breakdown of larger aggregates and unfolding of the structures post shear treatment was reported (Farzi et al., 2015).

Similar to shear exposure, temperature treatment caused a reduction in viscosity at all shear rates in a temperature-dependent manner (**Figure 6.2**). The viscosity, at 1 s^{-1}, was reduced by ~15% after heating mamaku gum at 65°C for 30 mins, which drastically decreased by ~75% after heating at 75°C and ultimately decreased by ~99% after 115°C treatment. Simultaneously, η_{max}/η_{crit} was reduced by ~10% after heating at 75°C with a further reduction by ~97% at 95°C, finally losing the shear thickening behaviour at 115°C. Furthermore, the $\dot{\gamma}_{crit}$ increased from ~1 s^{-1} for the control and 65°C treated samples, to ~4 s^{-1} and ~63 s^{-1} for 75°C and 95°C treated samples, respectively (**Table 6.3**). These changes in the viscosity profiles collectively suggest that there may be thermal degradation of the polysaccharide *i.e.*, breakdown leading to smaller chain fragments in a temperature-dependent manner.

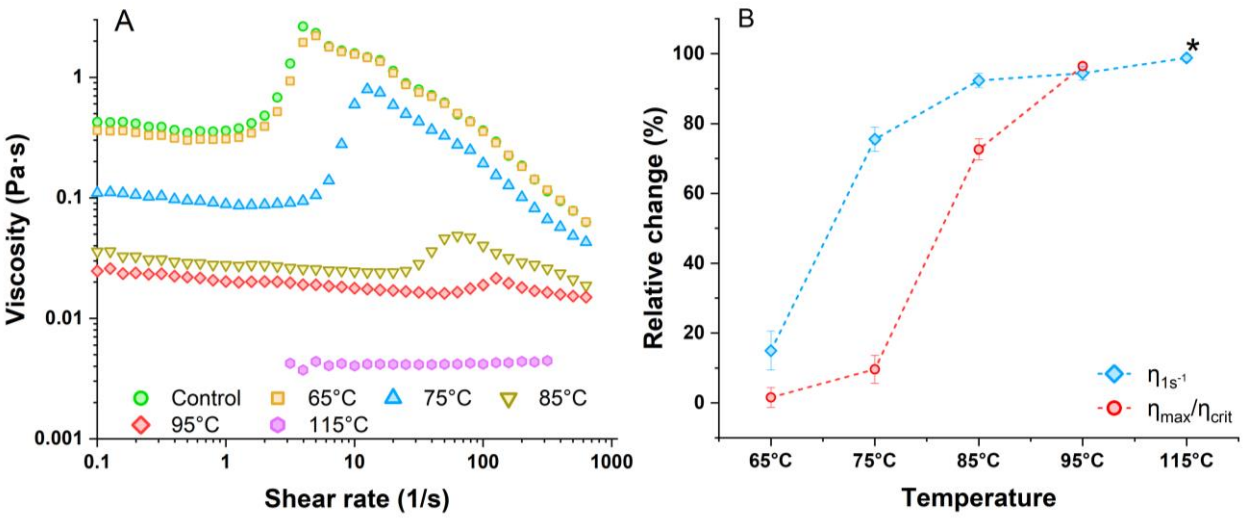


Figure 6.2: (**A**) Viscosity profiles of crude mamaku gum (2% w/w total solids) after temperature treatment between 65-115°C for 30 min. (**B**) Relative change (%) in viscosity at 1 s^{-1}, $\eta_{(1\,s^{-1})}$, and extent of shear-thickening, η_{max}/η_{crit}, after temperature treatment. (*): Newtonian behaviour at 115°C treatment. Values are plotted as means ± standard deviation (n=3). Measurements were taken using cup-and-bob geometry at 20°C. η_{max}, maximum viscosity (Pa.s); η_{crit}, critical viscosity (Pa.s).

Table 6.3: Comparison of viscosities and critical shear rate for crude mamaku gum (2% w/w total solids) after temperature treatment for 30 min.

	Control	65°C	75°C	85°C	95°C	115°C
$\eta_{(1\,s^{-1})}$	0.36	0.31	0.09	0.03	0.02	0.004*
η_{max}	2.64	2.21	0.79	0.049	0.004	-
$\dot{\gamma}_{crit}$	1.00	1.00	3.98	20.00	63.10	-
η_{crit}	0.36	0.31	0.12	0.02	0.02	-
η_{max}/η_{crit}	7.31	7.21	6.61	2.00	0.26	-

$\eta_{(1\,s^{-1})}$, viscosity at 1 s^{-1} (Pa.s); η_{max}, maximum viscosity (Pa.s); $\dot{\gamma}_{crit}$, critical shear rate (s^{-1}); η_{crit}, critical viscosity (Pa.s); η_{max}/η_{crit}, extent of shear-thickening. Data extrapolated from graph in **Figure 6.2A**. (*): Newtonian behaviour at 115°C treatment.

In addition to the viscosity profiles, the viscoelastic behaviour of the shear and temperature-treated samples was also studied within the linear region (**Figure 6.3**). It was observed that for the control, both—storage modulus, (G') and loss modulus, (G'')—increased with increasing frequency, with the 'liquid-like' behaviour ($G'' > G'$) dominating at low frequencies (< 0.5 Hz) and both moduli becoming equal above 0.5 Hz. With the shear and temperature treatments, a similar trend of an increase in G' and G'' with increasing frequency

was observed, but the values of G' and G'' were reduced with increasing treatment intensity, and the 'liquid-like' behaviour ($G'' > G'$) dominated over the 'weak-gel like' behaviour ($G' > G''$) over all the tested frequencies (up to 10 Hz). This is shown by an increase in the damping factor (ratio of G'' to G') (**Figure 6.4**), suggesting a decrease in elastic behaviour. In fact, above 95°C treatments, the elastic moduli were too weak to be detected by the rheometer, probably due to disruption of weak interactions such as H-bonds and degradation of longer polymer chains to shorter chains, limiting chain-chain interactions. A similar reduction in G' and G'' was observed for tragacanth gum after shear and temperature treatments attributed to polymer degradation (Keivanfard et al., 2022).

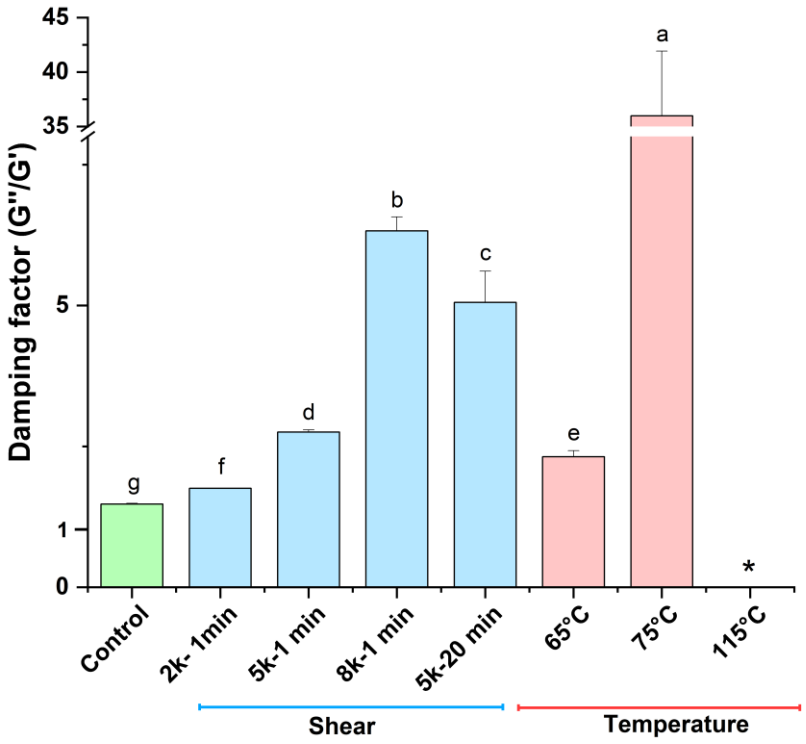


Figure 6.4: Damping factor (ratio of G'' to G') of crude mamaku gum (2% w/w total solid) after shear and temperature treatment at 0.1 Hz frequency. (*): G' was not detected. Values are plotted as means ± standard deviation (n=3). Measurements were taken using double gap geometry at 20°C. Bars with different letters are significantly different ($p \leq 0.05$).

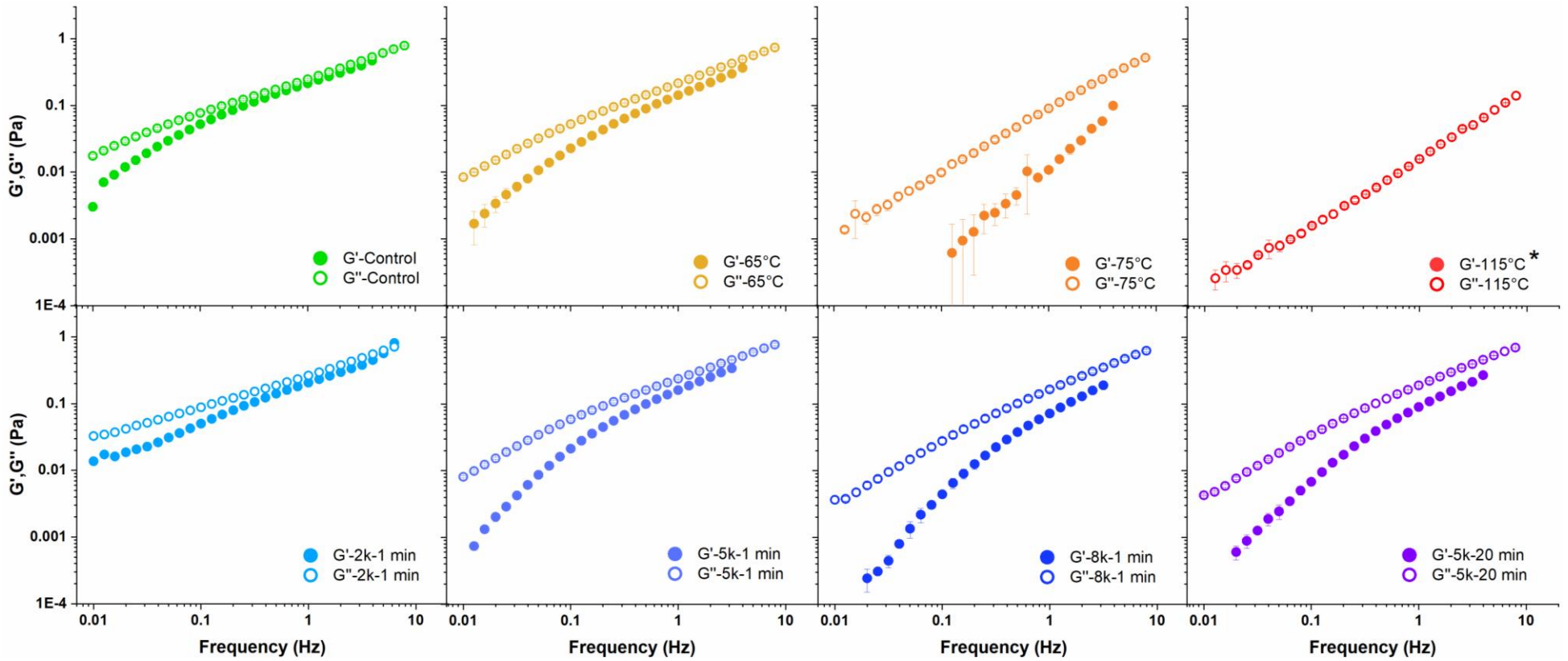


Figure 6.3: Storage modulus (G', filled symbols) and loss modulus (G'', empty symbols) of crude mamaku gum (2% w/w total solid) after shear and temperature treatment as a function of frequency. (*): G' was not detected. Values are plotted as means ± standard deviation (n=3). Measurements were taken using double gap geometry at 20°C.

6.3.2 Molecular weight and size of mamaku polysaccharide

The molecular parameters of MP such as weighted-average molecular weight (M_w), radius of gyration (R_g), polymer conformation and polydispersity were characterised *via* SEC-MALLS, after shear and temperature treatments. Surprisingly, the shear-treated samples did not show any significant changes in M_w after any applied shear (**Table 6.4** and **Figure E.1** in **Appendix E**). This suggests that the backbone structure of MP was retained after the shear treatment and the decrease in viscosity was not due to shear-induced depolymerisation. However, with increasing treatment intensity, a decreasing trend in R_g was observed which was statistically significant only at extreme conditions (~2.5% reduction at 8k- 1 min and 5k-20 min). These findings contrast with previously reported results where a clear decrease in M_w post shear treatment was observed for other gums such as acacia gums (Al-Assaf et al., 2009), scleroglucan (Zeng et al., 2021), pectin (Shpigelman et al., 2015), tamarind seed polysaccharide (Xie et al., 2021), chitosan (Kasaai et al., 2003) and methylcellulose (Floury et al., 2002).

In the present study, during sample preparation for molecular analysis, the polymer solutions were subjected to an ultracentrifugation step—to remove large aggregates which otherwise could block the SEC columns and detectors—and therefore some of the polysaccharide chains were lost. Thus, in a separate trial, mamaku gum was first ultracentrifuged and then subjected to shear treatment at 5k-20 min and 8k-1 min followed by directly injecting the samples into the SEC-MALLs—no difference in M_w was observed (**Table E.1** in **Appendix E**), confirming that the sample purification steps did not affect the results.

Figure 6.5 shows the chromatogram for the temperature-treated gum fractions with eluting time. The light scattering profiles clearly shifted to the right, indicating a decrease in M_w with an increase in the treatment temperature. When compared to the control, even at the lowest temperature of 65°C, a significant decrease in M_w and R_g was observed (from ~3.8x10^6 Da to ~3.6x10^6 Da and from ~150 nm to 145 nm, respectively) (**Table 6.5**). The M_w and R_g continued to significantly decrease as the temperature increased, reaching ~0.6x10^6 Da and ~50 nm (~84 and 67% reduction) after heating at 115°C (**Table 6.5**). Furthermore, it can also be observed

from **Figure 6.5**, that there was a shift to the right of the chromatogram from a monomodal peak (control and 65°C) to bimodal/shoulder peaks (75-95°C) and eventually, a monomodal peak at high temperature (115°C). This shift towards the right-hand side of the light scattering chromatogram is an indication of the degradation of the large native polymer chains to smaller chains as the temperature increases, indicating the high sensitivity of MP when the processing conditions are above 65°C. A change in molecular conformation (obtained from the slope of log M_w *vs* log R_g plot) was also observed with temperature, where the native polymers transited from an initial value of ~0.6 (implies a linear chain conformation in a good solvent) to ~0.55 (implies a reduction in extended chain conformation as intramolecular interactions dominates over intermolecular interaction, liken to linear random coils in a theta solvent[25]). This temperature-dependent reduction in M_w and R_g could explain the reduction in viscosity (**Figure 6.2**).

Table 6.4: Molecular parameters of purified mamaku gum after shear treatment analysed by size-exclusion chromatography coupled with multi-angle laser light scattering (SEC-MALLS).

	Weighted-average molecular weight, M_w x 10^6 (Da)	Radius of gyration, R_g (nm)	Slope from the plot of M_w against R_g	Polydispersity, M_w/M_n
Control	3.95±0.05^a	155.8±0.14^a	0.62±0.00^a	1.09±0.00^a
For 1 min				
2k	3.99±0.03^a	155.13±0.46^a	0.61±0.00^a	1.08±0.00^a
4k	3.99±0.03^a	154.4±0.37^b	0.61±0.01^a	1.08±0.01^a
5k	4.05±0.05^a	155.65±0.38^a	0.62±0.01^a	1.08±0.00^a
6k	3.98±0.03^a	154.6±0.79$^{a, b}$	0.62±0.01^a	1.08±0.00^a
8k	3.99±0.02^a	151.75±0.96^c	0.62±0.01^a	1.07±0.01^a
At 5k rpm				
1 min	4.05±0.05^a	155.65±0.38^a	0.62±0.01^a	1.08±0.00^a
5 min	4.02±0.06^a	156.125±0.01^a	0.61±0.01^a	1.07±0.00^a
20 min	4.07±0.08^a	152.15±0.35^c	0.6±0.01^a	1.08±0.01^a

Values are expressed as means ± standard deviation (n=3). Values in the same column denoted with the different superscript letters are significantly different ($p \leq 0.05$).

[25] A theta-solvent is a sufficiently poor solvent for a polymer, such that the polymer molecules have a low affinity for solvent and tend to move closer to neighbouring polymer molecules (*i.e.*, interactions between the polymer segments and the solvent are minimized and polymer-polymer interactions are maximized).

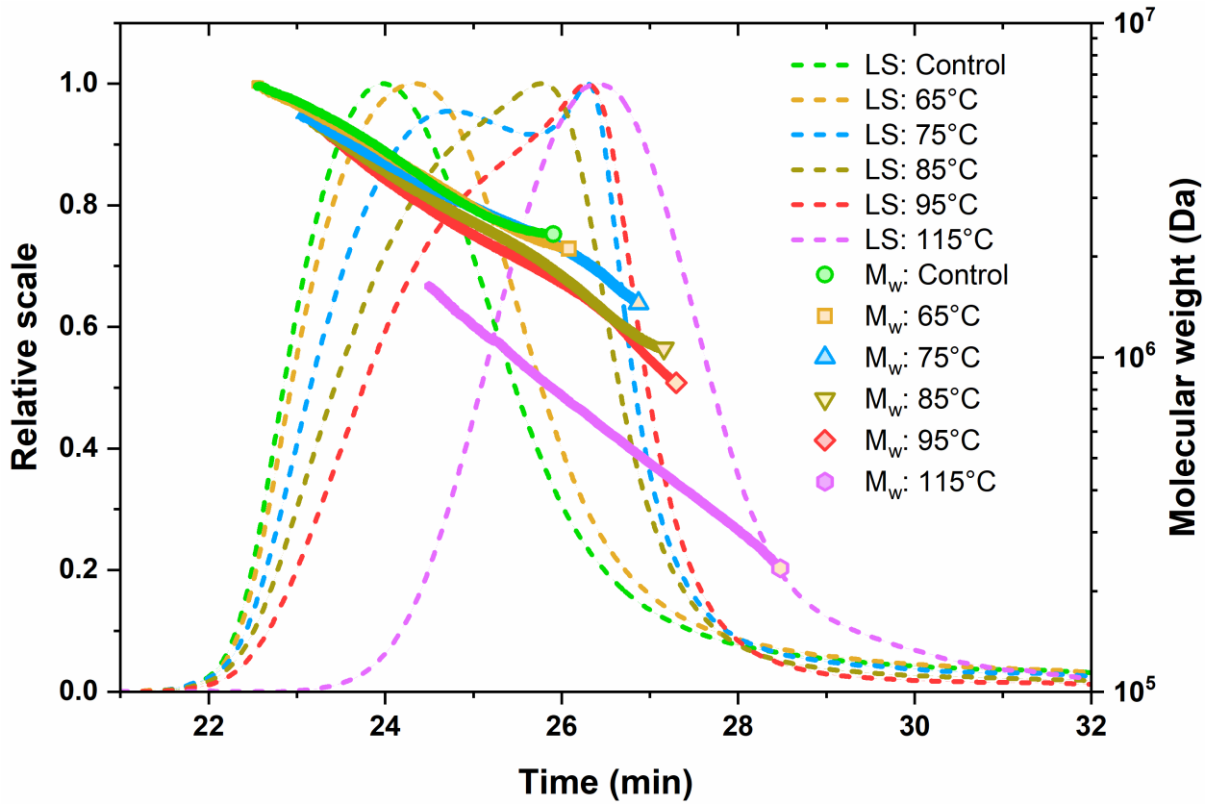


Figure 6.5: Light scattering (LS) signal and weighted-average molecular weight (M_w) analysis by size-exclusion chromatography coupled with multi-angle laser light scattering (SEC-MALLS) of purified mamaku gum after temperature treatment.

Table 6.5: Molecular parameters of purified mamaku gum after temperature treatment analysed by size-exclusion chromatography coupled with multi-angle laser light scattering (SEC-MALLS).

	Weighted-average molecular weight, M_w x 10^6 (Da)	Radius of gyration, R_g (nm)	Slope from the plot of M_w against R_g	Polydispersity, M_w/M_n
Control	3.78±0.04^a	149.53±0.61^a	0.61±0.00^a	1.1±0.00^e
65°C	3.59±0.01^b	144.85±0.86^b	0.6±0.01^a	1.11±0.00^e
75°C	2.79±0.06^c	121.95±0.50^c	0.55±0.01^b	1.13±0.00^d
85°C	2.39±0.02^d	113.05±0.83^d	0.55±0.01^b	1.17±0.01^c
95°C	1.99±0.03^e	103.93±0.74^e	0.56±0.01^b	1.23±0.01^a
115°C	0.6±0.00^f	49.65±0.32^f	0.62±0.01^a	1.21±0.00^b

Values are expressed as means ± standard deviation (n=3). Values in the same column denoted with the different superscript letters are significantly different ($p \leq 0.05$).

Similar to R_g, a decreasing trend was observed for z-average radius with increasing treatment intensity (**Figure 6.6**). A statistically significant decrease in z-average radius (from ~76 nm for control) was only detected at the extreme shear conditions *i.e.*, ~5% reduction at 8k-1 min (to ~72 nm) and 5k-20 min (to ~72.4 nm), while for the temperature-treated samples the decrease in the z-average became significant at 85°C (~22% reduction, to ~59.6 nm), with a further ~36% reduction (to 48.8 nm), at the highest temperature treatment (115°C).

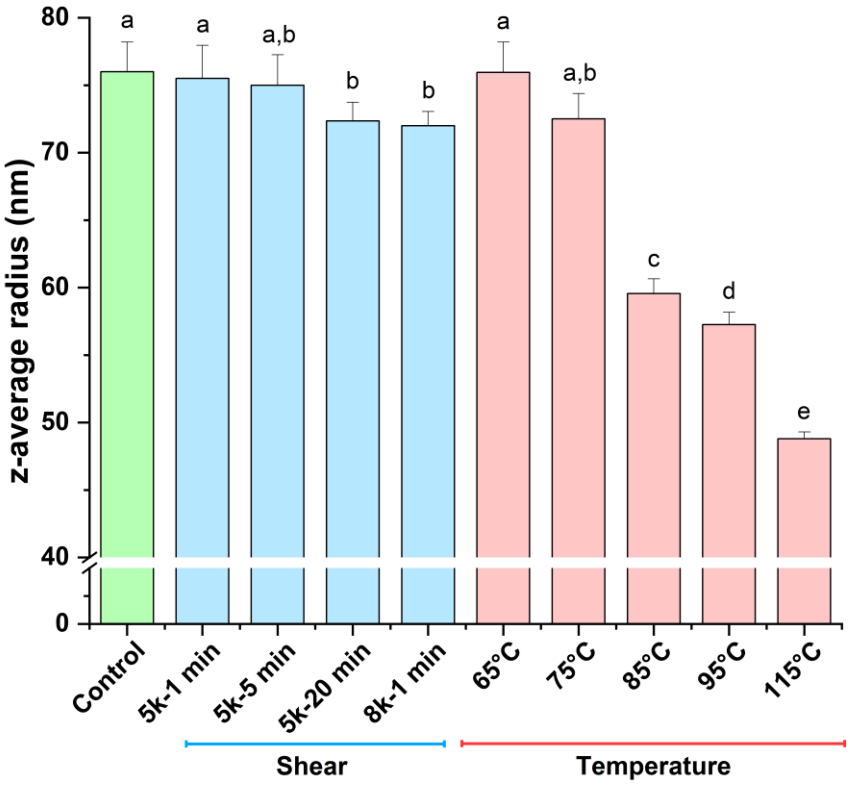


Figure 6.6: Effect of shear and temperature treatment on the z-average radius of purified mamaku gum. Values are plotted with mean ± standard deviation (n=5) obtained at 20°C. Bars with different letters are significantly different ($p \leq 0.05$).

6.3.3 Constituent sugar composition and nuclear magnetic resonance

Shear treatment (using high-pressure homogenisation) has been reported to induce side chain degradation in pectin from potato peel waste, while the main chain composition remained intact (Xie et al., 2018). The removal of some/specific monosaccharide units from the side chain may not significantly affect the M_w, as observed in our case, for the shear-

treated MP samples (**Table 6.4**), but may impair the hydrogen bonding between chains, thus, causing a reduction in viscosity. Constituent sugar analysis of both temperature and shear treated mamaku samples showed that the overall composition remained similar after all treatments (**Figure 6.7**). No changes in the monosaccharide composition for the temperature-treated samples indicate that the reduction in M_w after heat treatment was purely due to partial hydrolysis of the polysaccharide backbone, rather than the removal of individual monosaccharide units, which would have otherwise been lost *via* dialysis (molecular weight cut-off: 12,000-14,000 Da). Furthermore, NMR spectroscopy showed no discernible changes in the structure of the mamaku samples with either shear or temperature treatment (**Figure E.2** and **E.3** in **Appendix E**).

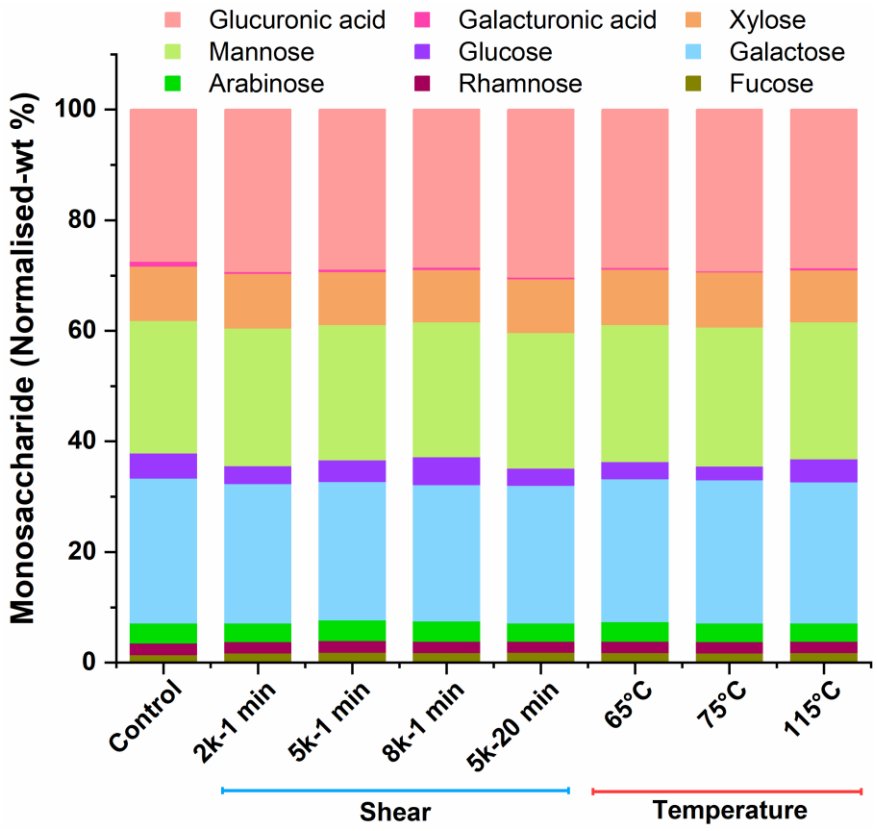


Figure 6.7: Constituent sugar composition of purified mamaku gum after shear and temperature treatment.

6.4 General Discussion

Treatment of natural polysaccharides by physical, chemical or enzymatic methods is often used to alter their physicochemical properties and physiological effects (Riaz, Iqbal, Jiang, & Chen, 2021; Wang, Xie, Shen, Nie, & Xie, 2018). The physical modification, by thermal, mechanical, and thermo-mechanical processes is more attractive to the industry than chemical modification, because problems of toxicity, separation and disposal that may be associated with chemicals are avoided. However, the modification of polysaccharides during processing may have undesirable effects, thereby limiting their use for some applications. Thus, in this study, the sensitivity of MP towards high shear and temperature treatments used during food manufacturing was investigated.

During shearing, the polysaccharide chains stretch and the molecules experience tension. When this tension reaches a critical level, the polymer chains break resulting in the formation of smaller fragments, which cause a reduction in viscosity. The mechanical scission *via* cleavage of strong glycosidic bonds in the backbone chain of a polymer is the primary reason vastly reported for the decrease in viscosity on exposure to shear (from mechanical action) (Belmiro, Tribst, & Cristianini, 2018; Eren et al., 2015; Laneuville et al., 2013). Villay et al. (2012) reported a reduction of ~87% for guar gum, ~60% for alginate and hydroxyethylcellulose and ~50% for CMC in M_w after using a high-pressure homogeniser (200 MPa, 2 cycles). Shearing may also cause changes in the primary structure of the polysaccharide, which could affect the molecular spatial structure and intermolecular interaction, causing a reduction in viscosity (Chen et al., 2012; Porto et al., 2015). However, in the present study, there were no changes detected in the chain length and the composition of the MP (**Table 6.4** and **Figure 6.7**). It is possible that the 'critical level of tension' was not achieved by the shear treatment used in this study, as the forces needed to break the covalent bonds in the main chain were insufficient. A similar resistance to shear-induced depolymerisation has been reported for polysaccharides from *Astragalus* (400 MPa, 10 min) (Zhu et al., 2016) and *Mesona chinensis* Benth (120 MPa, 6 cycles) (Huang et al., 2018). However, these authors reported an improvement in α-glucosidase inhibition and antioxidant activity after shear treatment and attributed it to changes in exposed groups due to an alteration in the secondary structure (using circular dichroism) (Zhu et al., 2016) and

morphology of the polysaccharide (using SEM) (Huang et al., 2018) without any reduction in M_w of the polysaccharide. This could imply conformation changes occurring intramolecularly which resulted in the exposure of side groups that were initially hidden in the polymer chains.

In the case of MP, on subjecting MP to shear treatment, a decrease in $\eta_{(1\,s^{-1})}$ and η_{max}/η_{crit} and an increase in $\dot{\gamma}_{crit}$ were observed depending on the severity of the treatment (**Figure 6.1, Tables 6.1** and **6.2**). The intrinsic viscosity, $[\eta]$, of a polymer (or the volume occupied by an individual polymer chain) is strongly governed by the M_w of the polymer ($[\eta] \propto M_w^a$, where "a" is a conformational factor), where the greater the M_w, the greater the $[\eta]$ and the greater the apparent viscosity of the polymer solution. The M_w of MP was unaffected after shear treatment and therefore, our initial hypothesis of polymer degradation due to shear is proven to be untrue, thus, a new hypothesis must be considered to interpret and explain the results. Based on the results obtained, the decrease in viscosity after shear treatment could be related to several phenomena that relate to chain rearrangements that resulted in a more compact folded chain. These could be the result of changes in the intermolecular, intramolecular, conformation and translational arrangement of MP chains. During shear treatment, MP chains experience shear forces that could disrupt intermolecular interactions among neighbouring chains. The individual chains are then unfolded and stretched by shear which could also disrupt intramolecular interactions (**Figure 6.8A**). Soon after the treatment, chains will continually rearrange into a new favoured state of equilibrium. It is plausible that MP chains, during this translational rearrangement, may undergo some changes in the packing of the three-dimensional units building up the macromolecule, which could consequently result in pockets of stronger intramolecular interactions giving it a more folded and compact structure (**Figure 6.8B**). These changes however are only picked up under extreme shear conditions where the R_g and the z-average radius were slightly reduced compared to the unsheared gum sample. During viscosity measurement, the shear-modified MP structure may resist the stretching of the chains because of the stronger intramolecular interactions and as a result, more energy was needed to unfold the chains to promote sufficient intermolecular hydrogen bonding to initiate the shear-thickening behaviour (thus, the increase in $\dot{\gamma}_{crit}$). Moreover, the chains may not unfold completely due to the stronger

intramolecular interactions limiting the sites for the formation of intermolecular interactions (thus, the decrease in η_{max}/η_{crit}) (**Figure 6.8C**).

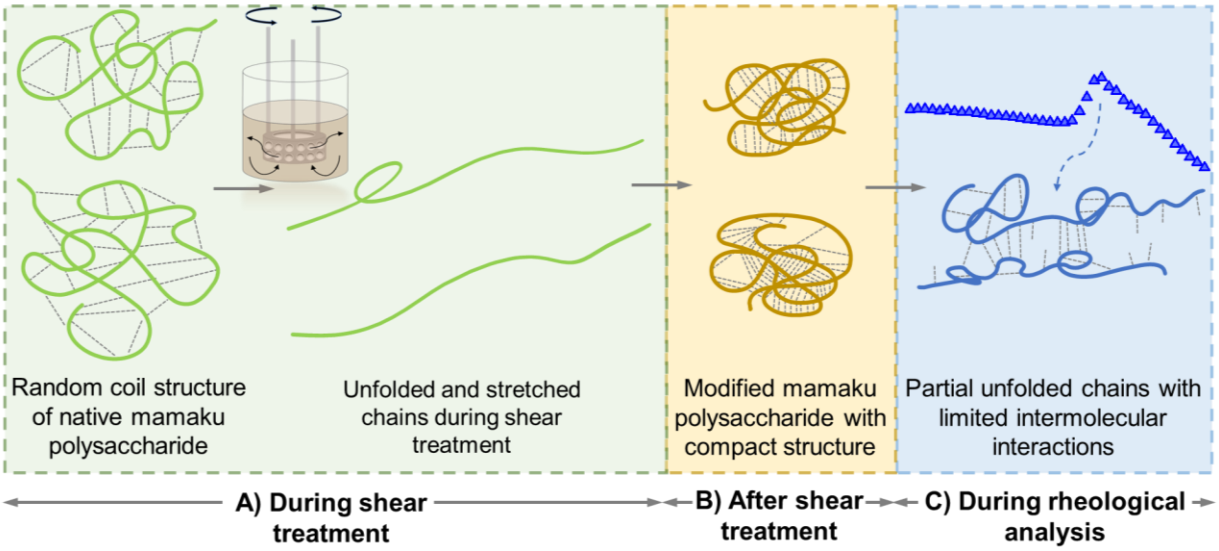


Figure 6.8: Schematic illustration showing the effect of (**A**, **B**) shear treatment on the packing of mamaku polysaccharide molecules and (**C**) consequently limiting the unfolding during the rheological analysis.

On the other hand, during thermal treatment, degradation *via* chain scission of the glycosidic linkage caused a reduction in M_w and viscosity in the mamaku gum (**Figures 6.2**, **6.5**, **Tables 6.3** and **6.5**). When the polymer chains are sufficiently heated the molecules get energised, and the bond between molecules vibrates and stretches, which eventually breaks, once the bond dissociation energy is achieved. A similar decrease in M_w and viscosity has been reported for mushroom *Inonotus obliquus* polysaccharide heated at 100°C for 3 h (Zhang, Chen, Ma, & Zhang, 2013) and waxy potato starch heated at 120-150°C for 30 min (Ang, Matia-Merino, Lim, & Goh, 2021). Lu, Li, Qiao, Qiu, and Liu (2018) also reported degradation in black garlic polysaccharide during thermal treatment at 70-90°C for 2-8 days.

Figure 6.9 shows the comparison of the rheological profiles for the extreme tested shear treatments *i.e.*, 5k-20 min and 8k-1 min and 75°C temperature treatment. Though the M_w for the shear-treated samples (~3.99 x 10^6 Da) was higher than the 75°C treated sample (~2.79 x

10^6 Da), three key conflicting observations can be made: (i) the viscosity (at 0.1-2 s^{-1}) was similar for all three samples; (ii) η_{max}/η_{crit} was significantly lower for the shear-treated samples (~2.8) compared to the 75°C treated sample (~6.6); and (iii) the $\dot{\gamma}_{crit}$ was higher for the shear-treated samples (~12-15 s^{-1}) than for the 75°C treated (~4 s^{-1}) sample. These rheological behaviours of the shear-modified MP could again be explained by the molecular rearrangement and the formation of a more compact structure (*i.e.*, strong intramolecular interactions leading to partial unfolding during rheological analysis). On the contrary, the smaller chains in the temperature-treated MP may be more easily unfolded due to weaker intramolecular interactions while exposing the sites for intermolecular interactions during the rheological analysis. Furthermore, the similar viscosity at low shear rates suggests that polymer-polymer and polymer-water interactions are comparable between all three samples (5k-20 min, 8k-1 min and 75°C). This would mean that at low shear rates when polymer molecules largely remain unperturbed, the extent of intermolecular interactions are similar despite the lower molar mass of the temperature treated MP. The rearrangements in shear modified MP may have resulted in a reduced amount of hydrogen bonding groups to be exposed and thereby, impairing the ability of the polymer to interact with neighbouring molecules and thus, reducing the viscosity of the solution. These results are in line with the subtle decrease in the z-average radius of the shear-treated MP mentioned above. The decrease in exposed groups of MP chains will also probably reduce the interaction with the water molecules. As a result, the Brownian motion of the MP-water complex will increase giving lower z-average radius ($\propto \frac{1}{diffusion\ coefficient}$). Changing the interaction between molecules of gum and water will change the rheology properties. Interestingly, the z-average radius for shear-treated (5k-20 min and 8k-1 min) samples was similar to the 75°C treated sample even though their molar masses differ. It is possible that conformational changes during shear treatment are a subtle intermediate stage between disentanglement and bond rupture, depending on shear intensity. The previous studies might have missed this intermediate stage as in most of them, the polymers were subjected to extreme shear from equipment such as a homogenizer or a microfluidizer. However, this cannot be concluded from the results of the present study.

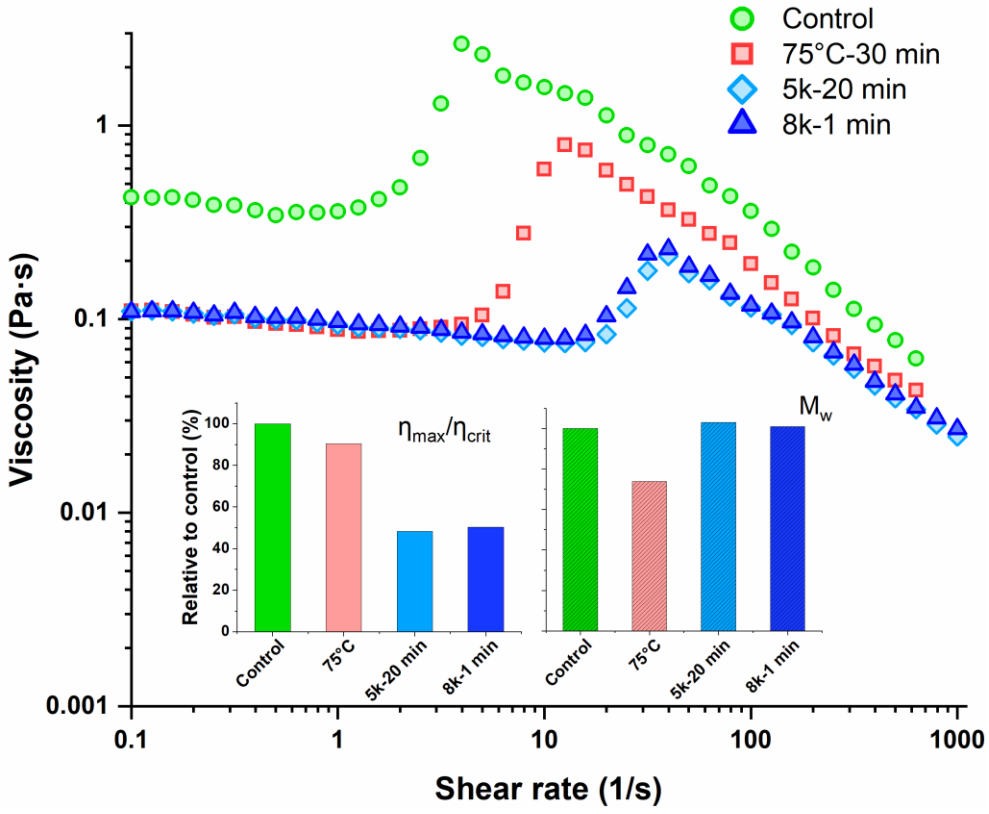


Figure 6.9: Comparison between shear (5k- 20 min and 8k-1 min) and temperature (75°C- 30 min) treated mamaku gum samples (2% w/w total solids). η_{max}/η_{crit}, extent of shear-thickening; M_w, weighted-average molecular weight.

Additionally, the rheological behaviour of shear-treated mamaku gum was analysed in the presence of urea, a commonly used hydrogen bond disrupter (**Figure 6.10**). If the more compact structure of shear-modified MP is due to increased intramolecular hydrogen bonds alone, then the urea should break them all, bringing the viscosity of the shear-modified MP closer to the control (due to similar M_w). However, this was not the case, as the viscosity of the control was still very different from the shear-treated samples, with the viscosity decreasing with greater treatment intensity. As previously observed for MP (Jaishankar et al., 2015), the shear-thickening behaviour was lost in all samples, suggesting that urea interferes with the intermolecular hydrogen bonding between MP chains. The results suggest that the compact structure of the shear-modified MP may not only be due to hydrogen bonds, but possibly other interactions mediated by mono, divalent and trivalent ions—given the presence of the high salt content in the mamaku gum extract.

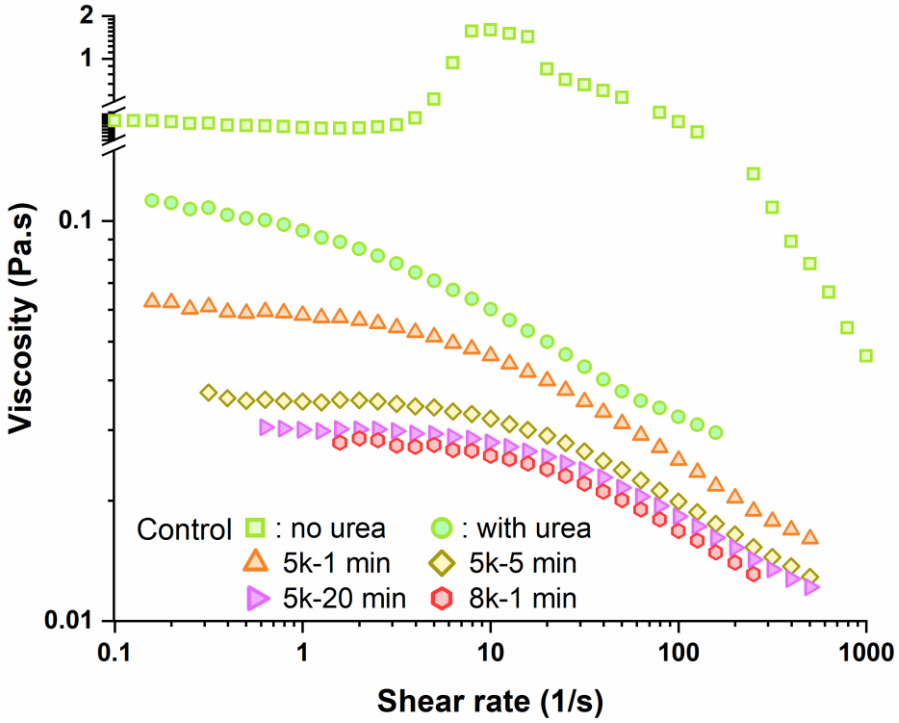


Figure 6.10: Effect of urea (5M) on the viscosity profile of shear-treated mamaku gum (2% w/w total solids). Measurements (n=3) were taken using cup-and-bob geometry at 20°C.

Overall, this study demonstrates the sensitivity of MP towards temperature and shear treatments. Temperature treatment caused thermal degradation of MP depending on the severity of treatment leading to a drastic loss in viscosity. A similar reduction in viscosity was observed after shear treatment without any polymer degradation. It is proposed that the shear-induced viscosity reduction could be related to the rearrangement of MP molecules and the formation of a more folded and compact structure. The results from this study are of high importance to the industry when processing conditions are considered since a decrease in viscosity will lead to texture modification of fluid and semi-solid foods which incorporate the MP. Further work on the effects of industrial treatments such as homogenisation and microfluidisation is needed to fully understand the sensitivity of MP to shear treatment. Also, further studies on structural changes should be carried out to gain more insights into the behaviour of MP during processing.

Chapter 7

Process-structure-function relationship for mamaku suspension: Effect of drying methods on powder functionality

7.1 Introduction

The pith from the fronds and trunk of the mamaku fern contains a water-soluble biomacromolecule called mamaku polysaccharide (MP), responsible for the uncommon shear-thickening behaviour of gum extract. The unique rheological behaviour of MP has been shown to alter the peristalsis contractions in an *ex-vivo* rat stomach model when compared with guar gum at a similar viscosity (Lentle et al., 2010). In a subsequent *in vivo* study, food consumption was reduced in rats gavaged with mamaku gum (Wee et al., 2017). The weight of the stomach content, retrieved after 2 h of final gavage, was significantly higher in the mamaku gum-treated group. In both these studies, mamaku gum was directly administrated into the stomach, but in reality, the gum needs to travel from the mouth *via* the oesophagus before it reaches the stomach; and in this case, the shear-thickening may develop in the oesophagus, which may pose an undesirable swallowing experience and choking hazard. Additionally, the physiological effects observed in these studies were at a high concentration of mamaku gum (more than ~15% w/w), which may not be a realistic concentration to deliver to humans if used in food systems. Lastly, as shown in **Chapter 6**, MP is sensitive to shear and temperature treatment, which may render its rheological properties ineffective in food products.

This chapter explores the potential of using the whole pith from mamaku fronds as an alternative to extracted gum for developing a food ingredient. Using the whole pith is a more sustainable way of utilising mamaku fern that will generate less waste, as opposed to the additional processing steps involved in extracting MP. Furthermore, the pith contains a high amount of fibres that may have additional physiological benefits (unpublished).

Fresh mamaku pith has a high moisture content, which makes it susceptible to microbial spoilage. However, drying can hinder microbial spoilage and prolong its shelf-life. Drying is a widely employed technology for the processing and preservation of high-moisture foods.

Oven-drying is a commonly used low-cost method, where a continuous flow of hot air is used to heat the product causing moisture to migrate within the matrix toward the surface by diffusion and/or hydrostatic pressure gradient (Karam et al., 2016). Freeze-drying is another method, used mostly for high-value products such as coffee, spices and herbs, where dehydration is achieved by sublimation of frozen products (Verma & Sharma, 2018). It is well established that the drying process can significantly affect the physicochemical properties of the product (**Table 2.4**). For example, freeze-dried sea buckthorn berries retained more carotenoids, vitamin C and phenolics than oven-dried (Araya-Farias, Makhlouf, & Ratti, 2011). It has also been reported that chokeberries had a higher porosity after freeze-drying than after oven-drying (Calín-Sánchez et al., 2015). The drying method also may cause deformation that can alter the structural matrix of food products and consequently affect their functionality. These dried products can be milled into powders for ease of transportation, storage and application.

Food powders are generally rehydrated in water before consumption. Several studies have reported the dynamic rehydration process for milk powders (Crowley et al., 2016; Ji et al., 2015; Ji et al., 2016) and hydrocolloids (Premathasan & Taylor, 2018; Wangler & Kohlus, 2017; Wangler, Teichmann, Konstanz, & Kohlus, 2019). However, there are limited studies on rehydration of powdered plant materials. The rehydration process for powders can be divided into four sequential steps: (i) wetting, (ii) sinking, (iii) dispersion and (iv) particle solubilisation into solutions, if soluble (**Figure 2.10**) (Crowley et al., 2016; Fang et al., 2007; Schubert, 1993; Wangler & Kohlus, 2018). Wetting refers to replacing the gaseous phase on the powder surface with water. Sinking refers to the submerging of powder below the surface of the water. Dispersion refers to the disintegration of wetted bulk powder particles and their dispersion throughout the bulk liquid. Solubilisation refers to the dissolution of the powder particles into the water to form a solution. These steps tend to overlap with each other and thus are difficult to study in isolation. An ideal food powder should be able to wet thoroughly, sink into the water rather than float on the surface, disperse and dissolve within a short time without forming any lumps. The rate of rehydration of powders *i.e.*, how quickly each step can be completed, mainly depends on the composition and physical properties (such as size, charge, porosity and morphology) of the powder, among others, which in turn may be affected by the drying method used (Gaiani et al., 2011; Li, Jin, &

Sheng, 2020). The surface composition will influence the hydrophilicity which will affect the wetting behaviour. Particles with high porosity enable water to penetrate easily into their structure. The morphology (size and shape) of particles can also impact how water penetrates the bulk powder (Yekeler, Ulusoy, & Hiçyılmaz, 2004).

With the motivation of developing a natural shear-thickening food ingredient using the whole mamaku pith, the process-structure-function relationship for the mamaku pith powder was investigated. It was hypothesised that, with an appropriate drying method, dried ground mamaku pith can confer similar shear-thickening properties as the extracted mamaku gum. The whole mamaku pith was firstly dried (oven- and freeze-drying) and then ground to powder using a pin mill. The resulting powders were characterised for changes in their physiochemical properties, rehydration behaviour in water, rheological behaviour and *in vitro* starch digestion.

7.2 Materials and Methods

7.2.1 Mamaku pith powder

The fully grown mamaku fronds (stage 2) were harvested, peeled to remove the external rind and cut into slices (~1 cm in thickness). The sliced pith was dried using either a freeze-dryer (FD18ISLA, Cuddon Freeze Dry, Blenheim, New Zealand) or an oven-dryer (Inoxtrend, Treviso, Italy) and ground using a pin mill (Grain Tech Engineering Ltd., Auckland, New Zealand, sieve size 650 μm) as described in **Section 3.1.2**. The freeze-dried pith powder (FDP) and oven-dried pith powder (ODP) have particles of size, d(0.5), 105.5±0.5 μm and 104.75±9.7 μm, respectively (**Figure 3.4**) and water activity (a_w) of 0.21±0.01 and 0.27±0.01, respectively.

7.2.2 Powder characterisation

7.2.2.1 Chemical composition

Moisture, protein, lipid and ash contents were determined using AOAC 950.46B, AOAC 968.06, AOAC 991.36 and AOAC 920.153 methods, respectively. Starch and dietary fibres were determined using Megazyme kits based on AOAC 996.11 and AOAC 991.43 methods, respectively. The mineral composition was determined using an inductively coupled plasma

(ICP)-optical emission spectrometer and sugar composition was analysed using gas chromatography. Uronic acid content was quantified spectrophotometrically using the *m*-hydroxydiphenyl method with glucuronic acid as the standard (Blumenkrantz & Asboe-Hansen, 1973). The chemical analyses were conducted by an accredited Nutrition Laboratory, Massey University, Palmerston North, New Zealand.

7.2.2.2 Colour

The surface colour was measured with a digital chroma meter (CR-400, Konica Minolta, Tokyo, Japan) in the CIE system (L^*: lightness, a^*: + redness, - greenness and b^*: + yellowness, - blueness). The browning index (BI, defined as brown colour purity) for each powder sample was calculated using:

$$\text{BI} = \frac{(x-0.31)}{0.17} \times 100 \qquad \textbf{Equation 7.1}$$

where, $x = \frac{(a^*+1.75\times L^*)}{(5.645\times L^*+a^*-3.012\times b^*)}$, while the total difference in powder samples (ΔE) was calculated using:

$$\Delta E = [(a^* - a_o^*)^2 + (b^* - b_o^*)^2 + (L^* - L_o^*)^2]^{1/2} \qquad \textbf{Equation 7.2}$$

where, a^*, b^* and L^* correspond to ODP and a_o^*, b_o^* and L_o^* correspond to FDP.

7.2.2.3 Density of powder

Powder samples were accurately weighed (5 g) into a 25 ml measuring cylinder (15x1.8 cm) and without disturbing the cylinder the volume was read to give the bulk volume of the powder. The cylinder with powder was then manually tapped until there was no further change in volume, giving the tapped volume of the powders. The bulk (ρ_b) or tapped density (ρ_t) were calculated as the ratio of the weight of powder to the bulk or tapped volume, respectively (Ermis & Özkan, 2021).

Particle density (ρ_s) was measured using the gas pycnometer (Ultrapycnometer 1000, Quantachrome Instruments, Boynton Beach, Florida, USA), where mamaku powders (~1 g) were placed in a sample cell and purged with nitrogen to degas the cell by ten pressurisation cycles to obtain the volume occupied by powders (Stange, Scherf-Clavel, & Gieseler, 2013).

The ratio of weight to volume was used to calculate ρ_s. Furthermore, porosity (ϕ) defined as the ratio of the volume occupied by voids to total volume, was calculated using:

$$\phi = \frac{\rho_s - \rho_b}{\rho_s} \text{ x } 100 \qquad \textbf{Equation 7.3}$$

where, ρ_s is particle density and ρ_b is bulk density.

7.2.2.4 Powder flow behaviour

The density of the ground mamaku powder samples was also used to characterise the flow behaviour. Based on the change in volume after tapping the bulk sample, compressibility or Carr index (CI) and Hausner ratio (H_R) were calculated using **Equations 7.4** and **7.5**, respectively:

$$\text{CI} = \left(1 - \frac{\rho_b}{\rho_t}\right) \times 100 \qquad \textbf{Equation 7.4}$$

$$H_R = \frac{\rho_t}{\rho_b} \qquad \textbf{Equation 7.5}$$

where, ρ_b is bulk density and ρ_t is tapped density.

In addition, the angle of repose measurement was carried out for FDP and ODP by freely flowing the powders (3 g) through a funnel clamped 10 cm from a paper surface (Nep & Conway, 2011). The height, h, and the radius, r, of the cone formed after the complete flow of powder were measured and θ was calculated using:

$$\tan(\theta) = \frac{h}{r} \qquad \textbf{Equation 7.6}$$

7.2.2.5 Scanning electron microscopy

The surface of the freeze-dried and oven-dried pith and their respective powders was analysed using scanning electron microscopy (SEM). The dried pith was cut into cubes (~0.5x0.5x0.5 cm) and mounted on aluminium stubs using double-sided tape, while the powder samples were uniformly spread on the double-sided tape adhered to the aluminium stub. The samples were then sputter coated with gold (~100 nm thickness) using Baltec SCD 050 sputter coater and viewed under FEI Quanta 200 environmental scanning electron

microscope (Field Electron and Ion Company, Hillsboro, Oregon, United States) at an accelerating voltage of 20 kV.

7.2.3 Powder rehydration

7.2.3.1 Wetting: Contact angle

The contact angle between FDP or ODP and water was analysed using the sessile drop technique as described by Ji et al. (2016). Briefly, powder samples were compressed to form the smooth disk under 281 bar pressure using a powder press (Vaneox Pressing Technology, Kleve, Germany). A 10 µl droplet of milli-Q water (at ~20°C) was placed on the disk surface using the auto-injector control system of the optical tensiometer (Biolin Scientific Attention theta flex, ATA Scientific Instruments, Sydney, Australia). The dynamic contact angle was measured every second till the droplet disappeared.

7.2.3.2 Sinking time

The time taken by FDP and ODP to immerse in water spontaneously without agitation was measured as described by Ji et al. (2016), with modifications. Briefly, 0.5 g of powder sample was placed evenly on the surface of the milli-Q water in a 400 ml beaker (~10x8 cm, containing 200 ml of water at ~20°C) and the time when all the powder immersed in water was recorded using a timer.

7.2.3.3 Dispersion: Particle size measurements

Dispersion of FDP and ODP was studied by monitoring the change in particle size as a function of time. Powder samples were dispersed in milli-Q water (1% w/w, ~20°C) and stirred at 150 rpm in a water bath (~20°C). The samples at different time points (0 to 1440 min) were added to the dispersion unit of Mastersizer 2000 (Malvern Instruments Ltd., Malvern, England) until a laser obscuration of ~10% was achieved. A general-purpose analysis model with a refractive index of 1.5 and 1.33 for powder particles and water, respectively, was used to calculate the particle size distributions.

7.2.3.4 Solubilisation

FDP and ODP samples (0.5 g) were dispersed in 50 ml of milli-Q water (1% w/w, ~20°C) in a beaker (~10x8 cm) and placed in a water bath (~20°C) with constant stirring at 150 rpm for different mixing times (0 to 1440 min). After mixing, the suspensions were transferred to 50 ml centrifuge tubes and centrifuged at 13,000 *g* for 30 min. The supernatant was collected, and the amount of solids was determined by drying in a hot-air oven at 105°C. Solubilisation (%) was calculated as the ratio of the amount of solids in the supernatant to the initial sample dry weight (Boucheham, Galet, Patry, & Zidoune, 2019).

7.2.4 Shear rotational rheology

FDP and ODP samples were hydrated in milli-Q water at different concentrations ranging from 0.5 to 8% (w/w) for ~15 h at ~20°C. Rheological measurements were performed in rotational mode using a Paar Physica MCR 302 rheometer (Anton-Paar, Graz, Austria) in a controlled shear rate (CSR) mode with a log-ramp profile from 15 s to 2 s (initial to final) at 20.0±0.1°C. Viscosity curves were measured using the cup-and-bob geometry (CC27 and C-PTD 200) or parallel plate (PP-40/Q1 and P-PTD200, gap = 1.5 mm) or double gap geometry (DG-26-7 and C-PTD 200), depending on the viscosity of the sample. Data were recorded using Rheoplus/32 software (Version 3.62).

7.2.5 Release behaviour of mamaku polysaccharide

FDP and ODP samples were weighed (0.5 g) and poured into 50 ml milli-Q water in a beaker (~9x4.5 cm, 1% w/w) at ~20°C. The samples were stirred using a magnetic stirrer initially at 600 rpm for 15 sec to create a vortex to disperse the powder and thereafter, stirred at 150 rpm for different rehydration times (0 to 1440 min). After a specific rehydration time, the samples were centrifuged at 13,000 *g* for 30 min to collect the supernatant. The whole suspension before centrifugation and the supernatant after centrifugation (*i.e.,* continuous phase) were characterised for viscosity and uronic acid content.

7.2.6 *In vitro* digestion of starch

The effect of FDP and ODP on the digestion of starch from WeetBix™ flaked wheat biscuit was studied as described previously (Monro, Mishra, & Venn, 2010). Briefly, FDP and ODP

suspensions (5% w/v) were prepared by hydrating the samples in water for ~18 h. WeetBix™ (WB; 2.5 g) was weighed into 70 ml specimen pots and mixed with 20 ml gastrointestinal salt solution (7 g/L of a stock mixture of 50 g NaCl, 4 g $CaCl_2$, 1 g $NaHPO_4$, 0.1 g $MgCl_2$), maleate buffer (5 ml, 0.1 M, pH 6.0) and powder suspension (25 ml) and volume adjusted to the 53 ml mark. A control pot of WeetBix™ alone (WB + water + buffer) was also prepared. Digestion was initiated by adding pancreatin (1 ml, 1% w/v, Sigma P1750, 4 x USP specifications, Saint Louis, Missouri, USA) and amyloglucosidase (0.1 ml, EAMG, Megazyme, Bray, Ireland) to the reaction pots, which were then installed in a rotary mixer (Heidolph REAX 2, Schwabach, Germany) placed in a heated cabinet (Heidolph INKUBATOR 1000 air heater, 37°C) for end-over-end rotation at 12 rpm to simulate physiological mixing. Digestion was timed from the start of the rotation. An aliquot (1 ml) was removed from each pot at 0, 10, 20 and 40 min and mixed with ethanol (4 ml) to stop digestion and precipitate undigested starch. After centrifuging a 0.5 ml sub-sample of supernatant was removed for analysis of reducing sugars by dinitrosalicylic acid (DNS) method (Englyst & Hudson, 1987).

7.2.7 Statistical analysis

All the experiments were performed at least in triplicate. The data are reported as mean ± standard deviation. Statistical analysis was performed using a one-way analysis of variance (ANOVA) with Tukey HSD post-hoc test at a 95% confidence level using SPSS software (IBM SPSS Statistics, Version 28.0.1.1(15)).

7.3 Results and Discussion

7.3.1 Chemical composition

The fresh mamaku pith had high moisture content (~94%), which was sufficiently reduced to ~5% dry weight using a freeze-dryer or oven-dryer, followed by grinding of the samples using a pin mill. The resulting mamaku pith powders contained a large proportion of dietary fibres (~36-40%) with the majority being insoluble dietary fibres (~23-27% of pith dry weight) (**Table F.1** in **Appendix F**). About 32-36% of the dietary fibre was soluble and of that about 32% was uronic acid (~4% of the dry weight of both powders), reflecting the large contribution of glucuronomannan to the soluble fibre fraction. The amount of sugar was also

high (~36-40%)—fructose (~17-19%) and glucose (~19-20%) were dominant sugars. The powder samples were relatively high in minerals (~8%), especially potassium, aluminium, sodium and calcium. Small amounts of fat (~1%) and protein (~2%) were present.

7.3.2 Powder characterisation

7.3.2.1 Colour

Colour is a critical quality attribute that is significantly affected by processing conditions. ODP had higher red and yellow Hue values and lower lightness than FDP (low L^*, high a^* and b^* for ODP), giving ODP a more brownish appearance (higher BI for ODP) (**Table 7.1**). The total colour difference (ΔE) between ODP and FDP was calculated as ~8. $\Delta E > 3$ suggests that the difference between samples is perceptibly different (Pathare, Opara, & Al-Said, 2013). The development of a darker colour for ODP could be a result of enzymatic and non-enzymatic browning reactions: oxidation of phenolic compounds by polyphenol oxidase and Maillard reaction between sugars and proteins at high temperature, respectively (Silva, Abreu, Silva, & Cardoso, 2019). On the contrary, the relatively low temperature involved during freeze-drying did not result in the browning of the mamaku powder. A similar observation that a darker colour was obtained after oven-drying as compared to freeze-drying, has been reported for black mulberries (Chen et al., 2017b), chokeberries (Samoticha, Wojdyło, & Lech, 2016), sugar beetroot (Ermis & Özkan, 2021), soy okra (Muliterno, Rodrigues, de Lima, Ida, & Kurozawa, 2017) and mushrooms (Argyropoulos et al., 2011).

7.3.2.2 Density and flow behaviour

Higher density (ρ_b, ρ_t and ρ_s) values were observed for ODP than for FDP (**Table 7.1**), which is in agreement with previous studies on mango (Caparino et al., 2012) and sugar beetroot (Ermis & Özkan, 2021) powders. The high particle density of ODP—and lower porosity—indicates the shrinkage and collapse of the pith structure during oven-drying. In addition to shrinkage, the difference in particle size distribution, surface structure and irregular shape may also affect the close packing of particles and therefore, the bulk and/or tapped packing density. Furthermore, the flow properties of the powders were predicted. A higher value of the angle of repose for FDP suggests that it is more cohesive than ODP. A similar trend was observed for CI and H_R, indicating relatively poor flow for FDP. Generally, from both CI and

H_R data, ODP was categorised as a poor flowing powder (CI: 26-31, H_R: 1.35-1.45), while FDP was categorised as a very, very poor flowing powder (CI: > 38, H_R: > 1.60). The relatively poor flow behaviour for FDP and ODP could be attributed to the high sugar content, which makes the powder highly hygroscopic rendering a greater tendency to stick and form clumps.

Table 7.1: Characterisation of freeze-dried (FDP) and oven-dried (ODP) mamaku pith powders.

	FDP	ODP
		
L^*	89.27±0.28^a	84.43±0.37^b
a^*	0.98±0.06^b	2.22±0.05^a
b^*	14.49±0.05^b	20.76±0.15^a
Browning index (BI)	18.12±0.06^b	29.65±0.24^a
Bulk density (ρ_b, g/cm^3)	0.14±0.01^b	0.26±0.01^a
Tapped density (ρ_t, g/cm^3)	0.25±0.01^b	0.38±0.01^a
Particle density (ρ_s, g/cm^3)	1.48±0.001^b	1.52±0.004^a
Porosity (ϕ, %)	90.95±0.03^a	82.40±0.01^b
Angle of repose (°)	38°±3^a	32°±2^b
Carr's index (CI)	44.53±3.47^a	31.05±1.89^b
Hausner ratio (H_R)	1.81±0.12^a	1.45±0.04^b

Values are expressed as means ± standard deviation (n=10). Values in the same row denoted with the different superscript letters are significantly different ($p \leq 0.05$).

7.3.2.3 Powder microstructure

The micrographs for freeze-dried and oven-dried whole pith and their respective powder surfaces are shown in **Figure 7.1**. Freeze-dried pith exhibited a more porous structure, while in oven-dried pith the porous structure appeared to collapse (pore size diminishes) somewhat resulting in a more compact and denser structure. In addition, the surface of FDP appeared smooth and flake-like while the ODP surface appeared thicker and wrinkled. The collapse in structure could be a result of heating the pith above its glass transition

temperature (T_g) leading to a soft and rubbery state where the solid food matrix can no longer support its own weight (Ratti, 2001). Izli and Polat (2019) reported a similar structural collapse on drying quince (45-75°C), and the degree of collapse of the tissue matrix increased with an increase in drying time. Air drying Kiwifruit (at 60°C) has also been reported to result in a tightly shrunken, thicker cellular structure and flattened surface when compared to freeze-dried samples (Zhang et al., 2019). The shrinkage and collapse in structure led to lower porosity for ODP (~8% lower than FDP) which is mainly responsible for the higher density of ODP compared to that of FDP (**Table 7.1**). Higher porosity after freeze-drying relative to oven-drying has also been reported for other plant materials (Calín-Sánchez et al., 2015; Ermis & Özkan, 2021; Michalska et al., 2017).

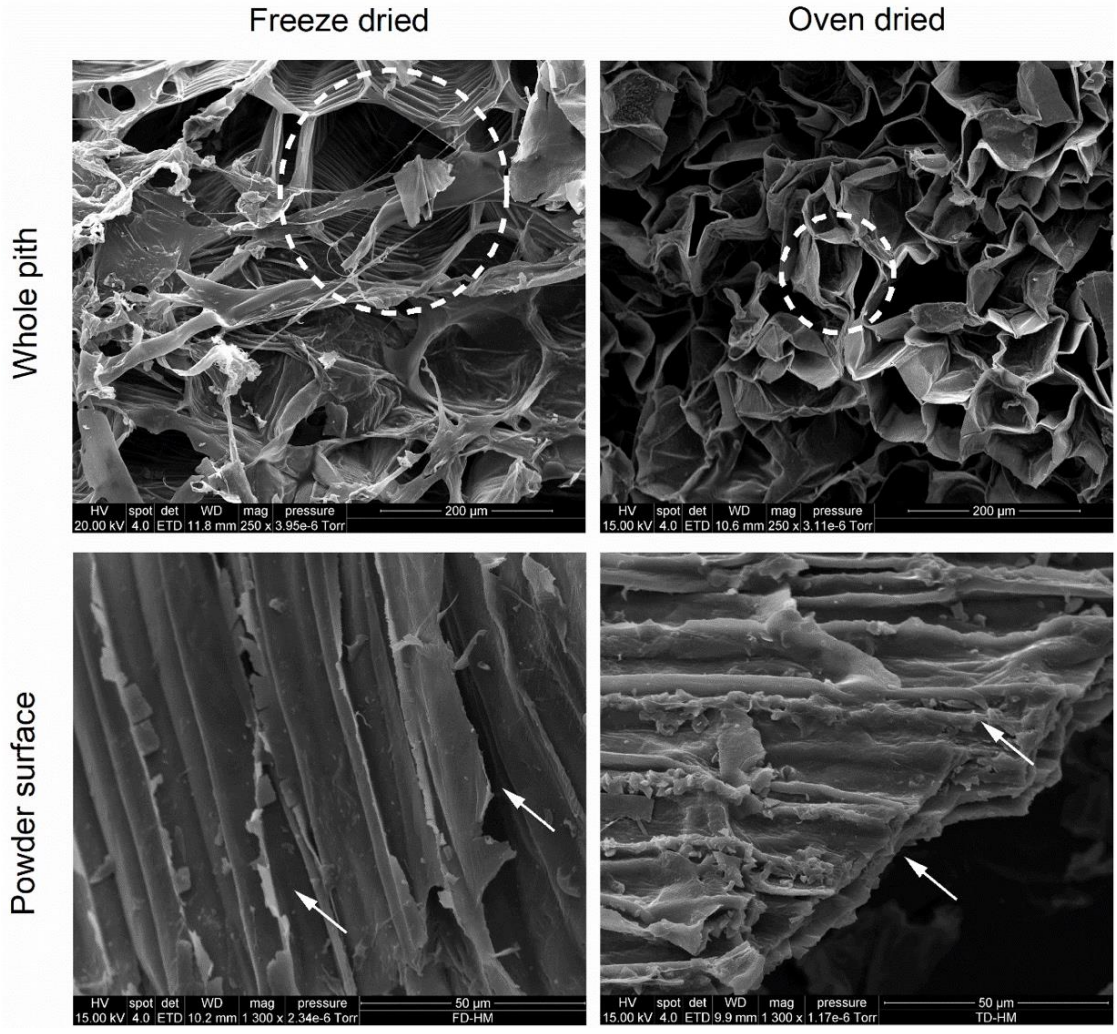


Figure 7.1: Micrographs of freeze-dried and oven-dried mamaku whole pith and their respective powder surfaces.

7.3.3 Rehydration behaviour of powders

7.3.3.1 Wetting

The wettability of powders is generally determined by measuring the contact angle formed by a droplet of water on the powder surface after spreading and reaching equilibrium by the balance of interfacial tensions between the solid (powder), the liquid (water droplet) and the gas (air). However, the contact angle measured on FDP and ODP using the current method changes over time as the water droplet once placed on the powder disk penetrates and gets absorbed into the powder bulk. A contact angle of 0-90° represents good wetting, whereas a contact angle above 90° represents poor wetting behaviour. **Figure 7.2A** shows the penetration of a water droplet into FDP and ODP at different time intervals. The contact angles for FDP and ODP were similar (~70°) at the start of the experiment, and they significantly reduced to ~20° within 5 s and 12 s, respectively (**Figure 7.2B**). A drastic decrease in contact angle suggests the hydrophilic nature of both powders. In the case of FDP, the presence of larger voids between particles generally facilitates easier movement of water into the powder bulk (Freudig, Hogekamp, & Schubert, 1999; Hogekamp & Pohl, 2003). Powders are commonly engineered to develop a porous agglomerated structure that improves the wetting behaviour (Forny et al., 2011; Ji et al., 2015). The compression of powders when filling the disk may cause some changes in the surface roughness, the structure of the bulk powder and the compaction pressure, thus, the contact angle should be treated as an apparent contact angle (Wangler & Kohlus, 2018). Furthermore, the contact angle measured using a powder disk may differ from the contact angle formed on individual powder particles.

7.3.3.2 Sinking

Once the gaseous phase around the powder is replaced by water, the water penetrates the powder particles, which will increase the particle density. As soon as the powder particles overcome the buoyant force exerted by the fluid, the powder will sink. It has been reported that food particles of size ≥100 μm and ρ_s ≈1.5 g/cm^3 could easily sink into water (Freudig et al., 1999). In the current study, both FDP and ODP are close to these generally accepted conditions, however, marked differences in the sinking behaviour were observed. The ODP

submerged into the water in ~2 min, while FDP continued to float on the surface (for the entire observation period of 60 min). Furthermore, a gelatinous layer around aggregates of powder particles was observed for the FDP (**Figure 7.3**). It is possible that due to the high porosity, water quickly penetrates the FDP particle surface (Forny et al., 2011; Hedenus, Mattsson, Niklasson, Camber, & Ek, 2000), and initiates the dissolution process before the particles sink and disperse (*i.e.*, a faster rate of water uptake than powder dissolution). This could lead to a poorly wetted centre, incomplete dissolution and formation of the viscous surface layer on the particle surface (Premathasan & Taylor, 2018; Wangler et al., 2019). The longer the FDP float on water, the polysaccharides (such as MP and cellulose) present in the wet surface layer of the powder particle may continue to interact with water and develop a viscous gelatinous layer, which could further delay the uptake of water (and the escape of entrapped air) and cause the formation of particle aggregates (Wangler & Kohlus, 2018; Wangler et al., 2019). On the other hand, ODP has a higher density and a lower porosity, which led to more rapid water uptake, thus enabling the particles to be wetted sufficiently and sink more easily than the FDP.

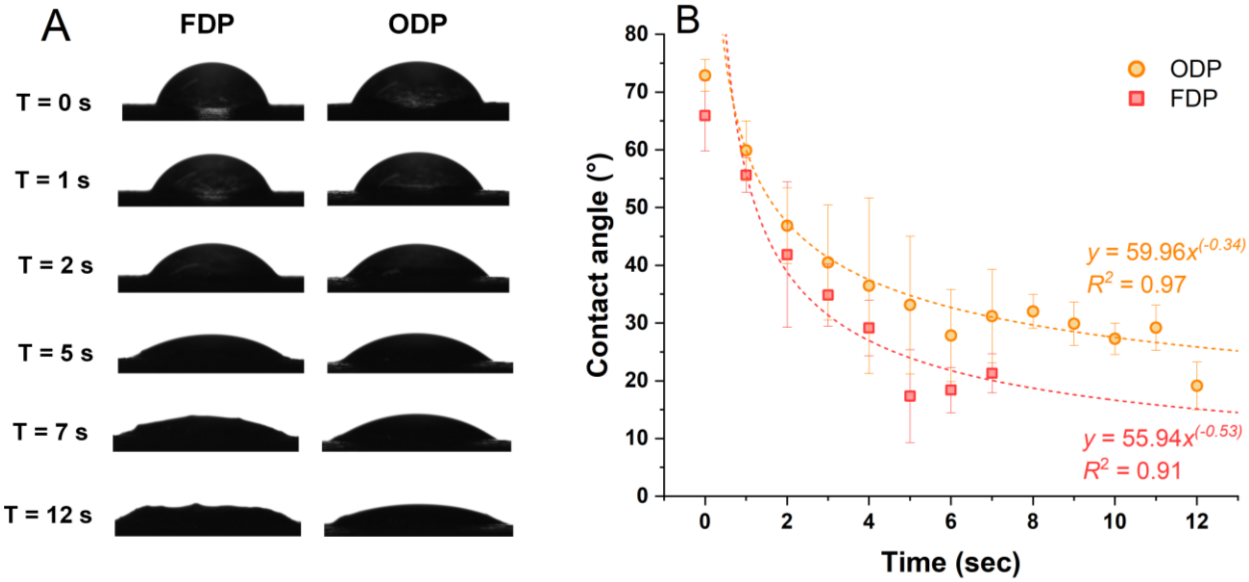


Figure 7.2: (**A**) Images showing the penetration of water droplet into freeze-dried (FDP) and oven-dried (ODP) mamaku pith powders at different time intervals. (**B**) Change in contact angle as a function of time at ~20°C. Values are plotted as means ± standard deviation (n=6).

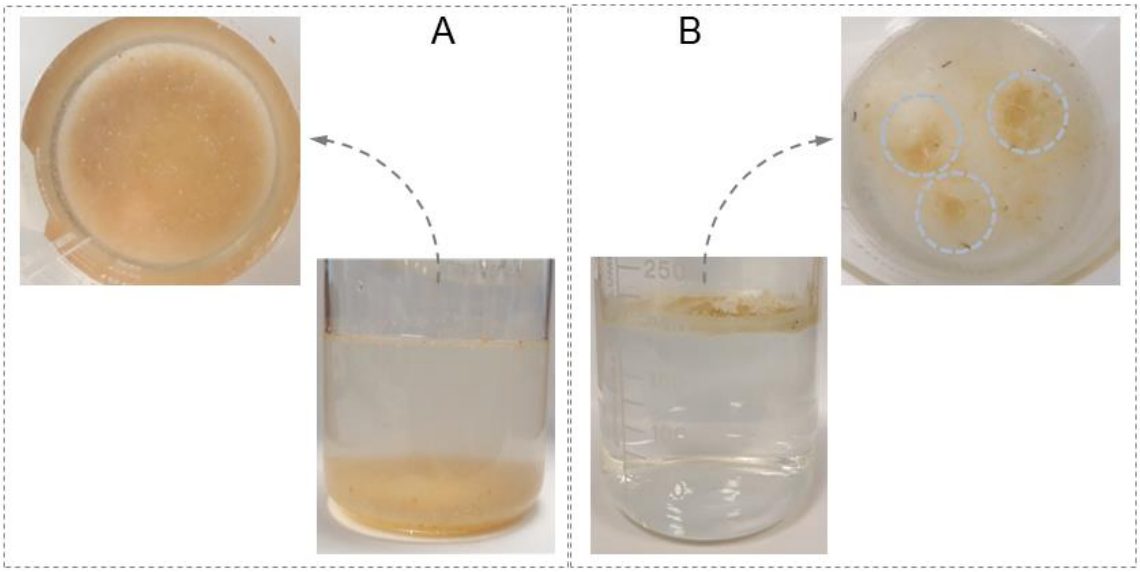


Figure 7.3: Pictures of (**A**) oven-dried (ODP) and (**B**) freeze-dried (FDP) mamaku pith powders at the end of the sinking experiment. A gelatinous layer with aggregates was observed for FDP powder with no sinking for 60 min.

7.3.3.3 Dispersion and solubilisation

In order to circumvent the poor sinking of the FDP powder, shear was applied (to both FDP and ODP) to facilitate a more effective dispersion. The change in particle size under the applied shearing conditions was monitored. Generally, as food powders are dispersed during reconstitution, the particle size reduces due to the breakdown of particles and the dissolution of water-soluble components such as sugars and polysaccharides into the bulk water phase (Ji et al., 2015). However, for FDP and ODP, the particle size was found to increase with time, suggesting swelling of the particle structure (**Figure 7.4A**). The increase in particle size was highest during the first 180 min for both FDP and ODP. FDP had a smaller particle size than ODP throughout the entire experiment. Similar swelling behaviour has been observed for different cereal and legume powders that contained fibrous materials (Boucheham et al., 2019). The swelling is related to the insoluble fraction within the particle structure which appears to occur simultaneously with the solubilisation of the water-soluble fraction of the particles (**Figure 7.4B**). The increase in solubilisation was also the most significant in the first 180 min of the experiment. The data show that the FDP was more soluble than ODP which could explain the lower particle size of FDP compared to ODP.

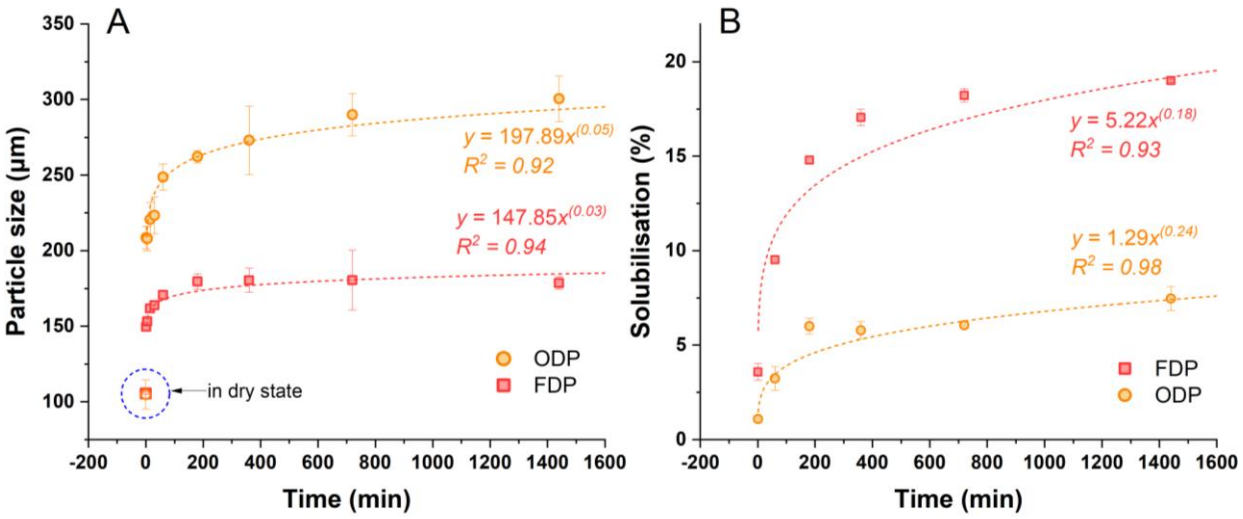


Figure 7.4: Change in (**A**) particle size (d 0.5) and (**B**) % solubilisation of freeze-dried (FDP) and oven-dried (ODP) mamaku pith powders in water at ~20°C as a function of time. Values are plotted as means ± standard deviation (n=6).

The swelling of powder particles starts as soon as the particles are brought in contact with the water and may have contributed to the poor sinking behaviour of FDP (Freudig et al., 1999; Hogekamp & Schubert, 2003). The swelling causes an increase in particle size that may lead to a drop in ρ_s, thus, impeding sinking (Wangler & Kohlus, 2017). The swelling of particles may also block the pores, which will hinder the ease with which water penetrates inside (Wangler & Kohlus, 2018), and as a result, powder particles will take longer to overcome the buoyant forces. The delay in the sinking may promote the diffusion of water-soluble compounds from the wet surface layer of the particles into the water phase (*i.e.,* solubilisation) before completing intermediate steps (*i.e.,* sinking and dispersion). The dissolution of compounds into bulk water will further reduce the density and delay sinking. Though the swelling was also observed for ODP, its impact on sinking was not as drastic as for FDP. This could be due to higher density (**Table 7.1**) and a lower solubilised fraction observed for the ODP (**Figure 7.4B**) which could easily contribute to a faster sinking.

7.3.4 Rheological characterisation

The FDP and ODP samples were hydrated overnight at a concentration ranging from 0.5 to 8% (w/w total solids) prior to viscosity measurements which are shown in **Figure 7.5**. The

FDP suspension (which consisted of the insoluble particle fraction + soluble MP) exhibited three distinctive regions: Newtonian behaviour at a low shear rate, shear-thickening at an intermediate shear rate, and shear-thinning at a higher shear rate (**Figure 7.5A**), which is the typical rheological profile of MP extracted from the pith (Goh et al., 2007). The ability of the FDP suspension to show similar viscosity profiles to MP indicates the strong contribution of the soluble MP in the continuous phase without marked interference from the insoluble particle fraction. As expected, the viscosity of FDP suspension increased with an increase in powder concentration. As the concentration of the powder increases, the volume fraction of the particles also increases correspondingly which leads to decreasing proximity, closer packing of particles and increasing particle-particle collisions. In addition to the particle concentration, MP concentration in the continuous phase also increases, which increases the viscosity of the continuous phase. The swollen insoluble fraction in the dispersed phase and the complex rheological behaviour of the continuous phase from the MP contributed to the overall unique rheological properties of the dispersion. Interestingly, at higher concentrations (5% and 8% w/w) the shear-thickening behaviour was lost.

The particle polymer suspension can give rise to three types of interactions: polymer-polymer, polymer-particle and particle-particle. The polymer-polymer interactions are dominant at dilute particle concentration, while particle-particle interactions become important with increasing concentration becoming dominant at very high concentrations. Intermediate to polymer-polymer and particle-particle interactions lies the polymer-particle interactions (Mazzanti & Mollica, 2020; Pryamitsyn & Ganesan, 2006). A concentrated suspension of hard particles, when particle-particle interactions are strong, can exhibit shear-thickening behaviour due to the formation of transient particle aggregates, called hydroclusters, as particles come in close proximity during shearing (Gürgen et al., 2016; Park, Rathee, Blair, & Conrad, 2019; Warren et al., 2015). However, the shear-thickening behaviour of the FDP suspension cannot be attributed to particle clustering because, at the higher concentrations of FDP (5% and 8% w/w), the shear-thickening behaviour was lost. The loss of shear-thickening behaviour could be due to several possible explanations including limited hydration of FDP that reduce the solubility of MP; reduced available space for the polymer chains to stretch upon shear and the interference from the insoluble powder fractions which disrupts the intermolecular interactions among the MP during shear.

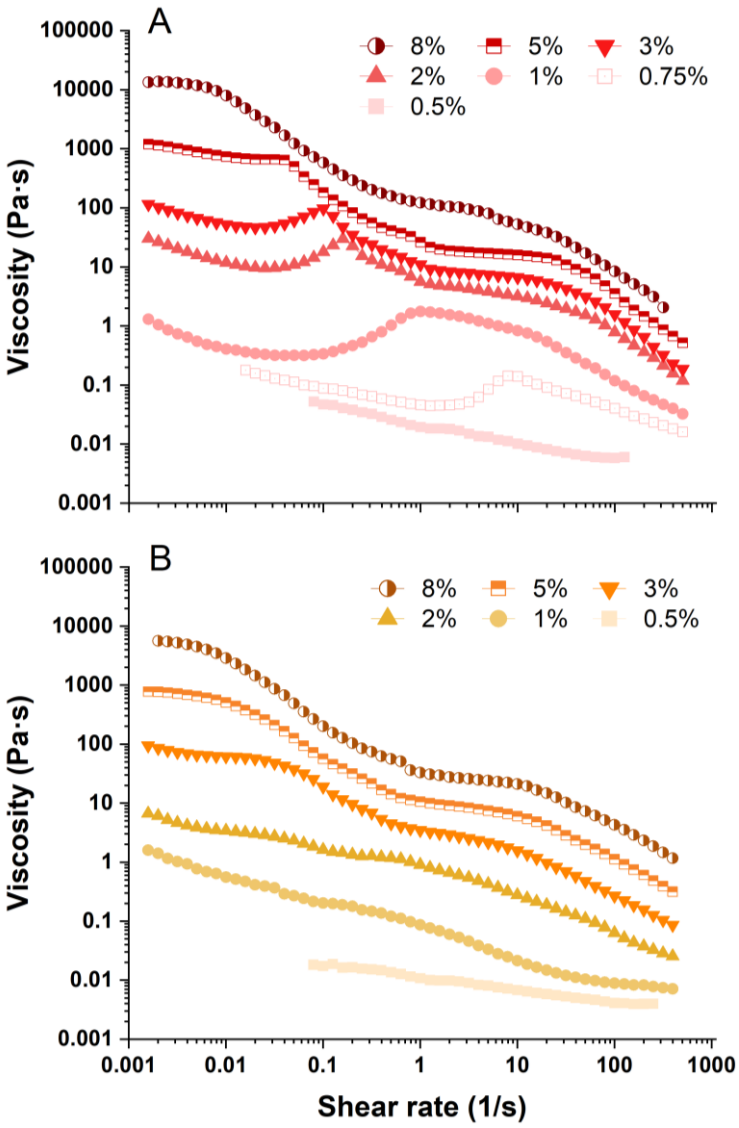


Figure 7.5: Viscosity profiles of (**A**) freeze-dried (FDP) and (**B**) oven-dried (ODP) mamaku pith powder suspensions (after 15 h hydration) as a function of shear rate. Values are plotted as means of triplicates (n=3). Measurements were taken using cup-and-bob geometry at 20°C. 8% (w/w) sample was measured using parallel plate geometry.

The ODP suspension, on the other hand, did not exhibit any shear-thickening region; rather a shear-thinning behaviour was observed (**Figure 7.5B**) at all concentrations. This further affirms that the shear-thickening behaviour in the FDP suspension is not because of particle clustering. The reason for the loss of shear-thickening behaviour in the ODP suspension was investigated by heating mamaku gum extract (2% w/w total solids) in the oven at ~50°C for 40 h (similar conditions used for preparing the ODP). However, the rheological profile of

mamaku gum was unaffected (**Figure F.1** in **Appendix F**), indicating that the drying regime used did not affect the shear-thickening properties of the MP. A plausible explanation for the loss of shear-thickening behaviour could be due to the entrapment of the MP within the dense structure of ODP resulting in insufficient MP being released in the continuous phase to exhibit the typical shear-thickening behaviour of the MP.

7.3.5 Release of mamaku polysaccharide from powder particles

The release of MP from FDP and ODP was studied by quantifying the amount of uronic acid in the continuous phase and monitoring the viscosity of suspension (1% w/w) and continuous phase over 1440 min of hydration. The amount of uronic acid released into the continuous phase increased with time for both powders; however, the amount released by FDP was significantly higher than for ODP at all time points (**Figure 7.6**). The amount of uronic acid increased exponentially in the continuous phase of FDP for the first 180 min, which then plateaued (as no marked increase was observed). On the contrary, the amount of uronic acid released by ODP, even after 1440 min of rehydration, was markedly lower than that released by FDP at 180 min.

The continuous phase of the reconstituted FDP exhibited shear-thinning behaviour at the beginning of the rehydration process. The shear-thickening behaviour only appeared at 180 min and became more prominent as the rehydration time increased (**Figure 7.7A'**). A similar trend in viscosity was observed for the FDP suspension (**Figure 7.7A**). On comparing the suspensions with their continuous phases, it can be observed that MP contributed to the rheological profile of the suspension while the particles increased the overall viscosity without altering the trend of the rheological properties. No shear-thickening behaviour was observed for the ODP suspensions and their continuous phases (**Figure 7.7B**, **B'**). However, on concentrating the continuous phase of the ODP collected after 1440 min of rehydration, the shear-thickening behaviour was observed (**Figure 7.7B'**). This demonstrates that the lack of shear-thickening is just a MP concentration effect as not enough gum was released from the ODP powder particles. However, when the gum in the continuous phase is concentrated, the shear-thickening is recovered, proving that the gum was not damaged during heat treatment.

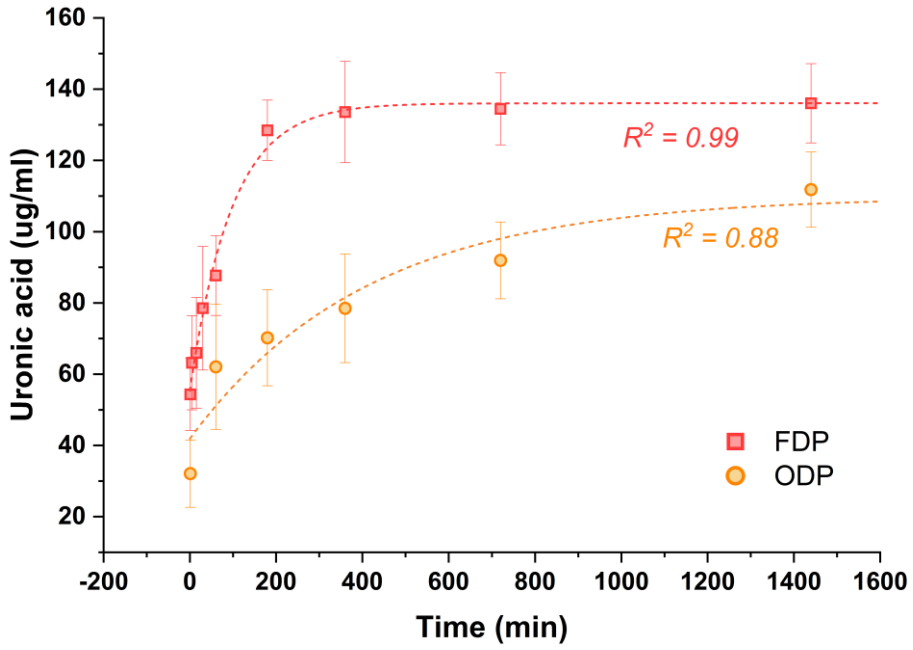


Figure 7.6: Amount of uronic acid in the continuous phase of freeze-dried (FDP) and oven-dried (ODP) mamaku pith powder suspension (1% w/w) as a function of hydration time at ~20°C. Values are plotted as means ± standard deviation (n=3).

For both FDP and ODP, the viscosity of the suspensions increased with rehydration time. This development of viscosity could be a net result of multiple events happening simultaneously such as the increasing release of MP in the continuous phase, the solubilisation of powder particles, the increase in particle size and possible changes in the size distribution and shape of particles. Once the MP is released in the continuous phase, MP may continue to interact with water to develop an interfacial hydrogen bond network *i.e.*, hydration of the individual polysaccharide chains (Grossutti & Dutcher, 2020), which may further contribute to viscosity enhancement. Although the understanding of the hydration of individual chains at the molecular level is limited, an increase in viscosity with polymer hydration time has been reported previously (Premathasan & Taylor, 2018; Wang et al., 2002; Wangler & Kohlus, 2018), which may be due to an increasing hydrodynamic volume and conformational changes.

One should be cautious while interpreting the true values of the amount of uronic acid and viscosity of the continuous phase because the loss of MP during centrifugation cannot be discharged. MP release behaviour was also studied for FDP and ODP of different particle

sizes (bigger > 105 µm > smaller), and similar trends in the amount of uronic acid and viscosity of the continuous phase were observed (**Figures F.2** and **F.3** in **Appendix F**). The consistency of these trends indicates that the results are reliable.

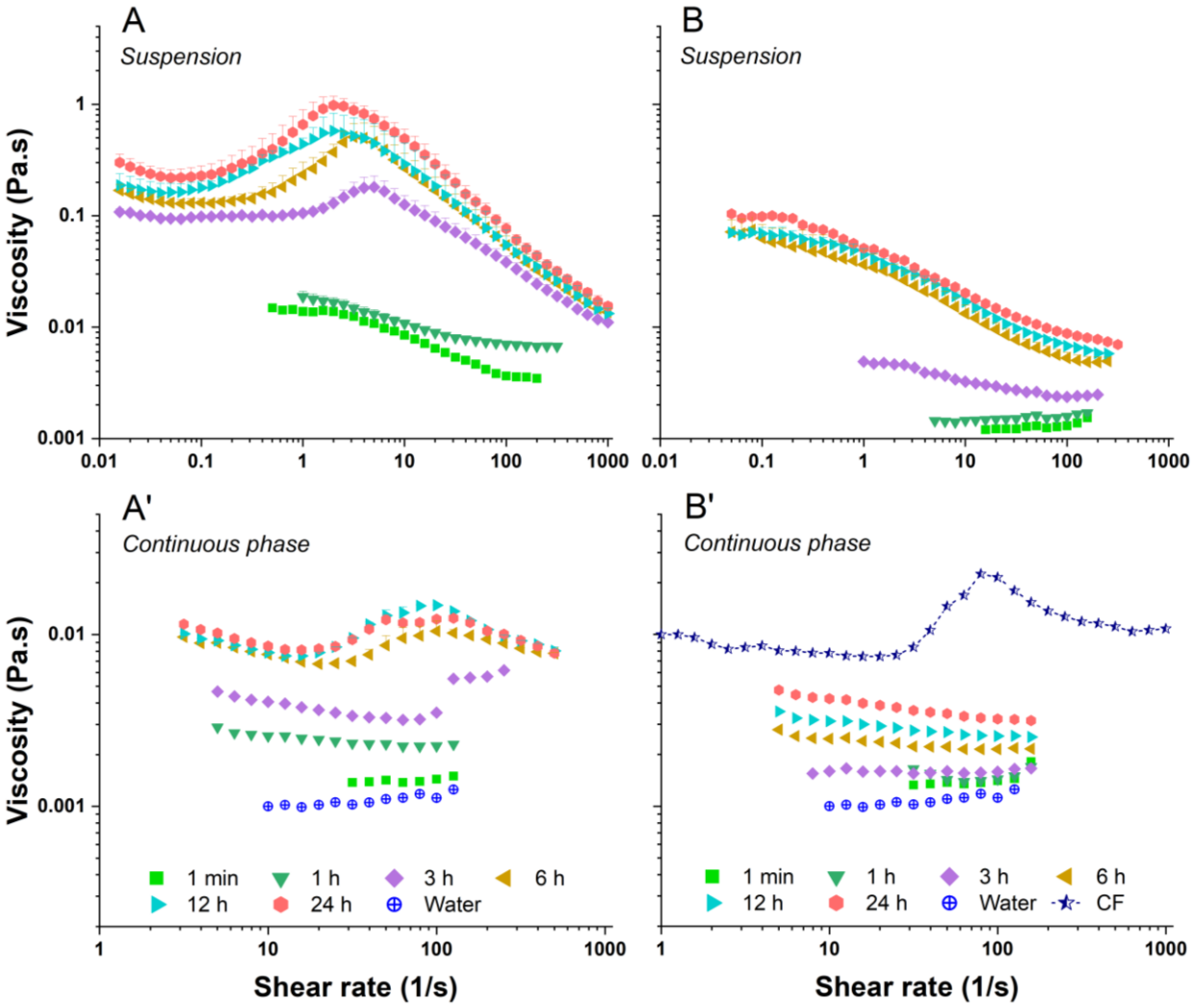
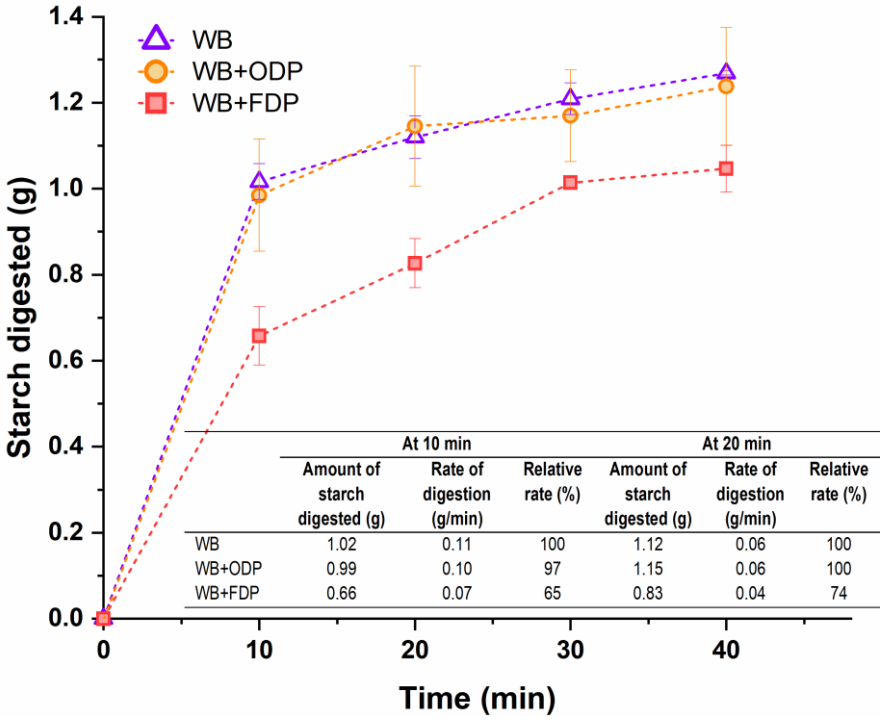


Figure 7.7: Time-dependent viscosity profiles of (**A**) freeze-dried (FDP) and (**B**) oven-dried (ODP) mamaku pith powder suspension (1% w/w) and their respective continuous phases (**A′**: FDP; **B′**: ODP). ODP continuous phase collected after 24 h of rehydration was concentrated using a vacuum evaporator: CF, concentrated fraction. Values are plotted as means ± standard deviation (n=3). Rheological measurements were taken using cup-and-bob (for suspension) or double gap geometry (for continuous phase) at 20°C.

7.3.6 Effect of hydrated powders on *in vitro* starch digestion

The digestion curves for WB in presence of FDP and ODP suspension are shown in **Figure 7.8**. FDP suspension decreased the digestion of WB by ~35% after 10 min, whereas the rate of digestion was hardly affected by the presence of the ODP suspension. A plausible reason for the difference in digestion rate could be the high viscosity and shear-thickening behaviour of FDP suspension (**Figure 7.5**), which may hinder the mixing of enzyme and substrate and/or delay the movement of the enzyme to substrate, leading to lower enzymatic activity (Brownlee, 2011; Edwards & Garcia, 2009). Mamaku pith suspension (with shear-thickening behaviour) can significantly reduce the rate of mixing and diffusion, and thus, the rate of digestion, as compared to guar gum and psyllium husk (no shear-thickening behaviour) (unpublished). Furthermore, it is possible that the MP released into the continuous phase from FDP may interact with the enzymes and may inhibit the enzyme activity by altering the enzyme conformation due to bonding or competing with the substrate for the enzyme's active site (**Chapter 5**) (Capuano, 2017).



	At 10 min			At 20 min		
	Amount of starch digested (g)	Rate of digestion (g/min)	Relative rate (%)	Amount of starch digested (g)	Rate of digestion (g/min)	Relative rate (%)
WB	1.02	0.11	100	1.12	0.06	100
WB+ODP	0.99	0.10	97	1.15	0.06	100
WB+FDP	0.66	0.07	65	0.83	0.04	74

Figure 7.8: *In vitro* digestion profiles for wheat biscuit alone (WB), and in the presence of 2.5% (w/v) freeze-dried (FDP) and oven-dried (ODP) mamaku pith powder. Values are plotted as means ± standard deviation (n=3).

7.4 General Discussion

Drying is a frequently used industrial operation for the preservation of perishable foods. The type of drying method used can affect the quality of the final product (process-structure relation), which consequently can limit the application of the product (structure-function relation). Here, the effect of the drying method (freeze-drying and oven-drying) on the structure and functionality of the mamaku pith powders are compared.

Process-structure: The fresh plant tissues have a very low T_g, [broccoli: -29°C (Xin, Zhang, & Adhikari, 2013); peas puree: -20 to -26°C (Lim, Wu, Breckell, & Birch, 2006); carrots: -50°C (Xu, Li, & Yu, 2014); potato: -47 to -53°C (Anglea, Karathanos, & Karel, 1993)] below which the high viscosity of the matrix limits the movements of molecules. On heating above T_g, as during oven-drying, the glassy matrix changes to a soft and rubbery state, which allows molecules to move more freely (Bhatta, Stevanovic Janezic, & Ratti, 2020). The rubbery state reduces the mechanical properties of the plant cellular matrix, which as a result cannot develop stress to balance the capillary stresses, leading to shrinkage (*i.e.*, structural collapse) (Achanta et al., 1997), as observed for mamaku pith. T_g is dependent on the moisture content of the plant product, and as drying continues, the moisture is removed, and subsequently, the plant cellular matrix transforms from a soft, rubbery state to a hard, glassy state (due to an increase in T_g) (Gulati & Datta, 2015). As the surface of the mamaku pith is exposed to heat during oven-drying, the surface temperature is higher than the inner temperature. Consequently, the rate of evaporation on the surface will be higher than the migration of the moisture from the inside of the matrix, leading to a faster transformation of the surface to a rigid glassy state, resulting in a stiff and denser structure on the surface (*i.e.*, causing case hardening) (Zhao et al., 2019). The phenomenon of collapse and case hardening during oven-drying leads to irreversible structural changes with shrunken capillaries; making the plant cellular matrix and subsequently ground powder denser, compact and rigid (**Table 7.1** and **Figure 7.1**). On the other hand, during freeze-drying, the majority of water is frozen to ice, and only a small amount of unfrozen water will contribute to the T_g of the mamaku pith (Roos, 1998). Thus, the T_g of the frozen mamaku pith will elevate, which helps prevent the structure of the food matrix during sublimation, leading to a porous structure with lower density (**Table 7.1** and **Figure 7.1**).

Structure-function: The changes in structure affect the interaction of powder particles with the environment (water). In the initial stage of hydration, the transfer of water from out to inside the powder is driven by capillary forces (Hedenus et al., 2000). Capillary forces depend on the porosity of the powder; thus, the porous FDP absorbs water faster than the denser ODP (**Figure 7.2A**, **B**). Over time, the capillary forces will decrease, and water will transfer *via* diffusion. Inside the particle, different constituents of the particle interact with water molecules causing the particles to swell and increase in particle size (**Figure 7.4A**). MP and other macromolecules present in the swollen (wet) layer of the particles formed a gelatinous layer around the particles (**Figure 7.3**). The swelling of particles and the formation of a gelatinous layer is known to delay the rate of rehydration (Wangler & Kohlus, 2018; Wangler et al., 2019). For FDP and ODP, the rehydration process was long, and most considerable changes happened over the first 180 min of rehydration (**Figures 7.4**, **7.6**, **7.7** and **7.9**). Simultaneously, the water-soluble compounds will diffuse from the wet layer of the powder into the bulk water as the driving force for diffusion is the concentration difference between these two. The concentration of soluble materials in bulk water will increase with time, which will reduce the rate of diffusion of MP (**Figure 7.6**) and other water-soluble compounds; as a result, the rate of solubilisation decreased with time, after 180 mins (**Figure 7.4B**). The diffusion of MP into the continuous phase and solubilisation of water-soluble compounds, in general, was significantly slower for ODP than for FDP (**Figure 7.4B**, **7.6** and **7.9A**). This difference could be due to the dense and hard structure (due to structural collapse and case hardening) formed during oven-drying. The inability of ODP to release enough MP in the continuous phase impaired its ability to form sufficient polymer-polymer interactions to exhibit shear-thickening behaviour (**Figure 7.5**) and did not have any effect on starch digestion (**Figure 7.8**). In general, crystallinity and surface properties of the powders can affect the rehydration process, however, no striking difference was observed in X-ray diffraction (XRD) and Fourier transform infrared (FTIR) for FDP and ODP (**Figure F.4** in **Appendix F**). Thus, the changes in functionality of ODP are most likely due to the formation of a hard and compact powder structure.

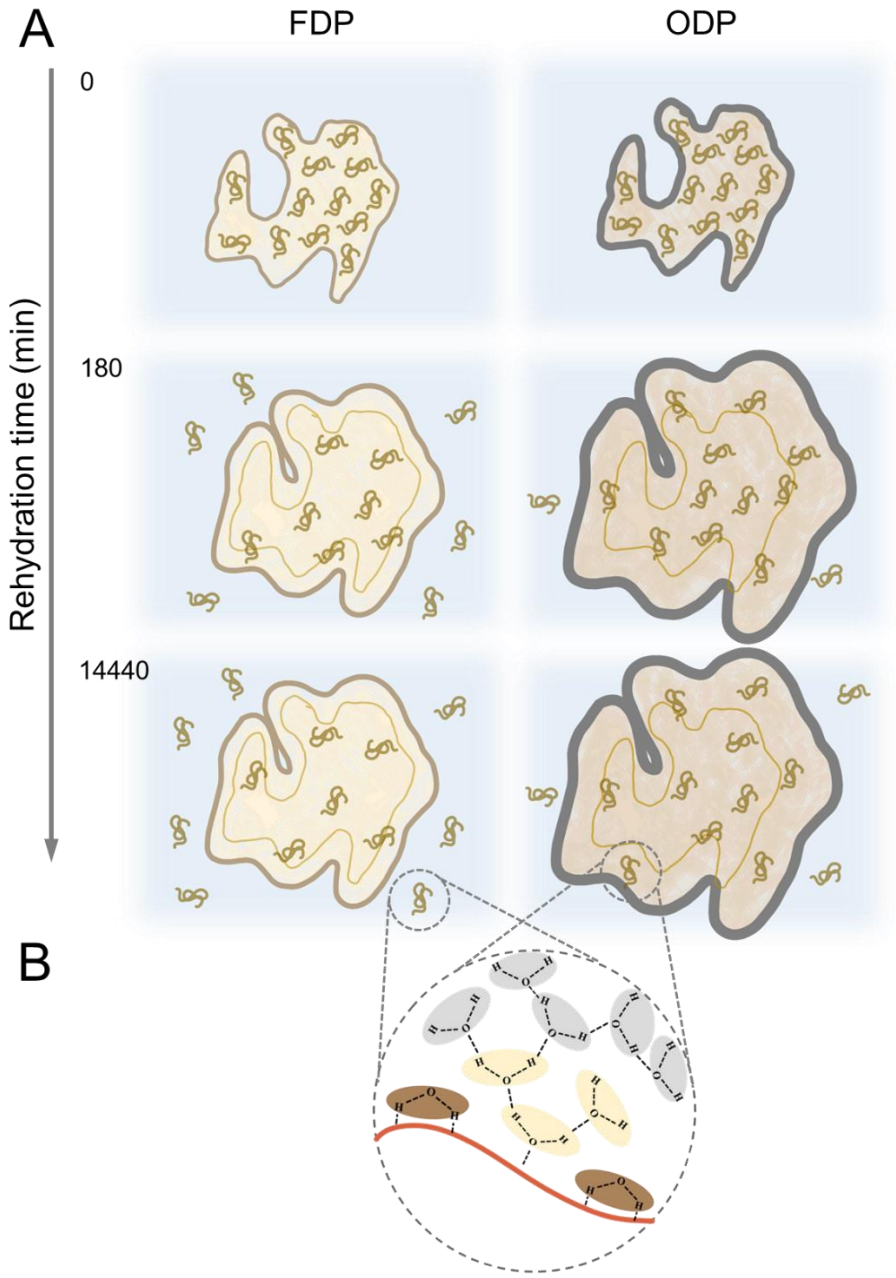


Figure 7.9: (**A**) Rehydration of freeze-dried (FDP) and oven-dried (ODP) mamaku pith powder and release of mamaku polysaccharide (MP). (**B**) Interaction of MP with water in and outside the powder particle.

Overall, this study shows the effect of freeze-drying and oven-drying methods on the physical and functional properties of mamaku pith powder. Oven-drying resulted in a dense powder surface that trapped the MP tightly within the matrix, limiting the release of MP in the continuous phase. Thus, no shear-thickening behaviour was observed for ODP

suspension. Freeze-drying, on the other hand, resulted in a porous structure that led to the rapid rehydration of powder and easy diffusion of MP into the continuous phase. The release of MP from FDP is a time-dependent process, and after sufficient MP is available in the continuous phase the shear-thickening behaviour is observed. These findings suggest that freeze-dried whole mamaku pith powder with retained shear-thickening behaviour can be used as an effective method for mamaku fronds to be made into a functional food ingredient as opposed to MP extract. Further work on improving the rehydration behaviour of powders, the stability of powders during storage and their incorporation into food systems is needed. Freeze-drying is a costly technique, so combining it with other drying methods such as microwave drying, and atmospheric freeze-drying may be advantageous but need further investigation.

Chapter 8

In vivo effects of mamaku pith powder on glycaemic, insulin and appetite responses and colonic fermentation

8.1 Introduction

Mamaku polysaccharide (MP) is a non-digestible biomacromolecule that can be ingested by humans in the form of mamaku pith. As shown in **Chapter 7**, the freeze-dried mamaku pith powder, upon hydration, releases the MP into the continuous phase which promotes viscosity development and shear-thickening behaviour. The shear-thickening behaviour of hydrated pith powder may cause a delay in gastric emptying, as reported for mamaku gum extract (Lentle et al., 2010; Wee et al., 2017). Furthermore, MP released in the continuous phase is also effective in reducing the activity of digestive enzymes (**Chapter 5**). The development of viscosity and shear-thickening behaviour, possible delay in gastric emptying and reduced digestive enzyme activity (particularly α-amylase) can affect the rate of intestinal digestion and absorption of food consumed together with this polysaccharide. A reduced rate of glucose absorption in the intestine has an important effect in lowering the blood glucose (glycaemic) response to starchy foods (Repin et al., 2017). It is therefore highly probable, but not yet studied, that mamaku pith powder may be able to reduce the glycaemic response to a carbohydrate food when consumed with it.

The ability to reduce blood glucose concentration is an extremely important health benefit. It is estimated that in 2012, 2.2 million deaths were attributed to high blood glucose and related comorbidities, with another 1.5 million directly attributed to diabetes (World Health Organisation, 2016). High blood glucose can promote the overproduction of reactive oxygen species resulting in increased oxidative stress, inflammation, hypercoagulability and elevation of blood pressure, which in the long-term can lead to diabetes and early cardiovascular disease (Ceriello et al., 1996; Louis Monnier et al., 2006; O'Keefe & Bell, 2007; O'Keefe, Gheewala, & O'Keefe, 2008; Vuksan et al., 2010). The secondary disorders may arise not only from chronically elevated blood glucose but also from transient states of high blood

glucose after carbohydrate-rich meals (Akasaka et al., 2017; Watt, Sanchez-Rangel, & Hwang, 2020).

Therefore, the first objective of this work was to determine, in a group of healthy people, the influence of mamaku pith powder on the postprandial glycaemic and insulin responses and appetite sensation when co-ingested with a carbohydrate-rich meal. It was hypothesised that mamaku pith powder would suppress the postprandial blood glucose response and suppress appetite similarly to guar gum, which was included as a positive control.

At the colonic level, soluble MP present in mamaku pith powder can act as a substrate for colonic microbes and produce beneficial short-chain fatty acids (SCFAs), as shown during *in vitro* fermentation (**Chapter 5**). The production of SCFAs during fermentation has been shown to depress postprandial glycaemic response, possibly by regulating several key hormones, such as glucagon-like peptide-1 (GLP-1, increases insulin secretion and satiety feelings) and peptide YY (PYY, increases satiety), upregulate glucose transporter type 4 (GLUT4, improves glucose uptake in skeletal muscle and adipose tissue), and decrease glycolysis[26] and gluconeogenesis[27] to increase glycogen synthesis (Cherta-Murillo et al., 2022; Salamone, Rivellese, & Vetrani, 2021). As colonic fermentation and SCFA production occurs mainly after the small intestine, the effect of SCFAs on blood glucose is usually observed only in the subsequent meal (*i.e.*, the second meal effect) (Brighenti et al., 2006). However, the question remains, will mamaku pith powder fermentation produce enough SCFAs which could lead to a second meal effect in humans?

The human trial performed to test the effect of mamaku pith powder on blood glucose was an acute study, not long enough to see effects on colonic microbiota and SCFAs production. Thus, a separate trial was performed using a rat faecal bulking index model to study the effects of mamaku pith powder on colonic fermentation. The rat faecal bulking index model has been proven to be very useful in the preliminary assessment of the effect of dietary fibres on hind gut fermentation and microbiota diversity (Monro & Paturi, 2020), and their survival during gut transit (Monro & Mishra, 2010). It was hypothesised that mamaku pith powder can modulate the growth of colonic microbiota and promote SCFAs production.

[26] The metabolic pathway that converts glucose into pyruvate.
[27] A process that transforms non-carbohydrate substrates (such as lactate, amino acids, and glycerol) into glucose.

8.2 Materials and Methods

Freeze-dried mamaku pith powder was prepared from fully grown mamaku fronds (stage 2) as described in **Section 3.1.2**. Freeze-dried mamaku pith powder was heat treated to make it microbially safe for consumption. Mamaku pith powder preparation was carried out in a certified food-grade facility (FoodPilot) in the School of Food and Advanced Technology, Massey University and the final powder was approved for human consumption by the manager (**Appendix G**).

8.2.1 Human trial: Effect of mamaku pith powder on glycaemic, insulin and appetite responses

An acute, randomised, single-blinded, placebo-controlled crossover intervention study involving healthy young and middle-aged adult participants was designed in accordance with the International Organization for Standardization method (ISO 26642:2010) to test the effect of mamaku pith powder ingestion on glycaemic, insulin and appetite responses (ISO, 2010). This study was approved by the New Zealand Health and Disability Ethics Committee (2022EXP12634) and was registered in Australia and New Zealand Clinical Trials Registry (ACTRN12622000629730). The study also complied with the guidelines/regulations outlined by the Biosafety Advisory, and Health and Safety Committee at Plant and Food Research Ltd. (**Appendices G** and **H**).

For the trial, four meals (treatments) were tested. All contained WeetBix™ (59.7 g, WB, Sanitarium, Auckland, New Zealand, purchased at a local supermarket) and blackcurrant flavouring (BF) (100 mg blackcurrant flavour plus 50 mg maltodextrin) and 250 ml water. WeetBix™ are wheat-based biscuits of compressed wheat flakes containing 67% carbohydrate of which 2.8% is sugar and the rest is readily digested starch (nutrient information panel). All meals delivered a dose of 40 g of available carbohydrate through WeetBix™, of which about 96% was readily digested starch and 4% sugar (calculated from the nutrient information panel). The available carbohydrate in WeetBix™ was previously estimated using an *in vitro* digestion model (Mishra, Edwards, Hedderley, Podd, & Monro, 2017). The mamaku pith powder treatments contributed an additional glycaemic equivalent of about 1 g glucose. The meals were:

Meal 1: WB + BF + 250 ml water (WB).

Meal 2: WB + BF + mamaku pith powder (5 g) + 250 ml water (WB+MD; not-pre-hydrated mamaku pith powder).

Meal 3: WB + BF + mamaku pith powder (5 g) dispersed in 250 ml water for 1 h before ingesting (WB+MH; pre-hydrated mamaku pith powder).

Meal 4: WB + BF + guar gum (3 g) + 250 ml water (WB+GG).

Guar gum (meal 4) was used as a positive control as it is shown to effectively suppress glycaemic response to WeetBix™ (Mishra et al., 2017). Pre-weighed mamaku pith powder and flavouring were prepared as sachets prior to the trial. Apart from meal 3, which required pre-hydration of the mamaku pith powder, the meal ingredients were mixed immediately before serving. All meals were subjected to microbial analysis as part of food safety requirements.

8.2.1.1 Participants

Volunteers willing to participate were invited to the clinical research facility at Plant and Food Research Ltd., Palmerston North, New Zealand and provided with an information sheet and briefed about the study (**Appendix H**). All respondents (n=24) were asked to complete an informed consent form and then screened to ensure that they met the necessary inclusion and exclusion criteria and were in good health. Volunteers' health was gauged by self-assessment and by their scores on the General Health Questionnaire (Goldberg & Hillier, 1979). As part of the screening, finger-prick measurements of blood glucose and HbA1c concentrations were made, which also familiarised participants with the blood sampling procedure used in the study. Anthropometric measurements of height, weight, waist circumference and blood pressure were also taken. Participants with fasting blood glucose >5.6 mmol/l, HbA1c >40 mmol/mol, allergic to or intolerant of wheat products, having a gastrointestinal disorder and type 1 or 2 diabetes or were unwilling or unable to provide informed consent or comply with the study procedures were excluded. All eligible participants (n=20) were 18-65 years old with BMI between 18 to 35 kg/m^2 and generally healthy from the general population in Palmerston North.

8.2.1.2 Study design

Each participant ingested each of the four meal treatments, with the order of treatments randomised for each individual. On trial days involving ingestion of test meals the participants were asked to arrive at the clinic fasted, *i.e.*, not having eaten since 10 pm the previous evening, and having had a moderate evening meal before then. The participants were asked to provide two baseline blood samples and rate their appetite on the visual analogue scale provided. They were then asked to ingest their test meal within 10 min of the baseline blood sampling. Blood samples were taken by finger prick at 15, 30, 45, 60, 90, 120 and 180 min from baseline (T=0). Ratings of appetite sensations were made at 15, 60, 120 and 180 min (**Figure 8.1**). Participants were given an additional 250 ml of water which could be consumed at any time during the study if needed. Participants consumed not more than two of the test meals per week with at least two days between each test meal. Participants and staff directly administering the meals were blinded to the differences between the meals.

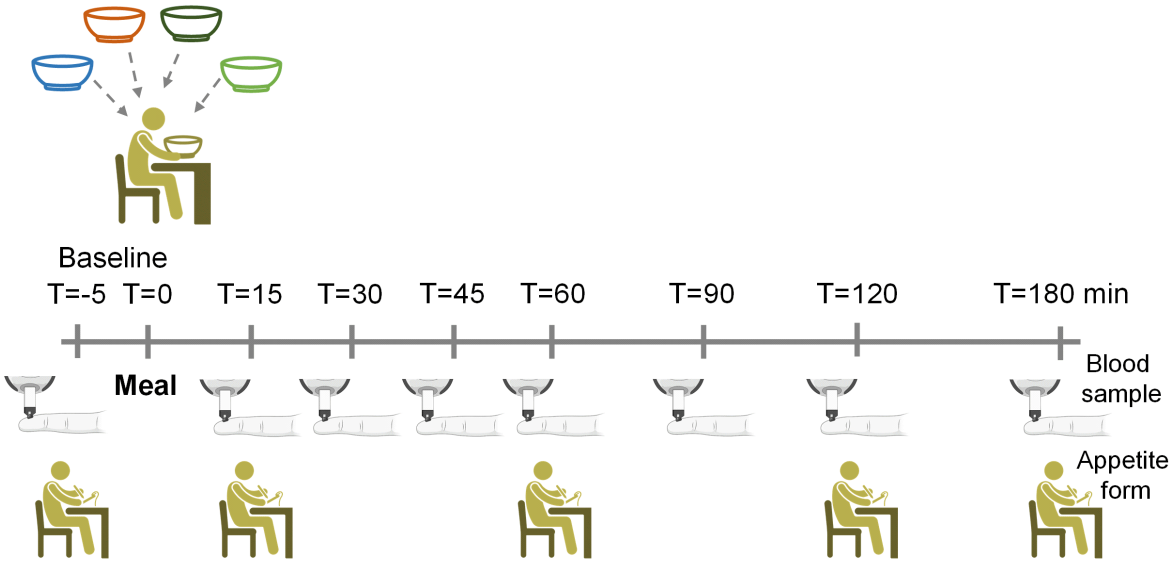


Figure 8.1: Trial design for mamaku pith powder testing in humans.

8.2.1.3 Data collection

Blood glucose and insulin were measured in capillary finger prick blood samples. Blood glucose was measured using a HemoCue Glucose 201 DM RT Analyser. For insulin

determination finger prick blood was drawn into a Lithium Heparin (LH) microvette tubes (CB 300 LH, Sarstedt AG & Co., South Australia, Australia), capped, inverted and stored on ice for a maximum of 1 h before centrifuging. The tubes were centrifuged at 2,000 *g* for 15 min at 4°C. Two 20 µl samples of the plasma were used to determine insulin by the assay procedure of the Human Insulin ELISA kit (EZHI-14K, EMD Millipore Corp., Burlington, Massachusetts, USA). Absorbance was read at 450 nm on a FLUOStar Optima® Plate reader (BMG Labtech, Victoria, Australia). A 4-parameter logistic (4PL) standard curve was fitted for each ELISA plate and used to calculate human insulin concentrations (µU/ml) of the plasma samples.

During each session, participants were also asked to rate their appetite sensation (hunger, fullness, satiety and desire to eat) by answering four questions: How hungry do you feel?, How full do you feel?, How satisfied do you feel? and How much food do you think you can eat? (Flint, Raben, Blundell, & Astrup, 2000). A visual analogue scale of a 10 cm long line ranging from 0 ("not at all") to 10 ("extremely") was used to record the response (**Appendix I**). Blood glucose response was the primary outcome, and associated insulin response and appetite were secondary outcomes.

8.2.2 Rat trial: Effect of mamaku pith powder on colon fermentation

Male Sprague-Dawley rats were raised on a standard commercial rat pellet diet post-weaning until they reached a weight of 200±20 g at about 6 weeks of age. For the experiment, rats were housed individually in hanging basket cages in a purpose-built small animal facility, in a room maintained at a temperature of 22±1°C, humidity of 60±5%, air exchanged 12 times/h, and a 12 h light/dark cycle. The cages were arranged in randomised blocks, with each block containing one cage from each treatment. The rats, n=8 per diet, were fed the five experimental diets for 21 days in a randomised parallel design (**Figure 8.2**). All diets were nutritionally complete, moderately high (20%) fat and all contained a background of 1% mixed dietary fibre (**Table 8.1**). The test materials were substituted into the 10% glucose portion of the baseline diet so that the raw starch content of all diets was the same. The final diets were 10% glucose (baseline), 10% wheat bran, 5% psyllium husk, 5% mamaku pith powder, and 10% mamaku pith powder. Each rat was allocated 25 g of diet per day and water was available *ad libitum*. Rats were weighed weekly during the 21 days, and at the

beginning and end of a 4-day balance period from day 18 to 21. During the balance period, the total faecal output of each rat was collected daily and freeze-dried. At the end of the trial, the rats were euthanised and samples of gut contents were removed for microbiota and short-chain fatty acids (SCFAs) analysis. Psyllium husk and wheat bran are low-fermentation fibres and are commonly used reference materials in animal trials for faecal bulking effects (Monro, 2000; Monro, Mishra, Redman, Somerfield, & Ng, 2016). Ethical approval for the study was obtained from the AgResearch (Ruakura) Animal Ethics Committee (Application no. 15329) according to the Animal Welfare Act 1999, New Zealand (**Appendix J**).

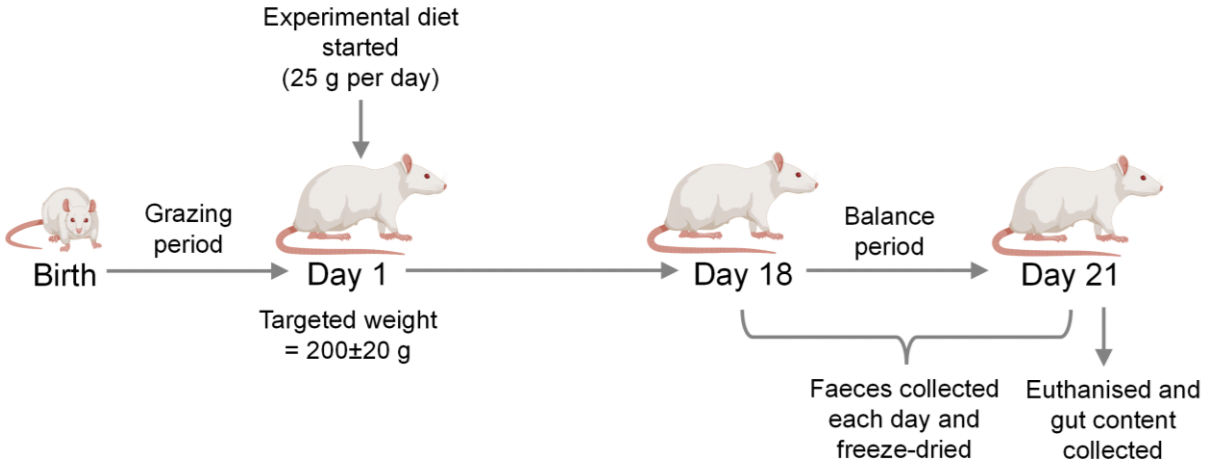


Figure 8.2: Trail design for mamaku pith powder colon fermentation in rats.

8.2.2.1 Colonic microbiota analysis

Post-caecal pre-faecal material was removed immediately after euthanasing the rats into plastic vials and frozen without delay to –80°C. The bacterial genomic DNA from rat colonic contents were extracted using QIAamp PowerFecal Pro DNA Kit (Qiagen, Auckland, New Zealand). The DNA samples were sequenced for the V3-V4 hypervariable region of the 16S rRNA gene as described in **Section 5.2.4.2**, and bioinformatic analysis was performed using Quantitative Insights Into Microbial Ecology 2 (QIIME 2, Version 2021.11) as described in **Section 5.2.4.3**. The alpha diversity (within a sample) was calculated using Faith's phylogenetic diversity (PD), Observed features, Pielou's evenness and Shannon diversity

metrics. The beta diversity (between samples) was calculated using unweighted UniFrac distances and plotted with principal coordinate analysis (PCoA).

Table 8.1: Composition of diets for rat trial.

	Diets				
	Glucose	Wheat bran	Psyllium	Mamaku pith powder	
	10%	10%	5%	5%	10%
Starch	380	380	380	380	380
Protein[1]	200	200	200	200	200
Milk fat[2]	150	150	150	150	150
Oil (Corn)	50	50	50	50	50
Vitamins[3]	50	50	50	50	50
Minerals[4]	50	50	50	50	50
Cholesterol	10	10	10	10	10
Fibre mix[5]	10	10	10	10	10
Glucose	100	0	50	50	0
Test material	0	100	50	50	100
Total	1000	1000	1000	1000	1000

[1]Lactic casein.

[2]Eclipse Dairy Ghee, Milligan's Food Group Ltd, Oamaru, New Zealand.

[3]Vitamin: Mixture contains the following components: (mg/kg diet) – retinol acetate 5.0, DL-α-tocopheryl acetate 100.0, menadione 3.0, thiamin hydrochloride 5.0, riboflavin 7.0, pyridoxine hydrochloride 8.0, D-pantothenic acid 20.0, folic acid 2.0, nicotinic acid 20.0, D-biotin 1.0, myo-inositol 200.0, choline chloride 1500.0; (µg/kg diet) – ergocalciferol 25.0, cyanocobalamin 50.0.

[4]Minerals: Mixture contains the following components: (g/kg diet) – Ca 6.29, Cl 7.79, Mg 1.06, P 4.86, K 5.24, Na 1.97; (mg/kg diet) – Cr 1.97, Cu 10.7, Fe 424.0, Mn 78.0, Zn 48.2; (µg/kg diet) – Co 29.0, I 151.0, Mo 152.0, Se 151.0.

[5]Fibre mix: Contains equal quantities of citrus fibre (Herbacel AQ Plus Citrus, Herbafood Ingredients GmbH, Germany), apple fibre (VITACEL Apple fibre AF 401, J. Rettenmaier & Sohne GmbH & Co. KG, Rosenberg, Germany); potato fibre (J. Rettenmaier & Sohne GmbH & Co. KG, Rosenberg, Germany), wheat fibre (VITACEL wheat fibre WF 600, J. Rettenmaier & Sohne GmbH & Co. KG, Rosenberg, Germany) and wheat bran (1:1:1:1:1).

8.2.2.2 Quantification of caecal short-chain fatty acids

Caecum digesta were weighed into 15 ml Eppendorf tubes and diluted with 0.01 M phosphate buffered saline (1:9) containing 2-ethylbutyric acid (5.56 mM) as an internal standard (for a final concentration of 5 mM 2-ethylbutyric acid). The samples were allowed to thaw slightly on ice and vortexed into a slurry before centrifuging at 3,000 *g* for 10 min (4°C). The supernatant (500 µl) was acidified with 250 µl concentrated hydrochloric acid

before 1000 µl of diethyl ether was added. Following a vortex, to allow acids to transfer to the diethyl ether phase, the sample was centrifuged at 10,000 *g* for 10 min (4°C). The diethyl ether phase was stored at -80°C until analysis on gas chromatography (GC). Further derivatization and GC analysis was performed as described in **Section 5.2.4.1**.

8.2.2.3 Faecal uronic acid determination

Loss of MP by hind gut fermentation was gauged by comparing total dietary uronic acid intake with faecal uronic acid output over the four-day balance period of faecal collection. Uronic acid is the primary constituent of MP, so was used as a measure of MP. Faeces from baseline diets were included as a control for background uronic acid content.

Uronic acid was determined using the spectrophotometric *m*-hydroxydiphenyl method (Blumenkrantz & Asboe-Hansen, 1973). Samples of mamaku pith powder (0.25 g) or faeces (0.5 g) were accurately weighed into 50 ml Falcon tubes, the tubes were filled to 50 ml with water and placed in a refrigerator overnight to hydrate. They were then homogenised (OMNI International, Marietta, Georgia, USA) with an S18N-19G dispersing element, accurately adjusted to 50 ml, the lids screwed on and the tubes rotated end over end for 2 h before centrifuging at 3,000 rpm for 10 min. Duplicate aliquots (0.1 ml) of supernatant were removed and made to 0.5 ml with water, alongside standards of 0.5 ml of 50 µg/ml glucuronic acid. Concentrated H_2SO_4 /0.0125 M sodium tetraborate (3 ml) was added with immediate mixing and the tubes were placed in ice water. The tubes were heated at 100°C for exactly 5 min, then cooled in ice water. *m*-hydroxydiphenyl reagent (0.1 ml of 0.15% *m*-hydroxydiphenyl in 0.5% NaOH) was added, the tubes immediately mixed, and read after 15 min at 520 nm. Blanks for each sample were run by using 0.1 ml of 0.5% NaOH in place of *m*-hydroxydiphenyl reagent. Fermentation of the MP during gut transit was estimated as uronic acid in faeces collected during the four-day balance period as a percentage of uronic acid consumed in the diets during the same period.

8.2.3 Rotational rheology

Guar gum (3 g) and mamaku pith powder (5 g) were each hydrated in milli-Q water (250 ml) at 37°C for varying time points (between 0-24 h). Rheological measurements were performed in rotational mode using a Paar Physica MCR 302 rheometer (Anton-Paar, Graz, Austria) in a

controlled shear rate (CSR) mode with a log-ramp profile from 30 s to 2 s (initial to final) at 37.0±0.1°C. Viscosity curves were measured using the cup-and-bob geometry (CC27 and C-PTD 200) and data was recorded using Rheoplus/32 software (Version 3.62).

8.2.4 Data processing and statistical analysis

Incremental blood glucose/ insulin responses (*i.e.*, above baseline level) were calculated by subtracting each individual's baseline value from subsequent measurements (post-ingestion of a treatment meal) and were then used to determine the incremental area under the curve (iAUC) for each individual by trapezoid summation. iAUCs were not calculated beyond the first time the blood glucose and insulin returned to baseline levels. The highest postprandial blood glucose/ insulin peak for each individual, irrespective of the time of occurrence was used to determine the mean peak height for each meal.

The rating of appetite sensation was measured manually as the distance from 0 ("not at all") point and is expressed as distance on the scale (cm).

The data were checked for normality using the Shapiro-Wilk test. The differences among the treatments at a given time point were assessed using non-parametric Kruskal-Wallis test at a 95% confidence level using SPSS software (IBM SPSS Statistics, Version 28.0.1.1(15)). The significant differences in alpha and beta diversity metrics for colonic microbiota were calculated using the Kruskal-Wallis test and permutational multivariate analysis of variance (PERMANOVA), respectively. The results are expressed as mean ± standard error mean.

8.3 Results

8.3.1 Human trial: Effect of mamaku pith powder on glycaemic, insulin and appetite responses

Twenty-four participants were assessed for eligibility, of which four participants were excluded from the study for not meeting the inclusion criteria. Twenty participants were allocated to intervention and 17 of them finished all treatments (**Figure 8.3**). The subject number exceeded the minimum number (n=10) specified by the current ISO method

(ISO26642:2010) for the glycaemic index (ISO, 2010). Data from all 17 participants were used for the analysis without any outliers.

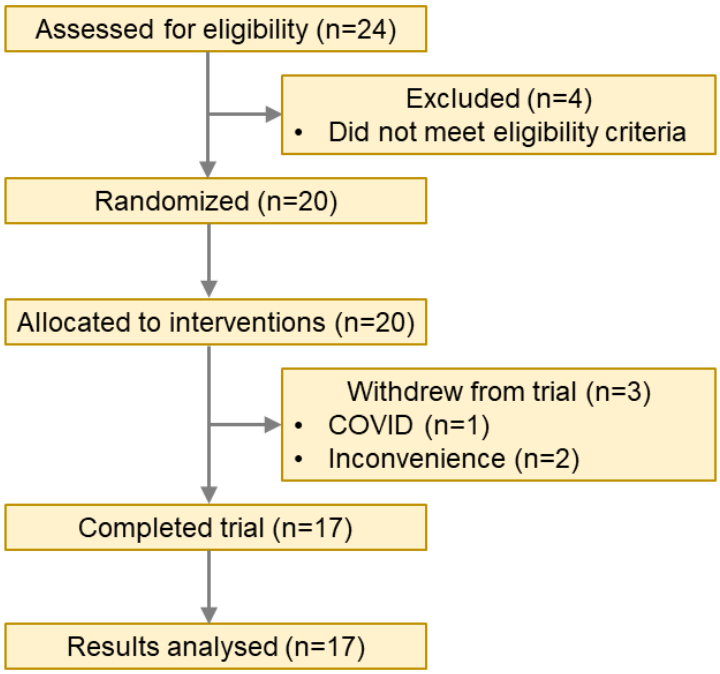


Figure 8.3: Consolidated Standards of Reporting Trials (CONSORT) diagram for the study trial.

8.3.1.1 Postprandial blood glucose response

The baseline blood glucose value for different treatment groups was very similar (~4.5-4.6 mmol/l). The changes in incremental blood glucose responses after ingestion of WB, WB+MD, WB+MH and WB+GG are shown in **Figure 8.4**. Compared with the baseline, an initial increase in the postprandial blood glucose that peaked at T=45 min was observed for all meals, followed by a gradual decrease. However, the peak heights differed significantly between some treatments. Compared with the WB control, pre-hydrated mamaku pith powder (WB+MH) and guar gum (WB+GG) treatments caused significant depression in peak height ($p<0.001$) by 20.5% and 27.4%, respectively. In contrast, the decrease in peak height by not-pre-hydrated mamaku pith powder treatment (WB+MD, 4.8%) was not statistically significant (**Table 8.2**). Furthermore, all treatments but guar gum reached the baseline in 120 min and then proceeded to track slightly below baseline. The statistical differences in the period 120 to 180 min were solely due to guar gum delaying the return to baseline.

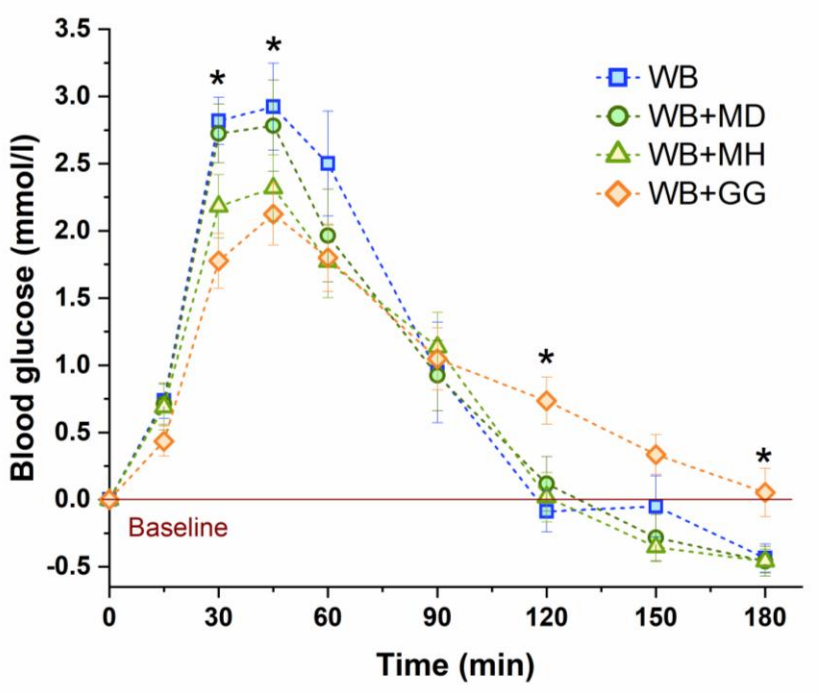


Figure 8.4: Mean incremental change in blood glucose concentrations over baseline (T=0) after the consumption of wheat biscuit alone (WB), WB+ not-pre-hydrated mamaku pith powder (WB+MD), WB+ pre-hydrated mamaku pith powder (WB+MH) and WB+ guar gum (WB+GG). Values are reported as mean ± standard error mean (n=17). (*): Significant different observed ($p \leq 0.05$).

Table 8.2: Peak height and mean incremental area under the blood glucose curve (iAUC) to 120 min and 180 min for meals.

Treatment	Peak height† (mmol/l)	iAUC			
		To 120 min		To 180 min	
		Mean iAUC (mmol.min/l)	Change‡ (%)	Mean iAUC (mmol.min/l)	Change‡ (%)
WB	2.9±0.3[a]	188.4±25.5[a]	-	194.8±26.9[a]	-
WB+MD	2.8±0.4[a]	172.6±22.8[a]	8.4	180.5±25.7[a]	7.3
WB+MH	2.3±0.3[b]	156.0±14.7[a]	17.2	161.9±15.7[a]	16.9
WB+GG	2.1±0.2[b]	148.8±17.6[a]	21.0	177.7±19.1[a]	8.9

†: Peak height from incremental blood glucose response (after subtracting the baseline).

‡: Change in the mean incremental area under the curve (iAUC) compared to WB control.

Meals were wheat biscuit alone (WB), WB+ not-pre-hydrated mamaku pith powder (WB+MD), WB+ pre-hydrated mamaku pith powder (WB+MH) and WB+ guar gum (WB+GG). Values are reported as mean ± standard error mean (n=17). Values in the same column with the different superscript letters are significantly different ($p \leq 0.05$).

Despite the differences in peak height and the attenuation of glycaemic response curves, treatments did not induce statistically significant differences in iAUC either up to 120 min, which excluded the tail of the glycaemic response with guar gum, or up to 180 min which include the full data set. Nonetheless, compared with the WB control, the mean iAUC to 120 min was reduced by 21% after guar gum (WB+GG) and by 17.1% after pre-hydrated mamaku pith powder (WB+MH) treatments and mean iAUC up to 180 min (with the 120-180 min tail included) was reduced by 8.9% and 16.9%, respectively (**Table 8.2**).

8.3.1.2 Postprandial insulin response

The effect of all treatments on insulin responses with time followed a similar pattern to that of blood glucose responses (**Figure 8.5**). The pre-hydrated mamaku pith powder (WB+MH) suppressed the insulin response more than the non-pre-hydrated (WB+MD), however, was not significantly different. The guar gum (WB+GG) had the greatest suppressive effect and was the only treatment for which the reduction compared to the WB control was statistically significant (**Table 8.3**). Despite the high inter-individual variability inherent in blood glucose and insulin responses the mean peak blood glucose and insulin responses across the four treatments correlated closely ($R^2 = 0.89$) (**Figure 8.6**).

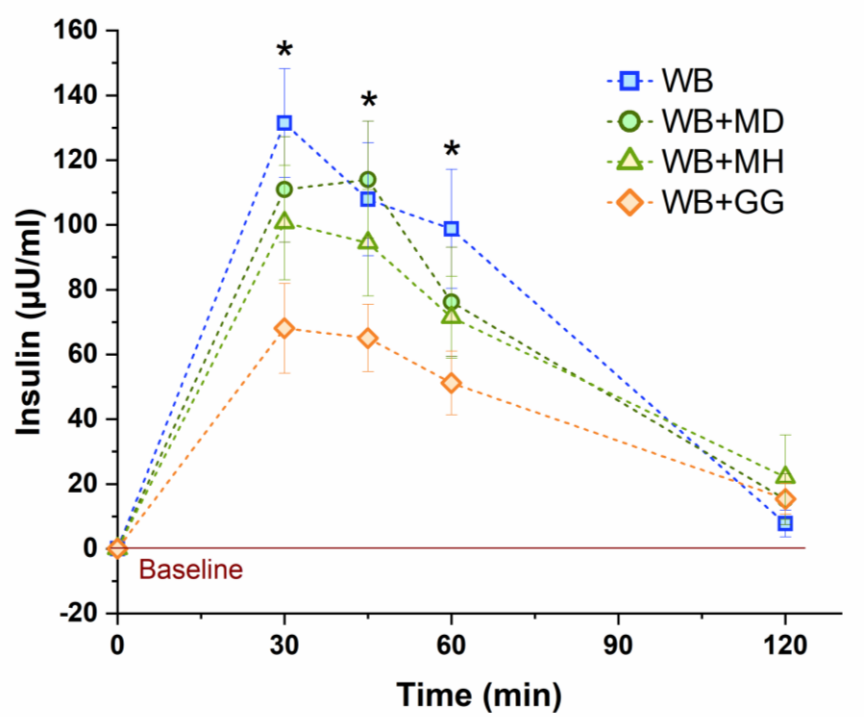


Figure 8.5: Mean incremental change in blood insulin concentrations over baseline (T=0) after the consumption of wheat biscuit alone (WB), WB+ not-pre-hydrated mamaku pith powder (WB+MD), WB+ pre-hydrated mamaku pith powder (WB+MH) and WB+ guar gum (WB+GG). Values are reported as mean ± standard error mean (n=17). (*): Significant different observed ($p \leq 0.05$).

Table 8.3: Peak height and mean incremental area under the insulin curve (iAUC) for meals.

Treatment	Peak height† (µU/ml)	iAUC to 120 min	
		Mean iAUC (mU.min/ml)	Change‡ (%)
WB	131.5±16.8[a]	8.4±1.3[a]	-
WB+MD	113.9±18.1[a]	7.4±1.4[a]	10.8
WB+MH	100.7±17.7[a]	7.1±1.3[a]	15.5
WB+GG	68.1±13.8[b]	4.9±0.9[b]	41.4

†: Peak height from incremental insulin response (after subtracting the baseline).
‡: Change in the mean incremental area under the curve (iAUC) compared to WB control.
Meals were wheat biscuit alone (WB), WB+ not-pre-hydrated mamaku pith powder (WB+MD), WB+ pre-hydrated mamaku pith powder (WB+MH) and WB+ guar gum (WB+GG). Values are reported as mean ± standard error mean (n=17). Values in the same column with the different superscript letters are significantly different ($p \leq 0.05$).

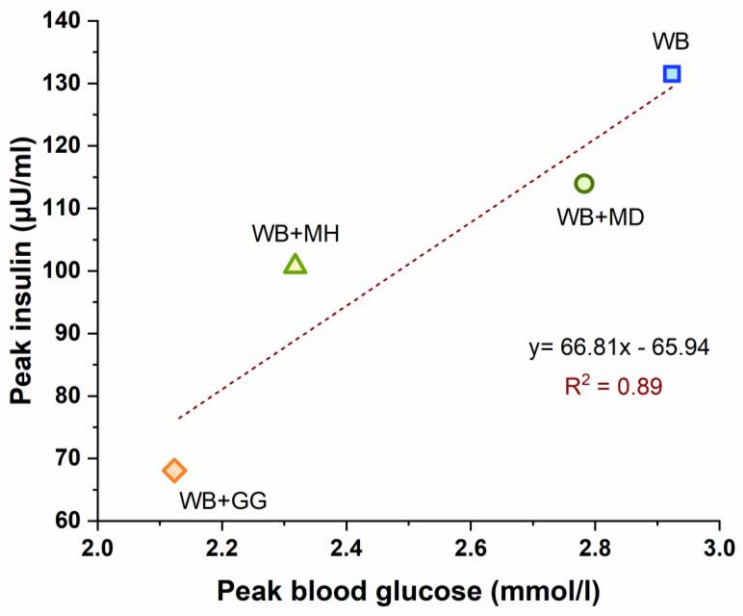


Figure 8.6: Correlation between peak blood glucose and peak insulin responses for all four meals tested. WB, wheat biscuit alone; WB+MD, WB+ not-pre-hydrated mamaku pith powder; WB+MH, WB+ pre-hydrated mamaku pith powder; WB+GG, WB+ guar gum.

8.3.1.3 Subjective rating of appetite sensation

After ingestion of either meal, participants felt fuller and more satisfied (T=15 min) which gradually reduced with time and subsequently increased the feeling of hunger and desire to eat a large amount (**Figure 8.7**). None of the treatments containing mamaku pith powder (WB+MD and WB+MH) differed drastically from one another or from the negative control (WB) or positive control (WB+GG) on any of the appetite dimensions at any time point. Similarly, the negative and positive controls did not differ significantly. However, guar gum was consistently one of the most satiating treatments and WB control was the least satiating, but the differences did not reach statistical significance at any point in the present study (**Figure 8.7A**).

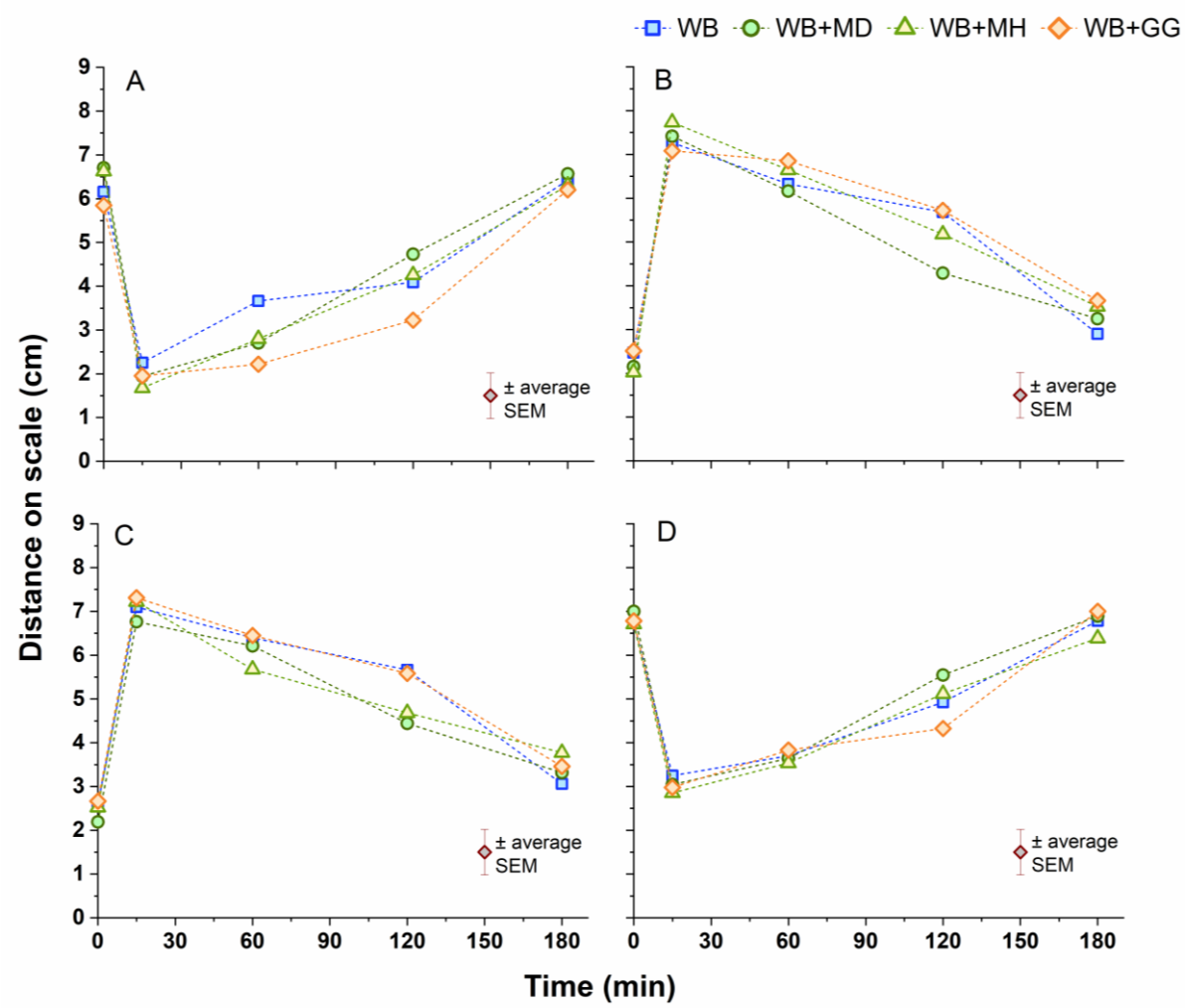


Figure 8.7: Changes in (**A**) hunger, (**B**) fullness, (**C**) satisfaction and (**D**) desire to eat after the consumption of wheat biscuit alone (WB), WB+ not-pre-hydrated mamaku pith powder (WB+MD), WB+ pre-hydrated mamaku pith powder (WB+MH) and WB+ guar gum (WB+GG). Values are reported as mean (n=17).

8.3.2: Rat trial: Effect of mamaku pith powder on colon fermentation

8.3.2.1 Colonic microbiota

The 16S rRNA gene sequencing of rat colonic microbiota from 40 samples (5 groups, n=8) generated a total of 11,118,336 reads. For each sample, reads ranged from 164,724 to 388,975 with an average of 277,958. The reads were denoised, filtered and clustered, resulting in 825 features. The alpha and beta diversity analyses are shown in **Figure 8.8**. The alpha diversity metrics showed a similar trend for rats fed glucose or psyllium diet having significantly lower alpha diversity than the others (**Figure 8.8A**, **B**, **C**, **D**). Rats fed with 5 and 10%

mamaku pith powder did not differ significantly. The beta diversity analysis revealed significant differences in the colonic microbiota of rats fed experimental diets. The PCoA plot, with ~35% total variation, shows diet-induced separation in the composition of the colonic microbiota, with differences between the dietary treatments (**Figure 8.8E**). Further details on taxonomic profiling are given in **Appendix K**.

8.3.2.2 Short-chain fatty acids production

The experimental diets induced considerable changes in SCFAs production in the caecum of rats (**Table 8.4**). Amongst the treatments, rats fed 5% mamaku pith powder had significantly higher caecal butyrate concentrations than the 10% mamaku pith powder and 10% wheat bran diets. Propionate was significantly higher in rats fed psyllium. In general, the SCFAs concentrations differed between rats fed 5 and 10% mamaku pith powder diets, but the changes observed were not significantly different. Experimental diets did not induce significant changes to acetate and lactate concentrations.

Table 8.4: Short-chain fatty acids (SCFAs) in the caecum of rats fed the experimental diets.

SCFAs (μmol/g of caecal contents)	Glucose	Wheat bran	Psyllium	Mamaku pith powder	
				5%	10%
Acetate	27.9±1.7^{a}	24.8±0.9^{a}	25.7±1.9^{a}	22.2±1.0^{a}	21.1±2.9^{a}
Butyrate	6.2±0.8^{ab}	3.9±0.3^{b}	7.0±0.8^{ab}	10.1±2.7^{a}	4.5±0.5^{b}
Isobutyrate	1.4±0.0^{a}	1.0±0.0^{b}	1.2±0.1^{ab}	1.1±0.1^{ab}	0.9±0.1^{b}
Formate	2.8±0.4^{a}	2.8±0.3^{a}	2.9±0.4^{a}	3.3±0.3^{a}	3.0±0.4^{a}
Lactate	1.9±0.3^{a}	0.8±0.1^{a}	2.0±0.6^{a}	1.4±0.3^{a}	1.2±0.3^{a}
Propionate	7.3±0.8^{ab}	7.0±0.5^{ab}	9.7±1.1^{a}	6.0±0.6^{ab}	5.6±1.0^{b}
Succinate	30.8±4.6^{a}	19.7±3.1^{ab}	24.4±5.7^{ab}	17.6±2.4^{ab}	7.6±1.76^{b}
Valerate	1.0±0.2^{a}	0.4±0.0^{a}	0.9±0.2^{a}	0.5±0.1^{a}	0.5±0.1^{a}
Isovalerate	0.5±0.0^{a}	0.2±0.0^{b}	0.3±0.1^{ab}	0.3±0.1^{ab}	0.2±0.1^{b}

Values are expressed as means ± standard error mean (n=8). Values with the different superscript letters in a row are significantly different ($p \leq 0.05$). Hexanoate and heptanoate acids were not detected; the limit of detection is 0.2 μmol/g of caecal contents.

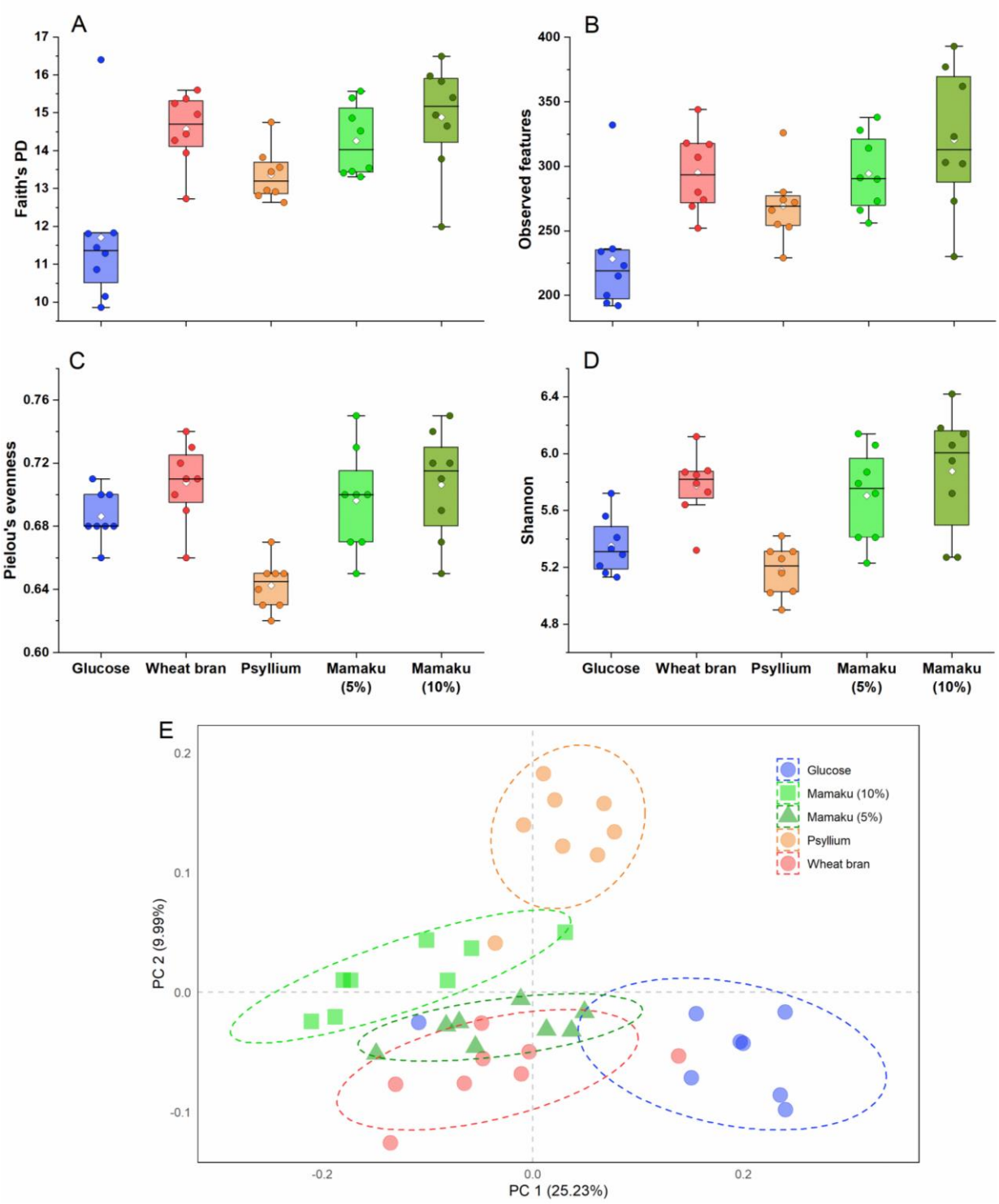


Figure 8.8: Alpha diversity analysis of colonic microbiota using (**A**) Faith's phylogenetic diversity (PD), (**B**) Observed features, (**C**) Pielou's evenness and (**D**) Shannon diversity metrics in rats fed experimental diets. (**E**) Beta diversity by principal coordinate analysis (PCoA) plot projecting unweighted UniFrac distances ($p < 0.001$).

8.3.2.3 Mamaku polysaccharide in faeces

Fermentation of the MP in the rat hind gut was estimated from the disappearance of uronic acid during gut transit. Compared with intakes of 203 mg and 410 mg of uronic acid per rat measured in the 5% mamaku and 10% mamaku pith powder diet groups respectively, 114 mg and 270 mg were retained in the faeces over the four-day balance period, representing 50% and 63% of the ingested uronic acid (**Table 8.5**). In other words, 50% and 37% of MP uronic acid from the 5% mamaku and 10 % mamaku pith powder diets, respectively was utilised in gut.

Table 8.5: Survival of mamaku polysaccharide (MP) during gut transit estimated from dietary and faecal uronic acid.

Diet	Uronic intake (mg)	Faecal uronic output (mg)	Recovery (%)
Glucose baseline	-	13.4±1.5	-
5% mamaku pith powder	203.2±2	114±6.5	50±3.7
10% mamaku pith powder	410.2±5.7	270±5.1	63±1.4

Values are expressed as means ± standard error mean (n=8).

8.4 Discussion

Ingestion of available carbohydrates is known to increase postprandial glucose and insulin levels in the blood. High postprandial and chronic blood glucose level, is recognised as a global public health problem, associated with several medical complications (Monnier & Colette, 2015). The spike in postprandial blood glucose is affected by several dietary factors such as the amount of available carbohydrates, the nature of starch, the amount of fat and protein, the method of food processing and the addition of dietary fibre (Kaur, Koh, Ponnalagu, & Henry, 2020), and any other influences that cause a delay in gastric emptying. The present study, for the first time, demonstrates the effect of co-consuming mamaku pith powder (pre-hydrated and not-pre-hydrated) with carbohydrate-rich meal on postprandial glycaemic, insulin and appetite response in healthy subjects.

Two mamaku pith powder meals *i.e.,* pre-hydrated and not-pre-hydrated were included in the study to test the importance of proper hydration and release of MP in the continuous phase for the desired biological functionality. As reported in **Chapter 7**, the hydration of mamaku pith powder and the release of MP into the continuous phase, and consequently the development of viscosity and shear-thickening behaviour is a time-dependent process (requires 2-3 h of hydration for the onset of shear-thickening). In the present study, a cautious approach was taken in terms of participant safety. The amount of mamaku pith powder ingested and the duration of its pre-hydration was limited to the minimum amount that *in vitro* studies had indicated would cause thickening responsible for the depression of glycaemic response (unpublished), without the risk that the shear-thickening property of hydrated powder would make swallowing difficult. The results of the present study showed that the combination of the amount of mamaku pith powder (5 g) and time of hydration (1 h) was just enough to detect an anti-glycaemic effect. A significant depression in glycaemic response amplitude (*i.e.,* peak height) was observed for the pre-hydrated mamaku pith powder treatment (WB+MH) but not for not-pre-hydrated mamaku pith powder treatment (WB+MD) (**Figure 8.4** and **Table 8.2**). The effectiveness of the pre-hydrated mamaku pith powder in suppressing glycaemic response was confirmed by the parallel suppression of insulin response (higher mean peak values for WB+MD than WB+MH), even though the response effect was not sufficient to achieve statistical significance (**Figure 8.5** and **Table 8.3**). These results confirm that the inability to release sufficient MP in the early stage of digestion would make it functionally ineffective as an anti-glycaemic agent. The results can also be extrapolated to powder prepared using other drying methods such as oven-drying, where the shear-thickening behaviour is not observed due to limited release of MP in continuous phase over 24 h of hydration, and therefore it may not be a good delivery medium and was not tested in this study.

A similar postprandial blood glucose and/or insulin-lowering effect has been reported after consumption of other dietary fibres, such as β-glucan from oat and barley (Tosh, 2013), soluble fibres from brewer's spent grains (Ullah et al., 2022), guar gum (Galali, Rees, & Kuri, 2022) and psyllium (Gibb, McRorie Jr, Russell, Hasselblad, & D'Alessio, 2015). The beneficial effect of fibres on postprandial glycaemic and insulin response can be related to different mechanisms acting simultaneously. Fibres may increase the viscosity of gastric and intestinal

contents, retard the diffusion and mixing processes, retard gastric emptying, alter the gut transit time, hinder enzyme-substrate complex and delay the absorption of glucose (de Carvalho et al., 2017).

Mamaku gum extract with shear-thickening behaviour was shown to significantly alter the muscular activity of the rat stomach wall when compared with guar gum at similar viscosity (Lentle et al., 2010). Mamaku pith powder suspension with similar shear-thickening behaviour may also alter the gut wall activity and affect the gut transit time. Also, overnight hydrated mamaku pith powder can significantly retard the *in vitro* diffusion and mixing processes compared to guar gum (unpublished). However, in the present study pre-hydrated mamaku pith powder was less effective in reducing postprandial blood glucose and insulin than guar gum (**Figures 8.4**, **8.5**, **Tables 8.2** and **8.3**). A possible reason for this could be the higher viscosity of guar gum than the pre-hydrated mamaku pith powder suspension, throughout the 3 h of the trial (**Figure 8.9**). Guar gum treatment effectively suppressed the glycaemic response amplitude as well as prevented the hypoglycaemic overcorrection (*i.e.*, blood glucose was above baseline blood glucose between 120-180 min, **Figure 8.4**) that may occur after an acute blood glucose load has been resolved by insulin-driven glucose disposal. Both reduction in response amplitude and avoidance of inter-meal hypoglycaemia have benefits. Lowering response amplitude reduces the damage caused by metabolic side reactions and hyperglycaemia-induced oxidative stress while avoiding hypoglycaemia averts depression of cognitive function and delays the onset of hunger (Warren & Frier, 2005). In the present study, the mamaku pith powder did not have the same glycaemia-attenuating effect as guar gum even though it significantly reduced the response amplitude. It is possible that the concentration of mamaku pith powder used was too small for its effect to extend from retardation of gastric emptying to retardation of uptake in the small intestine.

Bearing in mind that the amount of mamaku pith powder ingested in the meals and its degree of hydration were chosen to allow a safe test, rather than a test of maximum effect, the experiment suggests that mamaku pith powder has potential as a functional ingredient for reducing glycaemic impact and that further research to identify the conditions under which the effect of mamaku pith powder can be safely amplified is justified. Lastly, all four

meals tested in the present study affected all dimensions of appetite, but no significant differences between meals were observed (**Figure 8.7**).

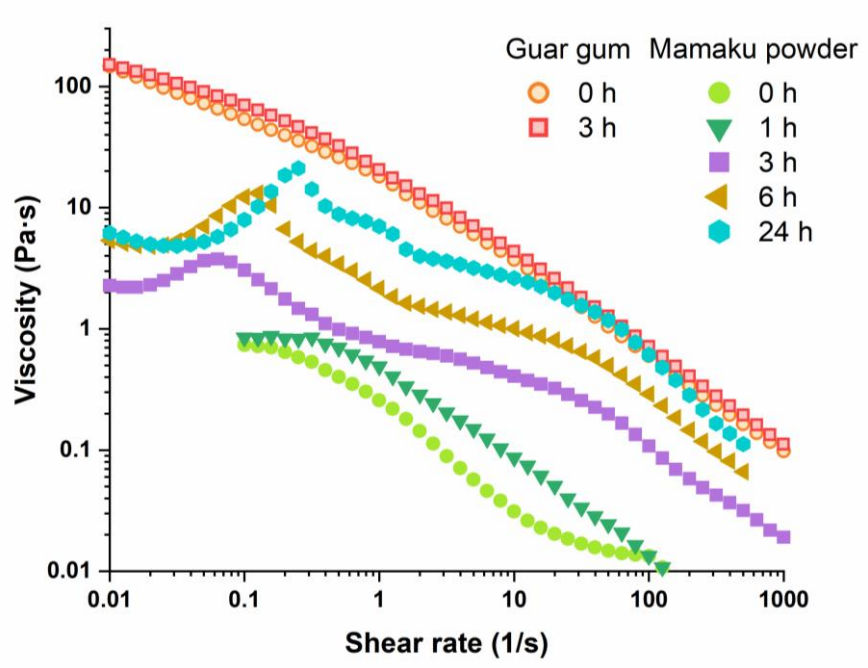


Figure 8.9: Viscosity profiles of guar gum (3 g in 250 ml water) and mamaku pith powder (5 g in 250 ml water, pre-hydrated at 37°C) at different time points (0, 1, 3, 6 and 24 h). Measurements were taken using cup-and-bob geometry at 37°C.

One of the merits of the study was the use of a robust crossover design where participants were their own control and underwent each of the treatments, therefore a smaller sample size was required for the same level of significance than if a parallel group design had been used. A broad participant range (young and middle-aged adults with BIM between 18 to 35 kg/m^2) was used in this study, but the generalisability of the findings to other populations *e.g.*, prediabetics and abnormal blood glucose, needs to be examined in the future. The sample size of 17 participants, although validated for measuring postprandial glucose responses, may not have been large enough to show statistically significant effects on insulin and appetite responses after ingestion of mamaku pith powder meals. Finally, no biomarkers were measured for satiety and appetite, as this study was designed to be an exploratory study.

After transit through the small intestine the undigested fraction of mamaku pith powder enters the colon for fermentation. The effect of mamaku pith powder on colonic fermentation was investigated using a rat model. Interestingly, the low fermentability of MP as observed during *in vitro* colonic fermentation (**Chapter 5**) was confirmed from the retention of about 50-65% of MP uronic acid in the faeces after gut transition (**Table 8.5**), suggesting that mamaku pith powder may be useful in faecal hydration and bulking, and warrants further study. During fermentation mamaku pith powder (5 and 10%) could significantly alter the colonic microbiota composition (**Figure 8.8**), without any significant increase in SCFAs production when compared with the glucose diet (**Table 8.4**). This is opposite to *in vitro* fermentation of mamaku gum where an increase in SCFAs production was observed (**Chapter 5**). Discrepancies between *in vitro* and *in vivo* SCFAs production could be because of multiple factors such as different sample types, low quantity of MP available freely as substrate, viscosity difference during fermentation, heterogeneity of colonic microbiome responsible for fermentation in different models (caecal fermentation in rat and human faecal for *in vitro* fermentation) and absorption of SCFAs during *in vivo* fermentation which was not mimicked during *in vitro* fermentation.

All in all, mamaku pith powder has the potential to be safely used as an anti-glycaemic agent which acts by suppressing the glycaemic response to co-consumed available carbohydrate. Mamaku pith powder can also modulate the gut microbiota. The results point to further research to establish an effective dose of mamaku pith powder and its hydration conditions to achieve functional efficacy. Investigations to determine how to best use mamaku pith powder within palatable food systems are needed.

Chapter 9

Overall conclusions and recommendations for future work

9.1 Conclusions

This thesis provides some technical understanding for developing a natural shear-thickening ingredient with proven functionality in humans. Two different fractions *i.e.,* water-soluble mamaku gum extract and the whole pith tissue were obtained from mamaku fronds. Both these fractions contain mamaku polysaccharide (MP) which is responsible for the atypical shear-thickening behaviour. The effect of mamaku frond harvesting age, sensitivity to high shear and temperature treatments and possible physiological actions were investigated at the fundamental level using the gum extract, while the physiological effects in humans were tested using mamaku pith powder, showing the potential of using the whole pith tissue for safe delivery of MP in humans under controlled hydration conditions, as an alternative to the mamaku gum extract. The following research questions were answered:

9.1.1 Does the harvesting age of mamaku frond matter?

In order to investigate age effect, mamaku gum was extracted from fronds of three different age groups, namely stages 1, 2 and 3 corresponding to young, fully grown and old fronds. The gum extract was characterised in terms of physicochemical properties and *in vitro* gastrointestinal and fermentation behaviours.

9.1.1.1 How does the structure and rheology of mamaku gum change with age? (Chapter 4)

- The proportion of constituent sugars that make up the MP was similar in all three gum extracts, with no distinguishing NMR spectra. However, the size of the MP decreased with increasing harvesting age. The molecular weight (M_w) reduced from ~4.1x10^6 to ~2.1 x10^6 Da, while the radius of gyration (R_g) decreased from ~147 nm to ~108 nm from stage 1 to stage 3, respectively.

- An age-dependent decrease in the shear viscosity (η_s) of MP was observed at all shear rates with $\eta_{s-Stage\,1} > \eta_{s-Stage\,2} > \eta_{s-Stage\,3}$. The shear-thickening behaviour was lost in the stage 3 sample.
- During extensional rheology measurements, stage 2 gum extract showed a longer capillary breaking time than stage 1. The stage 3 sample had the shortest capillary breaking time.

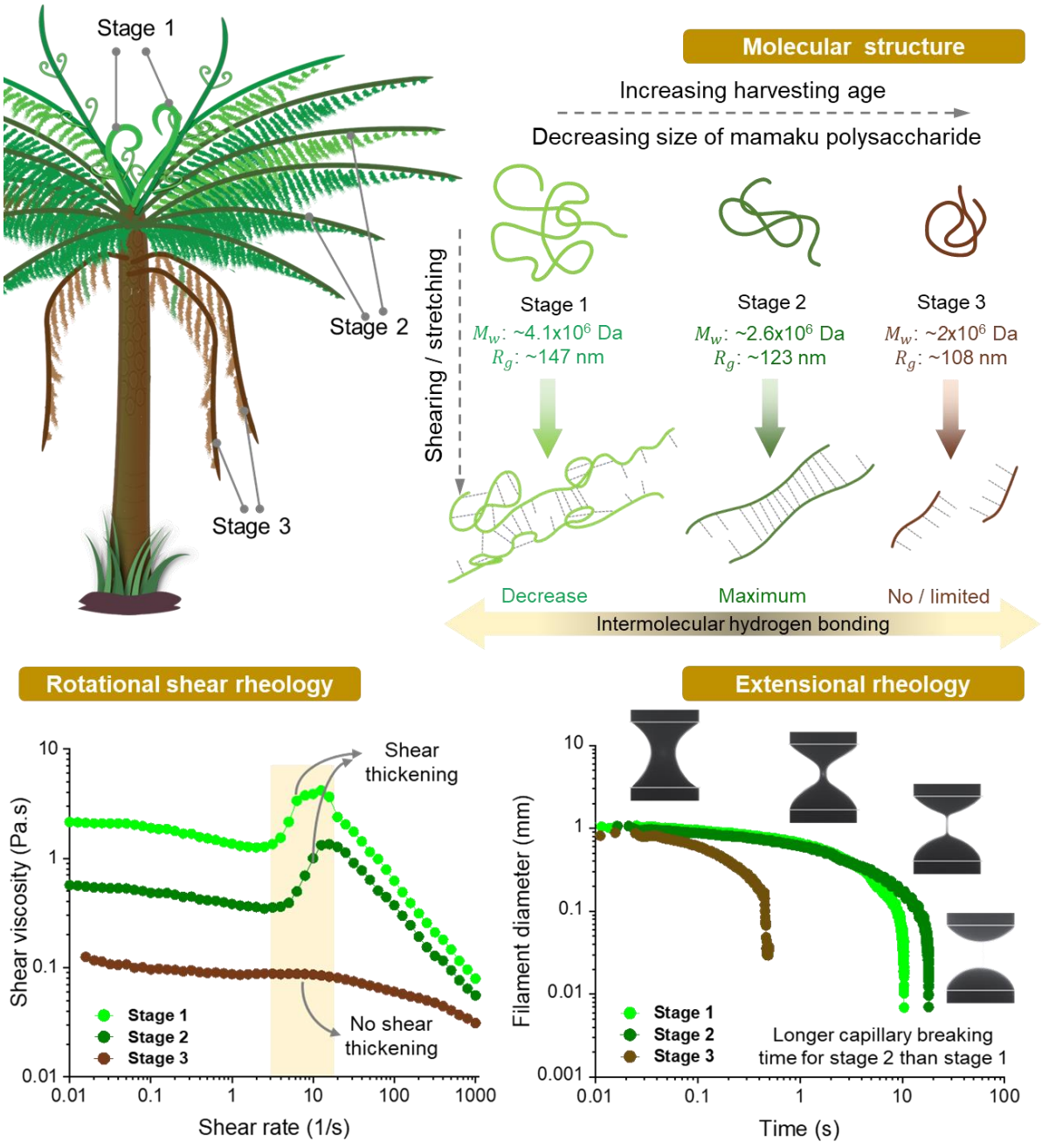


Figure 9.1: Schematic illustration showing the changes in size and rotational and extensional rheology of mamaku polysaccharide from different age fronds. Stage 1, young fronds; stage 2, fully grown fronds; stage 3, old fronds; M_w, weighted-average molecular weight; R_g, radius of gyration.

- The capillary breaking time behaviour corresponded with the higher extent of shear-thickening in the stage 2 sample than in stage 1. This could be explained by greater intermolecular interaction between MP chains from stage 2 than stage 1 on shearing or stretching the mamaku chains.
- It is proposed that there is a critical chain length of the polysaccharide where maximum intermolecular hydrogen bonding is achieved, resulting in stronger shear-thickening and extensional behaviours. Above and below this critical length the intermolecular interactions decrease which may reduce the shear-thickening and extensional behaviours.

9.1.1.2 How does mamaku gum affect the in vitro gastrointestinal function and colonic fermentation as a function of age? (Chapter 5)

- MP is not digestible as there was no decrease observed in the M_w of the polymer during simulated gastric and small intestinal digestion.
- In the upper gut, mamaku gum during its transit through the stomach and small intestine can inhibit the *in vitro* activity of digestive enzymes (α-amylase, pepsin and lipase). The effects were observed to be more pronounced in the presence of stage 1 and 2 gum samples than in stage 3 gum. Mamaku gum also binds bile acids, but no difference was observed between different age gum samples.
- In the lower gut, during *in vitro* colonic fermentation, human faecal microbiota utilised the mamaku gum and promoted the production of short-chain fatty acids (SCFAs) and reduced the pH. Furthermore, mamaku gum altered the composition of colonic microbiota, specifically reducing the ratio of Firmicutes to Bacteroidetes and increasing the relative abundance of *Bacteroides*, *Enterococcus*, *Paraprevotella* and *Parabacteroides* genera. No obvious difference between mamaku gum samples from stage 1, 2 and 3 was observed during fermentation.
- The changes in SCFAs and pH for mamaku gum groups were less prominent than in inulin and guar gum groups, suggesting lower fermentability of mamaku gum compared to the latter two.

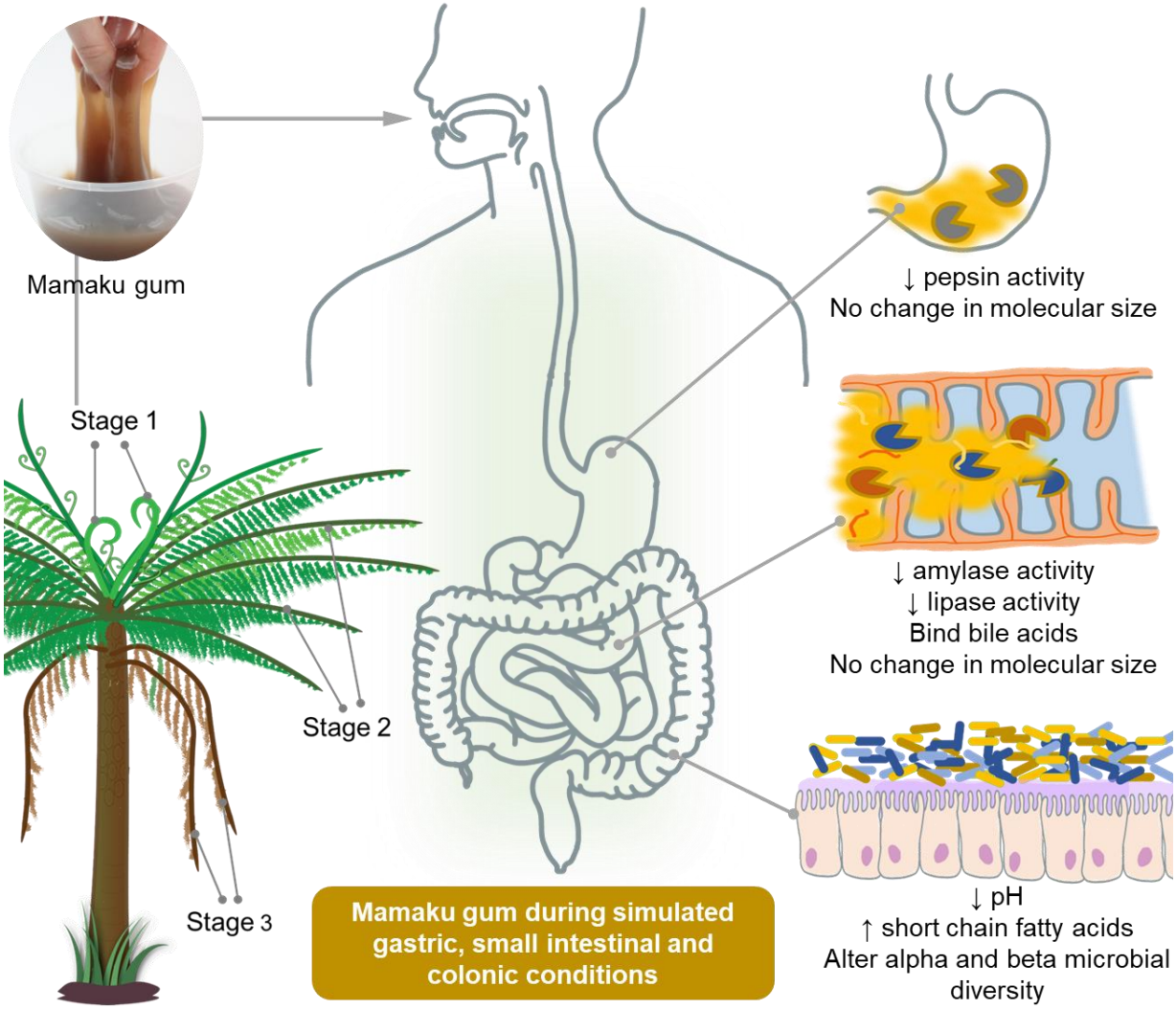


Figure 9.2: Schematic illustration showing the effects of mamaku gum in simulated gastric, small intestinal and colonic conditions.

Collectively, these results suggest that the harvesting age of the mamaku frond does matter. Stage 1 and 2 gum samples exhibit unique shear-thickening behaviour and stronger extensional properties and may modulate the host gut functionality by reducing enzyme activity, better than the stage 3 sample. The effects on colonic fermentation were similar between different age samples.

9.1.2 Can mamaku gum/pith withstand industrial operations without compromising the shear-thickening behaviour?

The sensitivity of MP towards shear and temperature treatments was studied by subjecting mamaku gum to high shear (between 1,000-8,000 rpm for various times using a lab-scale

high-shear mixer) and temperature (between 65 to 115°C, for 30 min) and changes in molecular structure and rheological properties were studied. The effect of drying methods on the functionality of mamaku pith powder was investigated by subjecting fresh pith tissue in a freeze-dryer or an oven-dryer, grinding them to powders and then characterising for physical properties, rehydration behaviour, rheology and *in vitro* digestion.

9.1.2.1 Is mamaku gum sensitive to high shear and temperature treatments? (Chapter 6)

- A marked irreversible decrease in viscosity was observed post shear and temperature treatments. The extent of shear-thickening decreased and the damping factor increased. The changes in rheological behaviour increased with increasing treatment intensity.
- For temperature-treated samples, the viscosity, at 1 s^{-1}, was reduced by ~15% after heating mamaku gum at 65°C for 30 mins, and drastically by ~75% after heating at 75°C and ultimately by ~99% after 115°C treatment. These decreases in viscosity were due to the depolymerisation of MP. The M_w decreased by ~5%, ~26% and ~84%, respectively. No shear-thickening behaviour was observed after heating at 115°C for 30 min.
- For shear-treated samples, the viscosity, at 1 s^{-1}, was reduced by ~9% after shearing mamaku gum at 2,000 rpm for 1 min, by ~44% after shearing at 5,000 rpm for 1 min, and ultimately by ~65% after 8,000 rpm for 1 min and 5,000 rpm for 20 min. However, interestingly, no evidence of depolymerisation was observed as the M_w, constituent sugars composition and NMR spectra remain unchanged. At extreme shear treatments (5,000 rpm for 20 min and 8,000 rpm for 1 min) a subtle decrease in z-average radius was observed.
- On comparing temperature and shear treatment results, the temperature treatment at 75°C for 30 min resulted in MP with a smaller size than samples subjected to extreme shear treatments, but the former had a higher extent of shear-thickening than the latter. Both these temperature and shear treated samples had similar viscosities at low shear rates (0.1- 3 s^{-1}).

- It is proposed that high shear treatment led to a compact and folded structure of MP due to increased intramolecular interactions which limit the unfolding of chains during rheological measurement and as a result a decrease in viscosity was observed.

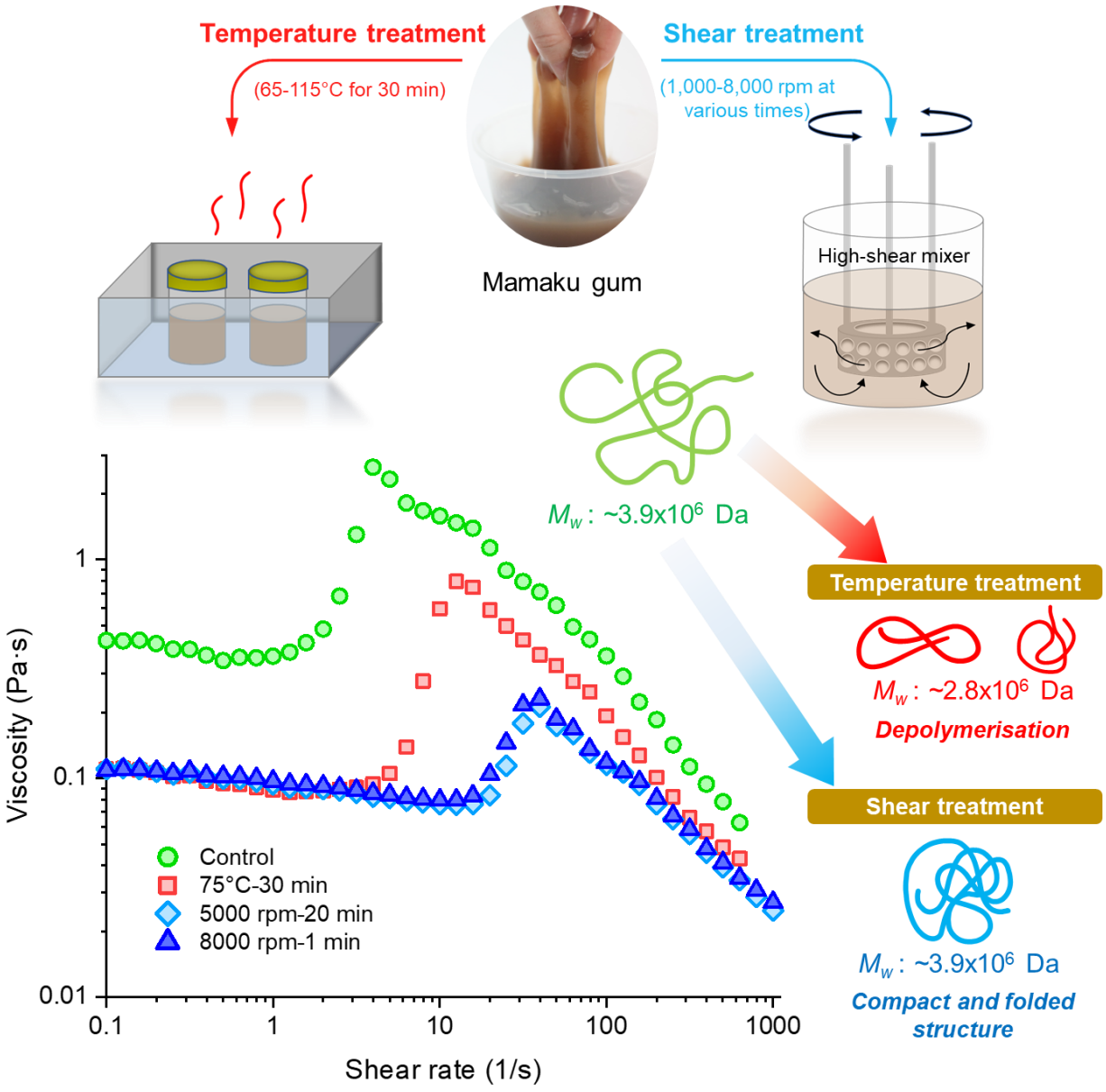


Figure 9.3: Schematic illustration showing the effects of shear and temperature treatments on mamaku gum.

9.1.2.2 How does the drying method affect the functionality of the pith powder? (Chapter 7)

- Oven-drying of mamaku pith resulted in a compact and dense structure of powder with a darker colour than freeze-drying.
- Upon rehydration with water, both freeze-dried and oven-dried mamaku pith powders absorbed water, causing the powder particles to swell and release the water-soluble compounds into the continuous phase.
- The ability of the freeze-dried powder to release enough water-soluble MP into the continuous phase resulted in a shear-thickening behaviour of the powder suspension similar to mamaku gum extract. The MP released into the continuous phase contributed to the rheological profile of the suspension while the insoluble particles increased the overall viscosity without altering the trend of the rheological properties.
- The development of viscosity and shear-thickening behaviour is time-dependent. A minimum of 1-3 h hydration time is required before observing shear-thickening behaviour.
- No shear-thickening was observed in oven-dried pith powder suspension because not enough MP was available in the continuous phase due to its compact and denser structure thereby limiting polymer-polymer interactions.
- *In vitro* digestion of wheat biscuits mixed with hydrated freeze-dried pith powder suspension reduced starch digestion by ~35% after 10 min, but starch digestion was unaffected by oven-dried pith powder suspension.

The results, therefore, show that the rheological behaviour of mamaku gum is sensitive to both high shear and temperature treatments. The sensitivity of MP molecules when using similar industrial processes should be considered as it may adversely affect the rheological properties of the product where MP is incorporated. Furthermore, using an appropriate method for drying the mamaku pith is key, as it can alter the structural characteristics of the powder samples, thus impacting the expected rheological and physiological behaviour.

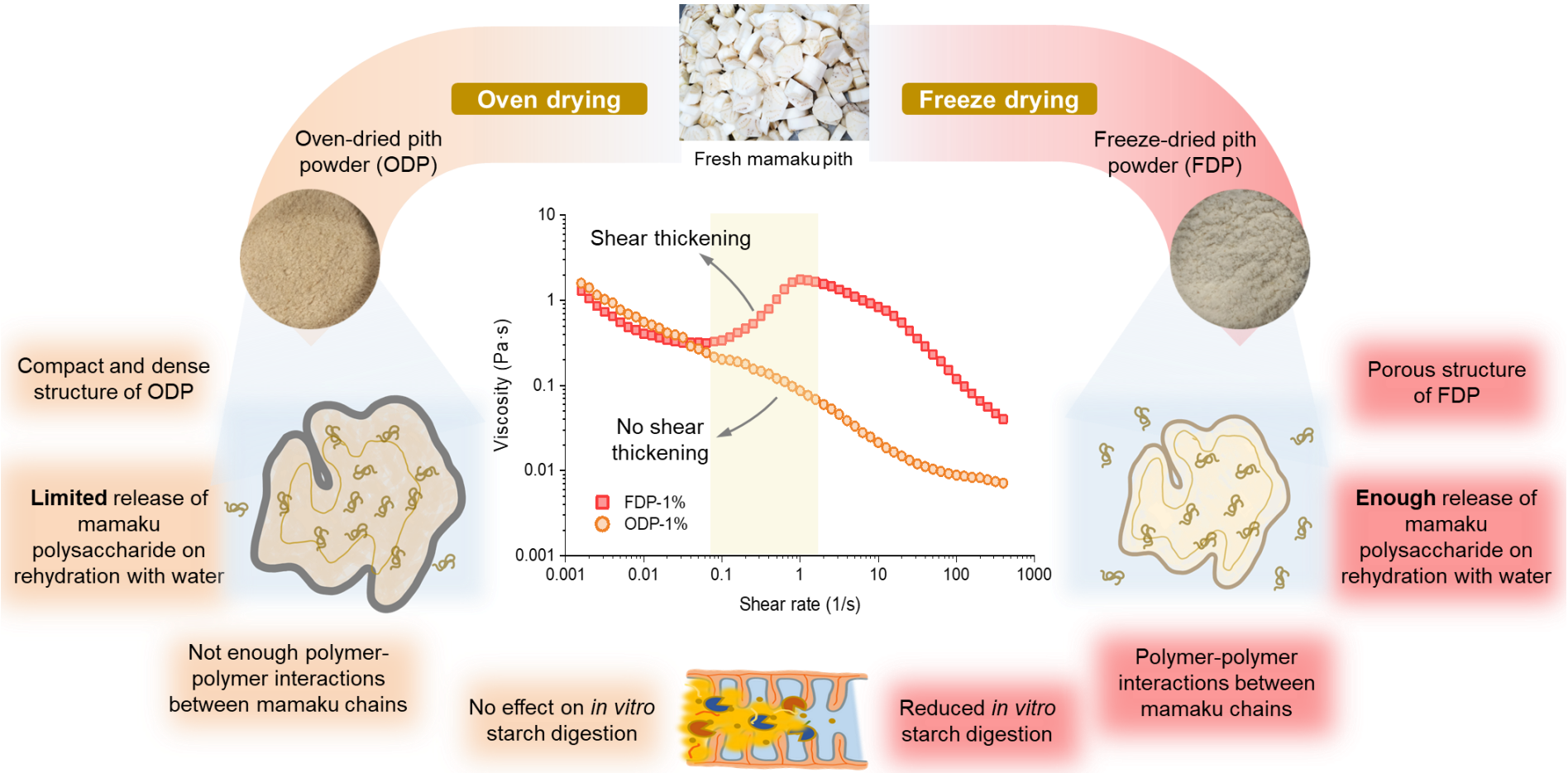


Figure 9.4: Schematic illustration showing the effects of freeze-drying and oven-drying methods on the functionality of mamaku pith powder.

9.1.3 Will mamaku pith have an impact *in vivo*?

The *in vivo* effects of freeze-dried mamaku pith powder were studied in human and rat trials. Human participants co-consumed freeze-dried mamaku pith powder (either pre-hydrated for 1 h or not-pre-hydrated) with a carbohydrate-rich meal and subsequent glycaemic response was monitored. The rats were fed a diet containing freeze-dried mamaku pith powder and the effects on colonic fermentation were studied.

9.1.3.1 Can the consumption of pith powder have an impact on glycaemic response and colonic fermentation? (Chapter 8)

- Compared with the control, consumption of pre-hydrated mamaku pith powder meal reduced postprandial peak blood glucose by ~21%. However, no significant decrease in peak blood glucose was observed after consuming a not-pre-hydrated pith powder meal.
- The mean incremental area under the blood glucose curve decreased after consuming pre-hydrated and not-pre-hydrated mamaku pith powder meals but was not significantly different.
- No significant differences were observed in postprandial insulin response for either of the two mamaku pith powder meals.
- Meals containing guar gum had a more pronounced decrease in postprandial blood glucose and insulin responses than the mamaku pith meals. This could be due to the higher viscosity of guar gum throughout the test period than mamaku pith powder suspensions.
- Consumption of mamaku pith powder altered the composition of colonic microbiota in rats.
- More than 50% of MP survived the gut transit and was recovered in rat faeces.

The consumption of mamaku pith powder can promote the host health. However, proper pre-hydration of mamaku pith powder is critical, so enough MP is released, to have an impact on postprandial blood glucose. Retention of MP in the rat faeces suggests that it could be used as a laxative.

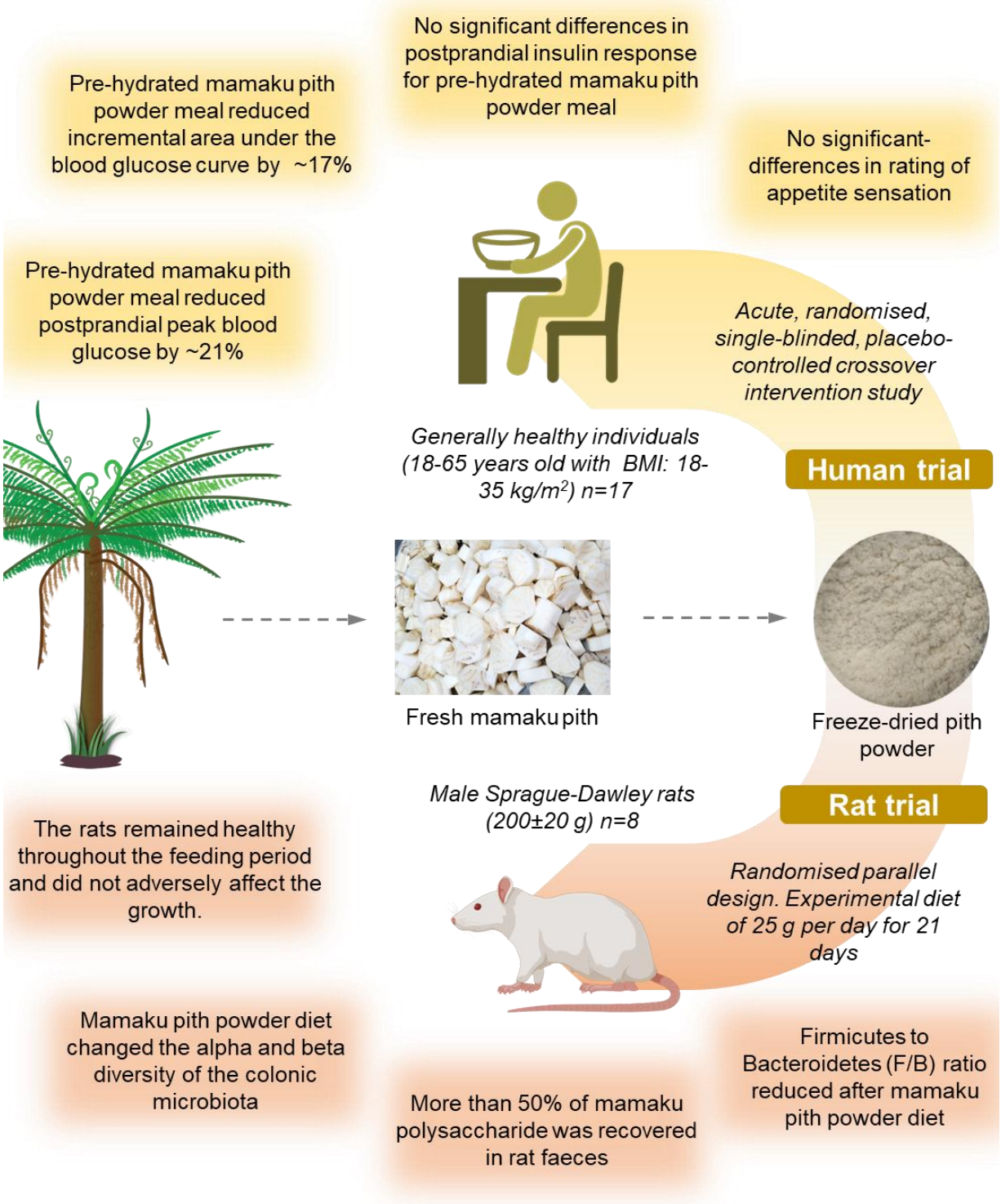


Figure 9.5: Schematic illustration showing *in vivo* effects of consuming mamaku pith powder in humans and rats.

9.2 Recommendations

The current study has produced new information towards understanding the processing of mamaku as a food ingredient and its physiological benefits, however, there are some new questions to be answered in future studies. These are outlined as follows:

- *Other New Zealand fern polysaccharides*

New Zealand has a diverse wealth of flora that offers an opportunity to discover new compounds with novel biological and/or chemical properties, making it possible to explore novel applications and develop extracts with various functionalities. Mamaku extract with novel shear-thickening behaviour is one such example. It is worth exploring gum extracts from other ferns such as ponga (silver fern, *Cyathea dealbata*), kātote (soft tree fern, *Cyathea smithii*), whekī ponga (golden tree fern, *Dicksonia fibrosa*), whekī (rough tree fern, *Dicksonia squarrosa*) and kiokio (palm-leaf fern, *Blechnum novae-zelandiae*) for their rheological, structural and physiological characterisations. It will also help us to understand if the shear-thickening behaviour is common in New Zealand ferns or unique only to mamaku fern.

- *Further rheological and structural characterisation of mamaku polysaccharide*

The rheological methods employed in the thesis provide sufficient details to understand the rheological behaviour of MP. Further methods such as stress relaxation, yield stress, large amplitude oscillatory shear (LAOS), and steady-state extensional viscosity using the filament stretching extensional rheometer (FiSER) or cross-slot extensional rheometer may be used for deeper understanding.

The chemical structure of MP was proposed partly based on the similar glucuronomannans reported in the literature. It is vital to confirm the exact sequence and arrangement of constituent sugars in the polymer chain to better explain the intermolecular interactions. Furthermore, the specific sites responsible for intermolecular hydrogen bonding leading to shear-thickening behaviour should also be investigated. This may be done by coupling the rheological measurements with other characterisation techniques such as rheo- nuclear magnetic resonance (rheo-NMR), rheo- small angle neutron scattering (rheo-SANS) and rheo-optics.

- *Mechanism for the shear sensitivity of mamaku polysaccharide*

In this study, the high shear sensitivity of MP was reported, however, the reason for viscosity reduction upon high shear treatment remains unclear. The proposed mechanism of re-arrangement of MP leading to a compact and folded structure due to increased intramolecular interactions on high shear treatment should be studied further possibly using techniques such as atomic force microscopy (AFM), and extensional rheology.

Also, during industrial processing, the shear experienced by MP could be much greater than what was tested here. Therefore, sensitivity to shear produced during operations such as homogenisation and microfluidisation should be assessed. The greater shear during these operations may lead to the degradation of MP, a phenomenon commonly reported in the literature.

- *Sensitivity of mamaku polysaccharide to other industrial treatments*

In addition to shear and temperature treatments, other techniques such as high hydrostatic pressure, ultraviolet (UV) and ultrasound technologies, are reported to affect the structure and functionality of biopolymers. However, their effects on MP have not yet been explored.

- *Faster release of mamaku polysaccharide from pith powder*

As reported here, the shear-thickening behaviour of rehydrated mamaku pith powder suspension was dependent on the release of MP from the pith tissue. Once enough MP was available in the continuous phase the shear-thickening behaviour was observed. The release of MP from pith tissue may be improved to generate an early shear-thickening effect. This could be achieved by freeze-thawing the fresh mamaku pith before drying which may lead to tissue rupture and thus may improve the MP release. Furthermore, reducing the thickness of the pith slices before drying may help to reduce the structural changes during drying. The effect of environmental conditions such as temperature during rehydration may also affect the release kinetics of MP.

- *Particle-polysaccharide systems and their physiological effects*

The presence of insoluble pith particles enhanced the viscosity of the continuous phase (containing MP) upon rehydration of freeze-dried pith powder in water. This suggests that the addition of particles to MP may be utilised to improve viscosity and shear-thickening behaviour in the gut at a lower dose of MP, as opposed to the high (>15% w/w) gum concentration used in previous studies. The particle-polysaccharide systems are complex and must be systematically characterised for rheological behaviour using the well-controlled size and volume fraction of particles and polymers. Different types of powder particles may have different effects on the rheological behaviour. Once the rheological properties of particle-polysaccharide systems are investigated, *ex vivo* stomach and intestine and the dynamic model for digestion (such as human gastric simulator, HGS, used to mimic the gastric conditions of humans) may be used to study physiological effects such as gastric emptying, gut transit and rate of digestion. This concept may further be developed to incorporate mamaku gum in meals (after mitigating the possible choking risk) where the food particles may naturally enhance the rheological behaviour of MP.

- *Delivery in stomach*

Possible physiological benefits of consuming mamaku gum/ pith powder are shown in this thesis. Safe delivery of mamaku ingredients to the stomach is the key to attaining these benefits. The delivery of the fresh gum into the stomach may be achieved by encapsulation or by interacting MP with other polysaccharides/proteins in a soft gel network which may disintegrate in gastric conditions and release free MP. Also, the development of functional food products with mamaku ingredients will be advantageous for both the consumer and the industry.

- *Targeting safe swallowing and dysphagia*

Texture modifications of foods or the thickening of fluids is a commonly recommended treatment for individuals with difficulty in swallowing, known as dysphagia. Improving the cohesiveness, the strength of internal bonds making up the product or the ability of particles to stick together in food/fluids can help maintain the integrity of the bolus and increase its pharyngeal transit time without fragmenting and promote safe swallowing. The

cohesiveness of the bolus is highly correlated with its extensibility (extensional behaviour) as opposed to traditional shear viscosity; though the extensional rheology in swallowing is not fully understood. As evident from the result of this thesis, MP has extremely strong extensional behaviour which could be useful in designing products targeting safe swallowing.

- *Anti-inflammatory potential of mamaku gum*

The traditional use of mamaku gum to treat skin conditions is thought to be related to its anti-inflammatory effect, however, it has not been investigated. In addition to anti-inflammatory effects, other pharmacological effects such as anti-oxidant, anti-bacterial and anti-cancer may also be present. On delivering mamaku gum to the gut, it is possible that these pharmacological effects (if any) may help to promote host health by repairing epithelial cell lines in the stomach and intestine.

- *Delay colonic fermentation and bowel health*

In general, most of the fermentation takes place in the proximal colon, producing SCFAs and gas. The gas produced during rapid fermentation, such as in the presence of inulin, causes the intestinal walls to stretch and expand, resulting in common irritable bowel syndrome (IBS) symptoms such as pain, bloating, and flatulence. Thus, the mixing of rapidly fermentable fibre with non-fermentable (or less fermentable) fibres that can increase the viscosity of digest could possibly delay the fermentation and limit the sudden increase in gas production. Also, the delay in fermentation will ensure the delivery of SCFAs to the distal colon. SCFAs are otherwise mostly produced and utilised in the proximal colon. Thus, delayed fermentation can also help in managing inflammatory bowel disease (IBD).

Delaying fermentation so that fermentable carbohydrate reaches the distal colon as a substrate for colonic bacteria also helps to delay protein putrefaction, reducing the risk of colorectal cancer.

Mamaku pith (and MP) is not very fermentable, as evident by the presence of more than 50% uronic acid in rat faeces after consuming the mamaku pith powder diet, and thus can be mixed with digesta to increase the viscosity of the digesta in the colon. This consequently

could delay the rate of fermentation of otherwise rapidly fermentable carbohydrates. Therefore, mamaku has the potential to be used in reducing the discomfort in individuals with IBS and IBD diseases, which has been manifested as a growing health problem.

- *Laxative agent*

The balance of insoluble fibres and low-fermentable soluble MP in the mamaku pith suggests a laxative function. Mamaku pith may combine the faecal bulking effects of cell wall structures, as observed with wheat bran, with the faecal hydrating/bulking and lubricating effects of hydrating hydrocolloids such as psyllium husk polysaccharide and have the potential to be an effective natural laxative. Mamaku pith, therefore, may be valuable as a partial substitute or replacement for wheat bran in products for large bowel health. It is a colourless product with a mild taste that can easily be masked. It is also free of gluten, making it more acceptable than wheat bran to a large segment of the market.

- *Further human trails*

The human trial presented in this thesis is the first key step toward studying the effect of mamaku pith powder on postprandial blood glucose response. Further trials are warranted to maximise this effect by achieving the appropriate rehydration time and dose. Along with measuring blood glucose, gastric emptying could also be studied in the same trial using no-invasive methods such as magnetic resonance imaging (MRI) scans. It will be interesting to see if the long-term consumption of mamaku ingredients can have an impact on weight management and thereby obesity. Mamaku ingredients could be used to design the next-generation natural food products to manage the growing epidemic of diabetes and obesity.

References

Achanta, S., Okos, M. R., Cushman, J. H., & Kessler, D. P. (1997). Moisture transport in shrinking gels during saturated drying. *AIChE Journal, 43*(8), 2112-2122.

Ahmed, J., Thomas, L., & Khashawi, R. (2020). Influence of hot-air drying and freeze-drying on functional, rheological, structural and dielectric properties of green banana flour and dispersions. *Food Hydrocolloids, 99*, 105331.

Akasaka, T., Sueta, D., Tabata, N., Takashio, S., Yamamoto, E., Izumiya, Y., . . . Matsui, K. (2017). Effects of the mean amplitude of glycemic excursions and vascular endothelial dysfunction on cardiovascular events in nondiabetic patients with coronary artery disease. *Journal of the American Heart Association, 6*(5), e004841.

Al-Assaf, S., Sakata, M., McKenna, C., Aoki, H., & Phillips, G. O. (2009). Molecular associations in acacia gums. *Structural Chemistry, 20*(2), 325-336.

Allen, T. (1981). Particle size, shape and distribution. In *Particle size measurement* (pp. 103-164): Springer.

Amid, B. T., Mirhosseini, H., & Kostadinović, S. (2012). Chemical composition and molecular structure of polysaccharide-protein biopolymer from *Durio zibethinus* seed: Extraction and purification process. *Chemistry Central Journal, 6*(1), 1-14.

Ang, C. L., Goh, K. K. T., Lim, K., & Matia-Merino, L. (2021). Rheological characterization of a physically-modified waxy potato starch: Investigation of its shear-thickening mechanism. *Food Hydrocolloids, 120*, 106908.

Ang, C. L., Matia-Merino, L., Lim, K., & Goh, K. K. T. (2021). Molecular and physico-chemical characterization of de-structured waxy potato starch. *Food Hydrocolloids, 117*, 106667.

Anglea, S. A., Karathanos, V., & Karel, M. (1993). Low-temperature transitions in fresh and osmotically dehydrated plant materials. *Biotechnology Progress, 9*(2), 204-209.

Anna, S. L., & McKinley, G. H. (2001). Elasto-capillary thinning and breakup of model elastic liquids. *Journal of Rheology, 45*(1), 115-138.

Araya-Farias, M., Makhlouf, J., & Ratti, C. (2011). Drying of seabuckthorn (*Hippophae rhamnoides L.*) berry: Impact of dehydration methods on kinetics and quality. *Drying Technology, 29*(3), 351-359.

Argyropoulos, D., Heindl, A., & Müller, J. (2011). Assessment of convection, hot-air combined with microwave-vacuum and freeze-drying methods for mushrooms with regard to product quality. *International Journal of Food Science & Technology, 46*(2), 333-342.

Arnolds, O., Buggisch, H., Sachsenheimer, D., & Willenbacher, N. (2010). Capillary breakup extensional rheometry (CaBER) on semi-dilute and concentrated polyethyleneoxide (PEO) solutions. *Rheologica Acta, 49*(11), 1207-1217.

Arora, T., Sharma, R., & Frost, G. (2011). Propionate. Anti-obesity and satiety enhancing factor? *Appetite, 56*(2), 511-515.

Aspinall, G. O., Carlyle, J. J., McNab, J. M., & Rudowski, A. (1969). *Anogeissus leiocarpus* gum. Part II. Fractionation of the gum and partial hydrolysis of *leiocarpan A*. *Journal of the Chemical Society C: Organic* (5), 840-845.

Aspinall, G. O., Hirst, E. L., & Wickstrøm, A. (1955). Gum ghatti (Indian gum). The composition of the gum and the structure of two aldobiouronic acids derived from it. *Journal of the Chemical Society (Resumed)*, 1160-1165.

Aspinall, G. O., Puvanesarajah, V., Reuter, G., & Schauer, R. (1984). Selective cleavage of β-D-glucopyranosiduronic acid linkages in methylated polysaccharide acids from *Drosera* species. *Carbohydrate Research, 131*(1), 53-60.

Asthana, R. (2000). Dissolutive capillary penetration with expanding pores and transient contact angles. *Journal of Colloid and Interface Science, 231*(2), 398-400.

Astorg, P., Boutron-Ruault, M. C., Andrieux, C., Blachier, F., Blottière, H., Bonithon-Kopp, C., . . . Clavel-Chapelon, F. (2002). Dietary fibers and colorectal cancer. Experimental studies, epidemiology, mechanisms. *Gastroenterologie Clinique et Biologique, 26*(10), 893-912.

Ayyash, M., Abu-Jdayil, B., Itsaranuwat, P., Almazrouei, N., Galiwango, E., Esposito, G., . . . Najjar, Z. (2020). Exopolysaccharide produced by the potential probiotic *Lactococcus garvieae C47*: Structural characteristics, rheological properties, bioactivities and impact on fermented camel milk. *Food Chemistry, 333*, 127418.

Bae, J. H., Kim, L. K., Min, S. H., Ahn, C. H., & Cho, Y. M. (2018). Postprandial glucose-lowering effect of premeal consumption of protein-enriched, dietary fiber-fortified bar in individuals with type 2 diabetes mellitus or normal glucose tolerance. *Journal of Diabetes Investigation, 9*(5), 1110-1118.

Bag, M. A., & Valenzuela, L. M. (2017). Impact of the hydration states of polymers on their hemocompatibility for medical applications: A review. *International Journal of Molecular Sciences, 18*(8), 1422.

Ballard, M. J., Buscall, R., & Waite, F. A. (1988). The theory of shear-thickening polymer solutions. *Polymer, 29*(7), 1287-1293.

Barbosa-Canovas, G. V., Ortega-Rivas, E., Juliano, P., & Yan, H. (2005a). Bulk properties. In *Food powders: Physical properties, processing, and functionality* (pp. 55-90). New York: Kluwer Academic/Plenum Publishers.

Barbosa-Canovas, G. V., Ortega-Rivas, E., Juliano, P., & Yan, H. (2005b). Drying. In *Food powders: Physical properties, processing, and functionality* (pp. 271-304). New York: Kluwer Academic/Plenum Publishers.

Barbosa-Canovas, G. V., Ortega-Rivas, E., Juliano, P., & Yan, H. (2005c). Particle properties. In *Food powders: Physical properties, processing, and functionality* (pp. 19-54). New York: Kluwer Academic/Plenum Publishers.

Barone, G., Corsaro, M. M., De Castro, C., Lanzetta, R., Mangoni, L., & Parrilli, M. (1994). Structural investigation of *Ceratozamia spinosa* mucilage. *Carbohydrate Research, 260*(2), 259-270.

Barone, G., Corsaro, M. M., Giannattasio, M., Lanzetta, R., Moscariello, M., & Parrilli, M. (1996). Structural investigation of the polysaccharide fraction from the mucilage of *Dicerocaryum zanguebaricum Merr*. *Carbohydrate Research, 280*(1), 111-119.

Baudelaire, E. D. (2013). Grinding for food powder production. In B. R. Bhandari, N. Bansal, M. Zhang, & P. Schuck (Eds.), *Handbook of food powders: Processes and properties* (pp. 132-149): Elsevier.

Bautista, F., Tepale, N., Fernández, V. V. A., Landázuri, G., Hernández, E., Macías, E. R., . . . Puig, J. E. (2016). A master dynamic flow diagram for the shear-thickening transition in micellar solutions. *Soft Matter, 12*(1), 165-170.

Bazzano, L. A., He, J., Ogden, L. G., Loria, C. M., Vupputuri, S., Myers, L., & Whelton, P. K. (2002). Fruit and vegetable intake and risk of cardiovascular disease in US adults: The first national health and nutrition examination survey epidemiologic follow-up study. *The American Journal of Clinical Nutrition, 76*(1), 93-99.

Beer, M. U., Wood, P. J., & Weisz, J. (1999). A simple and rapid method for evaluation of Mark–Houwink–Sakurada constants of linear random coil polysaccharides using molecular weight and intrinsic viscosity determined by high performance size exclusion chromatography: Application to guar galactomannan. *Carbohydrate Polymers, 39*(4), 377-380.

Beisel, C. L., & Afroz, T. (2016). Rethinking the hierarchy of sugar utilization in bacteria. *Journal of Bacteriology, 198*(3), 374-376.

Belmiro, R. H., Tribst, A. A. L., & Cristianini, M. (2018). Application of high-pressure homogenization on gums. *Journal of the Science of Food and Agriculture, 98*(6), 2060-2069.

Berggren, A. M., Björck, I. M., Nyman, E. M. G., & Eggum, B. O. (1993). Short-chain fatty acid content and pH in caecum of rats given various sources of carbohydrates. *Journal of the Science of Food and Agriculture, 63*(4), 397-406.

Berret, J.-F., Gamez-Corrales, R., Lerouge, S., & Decruppe, J.-P. (2000). Shear-thickening transition in surfactant solutions: New experimental features from rheology and flow birefringence. *The European Physical Journal E, 2*(4), 343-350.

Berret, J.-F., Gamez-Corrales, R., Séréro, Y., Molino, F., & Lindner, P. (2001). Shear-induced micellar growth in dilute surfactant solutions. *EPL (Europhysics Letters), 54*(5), 605.

Best, E. (1977). Mamaku. In *Forest lore of the Maori: With methods of snaring, trapping, and preserving birds and rats, uses of berries, roots, fern-root, and forest products, with mythological notes on origins, karakia used, etc* (pp. 92-96): Te Papa Press.

Bhandari, B. (2013). Introduction to food powders. In B. R. Bhandari, N. Bansal, M. Zhang, & P. Schuck (Eds.), *Handbook of food powders: Processes and properties* (pp. 1-26): Elsevier.

Bhandari, B., & Howes, T. (1999). Implication of glass transition for the drying and stability of dried foods. *Journal of Food Engineering, 40*(1-2), 71-79.

Bhardwaj, A., Miller, E., & Rothstein, J. P. (2007). Filament stretching and capillary breakup extensional rheometry measurements of viscoelastic wormlike micelle solutions. *Journal of Rheology, 51*(4), 693-719.

Bhatta, S., Stevanovic Janezic, T., & Ratti, C. (2020). Freeze-drying of plant-based foods. *Foods, 9*(1), 87.

Bisanz, J. E. (2018). *qiime2R: Importing QIIME2 artifacts and associated data into R sessions*. Retrieved from https://github.com/jbisanz/qiime2R

Bisht, A., Goyal, A., Sachdev, D., & Pasricha, R. (2019). Aminopropyl functionalized ordered mesoporous silica as an efficient adsorbent for separation of widely used acidulant citric acid from expired juices. *Separation Science and Technology, 54*(17), 2853-2862.

Blumenkrantz, N., & Asboe-Hansen, G. (1973). New method for quantitative determination of uronic acids. *Analytical Biochemistry, 54*(2), 484-489.

Bokulich, N. A., Kaehler, B. D., Rideout, J. R., Dillon, M., Bolyen, E., Knight, R., . . . Gregory Caporaso, J. (2018). Optimizing taxonomic classification of marker-gene amplicon sequences with QIIME 2's q2-feature-classifier plugin. *Microbiome, 6*(1), 1-17.

Bolyen, E., Rideout, J. R., Dillon, M. R., Bokulich, N. A., Abnet, C. C., Al-Ghalith, G. A., . . . Asnicar, F. (2019). Reproducible, interactive, scalable and extensible microbiome data science using QIIME 2. *Nature Biotechnology, 37*(8), 852-857.

Boucheham, N., Galet, L., Patry, S., & Zidoune, M. N. (2019). Physicochemical and hydration properties of different cereal and legume gluten-free powders. *Food Science & Nutrition, 7*(9), 3081-3092.

Bourbon, A. I., Pinheiro, A. C., Ribeiro, C., Miranda, C., Maia, J. M., Teixeira, J. A., & Vicente, A. A. (2010). Characterization of galactomannans extracted from seeds of Gleditsia triacanthos and Sophora japonica through shear and extensional rheology: Comparison with guar gum and locust bean gum. *Food Hydrocolloids, 24*(2-3), 184-192.

BPJ. (2008). Demystifying rongoā Māori: Traditional Māori healing. *Best practice: Improving Māori health,* 32-36.

Bressa, C., Bailén-Andrino, M., Pérez-Santiago, J., González-Soltero, R., Pérez, M., Montalvo-Lominchar, M. G., . . . Larrosa, M. (2017). Differences in gut microbiota profile between women with active lifestyle and sedentary women. *PloS One, 12*(2), e0171352.

Brighenti, F., Benini, L., Del Rio, D., Casiraghi, C., Pellegrini, N., Scazzina, F., . . . Vantini, I. (2006). Colonic fermentation of indigestible carbohydrates contributes to the second-meal effect. *The American Journal of Clinical Nutrition, 83*(4), 817-822.

Brodkorb, A., Egger, L., Alminger, M., Alvito, P., Assunção, R., Ballance, S., . . . Carrière, F. (2019). INFOGEST static *in vitro* simulation of gastrointestinal food digestion. *Nature Protocols, 14*(4), 991-1014.

Brouns, F., Bjorck, I., Frayn, K., Gibbs, A., Lang, V., Slama, G., & Wolever, T. (2005). Glycaemic index methodology. *Nutrition Research Reviews, 18*(1), 145-171.

Brownlee, I. A. (2011). The physiological roles of dietary fibre. *Food Hydrocolloids, 25*(2), 238-250.

Buck, A., & Tsotsas, E. (2018). Drying in food materials in fluidized beds. In P. K. Nema, B. P. Kaur, & A. S. Mujumdar (Eds.), *Drying technology for foods: Fundamentals and applications* (pp. 283-296). Boca Raton: CRC Press, Taylor & Francis Group.

Buisson, G., Duee, E., Haser, R., & Payan, F. (1987). Three dimensional structure of porcine pancreatic alpha-amylase at 2.9 A resolution. Role of calcium in structure and activity. *The EMBO Journal, 6*(13), 3909-3916.

Buonocore, V., Poerio, E., Silano, V., & Tomasi, M. (1976). Physical and catalytic properties of α-amylase from *Tenebrio molitor L.* larvae. *Biochemical Journal, 153*(3), 621-625.

Burckbuchler, V., Kjøniksen, A.-L., Galant, C., Lund, R., Amiel, C., Knudsen, K. D., & Nyström, B. (2006). Rheological and structural characterization of the interactions between cyclodextrin compounds and hydrophobically modified alginate. *Biomacromolecules, 7*(6), 1871-1878.

Butt, M. S., Shahzadi, N., Sharif, M. K., & Nasir, M. (2007). Guar gum: A miracle therapy for hypercholesterolemia, hyperglycemia and obesity. *Critical Reviews in Food Science and Nutrition, 47*(4), 389-396.

Calín-Sánchez, Á., Figiel, A., Hernández, F., Melgarejo, P., Lech, K., & Carbonell-Barrachina, Á. A. (2013). Chemical composition, antioxidant capacity, and sensory quality of

pomegranate (*Punica granatum L.*) arils and rind as affected by drying method. *Food and Bioprocess Technology, 6*(7), 1644-1654.

Calín-Sánchez, Á., Kharaghani, A., Lech, K., Figiel, A., Carbonell-Barrachina, Á. A., & Tsotsas, E. (2015). Drying kinetics and microstructural and sensory properties of black chokeberry (*aronia melanocarpa*) as affected by drying method. *Food and Bioprocess Technology, 8*(1), 63-74.

Callahan, B. J., McMurdie, P. J., Rosen, M. J., Han, A. W., Johnson, A. J. A., & Holmes, S. P. (2016). DADA2: High-resolution sample inference from Illumina amplicon data. *Nature Methods, 13*(7), 581-583.

Canani, R. B., Di Costanzo, M., Leone, L., Pedata, M., Meli, R., & Calignano, A. (2011). Potential beneficial effects of butyrate in intestinal and extraintestinal diseases. *World Journal of Gastroenterology: WJG, 17*(12), 1519.

Caparino, O., Tang, J., Nindo, C., Sablani, S., Powers, J., & Fellman, J. (2012). Effect of drying methods on the physical properties and microstructures of mango (*Philippine 'Carabao' var.*) powder. *Journal of Food Engineering, 111*(1), 135-148.

Capuano, E. (2017). The behavior of dietary fiber in the gastrointestinal tract determines its physiological effect. *Critical Reviews in Food Science and Nutrition, 57*(16), 3543-3564.

Carnachan, S. M., Bootten, T. J., Mishra, S., Monro, J. A., & Sims, I. M. (2012). Effects of simulated digestion *in vitro* on cell wall polysaccharides from kiwifruit (*Actinidia spp.*). *Food Chemistry, 133*(1), 132-139.

Cassidy, Y. M., McSorley, E. M., & Allsopp, P. J. (2018). Effect of soluble dietary fibre on postprandial blood glucose response and its potential as a functional food ingredient. *Journal of Functional Foods, 46*, 423-439.

Cavalieri, L. F., & Rosenberg, B. H. (1959). Shear degradation of deoxyribonucleic acid. *Journal of the American Chemical Society, 81*(19), 5136-5139.

Ceriello, A., Taboga, C., Tonutti, L., Giacomello, R., Stel, L., Motz, E., & Pirisi, M. (1996). Post-meal coagulation activation in diabetes mellitus: The effect of acarbose. *Diabetologia, 39*, 469-473.

Chajès, V., & Romieu, I. (2014). Nutrition and breast cancer. *Maturitas, 77*(1), 7-11.

Changrue, V., Raghavan, V. G., Orsat, V., & Vijaya Raghavan, G. (2006). Microwave drying of fruits and vegetables. *Stewart Postharvest Review, 2*(6), 1-7.

Chassenieux, C., Nicolai, T., & Benyahia, L. (2011). Rheology of associative polymer solutions. *Current Opinion in Colloid & Interface Science, 16*(1), 18-26.

Chater, P. I., Wilcox, M. D., Brownlee, I. A., & Pearson, J. P. (2015). Alginate as a protease inhibitor *in vitro* and in a model gut system; selective inhibition of pepsin but not trypsin. *Carbohydrate Polymers, 131*, 142-151.

Chen, D., Chen, G., Wan, P., Hu, B., Chen, L., Ou, S., . . . Ye, H. (2017a). Digestion under saliva, simulated gastric and small intestinal conditions and fermentation *in vitro* of polysaccharides from the flowers of *Camellia sinensis* induced by human gut microbiota. *Food & Function, 8*(12), 4619-4629.

Chen, H., Liu, W., Hong, M., Zhang, E., Dai, X., Chen, Q., . . . Ji, X. (2019). Associative behavior of polyimide/cyclohexanone solutions. *RSC Advances, 9*(47), 27455-27463.

Chen, J., Liang, R.-H., Liu, W., Liu, C.-M., Li, T., Tu, Z.-C., & Wan, J. (2012). Degradation of high-methoxyl pectin by dynamic high pressure microfluidization and its mechanism. *Food Hydrocolloids, 28*(1), 121-129.

Chen, Q., Li, Z., Bi, J., Zhou, L., Yi, J., & Wu, X. (2017b). Effect of hybrid drying methods on physicochemical, nutritional and antioxidant properties of dried black mulberry. *LWT-Food Science and Technology, 80*, 178-184.

Cheng, H., & Neiss, T. G. (2012). Solution NMR spectroscopy of food polysaccharides. *Polymer Reviews, 52*(2), 81-114.

Cherta-Murillo, A., Pugh, J. E., Alaraj-Alshehhi, S., Hajjar, D., Chambers, E. S., & Frost, G. S. (2022). The effects of SCFAs on glycemic control in humans: A systematic review and meta-analysis. *The American Journal of Clinical Nutrition, 116*(2), 335-361.

Choi, H., Mitchell, J. R., Gaddipati, S. R., Hill, S. E., & Wolf, B. (2014). Shear rheology and filament stretching behaviour of xanthan gum and carboxymethyl cellulose solution in presence of saliva. *Food Hydrocolloids, 40*, 71-75.

Chuang, S.-C., Norat, T., Murphy, N., Olsen, A., Tjønneland, A., Overvad, K., . . . Kaaks, R. (2012). Fiber intake and total and cause-specific mortality in the European prospective investigation into cancer and nutrition cohort. *The American Journal of Clinical Nutrition, 96*(1), 164-174.

Clasen, C., Plog, J., Kulicke, W.-M., Owens, M., Macosko, C., Scriven, L., . . . McKinley, G. H. (2006). How dilute are dilute solutions in extensional flows? *Journal of Rheology, 50*(6), 849-881.

Codex Alimentarius. (2010). Guidelines on nutrition labelling CAC/GL 2-1985 as last amended 2010. *Joint FAO/WHO Food Standards Programme, Secretariat of the Codex Alimentarius Commission, FAO, Rome*

Corradini, C., Cavazza, A., & Bignardi, C. (2012). High-performance anion-exchange chromatography coupled with pulsed electrochemical detection as a powerful tool to evaluate carbohydrates of food interest: Principles and applications. *International Journal of Carbohydrate Chemistry, 2012*

Corredig, M., & Wicker, L. (2001). Changes in the molecular weight distribution of three commercial pectins after valve homogenization. *Food Hydrocolloids, 15*(1), 17-23.

Courtois, F. (2013). Roller and drum drying for food powder production. In B. R. Bhandari, N. Bansal, M. Zhang, & P. Schuck (Eds.), *Handbook of food powders: Processes and properties* (pp. 85-104): Elsevier.

Crowe, A. (2004). *A field guide to the native edible plants of New Zealand*. Auckland: Godwit.

Crowley, S., Kelly, A., Schuck, P., Jeantet, R., & O'mahony, J. (2016). Rehydration and solubility characteristics of high-protein dairy powders. *Advanced Dairy Chemistry*, 99-131.

Cui, Y., Zhang, L., Wang, X., Yi, Y., Shan, Y., Liu, B., . . . Lü, X. (2022). Roles of intestinal *Parabacteroides* in human health and diseases. *FEMS Microbiology Letters, 369*(1), fnac072.

Cummings, J., & Macfarlane, G. (1991). The control and consequences of bacterial fermentation in the human colon. *Journal of Applied Bacteriology, 70*(6), 443-459.

de Carvalho, C. M., de Paula, T. P., Viana, L. V., Machado, V. M., de Almeida, J. C., & Azevedo, M. J. (2017). Plasma glucose and insulin responses after consumption of breakfasts with different sources of soluble fiber in type 2 diabetes patients: A randomized crossover clinical trial. *The American Journal of Clinical Nutrition, 106*(5), 1238-1245.

De Ruiter, G. A., Schols, H. A., Voragen, A. G., & Rombouts, F. M. (1992). Carbohydrate analysis of water-soluble uronic acid-containing polysaccharides with high-performance anion-exchange chromatography using methanolysis combined with TFA hydrolysis is superior to four other methods. *Analytical Biochemistry, 207*(1), 176-185.

Dehmoune, J., Decruppe, J.-P., Greffier, O., & Xu, H. (2007). Rheometric and rheo-optical investigation on the effect of the aliphatic chain length of the surfactant on the shear thickening of dilute worm-like micellar solutions. *Rheologica Acta, 46*(8), 1121-1129.

Deshpande, S., Sathe, S., Salunkhe, D., & Cornforth, D. P. (1982). Effects of dehulling on phytic acid, polyphenols, and enzyme inhibitors of dry beans (*Phaseolus vulgaris L.*). *Journal of Food Science, 47*(6), 1846-1850.

Despond, S., Espuche, E., Cartier, N., & Domard, A. (2005). Hydration mechanism of polysaccharides: A comparative study. *Journal of Polymer Science Part B: Polymer Physics, 43*(1), 48-58.

Dhital, S., Dolan, G., Stokes, J. R., & Gidley, M. J. (2014). Enzymatic hydrolysis of starch in the presence of cereal soluble fibre polysaccharides. *Food & Function, 5*(3), 579-586.

Dhital, S., Gidley, M. J., & Warren, F. J. (2015). Inhibition of α-amylase activity by cellulose: Kinetic analysis and nutritional implications. *Carbohydrate Polymers, 123*, 305-312.

Dikeman, C. L., & Fahey Jr, G. C. (2006). Viscosity as related to dietary fiber: A review. *Critical Reviews in Food Science and Nutrition, 46*(8), 649-663.

Ding, J., Tracey, P. J., Li, W., Peng, G., Whitten, P. G., & Wallace, G. G. (2013). Review on shear thickening fluids and applications. *Textiles and Light Industrial Science and Technology (TLIST), 2(4)*, 161-173.

Ding, Y., Yan, Y., Peng, Y., Chen, D., Mi, J., Lu, L., . . . Cao, Y. (2019). *In vitro* digestion under simulated saliva, gastric and small intestinal conditions and fermentation by human gut microbiota of polysaccharides from the fruits of *Lycium barbarum*. *International Journal of Biological Macromolecules, 125*, 751-760.

Dinic, J., Zhang, Y., Jimenez, L. N., & Sharma, V. (2015). Extensional relaxation times of dilute, aqueous polymer solutions. *ACS Macro Letters, 4*(7), 804-808.

Dongowski, G., & Lorenz, A. (1998). Unsaturated oligogalacturonic acids are generated by *in vitro* treatment of pectin with human faecal flora. *Carbohydrate Research, 314*(3-4), 237-244.

Dreher, M. L. (2015). Role of fiber and healthy dietary patterns in body weight regulation and weight loss. *Advances in Obesity, Weight Management & Control, 3*, 00068.

Dupont, D., Alric, M., Blanquet-Diot, S., Bornhorst, G., Cueva, C., Deglaire, A., . . . Lelieveld, J. (2019). Can dynamic *in vitro* digestion systems mimic the physiological reality? *Critical Reviews in Food Science and Nutrition, 59*(10), 1546-1562.

Duxenneuner, M. R., Fischer, P., Windhab, E. J., & Cooper-White, J. J. (2008). Extensional properties of hydroxypropyl ether guar gum solutions. *Biomacromolecules, 9*(11), 2989-2996.

Eagles, P. F., Stephen, A. M., & Churms, S. C. (1993). Molecular structures of gum exudates from *Hakea* species. *Phytochemistry, 34*(3), 709-713.

Edwards, C. A., & Garcia, A. L. (2009). The health aspects of hydrocolloids. In G. O. Phillips & P. A. Williams (Eds.), *Handbook of hydrocolloids* (2 ed., pp. 50-81). Cambrridge: CRC Press.

Egres, R. G., Nettesheim, F., & Wagner, N. J. (2006). Rheo-SANS investigation of acicular-precipitated calcium carbonate colloidal suspensions through the shear thickening transition. *Journal of Rheology, 50*(5), 685-709.

Ellegard, L., & Andersson, H. (2007). Oat bran rapidly increases bile acid excretion and bile acid synthesis: An ileostomy study. *European Journal of Clinical Nutrition, 61*(8), 938-945.

Englyst, H., & Hudson, G. (1987). Colorimetric method for routine measurement of dietary fibre as non-starch polysaccharides. A comparison with gas-liquid chromatography. *Food Chemistry, 24*(1), 63-76.

Entov, V., & Hinch, E. (1997). Effect of a spectrum of relaxation times on the capillary thinning of a filament of elastic liquid. *Journal of Non-Newtonian Fluid Mechanics, 72*(1), 31-53.

Eren, N. M., Santos, P. H., & Campanella, O. (2015). Mechanically modified xanthan gum: Rheology and polydispersity aspects. *Carbohydrate Polymers, 134*, 475-484.

Ermis, E., & Özkan, M. (2021). Sugar beet powder production using different drying methods, characterization and influence on sensory quality of cocoa-hazelnut cream. *Journal of Food Science and Technology, 58*(6), 2068-2077.

Erni, P., Varagnat, M., Clasen, C., Crest, J., & McKinley, G. H. (2011). Microrheometry of sub-nanolitre biopolymer samples: Non-Newtonian flow phenomena of carnivorous plant mucilage. *Soft Matter, 7*(22), 10889-10898.

Esler, A. (1976). Succession of fronds of mamaku (*Cyathea medullaris*). *Wellington Botanical Society Bulletin, 39*, 41-43.

Fang, Y., Selomulya, C., Ainsworth, S., Palmer, M., & Chen, X. D. (2011). On quantifying the dissolution behaviour of milk protein concentrate. *Food Hydrocolloids, 25*(3), 503-510.

Fang, Y., Selomulya, C., & Chen, X. D. (2007). On measurement of food powder reconstitution properties. *Drying Technology, 26*(1), 3-14.

Farahmandfar, R., Tirgarian, B., Dehghan, B., & Nemati, A. (2020). Changes in chemical composition and biological activity of essential oil from Thomson navel orange (*Citrus sinensis L. Osbeck*) peel under freezing, convective, vacuum, and microwave drying methods. *Food Science & Nutrition, 8*(1), 124-138.

Farzi, M., Yarmand, M. S., Safari, M., Emam-Djomeh, Z., & Mohammadifar, M. A. (2015). Gum tragacanth dispersions: Particle size and rheological properties affected by high-shear homogenization. *International Journal of Biological Macromolecules, 79*, 433-439.

Fava, F., Lovegrove, J. A., Tuohy, K. M., & Gibson, G. R. (2009). The potential role of the intestinal gut microbiota in obesity and the metabolic syndrome. *Food Science & Technology Bulletin: Functional Foods, 5*, 71-92.

Feigl, K., & Tanner, F. X. (2022). Computational investigation of drop behavior and breakup in peristaltic flow. *Physics of Fluids, 34*(1), 012111.

Fernández, P. P., Otero, L., Guignon, B., & Sanz, P. D. (2006). High-pressure shift freezing versus high-pressure assisted freezing: Effects on the microstructure of a food model. *Food Hydrocolloids, 20*(4), 510-522.

Feskens, E. J., Sluik, D., & Du, H. (2014). The association between diet and obesity in specific European cohorts: DiOGenes and EPIC-PANACEA. *Current Obesity Reports, 3*(1), 67-78.

Fitzpatrick, J. (2013). Powder properties in food production systems. In B. R. Bhandari, N. Bansal, M. Zhang, & P. Schuck (Eds.), *Handbook of food powders: Processes and properties* (pp. 283-308): Elsevier.

Flavel, M., Jois, M., & Kitchen, B. (2021). Potential contributions of the methodology to the variability of glycaemic index of foods. *World Journal of Diabetes, 12*(2), 108.

Flint, A., Raben, A., Blundell, J., & Astrup, A. (2000). Reproducibility, power and validity of visual analogue scales in assessment of appetite sensations in single test meal studies. *International Journal of Obesity, 24*(1), 38-48.

Floury, J., Desrumaux, A., Axelos, M. A., & Legrand, J. (2002). Degradation of methylcellulose during ultra-high pressure homogenisation. *Food Hydrocolloids, 16*(1), 47-53.

Forny, L., Marabi, A., & Palzer, S. (2011). Wetting, disintegration and dissolution of agglomerated water soluble powders. *Powder Technology, 206*(1-2), 72-78.

Foster, T. (2008). *Plant heritage New Zealand: Te whakapapa o nga rakau: Interpreting the special features of native plants*. North Shore: Raupo.

Franco, B. M., Latre, M. L., Esteban, E. M. A., Ordovás, J. M., Casasnovas, J. A., & Peñalvo, J. L. (2014). Soluble and insoluble dietary fibre intake and risk factors for metabolic syndrome and cardiovascular disease in middle-aged adults: The AWHS cohort. *Nutricion Hospitalaria, 30*(6), 1279-1288.

Franková, L., & Fry, S. C. (2013). Biochemistry and physiological roles of enzymes that 'cut and paste' plant cell-wall polysaccharides. *Journal of Experimental Botany, 64*(12), 3519-3550.

Freudig, B., Hogekamp, S., & Schubert, H. (1999). Dispersion of powders in liquids in a stirred vessel. *Chemical Engineering and Processing: Process Intensification, 38*(4-6), 525-532.

Fringant, C., Desbrieres, J., Milas, M., Rinaudo, M., Joly, C., & Escoubes, M. (1996). Characterisation of sorbed water molecules on neutral and ionic polysaccharides. *International Journal of Biological Macromolecules, 18*(4), 281-286.

Funami, T., & Nakauma, M. (2021). Instrumental characteristics from extensional rheology and tribology of polysaccharide solutions. *Journal of Texture Studies, 52*(5-6), 567-577.

Fuwa, M., Nakanishi, Y., & Moritaka, H. (2016). Effect of xanthan gum on blood sugar level after cooked rice consumption. *Food Science and Technology Research, 22*(1), 117-126.

Gaiani, C., Boyanova, P., Hussain, R., Pazos, I. M., Karam, M., Burgain, J., & Scher, J. (2011). Morphological descriptors and colour as a tool to better understand rehydration properties of dairy powders. *International Dairy Journal, 21*(7), 462-469.

Gaiani, C., Burgain, J., & Scher, J. (2013). Surface composition of food powders. In B. R. Bhandari, N. Bansal, M. Zhang, & P. Schuck (Eds.), *Handbook of food powders: Processes and properties* (pp. 339-378): Elsevier.

Gaiani, C., Morand, M., Sanchez, C., Tehrany, E. A., Jacquot, M., Schuck, P., . . . Scher, J. (2010). How surface composition of high milk proteins powders is influenced by spray-drying temperature. *Colloids and Surfaces B: Biointerfaces, 75*(1), 377-384.

Galali, Y., Rees, G., & Kuri, V. (2022). The impact of waxy wheat flour, inulin and guar gum on post-prandial glycaemic and satiety indices, sensory attributes and shelf life of tandoori and pita breads. *Applied Sciences, 12*(7), 3355.

Gao, B., Chi, L., Zhu, Y., Shi, X., Tu, P., Li, B., . . . Schnabl, B. (2021). An introduction to next generation sequencing bioinformatic analysis in gut microbiome studies. *Biomolecules, 11*(4), 530.

Gao, J., Lin, L., Sun, B., & Zhao, M. (2017). Comparison study on polysaccharide fractions from *Laminaria japonica*: structural characterization and bile acid binding capacity. *Journal of Agricultural and Food Chemistry, 65*(44), 9790-9798.

Gao, W., Chen, F., Wang, X., & Meng, Q. (2020). Recent advances in processing food powders by using superfine grinding techniques: A review. *Comprehensive Reviews in Food Science and Food Safety, 19*(4), 2222-2255.

Garcia, A., Otto, B., Reich, S., Weickert, M., Steiniger, J., Machowetz, A., . . . Speth, M. (2007). Arabinoxylan consumption decreases postprandial serum glucose, serum insulin and plasma total ghrelin response in subjects with impaired glucose tolerance. *European Journal of Clinical Nutrition, 61*(3), 334-341.

Gibb, R. D., McRorie Jr, J. W., Russell, D. A., Hasselblad, V., & D'Alessio, D. A. (2015). Psyllium fiber improves glycemic control proportional to loss of glycemic control: A meta-analysis of data in euglycemic subjects, patients at risk of type 2 diabetes mellitus, and patients being treated for type 2 diabetes mellitus. *The American Journal of Clinical Nutrition, 102*(6), 1604-1614.

Girard, M., Turgeon, S. L., & Gauthier, S. F. (2002). Interbiopolymer complexing between β-lactoglobulin and low- and high-methylated pectin measured by potentiometric titration and ultrafiltration. *Food Hydrocolloids, 16*(6), 585-591.

Goh, K. K. T., Matia-Merino, L., Hall, C. E., Moughan, P. J., & Singh, H. (2007). Complex rheological properties of a water-soluble extract from the fronds of the black tree fern, *Cyathea medullaris*. *Biomacromolecules, 8*(11), 3414-3421.

Goh, K. K. T., Matia-Merino, L., Pinder, D. N., Saavedra, C., & Singh, H. (2011). Molecular characteristics of a novel water-soluble polysaccharide from the New Zealand black tree fern (*Cyathea medullaris*). *Food Hydrocolloids, 25*(3), 286-292.

Goldberg, D. P., & Hillier, V. F. (1979). A scaled version of the General Health Questionnaire. *Psychological Medicine, 9*(1), 139-145.

Good, R. J., & Lin, N.-J. (1976). Rate of penetration of a fluid into a porous body: II. Verification of the generalization of the washburn equation, for organic liquids in glass capillaries. *Journal of Colloid and Interface Science, 54*(1), 52-58.

Granfeldt, Y., Wu, X., & Björck, I. (2006). Determination of glycaemic index; some methodological aspects related to the analysis of carbohydrate load and characteristics of the previous evening meal. *European Journal of Clinical Nutrition, 60*(1), 104-112.

Grossutti, M., & Dutcher, J. R. (2020). Hydration water structure, hydration forces, and mechanical properties of polysaccharide films. *Biomacromolecules, 21*(12), 4871-4877.

Guillon, F., & Champ, M. (2000). Structural and physical properties of dietary fibres, and consequences of processing on human physiology. *Food Research International, 33*(3-4), 233-245.

Guiné, R. P., & Barroca, M. J. (2012). Effect of drying treatments on texture and color of vegetables (pumpkin and green pepper). *Food and Bioproducts Processing, 90*(1), 58-63.

Gulati, T., & Datta, A. K. (2015). Mechanistic understanding of case-hardening and texture development during drying of food materials. *Journal of Food Engineering, 166*, 119-138.

Gümüşay, Ö. A., Borazan, A. A., Ercal, N., & Demirkol, O. (2015). Drying effects on the antioxidant properties of tomatoes and ginger. *Food Chemistry, 173*, 156-162.

Gunness, P., Flanagan, B. M., & Gidley, M. J. (2010). Molecular interactions between cereal soluble dietary fibre polymers and a model bile salt deduced from 13C NMR titration. *Journal of Cereal Science, 52*(3), 444-449.

Gürgen, S., Li, W., & Kuşhan, M. C. (2016). The rheology of shear thickening fluids with various ceramic particle additives. *Materials & Design, 104*, 312-319.

Haleem, B. A., & Nott, P. R. (2009). Rheology of particle-loaded semi-dilute polymer solutions. *Journal of Rheology, 53*(2), 383-400.

Hallmark, B., Bryan, M., Bosson, E., Butler, S., Hoier, T., Magens, O., . . . Wibberley, S. (2016). A portable and affordable extensional rheometer for field testing. *Measurement Science and Technology, 27*(12), 125302.

Haque, M. A., Timilsena, Y. P., & Adhikari, B. (2018). Spray drying. In P. K. Nema, B. P. Kaur, & A. S. Mujumdar (Eds.), *Drying technology for foods: Fundamentals and applications* (pp. 113-132). Boca Raton: CRC Press, Taylor & Francis Group.

Hardacre, A. K., Yap, S.-Y., Lentle, R. G., & Monro, J. A. (2015). The effect of fibre and gelatinised starch type on amylolysis and apparent viscosity during *in vitro* digestion at a physiological shear rate. *Carbohydrate Polymers, 123*, 80-88.

Harrington, R., & Zimm, B. (1965). Degradation of polymers by controlled hydrodynamic shear. *The Journal of Physical Chemistry, 69*(1), 161-175.

Harte, F., & Venegas, R. (2010). A model for viscosity reduction in polysaccharides subjected to high-pressure homogenization. *Journal of Texture Studies, 41*(1), 49-61.

Hausken, T., Mundt, M., & Samsom, M. (2002). Low antroduodenal pressure gradients are responsible for gastric emptying of a low-caloric liquid meal in humans. *Neurogastroenterology & Motility, 14*(1), 97-105.

Haward, S. J., Odell, J. A., Berry, M., & Hall, T. (2011). Extensional rheology of human saliva. *Rheologica Acta, 50*, 869-879.

Haward, S. J., Sharma, V., Butts, C. P., McKinley, G. H., & Rahatekar, S. S. (2012). Shear and extensional rheology of cellulose/ionic liquid solutions. *Biomacromolecules, 13*(5), 1688-1699.

Hawkins, A. (1990). Characterizing the single particle. In M. J. Rhodes (Ed.), *Principles of powder technology* (pp. 9-34). Chichester: John Wiley & Sons.

Hedegaard, R. V., & Skibsted, L. H. (2013). Shelf-life of food powders. In B. R. Bhandari, N. Bansal, M. Zhang, & P. Schuck (Eds.), *Handbook of food powders: Processes and properties* (pp. 409-434): Elsevier.

Hedenus, P., Mattsson, M. S., Niklasson, G., Camber, O., & Ek, R. (2000). Characterisation of instantaneous water absorption properties of pharmaceutical excipients. *International Journal of Pharmaceutics, 202*(1-2), 141-149.

Ho, I. H., Matia-Merino, L., & Huffman, L. M. (2015). Use of viscous fibres in beverages for appetite control: A review of studies. *International Journal of Food Sciences and Nutrition, 66*(5), 479-490.

Hogekamp, S., & Pohl, M. (2003). Porosity measurement of fragile agglomerates. *Powder Technology, 130*(1-3), 385-392.

Hogekamp, S., & Schubert, H. (2003). Rehydration of food powders. *Food Science and Technology International, 9*(3), 223-235.

Holmes, Z. C., Silverman, J. D., Dressman, H. K., Wei, Z., Dallow, E. P., Armstrong, S. C., . . . David, L. A. (2020). Short-chain fatty acid production by gut microbiota from children with obesity differs according to prebiotic choice and bacterial community composition. *MBio, 11*(4), e00914-00920.

Holzwarth, G. (1978). Molecular weight of xanthan polysaccharide. *Carbohydrate Research, 66*(1), 173-186.

Hosseinpour-Niazi, S., Mirmiran, P., Mirzaei, S., & Azizi, F. (2015). Cereal, fruit and vegetable fibre intake and the risk of the metabolic syndrome: A prospective study in the Tehran lipid and glucose study. *Journal of Human Nutrition and Dietetics, 28*(3), 236-245.

Howarth, N. C., Saltzman, E., & Roberts, S. B. (2001). Dietary fiber and weight regulation. *Nutrition Reviews, 59*(5), 129-139.

Hu, J. L., Nie, S. P., Li, C., & Xie, M. Y. (2013). *In vitro* effects of a novel polysaccharide from the seeds of *Plantago asiatica L.* on intestinal function. *International Journal of Biological Macromolecules, 54*, 264-269.

Hu, J. L., Nie, S. P., Min, F. F., & Xie, M. Y. (2013). Artificial simulated saliva, gastric and intestinal digestion of polysaccharide from the seeds of *Plantago asiatica L. Carbohydrate Polymers, 92*(2), 1143-1150.

Hu, Y., Wang, S., & Jamieson, A. (1995). Rheological and rheooptical studies of shear-thickening polyacrylamide solutions. *Macromolecules, 28*(6), 1847-1853.

Huang, D., Yang, P., Tang, X., Luo, L., & Sunden, B. (2021). Application of infrared radiation in the drying of food products. *Trends in Food Science & Technology, 110*, 765-777.

Huang, L., Shen, M., Zhang, X., Jiang, L., Song, Q., & Xie, J. (2018). Effect of high-pressure microfluidization treatment on the physicochemical properties and antioxidant activities of polysaccharide from Mesona chinensis Benth. *Carbohydrate Polymers, 200*, 191-199.

Huang, Y. L., Chow, C.-J., & Tsai, Y. H. (2012). Composition, characteristics, and *in-vitro* physiological effects of the water-soluble polysaccharides from Cassia seed. *Food Chemistry, 134*(4), 1967-1972.

Hugenholtz, F., Mullaney, J. A., Kleerebezem, M., Smidt, H., & Rosendale, D. I. (2013). Modulation of the microbial fermentation in the gut by fermentable carbohydrates. *Bioactive Carbohydrates and Dietary Fibre, 2*(2), 133-142.

Hughes, S., Shewry, P., Li, L., Gibson, G., Sanz, M., & Rastall, R. (2007). *In vitro* fermentation by human fecal microflora of wheat arabinoxylans. *Journal of Agricultural and Food Chemistry, 55*(11), 4589-4595.

Hughes, S. A., Shewry, P. R., Gibson, G. R., McCleary, B. V., & Rastall, R. A. (2008). *In vitro* fermentation of oat and barley derived β-glucans by human faecal microbiota. *FEMS Microbiology Ecology, 64*(3), 482-493.

Hur, S. J., Lim, B. O., Decker, E. A., & McClements, D. J. (2011). *In vitro* human digestion models for food applications. *Food Chemistry, 125*(1), 1-12.

Iida, Y., Tuziuti, T., Yasui, K., Towata, A., & Kozuka, T. (2008). Control of viscosity in starch and polysaccharide solutions with ultrasound after gelatinization. *Innovative Food Science & Emerging Technologies, 9*(2), 140-146.

ISO. (2010). ISO 26642: Food products—Determination of the glycaemic index (GI) and recommendation for food classification. In. Geneva: ISO.

Izli, N., & Polat, A. (2019). Freeze and convective drying of quince (*Cydonia oblonga Miller.*): Effects on drying kinetics and quality attributes. *Heat and Mass Transfer, 55*(5), 1317-1326.

Jaishankar, A., Wee, M. S. M., Matia-Merino, L., Goh, K. K. T., & McKinley, G. H. (2015). Probing hydrogen bond interactions in a shear thickening polysaccharide using nonlinear shear and extensional rheology. *Carbohydrate Polymers, 123*, 136-145.

Jankovie, M. (1993). Physical properties of convectively dried and freeze-dried berrylike fruits. *Faculty of Agriculture Belgrade, 38*(2), 129-135.

Ji, J., Cronin, K., Fitzpatrick, J., Fenelon, M., & Miao, S. (2015). Effects of fluid bed agglomeration on the structure modification and reconstitution behaviour of milk protein isolate powders. *Journal of Food Engineering, 167*, 175-182.

Ji, J., Fitzpatrick, J., Cronin, K., Maguire, P., Zhang, H., & Miao, S. (2016). Rehydration behaviours of high protein dairy powders: The influence of agglomeration on wettability, dispersibility and solubility. *Food Hydrocolloids, 58*, 194-203.

Jiang, T., & Zukoski, C. F. (2012). Role of particle size and polymer length in rheology of colloid–polymer composites. *Macromolecules, 45*(24), 9791-9803.

Jimenez, L. N., Dinic, J., Parsi, N., & Sharma, V. (2018). Extensional relaxation time, pinch-off dynamics, and printability of semidilute polyelectrolyte solutions. *Macromolecules, 51*(14), 5191-5208.

Jimenez, L. N., Martínez Narváez, C. D., & Sharma, V. (2020). Capillary breakup and extensional rheology response of food thickener cellulose gum (NaCMC) in salt-free and excess salt solutions. *Physics of Fluids, 32*(1), 012113.

Jin, W., Tang, H., Zhang, J., Wei, B., Sun, J., Zhang, W., . . . Zhong, W. (2020). Structural analysis of a novel sulfated galacto-fuco-xylo-glucurono-mannan from *Sargassum fusiforme* and its anti-lung cancer activity. *International Journal of Biological Macromolecules, 149*, 450-458.

Jonathan, M. C., van den Borne, J. J., van Wiechen, P., da Silva, C. S., Schols, H. A., & Gruppen, H. (2012). *In vitro* fermentation of 12 dietary fibres by faecal inoculum from pigs and humans. *Food Chemistry, 133*(3), 889-897.

Jones, M. A. (2015). *Effects of soybean pectin on blood glucose and insulin responses in healthy men.* University of Arkansas Fayetteville. Retrieved from https://scholarworks.uark.edu/etd/1325.

Karam, M. C., Petit, J., Zimmer, D., Djantou, E. B., & Scher, J. (2016). Effects of drying and grinding in production of fruit and vegetable powders: A review. *Journal of Food Engineering, 188*, 32-49.

Kasaai, M. R., Charlet, G., Paquin, P., & Arul, J. (2003). Fragmentation of chitosan by microfluidization process. *Innovative Food Science & Emerging Technologies, 4*(4), 403-413.

Kasehagen, L. J., & Macosko, C. W. (1998). Nonlinear shear and extensional rheology of long-chain randomly branched polybutadiene. *Journal of Rheology, 42*(6), 1303-1327.

Kaur, B., Koh, M., Ponnalagu, S., & Henry, C. J. (2020). Postprandial blood glucose response: Does the glycaemic index (GI) value matter even in the low GI range? *Nutrition & Diabetes, 10*(1), 15.

Kaur, B. P., Sharanagat, V. S., & Nema, P. K. (2018). Fundamentals of drying. In P. K. Nema, B. P. Kaur, & A. S. Mujumdar (Eds.), *Drying technology for foods: Fundamentals and applications* (pp. 1-17). Boca Raton: CRC Press, Taylor & Francis Group.

Keivanfard, N., Nasirpour, A., Barekat, S., & Keramat, J. (2022). Effects of heat and high-pressure homogenization processes on rheological and functional properties of gum tragacanth. *Food Hydrocolloids, 128*, 107593.

Kim, E. H.-J., Chen, X. D., & Pearce, D. (2002). Surface characterization of four industrial spray-dried dairy powders in relation to chemical composition, structure and wetting property. *Colloids and Surfaces B: Biointerfaces, 26*(3), 197-212.

Kim, E. H. J., Chen, X. D., & Pearce, D. (2009). Surface composition of industrial spray-dried milk powders: Changes in the surface composition during long-term storage. *Journal of Food Engineering, 94*(2), 182-191.

Kim, H. J., & White, P. J. (2010). *In vitro* bile-acid binding and fermentation of high, medium, and low molecular weight *β*-glucan. *Journal of Agricultural and Food Chemistry, 58*(1), 628-634.

Kim, W. J., & Yang, S.-M. (2000). Microstructures and rheological responses of aqueous CTAB solutions in the presence of benzyl additives. *Langmuir, 16*(15), 6084-6093.

Kirchberg, S., Abdin, Y., & Ziegmann, G. (2011). Influence of particle shape and size on the wetting behavior of soft magnetic micropowders. *Powder Technology, 207*(1-3), 311-317.

Kivelä, R., Pitkänen, L., Laine, P., Aseyev, V., & Sontag-Strohm, T. (2010). Influence of homogenisation on the solution properties of oat β-glucan. *Food Hydrocolloids, 24*(6-7), 611-618.

Kjøniksen, A. L., Hiorth, M., & Nyström, B. (2005). Association under shear flow in aqueous solutions of pectin. *European Polymer Journal, 41*(4), 761-770.

Kochar, J., Gaziano, J. M., & Djoussé, L. (2011). Dietary factors and the risk of coronary heart disease. *Aging and Disease, 2*(2), 149.

Koga, T., & Tanaka, F. (2005). Molecular origin of shear thickening in transient polymer networks: A molecular dynamics study. *The European Physical Journal E, 17*(2), 115-118.

Kolde, R. (2012). Pheatmap: pretty heatmaps. *R Package Version, 1*(2), 726.

Kong, F., & Singh, R. P. (2010). A human gastric simulator (HGS) to study food digestion in human stomach. *Journal of Food Science, 75*(9), E627-E635.

Kongjaroen, A., Methacanon, P., & Gamonpilas, C. (2022). On the assessment of shear and extensional rheology of thickened liquids from commercial gum-based thickeners used in dysphagia management. *Journal of Food Engineering, 316*, 110820.

Kosikova, B., Slamenova, D., Mikulasova, M., Horvathova, E., & Labaj, J. (2002). Reduction of carcinogenesis by bio-based lignin derivatives. *Biomass and Bioenergy, 23*(2), 153-159.

Kousaka, Y., & Endo, Y. (2006). Particle density. In M. Hiroaki, H. Ko Higashitani, & Y. Hideto (Eds.), *Powder technology handbook* (3 ed., pp. 49-52): CRC Press.

Kozich, J. J., Westcott, S. L., Baxter, N. T., Highlander, S. K., & Schloss, P. D. (2013). Development of a dual-index sequencing strategy and curation pipeline for analyzing amplicon sequence data on the MiSeq Illumina sequencing platform. *Applied and Environmental Microbiology, 79*(17), 5112-5120.

Krawczyk, B., Wityk, P., Gałęcka, M., & Michalik, M. (2021). The many faces of *Enterococcus spp.*—commensal, probiotic and opportunistic pathogen. *Microorganisms, 9*(9), 1900.

Kristensen, M., & Jensen, M. G. (2011). Dietary fibres in the regulation of appetite and food intake. Importance of viscosity. *Appetite, 56*(1), 65-70.

Kumar, A., & Chauhan, G. S. (2010). Extraction and characterization of pectin from apple pomace and its evaluation as lipase (steapsin) inhibitor. *Carbohydrate Polymers, 82*(2), 454-459.

Lacombe, C., & Essabbah, H. (1981). Comparative haemorheology of pathological blood. *Scandinavian Journal of Clinical and Laboratory Investigation, 41*(sup156), 249-250.

Lai, L.-S., & Liang, H.-Y. (2012). Chemical compositions and some physical properties of the water and alkali-extracted mucilage from the young fronds of *Asplenium australasicum* (J. Sm.) Hook. *Food Hydrocolloids, 26*(2), 344-349.

Laneuville, S. I., Turgeon, S. L., & Paquin, P. (2013). Changes in the physical properties of xanthan gum induced by a dynamic high-pressure treatment. *Carbohydrate Polymers, 92*(2), 2327-2336.

Langille, M. G., Zaneveld, J., Caporaso, J. G., McDonald, D., Knights, D., Reyes, J. A., . . . Knight, R. (2013). Predictive functional profiling of microbial communities using 16S rRNA marker gene sequences. *Nature Biotechnology, 31*(9), 814-821.

Lavi, B., & Marmur, A. (2006). The capillary race: Optimal surface tensions for fastest penetration. *Colloids and Surfaces A: Physicochemical and Engineering Aspects, 282*, 263-271.

Le Chatelier, E., Nielsen, T., Qin, J., Prifti, E., Hildebrand, F., Falony, G., . . . Kennedy, S. (2013). Richness of human gut microbiome correlates with metabolic markers. *Nature, 500*(7464), 541-546.

Lele, A. K., & Mashelkar, R. A. (1998). Energetically crosslinked transient network (ECTN) model: Implications in transient shear and elongation flows. *Journal of Non-Newtonian Fluid Mechanics, 75*(1), 99-115.

Lentle, R. G., & Janssen, P. W. M. (2011). Local motility and flow in segments that exhibit volume retention. In *The physical processes of digestion*: Springer Science & Business Media.

Lentle, R. G., Janssen, P. W. M., Goh, K. K. T., Chambers, P., & Hulls, C. (2010). Quantification of the effects of the volume and viscosity of gastric contents on antral and fundic activity in the rat stomach maintained *ex vivo*. *Digestive Diseases and Sciences, 55*(12), 3349-3360.

Lentle, R. G., & Janssen, P. W. M. (2008). Physical characteristics of digesta and their influence on flow and mixing in the mammalian intestine: A review. *Journal of Comparative Physiology B, 178*(6), 673-690.

Levi, G., & Karel, M. (1995). Volumetric shrinkage (collapse) in freeze-dried carbohydrates above their glass transition temperature. *Food Research International, 28*(2), 145-151.

Li, H. P., Hou, W. G., & Zhang, Y. Z. (2011). Rheological properties of aqueous solution of new exopolysaccharide secreted by a deep-sea mesophilic bacterium. *Carbohydrate Polymers, 84*(3), 1117-1125.

Li, L. L., Wang, Y. T., Zhu, L. M., Liu, Z. Y., Ye, C. Q., & Qin, S. (2020). Inulin with different degrees of polymerization protects against diet-induced endotoxemia and inflammation in association with gut microbiota regulation in mice. *Scientific Reports, 10*(1), 978.

Li, P., Jin, Y., & Sheng, L. (2020). Impact of microwave assisted phosphorylation on the physicochemistry and rehydration behaviour of egg white powder. *Food Hydrocolloids, 100*, 105380.

Li, Q. Y., Dou, Z. M., Chen, C., Jiang, Y. M., Yang, B., & Fu, X. (2022). Study on the effect of molecular weight on the gut microbiota fermentation properties of blackberry polysaccharides *in vitro*. *Journal of Agricultural and Food Chemistry, 70*(36), 11245-11257.

Li, Z., Jiang, D., Bi, H., Liu, D., Jang, S., & Zhou, Y. (2012). Preparation of a novel glucuronomannan from *Auricularia auricala* and its immunological activity. *Natural Product Communications, 7*(11), 1934578X1200701124.

Liang, K., Han, P., Chen, Q., Su, X., & Feng, Y. (2019). Comparative study on enhancing oil recovery under high temperature and high salinity: Polysaccharides versus synthetic polymer. *ACS Omega, 4*(6), 10620-10628.

Lim, J., Yeap, S. P., Che, H. X., & Low, S. C. (2013). Characterization of magnetic nanoparticle by dynamic light scattering. *Nanoscale Research Letters, 8*, 1-14.

Lim, M., Wu, H., Breckell, M., & Birch, J. (2006). Influence of the glass transition and storage temperature of frozen peas on the loss of quality attributes. *International Journal of Food Science & Technology, 41*(5), 507-512.

Liu, G., Sun, H., Rangou, S., Ntetsikas, K., Avgeropoulos, A., & Wang, S.Q. (2013). Studying the origin of "strain hardening": Basic difference between extension and shear. *Journal of Rheology, 57*(1), 89-104.

Liu, H., Gong, F., Wei, F., & Wu, H. (2018). Artificial simulation of salivary and gastrointestinal digestion, and fermentation by human fecal microbiota, of polysaccharides from *Dendrobium aphyllum*. *RSC Advances, 8*(25), 13954-13963.

Liu, Y., Duan, X., Duan, S., Li, C., Hu, B., Liu, A., . . . Wu, W. (2020). Effects of *in vitro* digestion and fecal fermentation on the stability and metabolic behavior of polysaccharides from *Craterellus cornucopioides*. *Food & Function, 11*(8), 6899-6910.

Liu, Y., Li, Y., Ke, Y., Li, C., Zhang, Z., Wu, Y., . . . Wu, W. (2021). *In vitro* saliva-gastrointestinal digestion and fecal fermentation of Oudemansiella radicata polysaccharides reveal its digestion profile and effect on the modulation of the gut microbiota. *Carbohydrate Polymers, 251*, 117041.

Louis, P., Hold, G. L., & Flint, H. J. (2014). The gut microbiota, bacterial metabolites and colorectal cancer. *Nature Reviews Microbiology, 12*(10), 661-672.

Lovegrove, A., Edwards, C., De Noni, I., Patel, H., El, S., Grassby, T., . . . Butterworth, P. (2017). Role of polysaccharides in food, digestion, and health. *Critical Reviews in Food Science and Nutrition, 57*(2), 237-253.

Lu, S., Mei, Q., Chen, J., Wang, Z., Li, W., Feng, C., . . . Dong, J. (2022). Cryo-TEM and rheological study on shear-thickening wormlike micelles of zwitterionic/anionic (AHSB/SDS) surfactants. *Journal of Colloid and Interface Science, 608*, 513-524.

Lu, X., Li, N., Qiao, X., Qiu, Z., & Liu, P. (2018). Effects of thermal treatment on polysaccharide degradation during black garlic processing. *LWT-Food Science and Technology, 95*, 223-229.

Ma, S. X., & Cooper, S. L. (2001). Shear thickening in aqueous solutions of hydrocarbon end-capped poly (ethylene oxide). *Macromolecules, 34*(10), 3294-3301.

Mackenzie, K., & Jemmett, A. (1971). Polymer shear stability. *Wear, 17*(5-6), 389-398.

Madar, Z., & Stark, A. (1995). Possible mechanisms by which dietary fiber affect lipid metabolism. *Agro Food Industry Hi-Tech, 6*, 40.

Maki, K. C., Carson, M. L., Miller, M. P., Turowski, M., Bell, M., Wilder, D. M., . . . Reeves, M. S. (2008). Hydroxypropylmethylcellulose and methylcellulose consumption reduce postprandial insulinemia in overweight and obese men and women. *The Journal of Nutrition, 138*(2), 292-296.

Malvern Panalytical Ltd. (2020). *Mastersizer 3000 User guide*.

Malvern Panalytical Ltd. (2023). Zetasizer advance range. Retrieved 20 March 2023 from https://www.malvernpanalytical.com/en/products/product-range/zetasizer-range/zetasizer-advance-range.

Mao, T., Huang, F., Zhu, X., Wei, D., & Chen, L. (2021). Effects of dietary fiber on glycemic control and insulin sensitivity in patients with type 2 diabetes: A systematic review and meta-analysis. *Journal of Functional Foods, 82*, 104500.

Marciani, L., Gowland, P. A., Spiller, R. C., Manoj, P., Moore, R. J., Young, P., & Fillery-Travis, A. J. (2001). Effect of meal viscosity and nutrients on satiety, intragastric dilution, and emptying assessed by MRI. *American Journal of Physiology-Gastrointestinal and Liver Physiology, 280*(6), G1227-G1233.

Marconati, M., & Ramaioli, M. (2020). The role of extensional rheology in the oral phase of swallowing: An *in vitro* study. *Food & Function, 11*(5), 4363-4375.

Marín-Santibáñez, B. M., Pérez-González, J., & Rodríguez-González, F. (2014). Origin of shear thickening in semidilute wormlike micellar solutions and evidence of elastic turbulence. *Journal of Rheology, 58*(6), 1917-1933.

Maskan, M. (2001). Drying, shrinkage and rehydration characteristics of kiwifruits during hot air and microwave drying. *Journal of Food Engineering, 48*(2), 177-182.

Masters, K. (1985). Analytical methods and properties of dried dairy products. *Evaporation, membrane filtration and spray drying in milk powder and cheese production. North European Dairy Journal, Vanlose, Denmark*, 393-403.

Matia-Merino, L., Goh, K. K. T., & Singh, H. (2012). A natural shear-thickening water-soluble polymer from the fronds of the black tree fern, *Cyathea medullaris*: Influence of salt, pH and temperature. *Carbohydrate Polymers, 87*(1), 131-138.

Mazzanti, V., & Mollica, F. (2020). A review of wood polymer composites rheology and its implications for processing. *Polymers, 12*(10), 2304.

McCleary, B., & Matheson, N. (1974). α-D-Galactosidase activity and galactomannan and galactosylsucrose oligosaccharide depletion in germinating legume seeds. *Phytochemistry, 13*(9), 1747-1757.

McGowan, R. E. (2014). *Rongoa Maori: A practical guide to traditional Maori medicine*: Robert McGowan.

McKinley, G. H., & Tripathi, A. (2000). How to extract the Newtonian viscosity from capillary breakup measurements in a filament rheometer. *Journal of Rheology, 44*(3), 653-670.

McMurry, J. (2008). Structure determination: Nuclear magnetic resonance spectroscopy. In *Organic chemistry* (7e ed., pp. 440-481): Thomson Learning Inc.

Metzker, M. L. (2010). Sequencing technologies—the next generation. *Nature Reviews Genetics, 11*(1), 31-46.

Michalska, A., Wojdyło, A., Lech, K., Łysiak, G. P., & Figiel, A. (2017). Effect of different drying techniques on physical properties, total polyphenols and antioxidant capacity of blackcurrant pomace powders. *LWT-Food Science and Technology, 78*, 114-121.

Minekus, M., Alminger, M., Alvito, P., Ballance, S., Bohn, T., Bourlieu, C., . . . Dupont, D. (2014). A standardised static *in vitro* digestion method suitable for food–an international consensus. *Food & Function, 5*(6), 1113-1124.

Mishra, S., Edwards, H., Hedderley, D., Podd, J., & Monro, J. A. (2017). Kiwifruit non-sugar components reduce glycaemic response to co-ingested cereal in humans. *Nutrients, 9*(11), 1195.

Mishra, S., & Monro, J. A. (2012). Wholeness and primary and secondary food structure effects on *in vitro* digestion patterns determine nutritionally distinct carbohydrate fractions in cereal foods. *Food Chemistry, 135*(3), 1968-1974.

Mishra, S., Monro, J. A., & Hedderley, D. (2008). Effect of processing on slowly digestible starch and resistant starch in potato. *Starch-Stärke, 60*(9), 500-507.

Mohapatra, D. (2018). Vacuum drying of foods. In P. K. Nema, B. P. Kaur, & A. S. Mujumdar (Eds.), *Drying technology for foods: Fundamentals and applications* (pp. 211-232). Boca Raton: CRC Press, Taylor & Francis Group.

Monnier, L., & Colette, C. (2015). Postprandial and basal hyperglycaemia in type 2 diabetes: Contributions to overall glucose exposure and diabetic complications. *Diabetes & Metabolism, 41*(6), 6S9-6S15.

Monnier, L., Mas, E., Ginet, C., Michel, F., Villon, L., Cristol, J.-P., & Colette, C. (2006). Activation of oxidative stress by acute glucose fluctuations compared with sustained chronic hyperglycemia in patients with type 2 diabetes. *JAMA, 295*(14), 1681-1687.

Monro, J. A. (2000). Faecal bulking index: A physiological basis for dietary management of bulk in the distal colon. *Asia Pacific Journal of Clinical Nutrition, 9*(2), 74-81.

Monro, J. A. (2001). Wheat bran equivalents based on faecal bulking indices for dietary management of faecal bulk. *Asia Pacific Journal of Clinical Nutrition, 10*(3), 242-248.

Monro, J. A., & Mishra, S. (2010). Digestion-resistant remnants of vegetable vascular and parenchyma tissues differ in their effects in the large bowel of rats. *Food Digestion, 1*(1-2), 47-56.

Monro, J. A., Mishra, S., Redman, C., Somerfield, S., & Ng, J. (2016). Vegetable dietary fibres made with minimal processing improve health-related faecal parameters in a valid rat model. *Food & Function, 7*(6), 2645-2654.

Monro, J. A., Mishra, S., & Venn, B. (2010). Baselines representing blood glucose clearance improve *in vitro* prediction of the glycaemic impact of customarily consumed food quantities. *British Journal of Nutrition, 103*(2), 295-305.

Monro, J. A., & Paturi, G. (2020). Kiwifruit skin and flesh contributions to fecal bulking and bacterial abundance in rats. *Plant Foods for Human Nutrition, 75*(4), 525-531.

Monro, J. A., Paturi, G., Butts, C. A., Young, W., De Guzman, C. E., McLachlan, A., . . . Ansell, J. (2012). Prebiotic effects of fermentable carbohydrate polymers may be modulated by faecal bulking of non-fermentable polysaccharides in the large bowel of rats. *International Journal of Food Science & Technology, 47*(5), 968-976.

Monro, J. A., Wallace, A., Mishra, S., Eady, S., Willis, J. A., Scott, R. S., & Hedderley, D. (2010). Relative glycaemic impact of customarily consumed portions of eighty-three foods measured by digesting *in vitro* and adjusting for food mass and apparent glucose disposal. *British Journal of Nutrition, 104*(3), 407-417.

Morris, G. A., Adams, G. G., & Harding, S. E. (2014). On hydrodynamic methods for the analysis of the sizes and shapes of polysaccharides in dilute solution: A short review. *Food Hydrocolloids, 42*, 318-334.

Mouécoucou, J., Villaume, C., Sanchez, C., & Méjean, L. (2004). Effects of gum arabic, low methoxy pectin and xylan on *in vitro* digestibility of peanut protein. *Food Research International, 37*(8), 777-783.

Mulet-Cabero, A.-I., Egger, L., Portmann, R., Ménard, O., Marze, S., Minekus, M., . . . Carrière, F. (2020). A standardised semi-dynamic *in vitro* digestion method suitable for food–an international consensus. *Food & Function, 11*(2), 1702-1720.

Muliterno, M. M., Rodrigues, D., de Lima, F. S., Ida, E. I., & Kurozawa, L. E. (2017). Conversion/degradation of isoflavones and color alterations during the drying of okara. *LWT-Food Science and Technology, 75*, 512-519.

Munoz-Tamayo, R., Laroche, B., Walter, E., Doré, J., Duncan, S. H., Flint, H. J., & Leclerc, M. (2011). Kinetic modelling of lactate utilization and butyrate production by key human colonic bacterial species. *FEMS Microbiology Ecology, 76*(3), 615-624.

Nachtigall, C., Berger, C., Kovanović, T., Wefers, D., Jaros, D., & Rohm, H. (2019). Shear induced molecular changes of exopolysaccharides from lactic acid bacteria. *Food Hydrocolloids, 97*, 105181.

Nachtigall, C., Rohm, H., & Jaros, D. (2021). Degradation of exopolysaccharides from lactic acid bacteria by thermal, chemical, enzymatic and ultrasound stresses. *Foods, 10*(2), 396.

Natividad, J. M., Lamas, B., Pham, H. P., Michel, M.-L., Rainteau, D., Bridonneau, C., . . . Chamignon, C. (2018). Bilophila wadsworthia aggravates high fat diet induced metabolic dysfunctions in mice. *Nature Communications, 9*(1), 2802.

Naumann, S., Haller, D., Eisner, P., & Schweiggert-Weisz, U. (2020). Mechanisms of interactions between bile acids and plant compounds—A review. *International Journal of Molecular Sciences, 21*(18), 6495.

Nazmi, A., Reinisch, T., & Hinz, H. (2008). Calorimetric studies on renaturation by $CaCl_2$ addition of metal-free α-amylase from *Bacillus licheniformis* (BLA). *Journal of Thermal Analysis and Calorimetry, 91*(1), 141-149.

Nep, E. I., Carnachan, S., Ngwuluka, N., Kontogiorgos, V., Morris, G., Sims, I., & Smith, A. M. (2016). Structural characterisation and rheological properties of a polysaccharide from sesame leaves (*Sesamum radiatum Schumach. & Thonn.*). *Carbohydrate Polymers, 152*, 541-547.

Nep, E. I., & Conway, B. R. (2011). Physicochemical characterization of grewia polysaccharide gum: Effect of drying method. *Carbohydrate Polymers, 84*(1), 446-453.

Nilsson, A. C., Ostman, E. M., Holst, J. J., & Bjӧrck, I. M. (2008). Including indigestible carbohydrates in the evening meal of healthy subjects improves glucose tolerance, lowers inflammatory markers, and increases satiety after a subsequent standardized breakfast. *The Journal of Nutrition, 138*(4), 732-739.

Nilsson, L., Leeman, M., Wahlund, K. G., & Bergenståhl, B. (2006). Mechanical degradation and changes in conformation of hydrophobically modified starch. *Biomacromolecules, 7*(9), 2671-2679.

O'Keefe, J. H., & Bell, D. S. (2007). Postprandial hyperglycemia/hyperlipidemia (postprandial dysmetabolism) is a cardiovascular risk factor. *The American Journal of Cardiology, 100*(5), 899-904.

O'Keefe, J. H., Gheewala, N. M., & O'Keefe, J. O. (2008). Dietary strategies for improving post-prandial glucose, lipids, inflammation, and cardiovascular health. *Journal of the American College of Cardiology, 51*(3), 249-255.

Owen, S. R., Tung, M. A., & Paulson, A. T. (1992). Thermorheological studies of food polymer dispersions. In *Rheology of foods* (pp. 39-53): Elsevier.

Oyinloye, T. M., & Yoon, W. B. (2020). Effect of freeze-drying on quality and grinding process of food produce: A review. *Processes, 8*(3), 354.

Pal, A., Indireshkumar, K., Schwizer, W., Abrahamsson, B., Fried, M., & Brasseur, J. G. (2004). Gastric flow and mixing studied using computer simulation. *Proceedings of the Royal Society of London. Series B: Biological Sciences, 271*(1557), 2587-2594.

Panagiotopoulos, C., & Sempéré, R. (2005). Analytical methods for the determination of sugars in marine samples: A historical perspective and future directions. *Limnology and Oceanography: Methods, 3*(10), 419-454.

Park, N., Rathee, V., Blair, D. L., & Conrad, J. C. (2019). Contact networks enhance shear thickening in attractive colloid-polymer mixtures. *Physical Review Letters, 122*(22), 228003.

Parkar, S. G., Rosendale, D., Paturi, G., Herath, T. D., Stoklosinski, H., Phipps, J. E., . . . Ansell, J. (2012). *In vitro* utilization of gold and green kiwifruit oligosaccharides by human gut microbial populations. *Plant Foods for Human Nutrition, 67*, 200-207.

Parkar, S. G., Simmons, L., Herath, T. D., Phipps, J. E., Trower, T. M., Hedderley, D. I., . . . Sutton, K. H. (2018). Evaluation of the prebiotic potential of five kiwifruit cultivars after simulated gastrointestinal digestion and fermentation with human faecal bacteria. *International Journal of Food Science & Technology, 53*(5), 1203-1210.

Pathare, P. B., Opara, U. L., & Al-Said, F. A. J. (2013). Colour measurement and analysis in fresh and processed foods: A review. *Food and Bioprocess Technology, 6*(1), 36-60.

Payling, L., Fraser, K., Loveday, S., Sims, I., Roy, N., & McNabb, W. (2020). The effects of carbohydrate structure on the composition and functionality of the human gut microbiota. *Trends in Food Science & Technology, 97*, 233-248.

Pera, P., Bucca, C., Borro, P., Bernocco, C., De Lillo, A., & Carossa, S. (2002). Influence of mastication on gastric emptying. *Journal of Dental Research, 81*(3), 179-181.

Pereira, R., Oliveira, J., & Sousa, M. (2020). Bioinformatics and computational tools for next-generation sequencing analysis in clinical genetics. *Journal of Clinical Medicine, 9*(1), 132.

Philip, W. (2003). Light scattering and the solution properties of macromolecules, handbook of size exclusion chromatography and related techniques. In: CRC Press.

Piermaría, J., Bengoechea, C., Abraham, A. G., & Guerrero, A. (2016). Shear and extensional properties of kefiran. *Carbohydrate Polymers, 152*, 97-104.

Porto, B. C., Augusto, P. E. D., Terekhov, A., Hamaker, B. R., & Cristianini, M. (2015). Effect of dynamic high pressure on technological properties of cashew tree gum (*Anacardium occidentale L.*). *Carbohydrate Polymers, 129*, 187-193.

Premathasan, N., & Taylor, S. E. (2018). Viscometric analysis of the hydration of a surface cross-linked EM-HEC polymer. *European Polymer Journal, 102*, 111-119.

Pruesse, E., Quast, C., Knittel, K., Fuchs, B. M., Ludwig, W., Peplies, J., & Glöckner, F. O. (2007). SILVA: A comprehensive online resource for quality checked and aligned ribosomal RNA sequence data compatible with ARB. *Nucleic Acids Research, 35*(21), 7188-7196.

Pryamitsyn, V., & Ganesan, V. (2006). Mechanisms of steady-shear rheology in polymer-nanoparticle composites. *Journal of Rheology, 50*(5), 655-683.

Quast, C., Pruesse, E., Yilmaz, P., Gerken, J., Schweer, T., Yarza, P., . . . Glöckner, F. O. (2012). The SILVA ribosomal RNA gene database project: Improved data processing and web-based tools. *Nucleic Acids Research, 41*(D1), D590-D596.

Queenan, K. M., Stewart, M. L., Smith, K. N., Thomas, W., Fulcher, R. G., & Slavin, J. L. (2007). Concentrated oat β-glucan, a fermentable fiber, lowers serum cholesterol in hypercholesterolemic adults in a randomized controlled trial. *Nutrition Journal, 6*(1), 1-8.

Rademaker, M., Davis, T., & Harris, P. (2022). Mamaku (New Zealand black tree fern) extract as a potential treatment for atopic dermatitis. *The Australasian Journal of Dermatology*.

Rahman, M. S. (2009). Dehydration and microstructure. In C. Ratti (Ed.), *Advances in food dehydration* (pp. 97-122). Boca Raton: CRC Press.

Ranjan, R., Rani, A., Metwally, A., McGee, H. S., & Perkins, D. L. (2016). Analysis of the microbiome: Advantages of whole genome shotgun versus 16S amplicon sequencing. *Biochemical and Biophysical Research Communications, 469*(4), 967-977.

Rastogi, N. K., Adsare, S. R., Karley, D., Raghavarao, K. S. M. S., & Niranjan, K. (2018). Osmotic dehydration applications and recent advances. In P. K. Nema, B. P. Kaur, & A. S. Mujumdar (Eds.), *Drying technology for foods: Fundamentals and applications* (pp. 29-56). Boca Raton: CRC Press, Taylor & Francis Group.

Ratti, C. (2001). Hot air and freeze-drying of high-value foods: a review. *Journal of Food Engineering, 49*(4), 311-319.

Ratti, C. (2013). Freeze drying for food powder production. In B. R. Bhandari, N. Bansal, M. Zhang, & P. Schuck (Eds.), *Handbook of food powders: Processes and properties* (pp. 57-84): Elsevier.

Redgwell, R. J., O'Neill, M. A., Selvendran, R. R., & Parsley, K. J. (1986). Structural features of the mucilage from the stem pith of kiwifruit (*Actinidia deliciosa*): Part I, structure of the inner core. *Carbohydrate Research, 153*(1), 97-106.

Rehage, H., & Hoffmann, H. (1982). Shear induced phase transitions in highly dilute aqueous detergent solutions. *Rheologica Acta, 21*(4), 561-563.

Reid, J. S. G., & Meier, H. (1973). Enzymic activities and galactomannan mobilisation in germinating seeds of fenugreek (*Trigonella foenum-graecum L. Leguminosae*). *Planta, 112*(4), 301-308.

Rendón-Huerta, J. A., Juárez-Flores, B., Pinos-Rodríguez, J. M., Aguirre-Rivera, J. R., & Delgado-Portales, R. E. (2012). Effects of different sources of fructans on body weight, blood metabolites and fecal bacteria in normal and obese non-diabetic and diabetic rats. *Plant Foods for Human Nutrition, 67*, 64-70.

Repin, N., Kay, B. A., Cui, S. W., Wright, A. J., Duncan, A. M., & Goff, H. D. (2017). Investigation of mechanisms involved in postprandial glycemia and insulinemia attenuation with dietary fibre consumption. *Food & Function, 8*(6), 2142-2154.

Reynolds, A. J., Temple, J. A., Robertson, D. L., & Mann, E. A. (2001). Long-term effects of an early childhood intervention on educational achievement and juvenile arrest: A 15-year follow-up of low-income children in public schools. *JAMA, 285*(18), 2339-2346.

Riana, L. M., Sims, I. M., & Matia-Merino, L. (2022). Emulsification properties of puka gum–An exudate of a native New Zealand tree (*Meryta sinclairii*): Effect of shear rate and gum concentration. *Food Hydrocolloids, 124*, 107263.

Riaz, T., Iqbal, M. W., Jiang, B., & Chen, J. (2021). A review of the enzymatic, physical, and chemical modification techniques of xanthan gum. *International Journal of Biological Macromolecules, 186*, 472-489.

Richardson, A., Calder, A., Stewart, C., & Smith, A. (1989). Simultaneous determination of volatile and non-volatile acidic fermentation products of anaerobes by capillary gas chromatography. *Letters in Applied Microbiology, 9*(1), 5-8.

Rideout, T. C., Harding, S. V., Jones, P. J., & Fan, M. Z. (2008). Guar gum and similar soluble fibers in the regulation of cholesterol metabolism: Current understandings and future research priorities. *Vascular Health and Risk Management, 4*(5), 1023.

Riley, M. (1994). *Māori healing and herbal: New Zealand ethnobotanical sourcebook*. Auckland: Viking Sevenseas N.Z.

Robal, M., Truus, K., Volobujeva, O., Mellikov, E., & Tuvikene, R. (2017). Thermal stability of red algal galactans: Effect of molecular structure and counterions. *International Journal of Biological Macromolecules, 104*, 213-223.

Rodd, L. E., Scott, T. P., Cooper-White, J. J., & McKinley, G. H. (2005). Capillary break-up rheometry of low-viscosity elastic fluids. *Applied Rheology, 15*(1), 12-27.

Rohrer, J. (2021). *Technical note 20: Carbohydrate analysis by high-performance anion-exchange chromatography with pulsed amperometric detection (HPAE-PAD)*.

Roos, Y. H. (1998). Role of water in phase-transition phenomena in foods. In M. A. Rao & R. W. Hartel (Eds.), *Phase/state transitions in foods: Chemical, structural and rheological changes* (pp. 57-86). New York: Marcel Dekker, Inc.

Rosendale, D., Cookson, A., Roy, N., & Vetharaniam, I. (2011). Opportunities for predictive modelling and gut health conceptually exploring an in silico tool for quantifying the benefits of dietary fibre consumption. *Agro Food Industry Hi-Tech, 22*(6), 18-22.

Ross, G. S., Redgwell, R. J., & MacRae, E. A. (1993). Kiwifruit β-galactosidase: Isolation and activity against specific fruit cell-wall polysaccharides. *Planta, 189*(4), 499-506.

Rost, K., & Schauer, R. (1977). Physical and chemical properties of the mucin secreted by *Drosera capensis*. *Phytochemistry, 16*(9), 1365-1368.

Rozali, S. N. M. (2019). *Atomization of fruit juice with fibres as drying aid: nozzle* (Doctor of Philosophy), Massey University, Palmerston North, New Zealand.

Rudin, A. (1998). *Elements of Polymer Science & Engineering: An Introductory Text and Reference for Engineers and Chemists*: Elsevier.

Rudin, A., & Schreiber, H. P. (1983). Shear modification of polymers. *Polymer Engineering & Science, 23*(8), 422-430.

Sabatie, J., Choplin, L., Paul, F., & Monsan, P. (1986). Shear-induced structure in enzymatically-synthesized dextran solutions. *Rheologica Acta, 25*(3), 287-295.

Saggin, R., & Coupland, J. (2002). Ultrasonic monitoring of powder dissolution. *Journal of Food Science, 67*(4), 1473-1477.

Sahana, T. G., & Rekha, P. D. (2019). A bioactive exopolysaccharide from marine bacteria *Alteromonas sp.* PRIM-28 and its role in cell proliferation and wound healing *in vitro*. *International Journal of Biological Macromolecules, 131*, 10-18.

Salamone, D., Rivellese, A. A., & Vetrani, C. (2021). The relationship between gut microbiota, short-chain fatty acids and type 2 diabetes mellitus: The possible role of dietary fibre. *Acta Diabetologica, 58*(9), 1131-1138.

Salleh, N., Goh, K. K. T., Waterland, M. R., Huffman, L. M., Weeks, M., & Matia-Merino, L. (2022). Complexation of anthocyanin-bound blackcurrant pectin and whey protein: Effect of pH and heat treatment. *Molecules, 27*(13), 4202.

Salvador, V., Cherbut, C., Barry, J. L., Bertrand, D., Bonnet, C., & Delort-Laval, J. (1993). Sugar composition of dietary fibre and short-chain fatty acid production during *in vitro* fermentation by human bacteria. *British Journal of Nutrition, 70*(1), 189-197.

Samoticha, J., Wojdyło, A., & Lech, K. (2016). The influence of different drying methods on chemical composition and antioxidant activity in chokeberries. *LWT-Food Science and Technology, 66*, 484-489.

Sánchez-Moya, T., López-Nicolás, R., Planes, D., González-Bermúdez, C., Ros-Berruezo, G., & Frontela-Saseta, C. (2017). *In vitro* modulation of gut microbiota by whey protein to preserve intestinal health. *Food & Function, 8*(9), 3053-3063.

Schubert, H. (1993). Instantization of powdered food products. *International Chemical Engineering, 33*(1), 28-45.

Schulze, K. (2006). Imaging and modelling of digestion in the stomach and the duodenum. *Neurogastroenterology & Motility, 18*(3), 172-183.

Scott, R. W. (1979). Colorimetric determination of hexuronic acids in plant materials. *Analytical Chemistry, 51*(7), 936-941.

Selomulya, C., & Fang, Y. (2013). Food powder rehydration. In B. R. Bhandari, N. Bansal, M. Zhang, & P. Schuck (Eds.), *Handbook of food powders: Processes and properties* (pp. 379-408): Elsevier.

Shah, U. V., Karde, V., Ghoroi, C., & Heng, J. Y. (2017). Influence of particle properties on powder bulk behaviour and processability. *International Journal of Pharmaceutics, 518*(1-2), 138-154.

Shao, P., Qin, M., Han, L., & Sun, P. (2014). Rheology and characteristics of sulfated polysaccharides from chlorophytan seaweeds Ulva fasciata. *Carbohydrate Polymers, 113*, 365-372.

Sharma, V., Haward, S. J., Serdy, J., Keshavarz, B., Soderlund, A., Threlfall-Holmes, P., & McKinley, G. H. (2015). The rheology of aqueous solutions of ethyl hydroxy-ethyl cellulose (EHEC) and its hydrophobically modified analogue (hmEHEC): Extensional flow response in capillary break-up, jetting (ROJER) and in a cross-slot extensional rheometer. *Soft Matter, 11*(16), 3251-3270.

Shimura, S., Tsuzuki, W., Kobayashi, S., & Suzuki, T. (1992). Inhibitory effect on lipase activity of extracts from medicinal herbs. *Bioscience, Biotechnology, and Biochemistry, 56*(9), 1478-1479.

Shpigelman, A., Kyomugasho, C., Christiaens, S., Van Loey, A. M., & Hendrickx, M. E. (2015). The effect of high pressure homogenization on pectin: Importance of pectin source and pH. *Food Hydrocolloids, 43*, 189-198.

Silanikove, N., Perevolotsky, A., & Provenza, F. D. (2001). Use of tannin-binding chemicals to assay for tannins and their negative postingestive effects in ruminants. *Animal Feed Science and Technology, 91*(1-2), 69-81.

Silva, A. F., Abreu, H., Silva, A. M., & Cardoso, S. M. (2019). Effect of oven-drying on the recovery of valuable compounds from Ulva rigida, *Gracilaria sp.* and Fucus vesiculosus. *Marine Drugs, 17*(2), 90.

Silvestri, S., & Gabrielson, G. (1991). Degradation of tragacanth by high shear and turbulent forces during microfluidization. *International Journal of Pharmaceutics, 73*(2), 163-169.

Sims, I. M., & Newman, R. H. (2006). Structural studies of acidic xylans exuded from leaves of the monocotyledonous plants *Phormium tenax* and *Phormium cookianum*. *Carbohydrate Polymers, 63*(3), 379-384.

Singh, R. P., & Heldman, D. R. (2001). *Introduction to food engineering*: Gulf Professional Publishing.

Sisodia, M. S., Rajak, D. K., Pathak, A. K., & Guria, C. (2015). An improved estimation of shear rate for yield stress fluids using rotating concentric cylinder Fann viscometer. *Journal of Petroleum Science and Engineering, 125*, 247-255.

Slaughter, S. L., Ellis, P. R., & Butterworth, P. J. (2001). An investigation of the action of porcine pancreatic α-amylase on native and gelatinised starches. *Biochimica et Biophysica Acta (BBA)-General Subjects, 1525*(1-2), 29-36.

Slaughter, S. L., Ellis, P. R., Jackson, E. C., & Butterworth, P. J. (2002). The effect of guar galactomannan and water availability during hydrothermal processing on the hydrolysis of starch catalysed by pancreatic α-amylase. *Biochimica et Biophysica Acta (BBA)-General Subjects, 1571*(1), 55-63.

Soliman, G. A. (2019). Dietary fiber, atherosclerosis, and cardiovascular disease. *Nutrients, 11*(5), 1155.

Song, Y., Shen, H., Liu, T., Pan, B., De Alwis, S., Zhang, W., . . . Ma, W. (2021). Effects of three different mannans on obesity and gut microbiota in high-fat diet-fed C57BL/6J mice. *Food & Function, 12*(10), 4606-4620.

Srinivasan, R., Karaoz, U., Volegova, M., MacKichan, J., Kato-Maeda, M., Miller, S., . . . Lynch, S. V. (2015). Use of 16S rRNA gene for identification of a broad range of clinically relevant bacterial pathogens. *PloS One, 10*(2), e0117617.

Stange, U., Scherf-Clavel, M., & Gieseler, H. (2013). Application of gas pycnometry for the density measurement of freeze-dried products. *Journal of Pharmaceutical Sciences, 102*(11), 4087-4099.

Stewart, M. L., & Slavin, J. L. (2006). Molecular weight of guar gum affects short-chain fatty acid profile in model intestinal fermentation. *Molecular Nutrition & Food Research, 50*(10), 971-976.

Stojanov, S., Berlec, A., & Štrukelj, B. (2020). The influence of probiotics on the firmicutes/bacteroidetes ratio in the treatment of obesity and inflammatory bowel disease. *Microorganisms, 8*(11), 1715.

Surampudi, P., Enkhmaa, B., Anuurad, E., & Berglund, L. (2016). Lipid lowering with soluble dietary fiber. *Current Atherosclerosis Reports, 18*(12), 1-13.

Szopinski, D., Handge, U. A., Kulicke, W.-M., Abetz, V., & Luinstra, G. A. (2016). Extensional flow behavior of aqueous guar gum derivative solutions by capillary breakup elongational rheometry (CaBER). *Carbohydrate Polymers, 136*, 834-840.

Tam, K. C., Jenkins, R. D., Winnik, M. A., & Bassett, D. R. (1998). A structural model of hydrophobically modified urethane−ethoxylate (HEUR) associative polymers in shear flows. *Macromolecules, 31*(13), 4149-4159.

Tamargo, A., Cueva, C., Álvarez, M. D., Herranz, B., Bartolomé, B., Moreno-Arribas, M. V., & Laguna, L. (2018). Influence of viscosity on the growth of human gut microbiota. *Food Hydrocolloids, 77*, 163-167.

Tan, H., Tam, K. C., & Jenkins, R. D. (2001). Network structure of a model HASE polymer in semidilute salt solutions. *Journal of Applied Polymer Science, 79*(8), 1486-1496.

Tedelind, S., Westberg, F., Kjerrulf, M., & Vidal, A. (2007). Anti-inflammatory properties of the short-chain fatty acids acetate and propionate: A study with relevance to inflammatory bowel disease. *World Journal of Gastroenterology: WJG, 13*(20), 2826.

Tekade, R. K. (2018). *Dosage Form Design Considerations: Volume I*: Academic Press.

Theuwissen, E., & Mensink, R. P. (2008). Water-soluble dietary fibers and cardiovascular disease. *Physiology & Behavior, 94*(2), 285-292.

Thongngam, M., & McClements, D. J. (2005). Isothermal titration calorimetry study of the interactions between chitosan and a bile salt (sodium taurocholate). *Food Hydrocolloids, 19*(5), 813-819.

Tian, J., Wang, X., Zhang, X., Chen, X., Dong, M., Rui, X., . . . Li, W. (2023). Artificial simulated saliva, gastric and intestinal digestion and fermentation *in vitro* by human gut microbiota of intrapolysaccharide from *Paecilomyces Cicadae Tjj1213*. *Food Science and Human Wellness, 12*(2), 622-633.

Tirtaatmadja, V., McKinley, G. H., & Cooper-White, J. J. (2006). Drop formation and breakup of low viscosity elastic fluids: Effects of molecular weight and concentration. *Physics of Fluids, 18*(4), 043101.

Tobin, A. B., Mihnea, M., Hildenbrand, M., Miljkovic, A., Garrido-Bañuelos, G., Xanthakis, E., & Lopez-Sanchez, P. (2020). Bolus rheology and ease of swallowing of particulated semi-solid foods as evaluated by an elderly panel. *Food & Function, 11*(10), 8648-8658.

Torres, M. D., Hallmark, B., & Wilson, D. I. (2014). Effect of concentration on shear and extensional rheology of guar gum solutions. *Food Hydrocolloids, 40*, 85-95.

Tosh, S. (2013). Review of human studies investigating the post-prandial blood-glucose lowering ability of oat and barley food products. *European Journal of Clinical Nutrition, 67*(4), 310-317.

Tripathy, P. P. (2018). Solar drying. In P. K. Nema, B. P. Kaur, & A. S. Mujumdar (Eds.), *Drying technology for foods: Fundamentals and applications* (pp. 297-312). Boca Raton: CRC Press, Taylor & Francis Group.

Ullah, H., Esposito, C., Piccinocchi, R., De Lellis, L. F., Santarcangelo, C., Minno, A. D., . . . Piccinocchi, G. (2022). Postprandial glycemic and insulinemic response by a brewer's spent grain extract-based food supplement in subjects with slightly impaired glucose tolerance: A monocentric, randomized, cross-over, double-blind, placebo-controlled clinical trial. *Nutrients, 14*(19), 3916.

Vadillo, D. C., Mathues, W., & Clasen, C. (2012). Microsecond relaxation processes in shear and extensional flows of weakly elastic polymer solutions. *Rheologica Acta, 51*(8), 755-769.

Vasilyev, G. B., Dreval, V. E., Malkin, A. Y., & Kulichikhin, V. G. (2010). Rheology of linear and branched styrene–acrylonitrile copolymers. Similarities and differences. *Polymer Science Series A, 52*(11), 1142-1155.

Vega, C., & Roos, Y. (2006). Invited review: Spray-dried dairy and dairy-like emulsions—compositional considerations. *Journal of Dairy Science, 89*(2), 383-401.

Verma, R. C., & Sharma, G. P. (2018). Freeze drying. In P. K. Nema, B. P. Kaur, & A. S. Mujumdar (Eds.), *Drying technology for foods: Fundamentals and applications* (pp. 57-70). Boca Raton: CRC Press, Taylor & Francis Group.

Villay, A., De Filippis, F. L., Picton, L., Le Cerf, D., Vial, C., & Michaud, P. (2012). Comparison of polysaccharide degradations by dynamic high-pressure homogenization. *Food Hydrocolloids, 27*(2), 278-286.

Vojdani, J. (1996). Solubility. In M. G. Hal (Ed.), *Methods of testing protein functionality* (pp. 11-60). London: Blackie Academic & Professional.

Vuksan, V., Jenkins, A., Dias, A., Lee, A., Jovanovski, E., Rogovik, A., & Hanna, A. (2010). Reduction in postprandial glucose excursion and prolongation of satiety: Possible explanation of the long-term effects of whole grain Salba (*Salvia Hispanica L.*). *European Journal of Clinical Nutrition, 64*(4), 436-438.

Wagner, M. H., Bastian, H., Hachmann, P., Meissner, J., Kurzbeck, S., Münstedt, H., & Langouche, F. (2000). The strain-hardening behaviour of linear and long-chain-branched polyolefin melts in extensional flows. *Rheologica Acta, 39*(2), 97-109.

Wagner, R., Simas, F. F., Pereira, G. C. Z., Angeli, A., Brito, J. O., Woranovicz-Barreira, S. M., . . . Gorin, P. A. J. (2007). Structure of a glycoglucuronomannan from the gum exudate of *Vochysia tucanorum* (family Vochysiaceae). *Carbohydrate Polymers, 69*(3), 512-521.

Wagner, R., Simas, F. F., Sassaki, G. L., Iacomini, M., da Silva, M. A., & Gorin, P. A. J. (2008). A high-viscosity glycoglucuronomannan from the gum exudate of *Vochysia thyrsoidea*: Comparison with those of other *Vochysia spp*. *Carbohydrate Polymers, 72*(3), 382-389.

Wagner, R., Woranovicz-Barreira, S. M., Iacomini, M., Delgobo, C. L., Pimentel, N. M., & Gorin, P. A. J. (2004). Structure of a glycoglucuronomannan from the low-viscosity gum of *Vochysia lehmannii*. *Carbohydrate Polymers, 57*(3), 269-275.

Walker, L. M. (2001). Rheology and structure of worm-like micelles. *Current Opinion in Colloid & Interface Science, 6*(5-6), 451-456.

Wang, D., Yeats, T. H., Uluisik, S., Rose, J. K., & Seymour, G. B. (2018). Fruit softening: Revisiting the role of pectin. *Trends in Plant Science, 23*(4), 302-310.

Wang, F., Zhang, Z., Wei, Y., Zhou, T., Wang, X., & Zhang, G. (2021). Rheology study of wormlike micellar solution formed by 1-hexadecyl-3-methylimidazolium tetrafluoroborate ionic liquids in present of sodium salicylate. *Journal of Dispersion Science and Technology, 42*(11), 1601-1609.

Wang, Q., & Cui, S. W. (2005). Understanding the physical properties of food polysaccharides. *Food Carbohydrates: Chemistry, Physical Properties, and Applications*, 162-214.

Wang, Q., Ellis, P. R., & Ross-Murphy, S. B. (2002). Dissolution kinetics of guar gum powders. I. Methods for commercial polydisperse samples. *Carbohydrate Polymers, 49*(2), 131-137.

Wang, Q., Liang, J., & Liu, H. (2019). *In vitro* effects of four polysaccharides containing β-D-Glup on intestinal function. *International Journal of Food Properties, 22*(1), 1064-1076.

Wang, Q., Wood, P. J., Cui, W., & Ross-Murphy, S. B. (2001). The effect of autoclaving on the dispersibility and stability of three neutral polysaccharides in dilute aqueous solutions. *Carbohydrate Polymers, 45*(4), 355-362.

Wang, S. Q. (1992). Transient network theory for shear-thickening fluids and physically crosslinked networks. *Macromolecules, 25*(25), 7003-7010.

Wang, Y., Guo, X., Zhang, L., & Zhao, Y. (2021). Effects of deproteinization on rheological properties of polysaccharides from Rosa acicularis 'Lu He'and Rosa acicularis Lindl fruits. *Journal of Food Measurement and Characterization, 15*(3), 2500-2515.

Wang, Y., Li, D., Wang, L.-J., & Xue, J. (2011). Effects of high pressure homogenization on rheological properties of flaxseed gum. *Carbohydrate Polymers, 83*(2), 489-494.

Wang, Z., Xie, J., Shen, M., Nie, S., & Xie, M. (2018). Sulfated modification of polysaccharides: Synthesis, characterization and bioactivities. *Trends in Food Science & Technology, 74*, 147-157.

Wang, Z. Q., Zuberi, A. R., Zhang, X. H., Macgowan, J., Qin, J., Ye, X., . . . Cefalu, W. T. (2007). Effects of dietary fibers on weight gain, carbohydrate metabolism, and gastric ghrelin gene expression in mice fed a high-fat diet. *Metabolism, 56*(12), 1635-1642.

Wangler, J., & Kohlus, R. (2017). Dynamics of capillary wetting of biopolymer powders. *Chemical Engineering & Technology, 40*(9), 1552-1560.

Wangler, J., & Kohlus, R. (2018). Development and validation of methods to characterize rehydration behavior of food hydrocolloids. *Food Hydrocolloids, 82*, 500-509.

Wangler, J., Teichmann, H., Konstanz, E., & Kohlus, R. (2019). Experimental investigation and simulation of rehydration dynamics of biopolymer powders. *Powder Technology, 355*, 461-473.

Ward, O. P., Moo-Young, M., & Venkat, K. (1989). Enzymatic degradation of cell wall and related plant polysaccharides. *Critical Reviews in Biotechnology, 8*(4), 237-274.

Warren, F. J., Zhang, B., Waltzer, G., Gidley, M. J., & Dhital, S. (2015). The interplay of α-amylase and amyloglucosidase activities on the digestion of starch in *in vitro* enzymic systems. *Carbohydrate Polymers, 117*, 192-200.

Warren, J., Offenberger, S., Toghiani, H., Pittman Jr, C. U., Lacy, T. E., & Kundu, S. (2015). Effect of temperature on the shear-thickening behavior of fumed silica suspensions. *ACS Applied Materials & Interfaces, 7*(33), 18650-18661.

Warren, R. E., & Frier, B. M. (2005). Hypoglycaemia and cognitive function. *Diabetes, Obesity and Metabolism, 7*(5), 493-503.

Washburn, E. W. (1921). The dynamics of capillary flow. *Physical Review, 17*(3), 273.

Watt, C., Sanchez-Rangel, E., & Hwang, J. J. (2020). Glycemic variability and CNS inflammation: Reviewing the connection. *Nutrients, 12*(12), 3906.

Wee, M. S. M., Matia-Merino, L., & Goh, K. K. T. (2015a). The cation-controlled and hydrogen bond-mediated shear-thickening behaviour of a tree-fern isolated polysaccharide. *Carbohydrate Polymers, 130*, 57-68.

Wee, M. S. M., Matia-Merino, L., & Goh, K. K. T. (2015b). Time and shear history-dependence of the rheological properties of a water-soluble extract from the fronds of the black tree fern, *Cyathea medullaris*. *Journal of Rheology, 59*(2), 365-376.

Wee, M. S. M., Lentle, R. G., Goh, K. K. T., & Matia-Merino, L. (2017). The first of the viscoceuticals? A shear thickening gum induces gastric satiety in rats. *Food & Function, 8*(1), 96-102.

Wee, M. S. M., Matia-Merino, L., Carnachan, S. M., Sims, I. M., & Goh, K. K. T. (2014). Structure of a shear-thickening polysaccharide extracted from the New Zealand black tree fern, *Cyathea medullaris*. *International Journal of Biological Macromolecules, 70*, 86-91.

Wei, M., Lin, K., & Sun, L. (2022). Shear thickening fluids and their applications. *Materials & Design*, 110570.

Wexler, H. M. (2007). Bacteroides: The good, the bad, and the nitty-gritty. *Clinical Microbiology Reviews, 20*(4), 593-621.

Wickham, H., Averick, M., Bryan, J., Chang, W., McGowan, L. D. A., François, R., . . . Hester, J. (2019). Welcome to the Tidyverse. *Journal of Open Source Software, 4*(43), 1686.

Williams, B. A., Grant, L. J., Gidley, M. J., & Mikkelsen, D. (2017). Gut fermentation of dietary fibres: Physico-chemistry of plant cell walls and implications for health. *International Journal of Molecular Sciences, 18*(10), 2203.

Williams, B. A., Mikkelsen, D., Flanagan, B. M., & Gidley, M. J. (2019). "Dietary fibre": Moving beyond the "soluble/insoluble" classification for monogastric nutrition, with an emphasis on humans and pigs. *Journal of Animal Science and Biotechnology, 10*(1), 1-12.

Witten Jr, T. A., & Cohen, M. H. (1985). Crosslinking in shear-thickening ionomers. *Macromolecules, 18*(10), 1915-1918.

Wojdyło, A., Figiel, A., Legua, P., Lech, K., Carbonell-Barrachina, Á. A., & Hernández, F. (2016). Chemical composition, antioxidant capacity, and sensory quality of dried jujube fruits as affected by cultivar and drying method. *Food Chemistry, 207*, 170-179.

Woo, M. W., & Bhandari, B. (2013). Spray drying for food powder production. In B. R. Bhandari, N. Bansal, M. Zhang, & P. Schuck (Eds.), *Handbook of food powders: Processes and properties* (pp. 29-56): Elsevier.

World Health Organisation. (2016). *WHO Global report on diabetes*. Geneva.

Wu, F., Guo, X., Zhang, J., Zhang, M., Ou, Z., & Peng, Y. (2017). *Phascolarctobacterium faecium* abundant colonization in human gastrointestinal tract. *Experimental and Therapeutic Medicine, 14*(4), 3122-3126.

Wunderlich, T., Stelter, M., Tripathy, T., Nayak, B., Brenn, G., Yarin, A., . . . Durst, F. (2000). Shear and extensional rheological investigations in solutions of grafted and ungrafted polysaccharides. *Journal of Applied Polymer Science, 77*(14), 3200-3209.

Xiao, X., Tan, C., Sun, X., Zhao, Y., Zhang, J., Zhu, Y., . . . Zhou, X. (2020). Effects of fermentation on structural characteristics and *in vitro* physiological activities of barley *β*-glucan. *Carbohydrate Polymers, 231*, 115685.

Xie, F., Zhang, H., Nie, C., Zhao, T., Xia, Y., & Ai, L. (2021). Structural characteristics of tamarind seed polysaccharides treated by high-pressure homogenization and their effects on physicochemical properties of corn starch. *Carbohydrate Polymers, 262*, 117661.

Xie, F., Zhang, W., Lan, X., Gong, S., Wu, J., & Wang, Z. (2018). Effects of high hydrostatic pressure and high pressure homogenization processing on characteristics of potato peel waste pectin. *Carbohydrate Polymers, 196*, 474-482.

Xin, Y., Zhang, M., & Adhikari, B. (2013). Effect of trehalose and ultrasound-assisted osmotic dehydration on the state of water and glass transition temperature of broccoli (*Brassica oleracea L. var. botrytis L.*). *Journal of Food Engineering, 119*(3), 640-647.

Xu, C., Li, Y., & Yu, H. (2014). Effect of far-infrared drying on the water state and glass transition temperature in carrots. *Journal of Food Engineering, 136*, 42-47.

Xu, D., Hawk, J. L., Loveless, D. M., Jeon, S. L., & Craig, S. L. (2010). Mechanism of shear thickening in reversibly cross-linked supramolecular polymer networks. *Macromolecules, 43*(7), 3556-3565.

Xu, Y., Niu, X., Liu, N., Gao, Y., Wang, L., Xu, G., . . . Yang, Y. (2018). Characterization, antioxidant and hypoglycemic activities of degraded polysaccharides from blackcurrant (*Ribes nigrum L.*) fruits. *Food Chemistry, 243*, 26-35.

Yekeler, M., Ulusoy, U., & Hiçyılmaz, C. (2004). Effect of particle shape and roughness of talc mineral ground by different mills on the wettability and floatability. *Powder Technology, 140*(1-2), 68-78.

Yesilata, B., Clasen, C., & McKinley, G. H. (2006). Nonlinear shear and extensional flow dynamics of wormlike surfactant solutions. *Journal of Non-Newtonian Fluid Mechanics, 133*(2-3), 73-90.

Yuan, B., Ritzoulis, C., & Chen, J. (2018a). Extensional and shear rheology of a food hydrocolloid. *Food Hydrocolloids, 74*, 296-306.

Yuan, B., Ritzoulis, C., & Chen, J. (2018b). Extensional and shear rheology of okra polysaccharides in the presence of artificial saliva. *NPJ Science of Food, 2*(1), 20.

Yuan, Y., Li, C., Zheng, Q., Wu, J., Zhu, K., Shen, X., & Cao, J. (2019). Effect of simulated gastrointestinal digestion *in vitro* on the antioxidant activity, molecular weight and microstructure of polysaccharides from a tropical sea cucumber (*Holothuria leucospilota*). *Food Hydrocolloids, 89*, 735-741.

Zaitoun, A., Makakou, P., Blin, N., Al-Maamari, R. S., Al-Hashmi, A., Abdel-Goad, M., & Al-Sharji, H. H. (2012). Shear stability of EOR polymers. *SPE Journal, 17*(02), 335-339.

Zangenberg, N. H., Müllertz, A., Kristensen, H. G., & Hovgaard, L. (2001). A dynamic *in vitro* lipolysis model: I. Controlling the rate of lipolysis by continuous addition of calcium. *European Journal of Pharmaceutical Sciences, 14*(2), 115-122.

Zeng, W., Wang, J., Shan, X., Yu, S., & Zhou, J. (2021). Efficient production of scleroglucan by *Sclerotium rolfsii* and insights into molecular weight modification by high-pressure homogenization. *Frontiers in Bioengineering and Biotechnology*, 799.

Zhang, L., Qiao, Y., Wang, C., Liao, L., Liu, L., Shi, D., . . . Xu, Q. (2019). Effects of freeze vacuum drying combined with hot air drying on the sensory quality, active components, moisture mobility, odors, and microstructure of kiwifruits. *Journal of Food Quality, 2019*

Zhang, N., Chen, H., Ma, L., & Zhang, Y. (2013). Physical modifications of polysaccharide from *Inonotus obliquus* and the antioxidant properties. *International Journal of Biological Macromolecules, 54*, 209-215.

Zhao, Y., Bi, J., Yi, J., Njoroge, D. M., Peng, J., & Hou, C. (2019). Comparison of dynamic water distribution and microstructure formation of shiitake mushrooms during hot air and far infrared radiation drying by low-field nuclear magnetic resonance and scanning electron microscopy. *Journal of the Science of Food and Agriculture, 99*(6), 2826-2834.

Zhou, W., Yan, Y., Mi, J., Zhang, H., Lu, L., Luo, Q., . . . Cao, Y. (2018). Simulated digestion and fermentation *in vitro* by human gut microbiota of polysaccharides from bee collected pollen of Chinese wolfberry. *Journal of Agricultural and Food Chemistry, 66*(4), 898-907.

Zhou, Z., Cao, X., & Zhou, J. Y. (2013). Effect of resistant starch structure on short-chain fatty acids production by human gut microbiota fermentation *in vitro*. *Starch-Stärke, 65*(5-6), 509-516.

Zhu, X., Zhang, X., Sun, Y., Su, D., Sun, Y., Hu, B., & Zeng, X. (2013). Purification and fermentation *in vitro* of sesaminol triglucoside from sesame cake by human intestinal microbiota. *Journal of Agricultural and Food Chemistry, 61*(8), 1868-1877.

Zhu, Z. Y., Luo, Y., Dong, G. L., Ren, Y.-Y., Chen, L. J., Guo, M. Z., . . . Zhang, Y. (2016). Effects of the ultra-high pressure on structure and α-glucosidase inhibition of polysaccharide from Astragalus. *International Journal of Biological Macromolecules, 87*, 570-576.

Zimmermann, U., Zhu, J., Meinzer, F., Goldstein, G., Schneider, H., Zimmermann, G., . . . Webb, D. (1994). High molecular weight organic compounds in the xylem sap of mangroves: Implications for long-distance water transport. *Botanica Acta, 107*(4), 218-229.

Appendices

Appendix A: Protocol for harvesting mamaku fronds

Appendix B: Supplementary information for Chapter 4

Appendix C: Human ethics approval and related documentation for Chapter 5

Appendix D: Supplementary information for Chapter 5

Appendix E: Supplementary information for Chapter 6

Appendix F: Supplementary information for Chapter 7

Appendix G: Food safety related documentation for Chapter 8

Appendix H: Human ethics approval and related documentation for Chapter 8

Appendix I: Appetite sensations form used for human trail

Appendix J: Animal ethics approval for Chapter 8

Appendix K: Colonic fermentation of mamaku pith powder using a rat model

Appendix L: Copyright permissions to reprint figures and tables

Appendix M: Statement of contribution

Appendix N: Embargo approval

Appendix A: Protocol for harvesting mamaku fronds

The key elements of harvesting are:

1. Explain who you are and why you want to take the material.
2. Ask for the material, knowing that you are cutting from the fern an arm not a frond.
3. Thank the mamaku for the sacrifice.
4. Place the spare/waste material back around the truck.
5. Acknowledge the tree as you leave – kia ora Matua for your gift – don't just walk away.
6. And any waste material after processing must be returned to the Whenua (it should go back to the tree)
    a. If this can't be done then place it with respect back on the Whenua in a native planting somewhere near to home.
    b. This is CRITICAL to the kaupapa – it completes the circle.

Appendix B: Supplementary information for Chapter 4

Table B.1: Surface tension (σ) for crude mamaku gum samples from stage 1, stage 2 and stage 3 of harvesting age at 1, 3 and 5% (w/w) total solids concentration.

Concentration	Surface tension, σ (mN/m)		
	Stage 1	Stage 2	Stage 3
1%	66	70	70
3%	58	64	70
5%	55	61	65.5

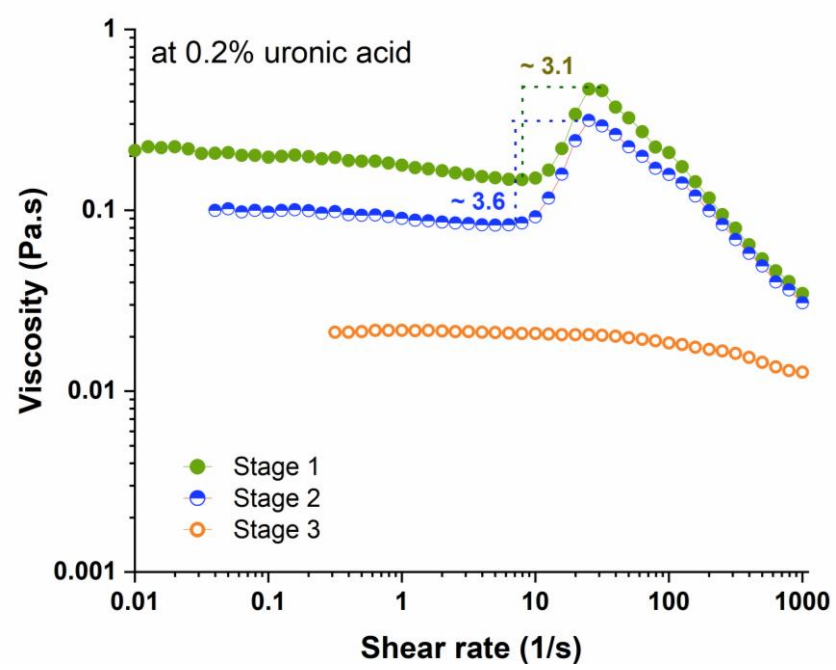


Figure B.1: Comparison of viscosity for crude mamaku gum extracted from different harvesting ages at 0.2% (w/w) uronic acid concentration, marked with η_{max}/η_{crit} ratios. η_{max}/η_{crit} is the extent of shear-thickening defined as the ratio of maximum viscosity, η_{max}, to viscosity at the onset of shear-thickening, η_{crit}.

Appendix C: Human ethics approval and related documentation for Chapter 5

C.1: Human ethics approval for collecting faecal samples for *in vitro* fermentation

MASSEY UNIVERSITY
TE KUNENGA KI PŪREHUROA
UNIVERSITY OF NEW ZEALAND

Date: 20 January 2021

Dear Akshay Bisht

Re: Ethics Notification - **SOA 20/51 - In vitro fermentation of Mamaku (Cyathia medullaris, tree fern).**

Thank you for the above application that was considered by the Massey University Human Ethics Committee: **Human Ethics Southern A Committee** at their meeting held on **Wednesday, 20 January,**

Approval is for three years. If this project has not been completed within three years from the date of this letter, reapproval must be requested.

If the nature, content, location, procedures or personnel of your approved application change, please advise the Secretary of the Committee.

Yours sincerely



Professor Craig Johnson
Chair, Human Ethics Chairs' Committee and Director (Research Ethics)

Research Ethics Office, Research and Enterprise
Massey University, Private Bag 11 222, Palmerston North, 4442, New Zealand **T** 06 350 5573; 06 350 5575 **F** 06 355 7973
E humanethics@massey.ac.nz **W** http://humanethics.massey.ac.nz

C.2: Māori consultation for *in vitro* fermentation study



To whom so ever it may concern

Dated; September 25th 2020

I advise that I have consulted with researchers Dr. Lara Matia-Merino and the PhD candidate Akshay Bisht regards possible cultural issues regarding the in-vitro trial designed as part of the study titled "**In vitro fermentation of Mamaku (*Cyathia medullaris*, tree fern)**". I see no cultural issues regarding the sampling and the disposal of the feces, however as this involves human waste, any engagement of Maori on the programme will need to ensure:

1. They have full disclosure of the purpose and use of the feces.
2. It is not used for any other purpose other than for this research.
3. It is disposed of according to their requirement as this can open them up to risk within the wairua space.
4. They are fully advised of the outcomes.

If you have any query, feel free to contact me.

Nga mihi.

Garry Watson

Chairman

Nga Uri o te Ngahere Trust.

C.3: Participant information sheet and consent form for collecting faecal samples for *in vitro* fermentation study

Participant Information Sheet

Study title: ***In vitro* fermentation of mamaku (*Cyathia medullaris*, tree fern)**

Locality: **Massey University, Palmerston North** Ethics committee ref.:

Lead investigator: **Akshay Bisht** Email: **A.bisht@massey.ac.nz**

Researcher introduction

My name is Akshay Bisht, and I am a PhD student at Massey University, School of Food and Advanced Technology. My supervisors are Dr. Lara Matia-Merino, A/Prof. Kelvin Goh and Dr. John Monro.

Invitation to participate in this research study

You are invited to take part in a study on *in vitro* fermentation of mamaku (*Cyathia medullaris*, tree fern). Whether or not you take part is your choice. If you don't want to take part, you don't have to give a reason, and it won't affect the care you receive. If you do want to take part now, but change your mind later, you can pull out of the study at any time.

This Participant Information Sheet will help you decide if you'd like to take part. It sets out why we are doing the study, what your participation would involve, what the benefits and risks to you might be, and what would happen after the study ends. We will go through this information with you and answer any questions you may have. You do not have to decide today whether or not you will participate in this study. Before you decide you may want to talk about the study with other people, such as family, whānau, friends, or healthcare providers. Feel free to do this.

If you agree to take part in this study, you will be asked to sign the Consent Form. You will be given a copy of both the Participant Information Sheet and the Consent Form to keep.

This document is 5 pages long. Please make sure you have read and understood all the pages.

What is the purpose of the study?

The New Zealand black tree fern (***Cyathea medullaris***), commonly known as mamaku in Maori and locally also called körau, katätä and pïtau, is one of the world's tallest tree fern grown across New Zealand.

Traditionally, the pith (*Medullaris* means "pithy") from the upper part of the trunk and fronds was consumed as a food source as fresh or boiled like vegetables. Mamaku was also widely used for its therapeutic benefits to treat gastric conditions and as dressings for a variety of skin conditions such as wounds and boils. The brownish-red exudate oozing from a trunk, upon solidification was chewed as a remedy for diarrhoea and could also be laxative. However, scientific literature supporting the possible health effects is limited.

The extrudate from mamaku is a non-starch polysaccharide made of the glucuronic acid backbone. Due to the lack of enzymes to digest the mamaku polysaccharide in the human gut, most of the polysaccharide will reach the colon. In the colon, mamaku may act as a substrate for the complex microbiome and result in a prebiotic effect. Prebiotic refers to a non-digestible dietary substance that can induce the growth or activity of beneficial microorganisms in the human gut. Thus, this study aims at testing the *in vitro* fermentability of mamaku in the presence of the microbiome from human faeces. In this study, your faeces sample will be collected and will be used to conduct a fermentation study in the laboratory. After fermentation, the production of short-chain fatty acids (SCFA) and the effect on the production of gut microbiota will be analyzed.

What will my participation in the study involve?

You have been chosen to participate in the study because you have met the criteria to be included in the study. The criteria include:

- Maori ethicality
- 18-40 years of age
- Generally healthy and not suffering from colon diseases
- Have not taken any antibiotics in the last 3 months
- Non-smoker
- Able to communicate in English

For this study, you (the participant) are required to collect your faeces sample (once) and provide it to the researcher at the School of Food and Advanced Technology, Massey University, Palmerstone North. You will be provided with a kit containing a scoop to collect your faeces sample, a sterile wide-mouth collection vial and a pair of gloves. An anaerobic bag, anaerobic sachet, a freezer pack and a polystyrene box will also be provided to store and transport the container containing faeces. A brown paper bag will be provided to dispose of your rubbish. You will be asked to wash hands before beginning the procedure; not to pass the faeces into the toilet and then collect; not to urinate or mix water with the faeces sample.

FAECES COLLECTION PROCEDURE:

1. Use disposable gloves while collecting the faeces sample.

2. Catch the faeces sample using the scoop provided before it reaches the toilet water (be careful not to contaminate the sample with any urine).

3. Using the scoop on the sterile container transfer some of the faeces samples to the sterile container provided (try to fill the container to at least a third full).

4. Ensure the lid on the sterile container is secure, then tightly seal the sterile container in the anaerobic bag provided with the white anaerobic sachet bag inside (remove the tinfoil outer packaging to reveal the white anaerobic sachet bag).

5. The anaerobic bag can then be put into the polystyrene box before putting it into the freezer. The faeces sample is triply contained and can be handled safely.

6. Put the contained faeces sample into the freezer, as well as the freezer pack (if it has not been put into the freezer already) so it is frozen when you transport the sample.

7. Excess faeces can be disposed of down the toilet and any used items can be put into the brown paper bag provided.

8. The brown paper bag can then be disposed of in the rubbish.

9. When transporting the faeces sample to the Massey University, for your study visit, put the frozen freezer pack into the polystyrene box with the contained faeces sample to ensure it stays frozen.

10. Deliver your box containing the sample to a member of the research team. Do not leave the sample at reception.

WHAT HAPPENS AFTER RECEPTION OF YOUR FAECES SAMPLE?

Upon reception of the faeces sample, it will be randomly coded using a 3-digit number and stored in a freezer. The sample will be processed for the *in vitro* fermentation study within two weeks of reception. At the end of the study, the residual faeces sample will be autoclaved and discarded in general lab waste, thereby no residual faeces sample will be retained after study.

If you wish to collect residual part of your sample, you must indicate that on the consent form and you will be asked to collect your residual samples on the 3rd week from reception of the sample from the researcher at the School of Food and Advanced Technology, Massey University, Palmerstone North.

What are the possible benefits and risks of this study?

Mamaku is a native plant to New Zealand and traditionally, it has been consumed by Maori people for its therapeutic effects. However, there is no scientific literature available on the same. This is the first study that will try to investigate the possibility of mamaku as a prebiotic under *in vitro* conditions. It can be satisfying to know that you are contributing to expanding the knowledge about Maori treasure, mamaku.

Further, unravelling the prebiotic effect of mamaku will strengthen the development of mamaku based products for health-conscious consumers, which in return will help in the marketing of

mamaku as a highly functional natural New Zealand food product with a strong whakapapa Māori, to support the development of a Mātauranga Māori-based Māori economy.

In addition, you can learn a lot about the processes that are involved in research by actively participating in it and get reimbursed for involvement in the study.

There is no cost to you, the participant, for taking part in this study. In recognition of your time and participation in this study, you will be reimbursed $25 after delivering your faeces samples.

It is highly unlikely that you will be injured during this study. However, one may feel uncomfortable in collecting and transporting their faeces samples and if you identify yourself as one, you are suggested not to take part in this study. If you were injured in this study, you would be eligible **to apply** for compensation from ACC just as you would be if you were injured in an accident at work or at home. This does not mean that your claim will automatically be accepted. You will have to lodge a claim with ACC, which may take some time to assess. If you have private health or life insurance, you may wish to check with your insurer that taking part in this study won't affect your cover.

What are my rights?

Participating in this study is completely voluntary and you are free to decline to participate, or to withdraw from the research at any time before providing your faeces samples, without experiencing any disadvantage. If you pull out of the study all the data that was related to you will be shredded.

You are welcome to discuss any concerns you have with the research team at any time, and you have free access to your data.

It is important to us that we maintain your privacy throughout this study. Your name and contact information will be held electronically and stored on the Principal Investigators computer only for data recording purposes. Your name will never be used in any report, correspondence or publication. Your involvement in this study is confidential.

The study data will be stored at a secure location at Massey University Palmerston North campus. Electronic data and records will be the responsibility of the Principal investigator. All data will be kept for 5 years, at which point it will be destroyed using University Security methods for removal of confidential material.

Who do I contact for more information or if I have concerns?

If you have any questions, concerns or complaints about the study at any stage, you can contact the following researchers involved in the study:

Dr. Lara Matia-Merino, Senior Lecturer, School of Food and Advanced Technology, Massey University.
Phone: +64-69516016
Email: L.Matia-Merino@massey.ac.nz

A/ Prof. Kelvin Goh, Program Director, SIT-Massey Food Technology, Singapore
Phone: +64-6 356 9099 ext. 86911
Email: K.T.Goh@massey.ac.nz

Akshay Bisht, PhD Student, School of Food and Advanced Technology, Massey University.
Phone: +64 276087945
Email: A.bisht@massey.ac.nz

If you want to talk to someone who isn't involved with the study, you can contact an independent health and disability advocate on:
Phone: 0800 555 050
Fax: 0800 2 SUPPORT (0800 2787 7678)
Email: advocacy@advocacy.org.nz
Website: https://www.advocacy.org.nz/

For Maori support please contact :
A/Prof. Nick Roskruge, Horticulture, School of Agriculture and Environment, Massey University.
Phone: 0272066850
Email: N.rosktuge@massey.ac.nz

This project has been reviewed and approved by the Massey University Human Ethics Committee: Southern A, Application 20/51. If you have any concerns about the conduct of this research, please contact Dr Negar Partow, Chair, Massey University Human Ethics Committee: Southern A, telephone 04 801 5799 x 63363, email humanethicsoutha@massey.ac.nz

Mamaku: A Māori Treasure

Mamaku is a native plant to New Zealand and traditionally, it has been consumed by the Māori people for its therapeutic effects; however, the scientific literature is limited. This is the first study that will investigate the possibility of mamaku as a prebiotic under *in vitro* conditions and expand the knowledge about Maori treasure, Mamaku.



You are needed, if you identify yourself as…

- A Māori
- Between 18-40 years age.
- Generally healthy and not suffering from colon diseases.
- Have not taken any antibiotics in last 3 months.
- Non-smoker
- Able to communicate in English.

Provide your faeces sample and get reimbursement of $25 for your time !

If you want to participate, feel free to contact:

Akshay Bisht
a.bisht@massey.ac.nz
0276087945

Mamaku: A Māori Treasure
Akshay Bisht
a.bisht@massey.ac.nz
0276087945

Consent Form

MASSEY UNIVERSITY

Please tick to indicate you consent to the following:

I have read and I understand the Participant Information Sheet.		
I have been given sufficient time to consider whether or not to participate in this study.		
I have had the opportunity to use a legal representative, whanau/ family support or a friend to help me ask questions and understand the study.		
I am satisfied with the answers I have been given regarding the study and I have a copy of this consent form and information sheet.		
I understand that taking part in this study is voluntary (my choice) and that I may withdraw from the study before delivering my faeces samples.		
I understand that my participation in this study is confidential and that no material, which could identify me personally, will be used in any reports on this study.		
I know who to contact if I have any questions about the study in general.		
I understand my responsibilities as a study participant.		
I wish to receive a summary of the results from the study.	Yes ☐	No ☐
I wish to collect the unused fraction of my faeces sample after the study.	Yes ☐	No ☐

Declaration by participant:

I hereby consent to take part in this study.

Participant's name:

Signature:	Date:

Declaration by member of research team:

I have given a verbal explanation of the research project to the participant, and have answered the participant's questions about it.

I believe that the participant understands the study and has given informed consent to participate.

Researcher's name:

Signature:	Date:

Appendix D: Supplementary information for Chapter 5

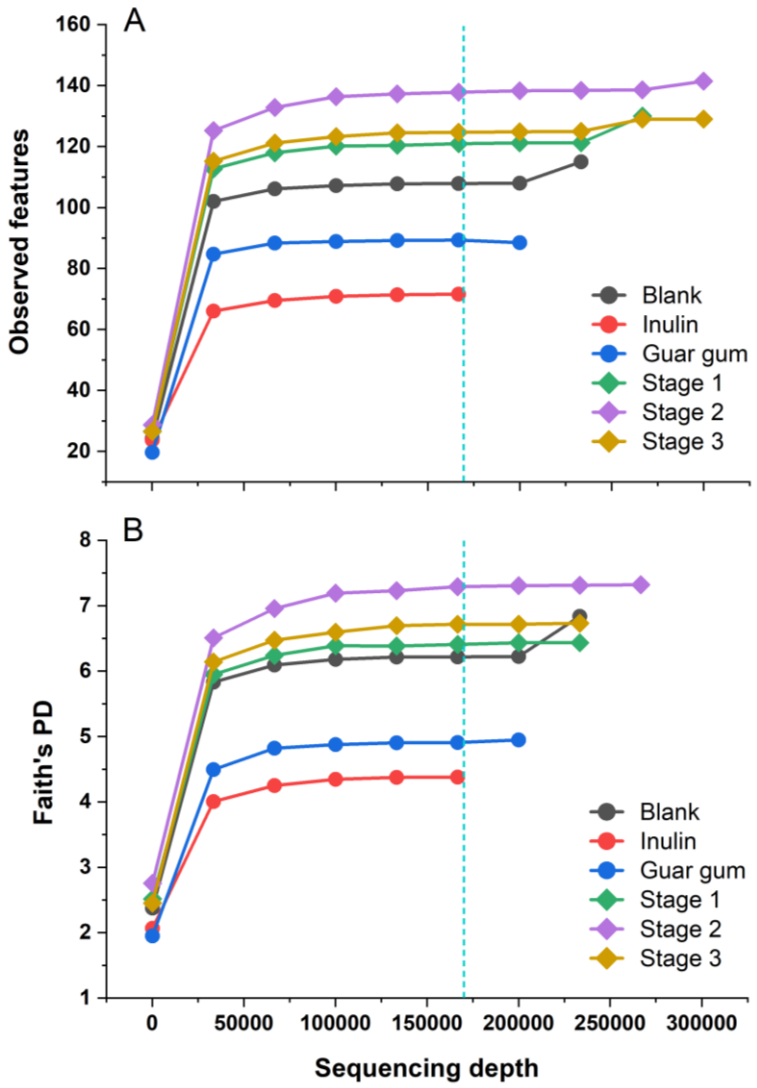


Figure D.1: Alpha rarefaction curve using (**A**) observed features and (**B**) Faith's phylogenetic diversity (PD). Dash line represents a sequencing depth of 172,862. Stage 1, 2 and 3 refers to the harvesting age of the mamaku fronds.

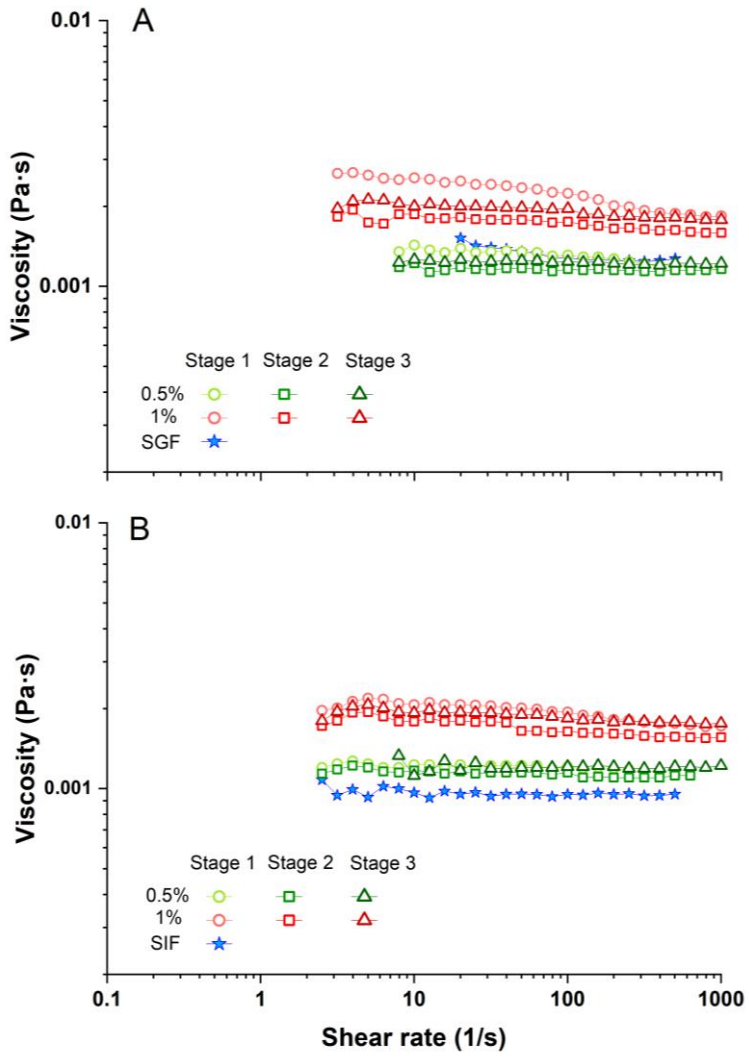


Figure D.2: Viscosity profiles of mamaku gum (0.5% and 1% w/w) in (**A**) simulated gastric fluid (SGF) and (**B**) simulated intestinal fluid (SIF) as a function of shear rate. Measurements were taken using double gap geometry at 20°C.

Appendix E: Supplementary information for Chapter 6

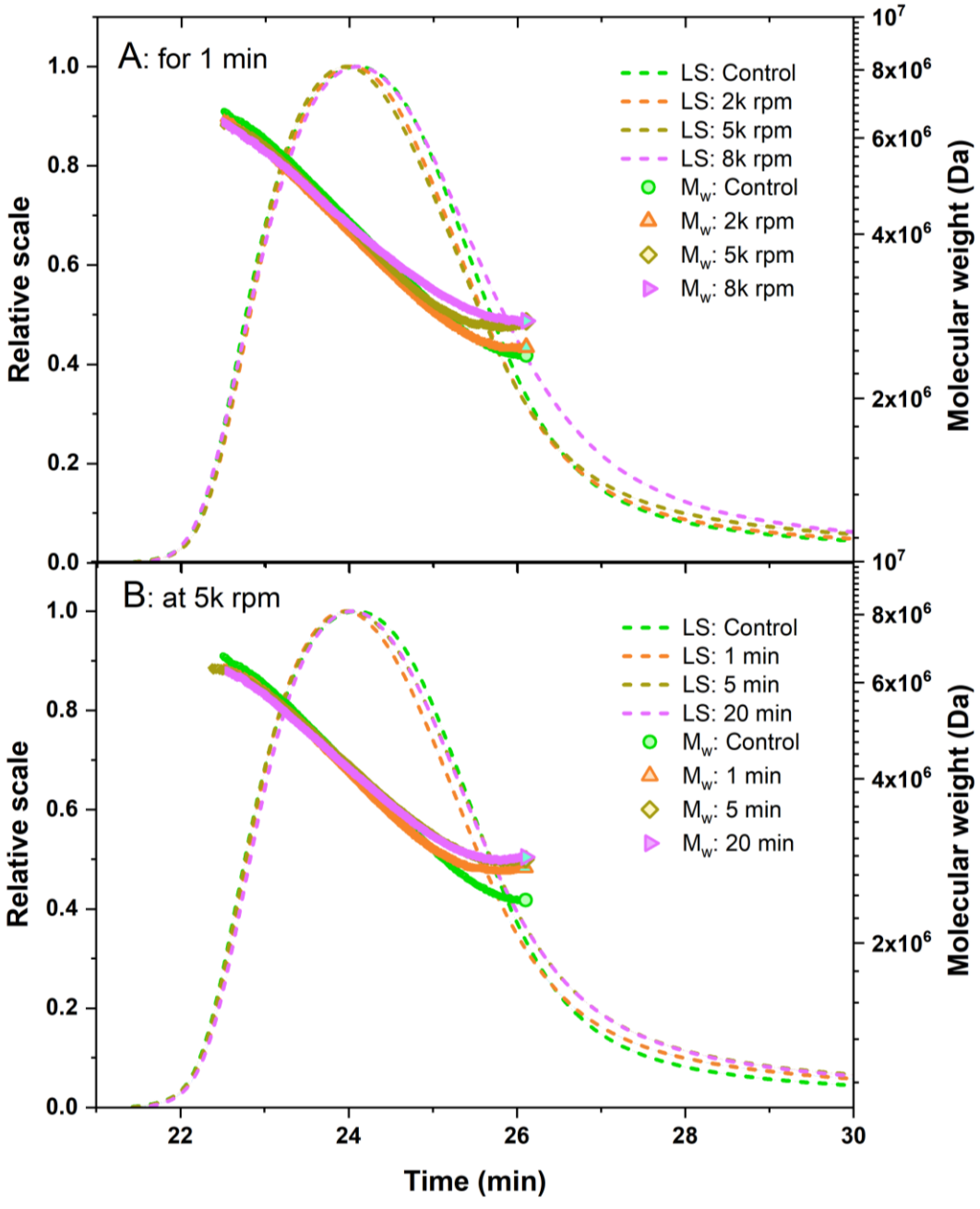


Figure E.1: Light scattering (LS) signal and weighted-average molecular weight (M_w) analysis by size-exclusion chromatography coupled with multi-angle laser light scattering (SEC-MALLS) of purified mamaku gum after shear treatment at (**A**) 2k, 5k and 8k rpm for 1 min and (**B**) 5k rpm for 1, 5 and 20 min.

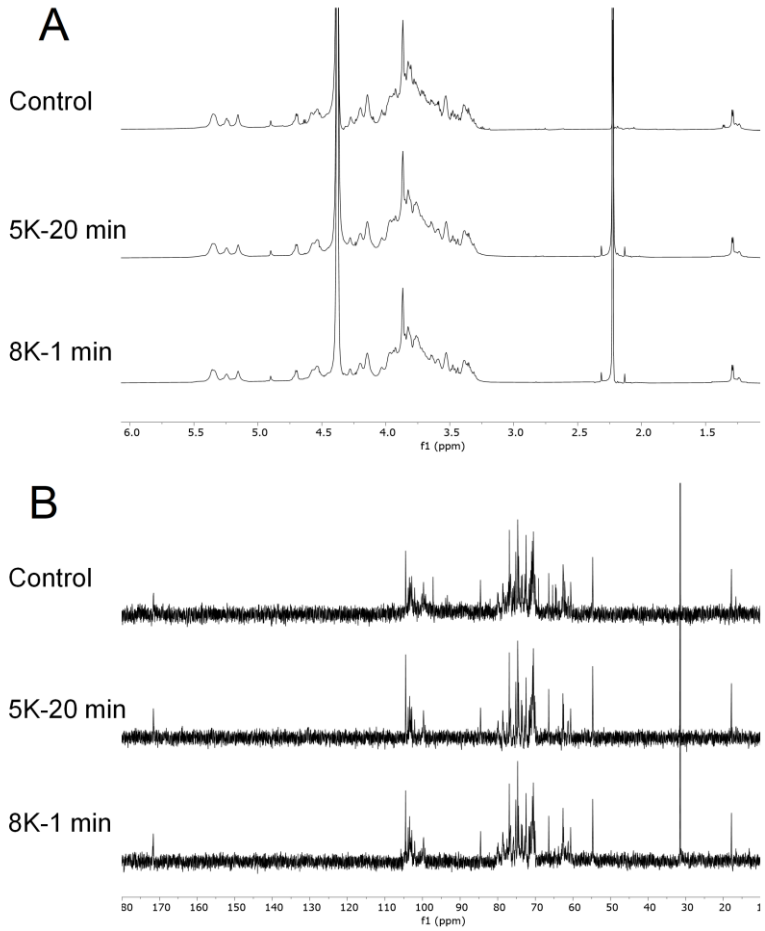


Figure E.2: (**A**) ^{1}H and (**B**) ^{13}C NMR spectra of purified mamaku gum after shear treatment.

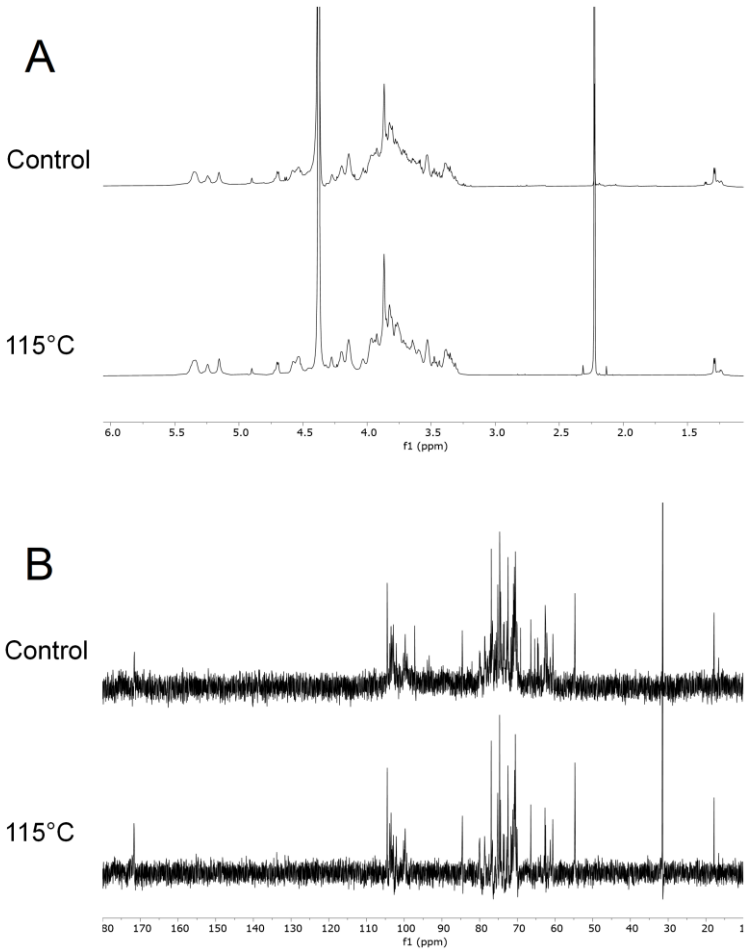


Figure E.3: (**A**) ^{1}H and (**B**) ^{13}C NMR spectra of purified mamaku gum after temperature treatment.

Table E.1: Molecular parameters of shear-treated purified mamaku gum by size-exclusion chromatography coupled with multi-angle laser light scattering (SEC-MALLS) *.

	Weighted-average molecular weight, M_w x 10^6 (Da)	Radius of gyration, R_g (nm)	Slope from the plot of M_w against R_g	Polydispersity, M_w/M_n
Control	3.95±0.05[a]	155.8±0.14[a]	0.62±0.00[a]	1.1±0.00[a]
5k-20 min	3.97±0.03[a]	151.25±1.08[b]	0.61±0.01[a]	1.07±0.01[a]
8k-1min	3.99±0.03[a]	151.4±0.37[b]	0.61±0.01[a]	1.08±0.01[a]

*Samples were purified first and then shear-treated followed by SEC-MALLS.
Values are expressed as means ± standard deviation (n=3). Values in the same column denoted with the different superscript letters are significantly different ($p \leq 0.05$).

Appendix F: Supplementary information for Chapter 7

Table F.1: Proximate and mineral composition of freeze-dried (FDP) and oven-dried (ODP) mamaku pith powders.

	FDP	ODP
Composition (% w/w)		
Moisture	5.1	5.8
Ash	8.3	8.0
Crude protein	2.0	2.1
Fat	0.9	0.6
Starch	3.1	1.9
Sugar	39.5	35.9
Fructose	18.5	16.9
Glucose	20.4	18.8
Galactose	0.3	0.3
Sucrose	0.2	<0.1
Total dietary fibres	36.2	39.8
Insoluble dietary fibres	23.0	27.0
Soluble dietary fibres	13.2	12.8
Uronic acid	4.2	4.2
Minerals (mg/kg)		
Potassium	34000	29000
Sodium	4500	6200
Calcium	2900	3500
Magnesium	610	690
Aluminium	620	700
Zinc	16.6	19.7
Manganese	3.5	4.2
Iron	13	14
Copper	2.7	2.4
Selenium	<0.02	<0.02
Lead	0.073	0.085
Mercury	<0.01	<0.01

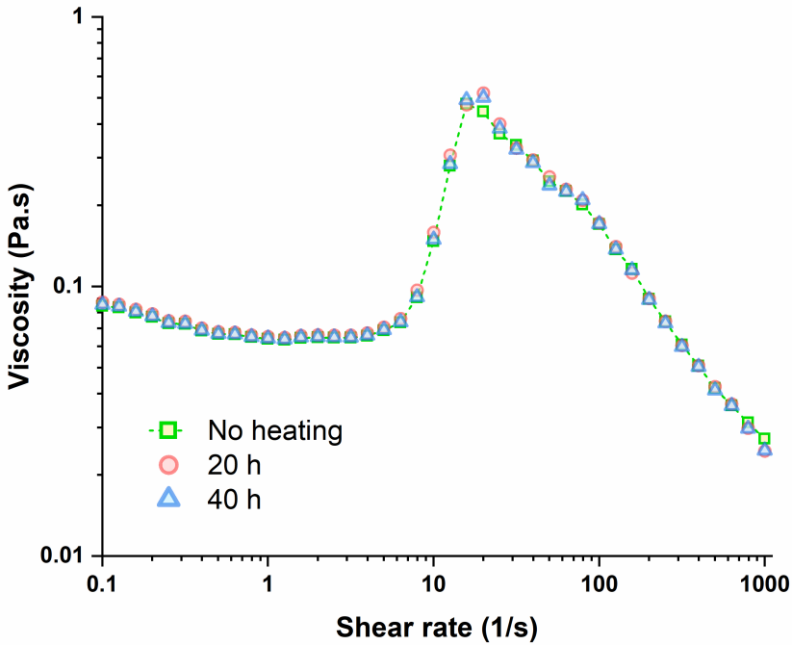


Figure F.1: Viscosity profiles of mamaku gum extract (2% w/w total solid) heated to 50°C for 20 h and 40 h. Measurements were taken using cup-and-bob geometry at 20°C.

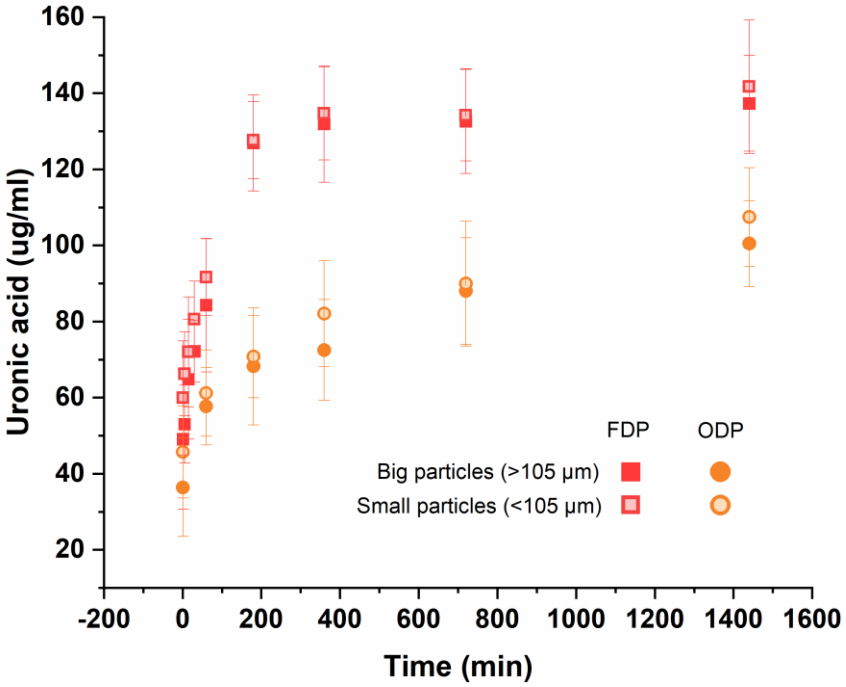


Figure F.2: Amount of uronic acid in the continuous phase of freeze-dried (FDP) and oven-dried (ODP) mamaku pith powder suspension (1% w/w) as a function of hydration time. Powder suspensions were centrifuged (13,000 *g* for 30 min) at different rehydration times, and the supernatant was collected to quantify uronic acid. Big particles size: FDP, 181 µm; ODP,171 µm; Small particles size: FDP, 48 µm; ODP, 97 µm.

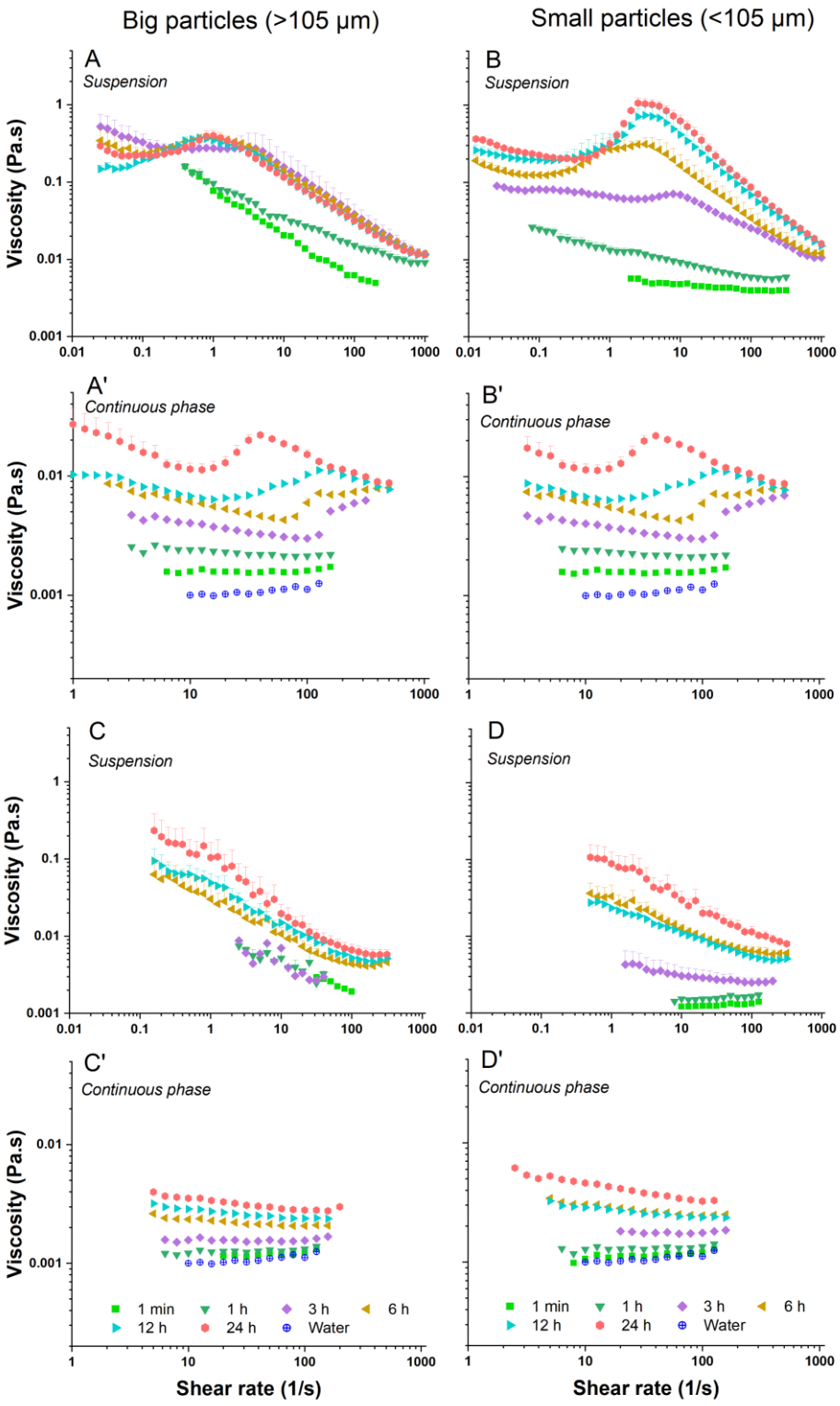


Figure F.3: Time-dependent viscosity profiles of (**A**, **B**) freeze-dried (FDP) and (**C**, **D**) oven-dried (ODP) mamaku pith powder suspension (1% w/w). Powder suspensions were centrifuged (13,000 *g* for 30 min) at different rehydration times, and the supernatant (*i.e.,* continuous phase) was collected to analyse viscosity profiles (**A′**, **B′**: FDP; **C′**, **D′**: ODP). Values are plotted as means ± standard deviation (n=3). Rheological measurements were taken using cup-and-bob (for suspension) or double gap geometry (for continuous phase) at 20°C. Big particles size: FDP, 181 µm; ODP,171 µm; Small particles size: FDP, 48 µm; ODP, 97 µm.

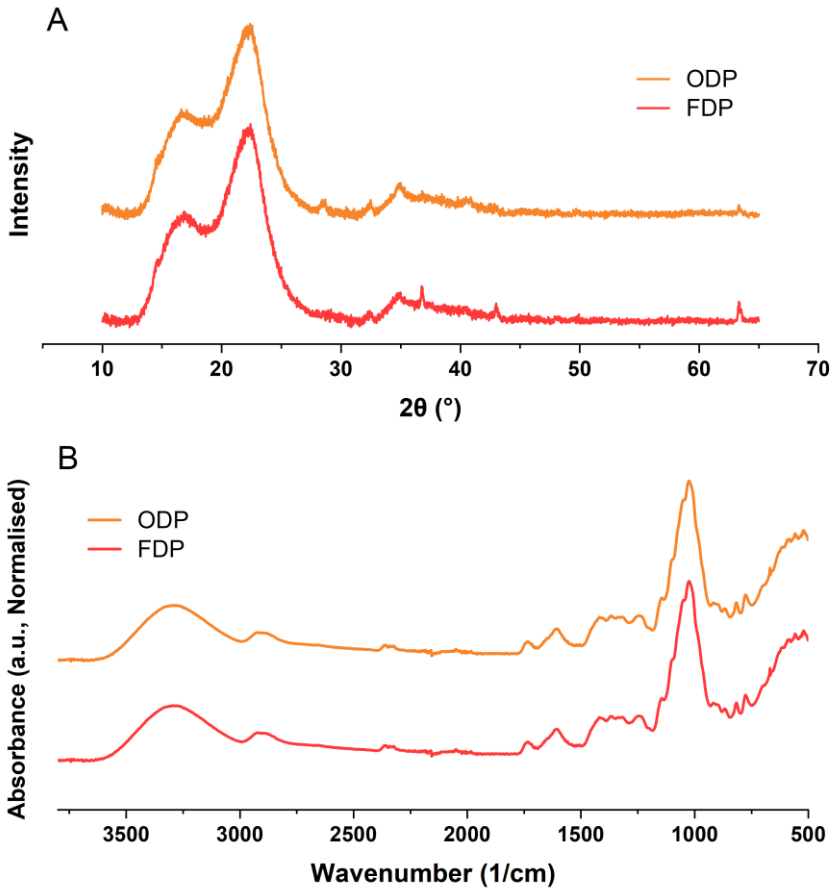


Figure F.4: (**A**) X-ray diffraction (XRD) and (**B**) Fourier transform infrared (FTIR) plots for freeze-dried (FDP) and oven-dried (ODP) mamaku pith powder. XRD (MiniFlex600-C, Rigaku Corporation, Tokyo, Japan) and FTIR (Thermo-Fisher Scientific, Waltham, Massachusetts, USA) analysis of powders were performed as described by Bisht, Goyal, Sachdev, and Pasricha (2019) and Salleh et al. (2022), respectively.

Appendix G: Food safety related documentation for Chapter 8

G.1: FoodPilot manager approval for human consumption of mamaku pith powder

The FoodPilot

R041 – Project Check

Version No: 004
Issue Date: 15/09/2021
Page 1 of 3

Authorised By: R. Naser

Check that the following information/tasks been completed, obtained, provided and /or attached (when possible).

Tick the box √ or if not applicable (NA)

6/05/2022

Name of Project Leader	Dr Lara Matia-Merino, Akshay Bisht
Training requirements /Competencies	√
Client (if applicable) and any specific requirements	NA
Trial records	√
Normal/critical process conditions/parameters	√
formulations of all batches processed, preferably in table format	√
Process flow diagram/chart outlining the process, including all equipment or plant used, all temperatures, holding times, homogenising pressures or other variables employed in the process	√
E-Dec (when applicable)	NA
CIP log sheet, cleaning and sanitation records	√
UHT/pasteuriser (or any alternative log sheet) if applicable	NA
COA for inwards goods, ingredients	NA
Temperature Records for inwards goods	NA
Records (thawing, tempering, heating, cooking etc)	√
Risk Assessment form (R036)	√
Food Safety step record, eg; heat treatments (time/temp), acidification (final pH), preservative level etc	√
Lab test results (eg; product, environment, water, etc)	√
Batch production Record (R018)	√
Product released documents	NA
Labels	√
Calibration or any other maintenance records	√
Validation reports / copies (eg; cleaning, process, shelf life, etc)	√
Verification or internal audit reports	NA

This document is the property of The FoodPilot. Once printed this document is uncontrolled version.

The FoodPilot

R041 – Project Check

Version No: 004
Issue Date: 15/09/2021
Page 2 of 3

Authorised By: R. Naser

Use this template to create a record of the project upon completion:

Manufactured date: 9th April 2022	**Time:** 10 am- 5pm
Current storage location	Fridge (4°C), PD lab, Riddet complex, Massey University
Booking Request number	1051
Intended use / purpose	Consumption - general population
List of ingredients used (as per the booking request otherwise the barcodes)	Mamaku, Maltodextrin, Blackcurrant flavour
Product movements within FoodPilot (indicate storage areas, length of time, quantities etc)	Stored in PD lab until 20th May 22- 1 bag
For export purposes only: • **Raised EDec (if applicable)** • **Raised export certificate:**	Not applicable
Product description	Freeze dried Mamaku fern pith powder flavoured with maltodextrin and blackcurrant.
Product Quantity	400g
Best before date	20th Dec 2022

This document is the property of The FoodPilot. Once printed this document is uncontrolled version.

The FoodPilot

R041 – Project Check

Version No: 004
Issue Date: 15/09/2021
Page 3 of 3

Authorised By: R. Naser

Analytical product tests (attach any results to this document)	Microbial analysis attached. (Aerobic PC, E. coli, Salmonella, staphylococcus, Clostridium, Bacillus, Coliforms and Listeria)
Product release criteria	• **Released Fit for human consumption** • **Released Not fit for consumption** • **Released fit for animal consumption** • **Disposed** • **ON HOLD for investigation** • **Failed (RA notified) if applicable**
How many batches Product ID (batch numbers) if applicable?	Single batch (Batch no.: 20220409-1051)

Product release food safety tests and criteria met			**Source document**
Tests undertaken	**Complies yes /No**	**Date -reference**	
Aerobic PC	yes	28 April 2022	Food standards Australia and New Zealand- Compendium of Microbiological Criteria for Food- March 2022
Bacillus cereus	yes	28 April 2022	
Total coliform	yes	28 April 2022	
E. coli	yes	28 April 2022	
Staph. Aureus	yes	28 April 2022	
Listeria monocytogenes	yes	28 April 2022	
Salmonella spp.	yes	28 April 2022	Job No # J22-98
Clostridium sp.	yes	28 April 2022	

Operator (delegates) signature	Bishay Bisht
FoodPilot Manager Signature	Rane 6/05/2022

This document is the property of The FoodPilot. Once printed this document is uncontrolled version.

MASSEY UNIVERSITY
COLLEGE OF SCIENCES
TE WĀHANGA PŪTAIAO

School of Food & Advanced Technology
Microbiology Laboratory
COLLEGE OF SCIENCES
Manager: Ann-Marie Jackson
T: +64 **6 951 7115**
Email: A.M.Jackson@massey.ac.nz

TO:	Garry Radford	AT:	Massey FoodPilot
SUBJECT:	Final Report **AMENDED** (combined 2 reports into 1)	REPORT DATE:	4/5/2022
MICRO JOB #:	J22-79	DATE/TIME Received at Lab:	28/3/2022 3:30pm
Sample Type:	pre-processing swabs for freeze-dryer project	DATE/TIME Processed:	28/3/2022 3:35pm
Lab Testing by:	Kylie Evans	Results Counted/Read by:	Kylie Evans

No	Sample Name	Solid / Liquid	Single / Composite	Aerobic PC cfu/swab	Anaerobic PC cfu/mL or g	*Bacillus cereus* cfu/mL or g	*Bifido-bacteria* cfu/mL or g	Coliforms		Enterobact-eriaceae cfu/swab
								Total cfu/swab	*E. coli* MPN/10mL or g	
1	Level 4 – freeze dryer internal surfaces: Environmental swab									< 1
2	Level 3 – floor of Extruder room: Environmental swab									< 1
3	Level 3 – drain #22 in Extruder room: Environmental swab									< 1
4	Freeze dryer internal surface: Hygiene swab			1				< 1		
5	Door glass internal surface: Hygiene swab			< 1				< 1		

No	Sample Name	Solid / Liquid	Single / Composite	*Listeria monocytogenes* Presence/Absence	*Salmonella spp.* Presence/Absence	*Staph. aureus* cfu/mL or g	Thermophiles cfu/mL or g	Yeasts & Moulds cfu/mL or g	Other
1	Level 4 – freeze dryer: Environmental swab			Not detected	Not detected				
2	Level 3 – floor of Extruder room: Environmental swab			Not detected	Not detected				
3	Level 3 – drain #22 in Extruder room: Environmental swab			Not detected	Not detected				
4	Freeze dryer internal surface: Hygiene swab								
5	Door glass internal surface: Hygiene swab								

MASSEY UNIVERSITY
COLLEGE OF SCIENCES
TE WĀHANGA PŪTAIAO

School of Food & Advanced Technology
Microbiology Laboratory
COLLEGE OF SCIENCES
Manager: Ann-Marie Jackson
T: +64 **6 951 7115**
Email: A.M.Jackson@massey.ac.nz

TO:	Akshay Bishit	AT:	Massey SF&AT
SUBJECT:	Final Report	REPORT DATE:	06/04/2022
MICRO JOB #:	J22-86	DATE/TIME Received at Lab:	31/03/2022 3.15pm
Sample Type:	Pre-processing swabs	DATE/TIME Processed:	31/03/2022 3.30pm
Lab Testing by:	Kylie Evans	Results Counted/Read by:	Kylie Evans

No	Sample Name Pre-processing swabs	Solid / Liquid	Single / Composite	Aerobic PC cfu/swab	Anaerobic PC cfu/mL or g	*Bacillus cereus* cfu/mL or g	*Bifido-bacteria* cfu/mL or g	Coliforms		Enterobact-eriaceae cfu/mL or g
								Total Cfu/swab	*E. coli* MPN/10mL or g	
1	Sieve			8				< 1		
2	Inside of box			2.3×10^2				< 1		
3	filter			3				< 1		
4	Hopper (pin mill)			16				< 1		
5	Outlet (pin mill)			<1				< 1		
6	Grinding area (pin mill)			17				< 1		

References / Methodology:

General Microbiological Testing: Compendium of Methods for the Microbiological Examination of Foods. 5th Edition. American Public Health Assoc. (APHA) 2015.

Aerobic Plate Count (APC): Standard Plate Count Agar for 48 hrs @ 30°C
Aerobic Plate Count (APC) for cosmetics: Bacteriological Analytical Manual, 8th Edition, Revision A, 1998. Chapter 23
Aerobic Plate Count on Petrifilm™: 3M™ Quickswab™ onto 3M AC Petrifilm™ for 48 hrs @ 30°C (milk/dairy products) or 35°C (other samples)
Anaerobic Plate Count (AnPC): Standard Plate Count Agar for 48 hrs @ 30°C under anaerobic conditions
Bacillus cereus: Mannitol Egg Yolk Polymixine (MYP) Agar 24hrs @ 30°C, +ve control NCTC 11143 (NZRM 3429)
Clostridium spp.: Tryptose Sulfite Cycloserine (TSC) Agar (w/o egg yolk) with overlay for 18-24hrs @ 35° under anaerobic conditions
Coliforms (Total): MPN method; Lauryl Sulphate broth with MUG (LST-MUG) 24-48hrs @ 35°C
Enterobacteriaceae: Violet Red Bile Glucose agar (VRBGA) 18-24 hrs @ 35°C. +ve control ATCC 25922
Enterobacteriaceae on Petrifilm™: 3M™ Quickswab™ onto 3M EB Petrifilm™ for 24 hrs @ 35°C
Escherichia coli: As for Total Coliforms, plus Eosine-Methylene Blue agar (EMB) 24hrs @ 35°C, and Kovac's Indole test for confirmation. +ve control ATCC 25922 (NZRM 916)

MASSEY UNIVERSITY
COLLEGE OF SCIENCES
TE WĀHANGA PŪTAIAO

School of Food & Advanced Technology
Microbiology Laboratory
COLLEGE OF SCIENCES
Manager: Ann-Marie Jackson
T: +64 **6 951 7115**
Email: A.M.Jackson@massey.ac.nz

TO:	Akshay Bisht	AT:	Massey SF&AT
SUBJECT:	Final Report **AMENDED**	REPORT DATE:	28/4/2022
MICRO JOB #:	J22-98	DATE/TIME Received at Lab:	14/4/2022 2:00pm
Sample Type:	powders	DATE/TIME Processed:	20/4/2022 10:00am
Lab Testing by:	Ann-Marie Jackson	Results Counted/Read by:	Ann-Marie Jackson

No	Sample Name	Solid / Liquid	Single / Composite	Aerobic PC cfu/g	Anaerobic PC cfu/mL or g	*Bacillus cereus* cfu/g	*Bifido-bacteria* cfu/mL or g	Coliforms		Enterobact-eriaceae cfu/mL or g
								Total MPN/g	*E. coli* MPN/g	
3	Mamaku 1 (10g used)	S		5		< 100		< 3	< 3	
4	Mamaku 2 (10g used)	S		5		< 100		< 3	< 3	

No	Sample Name	Solid / Liquid	Single / Composite	*Listeria monocytogenes*	*Salmonella spp.*	*Staph. aureus*	Thermo-philes cfu/mL or g	Yeasts & Moulds cfu/mL or g	*Clostridium spp.*
3	Mamaku 1 (10g used)	S		Not detected / 10g	Not detected / 10g	< 100			< 100
4	Mamaku 2 (10g used)	S		Not detected / 10g	Not detected / 10g	< 100			< 100

References / Methodology:

General Microbiological Testing: Compendium of Methods for the Microbiological Examination of Foods. 5th Edition. American Public Health Assoc. (APHA) 2015.

Aerobic Plate Count (APC): Standard Plate Count Agar for 48 hrs @ 30°C
Aerobic Plate Count (APC) for cosmetics: Bacteriological Analytical Manual, 8th Edition, Revision A, 1998. Chapter 23
Aerobic Plate Count on Petrifilm™: 3M™ Quickswab™ onto 3M AC Petrifilm™ for 48 hrs @ 30°C (milk/dairy products) or 35°C (other samples)
Anaerobic Plate Count (AnPC): Standard Plate Count Agar for 48 hrs @ 30°C under anaerobic conditions
Bacillus cereus: Mannitol Egg Yolk Polymixine (MYP) Agar 24hrs @ 30°C, +ve control NCTC 11143 (NZRM 3429)
Clostridium spp.: Tryptose Sulfite Cycloserine (TSC) Agar (w/o egg yolk) with overlay for 18-24hrs @ 35° under anaerobic conditions
Coliforms (Total): MPN method; Lauryl Sulphate broth with MUG (LST-MUG) 24-48hrs @ 35°C
Enterobacteriaceae: Violet Red Bile Glucose agar (VRBGA) 18-24 hrs @ 35°C. +ve control ATCC 25922
Enterobacteriaceae on Petrifilm™: 3M™ Quickswab™ onto 3M EB Petrifilm™ for 24 hrs @ 35°C

References / Methodology:

General Microbiological Testing: Compendium of Methods for the Microbiological Examination of Foods. 5th Edition. American Public Health Assoc. (APHA) 2015.

Aerobic Plate Count (APC): Standard Plate Count Agar for 48 hrs @ 30°C
Aerobic Plate Count (APC) for cosmetics: Bacteriological Analytical Manual, 8th Edition, Revision A, 1998. Chapter 23
Aerobic Plate Count on Petrifilm™: 3M™ Quickswab™ onto 3M AC Petrifilm™ for 48 hrs @ 30°C (milk/dairy products) or 35°C (other samples)
Anaerobic Plate Count (AnPC): Standard Plate Count Agar for 48 hrs @ 30°C under anaerobic conditions
Bacillus cereus: Mannitol Egg Yolk Polymixine (MYP) Agar 24hrs @ 30°C, +ve control NCTC 11143 (NZRM 3429)
Clostridium spp.: Tryptose Sulfite Cycloserine (TSC) Agar (w/o egg yolk) with overlay for 18-24hrs @ 35° under anaerobic conditions
Coliforms (Total): MPN method; Lauryl Sulphate broth with MUG (LST-MUG) 24-48hrs @ 35°C
Enterobacteriaceae: Violet Red Bile Glucose agar (VRBGA) 18-24 hrs @ 35°C. +ve control ATCC 25922
Enterobacteriaceae on Petrifilm™: 3M™ Quickswab™ onto 3M EB Petrifilm™ for 24 hrs @ 35°C
Escherichia coli: As for Total Coliforms, plus Eosine-Methylene Blue agar (EMB) 24hrs @ 35°C, and Kovac's Indole test for confirmation. +ve control ATCC 25922 (NZRM 916)
***E.coli*/Coliform Count on Petrifilm™**: 3M™ Quickswab™ onto 3M EC Petrifilm™ for 24 hrs @ 35°C (for Coliforms) then a further 24 hrs @ 35°C (48 hr total for *E.coli*) +ve control ATCC 25922 (NZRM 916)
Lactic Acid bacteria: Acidified MRS agar to pH 5.5; anaerobically incubated 72hrs @ 35°C: APHA - Method 19.522
Lactic Acid bacteria: (eg. *Bifidobacteria*) Standard Methods for the Examination of Dairy Products, 17th Edition, 2004
Listeria monocytogenes: Enriched in LEB, then Secondary incubation Fraser broth 24hrs @ 35°C, onto Oxford Agar 24hrs @ 35°C. +ve control NZRM 4230
Listeria monocytogenes count: Direct plating on Oxford medium for 48hrs@37°C colony confirmation by PCR +ve control NZRM 4230.
Mesophilic spore count: sample held @ 80°C for 10 mins, then plated as per APC
Psychrophiles: Standard Plate Count Agar for 7 days @ 7°C
pH: APHA 68.2
Salmonella spp.: Enriched in 2% P/W, then Secondary incubation on Rappaport-Vassiliadis (RVS) broth 24hrs @ 42°C, onto Brilliant Green agar (BGA) and Xylose-Lysine-Deoxycholate (XLD) agar 18-20hrs @ 37°C. +ve control NZRM 4030.
Staphylococcus aureus: Baird-Parker 48hrs @ 37°C, +ve control ATCC 25923 (NZRM 917)
Sterility Test: 7 days storage @ 30°C then conduct APC test; and @ 55°C then conduct Thermophiles test. Also look for swelling of bottles & test pH.
Thermophiles: Standard Plate Count Agar with overlay for 48hrs @ 55°C
Yeasts & Moulds (Y&M): Dichloran Rose Bengal Chloramphenicol (DRBC) 5 days @ 22 - 25°C; plates incubated upright

Signatures:

Ann-Marie Jackson
Lab Manager

Baizura Zain
Laboratory Technician

Kylie Evans
Laboratory Technician

Please note, although the University has taken all due care in preparing this information in a proper manner, it shall not be liable for any loss or damage incurred by the use of this opinion by persons or organisations. This report may not be reproduced except in full.

Samples will be discarded <u>one month</u> from date of this report unless otherwise requested by client.

G.2: Biosafety Advisory, and Health and Safety Committee application at Plant and Food Research

Food Safety Risk Assessment

For studies involving food that will be consumed or tasted by human participants.

This form must be completed for any research where human participants (including PFR employees) will taste or consume food. If multiple different product types/origins are to be used, complete separate forms for each product. Submit the completed forms online. The Biosafety team and Food Safety Co-ordinator will then receive notification of your application. Any queries please contact Sravani.Gupta@plantandfood.co.nz or Maree.Debenham@plantandfood.co.nz.

Food is defined as any substance tasted or consumed by a human. This can include but is not limited to: whole, parts or extracts of fruit, vegetables, plant, animal or seafood, food grade chemicals and ingredients. These foods can be purchased commercially or grown, extracted and processed by PFR or contractors.

Project and Facility Information

Project details

Project title	**Mamaku effects on blood glucose responses**
Project Number	
Principal Investigator	John Monro
Project team members	Akshay Bisht, Lara Matia-Merino, Hannah Dinnan, Suman Mishra, Sheridan, Sue Middlemiss-Kraak, John Monro
Who will be consuming the food? Have sensitive populations been screened out e.g., those younger than 5 years, older than 70 years, immune-compromised, pregnant or lactating). If these demographics are required for the test then an assessment of specific risks is required.	Healthy participants between 18- 65 years.
Who will be preparing the food?	Akshay Bisht
Who will be serving the food?	Sue Middlemiss-Kraak
Describe where the food will be	Preparation: The FoodPilot (operates under Risk Management

prepared, processed, stored and served.	Programme (RMP)), Massey University Stored: Plant and Food (in food-safe freezer) Served: Human Clinical Facility
Describe what you plan to do with any surplus food or raw ingredients.	Any surplus mamaku pith will be returned to Papatuanuku or retained for future use if necessary.
List the staff preparing and serving the food who have completed food safety training and describe their qualification? e.g., NZQA 167/168, advanced food safety qualifications, induction to the food safe facility.	Akshay Bisht, PhD student (Preparing food): Trained and inducted to operate in the Food Pilot Plant, at Massey university, by the pilot plant manager. Sue Middlemiss-Kraak (serving food). Food Safety training and induction: provided by the Food Development Lab Staff, with yearly updates as required on equipment and any safety concerns.
Who are the nearest first aiders and where is the Epi-pen and trained administrator located.	Nearest first aiders – Hannah Dinnan, Sheridan Martell, Dominic Lomiwes, Nayer Ngametua, Greg Sawyers. Epi-pen is stored in the cupboard in the waiting room (Clinical Facility)

Control of Physical, Microbial and Chemical Contaminants

Personal hygiene

Outline the protocols and provision for use of clean protective clothing such as footwear/dedicated food processing lab coats/overalls/ hair nets/gloves.	During food production: Overalls, gumboots, hair net, beard net will be worn at all times – available in changing area in the Food Pilot. Gloves will be changed regularly between tasks.
Describe how staff are following the protocols around ensuring hands and fingernails are clean. How do staff undertake sanitising procedures, such as washing after handling chemicals, soil, raw materials, and using the toilet? Is there a separate hand cleaning sink available?	Hands will be washed with warm water and dried thoroughly in a separate hand cleaning sink available at the entry of the pilot plant (at the beginning of work or re-entering after using toilet), and then sanitised using sanitiser. Hands will be washed similarly in the hand cleaning sink available in the pilot plant, after handling raw material. Fingernails will be maintained short, with no use of nail polish or fake nails.
When handling foods, describe the protocol that ensures staff remove jewellery, nail varnish and strong perfumes.	Jewellery will not be worn. Strong perfumes will be advised against. Fingernails will be maintained short with no use of nail polish or fake nails.
How are staff informed and how do they address the requirement to cover skin wounds, and not to work whilst sick.	Informed during induction to the Food Pilot Plant. All cuts and wounds will be covered with a

	wound strip or bandage (blue coloured and specially designed for food handlers) available from first aid kit. Disposable gloves will be worn over the top of the wound strip. The disposable gloves will be changed regularly between tasks. If vomiting/diarrhoea is experienced by anyone they must not return to the Food Pilot Plant for 72h after symptoms have passed. If anyone starts feeling unwell while in the plant, they should leave immediately.

Cleanliness of food safe work areas and equipment

Describe the procedure for cleaning all areas associated with food preparation, storage and participant tasting.	Workstations in the food preparation area must be cleaned and sanitised before and after work with sanitising solution.
Describe the procedure for sanitising equipment, serving vessels, utensils and food contact surfaces.	Freeze drier and pin mill will be thoroughly hand washed with hot water-detergent mix. All removable parts will be washed multiple times in dishwasher. Visual inspection will be carried out for evidence of any contamination. ATP measurements and microbial analyses (total count and total coliform) will be performed on different parts of equipment. Utensils will be washed multiple times in dishwasher. Autoclave will be first heat-sterilised and then samples will be loaded for mild heating.
Outline the rubbish disposal protocol.	All rubbish will be placed in plastic rubbish bins available in the food pilot facility.
Outline the pest control protocol for vermin and insects.	Pest control is managed by The Food Pilot Plant team under Risk Management Programme (RMP).

Food safe storage areas

How is prevention of contamination during storage mitigated? How are raw materials segregated from processed foods?	Soon after production, the food will be weighed and packed in aluminium bags in serving sizes, sealed and labelled. The packed food will be double contained in another plastic bag and stored in separate fridge.
Are cleaning products and other chemicals stored separately from food?	Yes
How is temperature monitoring undertaken?	Temperature monitoring is done with appropriate

How are chilled foods managed so they have limited time in the temperature danger zone (refer to USFDA 4/2 rule).	equipment in the FDL. Thermometers for cooking plus thermometers for freezers and fridges if required.
Describe how the shelf-life of stored material is monitored?	The product was previously tested for its microbial safety throughout the recommended shelf-life. Also, the product is a low water activity powder, which helps in keeping the product safe for longer.
Describe the labelling protocol of stored food items?	Each individual unit produced in the Food Pilot Plant is labelled with the Food pilot label, approved by the Manager. The label contains: Product description Contact person Best Before Batch number And a caution statement: 'The facility in which this product was manufactured also processes nuts, gluten, and other allergens'

Processed Foods

Processed Food: Food not in its natural state e.g. cooked apples, novel food products, bread, beverages. A processed food may have other substances added to it or undergo physical, chemical or biological changes.

What will participants be tasting / consuming?	Freeze-dried powdered mamaku pith (5 g) combined with small quantities of black currant flavouring (50 mg) and maltodextrin (100 mg) per treatment. The pith was extracted from surface-sterilised frond stem (stipe) sections by removing the external rind with a sharp knife under clean conditions, before freeze-drying and milling the pith to a powder.
What are all the ingredients in the food? Attach a formulation table listing all the ingredients, concentrations and suppliers.	Attached
Where is the food from?	The mamaku was harvested from mamaku trees growing in the Kahuterawa valley, near Palmerston North, with permission of the local council and local iwi authority.
Are all ingredients in the final food product to be tasted obtained from a commercial source?	No, mamaku powder will be prepared in the Food Pilot Plant.
Do the specification sheets or Certificate of Analyses for all ingredients contain any	Participants will be informed through the participant information sheet and in the case of WeetBix also

labelling declarations? (e.g. allergens, GM status, maximum concentrations allowed). How are participants informed of potential allergens in the food e.g. sulphites, gluten, shellfish, eggs, fish, milk, peanuts, soybeans, sesame seeds, tree nuts or lupin.	through the ingredient list and nutrient information panel on the WeetBix packaging.
Explain how the food will be processed or prepared. Specify what will be done with any surplus food or ingredients. Attach a processing flow diagram.	Attached The final product will be prepared by mixing mamaku powder, flavour and maltodextrin, then packaged and heat treated. The surplus ingredients will be stored at Massey University for later use.

Checklist of required attachments:

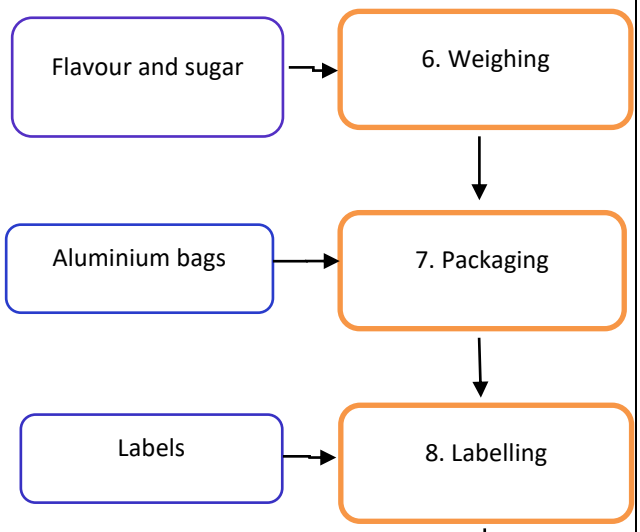
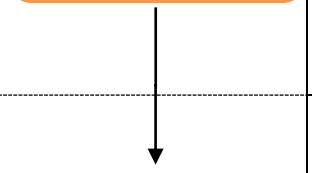
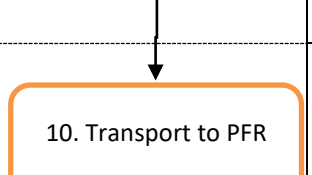
- A Supplier Product Specification sheet and Certificate of Analysis (COA) if available for each ingredient.
- Product formulation table listing all the ingredients, concentrations and suppliers.
- A flow diagram for processing conditions for ingredients and for the final food, including the steps to ensure food safety.
- If taking human samples for analysis please provide procedures around how these are handled i.e., Blood-collection procedure, storage if required, and disposal of samples.
- Participant information form including COVID contingency plan and if required, how participant's samples will be handled.
- Participant consent form.

List of ingredients

Ingredient	Amount	Supplier
Mamaku powder	5 g	Made in the Food Pilot, Massey University
Blackcurrant flavour	100 mg	Sensient Technologies New Zealand
Maltodextrin	50 mg	

Process flow diagram

Input	Process step	Food safety consideration
Raw material: Fresh mamaku fronds	1. Surface cleaning (during harvesting)	1) Fresh mamaku fronds will be surface cleaned with hydrogen peroxide (~ 2% w/w) to eliminate/ reduce the surface contaminants like microbes, dirt and insects. 2) The fresh fronds will be peeled to remove the external rind and the obtained pith. This will further reduce the possible surface contaminants like microbes, soil, dirt and insects. 3) Workstations will be cleaned and sanitised before and after work. 4) Personal hygienic practices will be followed in the Food Pilot.
	2. Peeling, and chopping (in the food pilot)	
	3. Transferring mamaku pith into plastic bags to be placed in freeze dryer.	1) The freeze drier will be thoroughly cleaned with the hot water-detergent mix. 2) ATP measurements will be performed after cleaning. 3) Trays to hold bags will be washed in a dishwasher. 4) Moisture content of about 5% (and water activity of about 0.25) will be achieved after drying, which stops microbial growth. 5) Workstations will be cleaned and sanitised before and after work. 6) Personal hygienic practices must be followed in the Food Pilot.
	4. Freeze drying	
	5. Grinding (Pin mill)	1) The pin mill will be thoroughly hand washed with the hot water-detergent mix, and all removable parts will be washed multiple times in the dishwasher. 2) Visual inspection for the absence of any contamination. 3) ATP measurements and microbial analysis (total count and total coliform) will be performed on different parts of the equipment. 4) Personal hygienic practices will be followed in the Food Pilot.

	1) Utensils will be washed multiple times in the dishwasher. 2) Workstation will be cleaned and sanitised before and after work. 3) Personal hygienic practices will be followed in the Food Pilot.
	1) The autoclave will be first heat sterilised and then samples will be loaded for mild heating. 2) Final product will be tested for Salmonella, Staphylococcus, Clostridium, Bacillus, Coliforms and Listeria and the total count, and only if within limits, will be transported.
	1) Final product will be transported in a clean and sterilised container.
	1) Storage space will be cleaned and sanitised.

Appendix H: Human ethics approval and related documentation for Chapter 8

H.1: Human ethics approval for testing the effect of mamaku pith powder on blood glucose, insulin and appetite responses

Health and Disability Ethics Committees

Health and Disability Ethics Committees
Ministry of Health
133 Molesworth Street
PO Box 5013
Wellington
6011
hdecs@health.govt.nz

Ethics reference: 2022 EXP 12634

17 May 2022

Dr John Monro

Private Bag 11600,
Palmerston North
4410
New Zealand

Tēnā koe Dr Monro

APPROVAL OF APPLICATION

Study title: Mamaku effects on postprandial glycaemic response to carbohydrate

I am pleased to advise that your application was **approved** by the Central Health and Disability Ethics Committee (the Committee) with non-standard conditions. This decision was made through the EXP pathway.

Conditions of HDEC approval

HDEC approval for this study is subject to the following conditions being met prior to the commencement of the study in New Zealand. It is your responsibility, and that of the study's sponsor, to ensure that these conditions are met. No further review by the Central Health and Disability Ethics Committee is required.

Standard conditions:

- Before the study commences at *any* locality in New Zealand, all relevant regulatory approvals must be obtained.
- Before the study commences at *any* locality in New Zealand, it must be registered in a clinical trials registry. This should be a registry approved by the World Health Organization (such as the Australia New Zealand Clinical Trials Registry, www.anzctr.org.au or https://clinicaltrials.gov/).
- Before the study commences at *each given* locality in New Zealand, it must be authorised by that locality in Ethics RM. Locality authorisation confirms that the locality is suitable for the safe and effective conduct of the study, and that local research governance issues have been addressed.

Non-standard conditions:

- Please remove the separate heading of "what will happen to my blood samples" as this is now covered elsewhere.
- Please add the full cultural statement instead of "We appreciate that blood is taonga and that donation of blood should be done in consultation with whanau, iwi and hapu".

"Cultural considerations: You may hold beliefs about sacred and shared values about your tissue samples and/or data originating from this tissue. The cultural issues associated with sending your tissue samples and data overseas and/or storing your tissue and data should be discussed with your family/whanau as appropriate. If you need cultural support this can be provided. Please let us know and we will arrange this for you, or you can ring the number at the bottom of this Participant Information Sheet and Consent Form. We respect the importance of these values and beliefs so please inform us if you wish to have whanau support present."

- Please also add the paragraph about not doing a karakia over the samples during sectruction here.
- Please put back the paragraph about: "what if something goes wrong" and remove the two paragraphs about ACC and physical harm on page 5 under "risks".

Non-standard conditions must be completed before commencing your study, however, they do not need to be submitted to or reviewed by HDECs.

If you would like an acknowledgement of completion of your non-standard conditions you may submit a post approval form amendment through the Ethics Review Manager. Please clearly identify in the amendment form that the changes relate to non-standard conditions and ensure that supporting documents (if requested) are tracked/highlighted with changes.

For information on non-standard conditions please see paragraphs 125 and 126 of the *Standard Operating Procedures for Health and Disability Ethics Committees (SOPs)*.

After HDEC review

Please refer to the *SOPs* for HDEC requirements relating to amendments and other post-approval processes.

Your next progress report is due by 17 May 2023.

Participant access to compensation

The Central Health and Disability Ethics Committee is satisfied that your study is not a clinical trial that is to be conducted principally for the benefit of the manufacturer or distributor of the medicine or item being trialed. Participants injured as a result of treatment received as part of your study may therefore be eligible for publicly-funded compensation through the Accident Compensation Corporation.

Further information and assistance

Please contact the HDECs Secretariat at hdecs@health.govt.nz or visit our website at www.ethics.health.govt.nz for more information, as well as our General FAQ and Ethics RM user manual.

Nāku noa, nā



Mrs Helen Walker

Chair

Central Health and Disability Ethics Committee

Encl: Appendix A: documents submitted

H.2: Australian New Zealand Clinical Trials Registry

Akshay Bisht

From: info@anzctr.org.au
Sent: Thursday, 28 April 2022 5:22 pm
To: Suman Mishra
Cc: John Monro
Subject: Your ACTRN (registration number): ACTRN12622000629730p

Dear Suman Mishra and John Monro,

Re: Mamaku effects on blood glucose response

Thank you for submitting the above trial for inclusion in the Australian New Zealand Clinical Trials Registry (ANZCTR).

Your trial has now been successfully registered and allocated the ACTRN: ACTRN12622000629730p

Web address of your trial: https://www.anzctr.org.au/ACTRN12622000629730p.aspx
Date submitted: 22/04/2022 7:39:56 AM
Date registered: 28/04/2022 3:21:58 PM
Registered by: Suman Mishra
Principal Investigator: John Monro

If you have already obtained Ethics approval for your trial, please send a copy of at least one Ethics Committee approval letter to info@anzctr.org.au or by fax to (+61 2) 9565 1863, attention to ANZCTR.

Note that updates should be made to the registration record as soon as any trial information changes or new information becomes available. Updates can be made at any time and the quality and accuracy of the information provided is the responsibility of the trial's primary sponsor or their representative (the registrant). For instructions on how to update please see https://www.anzctr.org.au/Support/HowToUpdate.aspx.

Please also note that the original data lodged at the time of trial registration and the tracked history of any changes made as updates will remain publicly available on the ANZCTR website.

The ANZCTR is recognised as an ICMJE acceptable registry (http://www.icmje.org/about-icmje/faqs/clinical-trials-registration/) and a Primary Registry in the WHO registry network (https://www.who.int/ictrp/network/primary/en/index.html).

If you have any enquiries please send a message to info@anzctr.org.au or telephone +61 2 9562 5333.

Kind regards,
ANZCTR Staff
T: +61 2 9562 5333
F: +61 2 9565 1863
E: info@anzctr.org.au
W: www.ANZCTR.org.au



Scanned by Trustwave SEG - Trustwave's comprehensive email content security solution.

H.3: Participant information sheet and consent form for testing the effect of mamaku pith powder on blood glucose, insulin and appetite responses

Participant Information Sheet

Mamaku effects on blood glucose response

Formal Study title: (*optional)* Mamaku pith effects on the postprandial glycaemic response to carbohydrate food

Sponsor (if applicable): National Science Challenges, High Value Nutrition.

Private Bag 11600, Palmerston North 4442, New Zealand.

Investigators

Principal Investigator: Dr John Monro.

Co-investigator: Dr Suman Mishra

Trial Coordinators: Hannah Dinan, Sheridan Martell.

Study Site: Plant & Food Research, Batchelar Road, Palmerston North.

Ethics committee ref.:

Introduction

You are invited to take part in a study on the effect of mamaku pith on the blood glucose response to carbohydrate consumed at the same time as the mamaku pith. Whether or not you take part is your choice. If you don't want to take part, you do not have to give a reason. If you do want to take part now, but change your mind later, you can pull out of the study at any time.

This Participant Information Sheet will help you decide if you would like to take part. It sets out why we are doing the study, what your participation would involve, what the benefits and risks to you might be, and what would happen after the study ends. We will go through this information with you and answer any questions you may have. You do not have to decide today whether or not you will participate in this study. Before you decide you may want to talk about the study with other people, such as family, whānau, friends, or healthcare providers. Feel free to do this.

If you agree to take part in this study, you will be asked to sign the Consent Form on the last page of this document. You will be given a copy of both the Participant Information Sheet and the Consent Form to keep.

This document is 11 pages long, including the Consent Form. Please make sure you have read and understood all the pages.

Voluntary participation and withdrawal from this study

Your participation in this study is completely voluntary. If you decide to take part, but later change your mind, you are free to withdraw at any time without having to give a reason.

We are happy for you to bring along a support person to each of the clinic appointments if you would like.

What is the purpose of the study?

The human responses under study are the post-meal blood glucose, insulin and hunger responses to a carbohydrate food. We will measure the effect of ingesting mamaku pith with the food on the blood glucose and insulin responses to the food, and on appetite for a period after consuming the food.

The purpose of the study is to test the effectiveness of mamaku pith as a natural indigenous meal component for reducing glycaemic response to food, and for controlling appetite. (Māori used it to help reduce hunger in times of famine.)

The study will help to show that the use of mamaku as a functional food, with health benefits, is supported by modern scientific analysis.

The results will help to confirm the traditional use of mamaku by Māori for its health benefits.

Showing a blood glucose and appetite suppressing effect of mamaku pith by thorough experimental and clinical analysis will help to provide a firm foundation for a Māori functional food enterprise based on mamaku, with economic benefits for Māori.

How is the study designed?

We will require 20 participants for the study.

There will be five different meals to be tested. You will be asked to consume all meals, one or two per week with at least two days between meals. So the trial will extend over a maximum of five weeks, and you will need to allow at least one full morning for each trial session. The order in which you receive the meals will be randomized, so the trial design is randomized crossover repeated measures design. The meals will be formulated to deliver 40 g of available carbohydrate (mainly starch) in 59.7 g of WeetBix, or approximately 4 biscuits.

The meals to be tested are:
1. WeetBix (59.7 g) plus 250 ml water plus blackcurrant flavouring.
2. WeetBix (59.7 g) plus dried mamaku pith (5 g) dispersed in 250 ml water just before consuming plus blackcurrant flavouring.

3. WeetBix (59.7 g) plus dried mamaku pith (5 g) dispersed in 250 ml water an hour before consuming plus blackcurrant flavouring.
4. WeetBix (59.7 g) plus undried mamaku pith (10 g) blended with 240 ml water just before serving plus blackcurrant flavouring.
5. WeetBix (59.7 g) plus guar gum (3 g) dispersed in 250 ml water just before serving plus blackcurrant flavouring.

To consume the meals you will mix the WeetBix with the water alone plus flavoring, or with the water plus flavoring after the mamaku or guar gum has been mixed into it. You will then be asked to ingest the moistened WeetBix within 10 minutes.

During a 3 hour period after the meals small blood samples will be taken by finger-prick sampling, for analysis of blood glucose and insulin, and you will be asked to record your subjective feelings of hunger using a simple pencil and paper scale.

Who can take part in the study?

Participants: Because this study is about comparing effects of meals on blood glucose response, and not about individual differences, we require a group of participants with normal blood glucose responses to carbohydrate foods. Therefore individuals will be chosen to participate in the study if they are considered to be generally healthy and within a healthy weight range (as obesity may affect glucose tolerance) and without problems with blood glucose control. Health status will be determined initially by the use of a health questionnaire, which asks about your current and past health issues.

Men and women will be suitable for the study. The age range is 20 to 65 years and the BMI range is 18 to 35 kg/m^2 (BMI is the abbreviated term of body mass index which is used to estimate a healthy weight range for individuals based on weight and height. BMI is determined by your weight in kilograms divided by your height (in metres squared).

All participants will need to:

- Have no known allergy to, or intolerance of wheat or mamaku.
- Have a BMI between 18 and 35
- Not suffer from glucose intolerance, as indicated by the fasting blood glucose and HbA1c screening test results or prior diagnosis of diabetes.
- Be healthy, as confirmed by a short medical questionnaire
- Be willing to fast from 10.00 pm the evening before a test.
- Be willing to consume only the supplied trial foods and water on the trial day until the last blood sample of the trial day (about noon).
- Be willing to not do any vigorous activity in the morning of test days

The research in this project will be undertaken in a culturally sensitive manner with all aspects of the trial explained in full to you in a manner most suitable to you. We will be available to answer questions throughout the study and will seek advice from appropriate advisory groups should it be necessary. You will be given access to interpreters at any time in the study should you require them. The opportunity for whanau support is available at all times.

You will be asked to consume a normal type of meal on the evening before each trial session, although preferably a similar one before each session, to refrain from heavy drinking, and to not eat anything after 10 pm on the evening before a trial session.

What will my participation in the study involve?

Pre-trial Screening: If you agree to take part in this study, we will make an initial appointment for you to come into Plant and Food Research in Palmerston North. At this appointment we will measure your height and weight and ask you some questions about your general health. This is so we can assess if you are eligible to participate in the study. If you are eligible we will ask you to have a quick blood test to check that your blood glucose is in the normal range and there is no evidence of diabetes. The test involves taking a small finger prick sample of blood and testing it, as is done routinely by people with diabetes at home.

Trial procedure: You will be asked to arrive at the clinic at 8.30 am on the morning of a trial session and then asked to rest for 15 mins, before 2 baseline blood samples (by finger prick) are taken. You will then be given one of the five test meals (all mainly WeetBix) to consume, from a standard bowl with a spoon, in a period of 10 mins. Small finger prick blood samples will be taken at 15, 30, 45, 60, 90, 120 and 180 min after eating the meal. Blood sampling involves use of a small pen-like finger prick device (as used by diabetics at home) which almost painlessly allows a small bead of blood to be massaged from the finger and used to monitor your blood glucose and insulin levels over the three hours after consuming the food. During the three hours you will be able to continue working if it is not strenuous (e.g., office work), and drink a set amount of water if thirsty. No food can be consumed until after the final blood test. Otherwise you will be asked to rest and do some non-strenuous activity such as reading.

You will be asked to rate your hunger five times; before consuming your breakfast test meal, immediately afterwards, and at hourly intervals after the meal, by placing a pencil mark on a simple scale.

If you agree to take part in the study, we would like you to be available on one morning per week, over five weeks, with each visit lasting a maximum of four hours. A follow up meeting will also be included to feed back the results of the study and answer any questions.

What will happen to my blood samples?

The samples will be placed in tubes labelled with the confidential code assigned to each participant. The samples will be analysed for insulin at Plant & Food Research laboratory.

Due to the small size of sample collected there is unlikely to be any remaining after analysis. If there is any remaining sample it will be disposed of according to necessary biohazard protocols. You will not be able to come in the laboratory and perform karakia when the blood sample is destroyed as the laboratory is a restricted working area.

What are the possible risks of this study?

This study focuses on the effects of natural food materials on blood glucose levels and does not use any pharmaceutical products. Due to the initial exclusion of subjects with a history of intolerance to wheat products it is unlikely that there will be any adverse reaction to the WeetBix component.

Intolerance of mamaku pith has not been formally tested in humans but mamaku has been widely consumed as part of the Māori diet for hundreds of years. It is also currently consumed in natural product smoothies that are promoted online. Testing of mamaku in animal (rat) trials has not revealed any toxic effects or impairment to rat growth or health at high intakes.

Guar gum is a form of dietary fibre that is widely used as a safe food ingredient by the food industry. The single dose ingested by each participant in this study is unlikely to have any adverse effects or effects noticeable beyond the trial session.

Considering the few materials consumed in the proposed study, the overall risk and the chance of side-effects is extremely small. However, if there is any indication that you are having an adverse reaction to any of the test meals the trial will be stopped immediately and the participants monitored until all signs of the reaction have faded.

The finger prick device used to draw a small bead of blood for glucose analysis is used daily by many people with diabetes. It is almost painless, but if it causes any discomfort, you will be given the opportunity to take a break, or if necessary stop participation in the study. The staff using the device have had many years of experience with it and have taken thousands of blood samples, so the chance of operator error is minuscule.

If you were injured as a result of treatment given as part of this study, which is unlikely, you will not be eligible for compensation from ACC. However, compensation would be available from Plant and Food Research in line with industry guidelines. We can give you a copy of these guidelines if you wish. You would be able to take action through the courts if you disagreed with the amount of compensation provided.

If you suffer physical harm from the mamaku being tested, or harm from any other aspects of the trial, for example from blood sampling by the researchers (very unlikely), liability is borne by Plant & Food Research subject to appropriate application or legal processes. If you have private health or life insurance, you may wish to check with your insurer that taking part in this study will not affect your cover.

You may obtain further information concerning medical treatment for injuries by contacting the Principal Investigator.

Should information become available on any possible adverse health effects of any of the meal components during the trial it will be immediately stopped, you will be informed of the nature of the adverse effects, and monitored as appropriate with medical input.

What are the possible benefits of this study?

An immediate benefit from the study is that you will receive instant feedback of an aspect of your health - glucose tolerance - during screening, and gain some understanding of your own relative blood glucose responsiveness to carbohydrate foods during the course of the trial.

The indirect benefit of the study, and the main aim of the study, is to show that mamaku is able to reduce the blood glucose response to a carbohydrate food, and therefore may be a valuable agent in blood glucose control, making it the basis of a range of functional food products. As mamaku is a Taonga plant and the project is being undertaken in partnership with a Māori trust the research may eventually benefit the Māori economy and in turn Māori communities.

Will any costs be reimbursed?

We will give you a $20 supermarket voucher for the initial screening visit and if you are accepted onto the study you will receive a further $20 voucher each time you participate in a test to partially compensate you for your travel and time. This will make a total of $120. If you decide to take part, but later change your mind, you are free to withdraw at any time without having to give a reason.

What if something goes wrong?

As this research study is for the principal benefit of the commercial partner [Ng Uri o te Ngahere Trust] if you are injured as a result of taking part in this study you will not be eligible for compensation from ACC.

However, Plant and Food Research has satisfied the Central Health and Disability Ethics Committee that approved this study that it has up-to-date insurance for providing participants with compensation if they are injured as a result of taking part in this study.

New Zealand ethical standards require compensation for injury to be at least ACC equivalent. Compensation should be appropriate to the nature, severity and persistence of your injury and should be no less than would be awarded for similar injuries by New Zealand's ACC scheme.

What will happen to my information?

During this study the scientists, clinical assistants and other Plant and Food staff will record information about you and your study participation – anthropometric data (such as height and weight), results of preliminary health screening, and blood glucose, insulin, and appetite responses during the trial. You cannot take part in this study if you do not consent to the collection of this information.

<u>Identifiable Information</u>
Identifiable information is any data that could identify you (e.g. your name, date of birth, or address). Only the clinical research staff will have access to your identifiable information. Identities of

participants are not required for analysis of the results of the trial as it is about comparison of meals, not people.

Access to your identifiable information would be given only under certain circumstances in the present trial:

- Plant and Food Research clinical staff to complete study assessments.
- Your usual doctor, if a study test gives an unexpected result that could be important for your health. This allows appropriate follow-up to be arranged.

De-identified (Coded) Information

To make sure your personal information is kept confidential, information that identifies you will not be included in any report generated by the report writer (Dr Monro) or any study information sent to the sponsor. Instead, you will be identified by a code. Dr Monro will keep a list linking your code with your name, so that you can be identified by your coded data if needed.

The following groups may have access to your coded information:

- Plant and Food Research staff involved in the trial, for the purpose of analysis and report writing.

The results of the study may be published or presented, but not in a form that would reasonably be expected to identify you.

Future Research Using Your Information.

Your coded information collected in this study will only be used for this study and will not be used for other medical and/or scientific research that is unrelated to the current study.

Security and Storage of Your Information.

Your identifiable information will be held on-site at Plant and Food Research during the study. After the study it is transferred to a secure archiving site and stored for at least 10 years, then destroyed. Only the Lead Researcher, Co-investigator and Trial Coordinators will have access to the health questionnaires used to assess your eligibility against the inclusion/exclusion requirements for participation in the study. Your coded study information will be kept by the sponsor in secure, cloud-based storage indefinitely. All storage will comply with local and/or international data security guidelines.

Risks.

Although efforts will be made to protect your privacy, absolute confidentiality of your information cannot be guaranteed. Even with coded and anonymised information, there is no guarantee that you cannot be identified. The risk of people accessing and misusing your information (e.g. making it harder for you to get or keep a job or health insurance) is currently very small, but may increase in the future as people find new ways of tracing information.

Rights to Access Your Information.

You have the right to request access to your information held by the research team. You also have the right to request that any information you disagree with is corrected.

Please ask if you would like to access the results of your screening and safety tests during the study. You may access other study-specific information before the study is over, but this could result in you being withdrawn from the study to protect the study's scientific integrity.
If you have any questions about the collection and use of information about you, you should ask Dr Mishra.

Rights to Withdraw Your Information.
You may withdraw your consent for the collection and use of your information at any time, by informing a Trial Coordinator.
If you withdraw your consent, your study participation will end, and the study team will stop collecting information from you.
Information collected up until your withdrawal from the study may continue to be used and included in the study with your consent, if it protects the quality of the study.

Ownership Rights.
Information from this study may lead to discoveries and inventions or the development of a commercial product. The rights to these will belong to the Nga uri o te Ngahere Trust. You and your family will not receive any financial benefits or compensation, nor have any rights in any developments, inventions, or other discoveries that might come from this information.

What happens after the study or if I change my mind?

You may withdraw from the study at any time but please inform one of the trial co-ordinators (Hannah Dinnan or Sheridan Martell).

If you withdraw your collected data up to the point of withdrawing may be used, with your agreement.
Any samples collected may be analyzed with other samples and the data used if suitable, subject to your permission.

The study material consumed is purely experimental at this stage, so will not be available after the study.

This is a "blinded" study, which means participants don't know which treatment they are having. However, you will be told at the end of the trial if you wish.

Blood collected from you in this study will not be passed on to anyone else outside this project and if there is any left after analysis it will be destroyed. If you decide to withdraw from the study your health questionnaire can be returned to you on request, otherwise it will be destroyed. Any blood sample collected from you will be destroyed and all data collected from you prior to your withdrawal from this study will not be included in the analysis and overall findings from this project.

The lead researcher will give you an overview of the main findings of the study and your personal results and answer any questions you may have about this research on request. A delay will inevitably occur between data collection and publication of results.

Can I find out the results of the study?

You may request the sponsor of the trial (Plant & Food Research/Nga uri o te Ngahere Trust) to provide you with a plain summary of the results.

The trial will be registered in the Australia New Zealand Clinical Trials Registry and may be accessed at http://www.anzctr.org.au/

Who is funding the study?

The trial is being funded by the Government's Ministry of Business Innovation and Employment (MBIE) in the High Value Nutrition Program of the National Science Challenges through a grant made to the Mamaku whakaoraora research project, jointly led by Plant and Food Research and the Nga uri o te Ngahere Trust.

The people who are running the trial are all staff of Plant and Food Research with no influence of the Nga uri o te Ngahere Trust, so there is no conflict of interest involved.

Who has approved the study?

This study has been approved by an independent group of people called a Health and Disability Ethics Committee (HDEC), who check that studies meet established ethical standards. The Central HDEC has approved this study.

Who do I contact for more information or if I have concerns?

If you have any questions, concerns or complaints about the study at any stage, you can contact:

Dr John Monro (Principal Investigator)
Phone: (06) 3556137
Email: john.monro@plantandfood.co.nz
Dr Suman Mishra (Co-Investigator)
Phone: (06) 3556146
suman.mishra@plantandfood.co.nz
Hannah Dinan, Sheridan Martell (Trial Coordinators)
Phone: (06) 3530962
Email: hannah.dinnan@plantandfood.co.nz, sheridan.martell@plantandfood.co.nz

For Māori health support please contact:

Chris Stack (Ngāti Tuwharetoa) (Māori support and advisor).
Phone: (06) 9537744
Email: chris.stack@plantandfood.co.nz

For Pacifica support please contact:

Nayer Ngametua
Phone: (06) 953 7744
Email: nayer.ngamatue@plantandfood.co.nz

If you want to talk to someone who isn't involved with the study, you can contact an independent health and disability advocate on:

Phone: 0800 555 050
Fax: 0800 2 SUPPORT (0800 2787 7678)
Email: advocacy@advocacy.org.nz
Website: https://www.advocacy.org.nz/

You can also contact the health and disability ethics committee (HDEC) that approved this study on:

Phone: 0800 4 ETHIC
Email: hdecs@health.govt.nz

Volunteers wanted

Plant & Food Research are looking for volunteers for a study investigating the effect of mamaku pith on blood glucose response.

Volunteers will be required to visit Plant & Food Research for a screening visit. If you are accepted for the study, you will have to attend our clinic for five testing sessions. Each testing session will take approximately 3.5 hours. Finger prick blood samples will be taken for blood glucose and insulin.

We require healthy people aged 18 to 60 years, with a BMI between 18 and 35.

You will be given a token of appreciation for your time and effort.



If you are interested and would like more information, please contact:

Hannah or Sheridan
(06) 353 0962 or
PN.Clinical@plantandfood.co.nz

plantandfood.co.nz

Plant & Food® Research
Rangahau Ahumāra Kai

ALJ | 04/22 | CBO-799

Consent Form

Mamaku effects on blood glucose response

Please tick to indicate you consent to the following

I have read, or have had read to me in my first language, and I understand the Participant Information Sheet.		
I have been given sufficient time to consider whether or not to participate in this study.		
I have had the opportunity to use a legal representative, whanau/ family support or a friend to help me ask questions and understand the study.		
I am satisfied with the answers I have been given regarding the study and I have a copy of this consent form and information sheet.		
I understand that taking part in this study is voluntary (my choice) and that I may withdraw from the study at any time without this affecting my medical care.		
I consent to the research staff collecting and processing my information, including information about my health.		
If I decide to withdraw from the study, I agree that the information collected about me up to the point when I withdraw may continue to be processed.	Yes ☐	No ☐
I consent to my GP or current provider being informed about my participation in the study and of any significant abnormal results obtained during the study.	Yes ☐	No ☐
I understand that my data will be stored for at least 10 years and will be the responsibility of the principal investigator, after which it will be destroyed.		
I understand that my participation in this study is confidential and that no material, which could identify me personally, will be used in any reports on this study.		
I agree to allow my coded information to be used for future research related to mamaku or blood glucose response.		
I am aware that I must call a study coordinator ahead of attending any		

session if I, or anyone I have had close personal contact with has COVID-19, is awaiting COVID-19 test results, has had close personal contact with COVID-19 patients, or is displaying symptoms of any transmissible illness.	
I am aware that if I, or anyone I have close personal contact with develop suspected COVID-19 or similar symptoms within three weeks of my visit to the Plant & Food Research Clinical Facility, I must notify the Principal Investigator (contact details above) by phone.	
I understand the compensation provisions in case of injury during the study.	
I know who to contact if I have any questions about the study in general.	
I understand my responsibilities as a study participant.	
I wish to receive a summary of the results from the study.	Yes ☐ No ☐

Declaration by participant:

I hereby consent to take part in this study.

Participant's name:

Signature: Date:

Declaration by member of research team:

I have given a verbal explanation of the research project to the participant, and have answered the participant's questions about it.

I believe that the participant understands the study and has given informed consent to participate.

Researcher's name:

Signature: Date:

Appendix I: Appetite sensations form used for human trail

Appetite sensations

Visual analogue scale for measuring appetite sensations.

Subject no.:

Date:

Diet:

Time: 0 minutes

How hungry do you feel?

Not at all hungry — Extremely hungry

How full do you feel?

Not at all full — Totally full

How satisfied do you feel?

Not at all satisfied — Extremely satisfied

How much food do you think you can eat?

Nothing at all — A large amount

Appendix J: Animal ethics approval for Chapter 8

J.1: Animal ethics approval for testing the effect of mamaku pith diet in rats

Akshay Bisht

From: John Monro <John.Monro@plantandfood.co.nz>
Sent: Thursday, 9 March 2023 11:09 am
To: Akshay Bisht
Subject: FW: AE Application number 15329 Response from AEC.

Animal ethics approval email

From: jim.webster@agresearch.co.nz <jim.webster@agresearch.co.nz>
Sent: Tuesday, 18 May 2021 9:35 am
To: John Monro <John.Monro@plantandfood.co.nz>; Chrissie Butts <Chrissie.Butts@plantandfood.co.nz>; Duncan Hedderley <Duncan.Hedderley@plantandfood.co.nz>; Sheridan Martell <Sheridan.Martell@plantandfood.co.nz>; Hannah Dinnan <Hannah.Dinnan@plantandfood.co.nz>; Susanne Middlemiss-Kraak <Susanne.Middlemiss-Kraak@plantandfood.co.nz>; ruakura.ethicschair@agresearch.co.nz; invermay.ethicssec@agresearch.co.nz; ruakura.ethicssec@agresearch.co.nz; ruakura.welfare@agresearch.co.nz; grasslands.welfare@agresearch.co.nz
Subject: AE Application number 15329 Response from AEC.

Message from the Animal Ethics Committee regarding: Application Number 15329 Mamaku effects in the rat model

APPROVED -Animal Manipulations described in the Form above have been APPROVED to start on the PROPOSED START DATE

If you are the APPLICANT, you must meet ALL REPORTING requirements for this Application.

REPORT A and STATISTICS forms are due after the Application END DATE and REPORT B is due within 6 months of the END DATE.

COMMITTEE NOTES:

Please add reporting due dates to your calendar so forms can be submitted promptly.

We appreciate your efforts to help refine the housing for this study and will continue to work with staff to find better alternatives long term.

AgResearch staff please go to
http://webapps2012/ethics/?Q=1&A=15329&V=S&P=Vi
other users please go to
https://ethics.agresearch.co.nz/?Q=1&A=15329&V=S&P=Vi

Attention: The information contained in this message is intended only for the persons or entities to which it is addressed and may contain confidential and/or privileged material. Any review, retransmission, dissemination or other use of, or taking of any action in reliance upon, this information by persons or entities other than the intended recipients is prohibited by AgResearch Limited. If you have received this message in error, please notify animalethicsoffice@agresearch.co.nz immediatly and erase the original message.

J.2: Māori consultation for the rat study

NGA URI O TE NGAHERE TRUST

Descendants of the Forest

PO BOX 5223 MT MAUNGANUI
Ph 07 575 8261, Fax 07 575 8261
ngaheretrust@xtra.co.nz

May 4th 2021

To Whom it May Concern
Mamaku Whakaoraora animal trial Ethics Approval.

This letter attests support for the animal trials our organisation and Plant and Food Research require to be conducted within our **Mamaku Whakaoraora** research kaupapa.

The animal work will provide an evidence-based foundation for establishing Mamaku (*Cyathia medullaris*, tree fern) as a highly functional natural food, with an indigenous whakapapa, and a strong capacity to improve a range of metabolic and gut health conditions. This research is co-led by myself, **Garry Watson,** as Chairman Nga Uri o te Ngahere Trust. The trials will assist in determining the processes for food safe preparation of Mamaku products and assess the properties of Mamaku under simulated *in vitro* gut conditions. Clinical trials with Mamaku products will be conducted to establish their safety and blood cholesterol-lowering potential as well as the effects on the colonic microbiota.
The animal trials are critical to this end stage of the research.

Nga Uri o te Ngahere Trust (NUOTN), specialises in ethnoscience and traditional health remedies in the Rongoa Rakau / Rongoa Māori space and they have a long track record in Mātauranga Māori based research kaupapa. As Chairman of the Trust, and as a co-owner of Trinty Bioactives we have sought and obtained consent from the ethics committee in the past for animal trials using Rongoa Rakau.

I am a kaumatua o Ngai Tai of Tainui and Tuhoe decent and I have approved the use of these trials to advance this research, which is so critically important to the health and wellbeing of our people. As a member of the MBIE College of Assessors [seconded as an expert in Mātauranga Māori] I frequently assess funding applications and research kaupapa where ethics approvals are required. Having viewed the research plan and methodologies [which we use in Trinity Bioactives Ltd in other research] I can verify that the research is ethically sound.

Please feel free to contact me directly if further detail is required.
Ngā mihi nui and kia kaha te Rangatahi.

Signed;

Chairman – NUOTN Trust

Appendix K: Colonic fermentation of mamaku pith powder using a rat model

The rats remained healthy, and the diet groups were very similar and not significantly different in their growth responses over the whole trial (**Table K.1**). Even the diet containing 10% dry mamaku pith powder, which would equate to a large intake of the fresh pith (6-8% dry matter) as traditionally consumed by Māori, did not adversely affect rat growth.

Table K.1: Growth responses of rats to diets containing different dietary fibre sources.

Parameters (g)	Glucose (Baseline)	Wheat bran	Psyllium husk	Mamaku pith powder	
				5%	10%
Feed intake	494±28	515±10	507±11	497±32	505±22
Wt gain	182±21	191±11	176±10	176±19	171±15
Wt gain/100 g feed	36.7±2.8	37.1±1.7	34.8±1.9	35.2±2.1	33.9±2.2

The taxonomic profiling suggests that colonic bacterial composition primarily belongs to Firmicutes, Bacteroidetes, Proteobacteria and Actinobacteria phyla, accounting for more than 95% of the total phyla in all five diet groups (**Figure K.1A**). Rats fed glucose or wheat bran diets had higher Firmicutes followed by Bacteroidetes, whereas rats fed psyllium or mamaku pith powder (5 and 10%) diets had higher Bacteroidetes followed by Firmicutes. The Firmicutes to Bacteroidetes (F/B) ratio was significantly reduced in rats fed psyllium and 10% mamaku pith powder, compared with glucose and wheat bran fed rats (**Figure K.1B**). Amongst all the diet groups, rats fed wheat bran had higher Actinobacteria.

Furthermore, at genus levels, 64 key genera were identified in all five groups (**Figure K.2**). Amongst these *Bacteroides*, *Muribaculaceae*, *Allobaculum*, *Romboutsia*, *Lactobacillus*, *Parasutterella*, *Coriobacteriaceae_UCG-002*, *Escherichia-Shigella*, *Dubosiella* and *Prevotellaceae_UCG-001* were prevailing genus. In order to compare the effect of diet on bacterial composition, genera with relative abundance below 0.5% were excluded. This resulted in 20 genera, of which 13 were significantly influenced by the diet (**Table K.2**). Compared with glucose fed diet, the relative abundance of *Bacteroides* increased and *Lactobacillus*, *Dubosiella*, *Terrisporobacter* and *Veillonella* decreased when fed with a psyllium diet. Rat fed wheat bran, had a higher relative abundance of *Bifidobacterium* and *Prevotella*

and a lower relative abundance of *Escherichia-Shigella*, *Terrisporobacter* and *Fusobacterium* than the glucose fed rats. Rats fed mamaku pith powder had a higher relative abundance of *Muribaculaceae*, *Parasutterella* (not in 5%) and *Prevotellaceae_UCG-001* and a lower relative abundance of *Escherichia-Shigella* (not in 5%), *Terrisporobacter*, *Fusobacterium*, *Parabacteroides* and *Veillonella* than the glucose fed rats. These results suggest that experimental diets with treatment fibres (wheat bran, psyllium or mamaku pith powder) may lead to significant diet-specific changes in the taxonomic composition of colonic microbiota in rats compared to baseline diet.

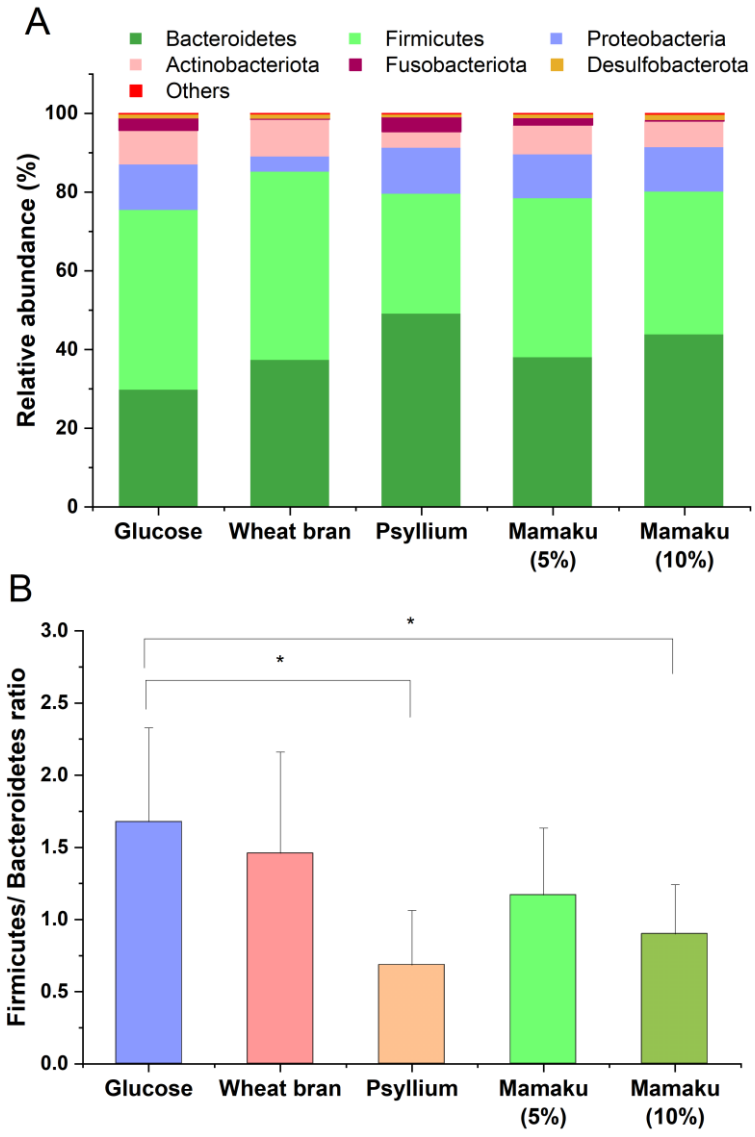


Figure K.1: (**A**) Relative abundance of bacteria in rat colon at the phylum level, (**B**) ratio of Firmicutes to Bacteroidetes in rats fed the experimental diets.

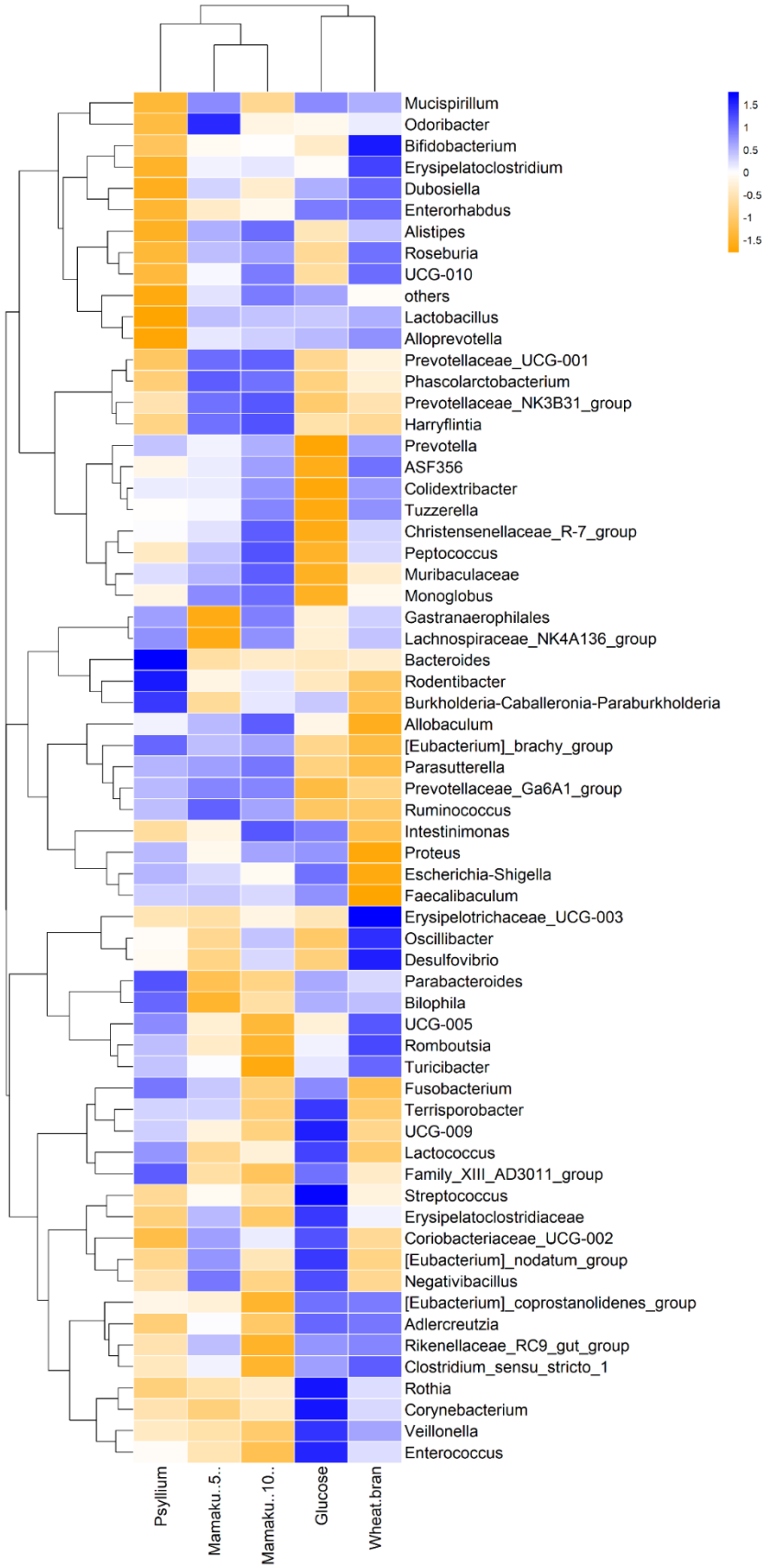


Figure K.2: Heatmap of gut microbial composition at genus level in rats fed the experimental diets.

Table K.2: Relative abundances of the top 20 genera in rats fed the experimental diets.

Genus	Diet (Relative abundance %)				
	Glucose	Wheat bran	Psyllium	Mamaku (5%)	Mamaku (10%)
Bacteroides	19.93±6.56^{b}	20.56±6.71^{b}	35.60±8.47^{a}	19.03±6.49^{b}	20.42±9.1^{b}
Muribaculaceae	5.91±3.25^{c}	8.51±2.93^{bc}	10.09±3.17^{abc}	10.92±1.51^{ab}	13.15±3.55^{a}
Allobaculum	8.47±3.61^{ab}	6.80±4.34^{b}	8.82±2.18^{ab}	9.35±1.07^{ab}	10.34±3.19^{a}
Romboutsia	8.08±4.87^{ab}	12.49±4.29^{a}	9.20±6.35^{ab}	6.81±3.09^{ab}	4.59±2.21^{b}
Lactobacillus	8.02±5.53^{a}	9.24±4.71^{a}	1.3±1.19^{b}	8.29±7.50^{a}	8.06±7.09^{a}
Parasutterella	3.35±2.05^{b}	2.87±1.28^{b}	5.63±2.81^{ab}	5.96±2.01^{ab}	6.67±2.74^{a}
Coriobacteriaceae_UCG-002	6.61±5.19^{a}	3.81±2.79^{a}	3.26±1.44^{a}	5.64±4.33^{a}	4.82±4.37^{a}
Escherichia-Shigella	7.96±4.73^{a}	0.79±0.89^{c}	5.22±3.09^{ab}	4.18±1.80^{abc}	3.06±2.46^{bc}
Dubosiella	3.97±3.12^{ab}	5.88±2.26^{a}	0.76±0.67^{c}	3.28±1.50^{b}	1.99±1.29^{bc}
Prevotellaceae_UCG-001	0.78±0.40^{b}	1.37±0.53^{b}	0.55±0.27^{b}	5.22±2.61^{a}	5.57±2.79^{a}
Terrisporobacter	4.61±1.59^{a}	0.90±0.92^{b}	2.25±1.59^{b}	2.23±1.69^{b}	0.96±1.11^{b}
Fusobacterium	3.18±2.67^{ab}	0.30±0.36^{c}	3.79±1.32^{a}	1.88±1.46^{bc}	0.42±0.62^{c}
Bifidobacterium	1.08±0.88^{b}	4.99±1.65^{a}	0.59±0.23^{b}	1.36±0.71^{b}	1.42±1.04^{b}
Alloprevotella	1.60±1.91^{ab}	3.67±5.30^{a}	0.01±0.01^{b}	0.62±1.03^{b}	1.00±0.99^{ab}
Parabacteroides	1.13±0.72^{ab}	0.95±0.47^{bc}	1.66±1.01^{a}	0.39±0.13^{c}	0.47±0.29^{c}
Prevotella	0.00±0.00^{b}	1.71±2.06^{a}	0.79±0.46^{ab}	0.29±0.36^{b}	1.19±1.15^{ab}
UCG-005	0.56±0.71^{a}	1.23±1.15^{a}	1.01±1.08^{a}	0.56±0.58^{a}	0.31±0.30^{a}
Veillonella	1.31±0.99^{a}	0.84±1.05^{ab}	0.46±0.44^{b}	0.41±0.42^{b}	0.32±0.44^{b}
Faecalibaculum	0.69±0.53^{a}	0.23±0.33^{a}	0.58±0.52^{a}	0.58±0.36^{a}	0.55±0.52^{a}
Colidextribacter	0.26±0.47^{a}	0.66±0.42^{a}	0.53±0.34^{a}	0.53±0.61^{a}	0.68±0.41^{a}

Genus with a relative abundance of 0.5% and above. Values are expressed as means ± standard deviation (n=8). Values in the same row denoted with the different superscripts are significantly different ($p \leq 0.05$).

The effect of diet on the functional composition of rat colonic microbiota was analysed using Phylogenetic Investigation of Communities by Reconstruction of Unobserved States 2 (PICRUSt 2) pipeline based on Kyoto Encyclopedia of Genes and Genomes (KEGG) and MetaCyc databases. Carbohydrate, amino acid and nucleotide metabolisms were the most prevailing signalling pathways amongst all five experimental diets (**Figure K.3**). Wheat bran diet fed rats had a significantly higher abundance of nucleotide metabolism pathways (Pathway 3, 4, 6, 7, 10, 22 and 25) and carbohydrate metabolism pathways (12, 13 and 18), than glucose diet rats fed. Mamaku (5 and 10 %) diet fed rats had a higher abundance of amino acid metabolism pathways (Pathway 2, 17 and 28) and nucleotide metabolism pathway (Pathway 27), while psyllium diet fed rates had a higher abundance of carbohydrate metabolism pathway (Pathway 1), amino acid metabolism pathway (Pathway

16) and nucleotide metabolisms pathway (Pathway 25) than glucose diet fed rats. These results suggest that experimental diets with treatment fibres (wheat bran, psyllium or mamaku 5 and 10%) may lead to significant diet-specific changes in the taxonomic and functional composition of colonic microbiota in rats compared to baseline diet.

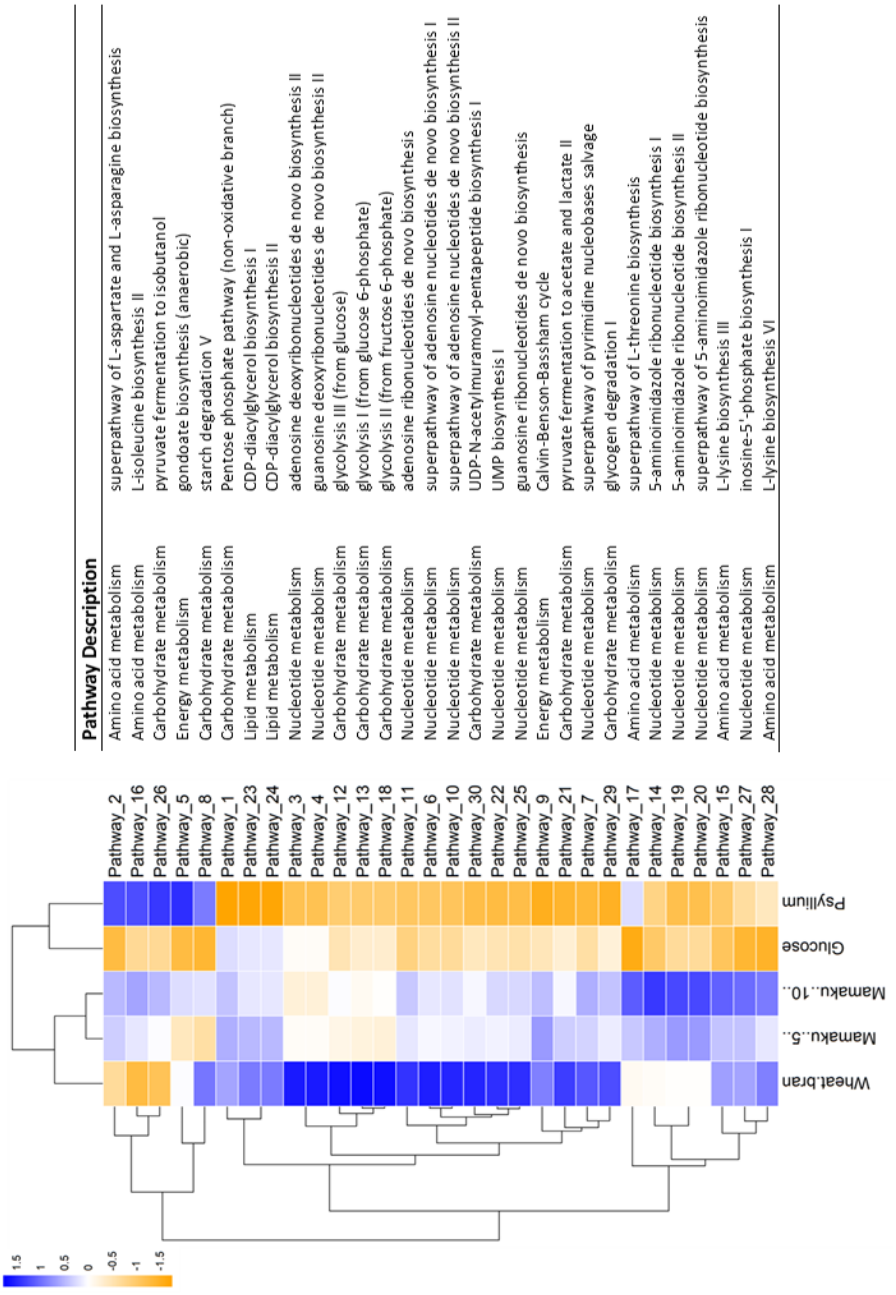


Figure K.3: Heatmap of pathways showing the top 30 abundant pathways of the gut microbiota in rats fed the experimental diets.

Appendix L: Copyright permissions to reprint figures and tables

L.1: Permission to reprint Table 2.1



CCC RightsLink

Home | Help | Email Support | Akshay Bisht

ACS Publications
Most Trusted. Most Cited. Most Read.

Complex Rheological Properties of a Water-Soluble Extract from the Fronds of the Black Tree Fern, Cyathea medullaris

Author: Kelvin K. T. Goh, Lara Matia-Merino, Christopher E. Hall, et al
Publication: Biomacromolecules
Publisher: American Chemical Society
Date: Nov 1, 2007

Copyright © 2007, American Chemical Society

PERMISSION/LICENSE IS GRANTED FOR YOUR ORDER AT NO CHARGE

This type of permission/license, instead of the standard Terms and Conditions, is sent to you because no fee is being charged for your order. Please note the following:

- Permission is granted for your request in both print and electronic formats, and translations.
- If figures and/or tables were requested, they may be adapted or used in part.
- Please print this page for your records and send a copy of it to your publisher/graduate school.
- Appropriate credit for the requested material should be given as follows: "Reprinted (adapted) with permission from {COMPLETE REFERENCE CITATION}. Copyright {YEAR} American Chemical Society." Insert appropriate information in place of the capitalized words.
- One-time permission is granted only for the use specified in your RightsLink request. No additional uses are granted (such as derivative works or other editions). For any uses, please submit a new request.

If credit is given to another source for the material you requested from RightsLink, permission must be obtained from that source.

BACK CLOSE WINDOW

© 2022 Copyright - All Rights Reserved | Copyright Clearance Center, Inc. | Privacy statement | Data Security and Privacy | For California Residents | Terms and ConditionsComments? We would like to hear from you. E-mail us at customercare@copyright.com

L.2: Permission to reprint Figure 2.5

ELSEVIER LICENSE
TERMS AND CONDITIONS

Sep 27, 2022

This Agreement between Mr. Akshay Bisht ("You") and Elsevier ("Elsevier") consists of your license details and the terms and conditions provided by Elsevier and Copyright Clearance Center.

License Number	5392800387276
License date	Sep 19, 2022
Licensed Content Publisher	Elsevier
Licensed Content Publication	Carbohydrate Polymers
Licensed Content Title	The cation-controlled and hydrogen bond-mediated shear-thickening behaviour of a tree-fern isolated polysaccharide
Licensed Content Author	May S.M. Wee,Lara Matia-Merino,Kelvin K.T. Goh
Licensed Content Date	Oct 5, 2015
Licensed Content Volume	130
Licensed Content Issue	n/a
Licensed Content Pages	12
Start Page	57
End Page	68
Type of Use	reuse in a thesis/dissertation
Portion	figures/tables/illustrations
Number of figures/tables/illustrations	1
Format	both print and electronic
Are you the author of this Elsevier article?	No
Will you be translating?	No
Title	The tale of Mamaku from farm to gut.
Institution name	Massey University
Expected presentation date	Jan 2023
Portions	Fig. 9. Schematic illustration of possible groups which are responsible for hydrogen bonding during shear-thickening.
Requestor Location	Massey Halls Manawatu, Privat Bag 11222 Massey University Palmerston North, 4410 New Zealand Attn: Akshay Bisht
Publisher Tax ID	GB 494 6272 12
Billing Type	Invoice
Billing Address	Mr. Akshay Bisht 42, Forrest Hill Road Forest Hill, Auckland Auckland, New Zealand 0620 Attn: Mr. Akshay Bisht
Total	**0.00 USD**
Terms and Conditions	

L.3: Permission to reprint Figure 2.7

SPRINGER NATURE LICENSE
TERMS AND CONDITIONS

Sep 27, 2022

This Agreement between Mr. Akshay Bisht ("You") and Springer Nature ("Springer Nature") consists of your license details and the terms and conditions provided by Springer Nature and Copyright Clearance Center.

License Number	5396920871179
License date	Sep 27, 2022
Licensed Content Publisher	Springer Nature
Licensed Content Publication	Heat and Mass Transfer
Licensed Content Title	Freeze and convective drying of quince (Cydonia oblonga Miller.): Effects on drying kinetics and quality attributes
Licensed Content Author	Nazmi Izli et al
Licensed Content Date	Nov 9, 2018
Type of Use	Thesis/Dissertation
Requestor type	academic/university or research institute
Format	print and electronic
Portion	figures/tables/illustrations
Number of figures/tables/illustrations	1
Will you be translating?	no
Circulation/distribution	500 - 999
Author of this Springer Nature content	no
Title	The tale of Mamaku from farm to gut.
Institution name	Massey University
Expected presentation date	Jan 2023
Portions	Figure 6: SEM images of dried quince samples: freeze drying and convective drying
Requestor Location	Massey Halls Manawatu, Privat Bag 11222 Massey University Palmerston North, 4410 New Zealand Attn: Akshay Bisht
Total	**0.00 USD**
Terms and Conditions	

Appendix M: Statement of contribution

M.1: Chapter 4

MASSEY UNIVERSITY
TE KUNENGA KI PŪREHUROA
UNIVERSITY OF NEW ZEALAND

GRADUATE RESEARCH SCHOOL

STATEMENT OF CONTRIBUTION DOCTORATE WITH PUBLICATIONS/MANUSCRIPTS

We, the student and the student's main supervisor, certify that all co-authors have consented to their work being included in the thesis and they have accepted the student's contribution as indicated below in the Statement of Originality.

Student name:	Akshay Bisht
Name and title of main supervisor:	A/Prof. Dr. Lara Matia-Merino
In which chapter is the manuscript/published work?	Chapter 4
What percentage of the manuscript/published work was contributed by the student?	85%

Describe the contribution that the student has made to the manuscript/published work:
The candidate has contributed towards conceptualization, methodology, validation, investigation, formal analysis, visualization, data curation and writing - original draft.

Please select one of the following three options:

○	**The manuscript/published work is published or in press** Please provide the full reference of the research output:
○	**The manuscript is currently under review for publication** Please provide the name of the journal:
◉	**It is intended that the manuscript will be published, but it has not yet been submitted to a journal**

Student's signature:	Akshay Bisht Digitally signed by Akshay Bisht Date: 2023.05.11 14:11:13 +12'00'	Main supervisor's signature:	A.Prof. Lara Matia-Merino Digitally signed by A.Prof. Lara Matia-Merino DN: cn=A.Prof. Lara Matia-Merino, c=NZ, o=Massey University, ou=School of Food and Advanced Technology, email=l.matia-merino@massey.ac.nz Date: 2023.05.11 11:10:40 +00'00'

This form should be placed at the beginning of each relevant thesis chapter.

M.2: Chapter 5

MASSEY UNIVERSITY
TE KUNENGA KI PŪREHUROA
UNIVERSITY OF NEW ZEALAND

GRADUATE RESEARCH SCHOOL

STATEMENT OF CONTRIBUTION DOCTORATE WITH PUBLICATIONS/MANUSCRIPTS

We, the student and the student's main supervisor, certify that all co-authors have consented to their work being included in the thesis and they have accepted the student's contribution as indicated below in the Statement of Originality.

Student name:	Akshay Bisht
Name and title of main supervisor:	A/Prof. Dr. Lara Matia-Merino
In which chapter is the manuscript/published work?	Chapter 5
What percentage of the manuscript/published work was contributed by the student?	95%

Describe the contribution that the student has made to the manuscript/published work:

The candidate has contributed towards conceptualization, methodology, validation, investigation, formal analysis, visualization, data curation and writing - original draft.

Please select one of the following three options:

- ○ **The manuscript/published work is published or in press**
  Please provide the full reference of the research output:
- ◉ **The manuscript is currently under review for publication**
  Please provide the name of the journal:
  Food and Function
- ○ **It is intended that the manuscript will be published, but it has not yet been submitted to a journal**

Student's signature:	Akshay Bisht Digitally signed by Akshay Bisht Date: 2023.05.11 14:12:15 +12'00'	Main supervisor's signature:	A.Prof. Lara Matia-Merino Digitally signed by A.Prof. Lara Matia-Merino DN: cn=A.Prof. Lara Matia-Merino, c=NZ, o=Massey University, ou=School of Food and Advanced Technology, email=l.matia-merino@massey.ac.nz Date: 2023.05.11 11:11:26 +08'00'

This form should be placed at the beginning of each relevant thesis chapter.

M.3: Chapter 6

MASSEY UNIVERSITY
TE KUNENGA KI PŪREHUROA
UNIVERSITY OF NEW ZEALAND

GRADUATE RESEARCH SCHOOL

STATEMENT OF CONTRIBUTION DOCTORATE WITH PUBLICATIONS/MANUSCRIPTS

We, the student and the student's main supervisor, certify that all co-authors have consented to their work being included in the thesis and they have accepted the student's contribution as indicated below in the Statement of Originality.

Student name:	Akshay Bisht
Name and title of main supervisor:	A/Prof. Dr. Lara Matia-Merino
In which chapter is the manuscript/published work?	Chapter 6
What percentage of the manuscript/published work was contributed by the student?	85%

Describe the contribution that the student has made to the manuscript/published work:
The candidate has contributed towards conceptualization, methodology, validation, investigation, formal analysis, visualization, data curation and writing - original draft.

Please select one of the following three options:

- ○ **The manuscript/published work is published or in press**
  Please provide the full reference of the research output:
- ◉ **The manuscript is currently under review for publication**
  Please provide the name of the journal:
  Food Hydrocolloids
- ○ **It is intended that the manuscript will be published, but it has not yet been submitted to a journal**

Student's signature:	Akshay Bisht Digitally signed by Akshay Bisht Date: 2023.05.11 14:16:51 +12'00'	Main supervisor's signature:	A.Prof. Lara Matia-Merino Digitally signed by A.Prof. Lara Matia-Merino DN: cn=A.Prof. Lara Matia-Merino, c=NZ, o=Massey University, ou=School of Food and Advanced Technology, email=l.matia-merino@massey.ac.nz Date: 2023.05.11 11:11:57 +08'00'

This form should be placed at the beginning of each relevant thesis chapter.

M.4: Chapter 7

MASSEY UNIVERSITY
TE KUNENGA KI PŪREHUROA
UNIVERSITY OF NEW ZEALAND

GRADUATE RESEARCH SCHOOL

STATEMENT OF CONTRIBUTION DOCTORATE WITH PUBLICATIONS/MANUSCRIPTS

We, the student and the student's main supervisor, certify that all co-authors have consented to their work being included in the thesis and they have accepted the student's contribution as indicated below in the Statement of Originality.

Student name:	Akshay Bisht
Name and title of main supervisor:	A/Prof. Dr. Lara Matia-Merino
In which chapter is the manuscript/published work?	Chapter 7
What percentage of the manuscript/published work was contributed by the student?	85%

Describe the contribution that the student has made to the manuscript/published work:

The candidate has contributed towards conceptualization, methodology, validation, investigation, formal analysis, visualization, data curation and writing - original draft.

Please select one of the following three options:

- ○ **The manuscript/published work is published or in press**
  Please provide the full reference of the research output:
- ○ **The manuscript is currently under review for publication**
  Please provide the name of the journal:
- ◉ **It is intended that the manuscript will be published, but it has not yet been submitted to a journal**

Student's signature:	Akshay Bisht Digitally signed by Akshay Bisht Date: 2023.05.11 14:17:18 +12'00'	Main supervisor's signature:	A.Prof. Lara Matia-Merino Digitally signed by A.Prof. Lara Matia-Merino DN: cn=A.Prof. Lara Matia-Merino, c=NZ, o=Massey University, ou=School of Food and Advanced Technology, email=l.matia-merino@massey.ac.nz Date: 2023.05.13 12:28:59 +08'00'

This form should be placed at the beginning of each relevant thesis chapter.

M.5: Chapter 8

MASSEY UNIVERSITY
TE KUNENGA KI PŪREHOROA
UNIVERSITY OF NEW ZEALAND

GRADUATE RESEARCH SCHOOL

STATEMENT OF CONTRIBUTION DOCTORATE WITH PUBLICATIONS/MANUSCRIPTS

We, the student and the student's main supervisor, certify that all co-authors have consented to their work being included in the thesis and they have accepted the student's contribution as indicated below in the Statement of Originality.

Student name:	Akshay Bisht
Name and title of main supervisor:	A/Prof. Dr. Lara Matia-Merino
In which chapter is the manuscript/published work?	Chapter 8
What percentage of the manuscript/published work was contributed by the student?	40%

Describe the contribution that the student has made to the manuscript/published work:

The candidate has contributed towards conceptualization, design of study, ethics approval, diet preparation, interpretation of the results and writing - review & editing.

The candidate has performed data analysis and drafted the Chapter 8 separately from the publication.

Please select one of the following three options:

○	**The manuscript/published work is published or in press** Please provide the full reference of the research output:
○	**The manuscript is currently under review for publication** Please provide the name of the journal:
◉	**It is intended that the manuscript will be published, but it has not yet been submitted to a journal**

Student's signature:	Akshay Bisht Digitally signed by Akshay Bisht Date: 2023.05.11 14:47:52 +12'00'	Main supervisor's signature:	A.Prof. Lara Matia-Merino Digitally signed by A.Prof. Lara Matia-Merino DN: cn=A.Prof. Lara Matia-Merino, c=NZ, o=Massey University, ou=School of Food and Advanced Technology, email=l.matia-merino@massey.ac.nz Date: 2023.05.13 12:29:55 +08'00'

This form should be placed at the beginning of each relevant thesis chapter.

MASSEY UNIVERSITY
TE KUNENGA KI PŪREHUROA
UNIVERSITY OF NEW ZEALAND

GRADUATE RESEARCH SCHOOL

STATEMENT OF CONTRIBUTION DOCTORATE WITH PUBLICATIONS/MANUSCRIPTS

We, the student and the student's main supervisor, certify that all co-authors have consented to their work being included in the thesis and they have accepted the student's contribution as indicated below in the Statement of Originality.

Student name:	Akshay Bisht
Name and title of main supervisor:	A/Prof. Dr. Lara Matia-Merino
In which chapter is the manuscript/published work?	Chapter 8
What percentage of the manuscript/published work was contributed by the student?	15%

Describe the contribution that the student has made to the manuscript/published work:

The candidate has contributed towards design of study, diet preparation, interpretation of the results and writing - review & editing.

The candidate has performed bioinformatics analysis and drafted the Chapter 8 separately from the publication.

Please select one of the following three options:

- ○ **The manuscript/published work is published or in press**
  Please provide the full reference of the research output:
- ○ **The manuscript is currently under review for publication**
  Please provide the name of the journal:
- ◉ **It is intended that the manuscript will be published, but it has not yet been submitted to a journal**

Student's signature:	Akshay Bisht Digitally signed by Akshay Bisht Date: 2023.05.11 14:48:09 +12'00'	Main supervisor's signature:	A.Prof. Lara Matia-Merino Digitally signed by A.Prof. Lara Matia-Merino DN: cn=A.Prof. Lara Matia-Merino, c=NZ, o=Massey University, ou=School of Food and Advanced Technology, email=r.matia-merino@massey.ac.nz Date: 2023.05.11 11:09:47 +08'00'

This form should be placed at the beginning of each relevant thesis chapter.

Appendix N: Embargo approval